UNIVERSITY OF SOUTHAMPTON
Faculty of Engineering, Science and Mathematics
School of Geography

Exploring Equifinality in a Landscape Evolution Model

by

Nicholas Alan Odoni

Thesis submitted for the degree of
Doctor of Philosophy (Ph.D.)

March 2007

UNIVERSITY OF SOUTHAMPTON

ABSTRACT

FACULTY OF ENGINEERING, SCIENCE AND MATHEMATICS
SCHOOL OF GEOGRAPHY

Doctor of Philosophy

EXPLORING EQUIFINALITY IN A LANDSCAPE EVOLUTION MODEL

by Nicholas Alan Odoni

Model equifinality is the property by which very similar model outputs can be generated by many different combinations of model inputs. It is known in numerical models used in other disciplines, and is thought to be likely in landscape evolution models ("LEMs") also, as they incorporate many process parameters of uncertain value. LEM equifinality, if pervasive, would be a serious obstacle to falsifying working hypotheses and would frustrate landscape evolution research, but to date it has not been quantified. This is attempted here, by sampling a LEM's response in its parameter space. A well known LEM ('GOLEM', Tucker & Slingerland, 1994), used here as an exemplar, is applied to evolution of a *c.* 38 km^2, 4^{th} order catchment in the Oregon Coast Range. Ten of GOLEM's parameters are selected for variation, covering mass movement, channel formation, fluvial erosion and weathering processes, and value ranges appropriate for the catchment are established from published data and calibration. Parameter space sampling is then carried out using a response surface methodology approach which reduces by *c.* 3 orders of magnitude the simulation run size needed to explore the 10-D parameter space. Initial simulations are run sampling the space according to a central composite design of 149 targeted parameter value combinations, which afford estimation of all parameter main and two-way interaction effects. Model outputs at 100,000 years are summarised by four metrics (sediment yield, drainage density, sediment delivery ratio, and a topographic metric), which serve as landscape descriptors. Equations, or "metamodels", are derived by regression to describe each metric as a function of the GOLEM parameters, and further simulations allow testing and improvement of model fits (R^2 of *c.* 98% for the sediment yield, drainage density and sediment delivery ratio, and *c.* 92% for the topographic metric). The parameter space is then sampled rapidly and densely ($>>10^6$ times), using each metamodel to predict GOLEM's output at each sample point. Results are compared with a reference value for each metric, to obtain equifinal proportions in a range of permitted tolerance bands around the reference, and using a bootstrap to aid calculation of confidence intervals. The likelihood of obtaining an equifinal result is found to depend on the tolerance band and the metric e.g. the equifinal probabilities for drainage density are estimated to be *c.* 26% and 58% respectively in the 2% and 5% tolerance bands, compared with c. 68% and 99% for the sediment delivery ratio in the same bands. Where combinations of metrics are used, the polymetric equifinal probability is often lower (and never higher) than it would be for any of the component metrics used singly. Also, the equifinal probability for any metric and tolerance band usually decreases as the number of parameters employed in the model increases. More generally, equifinal probabilities are seen to result from the combinations of parameter main effects and interactions driving each metric, thus allowing equifinality to be explored through the use of metamodel archetypes. Further research using other LEMs is needed, and the response surface methodology is recommended for both its computational efficiency and clarity in this respect.

CONTENTS PAGE

LIST OF FIGURES PAGE

LIST OF TABLES PAGE

DECLARATION OF AUTHORSHIP

I, **Nicholas Alan Odoni**

declare that the thesis entitled

Exploring Equifinality in a Landscape Evolution Model

and the work presented in it are my own. I confirm that:

- this work was done wholly or mainly while in candidature for a research degree at this University;
- where any part of this thesis has previously been submitted for a degree or any other qualification at this University or any other institution, this has been clearly stated;
- where I have consulted the published work of others, this is always clearly attributed;
- where I have quoted from the work of others, the source is always given. with the exception of such quotations, this thesis is entirely my own work;
- I have acknowledged all main sources of help;
- where the thesis is based on work done by myself jointly with others, I have made clear exactly what was done by others and what I have contributed myself;
- none of this work has been published before submission.

Signed: NICHOLAS ALAN ODONI

Date: 3rd September, 2007 (as submitted 'post viva', with corrections)

Dedicated to my mother, to my brother David, and to my friend John, who all kept faith in me when I had none left, and were more patient with me than I thought possible ...

I said to my soul, be still, and wait without hope
For hope would be hope of the wrong thing; wait without love
For love would be love of the wrong thing; there is yet faith
But the faith and the love and the hope are all in the waiting.

(T. S. Eliot, 'East Coker Part III', from *Collected Poems 1909-1926*)

ACKNOWLEDGEMENTS

I wish to acknowledge, with grateful thanks, the help and guidance of my supervisor, Dr Steve Darby, of the School of Geography, University of Southampton, throughout the period of this research. The work took far longer than I had ever intended, and his unwavering commitment to it was invaluable. I should also like to thank Dr Greg Tucker, of the University of Colorado, for his permission to use GOLEM in this research, and for his technical assistance in using the model.

Statistical matters feature strongly in the research, and I wish to acknowledge and thank Professor Russell Cheng, of the School of Mathematics, University of Southampton, for his advice on experiment design, metamodelling and the application of the bootstrap technique, the latter applied most importantly to obtain the quantifications presented in Chapters 5 and 6. His more general comments and interest in this research were also much appreciated.

The work conducted here was made possible by access to the University of Southampton's 'Beowulf' computing cluster, and entailed running long and complicated batch jobs, involving many simulations with GOLEM, and subsequently many different routines to carry out the parameter space sampling with the metamodels. The technical support of Dr Ivan Wolton, assisted by Dr Oz Parchment, both of Information Systems Services, University of Southampton, was essential in this respect, in particular in the writing of batch job procedures, and in solving computational, source coding and compiling problems.

Regarding the data on the Smith River catchment, I should like to acknowledge the assistance of Professor David Montgomery, of the University of Washington, Seattle, and his advice on the method to derive drainage network parameters needed in the simulations, as explained in section 3.5 and Appendix C. Professor Montgomery also acted as my academic host, during my 'WUN' scholarship visit to the United States in summer, 2003, and facilitated my meeting Harvey Greenberg, also of the University of Washington, who provided me with maps and aerial photos of the Smith River catchment prior to my field visit. On the field visit, I was accompanied by Professor Richard Waring, of Oregon State University, Corvallis, who greatly assisted me in understanding the ecology and climate history of the site and its region, and provided additional advice and information subsequently, this information being used in the site description, in section 3.5.

I was also able to visit Professor Michael Church, of the University of British Columbia, and I should like to acknowledge his advice regarding suitable metrics to use to summarise GOLEM's output, particularly his suggestions regarding elevation metrics. His advice prompted the derivation of the topographic metric, used in Chapter 4, which was much more sensitive than the other elevation based metrics I had been considering using up to that time.

Although there are many others I should like to thank, I need particularly to acknowledge the help of Ilse Steyl, who extracted the Smith River DEM from the source CLAMS data, and variously Isobel Sargent, Matt Wilson, Karen Anderson and Jeff Neal, on technical matters related to the use of Matlab ®. Thanks are also due to Sally Priest, who was very supportive during times when writing was especially difficult, and to Alastair Brown and Leanne Franklin-Smith, whose goodwill and help were invaluable while I was preparing the first complete draft of this thesis, and then later when I was compiling the final revised version for submission. Finally, I wish to acknowledge and thank the University of Southampton itself, for providing the funding, via a University of Southampton High Peformance Computing Bursary, for the initial three years of this research.

CHAPTER 1: INTRODUCTION AND RESEARCH AIMS

"It's just like the same!"

An exclamation often used by Genevieve Odoni (the author's daughter) when she was aged about three and had excitedly noticed two similar things.

"The devil is in the detail."

A common saying.

1.1 GENERAL THEME

At any time in the landscape, varieties of form and feature are presented to the eye. At one scale, we may see gravel bars and meanders in rivers, which change with each passing season; at a wider scale, valleys sculpted by glaciers thousands of years ago may provide the setting, like a natural stage, for the places where we live; and at yet wider scales, blocks of country may be dominated by uplifted masses of rock, their weathered and eroded humps persisting long after tectonic forces began to bring them towards the surface. Since the earliest days of the earth sciences, observers have tried to account for these and other features and forms, devising theories to make sense of their evolution and of the processes working to create the wider landscape. They have also sought to bring these theories together in models, through which - it is hoped - the evolution of different landscapes across the world becomes explicable according to common laws, and the changes in form and feature over time become part of a complete story.

Up until the 1960s, landscape evolution models were qualitative, comprising descriptive writing supplemented by pictures or diagrams (e.g. Davis, 1899, 1902, 1909; King, 1957; 1962), and later standard texts still include reviews and commentary on them (e.g. Chorley and Kennedy, 1971; Pitty, 1971; Young, 1972; Chorley, Schumm and Sugden, 1984; Thorn, 1988). Over the last fifty years, however, geomorphology has become increasingly quantitative, and this has led in turn to the development of quantitative models, and latterly to the use of process-response models. These types of model allow processes and changes in form over time to be related to each other by mathematical relationships, and there continues to be much interest in how such models may be applied to geomorphological problems (e.g. Thorn, 1988; Bras *et al.*, 2003; Martin and Church, 2004; Willgoose, 2005;

Codilean *et al.*, 2006). Some of the earlier mathematical process-response models were clearly promising (e.g. Kirkby, 1971; Luke, 1972), although restricted in the way they could be used. Latterly, numerical versions of such models, run on computers, have proved more flexible, and have been able to generate simulated forms and features resembling those seen in real landscapes (e.g. Ahnert, 1976 and 1987; Willgoose *et al.*, 1991a; Howard, 1994; Tucker and Slingerland, 1994; Moglen and Bras, 1995; Rinaldo *et al.*, 1995; Kooi and Beaumont, 1996; Braun and Sambridge, 1997; Tucker *et al.*, 1997; Veldkamp and Van Dijke, 1998; Coulthard *et al.*, 1999; and numerous others). This is a considerable advance from the days of the largely qualitative descriptions still used only four decades ago.

Despite this success, however, landscape evolution models ("LEMs") are thought to suffer from a potentially serious defect, called *model equifinality* (e.g. Beven, 1996; Kirkby, 2000; Bras *et al.*, 2003). The concept of equifinality itself is derived from systems theory, and is explained below, in subsection 1.2.1. For the purposes herein, however, the term 'model equifinality' will be taken to mean the property of a model, and in particular of a numerical model, by which it may generate the same or very similar output in many different ways (e.g. Beven, 1996; Freer *et al.*, 1996; Kirkby, 2000; Beven and Freer, 2001). In this respect, there are many uncertainties associated with LEMs and LEM studies, each providing additional factors and conditions to any LEM simulation. Accordingly, each simulation can be likened to a working hypothesis which incorporates a specific combination of those factors and conditions, and which is used to explain a possible landscape or landform history; similarly, a set of different simulations can be likened to a group of such working hypotheses. Model equifinality is a problem because it obstructs falsification of working hypotheses. How this happens, and the relationship between uncertainty, multiple working hypotheses and model equifinality, are also discussed below, in subsection 1.2.2.

Although possible equifinality in LEMs has been recognised for some time (e.g. Ahnert, 1987; Armstrong, 1987), Beven in particular has highlighted the need to understand the extent to which numerical models, including LEMs, may be equifinal (Beven, 1996, 2002). Without quantitative research into the problem, however, our understanding of equifinality in LEMs must remain vague, and the problem hidden from us, like some ogre lurking in the dark. The author's general purpose in this thesis therefore is to attempt to quantify the extent to which LEMs are equifinal. Posing this as a question, can we move from a qualitative understanding of equifinality to a more quantitative one, and thereby detach some of the vagueness from the concept, at least as it applies to LEMs? This would be

useful for geomorphologists, and quite possibly in other sciences also, where similar types of model are frequently used to explore multiple working hypotheses (e.g. Pollack, 2003).

Given therefore that this is the general purpose of the thesis, this chapter provides more context for the problem of model equifinality in LEMs. The first part of the chapter comprises a brief review of equifinality as a concept. There is also a short review of the main sources of uncertainty in LEMs and LEM studies, and a summary of the relationship between these uncertainties, multiple working hypotheses and the problem of model equifinality. This is followed by a introductory review of how LEMs have actually been used in geomorphology, with examples of the association between model outputs and the scenarios and variables used in LEM research. These reviews together then lead to the formulation and statement of the main research aims. At the end of the chapter, there is also an outline of the thesis structure.

1.2 EQUIFINALITY AND MODEL EQUIFINALITY

1.2.1 Equifinality as a concept

The basic concept and its appeal in geomorphology

The first use of the term 'equifinality' is attributed to von Bertalanffy and is drawn from his work on systems theory (e.g. von Bertalanffy, 1968). von Bertalanffy argued that an open system could reach the same final state from different initial conditions and in different ways. In particular, if an open system attained a steady state, this would be equifinal for all initial conditions and wholly independent of them (*ibid.*).

The properties of open systems, and the possibility of dynamic equilibrium or other states being achieved within them, appealed to geomorphologists. A clear attraction of the systems idea was that landscapes could be treated as a kind of open system. For example, Leopold, Wolman and Miller (1964) commented on the usefulness of the drainage basin as a basic geomorphological system, the drainage divide acting as a natural system boundary to each basin; similarly, Chorley (e.g. Chorley and Kennedy, 1971) wrote specifically on the need to study geomorphological problems using a systems theory approach. Thorn (1988) also attributes an appreciation of the application of systems concepts to earlier researchers, in particular to Strahler in the 1950s, and before him, to Gilbert as early as 1877 (Thorn,

1988, pages 164-165). Moreover, some notion of equifinality has existed in geomorphology since its earliest days as a science, and can certainly be traced to the work of William Morris Davis even if he did not himself use the term 'equifinality' to describe it.

In this respect, Davis's idea of the peneplain as the final condition of humid temperate landscapes (before any renewal through uplift) is an example of how landscapes were thought to tend towards the same general state over time (e.g. Davis 1899, 1902 and 1909), despite their initial forms or geology, or the effects of intervening climate changes. Similar arguments could be made regarding the types of slope development theories proposed by Penck and King (e.g. Young, 1972). This illustrates a more widely accepted idea in geomorphology, namely that landforms can converge to the same state over time, even though they may begin from different states and have been changed by different processes and driving conditions (e.g. Kirkby, 1996).

Taking a somewhat different view, Haines-Young and Petch (1983), in an interesting discussion of equifinality, suggested that a helpful definition of the term would be,

> "A single landform type is said to exhibit equifinality when it can be shown to arise from a range of initial conditions through the operation of the same causal processes (physical laws)."
>
> (Haines-Young and Petch, 1983, page 465).

The authors are quite critical of the idea of equifinality, however, suggesting that it is an empty problem if two similar forms in different locations can indeed be shown to have evolved in different ways (*ibid.*). The authors are therefore arguing that provided the separate evolution paths of the landforms can be established, their similarity of present form is irrelevant in the investigation of their history. The difficulty with this approach, however, is that it still begs the question: how are the different evolution paths to be distinguished from each other if the only attribute against which the competing hypotheses are to be tested is the form itself? Haines-Young and Petch (1983) must therefore require that the working hypotheses enable predictions to be made of attributes other than the forms. If field data can be obtained which will permit falsification of one or more of those predictions, then presumably the different evolution paths of each slope may be more clearly distinguished from each other, despite their similarities in form.

The idea of using many attributes rather than just the form is incorporated by Culling (1987), who took a broadly similar view to Haines-Young and Petch, albeit from a mathematical standpoint. He suggested that there may be properties of systems which lead to an appearance of equifinality, although the final characteristics may not be equifinal in every detail, and the resemblance depends on the characteristic behaviour of the system. Young (1972) was also sceptical that landforms are truly equifinal, commenting as follows:

> "In theoretical discussions of slope evolution assumptions are frequently made about the properties of the regolith for which there has, until recently, been little observational basis. A further application is in deductive work using process-response models. When comparing the results of such models with actual slope form, the difficulties caused by equifinality … are lessened if, in addition to the shape of the ground surface, observations of the regolith are available."
>
> (Young, 1972, page 194)

Again, it will be seen here that Young suggests that we include additional attributes of the system, in this instance details relating to the sediment or soil. To follow Young's recommendation, therefore, models predicting the evolution paths of the slope can be made more discriminating if, within the overall form, the model structures allow a distinction to be made between the bedrock and the regolith, or between different layers of the regolith.

With respect to model equifinality rather than equifinality in real landscapes, Bras *et al.* (2003) pose a wider question, namely whether "truly different" landscape models can lead to the same outcome. They suggest that such an occurrence should be very rare if the outcome is by reference to every facet of the system whose behaviour is being modelled. This may indeed be true, and perhaps possible if each cell in the modelled landscape is treated individually (e.g. Kirkby, 2000), but it may not be an efficient or practical way to approach the problem given that a modelled landscape may typically number 10^3-10^5 cells (reviewed in Chapter 2). Church (2003), in the same volume, discusses the matter in a slightly different way, saying that researchers need to use new and more demanding statistical measures, which combine various landscape metrics, whether from real or modelled landscapes. By such means, Church argues, we should be clearer about what constitute similar (or dissimilar) landscapes, whether real or simulated (*ibid.*). Willgoose (2003), in the same volume, makes a similar point, proposing that suites of metrics should be used, so as to make tests of model predictions more demanding.

Approaching the evolution of systems in a different manner, Phillips (1997, 1999, 2006) deduces from a mathematical analysis that the inclusion of more factors should make results, such as LEM output, 'more singular'. One way to interpret this is to say that the existence of many possible factors in the evolution of landscapes, whether real or modelled, should reduce the likelihood of equifinality. Beven, by contrast, holds a different view, namely that increasing the completeness of models will always require the inclusion of more parameters of uncertain value, and this in turn will increase the likelihood of equifinal output being generated (e.g. Beven, 1996). In addition to these conflicting views, there is a need to keep simulation work tractable, so it can be completed using available computing resources. This means practically that researchers generally have to concentrate on demonstrating the effects of the more important factors or variables, but likewise implies that there may be some loss of discrimination between different simulations - and hence some increase in model equifinality - as a result.

It appears from the foregoing that although equifinal behaviour in LEMs is likely, and probably unavoidable, there may be ways to reduce it. It is also interesting to note from the above that authors do not insist that it is a problem only of 'final' forms or states. Indeed, the concept was sometimes formerly termed 'convergence', and was still being referred to as such until quite recently (e.g. Pitty, 1971; Chorley, Schumm and Sugden, 1984), which implies that finality of a form is not crucial when applying equifinality as a concept. However, although 'equifinality' is the term often used by most authors nowadays (e.g. Ahnert, 1987; Summerfield, 1991; Kooi and Beaumont, 1996; Beven, 1996; Bras *et al.*, 2003), the matter is not wholly settled and some comment on the use of terms is needed before going further. It is also important to be clear about what quantities are to be compared with each other, and the role of location or place.

Equifinality, 'convergence' and place

In dealing with the appropriate terminology, it is helpful to consider some general issues in geomorphology. It is widely recognised that landscapes often contain relict landforms and other features, sometimes formed by events and conditions that lie far in the past (e.g. Schumm and Lichty, 1965; Brunsden, 1993; Ahnert, 1994; Phillips, 1999; Thomas, 2001; and numerous others). It follows that if it takes time for a landscape to adjust to changes in driving factors, such as the climate, uplift and so on, and if these changes are rapid, then full

adjustment of the landscape may not occur before the onset of the next such change. This means that many landscapes are seldom if ever wholly in equilibrium with the forces shaping them. The persistence of past forms and the episodic nature of major formative events also suggest that the concept of equilibrium, although useful at smaller scales, is not likely to be encountered at larger scales, such as over whole mountain ranges or amongst groups of adjoining drainage basins (e.g. Craig, 1982; see also Thorn, 1988). Geomorphologists are therefore more likely than not to be engaged in studies of transient landscapes and landforms, and LEM studies will necessarily reflect this.

It could be argued from the above that the idea of 'convergence' is perhaps the more useful one in geomorphological research, rather than equifinality in its strict sense. However, where convergence is discussed, the emphasis is often on the convergence of *forms* rather than of other landscape attributes, such as the sediment yield or drainage density (e.g. Pitty, 1971; Chorley, Schumm and Sugden, 1984). The author would suggest that there is no need for this limitation when using the term 'equifinality', and that the concept can be applied to any measure of a landscape and its behaviour, such as the sediment yield, or the mean depth of the regolith, or the drainage density, and so on. In addition, it can be seen that this point applies as much to modelled slopes and landscapes as it does to real ones; it also applies, moreover, to simulations applied to the same landscape and not simply to similar forms emerging in different locations, in the manner envisaged and discussed by Haines-Young and Petch (1983). In this way, the problem of similar forms evolving (via the LEM) at different locations is subordinate to the problem that similar forms may evolve at the same location, by using different variables and parameter values in the same LEM, or even by using different combinations of the same in different LEMs applied to the same landscape.

Taking these points together, for the purposes of this thesis the term 'equifinality' rather than convergence will be used, with the intention that it should be applicable to any attribute of a landscape and not simply to the landforms or the topography. The term 'equifinality' will also be used to refer to both transient and equilibrium states, depending upon the context, rather than only to equilibrium states. The only requirement in either instance is that there is a stipulated time at which to make comparisons of LEM output, whatever the reference measure or quantity of interest.

Having introduced the concept of equifinality and how the term itself will be used in the thesis, a brief review of why equifinality is thought to occur in LEMs now follows. This is

related to uncertainties in LEMs and LEM studies, which are also considered here. The possibility of equifinality in LEMs is further considered at the end of Chapter 2.

1.2.2 Uncertainty and the possibility of equifinality in LEMs

Development of LEMs, and sources of uncertainty in LEMs and LEM studies

The use of quantitative models to demonstrate theories of landscape evolution can be traced to process-response modelling work in the 1960s and 70s, and particularly to the pioneering slope evolution models of Michael Kirkby and Frank Ahnert (Thorn, 1988; see also Martin and Church, 2004; and Willgoose, 2005). Kirkby (1971) in particular was able to show that a range of realistic slope forms could be generated from the operation of just a small number of generalised processes, covering weathering, detachment and transport. Kirkby's work held the promise that process rate equations such as those he used could be extended beyond slope modelling to the simulation of landscapes as a whole. However, his analytical methods could only be applied in a limited way to whole landscapes (e.g. Luke,1972 and 1974). It was necessary to adopt numerical approximation, using computers, in order to simulate evolution of areas or drainage basins, the work of Frank Ahnert being amongst the first developments in this respect (Thorn, 1988). Ahnert's numerical modelling work was published in a series of papers in the late 1960s and early 1970s, culminating in Ahnert (1976), in which the principles underlying his slope model were extended to simulation of landscape evolution. Amongst other things, Ahnert was able to show how spatial variations in the modelled domain could be incorporated to take into account different bedrock types and their weathering, detachment and mass failure properties. This allowed him to show the influence of different process rates at different locations (*ibid.*), and the effects of uplift and other factors.

The modelling development that has occurred since that time has in essence not changed in its basic approach, in that the object is to simplify process equations and discretise time and space, so that evolution can be simulated by a stepwise, numerical method. Using models of this kind, geomorphologists have explored a range of problems, and examples of these are summarised in Table 1. Despite these sophisticated developments, however, the equations used in LEMs are largely generalised relationships, incorporating variable empirical parameters whose values are uncertain (Beven, 1996). There are further

uncertainties relating to the process formulations that are used to simulate the geomorphic processes of interest: although researchers aim to make these as physically based as practical, they are not wholly correct, and some mismatch between the formulation and reality cannot be avoided (e.g. Kirkby, 1996; Beven, 1996). To these uncertainties must be added general uncertainties relating both to the initial form of the landscape, including its distribution of soil and sediment, and to the past climate, uplift and other driving conditions which have affected the landscape over time. Finally, all such uncertainties are embedded in the cell gridding and time step schemes within which the LEM's calculations are made. These also cannot be wholly correct, and there are interesting examples of how variants can make important differences to model output (e.g. Braun and Sambridge, 1997).

It will be appreciated from the foregoing that the different sources of uncertainty in LEMs and LEM studies may not be easy to distinguish from each other. Some are derived from the initial and driving conditions; others, on the other hand, relate more directly to LEM structure and architecture. To clarify these aspects, a summary of the main sources of uncertainty is shown in Figure 1.1.

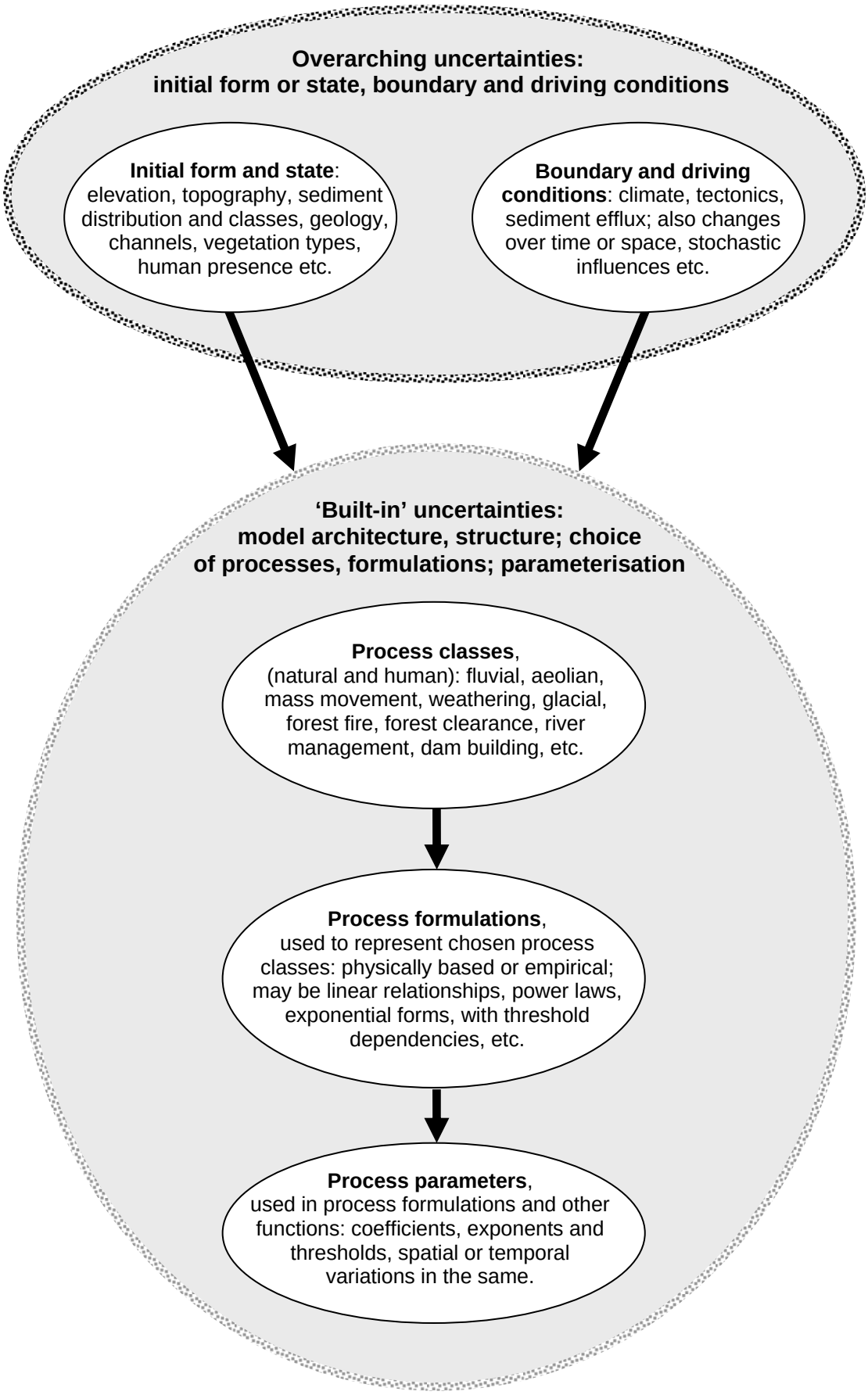

Figure 1.1: Main sources of uncertainty in LEMs and LEM studies (see text).

In the figure, the uncertainties are shown as a hierarchy. Those relating to initial form or state, and to the boundary and driving conditions, are separated from those more closely associated with the 'structure' and 'architecture' of the LEM (these terms explained below).

To begin with, as regards the initial form and the boundary and driving condition uncertainties, these are seen as 'overarching', in that they are present whatever the LEM or LEMs being used, and often the main focus of the research. For example, if the study begins with a present day landscape, with the aim of understanding the effects of climate change, there will be errors in the DEM and other initialising data, and errors in the projected climate itself, and also in the predicted vegetation succession and so on; similarly, if the LEM is used to understand the evolution of a landscape since a specified but distant past time, before historical records, then the initial landscape and its sediment cover will have to be hypothesised, and probably the climate and other driving conditions also to some extent, the uncertainties in the latter depending upon the availability and accuracy of past climate proxy data and related information.

By contrast with the overarching uncertainties, the 'built-in' uncertainties are seen largely as model dependent (e.g. Haff, 1996; Kirkby, 2000; Beven, 2002). More specifically, and for the purposes here, the term 'model structure' is intended to mean the theoretical representation of the system itself, as signified by the things being modelled, in particular, the state variables and processes, and the links between them. Architecture, on the other hand, is intended to mean the manner in which that structure is arranged and divided for computational purposes, both over time and space. It follows that the same model structure might be represented by a range of different architectures; similarly, it could be possible for the same architecture to be used for discretisation of a range of different model structures. These matters are reviewed in more detail in Chapter 2.

It will be appreciated from this that built-in uncertainties are likely to be more or less fixed, in that there is little a researcher can do to change them or improve on them once a LEM has been selected, or built, for a research purpose. Admittedly, some LEMs permit a choice between different process classes or process formulations[1], and others incorporate self-adjusting time steps and grid cell sizes (e.g. Braun and Sambridge, 1997; Coulthard *et al.*, 1999), but this flexibility has to be limited, to keep model size and coding practical.

[1] For example, as will be noted in Chapter 3, GOLEM (e.g. Tucker and Slingerland, 1997) allows a researcher to select one of four different process equations to model fluvial sediment transport.

The hierarchical relationship between the built-in uncertainties is particularly evident in Figure 1.1. Specifically, the choice of process classes in a LEM will be strongly influenced by the climate being applied to the modelled landscape; for example, aeolian processes are not likely to be needed in simulations of humid environments, nor are nival processes likely to be needed in simulations of warm environments. Once the main process classes of interest have been chosen, process formulations will be needed to represent them, so the formulations employed will be stem from the process class choices. In this respect, although past studies may guide a researcher which process formulation to prefer (assuming the LEM allows a choice), the matter is still subjective to some extent. In addition, whichever formulation is chosen to represent a process or other LEM function, it will almost certainly not be wholly physically based, and must therefore be empirical in some respect (Thorn, 1988).

Continuing with the hierarchy, the process parameters required in the simulations follow inevitably from the selected process formulations. As explained above, the parameters are mostly empirical and of uncertain value. It should also be noted here, however, that as the number of different model functions increases, so too does the number of parameters needed to implement them (e.g. Beven, 1996; Kirkby, 1996). Whatever the other uncertainties, therefore, most LEMs have a large process parameter space, which comprises large dimensionality (the number of parameters) and value uncertainty (the combined ranges of acceptable value for each parameter). This is considered again at the end of Chapter 2, and the implications of large LEM parameter spaces on simulation work are reviewed in Chapter 3.

With a number of uncertain parameters, and possibly many of them, how are model scenarios to be set up in a simulation experiment? In some cases, reviews and related sources will be able to suggest value ranges for the process parameters (for example, process rate coefficients in Saunders and Young, 1983, and Young and Saunders, 1986; similarly, fluvial process exponents in Prosser and Rustomji, 2000). If published sources are not available, then model calibration may allow value ranges and central or base case values of parameters to be estimated. However, the exercise is not simple, and there is always the difficulty that calibrating for several parameters' values simultaneously will lead to poorly estimated ranges for each of them, particularly if some of the parameters have little influence on the output (Beven, 1996). In such circumstances, it may be more appropriate to hypothesise central or 'base case' values for those parameters whose effects

appear to be small[2], and vary in the simulation only those whose effects are greater, departing from this if the results appear problematical for some reason.

Having reviewed the main sources of uncertainty, the argument is now expanded to consider the associations between uncertainty, multiple working hypotheses and model equifinality.

Uncertainty, model equifinality and multiple working hypotheses

The discussion above outlines how the uncertainties in LEMs and LEM studies arise, both in the way LEMs are constructed and in the manner in which they are used. The difficulties posed by having such uncertainties become especially troublesome where LEMs are used to investigate *inverse* problems (e.g. Pollack, 2003), that is, where the aim is to explain the most likely evolution path of a present day landscape since a particular time in the past. If the model can be designed with a strong physical basis, e.g. as in geophysical research, then the main uncertainties in an inverse problem will be the initial state, the boundary and driving conditions, and the observation errors (*ibid.*). However, in LEMs, because of their semi-empirical basis, many of the built-in uncertainties cannot be avoided, and these uncertainties present any researcher with many possible variables. The term 'variable' is used here in a wide sense, namely to mean any factor, condition, parameter and so on, which may be altered at a researcher's discretion, whether using just the one LEM, or more. With so many variables, LEM simulations can be run in many different ways (e.g. Beven, 1996; Kirkby, 2000). Moreover, this applies whether one is using just a single LEM, or if the aim is to contrast output from one LEM with another.

Why might this be a problem? The argument here is twofold. Firstly, given the general uncertainties, any simulation with a model will only be one of a number of possible explanations of reality (e.g. Freer *et al.*, 1996; Beven and Freer, 2001; Helton, 2004; Oberkampf *et al.*, 2004; Spear, 1997; and numerous others. See also Giere, 1999, and Pollack, 2003, for more philosophical discussions). Some of these will be better than others, however, in that their output closely resembles field or other relevant data to some degree, and out of these simulations, there may well be a selection generating the same or very similar output (Beven, 1996), thus demonstrating model equifinality.

[2] The ideas of a parameter's 'effect', and the identification of parameter effects more generally, are reviewed in detail in Chapter 3.

Secondly, the use of LEMs can be likened to the demonstration of *multiple working hypotheses* (e.g. Platt, 1964; Haines-Young and Petch, 1983 and 1986; Schumm, 1991; Baker, 1996; Pollack, 2003; Inkpen, 2005). In this respect, each simulation with a LEM can be viewed as a working hypothesis in its own right, each aspect of the overarching and built-in uncertainties combining to form the overall hypothesis; likewise, a suite of different simulations can be treated as a set of such hypotheses. Where model equifinality occurs, however, the different evolution paths drawn by each simulation converge, and this makes falsification of any of the hypotheses problematic. Such a situation is shown graphically, in Figure 1.2, adapted from Church (2003).

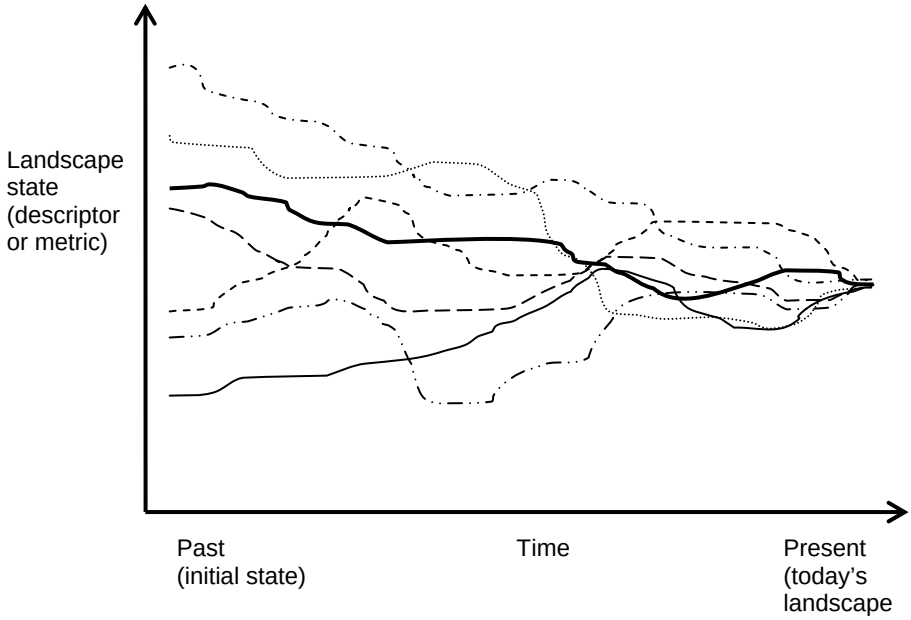

Figure 1.2: LEM evolution paths represented as multiple working hypotheses (adapted from Church, 2003). The bold line represents the true evolution path of the landscape; the other lines signify the evolution paths generated by different LEM simulations, each of which represents a different working hypothesis. In the figure, these are equifinal and converge on the present state, which cannot alone be used as a measure to falsify any of the hypotheses.

In the figure, each working hypothesis relates to a simulation and is shown by its own 'evolution path' over time, this taken to be identified by some descriptor or metric of the landscape state. Whether the metric is simply a single property, such as the drainage density, or a composite of different landscape properties, in the manner discussed by Church (2003), the path of the true landscape state over time is shown by the bold black line. This is assumed here to be the major unknown, and the target which the researcher is seeking to simulate.

Ideally, all of the working hypotheses would be clearly distinguishable from each other, particularly in their final result, so that by the end of the simulations, any 'wrong' hypotheses would clearly differ from the real landscape (as measured by the descriptor or metric). In the Figure 1.2, however, model equifinality is present, and all of the hypothesised evolution paths converge on the present state. In such a situation, the present state alone cannot be used to identify which evolution paths are wrong, and hence which of the multiple working hypotheses can be falsified.

As discussed in subsection 1.2.1, the possibility arises of using more descriptors from the real landscape. In this way, equifinality to one descriptor may not be a problem if the model predictions are not equifinal for the others. However, there may still be difficulties caused by observation errors relating to the present day landscape, so that what constitutes an equifinal result itself becomes uncertain. If the simulations are run stochastically, using climate variations for example, the position may become yet more uncertain and blurred. Model equifinality to multiple measures therefore still presents potentially serious problems.

As a variant of the situation pictured in Figure 1.2, Figure 1.3 shows model equifinality occurring where a common initial state is used for each LEM simulation.

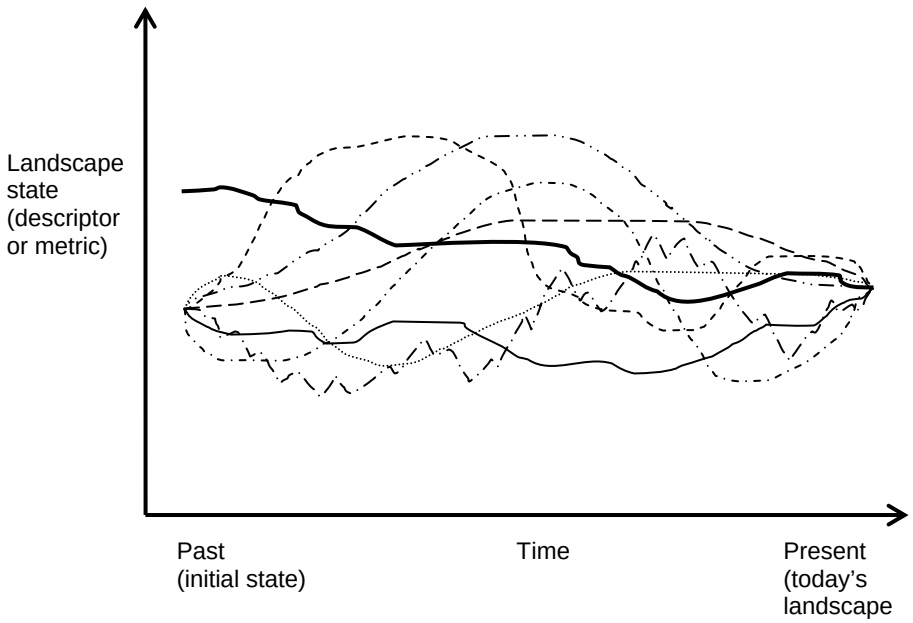

Figure 1.3: LEM evolution paths represented as multiple working hypotheses (adapted from Church, 2003), but this time beginning with a common initial condition. As before, the bold line represents the true evolution path of the landscape and the other lines signify the evolution paths generated by different LEM simulations. These are equifinal, so the measure of the present state alone cannot be used to falsify any of the simulation hypotheses.

In the figure, different system states emerge, as the evolution paths for each simulation at first diverge from each other. However, the paths converge later in the simulation, in this example all meeting at the present state of the real landscape. Presumably, variants and combinations of Figures 1.2 and 1.3 could be drawn, including representations with observation and other errors. However, it will be appreciated that if the type of equifinality seen in Figure 1.3 can be shown to occur in LEMs, then that seen in Figure 1.2 must occur also[3]. It will also be appreciated from Figure 1.3 that even if a researcher happened to hypothesise the initial state correctly, so it coincided with the true initial state, then it would still not be possible from the final state alone to falsify the wrong hypotheses.

Researchers are probably well aware of the uncertainties in model studies, and of the latent difficulties posed by LEM equifinality. However, once the problem is understood in the terms states above, and despite the comments by some of the authors cited in the discussion, the potential for equifinality in LEM studies appears to be huge. If it is common, it implies that we cannot "… secure the survival of the fittest theory by the elimination of those which are less fit." (Popper, 1969, page 313). We are also prevented from pursuing that "iterative back-and-forth interplay" between observations and models, which "… generally improves understanding of a system" (Pollack, 2003). Ubiquitous model equifinality in LEMs would therefore both obviate their use and frustrate progress in the discipline.

Given this conclusion, it clearly becomes necessary to consider how model equifinality can be dealt with. Although the problem appears difficult to manage, it may not be insuperable. In particular, if it can be assumed that LEM outputs are generally not due to inconsistencies in the calculating procedures or algorithms, nor to numerical instabilities of some kind, then they must represent a response to the model variables, manifested through their influence on the modelled landscape. As can be seen from Figure 1.1, these variables may stem from any of the sources of uncertainty in LEM studies. By examining LEM output for the influences of these variables, it should be possible to clarify whether equifinality does indeed occur, and the variables most likely to cause it. In addition, it may be possible to express the responses mathematically, thus clarifying how each variable affects model equifinality. An important preliminary step, therefore, before formulating the research aims, is to consider the range of variables used in LEM studies, and to examine their influence on LEM output. These matters are now briefly reviewed.

[3] In this way, Figure 1.2 is equivalent to assuming that the simulations in Figure 1.3 begin at a somewhat later time (nearer the present), when the landscape states have all diverged and are different from each other.

1.3 VARIABLES USED IN LEMS AND THEIR INFLUENCE ON OUTPUT

1.3.1 Table of example LEM studies

Table layout

To review all the findings of researchers who have used LEMs is a near impossible task, such has been the rate of increase in the use of LEMs over the last twenty years. The author has therefore taken examples from the literature to demonstrate the range of topics in geomorphology to which LEMs have been applied, and these are summarised in Table 1. The table also includes some studies with numerical slope evolution models, as these models work in an equivalent way to LEMs, and indications of equifinality in such studies would indicate that similar results in LEM studies are possible.

The table is divided into columns so as to distinguish between the simulation scenarios and variables, listed in column 2, and the main influences exhibited in the simulations, listed in column 3. The information in column 2 also highlights both the relative frequency of certain research themes in LEM studies generally, and the main variables of interest used in each of the listed studies. The information in column 3 is a summary of the results from each study, thus allowing variables and results to be seen side by side. It should be noted, however, that in summarising model results in column 3, the author's focus on influences of the variables gives the results a different emphasis to that given to them by the original authors. This is deliberate, for the purposes of introducing the equifinality problem, and is not meant to detract in any way from the work as it was originally reported. Another difference from the original papers is that each study is summarised in terms of the 'influences' of the variables, rather than their 'effects'. This is also deliberate, as the term 'effect' is used in a specific way in this thesis, particularly from Chapter 3 onwards, and this is rather different from the way effects are commonly described in LEM studies. Finally, before turning to the particular variables and influences listed in the table, it is also helpful to comment on the temporal focus of the studies and certain aspects of the presentation. For convenience here, references are cited by using the reference numbers in the table corresponding to the particular paper or study.

Table 1: Examples of studies with LEMs and slope evolution models, summarising the main variables and their influence on model output.

Reference	Main variables or scenario	Main influences on results
1. Ahnert (1987)	Process rate parameter values, geology	Differences in balance between processes and rates at different places strongly influences resulting forms.
2. Armstrong (1987)	Different initial slope forms, process classes and rates, rates of basal removal	Large differences in the initial form have a strong influence on the evolution of transient slope forms. Combinations of different processes can produce very similar transient forms, suggesting equifinality and convergence. Low weathering rates limit erosion and strongly influences slope form evolution; high rates have little or no influence. Rate of basal removal influences eventual slope forms and the depth of lower slope sediments. Different erosion processes produce different patterns of deposition on lower slopes, whatever the eventual slope form.
3. Bogaart *et al.* (2003a)	Climate and process parameters	Climate strongly influences surface runoff generation, areas draining into channel heads, and sediment yield. Change of climate from cold to warm reduces sediment yield. Change of climate from warm to cold increases drainage density, and sediment yield until ready supplies are exhausted.
4. Bogaart *et al.* (2003b)	Climate and process parameters	Variables have a strong influence on hillslope erosion, fluvial sediment transport, deposition and related output measures. Strength of influences changes over time.
5. Braun & Sambridge (1997)	Cell geometries, size and number	Cell grid scheme influences routing of channels and sediment, sinuosity, drainage density, and over time, topography.
6. Clevis *et al.* (2003)	Bedrock erodibility, rate of thrust displacement, temporal tectonic and sea level (base level) fluctuations	Bedrock erodibility strongly influences sedimentation rates, although effect changes over time.
7. Coulthard & Macklin (2005)	Different study sites, same long term general climate signals per site	Shifts to a wetter climate have a strong and almost immediate influence on sediment yield from the catchment as a whole. Land cover (forest) influences peaks in the sediment yield in response to the same climate conditions. Pattern of sediment movement within catchments is strongly determined by location. Responses over time of erosion and sedimentation to the same climate forcing are 'noisy', with possible pulsations.
8. De Boer (2001)	Rainstorm area in inverse relation to rainstorm frequency	Frequency of rainstorms strongly influences the total sediment yield from the basin. (Note 1.) Area of storms influences the sediment yield, whereas position of storms influences the formation of relief and topography.
9. Fagherazzi *et al.* (2004)	Sea level oscillations, climate (runoff), initial topography	Oscillation amplitude of sea level change strongly influences river mouth incision. Small amplitude oscillations in sea level have little influence on lowering of river beds, whereas larger amplitude oscillations have a stronger influence, causing the formation of knickpoints that propagate upstream. Climate (via as an increase in runoff) strongly influences formation of new incisions and sediment delivery to the shelf. Initial topography strongly affects position of initial channels and subsequent development of channels and topography.
10. Fischer *et al.* (2004)	Uplift and tectonic rebound coupled to a surface process model (LEM)	Fluvial removal processes, rebound and base level changes together strongly influence formation of realistic relief.
11. Gargani *et al.* (2006)	Long term climate shifts, base level	Pattern of climate change strong affects sediment yield and fluvial erosion. Base level changes have little influence on fluvial erosion at certain stages of the climate cycle.
12. Gasparini *et al.* (1999)	Runoff, sediment classes and proportions thereof	Variations in runoff, slope and sediment characteristics influence downstream fining in eroding networks. Initial proportions of sediment classes have little influence on pattern of downstream fining that eventually emerges.
13. Gasparini *et al.* (2004)	Climate, uplift, grain sizes and mixing again	Sediment grain size strongly affects channel concavity and relief. Mixed grain sizes may offset the influences of climate and uplift on channel gradient, thus producing similar channel slopes.

Table 1 (cntd): Examples of studies with LEMs and slope evolution models, summarising the main variables and their influence on model output.

Reference	Main variables or scenario	Main influences on results
14. Hancock (2003)	Erosion parameters, catchment aspect ratio	Erosion parameters and aspect ratio both influence hypsometric curve, area-slope relationship, channel width function and cumulative area distribution, although influence of some parameters/variations is greater than others.
15. Howard (1994)	Uplift and climate scenarios, and different erosion law formulations	Form of fluvial erosion law has strong influence, in the presence of uplift, on locations and rates of stream erosion in transient landscapes
16. Kirkby (1989)	Different climatic conditions, initial forms, time periods, process classes and process rate parameters, land management systems	Combinations of land management practices and climate strongly influence the evolution of slopes and sediment profiles. Responses to different temperature, hydrology, land cover and weathering are made more complex depending upon type of main climate being applied. Influence of new climate or new land use on an otherwise near-stable soil profile may be strong and non-linear
17. Kooi & Beaumont (1996)	Forms of process law; also uplift and transport/erosion rates	Response time of the landscape (as determined by process rate coefficients, laws and so on) and tectonics have important influences on patterns of landscape evolution.
18. Lancaster *et al.* (2001)	Numerous process parameters and site variables, including woody debris supply	Debris dams have little influence on sediment yield from a catchment, but absence of dams or a low supply of wood strongly influences the degree of pulsing of sediment through the system and the formation of terraces. Combined influences of debris flows, wood supply and in-channel sediment storage may be complex and counter-intuitive.
19. Martin (2000)	Weathering rates, diffusivities, process formulations	Weathering strongly influences transport by mass movement on steep slopes, low rates limiting erosion by creep and slides. Diffusivities (incorporating both creep and slide) strongly influence slope forms, subject to limiting weathering rates.
20. Moglen & Bras (1995)	Soil erodibility, expressed as 'softness'	Variability in soil 'softness' strongly affects sinuosity and convex-concave slope variability. Vertical variation strongly affects shape of hypsometric curve, whereas horizontal variation strongly influences relief.
21. Niemann *et al.* (2001)	Uplift	Uplift rates strongly affect the vertical migration rates of knickpoints.
22. Rinaldo *et al.* (1995)	Cyclic variation in τ_c (surface resistance), to effect climate change	Change in climate over time has complex (lagged) influences on drainage density, valley density and (fractal) topography. Evidence of past climates is complicated by uplift, slope-dependent processes and amplitude of the changes. (Note 2)
23. Rosenbloom & Anderson (1994)	Diffusivities, weathering, forms of process law, stream incision parameter	Hillslope diffusivity rates have a strong influence on evolution of realistic forms. Weathering rates have little influence on slope evolution unless they are low and limiting. Stream incision parameter has a strong influence on the stream profile.
24. Schlunegger *et al.* (2001)	Climate and geology, tectonic response to unloading following erosion	Change in climate strongly influences erosion and sediment yield; sediment yield also changes with time. Different geologies/strata strongly influence re-routing of drainage network. Tectonic response to erosion (unloading) influences re-routing of channels, drainage density and sediment yield.
25. Tucker (2004)	Climate and uplift, use of threshold law	Over long time scales, absence of a threshold has a strong effect on pattern of slope retreat A threshold in the erosion-transport laws strongly influences scarp evolution response to tectonic and climate forcing. Influence of the erosion threshold appears to be greater where fewer than 50% of flood events can mobilise sediment.
26. Tucker & Bras (1998)	Contrasts between different process classes and formulations	Different process classes and formulations have strong but different influences on landscapes and produce different equilibrium or final forms.
27. Tucker & Bras (2000)	Short term climate – intensity, frequency, variability	Variability of climate (runoff) strongly affects erosion rates, drainage density and (over time) relief.

Table 1 (cntd): Examples of studies with LEMs and slope evolution models, summarising the main variables and their influence on model output.

Reference	Main variables or scenario	Main influences on results
28. Tucker & Slingerland (1994)	Process classes and formulations, uplift, initial forms, process rate parameters	Different process formulations strongly affect characteristic evolution of the landscape and drainage system, particularly where the weathering rate is limiting. The slope failure angle and bedrock erodibility strongly influence the pattern of scarp retreat. Uplift and rebound help to maintain steeper channel gradients and hillslopes near the highest part of the escarpment.
29. Tucker & Slingerland (1996)	Uplift scenarios, variable geology (bedrock erodibility functions)	Variable geology strongly influences sediment yields, drainage density, patterns of erosion and sedimentation within the basin or range, and consequently affects the evolution of relief; uplift and rebound exert additional influences.
30. Tucker & Slingerland (1997)	Changes in intensity of runoff, overall runoff and erosion threshold (τ_c).	Runoff intensity strongly influences erosion, deposition, channel heads, drainage density, and hillslope gradients over time. Change in erosion threshold also influences the above, but less markedly than changes in runoff intensity. Weathering and sediment supply to channels exert a limiting influence under some climate conditions.
31. Tucker & Whipple (2002)	Influence of slope exponent in detachment-limited erosion law	Value of slope exponent in detachment-limited stream erosion law strongly influences form of slope retreat, rates and locations of erosion, positions of knickpoints and eventual slope profiles.
32. Whipple & Tucker (1999)	Uplift rate, ratio of m/n in stream erosion law.	Ratio of m/n has a strong influence on relationship between elevation and distance from the divide in equilibrium forms. Slope exponent n and uplift rate together have strong influence on response time of landscape to sudden base level changes.
33. Willgoose (1994a)	Contrast dynamic and declining equilibrium (rate of base level change)	Rate of uplift determines slope-area relationship as the landscape approaches dynamic equilibrium or declining relief. Area and slope exponents (m and n) in transport laws also influence the area-slope relationship and the position in the curve indicating where dominance shifts from diffusive (hillslope) to fluvial processes.
34. Willgoose (1994b)	Uplift rates, including step changes; also climate	Slope-area relationship is sensitive in different ways to various uplift and climate change combinations, some of these combinations influencing the form of the curve more strongly than others.
35. Willgoose *et al.* (1991c)	Uplift and climate; also process parameters.	Balance between diffusive and fluvial processes strongly influences form of the area-slope relationship under dynamic equilibrium. Transient influences also noted.
36. Willgoose *et al.* (1991d)	Implemented distinct channels, contrasted different channel formation rules and influence of perturbations in initial landscape	Distinct channels influence sediment routing and evolution of morphology. Perturbations in initial landscape (elevation) strongly influence channel location and direction along which they extend. If fluvial processes are dominant, then increasing aridity has little influence on non-dimensional form of landscape, whereas if diffusive processes are dominant, then combinations of different uplift and diffusivity may produce similar, non-dimensional landscape forms.
37. Willgoose and Hancock (1998)	Uplift, process parameters	High diffusivities have a strong influence on the shape of the hypsometric curve in steady state or declining relief landscapes, whereas lower diffusivities have little influence. The aspect ratio influences the hypsometric curve in steady state landscapes. Subtler, more detailed influences of the erosion process exponents m and n also noted.
38. Willgoose *et al.* (2003)	Different parameter values and output metrics	Influences of different parameter values on a single output metric are too small to allow its sole use as a calibration measure, and the use of suites of output statistics is recommended in calibration work. (Note 3)

Notes:

1. De Boer applied a rule whereby the frequency of a storm of a particular size was inversely related to its area.
2. Rinaldo *et al's* paper is an interesting example of a study where the focus is on changes taking place over time. The implementation of their climate variation is considered again as part of the discussion, in subsection 7.4.3.
3. This would suggest that the results are similar or very similar for many parameter value variations, implying a degree of equifinality for the metric in question.

Temporal focus and use of variables in the example studies

Looking at the variables listed in column 2, and the research themes in more detail, many of the studies have been focused on the development of landscapes to a state of dynamic equilibrium or steadily declining relief, although there are also a selection of studies which can clearly be related to short term evolution and transient landforms (e.g. 1- 3, 7, 8, 15, 16, 18, 22, 27 and 30). Also, whereas some authors refer to both transient and equilibrium conditions in the same paper (e.g. numbers 22 and 35), the more general approach is to report the pattern of landscape evolution over time, rather than to concentrate on the state of the landscape at any one particular time, whether it be in the short or long term. This probably accounts in part for the way variables are used in the reviewed studies, namely that only a limited number of variables are changed, generally perhaps four or five at most in any one study (e.g. 1-4, 6, 24 and 30), and often fewer than this. Authors also draw on their wider knowledge and experience to comment on the influence of some variables, for example climate and uplift, rather than present results from specific simulations in which these variables are changed so that their influences can be identified. Table 1, therefore is intended to include all the important variables and their inferred influences, taking into account the original authors' comments and not simply whether an individual variable was changed in the experiments or not.

With these points made, it is now possible to consider the main research themes, variables and influences.

1.3.2 Research themes, and association of variables with model output

Themes and variables

Looking at particular themes and variables listed in Table 1, there has been great interest in understanding the influences of climate and uplift (e.g. 3, 4, 6, 7, 9, 11-13, 15-17, 21, 22, 24, 25, 27-30, 32-35 and 37). Of the other variables, the table shows that there has been less interest in studying the effects of different process formulations, although this is still a common theme (e.g. 15-17, 19, 23, 26, 28 and 31). However, the influences of some variables have only seldom been explored, in particular differences in initial landforms (2, 9, 16, 28 and 36), combinations of process classes (1, 2, 16, 26, 28 and 35), grid cell

architecture (number 5 only), geology (1, 24 and 29), soil spatial properties (number 20 only), sediment classes (12 and 13), spatially variable climate events (number 8 only), and tectonic rebound to erosion and unloading (10 and 17, and 24, 28 and 31 to a lesser extent). It is also interesting to note that there are no experiments specifically exploring the effects of different lengths of time step and numerical stabilising algorithms.

In addition to the above, most of the studies are focused on erosion and erosional forms, although there are some exceptions dealing particularly with deposition and depositional forms (e.g. 6, 9 and 18). The absence of some process classes, such as aeolian and glacial processes, is also noteworthy, as these are to a large extent driven by climate variables and would presumably have be used in studies of particularly dry environments (for aeolian processes) or cold environments (for glacial processes), the latter including high mountain ranges. There is also an absence from most studies of vegetation or land cover variables, and also variables relating to human intervention, except where the study includes an interest in changes over the short term ($< c.10^4$ years) (e.g. 16 and 18). No doubt further developments with LEMs will lead to these processes being included where the purpose of the study requires it.

Results and influences

Turning to the results or influences found in these studies, again, there are clearly some common properties. In particular, climate and uplift often appear to exert a strong influence on many measures of output, such as sediment yield (e.g. 3, 7, 8, 11, 18, 24 and 29), drainage density (e.g. 3, 5, 22, 24, 25, 29, and 30) and slope forms and morphology (e.g. 1, 6, 9, 16, 17, 22, 25, 27, 30, 34-36). However, initial forms appear to exert a strong influence on output in short term and transient form studies (e.g. 2, 9, 16 and 36), and geology and process formulation a dominant influence on forms in long term and equilibrium studies (e.g. 1, 10, 17, 19, 24-26, 28, 29, and 31-33). There are also a number of studies testing the influence of process parameters (e.g. 1, 2, 6, 14, 16, 18, 22, 29- 31, 36-38), such as coefficients, thresholds or exponents used in certain transport formulae. Although the importance and ever presence of these parameters has been commented on above, it is interesting to note that extensive process parameter explorations have not been conducted, the ones noted here being mostly confined to variation in two or three of the parameters only (*ibid.*). Notwithstanding this limitation, these studies indicate that changes

in the values of coefficients and thresholds appear always to have a strong influence on sediment movement and erosion rates, especially in transient and short-term studies, whereas variations in exponent term values appear to be more influential on morphology and topographical relationships over longer time periods, in a similar manner to the influences exerted by different process formulations. These observations could turn out to be important in understanding model equifinality, as they suggest that propensity to equifinality may be rather complex, depending in each case on a combination of the metrics of interest, the time scale of the study, and the parameters whose values are being varied. The different influences noted above for some of the other variables, such as initial form, geology and climate, also suggest a similar general picture.

1.3.3 Summary of introductory review

Given the absence of studies in which more than a few variables are tested together, and also the uncertainty in the selection of appropriate values to use for process parameters and other important variables, there would appear to be many unexplored possibilities for LEMs to generate equifinal results. What is also interesting is that although major variations, such as climate, uplift and geology, have often been used in the studies, few authors have explored the effects of process parameter value variation beyond two or three such parameters. Perhaps the only author to have investigated the influences of co-varying larger numbers of different parameter values has been Frank Ahnert (1987), in his study of slope form evolution in the Kall valley of the northern Eifel[4]. Ahnert's work apart, however, there is clearly a lack of research not only into model equifinality as a topic, but also into the range of model output that could be found simply by exploring a LEM's parameter space. It is argued here that this is an important omission, as the possibility of generating equifinal outcomes through combinations of uncertain parameter values will always be present, much of it 'built-in' to the LEM, as part of the built-in uncertainties discussed in section 1.2. The immediate focus of this research, therefore, is to quantify the extent to which a LEM may generate equifinal results through parameter value variation only, with the emphasis on process parameter variation.

[4] Interestingly, by employing an ergodic hypothesis and referring to the agreement separately of simulated forms with real slope profiles in six different locations along the Kall valley, Ahnert was able to constrain quite tightly the parameter values generating evolution of realistic slope forms. He also commented that the likelihood of the result being due to equifinality was small, although he did not attempt to quantify it.

With these points made, the aims of this research can now be formulated and stated in the next section, together with an outline of the structure of the thesis.

1.4 FORMULATION OF THE RESEARCH AIMS, AND THESIS STRUCTURE

In this introduction, the author has reviewed how the concept of equifinality, introduced by von Bertalanffy (e.g. von Bertalanffy, 1968), has been understood and adopted by geomorphologists. Although the concept is somewhat different from that of 'convergence', most authors now use the term 'equifinality' to cover both transient and equilibrium states, whether in real or modelled landscapes. The term 'equifinality' can also be applied to any landscape property, not simply to its form or topography.

Regarding model equifinality, this has been explained to arise out of the uncertainties inherent in model structures and the need for empiricism (e.g. Beven, 1996, 2002). More specifically, the uncertainties in LEMs and LEM studies can be divided between the 'overarching' uncertainties, deriving from the initial state of a landscape and the attribution of boundary and driving conditions, and the 'built-in' uncertainties, deriving from model structures and architectures used in LEMs (Figure 1.1 *q.v.*). Together, these uncertainties give rise to a large number of possible variables. The term 'variable' is used here in a wide sense, to mean any condition, parameter or other factor that may be changed at a researcher's discretion, so that one LEM simulation may differ from another.

With so many variables, simulations with a LEM (or LEMs) may be run in many different ways. Each simulation is equivalent to a working hypothesis that may describe the evolution of the landscape. Similarly, a set of different simulations can be likened to a set of such hypotheses. However, given that the any simulation is only an approximation of reality, a selection of simulations may generate the same landscape measures very closely, to the extent that they may be considered equifinal for those measures (Figure 1.2 and 1.3). In this situation, the reference measures alone cannot be used to falsify any of the hypotheses encapsulated in the simulations. Moreover, observational and other errors may blur discrimination in the results, but they do not alter the fundamental problem. Thus, if model equifinality in LEMs is common, it is a serious obstacle to progress in the discipline.

Based on the review of examples of LEM studies given in Table 1, some LEM variables have a strong influence on model output; similarly, certain measures of output are strongly

influenced by a range of different variables. The review further indicates that it is possible to generate similar output from different LEMs, which may employ different process formulations and parameters, and this emphasises LEM equifinality is a real rather than only a theoretical problem. However, although the potential for equifinality is widely recognised, there has been no quantitative research to assess the extent to which it occurs, and the likelihood of obtaining equifinal output from a LEM is still unknown.

More specifically, and particularly with regard to the built-in uncertainties, there are problems associated with choosing appropriate process formulations and parameter values when setting up any simulation experiment. Looking at the reviewed examples of LEM studies, although certain variables covering geology, climate, uplift and process formulations, are often used in simulation work, little research has been conducted to assess the influence of varying more than three or so parameters' values in the same experiment. This is an important omission, as parameter value uncertainty must impinge on not only the driving variables (such as climate and uplift) used in simulation scenarios, but also on all of rates of the geomorphic processes represented in a LEM. Therefore, the primary aim in this thesis is to conduct research into the possibility of a LEM generating equifinal results through varying parameter values only. If equifinal output can be found through such variations, then a number of research aims can then be pursued in more detail, and these are listed as follows:

1. To quantify the extent to which a LEM generates equifinal results;

2. To assess how LEM equifinality may be affected by using different measures of output;

3. To quantify whether LEM equifinality is due more to some parameters than to others;

4. To quantify how LEM equifinality varies with the number of introduced parameters;

5. To identify those parts of the parameter space emerging as equifinal solution regions; and

6. Based on the results relating to the above and their wider implications, to comment on factors which seem to increase or reduce the likelihood of equifinality in LEM studies, and hence to form a view on the extent to which equifinality is a problem in LEMs generally.

To pursue these research aims, more information is required on the range of LEMs available and the manner in which parameters are used in them, and this is considered in a wide

ranging review in Chapter 2. It will also be shown that a key difficulty arises in sampling the parameter space, in order to assess the equifinality of a LEM, but in a manner which is both effective and efficient. This is covered in Chapter 3, in which an innovative methodology to calculate equifinality is introduced; the methodology is further developed and explained in Chapter 4. The main body of results, covering aims 1 to 5 above, is then presented in Chapters 5 and 6. Finally, in Chapter 7, the methodology and the implications of the results are discussed in detail, addressing in particular the issues related to research aim 6. By this structure, the thesis is therefore brought full circle, with a return to the more general problem of model equifinality in LEMs, as introduced in this chapter. The main discussion points are then summarised and recommendations for further work are proposed. This is followed by a statement of the conclusions to the research, and with some final remarks, the thesis is to brought to a close.

CHAPTER 2: LANDSCAPE EVOLUTION MODEL PARAMETERS AND PARAMETER SPACES

2.1 INTRODUCTION

The aim in this chapter is to examine the size of the parameter space associated with a typical LEM, as this needs to be understood before designing an experiment to evaluate a LEM's output for equifinality. To do this requires separate reviews of different aspects of LEMs and how they function. The chapter therefore begins with an introductory review of the basic features of LEMs, to explain their general composition and to identify the role of adjustable parameters in how they perform their calculations. This shows that LEMs often include only two or three main classes of geomorphic process, and that adjustable parameters feature mostly in the equations used to represent those processes. Accordingly, three sections of this chapter comprise a review of the process representations themselves, and the findings from these sections are then summarised to show the typical parameter requirements of a LEM. Information is also drawn from various sources to develop a summary of the typical value ranges that are likely to be appropriate for each of the parameters in simulation work. These two components together – value uncertainty and dimensionality – therefore combine to form the parameter spaces typical of most LEMs.

In structuring the information in the chapter, the author has taken into account that LEMs and their use form an evolving discipline in geomorphology. In particular, new LEMs will continue to be developed and older ones enhanced or improved, so it is not possible to be to wholly up to date in a review of LEMs. There is also the problem of space, in that to review all LEMs in detail would probably be too big a task for the space permitted here. However, the issues arising in LEMs which relate to adjustable parameters should be common to all LEMs, regardless of their level of functionality and the roles of their parameters. For example, more recent LEMs may include more sophisticated functions, such as routines for implementing self-adapting grid cell sizes and lengths of time step, channel meandering, and multiple sediment size classes, and so on, but these routines and functions still all depend on semi-empirical parameters and rules to some extent. For these reasons, the LEM review presented in this chapter is current up to 2002, and the developments since then are not seen to alter materially the discussion and general argument. With this point made, the first requirement is the general review of example LEMs, and this now follows.

2.2 GENERAL CHARACTERISTICS OF LEMS

2.2.1 Table of reviewed models

The purpose in this section is to introduce a selection of LEMs in more detail, in order to show their usual composition, attributes and functionality, and to clarify the role of adjustable parameters in their operation. To this end, a selection of published LEMs has been reviewed, and their general characteristics are summarised in Table 2.1.

Regarding the models listed in Table 2.1 (column 1), the view has been taken that for a model to be classed as a landscape evolution model, it needs to be able to simulate the evolution of topography over an area, that is, across two dimensions of space, rather than simply along a transect. However, the slope evolution model study by Martin (2000) has also been included, as this represents use of a particularly interesting mass movement formulation. Similarly, although FLUVER2 (Veldkamp and van Dijke, 1998) does not simulate all of the study landscape in a single spatial array, it includes two-dimensional landscape elements at various points along the fluvial process transect.

Column 1 also lists the name of the model, where there is one, and the original source papers. Comment on the models is for the most part confined to how they were reported in the original papers, so Table 2.1 does not represent the last word on all of these models, as some continue to be updated and adapted. For details of some of the more recent developments, there have been a number of reviews of various aspects of LEMs and landscape evolution modelling (e.g. Coulthard, 2001; Dietrich *et al.*, 2003; Bras *et al.*, 2003; Martin and Church, 2004; Willgoose, 2005; Codilean *et al.*, 2006). However, none of these reviews includes a critical analysis of the use of parameters in LEMs as required for this research. For convenience, comments in the review are cross-referenced to the relevant column number, and, where indicated, additional notes are given in Appendix A.

The remainder of Table 2.1 is divided between matters related to model architecture (columns 2 and 3), and model structure (columns 4 to 10), the use of these having already been explained (subsection 1.2.2, *q.v.*). Model structure is in turn divided between state and driving variables (columns 4 to 6) and processes (columns 7 to 10). Regarding the latter, it will be noted from columns 8 to 10 that the main classes of geomorphic process in the reviewed LEMs are confined to weathering, mass movement, and fluvial erosion and transport. This reflects the emphasis by past researchers and model builders on applying

them to studies of landscape evolution in humid temperate or semi-arid environments. Admittedly, some models have also been applied to mountainous or periglacial settings (e.g. Bogaart *et al.*, 2003a and 2003b; Schlunegger *et al.*, 2001), where one might expect processes driven by ice and snow to be effective, but most LEMs do not yet incorporate nival, glacial or aeolian processes.

Another point arising here is that the modelled landscapes are generally used for simulation of drainage basin or smaller catchment evolution. This reflects the importance of fluvial processes in the climatic settings referred to above. In these circumstances, the drainage divide provides a natural boundary to the catchment or basin, across which no material may be transported into or out of the landscape. The only exception normally is at the drainage outlet. If the model is of a single basin or catchment, there is normally a single outlet cell, via which fluvially transported material may be removed. However, some models permit representation and modelling of a number of adjoining basins, and have multiple fluvial outlet cells for this purpose (e.g. CASCADE, Braun and Sambridge, 1997; GOLEM, e.g. Tucker and Slingerland, 1996).

Finally, all the LEMs represent in some manner the elevation of the landscape using an array of cells, and simulate the movement of material (sediment, bedrock and so on) across the landscape by calculating changes in the cell values over a series of units of time. It follows that the divisions of space and time, and the allocation of suitable state variables for landscape properties, are common requirements in all LEMs, so some comment on these is made next.

Table 2.1 Table of reviewed landscape evolution models (current to 2002 – see notes and main text)

NAME, SOURCE	ARCHITECTURE		← STRUCTURE →						
			← State and driving variables →			← Processes →			
1.	2.	3.	4.	5.	6.	7.	8.	9.	10.
	Time scale; time step (Note 1)	**Spatial scale; cell no.**	**State variables (Note 2)**	**Driving conditions/parameters**		**Wea-thering**	**Mass movement**	**Fluvial erosion and transport**	**Explicit spatial variations**
				Uplift; tectonism	**Climate; land cover**				
SLOP3D Ahnert (1976, 1987)	1 million years 2,500 years	< 100 km^2 100 cells (10 x 10)	Regolith depth Bedrock elevation	Variable base level, uplift	Constant climate No vegetation	Physical Solution possible	Creep Splash Slow flows Deep and shallow slides	Wash No channels Mixed load Deposition allowed	Bedrock types (weathering rates, critical slopes, erodibility)
Armstrong (1976)	20,000 years 1 year	c. 0.04 km^2 1,600 cells (40 x 40)	Regolith depth Bedrock elevation	Constant base level	Constant climate No vegetation	Physical only	Creep	Fixed channels Mixed load Deposition allowed	-
CASCADE Braun & Sambridge (1997)	1 million years 100 years	< 10,000 km^2 10,000 cells, variable	Regolith depth Bedrock elevation	Variable base level, uplift Tilting and warping	Climate variable in time and space No vegetation	-	Diffusive, general process which combines creep and slides	Inferred channels Mixed load Deposition allowed	Bedrock types (critical slopes, erodibility)
CAESAR Coulthard *et al.* (1999, 2000, 2002)	1,000 years Hours to micro-seconds	< 10 km^2 Millions of cells	Regolith depth (multiple) Discharge Flow depth	Not indicated	Event based climate Variable vegetation	-	Diffusive slow or general process Shallow slides	Explicit channels Loads separated by sed. size class Deposition, stratification	Bedrock types (erodibility)
Howard (1994, 1997)	Graded/ cyclic	Unspecified	Regolith depth (elevation)	Variable base level, uplift	Not indicated	-	Two processes: slow, diffusive and fast, quasi-diffusive	Inferred channels Mixed load Deposition allowed	-
Kooi & Beaumont (1996)	Graded/ cyclic	Basin/range	Regolith depth (elevation)	Variable base level, uplift Tilting, warping	Not indicated	-	Diffusive slow or general process	No channels Mixed load Deposition allowed	-
Martin (2000)	30,000 years 1 year	Profiles, < 3 km Cell no. not indicated	Regolith depth Bedrock elevation	Falling base level	Constant climate No vegetation	Physical only	Creep Shallow slides Also combined slope process	-	-

Table 2.1 (continued) Table of reviewed landscape evolution models (current to 2002 – see notes and main text)

NAME, SOURCE	ARCHITECTURE		← STRUCTURE →						
			← Variables →			← Processes →			
1.	2.	3.	4.	5.	6.	7.	8.	9.	10.
	Time scale; time step (Note 1)	**Spatial scale; cell no.**	**State variables (Note 2)**	**Driving variables**		**Weath-ering**	**Mass movement**	**Fluvial erosion and transport**	**Explicit spatial variations**
Moglen & Bras (1995)	Graded/ cyclic	Unspecified	Regolith depth (elevation)	Variable base level	Not indicated	-	Diffusive slow or general process	Inferred channels Mixed load Deposition allowed	Bedrock types (erodibility)
Rinaldo *et al.* (1995)	Graded/ cyclic	Unspecified	Regolith depth (elevation)	Constant base level	Variable climate Variable cover	-	Diffusive slow or general process	Wash No channels Mixed load No deposition	-
GOLEM Tucker & Slinger-land (1994, 1996, 1997); Tucker & Bras (1998)	100,000 years 10 years	<200 km^2 10,000 cells (100 x 100)	Regolith depth Bedrock elevation	Variable base level, isostatic rebound Tilting, warping	Variable climate Vegetation optional	Physical only	Diffusive slow process Deep and shallow slides	Inferred channels Mixed load Deposition allowed	Bedrock types (weathering rates, critical slopes, erodibility)
CHILD Tucker *et al.* (1997, 2001a, 2001b)	100,000 years 10 years	<200 km^2 10,000 +, dynamic array	Regolith depth Bedrock elevation	Variable base level, isostatic rebound Tilting, warping	Variable climate Vegetation optional	Physical only	Diffusive slow process	Explicit channels Separate sand and gravel loads Deposition, stratification	Bedrock types (weathering rates, critical slopes, erodibility)
FLUVER2 Veldkamp & van Dijke (1998)	2 million years 100 years	> 1000 km^2 Cell no. not indicated	Regolith elevation	Variable base level Tilting, warping	Variable climate No vegetation	-	Diffusive general process Deep and shallow slides	Inferred channels Mixed load Deposition allowed	Bedrock types (critical slopes, erodibility)
SIBERIA Willgoose *et al.* (1991a-d)	2,000 years 1 year	< 10 km^2 Cell no. not indicated	Regolith elevation	Variable base level	Not indicated No vegetation	-	Diffusive slow or general process	Inferred channels Mixed load Deposition allowed	-

Notes:

1. The time step listed is that which might be used typically for computation, as explained in subsection 2.2.2. However, some LEMs, for example CAESAR, GOLEM and CHILD (references as cited in the table above) include a routine to subdivide the time step, so as to maintain numerical stability.
2. The state variables listed here are *dynamic*, in that their values are only changed by processes from one time step to the next, as described in subsection 2.2.2.

2.2.2 Spatial domain, time steps and state variables

Regarding the time intervals and overall time spans listed in Table 2.1 (column 2), these are indicative only, and are intended to represent the typical range of each model's capabilities. Likewise, the spatial scales and cell sizes (column 3) are also only intended to represent the typical ranges of space and resolution to which the model might be applied.

With respect to grid cells, these may all be of the same size and shape (e.g. Howard, 1994; Moglen and Bras, 1995; SIBERIA, Willgoose *et al.*, 1991a; GOLEM, Tucker and Slingerland, 1997), or of variable size and shape (e.g. CASCADE, Braun and Sambridge, 1997; CHILD, Tucker *et al.*, 2001a). Some models also include routines to allow the cell size and shape to be altered while the simulation proceeds in response to process rates and local conditions (e.g. CASCADE, Braun and Sambridge, 1997). Each method has advantages and disadvantages in the coding required to implement the type of cell grid. However, it is acknowledged that regular grid cell arrangements may introduce bias in the output (e.g. Howard, 1997; Braun and Sambridge, 1997; Codilean *et al.*, 2006), by driving processes in certain directions and not others. These effects can be overcome to some extent by adopting irregular or self-adapting grids.

Regarding time steps, most LEMs use fixed length time steps, but CAESAR is able to operate with variable time steps (e.g. Coulthard *et al.*, 1999, 2000, 2002). No doubt this feature will become common to more LEMs as they become more sophisticated, and modellers try to improve the physical basis of representations of climate and geomorphic processes. With this in mind, it is worth noting that in some studies, the models are run so as to be dimensionless in time, space or both, in order to demonstrate patterns of system behaviour which may be shown to be scale independent (e.g. Willgoose *et al.*, 1991b; Howard, 1994, 1997).

Besides the temporal and spatial discretisation, another fundamental part of each LEM is the allocation of state variables (column 4). The key attribute of a state variable is that its value is stored from one time step to the next, and is only altered by the geomorphic processes acting on the landscape. Generally, the values of all the state variables are set explicitly once only, at the beginning of a simulation, and thereafter are altered solely as the processes determine. State variables also have particular properties; for example, bedrock may be affected by weathering but not creep, and regolith by fluvial transport but not weathering. As will be seen from column 4, most LEMs have only one state variable, namely the

elevation of the cell above some datum, although some have more. For example, in GOLEM (e.g. Tucker and Slingerland, 1997), there are two state variables, bedrock elevation and regolith depth, and in CAESAR (e.g. Coulthard *et al.*, 1999, 2000, 2002) up to nine state variables, each for a different size class of sediment.

In addition to the state variables for rock or sediment, some versions of GOLEM and CHILD can also include vegetation as a state variable (Greg Tucker, 2003, personal communication), but this functionality is not explored here. Similarly, CAESAR includes water as a state variable, using TOPMODEL (Beven and Kirkby, 1979) to simulate the movement of water through the landscape. CAESAR therefore works as two sub-models running side by side, exchanging hydrological and geomorphological information. The use of TOPMODEL in this way also permits a more realistic implementation of climate than is usual in most LEMs. Since climate is an important driving variable, and with uplift is most likely to be implemented using parameters of some kind, the types of implementation and the parameter requirements they necessitate are considered next.

2.2.3 Driving conditions – climate, base level and uplift

Climate is usually simulated in LEMs as runoff or effective precipitation, assumed as a first approximation to be by overland flow. This assumption greatly simplifies matters, in that factors related to vegetation, evaporation and precipitation do not need to be modelled separately. In the simplest representations, a notional runoff rate per time step is applied to each cell, which may be spatially uniform (used in most of the models), or spatially variable, so as to reflect climatic variations that may arise over distance or altitude (e.g. in CASCADE, Braun and Sambridge, 1997; in FLUVER2, Veldkamp and Van Dijke, 1998). De Boer (2001) also introduced spatially variable storm events in a novel and interesting way, but his approach has not been repeated in the other LEMs reviewed here.

Temporally, the runoff is usually meant to represent a dominant or representative discharge for the catchment or basin. Where this is used in a LEM, the climate implementation in effect represents an average condition over each time step rather than individual rainfall events. The runoff input may itself be varied over time, to represent changes in the overall climate, or in the intensity of storms and showers, although the separate climate events are still not modelled (e.g. in GOLEM, Tucker and Slingerland, 1997; in SLOP3D, Ahnert,

1976; in Rinaldo *et al.*, 1995). This general, climate averaging approach is used in most of the LEMs, but in both CHILD (e.g. Tucker *et al.*, 2001b) and CAESAR (e.g. Coulthard *et al.*, 1999) short time steps (hours or less) are permitted and may allow for finer resolution in simulating the effects of individual showers and storms. CAESAR is also rather different from the other models, in that the hydrology of the catchment is simulated using longer time steps - generally in hours - whereas the geomorphic response to the modelled flows is updated in step lengths from minutes down to *c.* 10^{-4} seconds, depending on the rate of the flow discharge (J. Wheaton, 2006, personal communication). Summarising these points, the simplest climate conditions require just one parameter, for the runoff rate, and more sophisticated variations require more, to cover intensity or stochastic or cyclic variations.

Regarding base level changes and uplift, the number of parameters needed to implement these functions in a LEM also depends upon the complexity of the changes to be simulated. In this respect, just one base level parameter may be enough to cover a variety of conditions, such as a constant base level, or a steady efflux rate at the basin outlet. Additional parameters may be used to vary the base level over time. Similarly, uplift rates may be applied to the catchment and varied over time, and additional spatial influences, such as tilting, warping, and rebound (in response to unloading) may be applied through the use of other parameters (e.g. in CASCADE, Braun and Sambridge, 1997; in GOLEM, Tucker and Slingerland, 1994, 1996; in SLOP3D, Ahnert, 1976, 1987). Generally, however, the simplest base level and uplift variations require one parameter, to specify either the uplift rate relative to a fixed base level, or a particular efflux rate.

The other main classes of parameters in LEMs are those used in the geomorphic process equations and related functions. These are reviewed in detail in sections 2.4 to 2.6. Before doing so, however, some comment is needed on the general types of process and other functions used in LEMs, and the way the process relationships are bound, in mathematical terms, within the principle of mass continuity. These matters are now briefly considered.

2.3 PROCESS PARAMETERS AND MASS CONTINUITY

Regardless of the class of process in a LEM, or of the nature of the movement of material, any mass that is moved by the process will have to be accounted for in some way. It is therefore appropriate to review first the mass continuity relationships which bind together

the effects of the different driving conditions and processes. The basic form of the mass continuity equation (e.g. Kirkby, 1971; Carson and Kirkby, 1972) is given by:

$$\frac{\partial z}{\partial t} + \frac{\partial q_s}{\partial x} = 0, \qquad 2.01$$

where z is the elevation of a point above datum, and q_s represents the volumetric rate of sediment transport per unit width. By convention, equation 2.01 is often recast as:

$$\frac{\partial z}{\partial t} = -\frac{\partial q_s}{\partial x} \qquad 2.02$$

Since nearly all of the models being considered here simulate landscape evolution over two dimensions, equation 2.02 is often written in vectoral form, thus:

$$\frac{\partial z}{\partial t} = -\nabla \mathbf{q}_s \qquad 2.03$$

As discussed in subsection 2.2.3, the landscape may be affected also by uplift, which is incorporated in equation 2.03 as follows:

$$\frac{\partial z}{\partial t} = U - \nabla \mathbf{q}_s, \qquad 2.04$$

where U is the rate of uplift.

As will be seen from Table 2.1, in some LEMs no distinction is made between regolith and bedrock. However, a more complete approach is to model regolith and bedrock separately. This requires separate equations to take into account the processes affecting each state variable. Beginning with the elevation of any point in the landscape, the total elevation is found from:

$$z = B + G, \qquad 2.05$$

where B is the depth of bedrock above datum, and G is the thickness of regolith above the bedrock. This equation can be restated in terms of a rate of change, thus:

$$\frac{\partial z}{\partial t} = \frac{\partial B}{\partial t} + \frac{\partial G}{\partial t} \qquad 2.06$$

If the assumption is made that bedrock is only affected by weathering and uplift, then the bedrock component of equation 2.06 can be stated as:

$$\frac{\partial B}{\partial t} = U - W \,, \qquad 2.07$$

where W is the rate of weathering[1]. Substituting the right hand side of this into equation 2.06 gives a more complete form of continuity equation, thus:

$$\frac{\partial z}{\partial t} = U - W + \frac{\partial G}{\partial t} \qquad 2.08$$

Regarding the weathering term in this equation, weathering losses may be in part by solution and in part by fragmentation. The proportion of bedrock which is dissolved may be assumed to be lost from the landscape altogether, whereas the proportion subject to fragmentation is converted into regolith. This therefore increases the thickness of regolith at the same point in the landscape, and needs to be incorporated in the overall regolith mass continuity relationship. The mass continuity of regolith is then found from:

$$\frac{\partial G}{\partial t} = \lambda W - \nabla \mathbf{q}_s \,, \qquad 2.09$$

where λ is the proportion of weathered rock which contributes to the regolith. Regarding the sediment transport term, $\mathbf{q}_s$, this can be treated as the sum of fluvial and mass movement components, thus:

$$\mathbf{q}_s = \mathbf{q}_m + \mathbf{q}_f \,, \qquad 2.10$$

where $\mathbf{q}_m$ is the rate of mass movement and $\mathbf{q}_f$ is the rate of fluvial transport. Substituting the corresponding rate terms for $\nabla \mathbf{q}_s$ in equation 2.09, the continuity of regolith can now be more fully stated as:

$$\frac{\partial G}{\partial t} = \lambda W - \nabla \mathbf{q}_m - \nabla \mathbf{q}_f \,, \qquad 2.11$$

Finally, the right hand side of this relationship can be substituted for the regolith rate term in equation 2.08, to give a more complete mass continuity equation:

$$\frac{\partial z}{\partial t} = \left(U - W\right) + \left(\lambda W - \nabla \mathbf{q}_m - \nabla \mathbf{q}_f\right) \qquad 2.12$$

This is more informative than the basic equation (equation 2.01), as the roles of the separate classes of geomorphic process are clearly distinguished from each other. It is also important

[1] This is a very simple form of the equation, but it could appear with more terms, for example if fluvial bedrock erosion were included in the model, as in GOLEM (e.g. Tucker and Slingerland, 1997).

to note that the terms affecting each state variable are grouped in brackets and separated; thus, the first bracketed component refers to bedrock continuity, and the second to regolith continuity. With this equation in mind, the equations used in LEMs for implementing geomorphic processes will now be considered in more detail, beginning with a review of those used for the implementation of weathering.

2.4 WEATHERING

2.4.1 Basic processes and form of mathematical relationship

Although most of the LEMs listed in Table 2.1 do not incorporate weathering processes, for the few that do, the literature shows that weathering processes are highly complex (Ollier, 1984). To make matters simpler, most authors divide them into two categories, namely physical weathering and chemical weathering (Ollier, 1984; Selby, 1993). In LEMs, this categorisation is further simplified, with a general assumption that weathering may be treated as a physical detachment process, which lowers the bedrock surface and leaves the detached, solid fraction *in situ*. Solution and specific chemical processes are omitted, and no allowance is made for continued fragmentation of the regolith or its chemical alteration. Spatial factors, such as slope and sub-surface flow convergence, are also ignored, as are changes in the bulk density of the regolith as compared with that of the bedrock. The depth of the regolith, however, is generally assumed to affect the weathering rate, and Cox (1980) outlines conditions that ought to apply to most weathering rate equations. The general form of weathering rate equation suggested by Cox (1980) is:

$$W = W_0 e^{-k_w R}\left(1 + cR\right), \tag{2.13}$$

where W is the rate of weathering, W_0 is the base rate of weathering, assumed to apply to bare bedrock, k_w is a decay rate constant (assumed to be always greater than zero), R is the regolith depth, and c is another constant. Most researchers use variants of this equation, as reviewed below. As a general point, the symbols and forms of equation used by authors in representing weathering vary from paper to paper, and from model to model. This makes direct comparison of the equations and parameters awkward, so the different equations will be presented separately. A common form will then be derived from them, which allows a clear summary of the parameters typically required in weathering equations.

2.4.2 Weathering process equations and adjustable parameters

Weathering itself is included in five of the reviewed models (Table 2.1, column 7), as follows:

(i) in Armstrong (1976, 1987),

$$\frac{\partial B}{\partial t} = -W_0 e^{-k_w R}, \tag{2.14}$$

where B is the state variable for bedrock elevation, R is the state variable for regolith depth, W_0 and k_w are respectively the base rate of weathering for bare bedrock and the decay rate constant, and the minus sign before the W_0 indicates that weathering lowers the weathering front;

(ii) in GOLEM (e.g. Tucker and Slingerland, 1994, 1996, 1997),

$$\frac{\partial R}{\partial t} = k_w e^{-C/m_w}, \tag{2.15}$$

where R now refers to the bedrock, k_w is now the coefficient of the base rate of weathering, C is the regolith depth and m_w is a depth characterising the decay of the weathering rate curve;

(iii) in CHILD (e.g. Tucker e*t al.*, 1997),

$$\left.\frac{\partial C}{\partial t}\right|_{weathering} = k_w \exp\left(-\frac{C}{C_0}\right), \tag{2.16}$$

which is now given in terms of the rate of increase in the regolith depth, C, where C_0 is the decay rate depth, and presumably the bedrock weathering front is assumed to be lowered at the same rate as that at which the regolith increases in thickness;

(iv) in Martin (2000), based on Heimsath *et al.* (1997),

$$\frac{\partial h_b}{\partial t} = r_0 \exp\left[\beta\left(h_s - h_b\right)\right], \tag{2.17}$$

where h_b is the state variable for bedrock, r_0 the coefficient of the base rate of weathering, β an empirical constant, and h_s the overall elevation (equal to h_b plus the thickness of any overlying regolith); and

(v) in SLOP3D (e.g. Ahnert, 1976, 1987), based on Ahnert's written description of the relationship and casting this in the following form, adapted from the generic equation proposed by Cox (1980):

$$\frac{\partial B}{\partial t} = -W_0\left[\alpha F_p + (1-\alpha)F_c\right], \qquad 2.18$$

where F_p is a function for the rate of physical weathering, F_c a function for solution, and α is a proportionality constant dividing the balance between the two processes, and whose value could be set between 0 and 1 as desired. Thus, if α is set to 1, weathering is modelled solely as a physical detachment process; alternatively, reducing α increases the effects of solution and makes the weathering rate curve more humped. Regarding the two processes, F_p and F_c, Ahnert (1976) described the processes but gave no equations in his paper. However, F_p is likely to be the same as the physical detachment process given in Ahnert (1987) by:

$$\frac{W}{\Delta t} = \frac{W_0}{\Delta t} e^{-k_1 C}, \qquad 2.19$$

which, if cast in similar form to equation 2.14 (or 2.16), is equivalent to

$$\frac{\partial B}{\partial t} = W_0 e^{-k_1 C}, \qquad 2.20$$

where k_1 is the decay rate constant and C the regolith depth. Regarding the chemical process, Figure 2 in Ahnert (1976) showed a humped curve of the kind proposed by Cox(1980), suggesting that Ahnert's solution process was similar to the general form:

$$\frac{\partial B}{\partial t} = W_0 C e^{-k_1 C} \qquad 2.21$$

The contribution made by the physical and chemical weathering rates calculated in equations 2.20 and 2.21 could then be further modified by the value of α used in equation 2.18.

A common feature of all these equations is that the weathering process is always assumed to attack the bedrock alone. Although Ahnert (1976) indicated a possible way of allowing for solution of regolith, no attempt has been made otherwise to model weathering of the regolith separately. Similarly, although they do not specifically model chemical processes or density changes, Tucker and Slingerland (1994) state that "the change in density upon

conversion of rock to sediment is compensated for by the removal of mass in solution". These points aside, in summarising the foregoing, closer examination of equations 2.14 to 2.17 shows that they can all be recast in the same common form, thus:

$$\frac{\partial B}{\partial t} = -k_w e^{-G/m_w}, \qquad 2.22$$

where B is the elevation of the bedrock, k_w the base rate of weathering, G the regolith depth and m_w the decay depth. With reference to Ahnert's more sophisticated formula (equation 2.18), if the solution weathering rate is assumed to be zero, then the equation is equivalent to Ahnert's physical weathering formula (equation 2.20), which in turn can be reduced to the two parameter common form above (equation 2.22).

With this in mind, the right hand side of equation 2.22 may be substituted for the weathering rate terms in the basic LEM mass continuity equation (equation 2.12), and the solution component may be ignored (therefore $\lambda = 1$). Of the two remaining geomorphic processes included in equation 2.12, those relating to mass movement are somewhat simpler to implement, so the modelling of these processes is considered first.

2.5 MASS MOVEMENT

2.5.1 Movement mechanisms, material type and dispersal

Basic mechanisms

Detailed consideration of mass movement mechanisms and the factors influencing them are given in standard texts (e.g. Young, 1972; Carson and Kirkby, 1972; Selby, 1993). A review of this literature shows that there are many types of mass movement, and that each type of movement has its own complex causes and behaviour (*ibid.*). In simplifying mass movement processes, modellers focus mainly on factors controlling the manner of distribution of the material and its speed of dispersal. For this purpose, the scheme proposed by Carson and Kirkby (1972) is particularly useful, in that it shows how each type of mass movement can be categorised according to the dominant movement mechanism, the speed of the movement, and the amount of water mixed in with the material. Carson and Kirkby's scheme is shown below, in Figure 2.1.

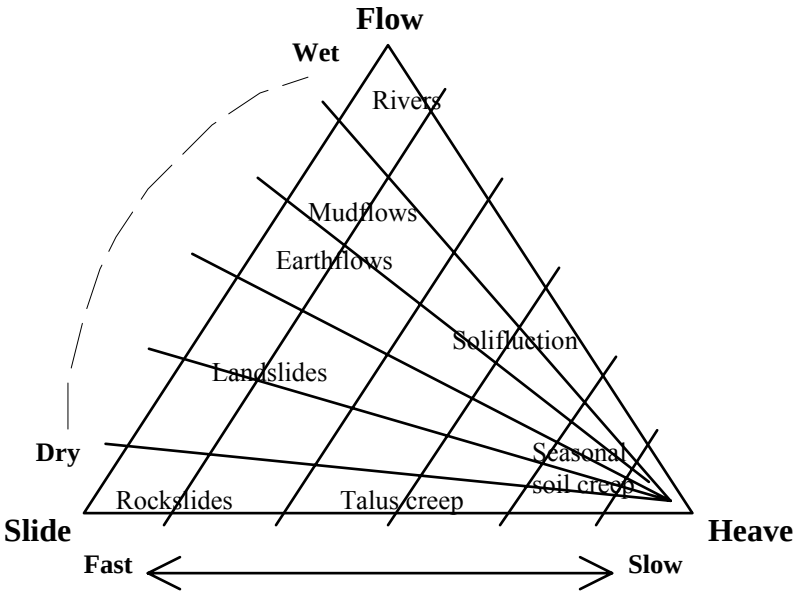

Figure 2.1: Illustration of mass movement types, characterised by their speed, water content and dominant mechanism. (Adapted from Carson and Kirkby, 1972)

According to Carson and Kirkby (1972), there are three basic movement mechanisms, heave, flow and slide. A feature of slide and flow mechanisms, of whatever speed, is that their inception is generally controlled by a threshold of some kind (Carson and Kirkby, 1972; Selby, 1993). Once the threshold is exceeded, material begins moving, and the movement continues until friction or physical obstacles bring it to a halt. For faster movements, material may be transported far away from its original source, and the momentum acquired during its descent may allow the material to rise up opposing slopes or over barriers before it comes to rest (*ibid.*). Movements controlled by thresholds are also likely to be episodic and confined to particular zones in the landscape where other factors promote their occurrence (*ibid.*).

Taking these points into account, although most modellers try to make their process relationships more physically based, in the reviewed LEMs this generally goes no further than making mass movements slope dependent in some way, usually with a critical slope threshold controlling inception and speed. However, there are differences relating to the type of material moved and the manner of dispersal, and these matters need comment.

Material type and dispersal methods

Regarding the type of material, mass movements in most LEMs are usually assumed to be shallow, and to affect the regolith only provided there is enough supply for the movement to take place (e.g. Ahnert, 1976; Tucker and Slingerland, 1994). Some models also allow for mass movement of bedrock, usually in the form of bedrock sliding (e.g. Tucker and Slingerland, 1994, 1996). In this instance, there is no initial supply limitation, as there would always be bedrock underlying the landscape. In either case, all that is required is a suitable algorithm for distribution of the material in the manner stipulated in the model.

The first and simplest of these is through transfer of material to cells immediately adjoining the source of the movement, a method which is here termed "nearest neighbour" dispersal. This is equivalent to a numerical solution to an underlying partial differential equation, such as equation 2.26 (introduced in subsection 2.5.2). The dispersal itself is effected during the model's time step, without the need for an algorithm to correct for super critical slopes. This dispersal method is particularly used for slower types of movement, which are unlikely to be controlled by a threshold. Also, the distribution of material subject to the movement is always down the slope.

A second and more complicated method of transfer, which is here termed "extended dispersal", is effected by distributing material over longer distances from the source, often in directions constrained by the local topography. This type of movement is made between the model's time steps, using an algorithm to calculate the number of cells over which the material should be spread. This dispersal method is particularly used for faster, threshold controlled movements, where distribution of the material would be expected to be virtually instantaneous compared with the length of the model's time step.

A feature of extended dispersal is that material may be allowed to spread laterally, so as to ensure that the slope threshold is not exceeded once distribution of the mobilised material is complete. However, there is a particular problem in trying to model runout effects of rapid flows and slides. Some more physically based formulations are now available in order to do this, based on research by Iverson and his co-workers (e.g. Iverson, 2003). These formulations go somewhat beyond the main research focus of this thesis, however, and will not be considered further. Regarding the implementation of the simpler formulations in LEMs, nearest neighbour dispersal is easier to describe and is included in most LEMs, so these are now reviewed, beginning with the basic equations used by modellers.

2.5.2 Nearest neighbour dispersal – basic equations

Nearest neighbour dispersal has been used mostly to implement slow movements dominated by heave mechanisms, of which creep is a good example. Based on research by Kirkby (e.g. Carson and Kirkby, 1972) and other workers, the rate of such slow movements is given by the equation:

$$q_m = -k_m \sin\theta , \qquad 2.23$$

where q_m is the volumetric rate of movement per unit width, k_m is the coefficient of slow mass movement, usually called the *diffusivity*, and θ is the slope angle. Since, for small slope angles, $\sin\theta \approx \tan\theta$, the tangent substitution is normally used, so that equation 2.23 may be more simply written either as:

$$q_m = -k_m \frac{\partial z}{\partial x}, \qquad 2.24$$

for the slope profile model form, or as:

$$q_m = -k_m \nabla \mathbf{z} , \qquad 2.25$$

for the whole landscape form. The use of vector symbols in the latter will be noted.

Both of these equations may also be recast as mass continuity relationships, to give, for equation 2.24:

$$\left.\frac{\partial z}{\partial t}\right|_m = -k_m \frac{\partial^2 z}{\partial x^2} , \qquad 2.26$$

and for equation 2.25:

$$\left.\frac{\partial z}{\partial t}\right|_m = -k_m \nabla^2 \mathbf{z} , \qquad 2.27$$

where in each case $\left.\frac{\partial z}{\partial t}\right|_m$ refers to the rate of change of elevation arising from mass movement only.

Variants of one of these equations are used in most LEMs, the number of parameters required depending upon the type of process being modelled and the particular form of the process equation. These variants and their parameter requirements are now considered separately.

2.5.3 Nearest neighbour representations of slow mass movement

Slow mass movement is modelled as a nearest neighbour mechanism in all of the reviewed LEMs (Table 2.1, column 8). Nearly all of the models use the tangent rather than the sine of the slope angle, so equations 2.24 to 2.27 show the general forms of equation used. Having made this point, the different forms of equation – used in Armstrong (1976) and Ahnert (1976, 1987) – need to be commented on. Both authors used the sine of the slope angle, Armstrong (1976) representing slow mass movement with:

$$C = K_s \sin\theta , \qquad 2.28$$

where C is the volumetric rate of movement per unit width and K_s the diffusivity. Ahnert's (1976) equation is slightly different from this, and was intended to represent what he called 'viscous flow', given by:

$$R_{visc} = K_{visc} C^m \sin\theta , \qquad 2.29$$

where R_{visc} is equivalent to C in equation 2.28, K_{visc} is the diffusivity, C is the regolith depth, and m is an empirical parameter, taken to be between 0 and 1. Ahnert (1987) simplified this to a form equivalent to Armstrong's (equation 2.28) i.e. $K_{visc}C^m = K_s$. Ahnert's (1976) equation (equation 2.29) requires that, for a given slope angle, the rate of movement declines as the regolith cover gets thinner. This accords with many observations (e.g. Young, 1978; Selby, 1993), and a similar depth restriction was also used by Rosenbloom and Anderson (1994) in their study of coastal scarp development. It does not occur in other LEMs, however, although the overall amount transferred downslope, rather than the rate itself, may be limited by the supply of regolith (e.g. Tucker and Slingerland, 1997).

The diffusivity coefficient may also be spatially variable in some models. In Moglen and Bras (1995), it was varied from cell to cell, and in FLUVER2 (Veldkamp and Van Dijke, 1998) it was varied with altitude, to simulate higher diffusivities caused by seasonal solifluction and talus creep[2]. The same theoretical relationship is also used in SIBERIA (e.g. Willgoose *et al.*, 1991a)[3]. Martin (2000) also used a similar linear relationship, cast in mass continuity form, but this was applied to mixed speeds of movement, and is discussed in subsection 2.5.4.

---

[2] Equation 2.26 is slightly different from the form of equation stated in Veldkamp and Van Dijke's (1998) paper, but closer inspection shows the two forms to be equivalent.

[3] The form of presentation of the equation is somewhat different from that used for the others considered here, in that the authors refer to $\boldsymbol{x}$ and $\boldsymbol{y}$ components of slope, but their theoretical bases are the same.

In summary, the equations used to implement slow mass movement in most models can be reduced to the common forms shown in equations 2.26 and 2.27, leaving the rate of movement to be constrained by just one parameter, k_m. A consideration of combined and fast movements, also implemented using nearest neighbour dispersal, now follows.

2.5.4 Nearest neighbour representations of combined speed and fast mass movements

Single parameter relationships

Intermediate speed and fast mass movements are usually controlled by a threshold, often manifested as a critical slope angle, and the main mechanisms of movement are slides or flows (Carson and Kirkby, 1972; Selby, 1993). In the simplest representations of fast movement, the threshold is ignored, and a linear, diffusive relationship is used to implement a combined process for creep and faster movements. For example, in Kooi and Beaumont (1996), CASCADE (Braun and Sambridge, 1997), and Rinaldo *et al.* (1995), there is no distinction between the speed or type of movement and no preferred directionality, other than that material may be transferred to any adjoining downslope cells. Kooi and Beaumont (1996) and Braun and Sambridge (1997) both used a mass continuity form of equation, as in equation 2.27, whereas Rinaldo *et al.* (1995) used a transport rate form[4], as in equation 2.25.

However, some workers (e.g. Howard, 1994; Roering *et al.*, 1999; Martin and Church, 1997) have used more sophisticated forms of relationship, which include more parameters, and these also need to be considered.

Relationships using more than one parameter

Regarding mass movement relationships in which the types of movement are differentiated from each other, Martin and Church (1997) suggested that slow and fast mass movements would be better represented with an equation of the form:

$$\frac{\partial z}{\partial t} = (\alpha + \beta)\left[\frac{\partial^2 z}{\partial x^2}\right], \qquad 2.30$$

[4] This has been inferred from the process description in the original paper, as the equation itself is not stated.

where α is the diffusivity for slow, creep-like movement, and β the diffusivity for fast, slide- and flow-like movement. The β term also includes a threshold, so that fast movement cannot occur unless a particular gradient has been exceeded, but the combined process is still implemented using nearest neighbour dispersal. Extending this work in a slope profile model, Martin (2000) modelled creep using a relationship of the form of equation 2.26, whereas slides were modelled using the equation:

$$q = K_0 + \left[0.5 \times (K_1 - K_0) \times \left(1 + \tanh\left(\frac{abs(\partial h / \partial x) - h_1}{h_2} \right) \right) \right], \qquad 2.31$$

where q is the rate of movement per unit width by slide, K_0 and K_1 are diffusivities, and h_1 and h_2 dimensionless adjustable scale parameters, all based on her field data. A feature of Martin's results was that rates of transport by landsliding were negligible in slopes below 30°, increased sharply thereafter in steeper slopes, but reached a maximum in slopes of about 55°, where, Martin hypothesised, the weathering rate became a limiting factor (*ibid.*).

Howard (1994, 1997) took a similar approach to Martin's, using separate process functions for slow and fast mass movements. His slow process, covering creep and splash, was modelled using a linear relationship equivalent to equation 2.27, but his fast, slide-like movement, was modelled using an equation of the form[5]:

$$q = -K_f \left[\frac{1}{1 - K_x |S|^a} - 1 \right] \boldsymbol{s}, \qquad 2.32$$

where K_f and K_x are constants, S is the gradient, a is an exponent (assumed to be spatially uniform and temporally constant), and $\boldsymbol{s}$ is the unit vector in the direction of the slope. This equation may be simplified and re-cast, so that it becomes:

$$q = -K_g \left[\frac{|\nabla z|^a}{1 - \left(|\nabla z| / S_c \right)^a} \right], \qquad 2.33$$

where S_c is the critical gradient, and K_g is a constant equal to $\frac{K_f}{S_c{}^a}$.

Howard applied this equation in seeking to explain badland morphology, in which small slope failures (relative to the model's cell size) could be assumed to occur more or less

[5] Taken direct from equation 2 in Howard (1997), without the linear (creep) term. Eq. 6 in Howard (1994) omits the -1 within the square bracket; this is a misprint, however, as the formula makes no sense without it.

continuously, and almost everywhere in the spatial domain. Interestingly, equation 2.33 is very similar to one derived from field evidence by Roering *et al.*, (1999), in a study of movement rates on steep, well-vegetated hillslopes in the Oregon Coast Range. Roering *et al.*'s formulation is the simpler, as both fast and slow movements are included in the same equation. However, both relationships model the movement so that mass transfer is heavily biased towards the steeper slopes, particularly as gradients approach the critical threshold. This gives the movement concentrative characteristics, so that it is quasi-diffusive, rather than purely diffusive in the manner of the formulations reviewed in subsection 2.5.3.

A feature of the formulations by Martin, Howard and Roering *et al.* is that the threshold is used to determine the *rate of transport* rather than *occurrence* of the movement itself. The movement is therefore modelled as a continuous rather than an episodic process. The only LEM in which intermediate or fast mass movements have been modelled by nearest neighbour transfer but in an episodic fashion is in SLOP3D (Ahnert, 1976). In this model, Ahnert included a plastic flow process, given by an equation of the following form:

$$q_p = k_p\left(R^m \sin\theta - \mathrm{T}_p\right), \qquad 2.34$$

where q_p is the volumetric rate of transport by plastic flow per unit width, k_p is a plastic flow constant, R the regolith depth, m an exponent (assumed constant), and T_p a threshold value for plastic flow. Plastic flow was therefore assumed to occur only where $R^m \sin\theta$ was greater than T_p. In this way, thinner soils might prevent occurrence of such movement on a given slope; conversely, lower slope angles might prevent occurrence of such movement even where soils are quite thick. Ahnert's plastic flow process is interesting, not least because it allows the possibility of modelling intermediate rate mass movements, such as earthflows and solifluction, which may be accommodated using nearest neighbour dispersal. However, he did not use this process in Ahnert (1987), and there is no similar process in any of the other LEMs reviewed here.

In summary, of the nearest neighbour formulations reviewed here, Martin (2000) uses four parameters (two coefficient terms, K_1 and K_0, and two scaling terms, h_1 and h_2, as in equation 2.31), and Howard (1994, 1997) and Ahnert (1976) three parameters (Howard: one coefficient, K_g, one exponent, a, and one threshold, S_c, as in equation 2.33; Ahnert, one coefficient, k_p, one exponent, m, and one threshold, T_p, as in equation 2.34). Mass movement modelled by extended dispersal is now considered.

2.5.5 Extended dispersal representations of mass movement

Extended dispersal is used to implement fast mass movement in four of the reviewed LEMs (Table 2.1, column 8), these being GOLEM (e.g. Tucker and Slingerland, 1997), FLUVER2 (Veldkamp and Van Dijke, 1998), SLOP3D (e.g. Ahnert, 1976), and CAESAR (e.g. Coulthard *et al.*, 1999). It might be thought that extended dispersal would allow an opportunity for a more physically based approach to modelling mass movements, particularly of the factors influencing the failure threshold and the speed and length of runout. The review shows this is not so, however[6]. The extended dispersal movements are therefore, with one main exception, solely controlled both in their occurrence and distribution by a critical slope threshold. The exception to this was used by Tucker and Bras (1998), who adapted GOLEM to include, in one of their scenarios, the effects of raised pore water pressures on landsliding. Based on work by Montgomery and Dietrich (1994), they derived a stability criterion for each cell, which relied on physical measurements and two parameters, the soil transmissivity and the internal friction angle of the soil. Although these are physical parameters, in that their values may be measurable in the field or laboratory, they are still adjustable for the purposes of a simulation with a LEM. In particular, there may be errors in the estimates of each parameter's value as originally measured, and the values cannot be expected to be uniform over the whole spatial domain. Montgomery and Dietrich (1994) also presumed that the relaxation slope threshold for such slides was half the internal friction angle. Their formulation, however, is not used in the other reviewed LEMs, although the idea of a separate threshold to constrain the runout has been considered by Kirkby (e.g. Kirkby, 1989).

Applying his ideas to the modelling of slope profiles, Kirkby's basic assumption was that the repose angle of the material will be somewhat less than the critical angle for initiation of the movement (*ibid.*). In this way, the movement causes an *overcorrection* of the slope. Intuitively, this makes sense, as such movements would be almost continuous in the same place if this were not so. However, there is the difficulty of how much overcorrection to allow for, and even this will be unable to model the complex piling up effects associated with certain movements, such as long run-out rockfalls or mudslides (e.g. Selby, 1993).

[6] The main obstacle seems to be associated with the model time step. To keep simulation times to a practical length, the LEM may require time step lengths of months or years, which require an averaging of the driving conditions. However, a slope may switch from a stable to an unstable state almost instantaneously, perhaps in response to an extreme event which cannot be simulated effectively by averaging the climate parameters.

In summary, where extended dispersal is used to represent fast mass movement, those LEMs that include it rely generally on one empirical parameter, the critical slope angle or gradient, which is used to control both inception of the movement and distribution of the material. The one exception found (in GOLEM, Tucker and Bras, 1998) relies on three parameters, the soil transmissivity, T, the internal friction angle of the soil, ϕ, and a slope relaxation threshold, presumed to be $\frac{1}{2}\phi$ but which could be set separately if desired, and which is used to control distribution of the material.

This section completes the review of the implementation of mass movement in LEMs, and therefore the formulations used to implement the $\nabla \mathbf{q}_m$ term in the basic LEM mass continuity equation (equation 2.12). Attention may now be directed to the last of the three process classes listed in Table 2.1, namely fluvial erosion and transport.

2.6 FLUVIAL EROSION AND SEDIMENT TRANSPORT

2.6.1 Driving conditions and general implementation

With the exception of the model by Martin (2000), all of the reviewed models include a representation of fluvial erosion and sediment transport (Table 2.1, column 9). This reflects the importance of fluvial processes in transporting solutes and sediment from real drainage basins. In this subsection, the methods used for routing of water through the landscape, and hence any fluvially transported material, are reviewed. In addition, three of the reviewed LEMs permit a distinction to be made between overland flow and flows through the soil (soil 'throughflow'), and another allows losses to groundwater, so these matters also need consideration.

Overland flow and soil throughflow

Once a rainfall or runoff input has been applied, according to the preferred climate condition, the total runoff rate for each cell needs to be calculated. This will be the sum of all runoff draining into the cell, plus the input for the cell itself, less any losses if these are modelled. In the simplest representation, all the runoff input is assumed to move through the catchment or basin by overland flow, and to reach the outlet without intervening losses.

Although this method is basic to all of the models, as a refinement, SLOP3D (Ahnert, 1976) permits losses to deeper groundwater, and GOLEM, CHILD and CAESAR allow for a proportion of the flow to take place as soil throughflow i.e. below the surface, subject to local soil properties (e.g. Tucker and Bras, 1998; Tucker *et al.*, 2001b; Coulthard *et al.*, 1999). In these LEMs, the model includes an algorithm to check how much water will flow across a cell during each time step. This is compared with the maximum amount that can be assumed to flow through the soil to lower slopes as throughflow. If the total cell runoff exceeds the soil throughflow, then the excess is assumed to flow over the surface, where it is available to erode and transport sediment (e.g. Tucker and Bras, 1998). In GOLEM and CHILD, the throughflow capacity is controlled by one parameter, the soil transmissivity (Tucker and Bras, 1998; Tucker *et al.*, 2001b). By contrast, in CAESAR, as the runoff at any point is determined using an adaptation of TOPMODEL (Beven and Kirkby, 1979), the apportioning of flow between surface and soil is controlled by two parameters, one controlling the temporal responsiveness of the soil water store and the other the hydraulic conductivity (Coulthard *et al.*, 1999). It will be appreciated that whilst soil transmissivity and hydraulic conductivity can be measured, they may be variable over space, reflecting local soil and regolith conditions. They are therefore still potentially adjustable values from the point of view of running a simulation.

Routing of runoff and fluvially transported sediment

As regards the routing of the runoff, this is assumed in the first instance in all LEMs to be in the direction of the steepest downslope flow path. A consequence of this routing method is that flow is concentrated down the catchment, tending to a maximum at the outlet. It follows that any fluvially transported sediment will be directed along the same flow paths. However, a LEM may also permit ponding of the runoff, or local 'drying ponds', to take into account local depressions along the flow routes. For example, in GOLEM (GOLEM glossary, Tucker, 1997), if the ponding option is activated, then local depressions may be assumed to fill with water until an outflow cell is found, from which routing of the runoff is resumed using the normal algorithm. Additionally, some of the transported sediment is allowed to accumulate in the ponds, so that they may fill up over time during a simulation. However, if the ponding option is de-activated, any runoff flowing into the depression is assumed to evaporate, leaving *in situ* all of the sediment that was being carried by the flow

to that point (*ibid.*). Kooi and Beaumont (1996) included a similar functionality in their model, in which alluvium could be stored in internal (isolated) drainage systems, and a similar process is possible in CASCADE (Braun and Sambridge, 1997), but it is not clear whether any of the other reviewed LEMs include this functionality.

As a final point regarding runoff and sediment routing, fluvial transport is generally modelled using just one mechanism, namely a cell to cell transfer. This is the same as the nearest neighbour transfer used for mass movement (ss 2.5.2 - 2.5.3 *q.v.*), except that fluvial processes are concentrative rather than diffusive. Ahnert (1976) included a separate mechanism which allows direct removal from the landscape and was intended to represent suspended load transport, but this was ancillary to the main cell to cell method outlined here.

Having covered runoff and sediment routing, the review now turns to implementation of transport equations in the LEMs themselves. There is now a large literature on fluvial transport processes, and this shows that despite attempts to improve the physical basis of transport equations, empirical parameters cannot be avoided. In addition, the inclusion of fluvial processes in LEMs is further constrained by the need to scale up the spans of time and space over which the equations must be applied. This makes fluvial processes the most difficult to implement in LEMs, compared with weathering and mass movement, and leads to some important simplifications in how the processes are represented. To understand these more fully, some of the basic ideas and simplifications are now reviewed.

2.6.2 Basic types of equation

Generally, researchers have tried to incorporate physical and other principles in sediment transport equations, to make them more physically based and give them better predictive power. A thorough treatment can be found in the standard literature (e.g. Leopold, Wolman and Miller, 1964; Knighton, 1998; Leeder, 1999), but as a first simplification, it should be noted that for the most part LEMs do not represent simultaneously transport by wash and in channels[7]. The term 'wash' is used here to mean a thin flow of water, like a sheet over the ground surface, which occurs on slopes and open surfaces (e.g. Summerfield, 1991). Channel flow, by contrast, is taken to mean flow in a discrete, erosional feature, with an

[7] An exception is to be found in SIBERIA (e.g. Willgoose *et al.*, 1991 a to d), which allows a soil wash process in addition to a channelled process. Also, other LEMs (e.g. GOLEM, Tucker and Bras, 1998), can be run using a general, water-driven process, inferred to be wash-like or channelled depending upon the type of simulation being run, although the two are not found to operate together in the same simulation.

identifiable bed and bounded by banks, in the manner preferred by Dietrich and Dunne (1993) in their comprehensive review.

Although research has been conducted into wash processes, there is no generally accepted law for wash transport (e.g. Dietrich *et al.*, 2003). Modellers have therefore generally relied on bedload equations, adapting these to cover a more generalised fluvial erosion process which also encompasses suspended load transport and wash transport. Looking at the main equations found in the literature, there are four basic types, all of which are used in some form in one or more of the reviewed LEMs[8]. The Du Boys formula (e.g. Thornes, 1979, page 238-239), is perhaps the simplest, taking the form[9]:

$$q_{sb} = B\tau(\tau - \tau_c), \qquad 2.35$$

where q_{sb} is the rate of bedload transport per unit width, B is an empirical constant for the bed material, τ is the bed shear stress, and τ_c the critical shear stress needed to entrain and transport the sediment. Under conditions of steady, uniform flow, the bed shear stress can be approximated by the formula (e.g. Leopold, Wolman and Miller, 1964):

$$\tau = \gamma RS, \qquad 2.36$$

where γ is the unit weight of water, R the hydraulic radius (equal approximately to the flow depth), and S the gradient of the bed. For simplicity, this will be referred to from here onwards as the 'bed shear equation'. A feature of this equation for modellers is that both γ and S are known at any time in a modelled landscape, whereas the hydraulic radius depends upon the modelled runoff (subsection 2.2.3, *q.v.*). This means that if this type of relationship (equation 2.36) is used in a LEM, the depth of the flow has to be calculated or inferred in some way, and this is discussed in subsection 2.6.3.

Another feature of the bed shear equation is that bed shear stress is often not itself directly measurable in real streams. Some workers have therefore preferred not to use it (for a review and comment, see Prosser and Rustomji, 2000), and have applied other formulae which incorporate direct stream measurements in some way. The Schoklitsch formula (Thornes, 1979, pp 239-240) has this advantage and is based on the Du Boys formula (*ibid.*), but relates transport rates to flow discharge as follows (adapted from Knighton, 1998):

---

[8] Some LEMs allow the researcher to choose which fluvial transport equation they wish to use. GOLEM, for example, has four basic equations, any one of which would implement fluvial transport in some manner.

[9] This is the form in which it is usually given (e.g. Thornes, 1979; Gomez and Church, 1989; Knighton, 1998). However, in Reid *et al.* (1997), there is no shear stress term outside the bracket.

$$q_{sb} = k_{sb} S^m (q - q_c), \quad 2.37$$

where k_{sb} is an empirical constant, m an empirical exponent, q the flow discharge per unit width, and q_c the critical discharge, again empirically derived, for the entrainment of the sediment. By contrast with this formula, Bagnold (1966) derived a transport equation from physical principles, treating the stream as an engine which had power to perform work moving the sediment, but could only do so at a certain efficiency. In his theory, the motivating agency of a stream was called its *stream power*, this being found from

$$\omega = \tau v, \quad 2.38$$

where ω is the stream power per unit area of the bed and v is the stream velocity.

Using the bed shear equation to substitute for the shear stress term in equation 2.38, and by other substitutions relating to the width and depth of the flow, this relationship can be re-written as:

$$\omega = \gamma q S, \quad 2.39$$

Similarly, the total stream power, Ω, is found by multiplying the unit stream power by the width of the stream, to give:

$$\Omega = \gamma Q S \quad 2.40$$

It will be noted that equations 2.39 and 2.40 both include the quantity qS or QS, which is a feature of stream power formulae. It follows that an equation which uses discharge and slope in this way, or which can be re-cast in this form, can be treated as an equation of the stream power type.

Having calculated the stream power, according to Bagnold (1966), the total rate of bed load transport, Q_{sb}, is then given by:

$$Q_{sb} = e_b \gamma Q S, \quad 2.41$$

where e_b is the stream efficiency for bedload transport (e.g. Bagnold, 1966) and Q is the total discharge. It will be noted here that the stream efficiency, e_b, is an empirical parameter. Similarly, for the rate of bed load transport per unit width of bed, q_{sb}, equation 2.41 can be restated as:

$$q_{sb} = e_b \gamma q S \quad 2.42$$

Bagnold also derived more theoretically complete formulae including particle size and flow depth terms, and these in turn can be adapted for mixed beds by introducing another empirical constant. The hydraulic radius can also substituted for flow depth, to give (adapted from Knighton, 1998):

$$q_{sb} \approx K(\omega - \omega_c)^{3/2} R^{-2/3}, \qquad 2.43$$

where K is a constant for bedload transport which *inter alia* accounts for stream efficiency and sediment size properties, and ω_c is the critical stream power. By substituting terms from equation 2.39 for ω and ω_c, equation 2.43 becomes more simply:

$$q_{sb} = k_{sb}(qS - \Phi)^{3/2} R^{-2/3}, \qquad 2.44$$

where k_{sb} is a general bedload transport rate coefficient, and Φ a threshold term, both parameters being related to the nature of the sediment. Equations 2.41 to 2.44 , however, are all bedload formulae, so modellers adapt these to model the total load, taking into account both suspended transport and wash processes. The topic is rather detailed and covered in elsewhere (e.g. Kirkby, 1971; Carson and Kirkby, 1972; Embleton and Thornes 1979; Knighton, 1998; Leeder, 1999), but these considerations together lead to a combined general equation for all fluvial transport, of the form:

$$q_s = k_s q^{\alpha} S^{\beta}, \qquad 2.45$$

where q_s is the rate of sediment transport per unit width, k_s is another empirical constant, and α and β are empirical exponents (e.g. Prosser and Rustomji, 2000). To distinguish this equation from those of the Schoklitsch, Du Boys and Stream power types, this will be referred to as the 'power law' equation from hereon.

In summary, all the LEMs apart from Coulthard's CAESAR model use equations which are based on the main types introduced here. Coulthard *et al.* (1999) by contrast used a type of bedload equation derived by Einstein (1950), which is quite unlike the other formulae, and more complex mathematically than the other equations considered above. However, by manipulation of its components, it can be recast in a general form which is quite similar to the other equations, as follows:

$$q_{sb,D} = k_D \left(\frac{dS}{\sqrt{D}} \right)^3, \qquad 2.46$$

where $q_{sb,D}$ is the rate of bed load transport for particles of diameter D, k_D is an empirical constant, and d is the depth of the flow.

Having introduced the main types of equation, the ones actually used in LEMs and the manner of their application may now be considered. For convenience during the discussion, the term 'cell discharge', or more simply 'discharge', will mean the discharge of water assumed to be leaving a particular cell.

2.6.3 Fluvial transport equations used in LEMs

LEMs incorporating power law type relationships

Of the equations considered above, the power law (equation 2.45) in some form provides the basis for the sediment transport relationships in SLOP3D (Ahnert, 1987), Moglen and Bras (1995), GOLEM (e.g. Tucker and Slingerland, 1994, 1996; Tucker and Bras, 1998), FLUVER2 (Veldkamp and Van Dijke, 1998), CHILD (e.g. Tucker *et al.*, 2001b) and SIBERIA (e.g. Willgoose *et al.*, 1991a). Strictly speaking, this equation should be simpler to use and encode than Du Boys-type shear stress formulae (equation 2.35), or depth-related stream power equations (equations 2.43 or 2.44), as flow depth is not needed in order to calculate the sediment transport rate. In these models, when calculating wash or channel processes, the key physical variables are therefore the slope and discharge per unit width. Slope is generally just the gradient and can be found directly from the cell elevations[10], and, for wash, discharge per unit width in any cell is the total runoff of the cell divided by the cell width. However, where a LEM allows for channelled transport, the channel width must be used instead, and this needs to be specified or calculated in some way, depending upon the rules adopted in the model. Channels and channel width adjustments are rather complex and are considered separately, in subsection 2.6.4. Also, despite the basic formula, depth calculations may be needed in practice, depending upon the particular substitutions used in the model implementation, similar to those discussed later in this subsection.

[10] Also, Ahnert (1987) used the sine of the slope angle, rather than the tangent. This makes the formulation more correct physically than the usual power law, and also likely to be more suitable for steeper slopes. It should also be noted that Ahnert (1976) used a type of shear stress formula rather than a power law.

LEMs incorporating relationships based on shear stress formulae

Rather than using the power law equation, some researchers prefer to use equations which, in their basic form, are cast in terms of the bed shear stress, similar to the Du Boys formula (equation 2.35). Shear stress formulae underpin the fluvial sediment transport calculations in the SLOP3D (Ahnert, 1976), Howard (1994, 1997), Rinaldo *et al.* (1995), GOLEM (Tucker and Slingerland, 1996, 1997) and CAESAR (e.g. Coulthard *et al.*, 1999). In CAESAR, although the Einstein (1950) formula appears to be quite different from the others, it can be recast in shear stress terms and will be treated as a shear stress type of equation[11]. Similarly, the formula used by Howard (1994, 1997) to calculate transport in alluvial channels is like an Einstein formula, and can also be expressed in shear stress terms. Regarding the formulation used by Ahnert (1976), although this is something of a hybrid, Ahnert using the sine of the slope angle, and referring to flow depth rather than shear stress, it is also like a shear stress type of equation and will be considered with the others here.

In these LEMs, therefore, whatever the basic form of equation used, the flow depth has to be estimated or specified to calculate the shear stress (equation 2.36), and hence the rate of sediment transport. This can be done either by the researcher setting the flow depth for the cells independently, or by the use of a model function which calculates flow depth according to spatial and other relationships, considered later in this sub-subsection. The only model in which the flow depth is stipulated independently is that by Armstrong (1976), and the formulation is reviewed in subsection 2.6.4.

Regarding flow depth quantified directly by calculation (in SLOP3D, Ahnert, 1976), an algorithm calculated flow depths for each cell after allowing for infiltration losses, which could be spatially varied. The flow depths were calculated iteratively until they were stable, or a set number of iterations had been performed, after which sediment transport for the time step was calculated using:

$$q_s = k_s d^m \sin^n \theta , \qquad 2.47$$

where θ is the slope angle, d is the flow depth, and m and n are empirical exponents, assumed to be constant. The transport coefficient, k_S, was spatially variable, and could also

[11] The Einstein formula may be treated as one of shear stress type by a straightforward rewriting of equation 2.46. By combining the sediment size and transport coefficients, and using the hydraulic radius, R, for flow depth, the equation becomes $q_{sb,D} \propto (RS)^3 = k_{sb,D}\tau^3$, with $k_{sb,D}$ as a coefficient appropriate for the sediment size.

be made dependent on the regolith depth, so as to simulate the presence of larger particles in deeper layers, which would be more difficult to entrain. This is a sophisticated spatial variation when compared with most of the more modern models[12].

Regarding the other LEMs needing flow depth in the fluvial transport calculations, a more direct calculation is made in CAESAR, where depth is found from the hydrological model which is run to simulate flow conditions (e.g. Coulthard *et al.*, 1999), in the manner described in subsection 2.6.1. The complete calculation also requires use of Manning's *n*, an empirical parameter[13], and erosion and deposition is apportioned in up to twelve active sediment layers for the sediment size classes being modelled. In the other LEMs, the calculation is more indirect, so it is helpful first to give the general form of equation from which the transport relationship in each model is derived. These equations are listed below:

(i) in Rinaldo *et al.* (1995) - $$q_s = f(\tau - \tau_c), \qquad 2.48$$

from which it is not clear whether the function of the excess shear stress is linear or otherwise;

(ii) in Howard (1994, 1997) - $$q_s = k_s(\tau - \tau_c), \qquad 2.49$$

which is a simple, linear relationship (of the excess shear), used to simulate erosion and transport in "nonalluvial channels" (e.g. Howard, 1994), as explained below; and

(iii) in GOLEM (e.g. Tucker and Slingerland, 1996, 1997) -

$$q_s = k_s(\tau - \tau_c)(\sqrt{\tau} - \sqrt{\tau_c}), \qquad 2.50$$

which is an adaptation of a Bagnold type equation, and is clearly non-linear. Tucker and Slingerland (1996, 1997) also use an excess shear equation, similar to equation 2.49, to simulate the erosion of bedrock (expressed as a rate of bedrock lowering). Howard's formula (equation 2.49) was applied to both regolith and bedrock channel erosion, although Howard (1994, 1997) also used a different equation to model erosion and transport in alluvial channels. The latter equation is first posed as a functional relationship between two parameters, similar to the Einstein (1950) equation, thus:

---

[12] It is also interesting that despite its being one of the oldest of the reviewed LEMs, SLOP3D was the only one which allowed for infiltration or groundwater losses of some kind, until the development of GOLEM, CHILD and CAESAR many years later.

[13] Manning's *n* and the Manning equation are discussed by Leopold, Wolman and Miller (1964, pages 157-159), and ranges of *n* for different stream types can be found in a number of sources, but a useful summary, with references, is given in Goudie (1997).

$$\phi = F\left(\frac{1}{\psi}\right), \qquad 2.51$$

where the function F is not specified, and the components ϕ and Ψ are defined by:

$$\phi = \frac{q_{sb}}{\zeta(1-\mu)D}, \qquad 2.52$$

and

$$\frac{1}{\psi} = \frac{\tau}{(\gamma_s - \gamma)D}, \qquad 2.53$$

where q_{sb} is the bed sediment transport rate per unit width, ζ is the fall velocity of the sediment grains, D is the sediment grain size, μ is the alluvium porosity, γ_s is the unit weight of the sediment grains, and γ the unit weight of water. Apart from q_{sb}, all the terms are physical quantities particular to the sediment, so both equations can be reduced as follows:

(i) equation 2.52, to $$\phi = k_1 q_{sb}, \qquad 2.54$$

and (ii) equation 2.53 to $$\frac{1}{\psi} = k_2 \tau, \qquad 2.55$$

where the coefficients k_1 and k_2 combine the values of the relevant physical quantities above. Substituting these expressions in equation 2.51 then gives:

$$\phi = k_1 q_{sb} = F(k_2 \tau) \qquad 2.56$$

Howard (1994) then introduced a critical threshold, ψ_c, an exponent p, and a coefficient, k_3, thus specifying the overall function F so that equation 2.51 can be restated as:

$$\phi = k_3 \left\{\frac{1}{\psi} - \frac{1}{\psi_c}\right\}^p, \qquad 2.57$$

Substituting from equations 2.54, 2.55 and 2.56, this can be restated in the shear stress form:

$$q_{sb} = k_4 (\tau - \tau_c)^p, \qquad 2.58$$

where the coefficient k_4 now takes into account the rearrangement and the other k_i terms. Following this, the similarity of equation 2.58 to equations 2.48 and 2.49 is evident.

For each of the shear stress equations (eqs 2.48-2.50, and 2.58) , to calculate shear stress, flow depth was inferred by resorting to equations which allow shear stress, flow discharge, flow velocity, channel width and depth, and contributing area (upslope area), to be related to each other. The bed shear equation (eq. 2.36 *q.v.*) allows shear stress to be related to flow

depth and gradient of the bed. However, flow depth and flow velocity can also be related to each other by mass continuity of the flow, given by:

$$Q = A_c v \approx wRv, \tag{2.59}$$

where A_c is the cross sectional area of the flow, and v, w and R are respectively the velocity, channel width and hydraulic radius as previously defined. For wide channels, the depth and hydraulic radius are effectively the same (e.g. Howard, 1994; Tucker and Slingerland, 1997). The flow velocity can then be found from well established relationships, for example using Manning's equation and Manning's n (e.g. as in Howard, 1994):

$$v = \frac{1}{n} R^{2/3} S^{1/2}, \tag{2.60}$$

or from the Darcy-Weisbach equation (e.g. as in Tucker and Slingerland, 1997):

$$v = \left(\frac{8gRS}{f} \right)^{1/2}, \tag{2.61}$$

where f is the Darcy-Weisbach friction factor (*ibid.*). Further substitutions can be made for the channel width, using either a total discharge relationship of the form:

$$w \propto Q^{m_1}, \tag{2.62}$$

where m_1 is an empirical exponent, or using a contributing area relationship of the form:

$$w \propto A^{m_2}, \tag{2.63}$$

where m_2 is another empirical exponent. There is some support for these relationships on both observational and theoretical grounds (e.g. Leopold and Maddock, 1953; Hairsine and Rose, 1992).

Now, referring again to the bed shear equation (equation 2.36), if R is used for depth, and other substitutions for velocity and channel width are made using equations 2.60-2.63, each of the shear stress equations (eqs 2.48-2.50, and 2.58) can be reduced to a general form. More details of the various steps required are provided in the endnotes to this chapter[I], but if the area substitution is made for channel width (equation 2.63), the general form is:

$$q_s = k_s A^{a_1} \left[k_A A^{a_2} S^{a_3} - \Phi_c \right]^{a_4}, \tag{2.64}$$

where Φ_c is a critical entrainment term, related to the critical shear stress, A is the upslope area (as in equation 2.63), k_s and k_A are empirical coefficients, and a_1, a_2, a_3, and a_4 are empirical exponents. Likewise, if the discharge substitution is made (equation 2.62), and assuming suitable adjustments for cell or channel width, the general form is:

$$q_s = k_s Q^{a_5} \left[k_q Q^{a_6} S^{a_7} - \Phi_c \right]^{a_8}, \qquad 2.65$$

where again k_s and k_q are empirical coefficients and a_5, a_6, a_7, and a_8 are empirical exponents. Types of equation similar to these are applied to wash and channelled transport in most of the reviewed LEMs[14]. It should also be mentioned here that equation 2.65 is rather an oversimplification of the final formula derived for use in GOLEM by Tucker and Slingerland (1997), as their initial transport equation (eq. 2.50) is not a simple function of the excess shear stress term, '$\tau - \tau_c$'. This aside, by further adjustments, to both the exponents and the coefficients, the same types of formulae have also been applied to incision into bedrock (e.g. Tucker and Slingerland, 1997; Howard, 1994), and for the simulation of detachment-limited rather than transport-limited conditions (e.g. Howard, 1997). As a further modification, CHILD (e.g. Tucker *et al.*, 2001b) incorporates equations similar to equation 2.65, but without the discharge term outside the bracket[15], and it will also be noted that equations 2.64 and 2.65 are similar to power law and Schoklitsch type formulae, although their derivation from shear stress considerations gives them a stronger physical basis.

LEMs incorporating stream power relationships

Stream power formulae are also often used in LEMs. Armstrong (1976) used such a formula, similar to equation 2.41, for discrete channels, as discussed in subsection 2.6.4. Braun and Sambridge (1997), in CASCADE, applied the same basic equation, but in an interesting application that allowed the rate of transport to be less than the capacity rate according to a certain entrainment length. In their model, transport capacity was given by:

[14] It is also possible to derive these forms using depth-discharge and depth-area empirical relationships, which are very similar to the width-discharge and width-area equations given here (eqs 2.62 and 2.63).

[15] CHILD uses the same basic form of equation to calculate a detachment capacity and a transport capacity for each class of sediment (e.g. Tucker *et al.*, 2001b). Each formulation needs its own parameters, namely two coefficients, three exponents and a threshold (*ibid.*). This model structure permits transport and detachment capacities to be different from each other in the same cell.

$$q_s = k_s q S, \qquad 2.66$$

where k_s is a general sediment transport coefficient, as in the equations discussed above. For any cell, the rate at which sediment was actually being transported, q_{act}, could be greater than, equal to, or less than the capacity[16] given by equation 2.66, entrainment or deposition occurring over the length of the cell depending upon whether capacity was exceeded or not, according to the equation:

$$\Delta q_{act} = \frac{q_s - q_{act}}{L} \Delta L, \qquad 2.67$$

where Δq_{act} is the change in sediment transport rate across the cell, L is the scale length for erosion or deposition, and ΔL the cell length. Braun and Sambridge (1997) suggested that for resistant alluvium or bedrock, L would have a larger value, and for the less resistant alluvium and rock, a lower value. This is a very interesting formulation, in that it connects ideas about downstream fining in channels, and sediment supply, with the variation in stream power observed in most rivers as they flow from upland to lowland areas (see, for example, Dade and Friend, 1998; Talling and Sowter, 1998; Gasparini *et al.*, 1999 and 2004; and Knighton, 1999). Moreover, Braun and Sambridge (1997) do not distinguish between channels and slopes, so the fluvial transport process in their model could represent wash or channelled transport. This is also the case in SLOP3D (Ahnert, 1976, 1987) and in Rinaldo *et al.* (1995). It is therefore of interest to note that all three models generate landscapes with the appearance of fluvially dissected forms, valley networks and so on. This therefore suggests that, at least as a first approximation over long time scales, the inclusion of channel transport in a LEM is not essential. However, other researchers have incorporated channel transport in their LEMs, so a review of how this is done now follows.

2.6.4 Channels and channelled transport in LEMs

Some of the papers describing LEMs with channelled transport are not clear about whether sediment can also be transported by a wash process as well as a channelled process *in the same simulation*. Regarding SIBERIA, Willgoose *et al.* (1991a) are specific: either a cell is a hillslope segment in which hillslope processes, including wash, may operate, or the cell

[16] The actual rate of transport is calculated from the rate at which sediment is being transported into the cell from any adjoining upslope cells.

contains a channel, with no separate wash process. Also, if a cell is designated a hillslope segment, the slope processes (creep, splash[17] etc.) operate together, so the wash element is added to the same general hillslope process function. However, if the cell is a channel, only channelled fluvial processes operate (*ibid.*). GOLEM (e.g. Tucker and Slingerland, 1994, 1996, 1997) and CAESAR (e.g. Coulthard *et al.*, 1999) also allow only hillslope or channel cells, again with no wash process separate from channel processes in the same simulation. Howard (1994, 1997), on the other hand, adopts something of a compromise, calculating the width of the channel in a particular cell, and from this the proportion of sediment transport which occurs by mass movement or fluvial processes within the same cell. As with the models above, the fluvial process is notionally a channelled one, although operationally (i.e. when analysing the model's output) he distinguishes between established channels, and ephemeral channels and small rills, where the transport may be more wash-like (discussed later is this subsection). For simplicity, therefore, it is assumed for the purposes herein that in the other models including channels, wash transport is not modelled as a separate process.

Where channels have been included, either they have been specified as fixed features (Armstrong, 1976), or inferred, and extended headwards, according to certain rules (e.g. Willgoose *et al.*, 1991a; Moglen and Bras, 1995), or they have been modelled less explicitly, but allowing for headward extension (e.g. Howard, 1994; Tucker and Slingerland, 1997), or for both extension and meandering (e.g. Tucker *et al.*, 2001b; Coulthard *et al.*, 1999, 2000). Armstrong's - the simplest representation - is considered first.

Fixed channels (Armstrong, 1976)

Armstrong (1976) specified channels of fixed width and length, in which sediment transport was calculated using a stream power equation of the form:

$$q_s = k_s e_s q S, \tag{2.68}$$

where k_s is a transport constant related to the type of sediment, and e_s is a stream efficiency term. The similarity of this equation with the equations 2.41 and 2.42 will be noted. Armstrong stipulated flow depths of 0.5m in the channels, and his model also allowed for streambed incision, the incision rate being directly proportional to the excess of transport

[17] The term 'splash' is taken to mean direct impact by water drops, usually direct from rainfall (e.g. Carson and Kirkby, 1972; Selby, 1993).

capacity over regolith supply in each cell. A limitation of using fixed channels, however, was that they could not extend dynamically i.e. in response to landform and process rate changes. To overcome this limitation, later researchers have tried to simulate the presence and headward extension of channels in a number of ways, and these are now considered.

LEMs with dynamic channels

Ideally, channel formation would be modelled from physical principles, using a relationship of the type proposed by Smith and Bretherton (1972). However, their result has not been implemented in any of the reviewed LEMs, possibly because the empirical formulations are easier to encode and implement. Of the LEMs including empirical channel functions, one of the first was SIBERIA (e.g. Willgoose *et al.*, 1991a). In this model, a cell indicator function determines whether a cell should be treated as a channel or part of a hillslope, the function itself using values generated by an equation representing an empirical channel formation rule. By this approach, the researcher chooses one out of three such rules, and their associated parameter values, to be used in a simulation. Each rule requires at least two parameters, namely a threshold and a coefficient (e.g. Willgoose *et al.*, 1991a). SIBERIA also includes procedures to prevent channel heads from cutting into the same cell, and to determine which cell should be used for extending the channel where more than one satisfies the channel extension criterion (*ibid.*).

Once a cell in SIBERIA is designated as channelled, then the channel width is calculated using a hydraulic geometry relationship (after Leopold and Maddock, 1953) of the form:

$$w = aQ^b, \tag{2.69}$$

where w is the channel width and a and b are empirically defined constants. Having calculated the width, this is then be used to calculate q and the associated rate of fluvial transport in the channel. In the model, transport is assumed to be at capacity, and there is no bedrock-regolith boundary (Willgoose *et al.*, 1991a).

In the model by Howard (1994, 1997), a channel is presumed to exist where the critical shear stress for erosion is exceeded. However, Howard distinguishes between channels in cells on headwater convex and linear portions of the landscape, where they are assumed to be ephemeral, and those in cells where slope curvature allows concentration of the flow, where fluvial processes are taken to dominate over diffusive (slope) processes (Howard

1994, page 2278). Similarly, although GOLEM can also be run using particular channel cell designation, as discussed in Chapter 3, in other applications of the model the presence of a channel is assumed more simply, occurring where the critical shear stress is exceeded (e.g. Tucker and Slingerland, 1997, page 2034).

In Howard (1994, 1997), as in SIBERIA, the channel width is found from hydraulic geometry relationships of the form given in equation 2.69. Operationally, Howard then establishes the drainage network by referring to a certain slope threshold and the slope curvature, such that a fluvial (as distinct from ephemeral) channel exists if:

$$\frac{\nabla^2 \mathbf{z}}{\overline{S}} \geq D_c, \qquad 2.70$$

where $\overline{S}$ is the mean gradient, the $\nabla^2 \mathbf{z}$ term is the slope curvature, and D_c is the threshold. If slope curvature is treated as a proxy for flow concentration, equation 2.70 is similar to an empirical relationship for channel head location found by Montgomery and Dietrich (1988). In this paper, the authors showed a clear relationship between the gradient at the channel head and the upslope drainage area, over three study sites with different relief, rock type and climate. The relationship is of the general form:

$$\ln|A| = \ln|A_0| - b \ln|S|, \qquad 2.71$$

where A is the upslope area i.e. the area draining into the channel head, A_0 and b are constants, and S is the ground slope (in the direction of the channel) at the channel head. This relationship may be recast as a function of discharge, using an equation of the form:

$$Q = k_a A^f, \qquad 2.72$$

where k_a and f are also assumed to be constant. Using this to substitute for A in equation 2.71, and recasting the relationship in non-logarithmic terms, discharge and slope at the channel head may then be related to a critical threshold, thus:

$$k_{ch} Q^l S^b = T_{ch}, \qquad 2.73$$

where k_{ch} is an empirical parameter, l an exponent, and T_{ch} the channel formation threshold, and all the parameter values are assumed constant for the particular climate, land cover and geology. This equation then provides a general condition for channel initiation in terms of cell discharge and slope. This form of relationship, using four adjustable parameters, can

be used as one of the possible process activating functions in GOLEM (discussed in more detail in Chapter 3), although further analysis shows that it can be simplified to

$$QS^{n_{ci}} = T_{ci}, \qquad 2.74$$

where n_{ci} and T_{ci} are the appropriate exponent and threshold parameters.

In contrast to the spatially invariate methods used above, Moglen and Bras (1995) adopted a completely different approach, suggesting that channel extension could depend instead upon the local erodibility of the regolith. In their model, each cell was randomly assigned a different erodibility, which could be greater or less than a specified mean value. Sediment transport rates were calculated using a simple power law, with no threshold term, and sediment was presumed to be transported at the detachment capacity in each cell. However, unlike the implementation in other LEMs, the transport coefficient, k_s, was varied from cell to cell to reflect the local erodibility of the sediment. Where all cells were assigned the same erodibility, Moglen and Bras' (1995) model produced channels which extended in straight lines. However, where variable erodibility was introduced, channels would extend upslope into the neighbouring cell which had the most easily erodible material. Increasing the overall range of erodibility about the mean also increased the complexity of the drainage network, which became more sinuous. An intriguing point here is that Moglen and Bras (1995) did not need to include arbitrary channelisation thresholds in their model. Their results therefore show how naturalistic fluvial networks may be produced by variable regolith qualities alone, rather than by the more formal rules required in SIBERIA, or in GOLEM if the latter's channel designation function is used[18].

Finally, it should be noted here that despite the success of these LEMs in producing naturalistic model landscapes, the channels included in them only extend upslope. There is therefore no mechanism to simulate lateral channel erosion and meandering. This omission has probably been a matter of program complexity and computer power as much as anything else, and more recent work has been directed towards making up for these omissions. Both CAESAR (e.g. Coulthard *et al.*, 1999) and CHILD (e.g. Tucker *et al.*, 2001b) offer a representation of these processes, the programs including routines for calculating the transport of different classes of sediment and the routing of channels.

[18] It is also of interest to see how the sinuosity of the network was produced using a regular, orthogonal grid, rather than the irregular grids used in CHILD (e.g. Tucker *et al.*, 2001b) or CASCADE (e.g. Braun and Sambridge, 1997). This suggests that the supposed advantages of irregular grids over the regular kind are not as certain as might be supposed, and the whole matter clearly merits further research.

Since the process representations in CAESAR and CHILD are quite complex[19] and sections 2.4 to 2.6 already include potentially a large number of adjustable parameters, the additional functionality in these two models will not be reviewed in detail. However, it should be noted that the equations used to implement the meandering and erosion routines incorporate empirical parameters as coefficient, threshold and exponent terms. CHILD also includes of an overbank sedimentation routine (e.g. Tucker *et al.*, 2001b). During a flood, this is made to vary as a function of both the distance from a primary channel and the local floodplain topography. For a given depth of flood, the sedimentation rate is dependent upon two parameters, one for the base rate of deposition and the other for the rate of its decay with distance from the channel, and the flood depth itself is based on an empirical relationship incorporating a further two adjustable parameters.

Detachment limited conditions and bedrock erosion formulations

In bringing this subsection to a close, brief comment is needed on process formulations intended to be applicable to detachment limited conditions (e.g. Howard, 1994; GOLEM, Tucker and Slingerland, 1997). These are usually expressed in terms of the rate of lowering of bedrock, rather than the volumetric rate of transport (*ibid.*). They also employ bed shear stress quantities based on similar calculations to those used in the transport formulae considered above, and for equivalent reasons also rely on empirical parameters in the form of thresholds, coefficients and exponents. Whilst noting (as reviewed in Chapter 1, Table 1) that the use of these forms of equation may lead to different patterns of landscape evolution, especially over longer timescales (e.g. Tucker and Whipple, 2002; Whipple and Tucker, 1999), for the purposes of this review, the author considers them to be qualitatively the same as the other types of equation, and therefore they will not be reviewed separately.

2.6.5 Section summary – fluvial transport, erosion, and related functions

In summary, this section has had to be more detailed than that required for reviewing weathering and mass movement. This reflects the complexities of fluvial processes and the difficulties of trying to model the interactions of two states of matter – liquid and solid – at

[19] CAESAR is additionally sophisticated in that the channel may occupy laterally more than one cell's width, whereas in the other LEMs, channels may not be more than one cell wide.

the same time. The review shows, however, that despite the greater or lesser physical bases to the particular transport equations used in LEMs, empirical parameters have to be included, equations 2.64 and 2.65 typifying the number and type of parameters required. The adaptations for channel activating functions, calculating the width of channels, flow depths, and in the later models, channel meandering and overbank deposition, also need parameters, and serve to emphasise the extent of parameter use for implementing fluvial erosion and transport in a LEM. However, the naturalistic modelled landscapes generated by some LEMs, for example SLOP3D (e.g. Ahnert, 1976) and the model by Rinaldo *et al.* (1995), suggest that simpler representation of fluvial processes may still yield useful insight into landscape evolution. It is not therefore easy to generalise the parameter requirements for implementing fluvial processes, except that for the transport process alone it would appear to be at least three (for example, as in equation 2.45, a transport coefficient, k_s, a discharge exponent, α and a slope exponent, β), and probably five to seven in most cases (for example, as in equation 2.65, two coefficients, k_s and k_q, four exponents, variously a_i, and a threshold, Φ), with more as required by any functionality used to model channels, different sediment sizes and so on. Therefore, in the context of the overall mass continuity relationship, as expressed in equation 2.12, the $\nabla \mathbf{q}_f$ term is deceptively simple and encompasses a wide range of possibilities.

This concludes those sections of the chapter reviewing process functionality in LEMs. It now remains for the main findings to be summarised, with comment on the ways of establishing suitable values for the adjustable parameters, and clarifying the typical parameter space associated with a LEM.

2.7 TYPICAL PARAMETER SPACES OF LEMs

2.7.1 Typical parameter requirements in LEMs

The review has shown that although LEMs to date have generally included the same main classes of geomorphic process, there are important differences in the manner by which these processes and related functions are represented. These differences lead in turn to differences in the number of parameters required. It is therefore difficult to form a representative picture of the number of parameters in a typical LEM, though the number of parameters can be seen as broadly related to the sophistication of the model. In this respect,

it is fair to say that the newer models, such as CAESAR and CHILD, are likely to need more parameters than the older ones, such as GOLEM or Howard's model, although the situation is more complicated than this. In particular, if separate hydrological and vegetation modules are included in the model structure, then more parameters are needed, whatever the initial requirement for the model's main geomorphic components[20].

With this in mind, the findings from the review are summarised in Table 2.2. It should be noted that the Table lists all the parameters that *might* be required, rather than all the parameters actually used in just one particular model. If fact, none of the reviewed LEMs uses all of the listed parameters together in the same model structure. However, it is also clear that many LEMs need half or more of the tabled parameters.

[20] Although perhaps an extreme example, Lancaster, Hayes and Grant (2001), when applying CHILD with a vegetation module to a catchment evolution study of a forest site in Oregon, used *47* parameters in the geomorphic, hydrological and vegetation process relationships and related functions.

Table 2.2: Number of parameters typically required in the geomorphic processes, related functions and driving conditions implemented in most LEMs

PROCESSES	NO. OF PARAMETERS	TYPE OF PARAMETER
Weathering:		
- physical process (e.g. equation 2.22)	Two	One coefficient, one exponent
- chemical or solution process (e.g. equation 2.13)	Two or three	One or two coefficients, one exponent
Mass movement:		
- slow or general diffusive process, by nearest neighbour dispersal (e.g. equations 2.24-2.27)	One	One coefficient
- combined intermittent or quasi-diffusive process, by nearest neighbour dispersal (e.g. equations 2.29-2.34)	Three or four	One or two coefficients, one exponent (or a prescribed function), one threshold
- medium to fast slide or flow dominated movements, by extended dispersal	One or more	One threshold, possibly also one relaxation threshold; other parameters as required to improve physical basis or runout
Fluvial transport:		
- general representation (e.g. equations 2.64 and 2.65)	From three to seven	One or two coefficients, one threshold, from one to four exponents
- channel initiation and extension rules (e.g. equations 2.73 and 2.74)	Two to four	One or two exponents, one threshold, possibly one coefficient
- supply limited conditions, bedrock erosion	Two to four	One coefficient, one threshold, possibly one or two exponents
Other functions:		
- hydrological variability (soil throughflow, losses to groundwater)	One to three	One or two coefficients for soil throughflow; one coefficient for groundwater losses
- channel meandering	Three	One coefficient, one exponent, one threshold
- overbank sedimentation	Three	One coefficient, one exponent, one threshold
- land cover, spatial variations in erodibility	As required	As many as required to modify spatially the process rate coefficients and thresholds listed for any of the processes above
External variables (drivers):		
- base level, tectonics	One or more	At least one outlet rate condition, and more as required for temporal or spatial variation
- runoff	One, two or more	At least one for quantity, possibly one for intensity, and more as required for temporal or spatial variation

The table reveals that a fairly basic LEM needs about fifteen parameters, including - for the processes - four coefficients (one each for weathering, slow mass movement, fluvial sediment transport and bedrock erosion), several thresholds (one each for fast mass movement, fluvial sediment transport and either bedrock erosion or channel formation) and four or five exponents (one for weathering, possibly one for intermediate speed mass movement, at least two for fluvial sediment transport, with more for bedrock erosion and one for channel formation if necessary)[21]. If threshold terms are omitted from the fluvial and bedrock erosion processes, the number can be reduced to perhaps twelve or thirteen. By contrast, as more functionality is included in a LEM, so the parameter requirement increases. For example, a LEM including additional relationships for soil throughflow, and a mass movement function similar to equation 2.33, would need about twenty parameters; similarly, a LEM with further functionality for channel meandering, overbank sedimentation and chemical weathering would probably require over thirty.

Table 2.2 also helps to draw attention to two other points. First, as indicated in Chapter 1 (section 1.2), the number of parameters needed to implement geomorphic processes and related functions typically exceeds the number needed to implement the driving conditions. Also, Figure 1.1 shows how the former stem from the built-in uncertainties in a LEM, whereas the latter derive from the overarching uncertainties. In particular, process mechanisms and formulations adopted in LEMs are highly simplified, these simplifications being needed to keep calculations practical for the scales of time and space which are of interest. Although attempts have been made to improve the physical bases of these model components (e.g. the inclusion of pore water pressure landsliding, in GOLEM, by Tucker and Bras, 1998; the use of TOPMODEL and the Einstein equation in CAESAR, by Coulthard et al., 1999), the parameter requirement in a typical LEM remains high.

The second main point from Table 2.2 is that, for the geomorphic processes and related functions, there are at least as many coefficients as there are exponents, but rather fewer thresholds. This helps to clarify ways in which equifinality might be expected to be generated when using a LEM. In particular, it has been shown here that the exponents often help to determine the structure or form of a process relationship, whereas the coefficients and thresholds determine its rate and occurrence. Therefore, holding the exponents constant

[21] The author has assumed here that a 'basic' LEM would be likely to include physical weathering (two parameters), one slow and one fast type of mass movement (also two parameters), fluvial sediment transport (four or five), bedrock erosion (three), a function to initiate and extend channels (two), and separate base level and runoff conditions (another two).

throughout a series of simulations is equivalent to treating the forms of process relationship as fixed, even though their rates and occurrence might still be varied. As Table 2.2 shows, there are perhaps between ten and twenty such coefficient and threshold terms in a typical LEM, a parameter space of high dimensions. There is therefore potential enough for running many different simulations with a LEM varying these parameters alone, without considering changes in the values of the exponents also.

Finally, it should be borne in mind that there is a difference between the number of parameters required, and the number of parameter *values* required in an experiment, as multiple values for the same parameter may be needed to represent spatial and temporal variations (e.g. soil properties, by Moglen and Bras, 1995; climate, by Rinaldo *et al.*, 1995). Whether such variations are required or not, however, values will have to be established for the parameters before the simulations can be run. This leads to the parameter values actually used in simulation work, which are considered next.

2.7.2 Table of parameter values appropriate in modelling studies

The point has already been made in Chapter 1 (subsection 1.2.2, *q.v.*) that the LEM parameter space comprises both the dimensionality of the space, and the combined value uncertainty of the parameters themselves. The need to use combinations of published values, field data, model calibration and accepted practice in order to establish suitable base values[22] and upper and lower limits, to constrain each parameter's value range, has also been commented on (same place). The matter of parameter value estimation will not be considered further, as it is a complex subject in its own right (e.g. Beven, 2002 and 2006) and beyond the main focus of this thesis. For the purposes here, appropriate parameter values and value ranges will be identified by reference to values used in previous LEM studies, and from other relevant sources. The author will assume, however, that by some means, researchers using LEMs will decide upon the best ranges of values to use in their experimental work. With this general point made, the author has summarised value ranges of parameters and their usual evaluation methods in Table 2.3.

[22] The author uses the term 'base' value in the sense of a central value, equivalent to a median, mean or similar measure, which may be used in simulations, and about which other values may be tested for their effect if desired. The usefulness of the idea of a base or central value will made evident in Chapter 3.

Table 2.3: Suggested value ranges for parameters typically incorporated in geomorphic processes and related functions used in LEMs and slope profile models. Values are sourced mainly from the LEM papers listed in Tables 1 and 2.1 and the references cited in subsection 2.7.2.

PROCESS OR FUNCTION	PARAMETER, UNITS	SUGGESTED RANGE	EVALUATION METHOD AND COMMENTS
WEATHERING:			
Physical process (eq. 2.22)	Coefficient for bare bedrock, m yr^{-1}	5 – 5,000 x 10^{-6}	Usually based on published data, or found by calibration against an expected or published denudation rate. The highest values probably apply only to mountains in areas of rapid uplift.
	Decay depth, m	0.2 – 5.0	Usually based on published data, but may also be found by calibration.
MASS MOVEMENT:			
Slow, diffusive, as for creep and splash (eqs 2.24-2.27)	Diffusivity, m^2 m^{-1} yr^{-1}	5 – 5,000 x 10^{-5}	Usually based on published data. High values probably relate to sites where mixed speed movements, caused by different mechanisms, have occurred, so caution is necessary to select the most suitable value (see below).
Mixed speed, diffusive, as for creep combined with flows and slides (also eqs 2.24-2.27)	Diffusivity, m^2 m^{-1} yr^{-1}	5 – 500 x 10^{-3}	Usually based on published data, but may also be based on observations.
Fast or combined speed, quasi-diffusive, as for slides and flows, with or without creep; also possibly for intermittent flow or slide dominated process (eqs 2.29-2.34)	Diffusivity, m^2 m^{-1} yr^{-1}	1 – 500 x 10^{-3}	May all be based on published data (see note). However, the critical slope may need to be based instead on study site observations, and the exponent may also have to be hypothesised or found by calibration.
	Critical slope threshold angle (gradient)	15 – 60° (0.27 – 1.73)	
	Critical slope exponent	1.0 – 3.0	
Fast slide or flow type, including bedrock failure (extended dispersal, s. 2.5.6)	Critical and relaxation slope threshold angle (gradient)	25 – 75° (0.47 – 3.7)	May be based on published data or study site observations. Relaxation threshold may also be hypothesised or set arbitrarily to a value less than the critical slope. Bedrock thresholds are typically 10-20° greater than those for regolith movements.

Note: The diffusivity range quoted here is based on the formula by Roering *et al.* (1999), assuming an exponent value of 2.

Table 2.3 (cntd) Suggested value ranges for parameters typically incorporated in geomorphic processes and related functions used in LEMs.

PROCESS OR FUNCTION	PARAMETER, UNITS	POSSIBLE RANGE	TYPICAL EVALUATION METHOD AND COMMENTS
FLUVIAL TRANSPORT:			
Generalised type of representation (e.g. eqs 2.64 and 2.65)	First discharge exponent	0.3 – 2.0	Care is needed, as the values are all to some extent correlated with each other. Thus, a high value for the excess shear exponent is often matched by lower values for the second discharge and slope exponents. Usually the values selected will all be hypothesised, sometimes based on values used by other authors in published work, or otherwise set by researchers as thought appropriate for their study.
	Second discharge exponent	0.3 – 2.0	
	Slope exponent	0.5 – 3.0	
	Excess shear exponent	1.0 – 3.0	
Bedrock erosion (e.g. eqs 2.35 or 2.49)	Discharge exponent	0.2 – 2.0	As above, care is needed, as the values are all to some extent correlated with each other. Thus, a high value for the excess shear exponent is often matched by lower values for the discharge and slope exponents. Usually the values selected will all be hypothesised, sometimes based on values used by other authors in published work, or otherwise set by researchers as thought appropriate for their study.
	Slope exponent	0.2 – 3.0	
	Excess shear exponent	1.0 – 3.0	
OTHER FUNCTIONS:			
Flow depth vs discharge (similar to eq. 2.62), can be used with shear stress fluvial equations (eqs 2.47-2.50)	Coefficient (for units, see comments)	0.2 – 0.75	Based on well known, downstream hydraulic geometry data (e.g. reviews in Leopold, Wolman and Miller, 1964; Knighton, 1998), but may be set arbitrarily for the purposes of a particular study. Units for the coefficient depend upon the value of the exponent, thus for a mid range exponent value of 0.333, units are $s^{0.333}$.
	Discharge exponent	0.25 – 0.5	
Channel initiation and extension rules (eqs 2.70, 2.73 and 2.74)	Slope exponent	0.2 – 2.0	May be based on published data, but more likely to be found from study site observations, with or without model calibration.
	Threshold area, m2	$2 – 20 \times 10^3$	
Channel width vs discharge (eq. 2.69), used with fluvial channel processes	Coefficient (for units, see comments)	1.5 – 6.0	Based on well known, downstream hydraulic geometry data (e.g. reviews in Leopold, Wolman and Miller, 1964; Knighton, 1998), but may be set arbitrarily for the purposes of a particular study. Units for the coefficient depend upon the value of the exponent, thus for a mid range exponent value of 0.5, units are $m^{-0.5} s^{0.5}$.
	Discharge exponent	0.35 – 0.60	
Hydrological soil or bedrock properties, to model soil through-flow or losses to groundwater	Transmissivity, m3 yr-1 (cell width)-1	$1 - 100 \times 10^4$	May be based on published data or set arbitrarily to a value that seems suitable for the study.
	Drainage constant, yr-1	$1 – 500 \times 10^{-3}$	

The table summarises process parameter value information from a wide range of sources, and in particular from all of the model study papers cited in Tables 1 and 2.1, and from various papers and texts including *inter alia* Carson and Kirkby (1972), Duijsings (1987), Kirkby (1971 and 1989), Embleton and Thornes (1979), Gomez and Church (1989), Knighton (1998), Leopold, Wolman and Miller (1964), Martin (2000), McKean *et al.* (1993), Montgomery and Dietrich (1988 and 1989), Morris and Williams (1999), Prosser and Rustomji (2000), Roering *et al.* (1999), Saunders and Young (1983), Scheidegger (1970), Selby (1993), Summerfield (1991), Trudgill and Wise (1997), Van Asch *et al.* (1989), Young and Saunders (1986) and Young (1972 and 1978). It should also be noted that the values listed in Table 2.3 are limited to those parameters incorporated in the more commonly used geomorphic process equations, and the relevant equation numbers from the reviews in sections 2.4, 2.5 and 2.6 are provided to facilitate cross-reference.

Regarding the parameter value ranges in Table 2.3, as summarised from the sources cited above, these represent possible values over a wide variety of climatic and landscape settings. It will be appreciated therefore that for a specific landscape evolution study, in a certain climatic and geological setting, the actual range will probably be rather less than that listed in the table. For these more focused studies, the review indicates that parameter value ranges are nearly always within one order of magnitude, and for most parameters within ± 50% of the selected base value.

A separate comment is required concerning fluvial transport and bedrock erosion rate coefficients and thresholds (for example, see equations 2.45-2.50, and 2.64-2.66), as values for these parameters have not been listed. The reason is these parameters' values are usually selected after model calibration. Since there are many different forms of fluvial transport and erosion equation, as explained in section 2.6, any values found by calibration will depend upon both the equation used and the exponent values selected. This makes it difficult to derive much meaning from direct comparisons between values used for the fluvial coefficient and threshold terms in the different modelling studies. An equivalent problem also applies to the thresholds and coefficients used in the various bedrock erosion equations. Notwithstanding this point, the review indicates that whatever form of equation is used, the likely range of parameter value for a particular study and climate setting will be similar to those for the other parameters, that is, within one order of magnitude, and probably rather less than this for most purposes.

These deficiencies aside, the values listed in Table 2.3 give a sense of the permissible range for each parameter, within which the (smaller) range appropriate for a particular study is likely to lie. Although there is little to add regarding the values listed, with so many parameters in even one of the simpler LEMs, and with the ranges of possible value, there is clearly a large parameter space to consider in any set of simulations. Moreover, even supposing that the acceptable ranges for each parameter are constrained to, say, ±50 % of each base case value, this is still a large region. There are therefore many decisions for a researcher to make regarding parameter values and how this region should be explored. It will also be clearly appreciated that parameter dimensionality further increases the parameter space, and the two elements, value uncertainty and dimensionality, together present a formidable challenge if a thorough exploration of the parameter space is to be attempted. How this might be done, and the implications for understanding LEM output more generally, are considered in Chapter 3.

[I] To derive equations of the form of equations 2.64 and 2.65, based on a shear stress transport equation similar to equations 2.35, 2.48-49 or 2.58.

Presuming a form similar to equation 2.58, and using equation 2.36, the transport equation can be recast as:

$$q_{sb} = k_4\left(\gamma RS - \gamma\left[RS\right]_c\right)^p = \gamma^p k_4\left(RS - \left[RS\right]_c\right)^p \qquad \text{I\_1}$$

Also, combining equations 2.59 and 2.60, the hydraulic radius may be found from

$$R = \left(nQw^{-1}S^{-1/2}\right)^{3/5} \qquad \text{I\_2}$$

An equivalent relationship can also be derived based on substitutions using equations 2.59 and 2.61.

Using equation I_2 in this instance for R in equation I_1 gives

$$q_{sb} = \gamma^p k_4\left(\left[nQw^{-1}S^{-0.5}\right]^{0.6} S - \Phi_c\right)^p \qquad \text{I\_3}$$

where Φ_c now represents the threshold for transport. Further terms for Q may be required outside the main bracket, depending upon the original form of the shear stress equation, and other substitutions for the width can then be made using width-area (eq. 2.63) or width-discharge (eq. 2.62) relationships. Similarly, Q itself can be replaced if desired with a contributing area term, A, for example by using the applied run off multiplied by the upslope area. Equations 2.64 and 2.65 can also be derived more directly i.e. without the above intervening steps, using empirical depth-discharge and depth-area relationships, similar to equations 2.62 and 2.63.

CHAPTER 3: METHODOLOGY – GENERAL APPROACH TO QUANTIFICATION AND PARAMETER SAMPLING

3.1 INTRODUCTION

Having established the parameter spaces typical of LEMs, and with this the apparent likelihood of LEMs to generate equifinal output, attention can now be shifted to the methodological issues entailed in quantifying model equifinality. At first glance, the basic requirement is for a thorough sampling of the parameter space, from which the proportion of simulations converging on a reference result - or selection of such results - can be calculated. Closer inspection shows that this is far from straightforward, however, as there are considerable practical limitations, discussed below, on how the research can be conducted. The first objective in this chapter is to outline these limitations and possible techniques for dealing with them. A preferred methodology is then adopted, and two following sections of the chapter cover further aspects of the methodology and related experiment design issues.

The focus is then turned to the choice of LEM to be used in the research, and a description of its main functions and capabilities is provided. The LEM also needs to be initialised, and set up for simulation work, so there is a section dealing with the chosen landscape setting, the parameters selected for use in the research, and the value ranges for those parameters. Finally, the details of the experiment design used in the initial sampling are explained. The chapter is therefore structured broadly as follows:

- overview of parameter space sampling issues and possible methods, and choice and description of the methodology to be used in this research;
- sampling and other experiment design issues related to the chosen methodology;
- choice and description of the LEM selected for the research;
- description of the chosen study landscape, and selection of parameters and their values; and
- description of the experiment design used for the initial parameter space sampling.

In addition to the above, supporting information relating to parameter values and the initial experiment design is given in Appendices B-E. The first step is to consider the choice of the methodology and its conceptual basis, and this now follows.

3.2 PARAMETER SPACE SAMPLING ISSUES, AND CHOICE OF METHODOLOGY AND ITS CONCEPTUAL BASIS

3.2.1 Parameter spaces, simulations and experiment run sizes

Any method designed to quantify the degree of model equifinality in essence involves undertaking multiple model simulations using different parameter value combinations, and thence establishing how many simulation results are equifinal to the output measures of interest. In the simplest terms, it is a matter of proportions, and can be expressed by:

$$Eq(y) = \frac{N_{eq.}}{N_t}, \qquad 3.01$$

where $Eq(y)$ is the proportion of equifinal solutions for the output measure y, $N_{eq.}$ is the number of simulations yielding equifinal solutions, and N_t is the total number of simulations run in the sample of the parameter space. It will be appreciated from equation 3.01 that the accuracy and the precision of the estimate of equifinality, $Eq(y)$, cannot be absolute, but will depend upon the rigour and density of the parameter space sampling.

The parameter space typical of any LEM, as reviewed in Chapter 2, therefore poses immediate practical problems to any researcher wishing to explore that parameter space. Firstly, each individual LEM simulation takes some time to complete, even on fast, modern PC's and computing clusters (typically from hours to days, or even weeks, for each simulation; Greg Tucker, 2002, and Joe Wheaton, 2006, personal communications). Secondly, to sample the parameter space rigorously, the number of parameters, and the number of values of interest for each, together generate a large number of possible combinations required in the simulations. Table 3.1 shows examples of the number of simulations needed to sample a parameter space of k dimensions at N value points per parameter. The total run size required by each combination is N^k simulations, and although the smaller run sizes may be completed in a reasonable time (compared with the usual time span of a PhD or similar project), if many computers are allocated to the task, it is clear that the larger run sizes require an infeasible number of LEM simulations given usual computing resources.

Table 3.1: Total simulation run sizes required to sample all combinations of *k* parameters sampled at *N* values for each. The shaded area denotes the run sizes required of a typical LEM on this basis, according to the parameter requirements listed in Table 2.2 (*q.v.*).

	Number of parameters, *k*:			
	5	**10**	**15**	**20**
Number of values used for each parameter, *N*:	**Total run size**			
2	32	1,024	32,768	1,048,576
3	243	59,049	14,348,907	*c.* 3.49×10^{9}
5	3,125	9,765,625	*c.* 3.05×10^{10}	*c.* 9.54×10^{13}
8	32,768	*c.* 1.07×10^{9}	*c.* 3.52×10^{13}	*c.* 1.15×10^{18}

Faced with these numbers, a researcher must employ methodologies that minimise the number of simulations required, while still retaining parameter space sampling that is dense enough to produce representative results for the whole parameter space. After an initial appraisal of possibilities, the author considered in detail two possible methods, 'GLUE' (Beven and Binley, 1992), and the use of a mediating function or 'metamodel' (e.g. Kleijnen, 1998; Law and Kelton, 1991;).

Regarding 'GLUE', this is the acronym for 'Generalised Likelihood Uncertainty Estimation', which has been developed as a method for calibrating numerical models that include many parameters (e.g. Beven and Binley, 1992; Beven, 1996; Beven and Freer, 2001; Beven, 2006). The method takes into account both parameter value and observation data uncertainties, and after many simulations provides an estimation of the likelihood that any particular set of parameter values provides a 'behavioural' calibration for the output measures of interest (*ibid.*). It has been applied mainly to problems in hydrology, where it has been observed that many different parameter value combinations can generate very similar output, thus demonstrating a high degree of model equifinality (*ibid.*). The random sampling of the parameter space used in GLUE, and the identification of parameter values more likely to generate certain solutions than others, suggested that an adaptation of a GLUE method for this research might be appropriate. However, it still requires a very large number of simulations with the LEM, probably 10^5 or more for a modest LEM parameter space of between 7 to 10 parameters (e.g. Beven and Freer, 2001). The problem of large run sizes would therefore not be solved by using GLUE, and accordingly, the method was not adopted for the research herein.

The use of a mediating function, also called a 'metamodel' (further explained in subsection 3.2.2 and section 3.3), which could act as a surrogate model for the full LEM simulations, is a well established method in engineering and operations research (e.g. Kleijnen, 1998;

Sanchez, 2006). Through the use of a suitable experiment design, the parameter space is first sampled sparsely and output measures from the simulations are obtained. By regression analysis, these measures may be then expressed as mathematical functions of the parameter values (*ibid.*). The method therefore provides an equation that can be solved as a single calculation, using a spreadsheet or other software, for any point in the parameter space within the designated parameter value limits. The equation may therefore be used to sample the parameter space as densely as required, generating a prediction of the LEM's output at each sample point. Provided the equation is sufficiently accurate (as indicated by R^2 and other regression statistics), the proportion of results equifinal for the measure of interest can then be calculated (equation 3.01, *q.v.*), thus providing a quantified estimate of the LEM's equifinality for that measure.

Although this method still requires a large number of simulations to be run in order to provide the data from which the equations are derived, the total is still two or more orders of magnitude fewer than would be required if using a GLUE or similar procedure (e.g. Beven and Freer, 2001). A potential disadvantage is that the LEM output may be noisy or in some way erratic, so that it is not possible to derive equations which are accurate enough to be useful. Also, for different measures of output, and different output reference times, other equations have to be derived through more regression analyses, which entails further work. Despite these disadvantages, however, the success of the method in other fields (e.g. Kleijnen *et al.*, 2005) suggested its adoption was appropriate for conducting the research herein. A detailed explanation of the concept underlying the 'metamodel' methodology now follows.

3.2.2 The 'metamodel' concept

A simulation model may be likened to a complex function, which transforms the input data into a set of outputs (e.g. Law and Kelton, 1991; Kleijnen, 1998). However, in the case of a complex, discretised, numerical model, such as a LEM, the exact mathematical representation of this function is not known (*ibid.*). Despite this, LEM outputs can be related to the inputs, including the parameter values, by which they have been generated. Specifically, at any particular reference time, the outputs can be summarised using a range of measures, here termed 'metrics', which may serve as descriptors of the simulated landscape. If the relationships between the parameter values and the (output) metrics are consistent, then it is possible to derive regression equations which quantify them.

Moreover, if these regression relationships are sufficiently accurate, then they may be used to predict the LEM's output, as expressed by the metrics, in terms of any parameter value combination within the parameter space of interest. A regression equation of this type is called a *metamodel*, as it can be used as a substitute or proxy for the full simulation with the numerical model (e.g. Kleijnen, 1998). Such tools have been widely applied in some branches of engineering and science (e.g. Kleijnen, 1998; Chen *et al.*, 2006; Sanchez, 2006) but there are very few examples of their use in the earth sciences[1], and none in geomorphology. Their key advantage is that they allow many possible model scenarios to be explored very quickly. In this research, therefore, solving the metamodel for any parameter value combination involves a single, rapid calculation, thus enabling the LEM's parameter space to be sampled very densely (*c.* 10^6 times), and certainly much more densely than would be practical if relying on full simulations. In summary, the overall concept of the research methodology is presented in Figure 3.1. It should be noted here that for clarity, and to distinguish it from other regression equations or models referred to in the thesis, the term 'metamodel' is used from hereon to mean a regression equation of the type described above i.e. an equation derived from numerical model output, with the aim that it should be used as a proxy for simulations with the full model.

[1] It is very difficult to be sure on this point, as the description of the types of model used in the literature makes metamodel approaches in the earth sciences very difficult to distinguish from the use of any other type of model, whether it be statistical, numerical, mathematical, a regression model fitted to field data, and so on. There does, however, appear to have been some interest in the use of metamodels in climatology and oceanography (e.g. Chapman *et al.*, 1994; Lynch *et al.*, 2001; Beringer *et al.*, 2002; Sexton *et al.*, 2003), and quite possibly the technique will be increasingly used in other disciplines as it becomes more widely known.

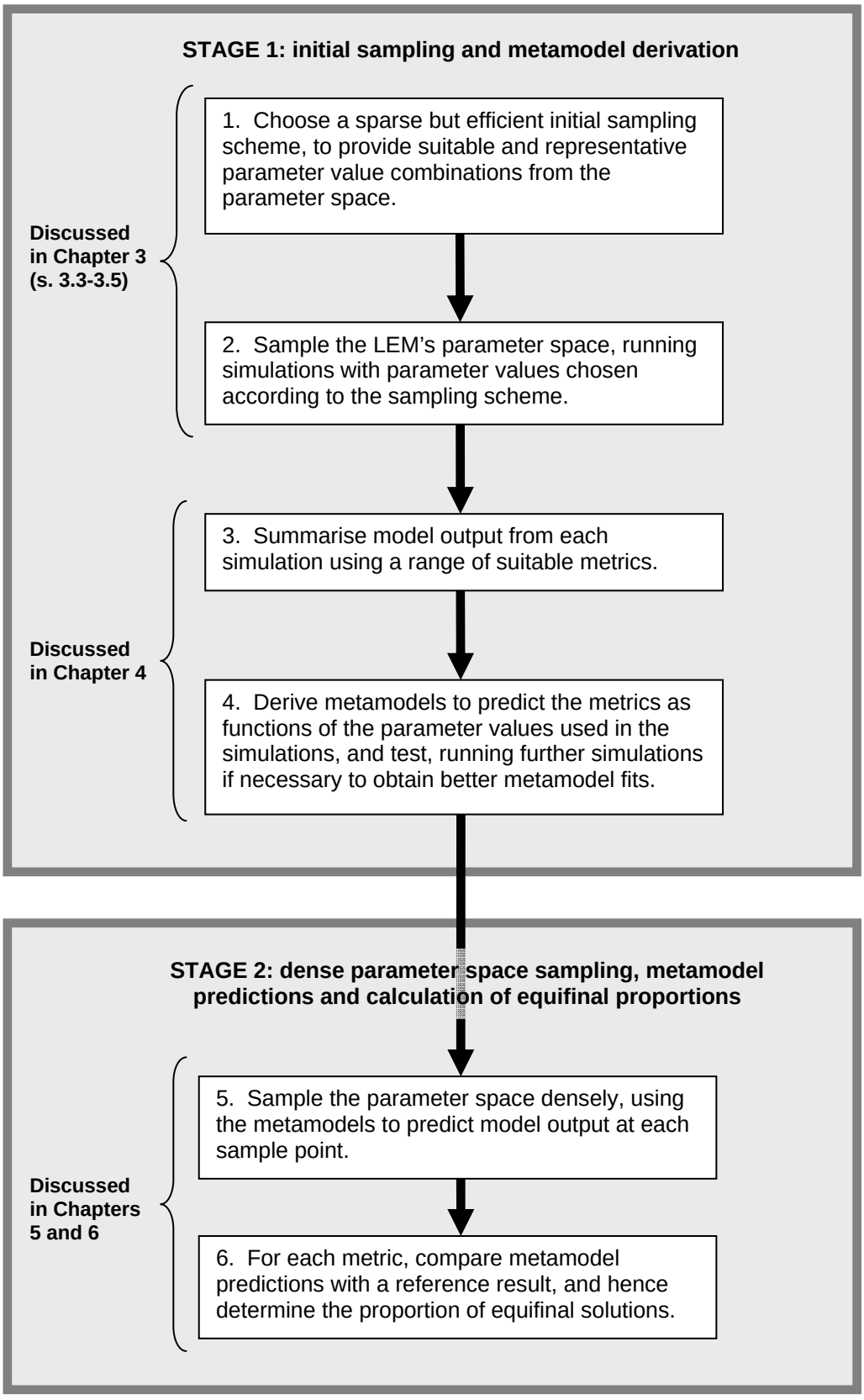

Figure 3.1: The metamodelling methodology, summarised as steps within a two stage process, and also showing the order of their discussion within the thesis. Step 5 generates large numbers (*c.* 10^6) of proxy solutions, which can be used to calculate equifinality.

Figure 3.1 shows that metamodel methodology is essentially a two stage sampling procedure. The first stage employs a sparse sampling of the parameter space and a limited number of simulations, from which the output can be used to derive the metamodels. Once these have been developed, they may be tested, by running additional test simulations, and improved if necessary, running further simulations as required. The metamodels may then be used to emulate the LEM, thus providing the basis for the second stage of the parameter space sampling. As explained above, predicted LEM output from very large sample sizes (*c.* 10^6 points) may then be obtained quickly from across the whole parameter space.
By this methodology, therefore, the problem of quantifying model equifinality may be treated in a different way, namely by focusing on how many simulations are required to derive accurate metamodels of the LEM's output. In particular, the initial sampling scheme must be efficient, so that it still adequately represents the parameter space even though there are only a limited number of initial sample points. In addition, the output metrics must be selected with care, and be appropriate for the landscape features and properties of interest. Finally, the derivation of the metamodels must be robust, and the method of their application in the second stage of sampling statistically rigorous. The first two steps, covering sampling and experiment design issues and setting up the LEM for the simulations, are considered in detail in this chapter, beginning with some comments on basic concepts and terminology. These are dealt with in some detail, as particular aspects turn out to be of great importance in the research more generally.

3.3 SAMPLING AND EXPERIMENT DESIGNS

3.3.1 Basic concepts

The choice of a suitable sampling scheme is a problem common to many enquiries in science and engineering, including modelling studies, and the design requirements are often satisfied using response surface methodology (explained below) or similar techniques, for which there is now a large standard literature (e.g. Box *et al.*, 1978; Box and Draper, 1987; Kleijnen, 1998; Law and Kelton, 1991; Vose, 1996; Wu and Hamada, 2000). The review of terminology and the related points here are therefore drawn from these references.

Responses, factors and sample points

In any experiment, whether the experimental unit is a real system or a model thereof, output (the *response*) is obtained under a particular set of conditions (a *run*). The response may be expressed in terms of different measures or 'metrics' (e.g. drainage density, sediment yield). The experiment, however, should identify whether variables changed during the run - the *factors* - have any effect on the response. In this context, the input parameters in a numerical simulation are equivalent to the factors changed in any experiment. Likewise, the parameter values used are equivalent to the *levels* of those factors. The concept of factor levels is crucial in experiment design (e.g. Box *et al.*, 1978; Wu and Hamada, 2000) and will be returned to in more detail in subsections 3.3.4 to 3.3.6. In this thesis, the term *parameter case* is used to mean any combination of parameter levels (or values) used in running a full simulation or in making a prediction with a metamodel[2].

Where two or more parameters' levels are varied, the particular combination of levels can be represented as a single point, called a *design* or *sample* point. The point can be thought of as being located at the end of a vector in the model's parameter space, the opposite end being at the origin, which represents all the central (base case) parameter levels. Where the model has two or three parameters only, the parameter space can be drawn as an area or volume, and the position of the design point is not difficult to visualise. As LEMs typically have twenty or more process parameters (Table 2.2 *q.v.*), their parameter spaces are hyper-dimensional, but the concept of a design or sample point still applies.

The use of appropriate combinations of design levels should therefore not only demonstrate which parameters are influencing the response, but also allow those influences to be quantified, including their strength, and any characteristic trend or form in the relationship between the response and the parameter values. (e.g. Box *et al.*, 1978; Box and Draper, 1987; Wu and Hamada, 2000). Quantifiable influences of this kind, which are generally related to a particular reference time, are usually called *effects*, and should be distinguished carefully from the wider, more usual use of the term 'effect' in geomorphology. Strictly speaking, in the sense used herein, quantified effects of geomorphological variables are not therefore identifiable if a simulation experiment uses only one value for that variable. The

[2] The author finds it helpful here to distinguish between parameter *cases* and parameter *sets*. Thus, two different LEMs will require different parameter *sets*, these comprising the coefficients, exponents and so on used in the different models; similarly, the same LEM may be applied using different parameter sets if the LEM permits alternative formulations to be used to implement the same process. By contrast, a parameter *case* is the combination of values used for the parameters within a particular set. By changing the parameter case, therefore, it is only the parameter values which are changed, rather than the parameters themselves.

point is considered again, in the discussion in Chapter 7, where the wider implications of this research are considered. The concepts applicable to quantified effects, in the manner being considered here, are explained next.

Main effects and interaction effects

If a parameter (or factor) has an influence which is clearly discernible in the response (i.e. it can be isolated from the influences of the other parameters or factors), then it is said to have a *main effect* (e.g. Box *et al.*, 1978; Law and Kelton, 1991; Wu and Hamada, 2000). Accordingly, in a LEM, to estimate whether a parameter has a linear main effect, at least two design points are required, with the parameter at one level in the first simulation, and at another level in the second (*ibid.*). To estimate effects which are non-linear, including those demonstrating curvature, more levels need to be used for each parameter, and the parameter space must be sampled with more design points (*ibid.*). It follows that although it is generally assumed that main effects are continuous i.e. with no break or sudden jump in the response as the parameter values are changed across the range of interest, additional sampling may be required to identify irregular and non-continuous effects.

If the size of the main effect of one parameter is increased or reduced by changing the levels of another, the two factors are said to have an *interactive effect*, or more simply an *interaction* (e.g. Box *et al.*, 1978; Law and Kelton, 1991). Where the interaction involves two factors only, this is called a *two-way* or *two-factor* interaction; likewise, a *higher-way* interaction may involve three factors or more. As with main effects, interactions may also be linear, curvilinear, or discontinuous.

One way to visualise the way in which two parameters affect a model's response is to plot the response as a surface. The resulting surface is called a *response surface*, and methods which exploit properties of the surface form the basis of *response surface methodology* ('RSM') (e.g. Box and Draper, 1987). Figure 3.2 shows an example of a 2-D response surface.

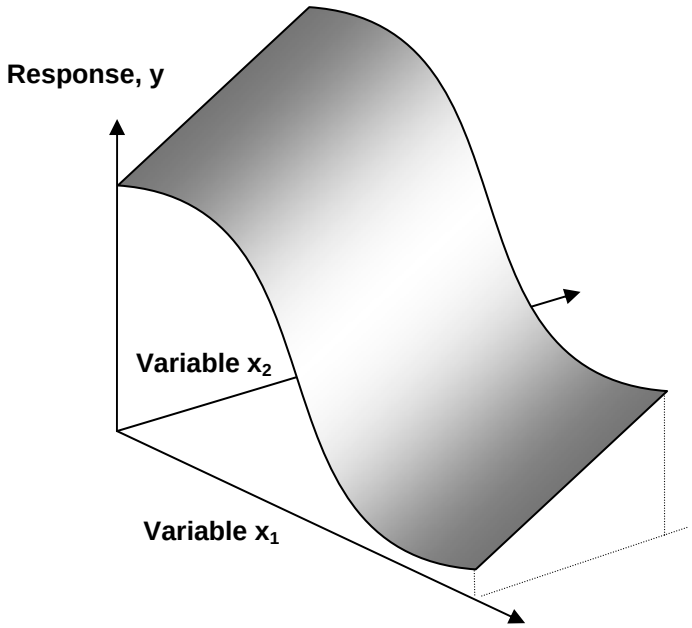

Figure 3.2: Example of a 2-D response surface, formed by the response, y, plotted against two variables, x_1 and x_2. (Arbitrary scales throughout)

Figure 3.2 shows a smooth, curved response surface, but responses may be more complicated than this, with steps and irregular features. A response surface also need not be confined to two variables or factors, but may exist in many dimensions mathematically, even though it is not possible to plot or visualise simply.

RSM has been widely applied in optimisation studies, where attention is focused on finding a region of the response surface with useful properties (e.g. Box and Draper, 1987; Wu and Hamada, 2000). However, it can also be used to obtain a better understanding of a system generally, and this may be achieved by spreading the sample points more widely, including to the intended limits of the parameter space. In these circumstances, and through the use of a *response surface model*, prediction of the response across the full (unsampled) parameter space may be based on interpolation of the response surface between the sampled points. Consequently, as more points are sampled, a more complete impression of the response surface is acquired.

In deriving a response surface model, the analysis will usually reveal a number of main effects and interactions which appear to be important, although some will be more statistically significant than others. If a researcher wishes to derive a parsimonious model demonstrating a good fit to the data, as evidenced by a high target R^2 score for example, there may be difficulties in deciding between main or interaction effect terms of broadly the

same significance. To simplify the choices, Wu and Hamada (2000) list three general principles to follow, listed below:

- **Hierarchical Ordering.** This principle comprises two elements, namely that (i) lower order effects are more likely to be important than higher order effects, and (ii) effects of the same order are equally likely to be important. For example, a linear term in a response surface model is to be preferred over a quadric or cubic term if the explanatory powers of each appear to be broadly the same; similarly, widely applied functions, such as logarithms or exponentials, are preferred to long and complex polynomials.
- **Effect sparsity.** This principle states that the variation exhibited in the data is primarily attributable to fewer of the effects, and therefore to fewer of the factors, rather than to all of them. This conforms with the idea of parsimony, or "Ockham's razor"[3].
- **Effect heredity.** This principle states that before including an interaction effect in a model, at least one of its contributing factors should demonstrate a significant main effect. Wu and Hamada (2000) comment that this is primarily useful in the model building phase of a study, as it provides a consistent reason for eliminating many of the possible two-factor and higher-way interactions from the analysis.

Taking these principles together, initial sampling should therefore give priority to estimation of main effects, two-factor and lower-way interactions, and to linear trends or simple curvature in either. Having covered these basic points and principles, specific methods of sampling are now reviewed.

3.3.2 Monte Carlo and Latin Hypercube sampling schemes

Monte Carlo methods

There is now an extensive literature on Monte Carlo methods, with useful introductions provided by Kalos and Whitlock (1986), Madras (2002) and Fishman (1996), among others. Kalos and Whitlock (1986, page 2) define it as any method "... that involves deliberate use of random numbers in a calculation that has the structure of a stochastic process", so the

[3] Also spelt 'Occam' in some texts, and named after the English Franciscan monk, William of Ockham (1285-1349), Ockham's razor is expressed as 'Entities are not to be multiplied beyond necessity' (Flew, 1983). The statement is more widely interpreted to mean that in any choice between two or more competing theories or models, of equivalent validity, the simplest is to be preferred. The principle of simplicity is both practical and philosophical, but should not be applied rigidly (e.g. Popper, 1969; Haines-Young and Petch, 1986; Baker, 1996). Interestingly, a statement of Ockham's razor itself is not found in any of William of Ockham's surviving works (Flew, 1983).

random element forms a key component of the sampling. Where the sampling is wholly random, each design point bears no predictable relation to any other, and hence sampling is not influenced by the researcher's own bias or preferences. It can therefore be argued (e.g. Iman and Helton, 1988) that Monte Carlo sampling offers more opportunity than regular designs to make surprising or challenging discoveries. This may be particularly valuable in risk analysis or similar studies (e.g. Fishman, 1996; Vose, 2000), but the method is not without difficulties. In particular, the random nature of the sampling means that some points may be clustered very close to each other in the parameter space, whilst other parts of the parameter space are sparsely sampled by comparison. If the most useful and important region turns out to be the latter, then additional sampling may be required there, whereas the denser sampling elsewhere may turn out to have been unnecessary. Latin Hypercube sampling is devised to overcome these difficulties, and is explained next.

Latin Hypercube sampling

As described previously, if a model parameter space of k parameters is to be explored, using N levels per parameter, then an experiment of all the intended parameter cases requires N^k simulations (Table 3.1 *q.v.*). The basis of Latin Hypercube ('LH') sampling is to divide each parameter into N intervals (usually according to a probability distribution of each parameter's values), and the parameter space into N^k hyper-dimensional boxes (*hypercubes*) or sample point locations (e.g. Vose, 2000; Iman and Helton, 1988). A sampling generator is used to select at random a parameter case from some point inside one of these hypercubes, or one more simply one of the designed sample points. This is used with a sampling memory, which ensures that new cases do not repeat too closely those already selected. The procedure is repeated until enough parameter cases have been chosen to make up the desired sample size. The problem of under-sampling in certain areas of the parameter space may also be solved by checking for correlation between sample points across the parameter space (for a wider discussion of this approach, see Iman and Helton, 1988; Helton and Davis, 2003; Sanchez, 2006). These techniques together generally mean that LH samples are only a tenth or so the size of those using wholly random sampling (e.g. Vose, 2000; Sanchez, 2006). However, there is still the risk that certain areas of the parameter space will be under-sampled, necessitating additional, more targeted runs later. In addition, the parameter space limits may not be explored thoroughly without deliberately positioning sample points at or near these locations, which rather obviates the random

element in the method. As alternatives to this approach, factorial, fractional factorial and central composite designs may be used to sample the parameter space limits from the outset, and these types of design are now considered.

3.3.3 Factorial, fractional factorial and central composite designs

Factorial designs

The N^k design introduced previously (Table 3.1) is an example of a *full factorial design*. Such a design allows detection of all the main effects and higher factor interactions of the k parameters, with curvature estimation of polynomials to the order of N-1 (Box and Draper, 1987; Wu and Hamada, 2000). However, by the hierarchical ordering principle, higher order effects are less likely to be important, so it is common for the sample size to be reduced by looking for linear effects only, using just 2 levels for each parameter, and thus requiring a 2^k factorial design. From the standard literature, nearly all of the regular experiment designs used in preliminary investigations are variants of the 2^k factorial type, and the standard texts include details of numerous case studies in engineering and science employing such designs (Box *et al.*, 1987; Box and Draper, 1978; Law and Kelton, 1991; Kleijnen, 1998; Wu and Hamada, 2000). Although curvature estimation is not possible using a 2^k factorial design, linear main effects and interactions may still be identified, thus providing a good first approximation of a system's response in many investigations (*ibid.*) A factorial design is usually laid out in a *design matrix*, in which the factor levels are shown by plus or minus signs rather than by their actual values, the latter usually listed in the *planning matrix*. In the design matrix, a '+' denotes the higher parameter level and a '-' the lower. Table 3.2 shows an example design matrix of a factorial design of three factors.

Table 3.2: Design matrix of a 2^3 factorial design

	Parameter number and design level		
Parameter case number	**1**	**2**	**3**
1	+	+	+
2	-	+	+
3	+	-	+
4	-	-	+
5	+	+	-
6	-	+	-
7	+	-	-
8	-	-	-

If it is necessary to estimate response curvature, then more design levels are needed, although generally it is unusual for full factorial designs to include more than 3 levels per factor, in a 3^k design (e.g. Wu and Hamada, 2000). This aside, it can be seen that full factorial designs follow a regular pattern, the '+' and '-' signs alternating down each column in a predictable way. However, they also have disadvantages, in particular it may still not be possible to run all the parameter cases, and designs in only two or three levels may not allow steps or jumps in the response to be detected (e.g. Iman and Helton, 1988). Moreover, if many higher-way interaction effects turn out to be negligible, in accordance with the effect heredity principle, some simulations will not have been needed. Fractional factorials may help to deal with this problem, and are reviewed next.

Fractional factorial designs

By convention (e.g. Box and Draper, 1987; Law and Kelton, 1991; Wu and Hamada, 2000), main effects and interactions are usually denoted using the number labels for each factor. Therefore, the 2^3 design of Table 3.2 allows detection of all three main effects - **1**, **2** and **3** - and of their two-factor interactions, **12**, **13** and **23**, and of the three-factor interaction, **123** (e.g. Law and Kelton, 1991; Wu and Hamada, 2000). Equivalent properties are found in experiments with more factors so that, for example, a full factorial experiment in five factors allows estimation of 10 three-factor interactions, 5 four-factor interactions and one five-factor interaction, **12345**. However, if the effects of the three-factor and higher-way interactions can reasonably be expected to be negligible, then a full factorial design is unnecessary, as some of the design matrix combinations are redundant. A fractional factorial allows simplification of the design without sacrificing the ability to estimate those lower-way interaction effects expected to be of interest. To illustrate how these designs are structured, Table 3.3 shows the design matrix of a 2^{5-1} fractional factorial experiment.

Table 3.3: Design matrix for a 2^{5-1} fractional factorial, using factors 1 to 4 to determine the design level of factor 5 in each parameter case.

	Parameter				
Parameter case number	**1**	**2**	**3**	**4**	**5**
1	+	+	+	+	+
2	-	+	+	+	-
3	+	-	+	+	-
4	-	-	+	+	+
5	+	+	-	+	-
6	-	+	-	+	+
7	+	-	-	+	+
8	-	-	-	+	-
9	+	+	+	-	-
10	-	+	+	-	+
11	+	-	+	-	+
12	-	-	+	-	-
13	+	+	-	-	+
14	-	+	-	-	-
15	+	-	-	-	-
16	-	-	-	-	+

In this design, the level of factor 5 in each parameter case is calculated from those used for the other four factors. This is achieved by multiplying the *signs* ascribed to the design levels of factors 1 to 4, treating each '+' as '+1', and each '-' as '-1'. The calculation is governed by a formula called a *design generator*, and is carried out row by row, working down the design matrix (Box and Draper, 1987; Wu and Hamada, 2000). In this example, the design generator for factor 5 is written as:

$$\mathbf{5}_i = \mathbf{1}_i \times \mathbf{2}_i \times \mathbf{3}_i \times \mathbf{4}_i \qquad 3.02$$

where $\mathbf{1}_i$ means the design matrix level of factor 1 in row i, $\mathbf{2}_i$ is the design matrix level of factor 2 in row i, and so on. By convention (e.g. Law and Kelton, 1991; Wu and Hamada, 2000), the labels and multiplication signs are omitted, so that 3.02 becomes:

$$\mathbf{5} = \mathbf{1234} \qquad 3.03$$

This design is called a *half-fraction*, as it requires only half the number of runs needed by the full factorial. Again, by convention, the number of factors determining the fraction is denoted by the symbol p, and the literature includes extensive tables of different 2^{k-p} fractional factorial designs (e.g. Box *et al.*, 1978; Box and Draper, 1987; Law and Kelton, 1991; Wu and Hamada, 2000).

Every fractional factorial has a certain *design resolution*, which determines how clearly the main effects and interactions can be estimated, and the standard texts explain what a researcher should expect from each 2^{k-p} design in this regard (*ibid.*). For example, equation 3.03 can be recast by multiplying each side of the equation by factor 5. By convention, any

factor multiplied by itself produces the identity factor, **I** (Wu and Hamada, 2000), so equation 3.03 can be restated as:

$$\mathbf{I = 12345} \qquad 3.04$$

This is called the design's *defining relation*. The above example has five factors' terms in it, so this is a *resolution five* design (*ibid.*). By convention, the resolution is indicated by a roman numeral, and so this example is therefore more formally labelled a 2^{5-1}_{V} fractional factorial (e.g. Box *et al*., 1978; Wu and Hamada, 2000). The resolution is important, as it indicates the degree to which 'aliasing' limits estimation of main effects and interactions. Aliasing is a complex problem, particularly if irregular or randomised designs are used, and some comment on it is needed here.

Aliasing, and 'clear' and 'strongly clear' effects

The number of simulations required in a fractional factorial experiment may be reduced by increasing the size of the fraction. For instance, a 2^{5-2} fractional factorial design would require only 8 runs, rather than the 16 required by the 2^{5-1} example shown above. However, the lower run size comes at the cost of a lower design resolution. In the 2^{5-2} example, some of the main effects and interactions are now indistinguishable from other main effects or interactions. This problem is called *aliasing* (e.g. Wu and Hamada, 2000) and it occurs in all fractional factorials. Thus, in any *resolution III* design, some of the main effects are aliased with two-factor interactions (e.g. Box and Draper, 1978; Law and Kelton, 1991; Wu and Hamada, 2000); likewise in any *resolution IV* design, some of the main effects are aliased with three-factor interactions, and some two-factor interactions are aliased with each other (*ibid.*). To summarise the main points, in a resolution IV design, all the main effects are *clear*, as no main effect is aliased with any other main effect. Similarly, in a resolution V design, all the main effects are *strongly clear*, because not only are they not aliased with each other, no main effect is aliased with any two-factor interaction. Likewise, the two-factor interactions in a resolution V design are all clear (Wu and Hamada, 2000), since they are only aliased with three-factor or higher-way interactions. Aliasing of three-factor interactions and above is not a problem if it can be assumed that the effect of such interactions is negligible (*ibid.*). In these circumstances, fractional factorials may be very efficient initial sampling designs, although there is still the problem of detecting curvature in main effects and interactions (e.g. Sanchez, 2006). A 3^{k-p} fractional factorial may provide

a way to include curvature estimation, but another class of design, called a *central composite design*, is likely to be much more efficient, as discussed next.

Central composite designs

The main features of central composite designs were first described in a landmark paper by Box and Wilson (1951), and are now covered in the standard statistics and experiment design literature (e.g. Box *et al.*, 1978; Box and Draper, 1987; Law and Kelton, 1991; Wu and Hamada, 2000). A geometrical conceptualisation of a three factor central composite design in two levels is shown in Figure 3.3.

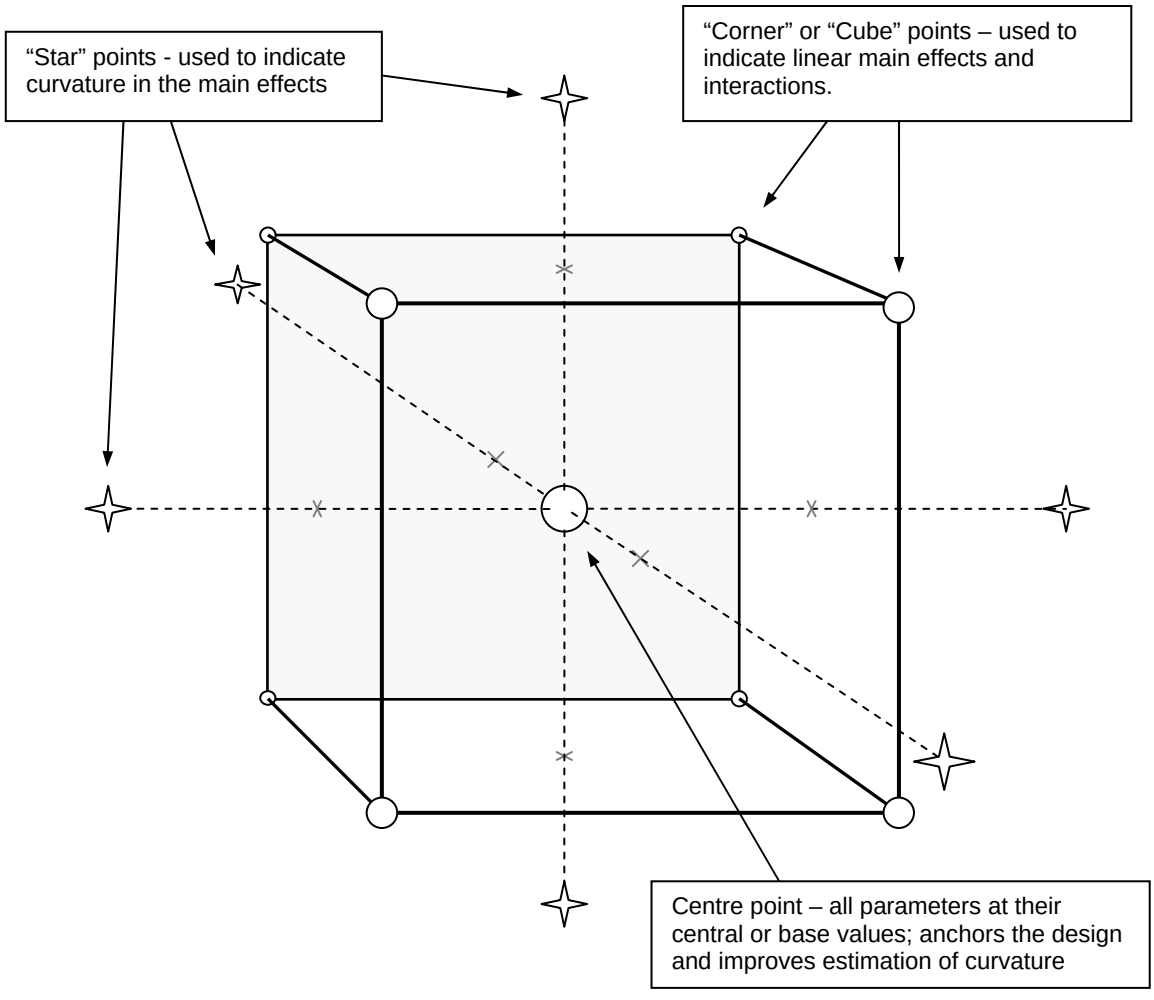

Figure 3.3: Diagram of a central composite design of three factors in two levels, showing star points, corner (or cube) points and the centre point (after Box and Wilson, 1951).

Figure 3.3 shows the three main components of central composite designs, namely:

- A centre point, representing the parameter case in which all the parameters are set at their central levels (base case values), usually denoted using a zero in the design matrix[4].
- A two-level, factorial or fractional factorial, of n_f design points, usually denoted by +1 and -1 in the design matrix. For two or three factor examples, these points may be visualised as being located respectively at the corners of a square or cube, giving them the names of *corner* or *cube* points. More generally, such points can be called *factorial* points, as they mark the limits of the factorial part of the design, or the *factorial space*.
- *Star* points, marking extreme upper and lower levels for each parameter. Each parameter has two such values, visualised as being located on lines passing through the centre point and extending some distance beyond the factorial space limits. Star point levels may be labelled nominally $+\alpha$ and $-\alpha$ in the design matrix, or denoted by their scale values (see equation 3.03 below), so as to distinguish them from the other design levels.
- A 2-level central composite design of this type allows estimation of linear and curved (quadratic) main effects and interactions (Box and Draper, 1987). Also, for economy of run size, most central composite designs incorporate a resolution V fractional factorial, which allows all two-factor interactions to be clearly estimated (*ibid.*).

The design levels are used to scale the values actually used in the experiment, and this is explained in more detail in Appendix E. Regarding the star points in particular, in design matrix terms, α should be greater than or equal to 1, but generally less than or equal to $\sqrt{k}$ (Wu and Hamada, 2000). If the design is fractionated, and in the absence of information to the contrary, the design level corresponding to α may be found from the Box and Hunter (1957) criterion, using:

$$\alpha = \sqrt[4]{n_f}, \qquad 3.05$$

and this value is used in scaling the actual values corresponding to the star points that should be used in the simulations.

In summary, a central composite design has advantages over factorial designs by using a fractional factorial, which gives economy of run size, and star points and a centre point,

[4] To stabilise estimation of variance, replication of runs at the centre point is recommended where the output is likely to vary with each run, for example where a model is being used stochastically (e.g. Box and Draper, 1987). Otherwise, only one run is needed using the centre point (*ibid.*).

which allow simple main effect and interaction curvature to be estimated[5]. As disadvantages, the response surface across the factorial space needs to be broadly smooth and continuous. In this respect, irregularities and step features may be better detected using Monte Carlo or Latin Hypercube sampling, although much will still depend upon where the sample points are placed.

Having reviewed the main sampling methods of interest, it is now possible to assess which is the most useful for the research purpose herein.

3.3.4 CHOICE OF SAMPLING METHOD

In making a final choice of which sampling method to use, Monte Carlo and full factorial designs were quickly excluded. Both methods were considered too computationally expensive given the large number of parameters potentially of interest in this study. This left Latin Hypercube, fractional factorial and central composite designs as possible sampling methods. The discussion here therefore concentrates on these methods, and their advantages and disadvantages are summarised in Table 3.4.

[5] It is interesting to note here that no examples of the use of central composite designs were found in the geomorphological literature, nor were any found in a wider search, encompassing some 35 journals from geology, geophysics, hydrology and the oceanographic and atmospheric sciences. By contrast, a search of the scientific literature generally yielded over 900 references, mainly in journals from chemistry, biology, medicine, electronics, engineering and related disciplines. Similarly, the author found no references to the use of factorial or fractional factorial designs in geomorphology, and very few examples from the geosciences more generally, compared with *c.* five thousand examples from the wider science literature, again many from engineering, biology, medicine, operational research and related disciplines.

Table 3.4: Summary of Latin hypercube, fractional factorial and central composite design sampling methods, with an assessment of their suitability for this study. *k* refers to the total number of parameters and *p* to the number included in any fraction (subsection 3.3.3 *q.v.*)

Sampling method	Number of factor levels	Number of simulations	Advantages	Disadvantages	Assessment for the purposes of this study
Latin hypercube	2 or more, randomised	Usually > 10*k*	- Run size sometimes more economical than when using fractional factorial or central composite designs - Randomised, so may show unforeseen results and discontinuities - Larger samples may allow estimation of curvature	- Complicated to execute (needs checks for sample point correlation) - Must be used incrementally, to check thoroughness of sampling - Additional sampling may be necessary, defeating initial run size economy - Need for additional sampling also implies some redundancy in the initial sample	- Initial detection of discontinuities is unnecessary, as metamodels will be tested anyway - Interim analysis, and possible additional sampling, demand both resources and time
2^{k-p} fractional factorial design	2, fixed	2^{k-p}	- Economy of run size - Ease of calculating the sample points - Resolution IV designs allow clear estimation of all linear main effects - High fractions useful in screening designs	- Cannot show curvature or discontinuities in main effects and interactions - Some redundancy inevitable	- *A priori* reasoning of GOLEM's response suggests that curvature in main effects should be expected - No interim analysis, so less resource and time demands than Latin hypercube
3^{k-p} fractional factorial design	3, fixed	3^{k-p}	- Ease of calculating the sample points - Suitable resolution allows estimation of curvature in both main effects and interactions	- Large run size compared with 2^{k-p} designs - Cannot show discontinuities - Some redundancy inevitable - Care needed to deal with complex aliasing	- *A priori* reasoning suggests curvature detection in main effects is useful - No interim analysis or sampling, so less time demanding than Latin hypercube - Run size likely to include more redundancy than all of the other methods considered here
Central Composite design	2, fixed, for cube points 3, fixed, for centre and axial points	1 central point, 2^{k-p} factorial points, and 2*k* star points	- Economy of run size - Ease of calculating the sample points - Allows estimation of curvature in the main effects - Resolution V designs allow clear estimation of all linear, two-factor interactions	- Needs more runs that a 2^{k-p} design - Cannot show discontinuities, or curvature in the interactions - Some redundancy inevitable	- *A priori* reasoning suggests curvature detection in main effects will be needed - No interim analysis or sampling, so less time demanding than Latin hypercube - Run size smaller than 3^{k-p}, and probably about the same as or smaller than Latin hypercube

Since curvature in the main effects was considered possible, the use of a 2^{k-p} fractional factorial was also quickly precluded. The possibility of curvature in the main effects was discerned partly through exploratory simulations with the chosen LEM (sections 3.4 and 3.5) during early stages of the research, and also through simple reasoning of the processes of interest in the landscape. The possibility of curvature in the interactions also arose, which again precluded use of a 2^{k-p} design, but suggested that a 3^{k-p} fractional factorial could be more appropriate. However, a 3^{k-p} design was also excluded, mainly because of the much larger run sizes needed by this sort of design compared with Latin Hypercube sampling or central composite designs.

This left a choice between these two types of experiment, namely Latin Hypercube sampling and use of a central composite design. To clarify matters, the author drew on examples from the literature (e.g. Iman and Helton, 1988; Bowman *et al.*, 1993; Chapman *et al.*, 1994; Sacks *et al.*, 1989) and also sought further advice from Professor R. Cheng, of the School of Mathematics, University of Southampton. Iman and Helton (1988) in particular recommend that Latin Hypercube sampling should be used in many situations; by contrast, the findings of Bowman *et al.* (1993) and Chapman *et al.* (1994) were much less conclusive, both groups needing interim analysis and additional samples to explore further areas of the parameter space which appeared interesting or problematical. On balance, it was decided that no design is ideal, but that a central composite design offered the best compromise. In particular, some additional sampling was thought almost certainly to be needed whatever the initial sampling method, in order to test each metamodel's accuracy. In this respect, the central composite design was seen to have the advantage that main effects could be identified separately if needed using just the centre and star points, and this would allow more robust estimation of any important two-factor interaction terms. By contrast, the LH sample would make it more difficult to derive a metamodel without using both main effect and interaction terms together throughout the regression analysis. In addition, the central composite design would explore the factorial space to its limits, whereas LH sampling would only do so if sample points were deliberately placed at or near those limits.

Having made this choice, the key issues became which LEM to use in the simulations, the choice of the landscape setting and parameters of most interest, and the parameterisation of that model for the simulation experiment. The choice of LEM was made first and is now discussed, with a description of the model as used in this research.

3.4 CHOICE OF LEM AND MODEL DESCRIPTION

3.4.1 Choice of model

One of the options considered in this research was to look for the equifinal responses exhibited by several models, so that output from different LEMs could be compared with each other. It became clear very quickly, however, that to do this would be a very demanding task, and the decision was made to conduct the simulations using just one model. Also, as discussed in Chapter 2, LEMs generally include classes of processes most suited to the modelling of landscapes in humid or semi arid environments, so the decision was made to apply the chosen LEM to a similar such landscape, where operation of all of the main process classes could be exploited. With these requirements in mind, of the models reviewed in Chapter 2, at the time of making the choice of model only GOLEM and CHILD included a representation of weathering. Of these, although CHILD had at that time some more realistic functionality (e.g. channel meandering), it was decided to use GOLEM because of its relative simplicity, and also because it has been used successfully in a number of studies (e.g. Tucker and Slingerland 1994, 1996, and 1997; Tucker and Bras, 1998). Having covered the decision to use GOLEM, a description of the model now follows.

3.4.2 Description of GOLEM

The Geomorphic/Orogenic Landscape Evolution Model, or "GOLEM", was designed and developed by Professor R. Slingerland and Dr G. E. Tucker, and was encoded in the computer programming language 'C' by Dr Tucker. Its intended use is the simulation of landscape evolution over time scales ranging from tens of thousands to millions of years, over spatial scales extending from small catchments to mountain ranges. The theoretical and computational bases of the model are described in Tucker and Slingerland (1994, 1996 and 1997). More details, including instructions and a glossary of terms may be found on Dr Tucker's main website, presently at: 'http://www.colorado.edu/geolsci/gtucker/Software/Golem/Golem.html'. The following description is drawn from these sources and personal communications with Dr Tucker.

Mode of operation, cell division and state variables

GOLEM can be used in large-scale or catchment mode. The large scale mode is intended for simulations where a coarse spatial resolution (*c.* >0·04 km^2 per grid cell) is acceptable. In this mode, GOLEM is able to simulate the evolution of a channel network, but the operation of hillslope processes is greatly simplified, and individual hillslope sections cannot be represented. Since the author thought that the operation of both hillslope and channel processes would be of interest in this study, the large-scale mode was not used and all simulations are made running the model in catchment mode.

The landscape in GOLEM is represented by square cells, set within an orthogonal grid. The edges of the grid can be treated in different ways, so as to simulate tectonic effects such as uplift, tilting and flexing. The boundary of the modelled landscape itself can be rectangular or irregular. Cells within the boundary are 'active', whereas cells outside the boundary are left unchanged. The domain may have a single or multiple drainage outlet cells, as required.

GOLEM represents the topography of the landscape using the elevation of each of the catchment cells above an arbitrary datum, set by the base of the lowest bedrock layer. The elevation is then found from the thickness of the bedrock and the depth of any overlying sediment. For convenience, rather than express the output in these terms, elevations are usually measured relative to the outlet, which is assumed to have a zero elevation.

Although GOLEM can account for spatial variations in bedrock, for simplicity, spatially uniform bedrock was assumed in all of the simulations undertaken herein. The sediment cover can be initialised in different ways. In this study, the landscape was assumed in an initialising simulation to begin with a uniform sediment depth of 0.5m. After 50,000 years of simulated time, the initial layer was redistributed by the processes acting on the landscape, providing a more realistic resemblance to real conditions. All subsequent simulations in this study were started using this modified landscape, with its redistributed sediment cover. Output from the initialising simulation is discussed with the other model output in Chapter 4.

Runoff and climate

GOLEM does not incorporate simulation of individual flood events. Rather, the cell discharge is calculated according to a notional runoff rate per cell and the flow routing rules. If the runoff rate per cell in a time step is P, then the cell discharge is given by:

$$Q = PA, \qquad 3.06$$

where Q is the cell discharge, and A is the area (i.e. the number of cells) draining into and including the cell. Flow out of any cell is routed along the steepest downslope flow path. All the runoff is assumed to be over the ground surface, unless soil transmissivity allows a proportion to flow below the surface, or to be lost to deeper groundwater. The incorporation of transmissivity was used by Tucker and Bras (1998) to represent the effects of saturation excess overland flow, but it is not explored further in this research.
The climate can be changed by altering the base runoff rate, P, either between one simulation and another, or during the course of a simulation as a function of the elapsed time. The transporting capacity of the discharge can be varied similarly by changing a runoff intensity factor, so as to allow for the effects of rainstorms of different volume and duration. This latter functionality is discussed in Tucker and Slingerland (1997) but, for simplicity, was not explored in this study.

Channel initiation and headward extension

GOLEM can be run with a channel initiation function, so that the model discriminates between cells which contain channels, in which the fluvial transport functions operate, and those which do not, in which only hillslope processes are active. The channel formation function is an adaptation of Montgomery and Dietrich's (1988) formula (subsection 2.6.4 *q.v.*). In GOLEM, channels are formed where:

$$k_{ci} A^{m_{ci}} S^{n_{ci}} > t_{ci}, \qquad 3.07$$

where k_{ci} is a constant, A is the area draining into the cell, S is the steepest downslope gradient, m_{ci} and n_{ci} are exponents relating to channel formation, and t_{ci} is a channel formation threshold. This is an adaptation of equation 2.73, using an area rather than a discharge term. To reduce the number of parameters varied in the simulations, the author simplified equation 3.07 by setting k_{ci} and m_{ci} both to 1, leaving only variations in n_{ci} and t_{ci} to be considered. The equation can then be recast in logarithmic form as:

$$\ln|A| = \ln|t_{ci}| - n_{ci} \ln|S|, \qquad 3.08$$

which is Montgomery and Dietrich's (1988) basic form (eq. 2.71).

Process classes and mass continuity relationships

As noted above, GOLEM may include state variables for bedrock and regolith. The mass continuity equations for these variables, and the processes affecting them, are summarised in Figure 3.4. The overview which follows is taken largely from Tucker and Slingerland (1997), albeit adapted for the processes used in the simulations herein. Specifically, simplifications aimed to reduce the number of parameters varied in this study are also explained here.

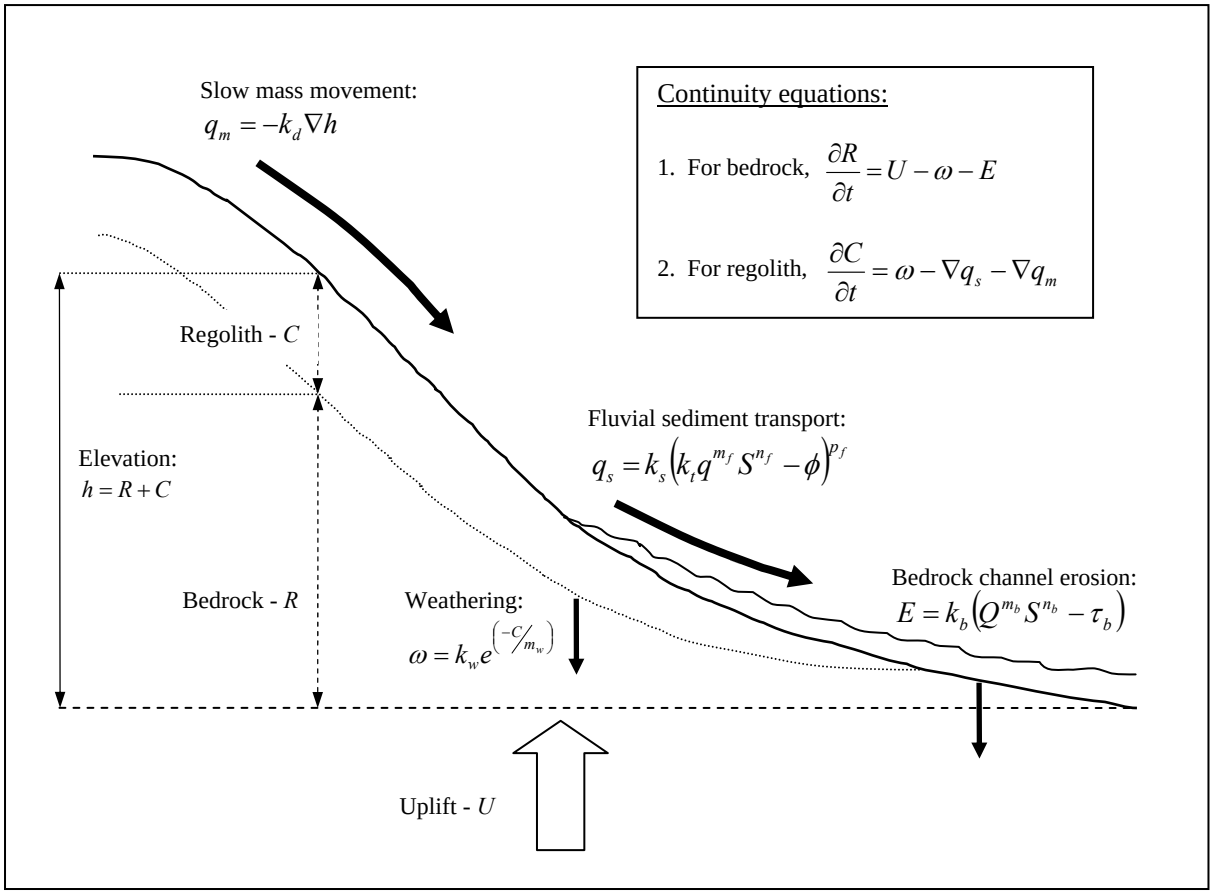

Figure 3.4: Summary of the key features of GOLEM (after Tucker and Slingerland, 1997), as adapted for the purposes of this study; full details given in the text.

Beginning with the state variables, the elevation at any time is found from:

$$h = R + C \,, \tag{3.09}$$

where h is the elevation of the cell above base level, R the elevation of the bedrock, and C the thickness of the regolith. The continuity equation for bedrock is given by:

$$\frac{\partial R}{\partial t} = U - \omega - E \,, \tag{3.10}$$

where U is the rate of uplift, ω is the rate of weathering, and E is the rate of bedrock channel erosion. The continuity equation for regolith is then given by:

$$\frac{\partial C}{\partial t} = \omega - \nabla q_s - \nabla q_m , \qquad 3.11$$

where q_s is the volumetric rate of sediment transported (per unit width) by fluvial processes, and q_m the volumetric rate of transport (also per unit width) by mass movement processes. If one excludes for the moment mass movement by landsliding, the last term can be restated in terms of height, so that equation 3.11 becomes:

$$\frac{\partial C}{\partial t} = \omega - \nabla q_s - k_d \nabla^2 h , \qquad 3.12$$

where k_d is a diffusivity for sediment transport per unit width for slow mass movement.

Process equations

The rate of weathering in equations 3.10 to 3.12 is represented by an equation very similar to equation 2.22:

$$\omega = k_w e^{\left(-C/m_w\right)}, \qquad 3.13$$

where k_w is the weathering rate coefficient for bare bedrock, and m_w is a characteristic depth which constrains how quickly the weathering rate declines as the depth of regolith increases. The rate of slow (diffusive) mass movement per unit width is expressed using:

$$q_m = -k_d \nabla h , \qquad 3.14$$

which is the vectoral representation, as in equation 2.25, and k_d is the diffusivity, as above. Erosion of bedrock channels, E, only occurs in channel cells stripped of sediment, and is calculated using:

$$E = k_b \left(\tau - \tau_b\right), \qquad 3.15$$

where k_b is a coefficient, τ is a shear stress term, and τ_b the critical shear stress threshold for the erosion of bare bedrock. Equation 3.15 can be restated as:

$$E = k_b \left(Q^{m_b} S^{n_b} - \tau_b\right), \qquad 3.16$$

where m_b and n_b are empirically derived exponents (e.g. Tucker and Slingerland, 1997). To keep the parameter space more manageable, the values for m_b and n_b were herein fixed at 0.3 and 0.7 respectively (Tucker and Slingerland, 1997)[6], so that equation 3.16 becomes:

$$E = k_b\left(Q^{0.3}S^{0.7} - \tau_b\right), \qquad 3.17$$

and the parameter variation is confined to k_b and τ_b. Also, it should be noted that E is given in terms of a rate of change of height i.e. the rate at which the bed is being lowered, rather than as a volumetric rate of transport per unit width.

Turning now to fluvial sediment transport, GOLEM does not include a function for calculating wash transport. However, the researcher has a choice of using one of four different fluvial sediment transport functions:

1. the Bagnold function (used in Tucker and Slingerland, 1997);
2. a power law, similar to equation 2.45 (used in Tucker and Bras,1998);
3. a threshold function, similar to the power law, but including a threshold term; and
4. the Meyer-Peter-Müller formula (e.g. Gomez and Church, 1989).

For simplicity, simulations in this research were conducted using the threshold function only (option 3 above). The general forms of such formulae have been reviewed in subsection 2.6.3, so this function can be stated as:

$$q_s = k_s\left(k_t q^{m_f} S^{n_f} - \phi\right)^{p_f}, \qquad 3.18$$

where q_s is the volumetric rate of sediment transport per unit width of channel, k_s is a sediment transport coefficient, k_t is another coefficient relating to the discharge-gradient term, q is the flow discharge per unit width, S is the channel gradient, ϕ is the threshold (below which sediment transport is zero), and m_f, n_f and p_f are empirically derived exponents. The implementation of the threshold function requires adjusting the basic transport formula to allow for the width of the channel. First, the width of the channel is estimated using empirically derived hydraulic geometry models, which relate channel width to flow discharge (e.g. Leopold, Wolman and Miller, 1964, p. 244):

$$W = bQ^{m_c}, \qquad 3.19$$

[6] Appropriate values for *m* and *n* have also been explored more widely (e.g. Whipple and Tucker, 1999; Tucker and Whipple, 2002; and Niemann *et al.*, 2001), but for simplicity here, the ones chosen were considered suitable.

where W is the width, b is an empirically derived coefficient, Q is the discharge (found here from eq. 3.06), and m_c is an empirically derived exponent, found typically to be in the range from 0.4 to 0.6 (*ibid.*). Substituting this into equation 3.18, we obtain:

$$Q_s = Wq_s = bQ^{m_c} k_s \left(k_t q^{m_f} S^{n_f} - \phi\right)^{p_f}, \tag{3.20}$$

where Q_s is the rate of sediment transport in the channel. It should be noted that the relation given in equation 3.19 also allows substitution for the q term within the bracket, thus:

$$q = \frac{Q}{W} = \frac{Q}{bQ^{m_c}}, \tag{3.21}$$

which, substituting in equation 3.20, gives:

$$Q_s = bk_s Q^{m_c} \left[k_t \left(\frac{Q}{bQ^{m_c}} \right)^{m_f} S^{n_f} - \phi \right]^{p_f} \tag{3.22}$$

This expression can be recast, as follows:

$$\begin{aligned}
Q_s &= bk_s Q^{m_c} \left[\frac{k_t Q^{m_f} S^{n_f}}{b^{m_f} Q^{m_c m_f}} - \phi \right]^{p_f} \\
&= bk_s Q^{m_c} \left[\frac{k_t Q^{m_f (1-m_c)} S^{n_f}}{b^{m_f}} - \phi \right]^{p_f} \\
&= bk_s Q^{m_c} \left[\frac{k_t}{b^{m_f}} \left(Q^{m_f (1-m_c)} S^{n_f} - \frac{b^{m_f} \phi}{k_t} \right) \right]^{p_f} \\
&= \frac{bk_s k_t^{p_f} Q^{m_c}}{b^{m_f p_f}} \left(Q^{m_f (1-m_c)} S^{n_f} - \frac{b^{m_f} \phi}{k_t} \right)^{p_f} \\
&= b^{(1-m_f p_f)} k_s k_t^{p_f} Q^{m_c} \left(Q^{m_f (1-m_c)} S^{n_f} - \frac{b^{m_f} \phi}{k_t} \right)^{p_f}
\end{aligned} \tag{3.23}$$

Further simplifications can then be made, using:

$$k_f = b^{(1-m_f p_f)} k_s k_t^{\ p_f}, \tag{3.24}$$

where k_f is a general sediment transport coefficient, and

$$\tau_c = \frac{b^{m_f} \phi}{k_t}, \tag{3.25}$$

where τ_c is a transport threshold. Together in equation 3.23, these give:

$$Q_s = k_f Q^{m_c} \left(Q^{m_f (1-m_c)} S^{n_f} - \tau_c \right)^{p_f}, \tag{3.26}$$

which is the general form of the transport equation implemented in the model in this research. If a stream power form of the transport law is assumed, similar to equation 2.44, but omitting the hydraulic radius term, then m_f and n_f are equal to 1, and p_f is equal to 1.5. The value of m_c is set to 0.5 and is not variable in the code as it is presently written, and both the code and input file (called upon at the start of each simulation) would need to be amended before variations in this parameter could be implemented. With this points covered, equation 3.26 becomes:

$$Q_s = k_f Q^{0.5} \left(Q^{0.5} S - \tau_c \right)^{1.5}, \qquad 3.27$$

which leaves only variations k_f and τ_c to be considered in this study.

Turning now to rapid mass movement, GOLEM includes functions for both bedrock and shallow landslides. The bedrock sliding function was not used herein, both for simplicity, and because it was not thought to be an important process in the study catchment (see section 3.5 below). The bedrock sliding threshold was accordingly set to a high value (2, equivalent to a failure angle of *c.* 63º) and not varied as part of the experiment. However, simple, slope-dependent, shallow landsliding, triggered when the threshold gradient, s_{cr}, is exceeded, was used in the simulations. Such landsliding is implemented by extended dispersal, as discussed in subsection 2.5.5. Area dependent landsliding is also possible, and was used in Tucker and Bras (1998) to represent the effects of shallow slides triggered by excess pore water pressures. Again, to keep the parameter space more manageable, this latter representation was not used.

Finally, GOLEM can also include a vegetation module, but this was not considered here.

3.5 IMPLEMENTATION IN GOLEM

3.5.1 Study catchment

Choice of site

Selection of a specific catchment for use in the simulations was governed by some general requirements. In particular, it was thought it was important that it should be located in an area which had been well studied previously, thereby aiding the selection of realistic values for process rate coefficients and thresholds. It was also important that the catchment should not have been glaciated or subject to aeolian processes, as these process classes are not

included in GOLEM (Table 2.1 *q.v.*). Similarly, catchments including chalk or limestone strata were avoided, to reduce the influence of solution weathering. Taking these requirements into account, and out of a number of possibilities, a catchment in the Oregon Coast Range ('OCR') was selected, around the headwaters of the Smith River (Figure 3.5). The OCR has been the focus of much research over the last twenty or so years, as it was believed to be an example of a region which is broadly in equilibrium with its climatic and uplift conditions (e.g. Reneau and Dietrich, 1991; Kobor and Roering, 2004). Recent research has suggested that the situation is much more complicated, with strong variations in erosion rates and uplift history across the region (e.g. Gendaszek *et al.*, 2005; Van Laningham *et al.*, 2006). These points were not thought to affect the usefulness of the Smith catchment and any related data sources, and all the simulations herein were therefore conducted using the Smith catchment.

The author visited the field site in 2003, during a research study visit to the U.S.A., during which various details concerning the climate, ecology and current land management of the site and its region were confirmed. The primary source data on the catchment were obtained from the 'CLAMS' website[7] ('http://www.fsl.orst.edu/clams/project.htm'), and the author was granted permission by the CLAMS group administrator to download a DEM of the Smith catchment for use in this research. The DEM of the catchment provided by CLAMS was of 30 m resolution, and smoothed, so as remove pits and spikes, with the elevations being rounded to the nearest metre. Additional information on ecology and climate were provided by Professor Richard Waring, of the Department of Forestry, Oregon State University, Corvallis, who also accompanied the author on the site visit. Figure 3.5 shows both a map of central and southern Oregon and an inset, with topographic and other details, of the Smith River study catchment.

[7] 'CLAMS' - **C**oastal **L**andscape **A**nalysis and **M**odeling **S**tudy, a partnership supported by the U.S. Forest Service (Pacific Northwest Research Station), Oregon State University (College of Forestry), and Oregon Department of Forestry. CLAMS co-ordinates research projects and hosts databases focused on understanding the relationships between the economy and the environment in the Oregon Coast Range and the coastal region.

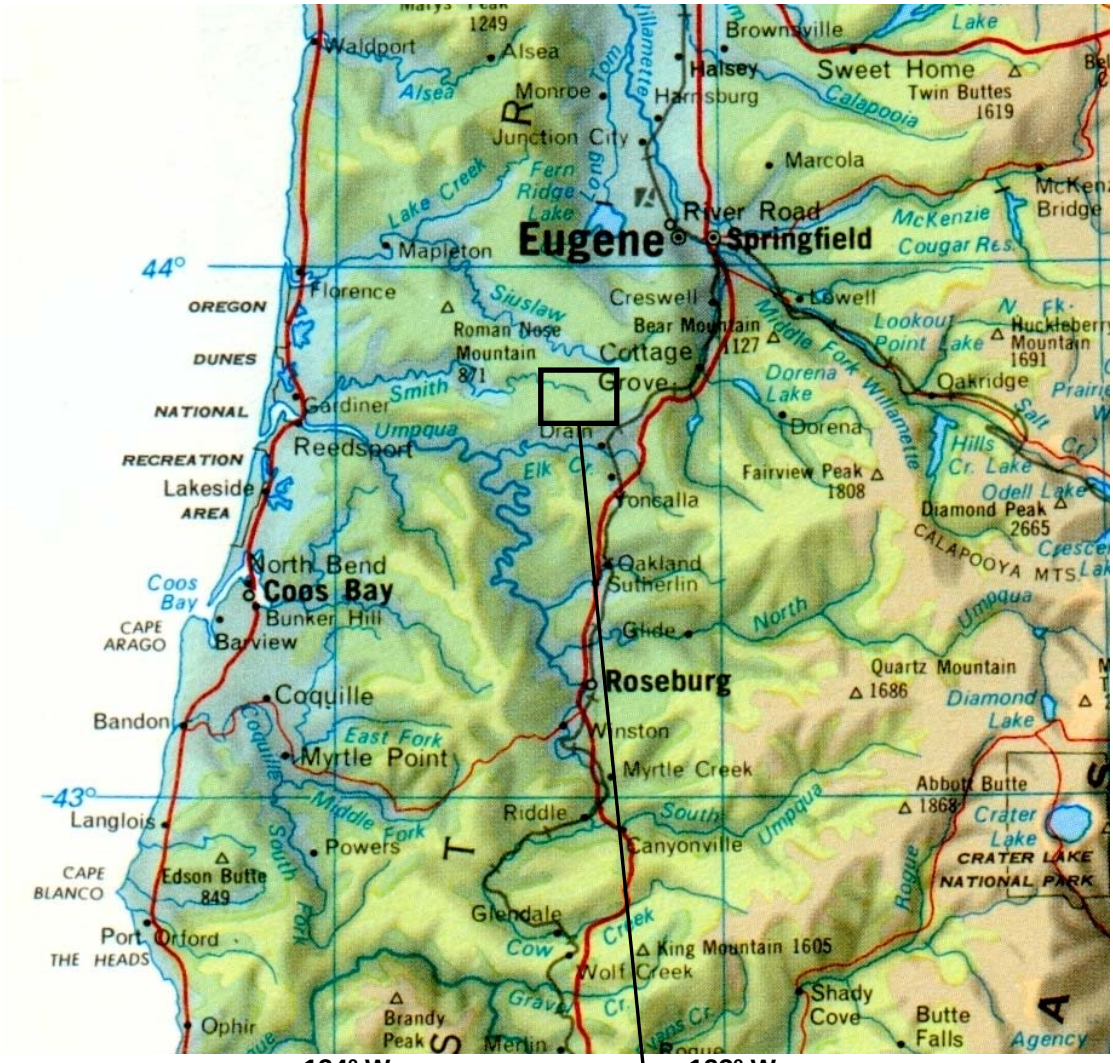

Catchment details:

Length:	9.78 km
Width:	7.05 km
Area:	38.7 km^2
No. of cells:	*c.* 43 x 10^3
Elev. (outlet):	237 m a.s.l.
Elev. (max):	497 m a.s.l.
Relief:	260 m
Mean slope (gradient):	10º (0.17)
Drain^{ge} dens^{y}:	2.5 km^{-1} (est.)
Stream order:	4 (est.)
Precipitation:	*c.* 2.2 m yr^{-1}
Est. runoff:	*c.* 1 m yr^{-1}

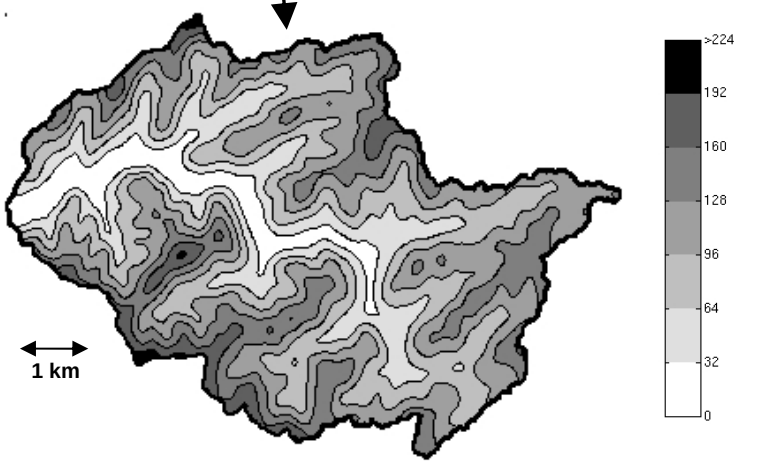

Figure 3.5: Map of part of Oregon, showing location of the Smith River headwaters catchment used in this research; also plot of the DEM of the study site, with contours at 32 m intervals, and showing additional basic details relating to the catchment.

Site description and related details

The Smith River flows into the Umpqua River near Reedsport (43º 42' N 124º 07' W), about 12 km from the Pacific Ocean. The lower reaches of the Smith are therefore tidal, and the whole river, along with the other rivers and coastal waters of this region, is important economically for both its freshwater and anadromous fish. There has been great concern over the last fifty years to maintain fish stocks and the health of both the coastal and inland fisheries, and to protect species which have been over-fished[8]. Land management practices, and particularly forestry, road building and the control of wild fires, are all factors influencing the supply of sediment to the rivers, and these topics continue to be the focus of much research (e.g. CLAMS; Lancaster *et al.*, 2003).

The headwaters region of interest herein is located some 55 km inland at approximately 43º 45' N 123º 20' W. The climate influencing the Smith changes mainly with distance from the ocean and with altitude, but there is also a north-south trend, the northerly locations being much wetter (CLAMS). In the study site area, the climate is of a Mediterranean type, with hot, dry summers, and cooler, wet winters. Most of the rainfall (2.2 m/yr, CLAMS, 2006) falls between November and April, when stream flows are markedly higher (Waring, 2003, personal communication). Extreme summer temperatures are also possible, however, often reaching 35-40º C or more[9], so there is a strong summer moisture deficit. USGS streamflow data[10] were used to estimate an annual runoff for the study area catchment of 1 metre per year, which was used in all of the simulations herein. Details of the streamflow sources and runoff calculations are given in Appendix B. The dominance of the winter floods also suggested that the dominant discharge type of climate simulation used by GOLEM (subsections 2.2.3 and 3.4.2) would be appropriate for the catchment, at least as a first approximation.

The principle land use in the study catchment is forestry, and evidence from the site visit indicated a logging return period of 50 or so years (Waring, 2003, personal communication). However, some dense and tall stands suggested that parts of the catchment had probably never been clear felled. Regarding the recent logging, aerial photographs showed a number of clear cuts spread about the catchment, amounting to 10% or so of the total study area

---

[8] For example, although there is a rich Salmon fishery on the Smith, the Coho salmon has had to be protected. Similar restrictions apply to coastal and sea fish to prevent catastrophic collapse, such as happened to the pilchard stocks after the Second World War.

[9] During the author's site visit, the temperature reached 38º C.

[10] All stations in Oregon, USGS gauging station code numbers 14311300, 14323100 and 14311200.

(Harvey Greenberg, University of Washington, 2003, personal communication). The main tree species are Douglas Fir (*Pseudotsuga menziesii*) and Western Red Cedar (*Thuja plicata*), with numerous examples of these trees well over 40 m tall and reaching nearly 2 m across, measured at breast height. Other common species include Western Hemlock (*Tsuga heterophylla*) and Bigleaf Maple (*Acer macrophyllum*), and also some Alder (*Alnus*), Yew (*Taxus*) and Ash (*Fraxinus*) species. The presence of older Western Hemlock is a good indicator that the catchment has not been subject to a major fire for some decades (Waring, 2003, personal communication). There were also many fallen trunks, in various stages of decay, lying across the forest floor, with some in or across the main river channel. The logging activity only occupies a small part of the catchment, however, and was not considered an important factor for the purposes of this research.

In the understorey, the chief shrubs are Oregon grape (*Berberis aquifolium*), Sword Fern (*Polystichum munitum*), and Himalayan Blackberry (*Rubus armeniacus*), the last named being a highly invasive, non-native species. Apart from the clear cuts, and areas in the central floodplain kept open for domestic animals, the tree cover and understorey are generally very dense and difficult to penetrate. The thickness of the tree cover and the density of the understorey together suggest that wash processes should be minimal in the catchment, and that operating GOLEM with a distinct fluvial channel function (subsection 3.4.2) would be appropriate.

The geology of the area comprises beds of the Tyee formation, a series of medium to fine grained, thickly bedded sandstones and micaceous siltstones, possibly of marine origin, with minor interbeds of tuff (Walker and Macherd, USGS, 1991). Observations of roadside cuts indicate that the bedrock is deeply weathered, to over 2 m in places, similar to the observations made by Reneau and Dietrich (1991). These depths, together with Reneau and Dietrich's (1991) data, were taken as an indication of the regolith thicknesses GOLEM should simulate over time in hillslope hollows and on lower slopes. Also, the absence of any limestone strata was welcome, for the reasons previously stated.

The flood plain deposits, as seen from exposed river bank sections, are two or more metres deep, and generally composed of a very fine, soft sand, lying above a coarse gravel layer of at least 30 cm thickness. However, it was not possible to explore the floodplain widely, and no cores were taken, so other deposits could well be much deeper than the ones observed.

Near the location of the study catchment's outlet, the main channel is 2½ to 3 metres wide, and it retains this width until near the source, where it declines to about 1 to 1½ m wide. In the central reaches, the river banks are generally 2 to 3 m above the river bed, and well

vegetated with trees of both deciduous and coniferous species. The banks in this zone are 6 to 7 m apart, mostly grassed, and steep or near vertical in places. Flood stage indicators (e.g. weed trapped in overhanging branches, still showing the flow direction) suggest that the previous winter's floods had reached at least 2 m above the river bed. By contrast, on the day of the visit, the flow in the main channel was estimated to be about a 1 $m^3 s^{-1}$or less. These observations further emphasised the likely dominance of winter flooding.

The river bed itself comprised mostly long sections (10-40 m) of bedrock, with patches of gravel and sand, interspersed with much shorter mixed gravel and sand sections. The gravel was mostly sub-angular or rounded, the larger clasts being typically about 8 cm (A-axis) by about 3 cm (B-axis), but quite flat (< 2 cm C-axis). The smaller gravel particles were more rounded, with a distinctly rough feel. There were also a number of gravel and cobble bars, some of them embanked at one side by fallen tree trunks. In addition, in some bedrock sections, thin slabs of the bedrock had been broken clear of the river bed, and these were associated with angular cobbles and gravel downstream. These observations indicated that the GOLEM simulations should include bedrock erosion, and that the initial simulations should be able to replicate to some extent the mix of bedrock and gravel channel sections.

Although the hillslopes, particularly near the source, appeared to be quite steep (*c.* 30º), no evidence was found of recent landslides near the main course of the river or in the slopes bounding the floodplain. This applied also to a cleared area of similar gradients, where the trees appeared to have been felled the year before. However, there were a number of tributaries which had steeper channel beds than the main channel, and which appeared to cut through steeper terrain. If landsliding does occur, it is more likely to do so in these locations. Also, landsliding is widely reported throughout the OCR (e.g. Reneau and Dietrich, 1991; Kobor and Roering, 2004). Accordingly, it was decided to include shallow landsliding in the simulations with GOLEM, the steeper observed slopes (somewhat variable, but estimated by clinometer to be about 30º) giving a good indication of the likely threshold angle for sliding. Similarly, in the clear cut areas, the hilltops were quite rounded and convex, so slow, diffusive processes were also included.

Finally, although the denudation rate near the Smith River latitudes has been estimated to be *c.* 0.065 mm yr^{-1} (Gendaszek *et al.*, 2005), this figure includes the much steeper and wetter areas of the North Fork Smith River, where erosion rates are much higher and landsliding frequent. The rate for the study catchment is taken to be less than this.

Having dealt with the choice of study site, the selection of processes and parameterisation of GOLEM are now considered.

3.5.2 Parameterisation of GOLEM for the Smith River simulations

Although GOLEM includes 20 or so adjustable parameters, this was considered too large a number for this study, and the final list was restricted to ten, using two each to implement variations in weathering, mass movement, channel formation, fluvial sediment transport and bedrock erosion processes. For simplicity, it was also decided in the fluvial process equations to vary the coefficient and threshold parameters only, keeping the exponents (e.g. as in equations 3.16 and 3.26) constant. The parameters varied in the simulations are listed in Table 3.5, and this also shows their base case, factorial point and star point values, to be used as required in the central composite design. All parameter values listed in the table are based on a model time step of one year, and the fluvial transport parameters, which were established by calibration, are based on the assumed runoff rate of 1 m per year, and a sediment yield of *c.* 20 $m^3 km^2 yr^{-1}$. The latter was estimated partly from the sources cited above (e.g. CLAMS, Gendaszek *et al.*, 2005), but taking into account the gentler slopes and lower rainfall in the study catchment, and also from results from calibration simulations (explained below). An uplift rate of 200 metres per million years, consistent with the uplift history of the region (e.g. Reneau and Dietrich, 1991), was applied in an initialising, 'warm up' simulation, the latter needed to allow a more realistic distribution of sediment in the modelled catchment. Subsequent simulations in the main experiment were conducted using the resulting modelled landscape, with the established drainage pattern and sediment distribution, but without uplift. More details of the results from the initialising and main simulations are presented in Chapter 4.

Table 3.5: List of parameters chosen for variation in the simulations, together with their design point values and main source of derivation. Other, more general parameter value sources used are cited in subsection 2.7.2.

			Parameter values corresponding to each level in the sampling design					
Process	**Parameter**	**Units**	**$-\alpha$** (star point)	**-1** (corner point)	**0** (central point)	**+1** (corner point)	**$+\alpha$** (star point)	**Main source**
Weathering	k_w - base rate coefficient	m yr^{-1}	180 x 10^{-6}	222 x 10^{-6}	240 x 10^{-6}	258 x 10^{-6}	300 x 10^{-6}	Heimsath *et al.* (2001)
	m_w - rate decay depth	m	0.23	0.30	0.33	0.36	0.43	Heimsath *et al.* (2001); calibration
Mass movement	k_d – diffusive rate coefficient	m^2 yr^{-1}	2.0 x 10^{-3}	3.12 x 10^{-3}	3.60 x 10^{-3}	4.08 x 10^{-3}	5.20 x 10^{-3}	Roering *et al.* (1999)
	s_{cr} – threshold gradient (landslides)	-	0.48	0.578	0.62	0.662	0.76	Reneau and Dietrich (1991); own data
Channel initiation	n_{ci} - gradient exponent	-	0.216	0.334	0.402	0.484	0.748	Slope-drainage area relationship (App. C)
	t_{ci} – threshold area	m^2	7,600	10,607	12,236	14,115	19,700	Slope-drainage area relationship (App. C)
Alluvial channels	k_f - transport rate coefficient	$yr^{0.25}$ $m^{-0.75}$	221 x 10^{-6}	376 x 10^{-6}	442 x 10^{-6}	509 x 10^{-6}	664 x 10^{-6}	Calibration
	τ_c – transport threshold	$m^{1.5}$ $yr^{-0.5}$	0	4.2	6.0	7.8	12	Calibration
Bedrock channels	k_b – erosion rate coefficient	$m^{0.1}$ $yr^{-0.7}$	3.75 x 10^{-6}	11.625 x 10^{-6}	15 x 10^{-6}	18.375 x 10^{-6}	26.25 x 10^{-6}	Tucker and Slingerland (1997); calibration
	τ_b - erosion threshold	$m^{0.9}$ $yr^{-0.3}$	0	2.8	4	5.2	8	Tucker and Slingerland (1997); calibration

Regarding the weathering (k_w and m_w) and mass movement (k_d and s_{cr}) parameter values, these were determined via a combination of published sources and the author's observations. Some trial simulations were also needed to gain a better estimate of m_w, the weathering rate decay parameter, in order to simulate more realistic regolith depths.

The values of the channel formation parameters, t_{ci} and n_{ci}, were based on morphometric data from the DEM of the catchment, in particular, the drainage areas feeding into flow convergence zones of maximum slope. At these locations, slope curvature switches from convex to concave, as fluvial processes become dominant over mass movement. The areas and slopes at these locations were then plotted, and a log|slope| versus log|area| relation was derived from the data, of the form reported by Montgomery and Dietrich (1988, 1992) and shown in equation 2.71. Although the values obtained by this method are somewhat different from those reported for other parts of the OCR, they appeared sensible for the study catchment and experimental purpose herein, and their method of derivation valid (David Montgomery, 2003, personal communication). More details on the values used and the calculations to derive these parameters' values are given in Appendix C.

The fluvial erosion and transport parameter values (for k_f, τ_c, k_b and τ_b) were derived by calibration. An immediate difficulty in doing this, however, was that it was not possible to initialise the modelled catchment with a realistic sediment distribution or channel network, resembling that of the catchment itself. As explained below, and also in Chapter 4, a warm up simulation was therefore required, during which a realistic sediment cover and network would evolve. When calibrating for the fluvial transport and bedrock erosion parameters, therefore, the runs were found to generate a rising trend in the sediment yield, in response to the evolving sediment cover and channel network (also explained in Chapter 4). Rather than extend the calibration exercise to achieve a wider range of values, it was decided that provided the modelled sediment yield was reasonable when compared with the available field data, this would be sufficient for the research purpose. These parameters were therefore calibrated to a value of *c.* 20 $m^3 km^{-2} yr^{-1}$, as explained above. Also, the thresholds, τ_c and τ_b, were included in the process formulations to account for the need for stronger flows (above a certain competence) to mobilise the larger gravel and cobbles present in the channels.

Having covered the parameterisation of GOLEM for the main experiment, details of the initial experiment design are now explained.

3.5.3 Experiment design details: design matrix, planning matrix and parameter cases

As previously discussed, the parameter space defined in section 3.3.3 was sampled using a central composite design. Specifically, the design incorporated a 2_{V}^{10-3} fractional factorial, which allows strongly clear estimation of all main effects and clear estimation of all two-factor interactions (subsection 3.3.3). To determine the design levels of the parameters to be used in each simulation, and in particular in the fractional factorial part of the design, each parameter was assigned a design number, and these are shown in Table 3.6.

Table 3.6: Design numbers assigned to each parameter, used in forming the design matrix.

Parameter	Design number	Parameter	Design number
k_w	1	n_{ci}	6
m_w	2	t_{ci}	7
k_d	3	s_{cr}	8
k_f	4	k_b	9
τ_c	5	τ_b	10

It should be noted that the allocation of design numbers shown above is quite arbitrary, as it is immaterial to layout of the design which parameter is allocated to which number; any of the parameters could therefore have been allocated to any of the design numbers. All that is required is that the design generators are applied correctly and consistently. Thus, if k_d is denoted by design number 3, and s_{cr} by design number 8, then these numbers must be applied, consistently in each row, throughout the preparation of both the design matrix and the planning matrix. The same point holds for the other parameters.

The design generators for fixing the design matrix levels are explained in Wu and Hamada (2000, p199). The generators were applied first to determine the design levels for s_{cr}, using:

$$\mathbf{8} = \mathbf{3456} \qquad 3.28$$

To determine the design levels for k_b, the following was used:

$$\mathbf{9} = \mathbf{13457} \qquad 3.29$$

Finally, the design levels for τ_b were determined using:

$$(\mathbf{10}) = \mathbf{12467} \qquad 3.30$$

By convention, the design level of factors numbered 10 or higher is placed in brackets.

The full design matrix comprises 1 simulation with all parameters at their central values, 20 simulations using the star points, and the 128 simulations which make up the fractional factorial, giving a total of 149 simulations to undertake the initial sampling of the parameter space. The full design matrix is too long to produce here, and appears in Appendix D, and the planning matrix, which shows the actual values used in the simulations, appears in Appendix E, together with an explanation of how the design levels are translated into actual parameter values. The parameter cases used in the simulations are also numbered, for ease of reference.

For all simulations, the simulation period was chosen arbitrarily as 100,000 years. Although this period is too short to enable the landscape to evolve to an equilibrium state (such evolution would take perhaps two weeks of computer time for each simulation), it was thought to be sufficiently long to reveal the effects of both the faster processes, such as landsliding and fluvial transport, and the slower processes, such as weathering and slow mass movement.

These points conclude Chapter 3, and step 1 of the methodology as summarised in Figure 3.1. The simulations with GOLEM (step 2) can now be conducted, and this prepares the way for analysis of the results, selection of the metrics, and derivation of the metamodels (steps 2 to 4). These matters are presented in Chapter 4.

CHAPTER 4: MODEL OUTPUT, CHOICE OF METRICS AND DERIVATION OF THE METAMODELS

4.1 INTRODUCTION

The author's aim in this chapter is to present the next steps of the methodology, namely the output from the simulations with GOLEM using the central composite design, the choice of metrics, and the derivation of the metamodels (steps 2, 3 and 4 in Figure 3.1, *q.v.*). The chapter therefore includes detailed presentation of the output from GOLEM obtained from the main experiment, focusing particularly on results from the base case simulation i.e. the parameter case where all of the parameters are at their base case values. Different output metrics are discussed and contrasted, from which four are selected as subjects for the metamodels. An approach to deriving initial metamodels for these metrics is also outlined, covering the type of preliminary model to be fitted, and the requirements to ensure both a satisfactory fit to the data and model parsimony.

Besides the choice of metrics and metamodel derivation, the work needed during this phase of the research also required additional simulations, used in testing the preliminary metamodels for three of the metrics, and subsequently in deriving the final form of the metamodel for each metric. In this respect, problems encountered in trying to derive a preliminary metamodel for the fourth metric, using the same approach applied in deriving the preliminary metamodels for the other three, led to a revision of the general approach to the regression analysis and the type of model to be fitted. This revision in turn allowed final metamodels for all four metrics to be developed satisfactorily, so the revision of the method is also explained. A particular feature of the revised regression approach was the proposed application of a *bootstrap* to the metamodel predictions. The principles of the bootstrap and the manner of its inclusion in the overall methodology are therefore also provided in this chapter.

Throughout the chapter, where possible, metrics and regression output data are summarised in plots and tables, supported by appendices with additional information where appropriate. Since output from the warm up and base case simulations is of key importance, the output from these simulations is discussed first and in some detail, beginning with evolution of topography.

4.2 OUTPUT FROM THE WARM UP AND BASE CASE SIMULATIONS

4.2.1 Evolution of topography

The warm up and base case simulations were run using the same parameter values. An uplift rate of 200 m Myr^{-1} was applied during the warm up, which was run for 50,000 years; the base case and other simulations were all run for 100,000 years, with no uplift. Output data were obtained from the simulations every 10,000 years, and examples from the topographic output are summarised as contour plots at specific time slices, in Figure 4.1. Elevations are measured relative to the outlet, which is assumed always to be zero.

a. Start of warm up simulation

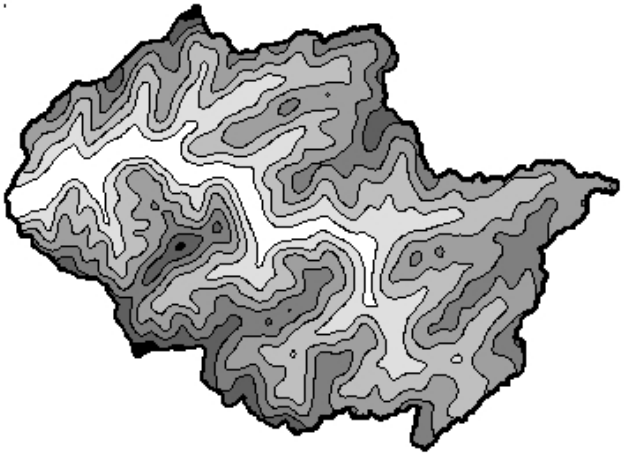

b. End of warm up simulation (start of base case simulation)

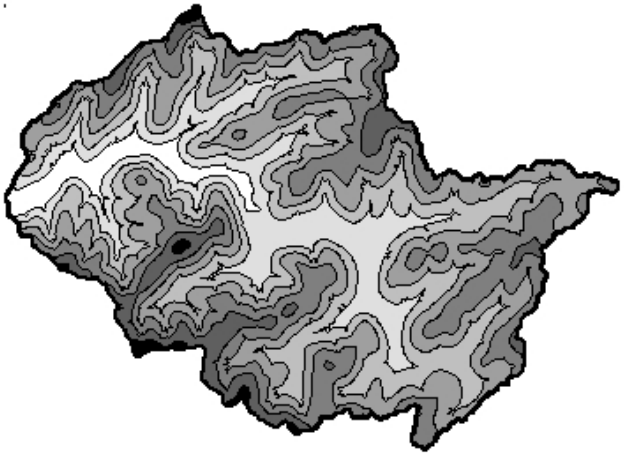

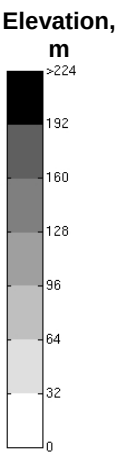

c. Base case simulation, after 50,000 years

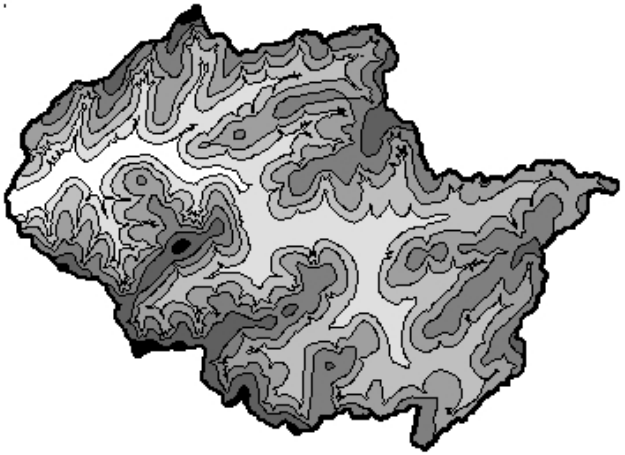

d. Base case simulation, after 100,000 years

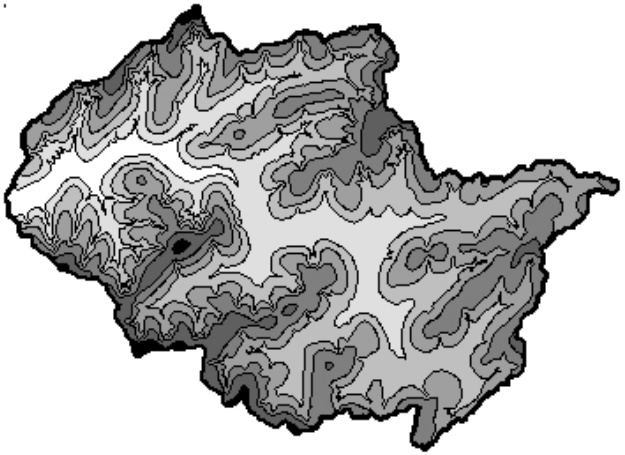

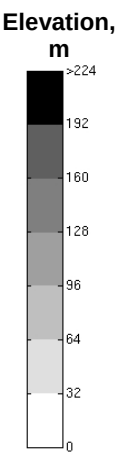

Figure 4.1, a-d: Contour plots showing evolution of the topography during the warm up and base case simulations.

Figure 4.1 clearly shows that the contours become more convoluted over time i.e. the catchment becomes more rugged, presumably as a result of fluvial processes (considered separately when examining evolution of the drainage network). Figure 4.1b shows evidence of an increase in maximum elevation compared with the start of the warm up simulation, caused by the applied uplift, and there is also evidence of valley infilling. For example, the area bounded by the lowest (32 m) contour has been reduced during the simulations, so that by the end of the base case, the area below this contour has been roughly halved since the start of the warm up.

As further evidence of changes in the catchment, Figure 4.2 shows the temporal trends in the mean elevation and the standard deviation of elevations. The maximum elevation is not shown, as this was found to shadow the mean trend almost exactly. The standard deviation of elevations, by contrast, gives an indication of the within catchment variability, which would not necessarily be expected to follow the trend in the mean.

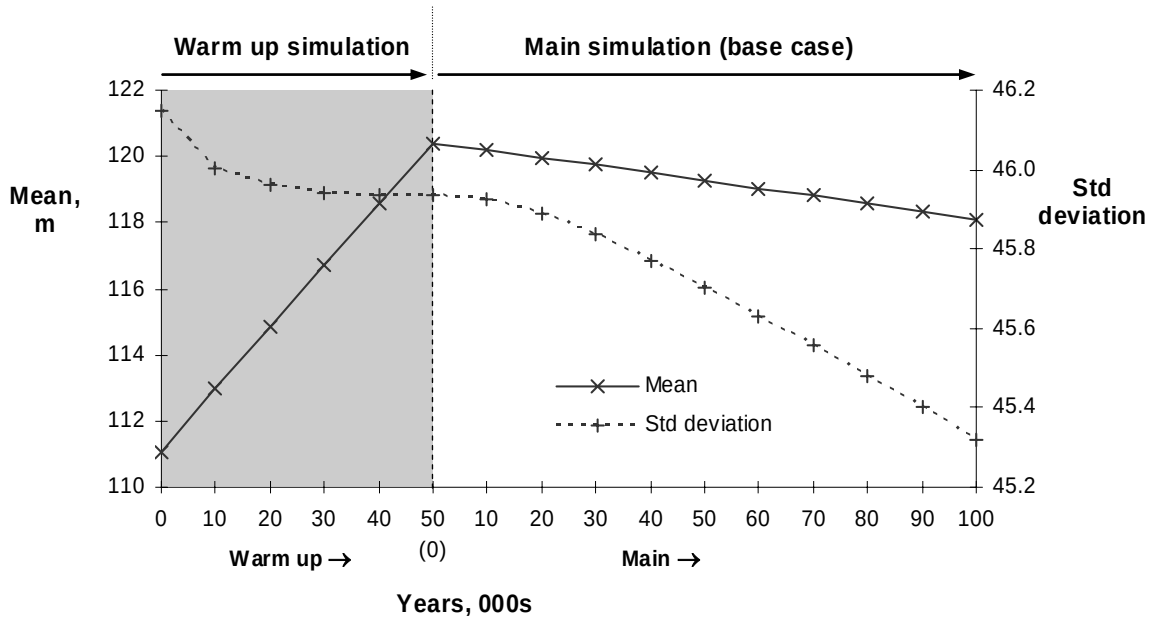

Figure 4.2: Mean and standard deviation of elevations during the warm up and base case simulations.

As expected, the mean elevation increased during the warm up phase, from about 111 m to over 120 m, but declined during the base case simulation, to about 118 m. The standard deviation declines from about 46.2 to 45.3 m, suggesting some flattening out of cells within the catchment over time i.e. more cells in the catchment have elevations clustered nearer the mean, possibly caused by sediment accumulating in these cells whilst the higher cells are being eroded. The elevation changes can also be examined as hypsometric curves of the

data at the same time slices, as shown in Figure 4.3. It should be noted that the elevations have not been normalised for the maximum elevation, as doing this obscures the differences between the curves. Even using the non-normalised data, the differences between them are small, particularly during the base case.

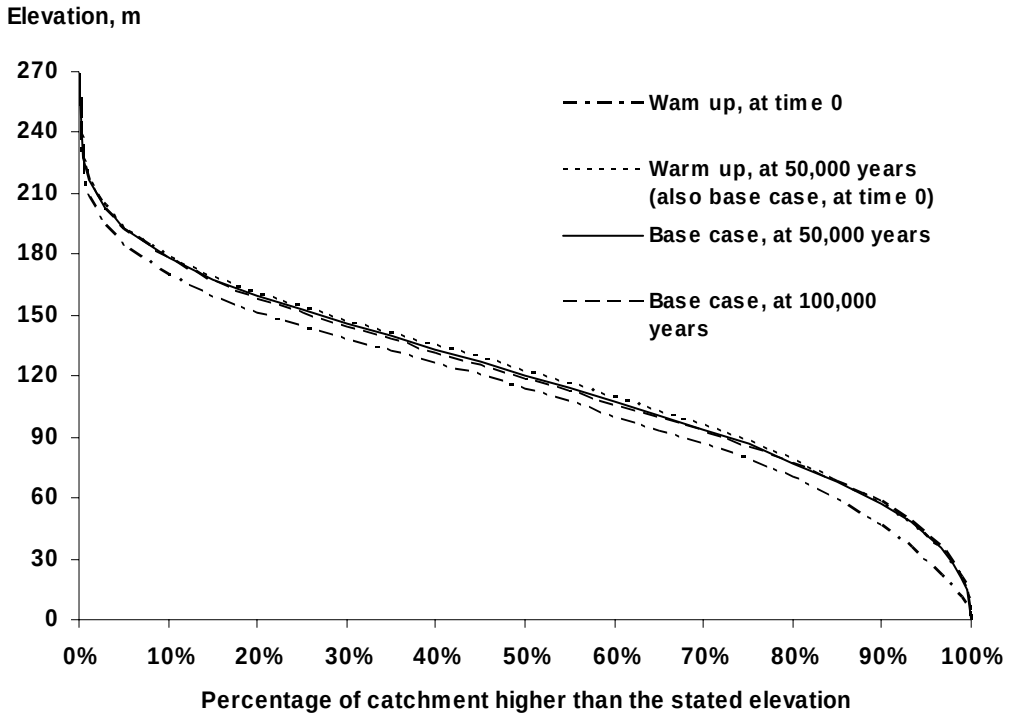

Figure 4.3: Hypsometric curves (non-normalised) of elevations during the warm up and base case simulations, using the same time slices as in Figure 4.1.

The main difference is between the curves at the start and end of the warm up simulation, resulting probably from the influence of uplift, although it is also likely that valley infilling has caused the slight rise in the middle portion of the warm up curve at 50,000 years. The base case curve at 100,000 years is generally lower than that at the start of the base case, evidencing net erosion of the catchment, but apart from these observations there is little to add regarding elevation changes. Attention is now turned to evolution of the drainage network.

4.2.2 Evolution of the drainage network

The channel network output is shown in Figure 4.4, the first time slice being at 10,000 years into the warm up simulation, and the later slices as for the elevation data. For greater clarity, the alluvial and bedrock channel sections are shaded differently.

a. Warm-up simulation after 10,000 years

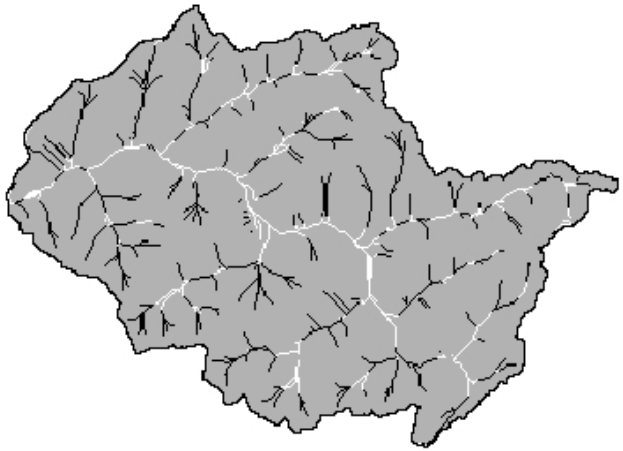

b. End of warm up simulation (start of base case simulation)

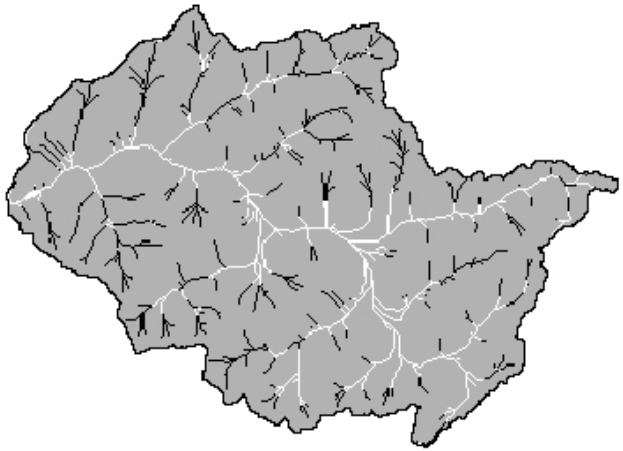

c. Base case simulation, after 50,000 years

d. Base case simulation, after 100,000 years

Figure 4.4, a-d: Evolution of the drainage network during the warm up and base case simulations, alluvial sections in white and bedrock in black.

The plots show that the catchment is dominated by bedrock sections during the warm up simulation, but that the alluvial channel sections become more extensive over time, extending mainly from the central floodplain towards the channel heads. By the end of the base case, bedrock sections are confined to short lengths at or near the channel heads. The network also appears to have become denser over time. Quantitatively, this is evidenced by the increase in the stream order, from 4 after 10,000 years of the warm up, to 5 at the end of the base case. There is also an increase in drainage density, and it interesting to contrast this with the change in the percentage of bedrock channels in the network (Figure 4.5).

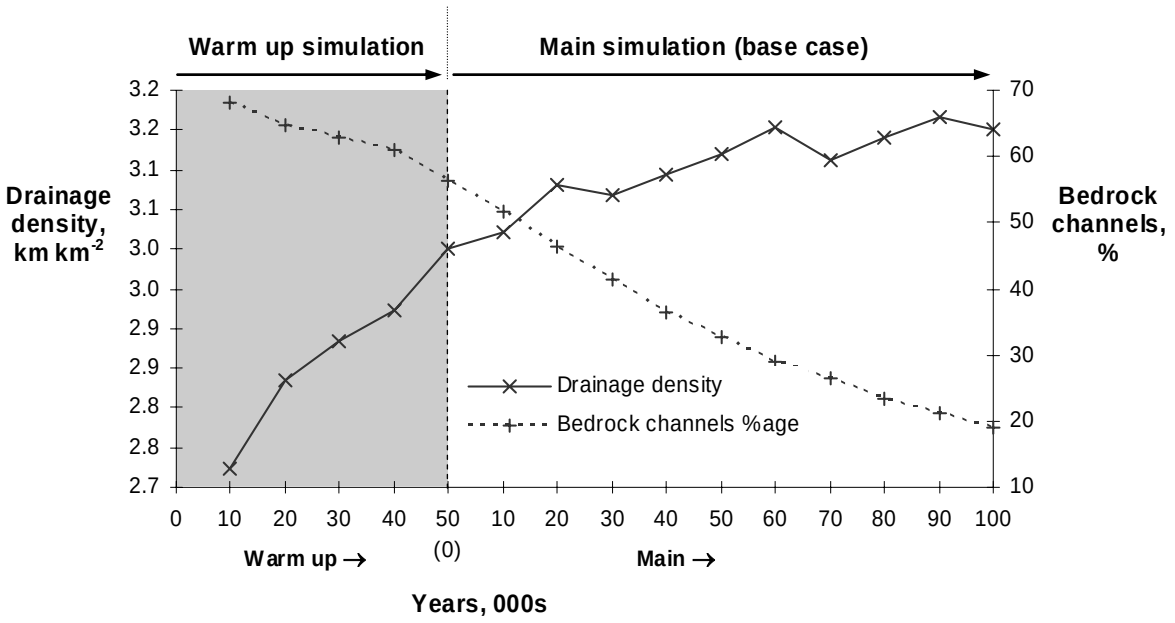

Figure 4.5: Drainage density and bedrock channel percentage during the warm up and base case simulations.

The data confirm that there is a marked change in the bedrock channel percentage, this declining from *c.* 70% of the network after 10,000 years of the warm up, to less than 20% of the network by the end of the base case. The drainage density, by contrast, increases from about 2.7 km^{-1} to 3.2 km^{-1} over the same period. As an aside, it is interesting to note that despite the parameter values being constant during the simulation, the decline in bedrock percentage is quite smooth, whereas the increase in drainage density is rather uneven.

The evolution of the sediment cover is now discussed.

4.2.3 Regolith depth and distribution of sediment

As with the elevation and drainage network output, examples from the sediment output are summarised as spatial plots (Figure 4.6). The first time slice is after 10,000 years of the warm up simulation, and the later time slices are the same as those used in plotting the elevation contours and drainage network. The distribution of sediment depths was found to be heavily skewed by a small number of cells with large values, and by a large number of cells which experienced little change during the simulations. Since neither a linear nor a log plot showed these values clearly, the depth scale has been set arbitrarily to emphasise spatial differences across the catchment.

a. Warm-up simulation after 10,000 years

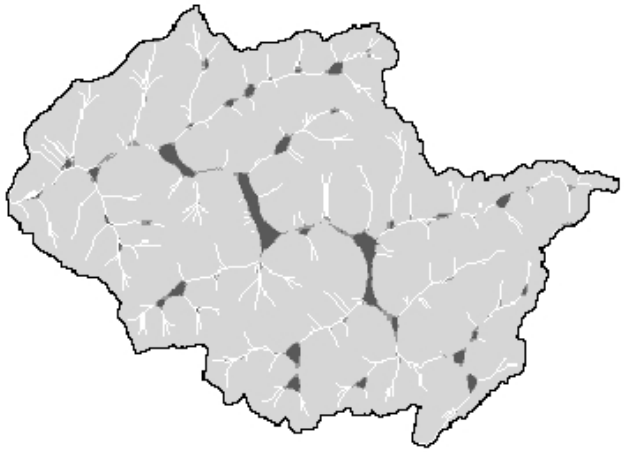

b. End of warm up simulation (start of base case simulation)

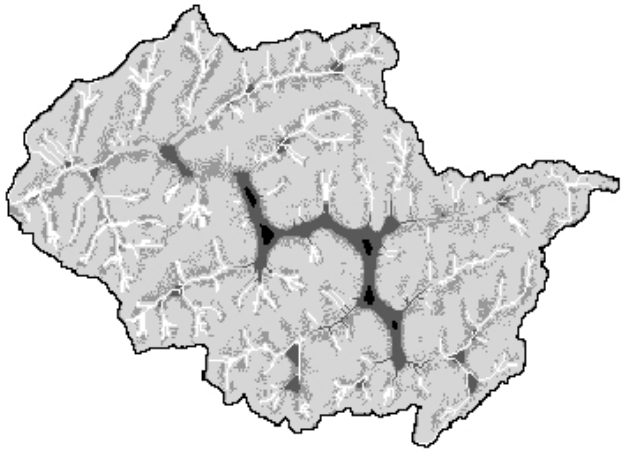

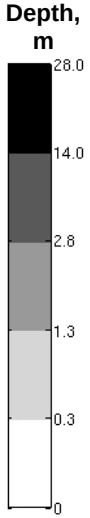

c. **Base case simulation, after 50,000 years**

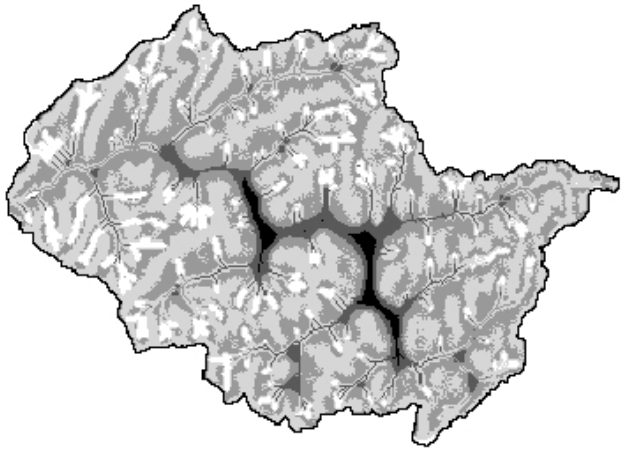

d. Base case simulation, after 100,000 years

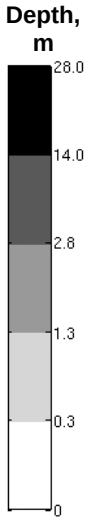

Figure 4.6, a-d: Regolith and sediment depths during the warm up and base case simulations.

Figure 4.6 shows that there is rapid sedimentation in stretches of the central floodplain, and in small sections along some of the channels, but that little variation in sediment depth occurs across the hillslopes until well into the base case. Some of the increase in sediment depth is likely to be due to weathering, although weathering rates will be slowed markedly as the depth of regolith increases[1]. After 50,000 years of the base case, however, there is a marked difference between regolith thicknesses near the tops and the bases of the hillslopes, arising from the influence of slope transport processes. Deposition in the central valley region also continues, probably driven by fluvial transport. By the end of the base case, the deepest areas of sediment are over 20 m thick in these areas. By contrast, the areas around the channel heads hold only a thin covering of regolith, or are even bare bedrock. Similarly, some of the cells bordering the channels have a thinner sediment cover than in either the hillslope cells immediately above them or in the channels cells below, the latter being silted up over time.

The temporal changes in regolith and sediment are also illustrated in figure 4.7.

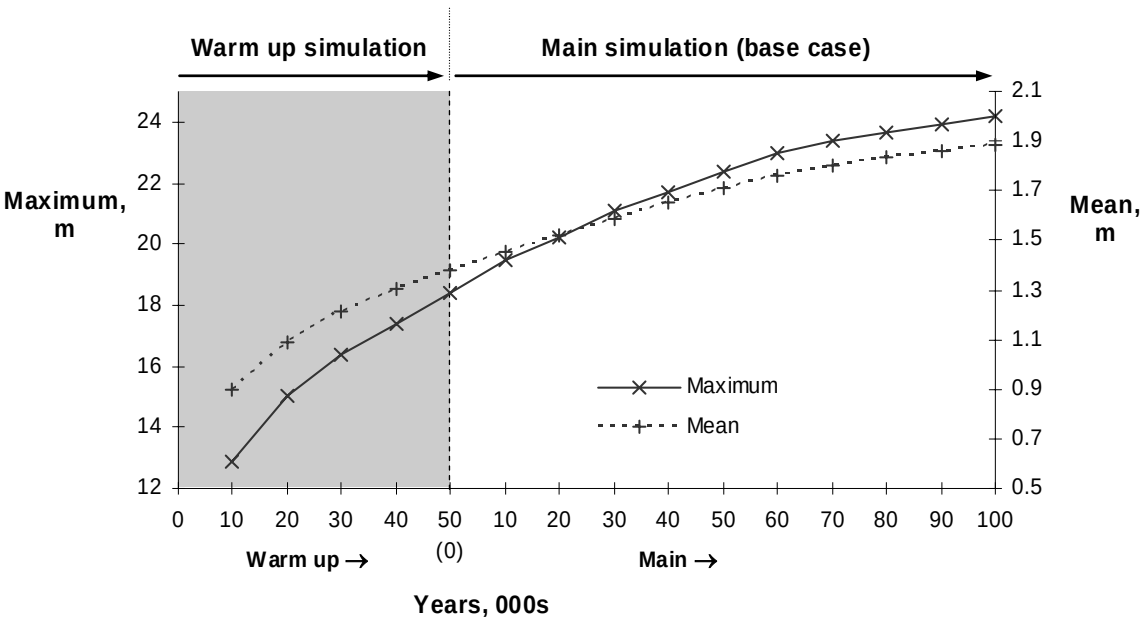

Figure 4.7: Maximum and mean regolith thickness (or sediment depths) during the warm up and base case simulations.

There is a marked difference between the maximum and mean values, these being about 24 m and 1.9 m respectively by the end of the base case simulation. The trends suggest that both the rate of deposition and the rate of accumulation by weathering are slowing over time during the base case simulation. The changes in sediment supply and distribution can also

[1] Using the base case values for k_w and m_w (Table 3.5, *q.v.*), increasing the regolith depth from 0.5m to 1m reduces the weathering rate from *c.* 53 x 10^{-3} m kyr^{-1} to *c.* 12 x 10^{-3} m kyr^{-1}.

be viewed by examining the trends in the sediment yield and sediment delivery ratio of the catchment. These quantities are derived from calculations using GOLEM's elevation and sediment output data, as explained in Appendix F, and are plotted in Figure 4.8.

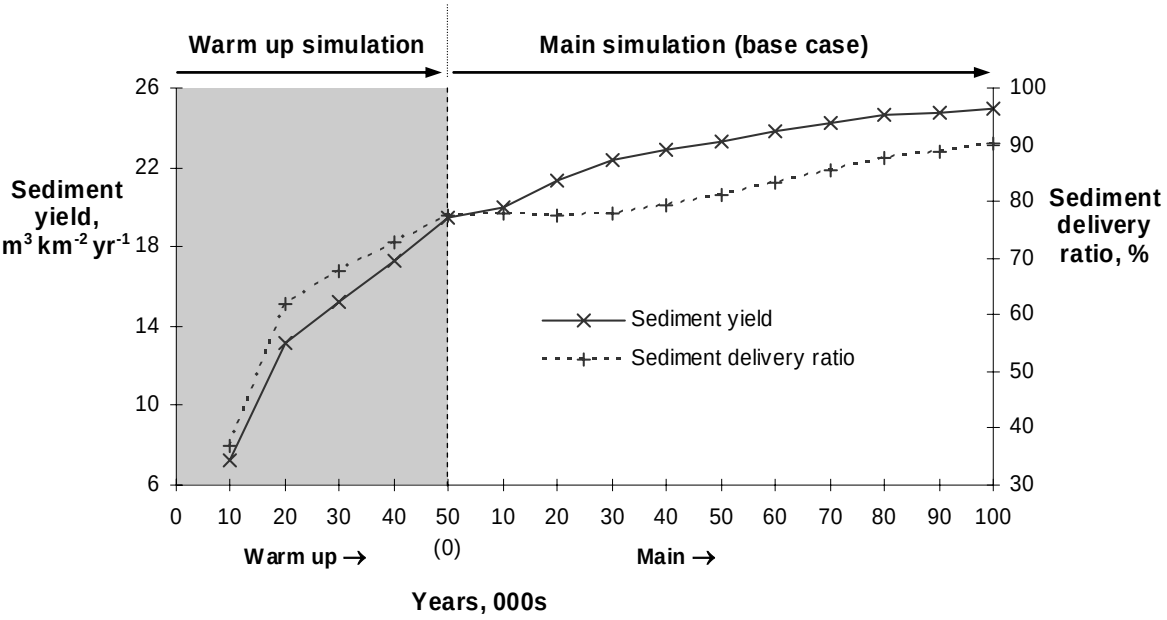

Figure 4.8: Sediment yield and sediment delivery ratio during the warm up and base case simulations.

The values for these metrics both increase over time, but the rate of increase is slowing towards the end of the base case. By then, the sediment yield is about 25 m^3 km^2 yr^{-1}, which, as explained previously, seems reasonable compared with the figure of *c.* 60 m^3 km^2 yr^{-1} obtained for the North Fork Smith River (subsections 3.5.1 and 3.5.2, *q.v.*). The sediment delivery ratio at the same time is about 90%, rather higher than might be expected normally (e.g. Richards, 1993). That it is so high is probably owing to the small size and ruggedness of the catchment, and to the processes and conditions applied during the simulations, in particular the constant climate and the absence of solution weathering.

4.2.4 Slope evolution and gradients

Examples from the slope output are summarised in the plots shown in Figure 4.9. The first time slice in the warm up simulation is at time zero, and the later time slices are the same as those used in the spatial plotting of the elevation, drainage network and sediment data.

a. Start of warm-up simulation

d. End of warm up simulation (start of base case simulation)

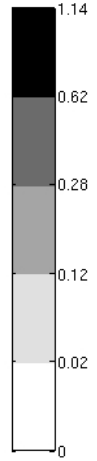

c. Base case simulation, after 50,000 years

d. Base case simulation, after 100,000 years

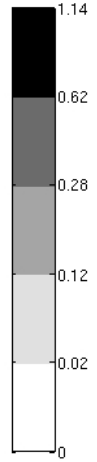

Figure 4.9, a-d: Evolution of slopes during the warm up and base case simulations.

As with the sediment data, the distribution of gradients is heavily skewed by a small number of high values. Also, the central floodplain experiences deposition during the warm up and early part of the base case simulations, leading to gentle gradients which are difficult to distinguish from each other. The gradient scale is therefore arbitrarily set, to emphasise the main differences over space. Changes in slopes over time are also illustrated (Figure 4.10), showing trends in the mean and maximum gradients.

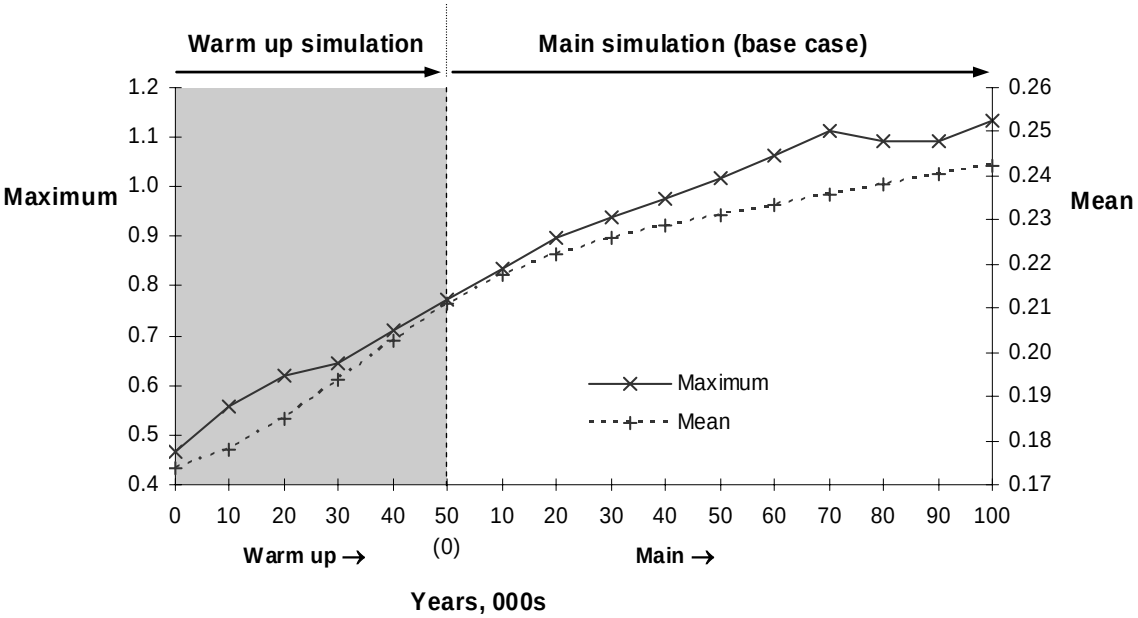

Figure 4.10: Maximum and mean gradient during the warm up and base case simulations.

Both mean and maximum gradients increase during the warm up and base case simulations, the rate of increase in the mean gradient declining slightly after about 20,000 years of the base case simulation. To obtain a better idea of the distribution of gradients across the catchment over time, the gradient data can also be presented in hypsometric style curves, as shown Figure 4.11.

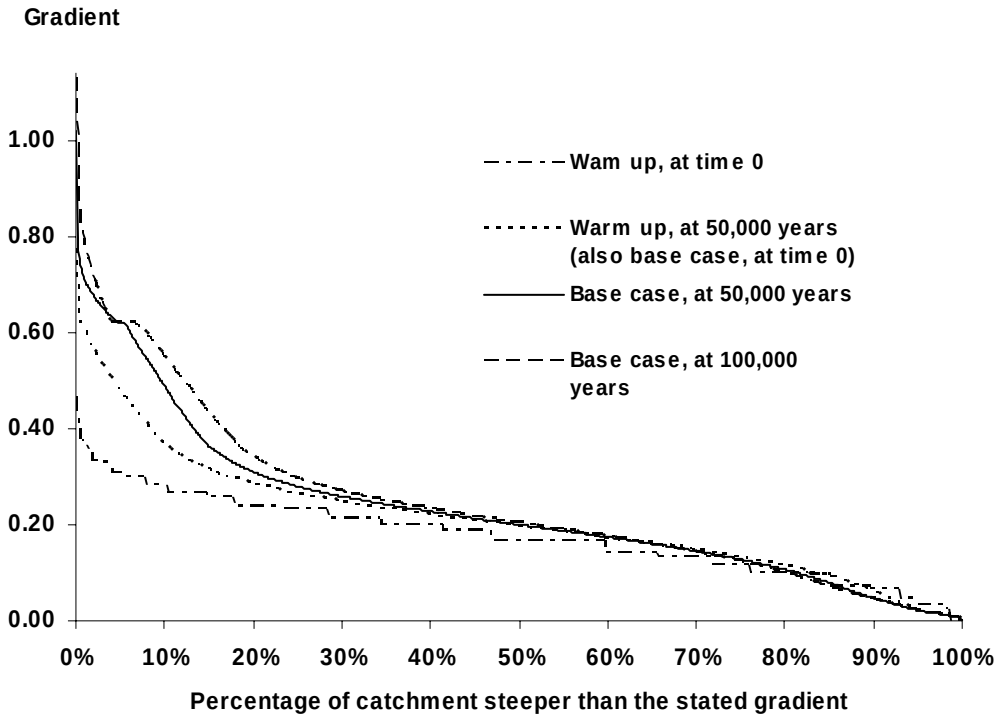

Figure 4.11: Hypsometric style curves of gradients (non-normalised) during the warm up and base case simulations, using the same time slices as in Figure 4.9.

Figure 4.11 shows that over most of the catchment, gradients generally increase during the warm up simulation, and rather less so during the base case. During the latter, only small changes in the proportion of cells with gradients of about 0.25 or lower occur, evidenced by small differences in the curves. However, for gradients of *c.* 0.25 and over, an increase over time occurs in the proportion of steeper gradients, the maximum rising to over 1 by the end of the base case. The knick in the base case curves at 50,000 and 100,000 years corresponds to a gradient of 0.62 - the threshold for shallow landsliding (Table 3.5 *q.v.*) - and indicates that landsliding is taking place in the catchment, some slopes being able to retain a cover of regolith, whilst steeper ones are left as bare bedrock. Looking at the slope and sediment plots in Figures 4.9 and 4.6 respectively, the active landsliding areas appear to be located around and near the channel heads, where channels are cutting back into the hillslopes[2].

This concludes the initial assessment of the evolution of the catchment. The discussion now turns to consideration of the output from the central composite design sample as a whole, and the selection of the metrics used to represent this output in the metamodels.

[2] This accords with the author's personal observations, reported in subsection 3.5.1. Slopes leading down to the channels near the channel heads were so steep that it was difficult to keep one's footing when clambering on them. Although undergrowth was too dense to permit a survey of the channel heads directly, that GOLEM should predict landsliding at or near the channel heads seems sensible.

4.3 RESULTS FROM THE CENTRAL COMPOSITE DESIGN SIMULATIONS AND CHOICE OF METRICS

4.3.1 Focus on factorial point results

In examining the results from the central composite design sample, the aim is to review the attributes of a selection of possible metrics, and make a choice of which ones to use as metamodel subjects. In this respect, the author could have considered simply selecting metrics at random, regardless of their sensitivity to the parameter values applied during the initial experiment. However, this would probably entail including some metrics whose responses are very insensitive to the parameters, thus indicating from the outset a high degree of model equifinality. There would be little point in expending effort deriving metamodels for such metrics, as the results from the parameter space exploration with the metamodel would probably only confirm the initial impression. By contrast, metrics which appear to be more sensitive to the parameter changes provide a better opportunity to explore how equifinality may differ between one metric and another, and how the use of different combinations of metrics and parameters may affect equifinal outcomes. For this reason, the metrics chosen here as metamodel subjects are those which appear to be the more sensitive ones, at least as compared with the others under consideration.

With this point made, the focus here is on landscape metrics at 100,000 years i.e. at the end of the base case simulation. For some metrics, which include time in their physical dimensions (e.g. sediment yield or sediment delivery ratio), output data are required from two time periods in order to calculate the metric. Such metrics are calculated herein using output from the 90,000 and 100,000 year time slices. Admittedly, this is a rather coarse time interval, but there were serious practical difficulties in trying to run the simulations so that output was saved more frequently, so finer temporal resolutions were not attempted.

In the initial examination of output from the model, the star point simulations have been omitted, this serving to emphasise variations exhibited by the base case and factorial point samples i.e. within the factorial space. Since it is impractical to visualise all the output metrics spatially, as in Figures 4.6 and 4.9 for example, the data are presented here using temporal plots. Besides making the presentation easier, the focus on temporal trends is also useful later in the thesis, and is discussed in Chapters 6 and 7. Metrics describing different elevation attributes are considered first.

4.3.2 Elevation results and metrics

Figure 4.12 shows the mean and standard deviation of elevations for the base case and all factorial point cases.

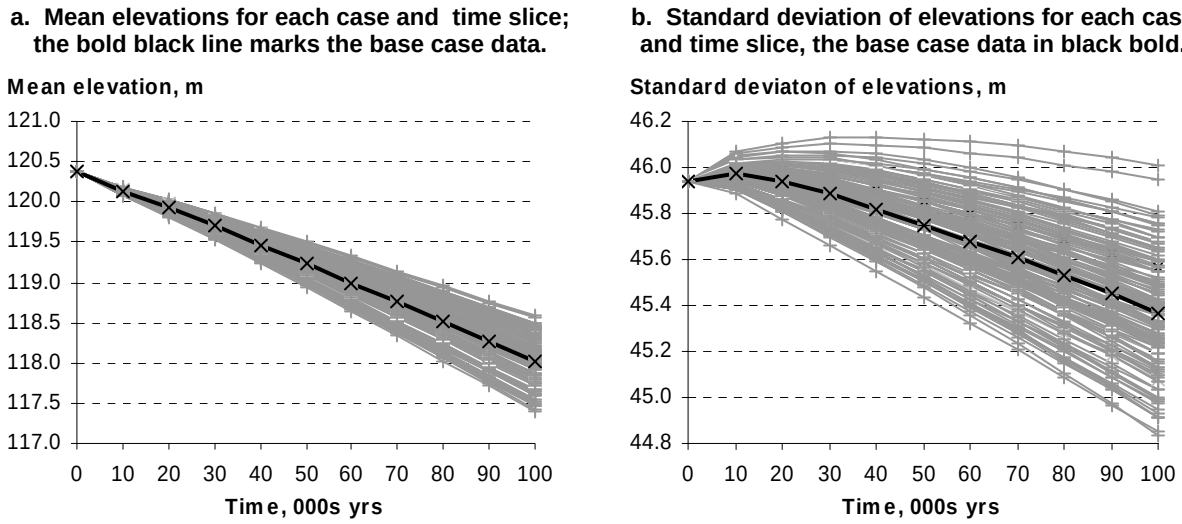

Figure 4.12, a and b: Mean and standard deviation of elevations for the base case and all factorial point cases in the central composite design sample.

The plots show that the base case response always lies broadly in the middle of each range of the factorial point results throughout the simulations, the range in the latter increasing over time. It is helpful to recall here that the factorial part of the central composite design comprises the 128 simulations using values corresponding to the +1 and -1 levels for each parameter, listed in Table 3.5, and used in the design level combinations listed in Appendix D, and actual value combinations listed in Appendix E. For both metrics plotted here, the range of results from these combinations at 100,000 years is still quite small, being only about 1.2 m for each. Expressed as percentages of the base case result, the ranges are *c.* 1.0% for the mean elevation data, and *c.* 2.6% for the standard deviation data.

Although there is some variation within the results for each of these metrics, they say little about any differences between the modelled landscapes generated by the factorial point and base case samples. In particular, in a geomorphological investigation, it can be easily envisaged that a LEM would be used to simulate the evolution of a landscape from a past time to the present, in the manner presented in Figures 1.2 or 1.3 (but not presuming the equifinality shown in those examples!). In such a situation, the present landscape forms the reference with which the simulations are to be compared. It is appropriate, therefore, to consider how the factorial point simulations would compare with a reference landscape. In

this instance, however, we do not have a real landscape to use as a 'target' for the simulations, and in the absence of such, the base case is used as the reference instead.

It will be appreciated that the use of a the base case as a common reference provides a constant condition for comparative purposes, as would indeed be true if a real landscape were being considered. Other metrics may therefore be devised which calculate directly a measure of the differences between each factorial point sample result and the base case. In this instance, the first step is to calculate the difference data, by subtracting the elevations of the base case, cell for cell, from those of each example parameter case. The difference data can then be analysed and manipulated to show the differences in various ways. As examples, Figure 4.13a shows the standard deviations of these differences, and Figure 4.13b the mean of the absolute values of the differences.

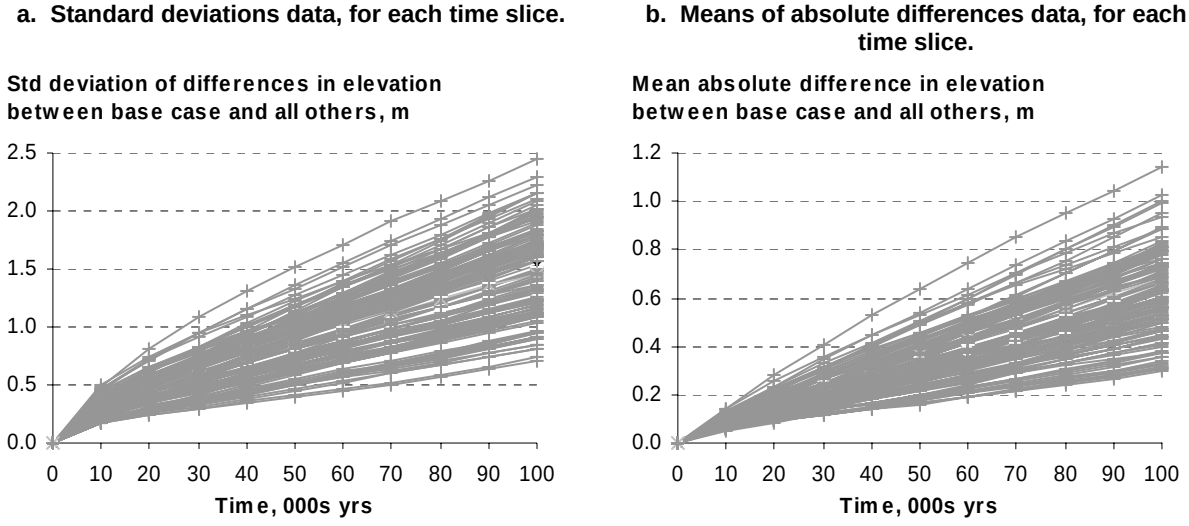

Figure 4.13, a and b: Standard deviation of differences and mean of absolute differences in elevation between the base case and each factorial point case in the central composite design sample.

In both plots, the range in the results clearly increases over time. However, it is difficult to assess what the spreads in the data at 100,000 years actually indicate, or how the sensitivity or otherwise of the metrics should be assessed. For example, if expressed as percentages of the mean elevation from the base case, the range in the data is *c.* 1.5% for the standard deviation of elevation differences at 100,000 years, and *c.* 0.8% for the mean of absolute differences at the same time, which suggests low sensitivity. These metrics also give no indication of how well the base case and other landscapes differ from each other over *space*. For example, a big standard deviation of the differences could mean that most of the elevation differences are small, but spread over a large extent of the landscape, or by

contrast, that the differences are large, but confined to a only small areas of the landscape. The mean absolute difference data could be interpreted similarly.

To try to incorporate an indication of differences over space, a different metric is devised, called the percentage topographic difference metric, or more simply the 'topographic metric'. This is calculated from the elevation difference data of the two landscapes, and requires a simple routine for counting the number of cells where the absolute difference is less than one metre. One metre is selected here as this is comparable with the error in the initialising DEM of the Smith River catchment (subsection 3.5.1 *q.v.*). Moreover, it is also considered quite demanding, in that a researcher would probably be very satisfied to have been able to generate a modelled landscape after 100,000 years which agrees with a real one to within ±1 m at every point.

Rather than express the total differences as a number of cells, the metric is calculated here as a proportion of the total catchment area, and converted to a percentage. The metric can thus be understood as stating that "x % of the landscape generated by parameter case *i* lies within ±1 m of the base case …". This greatly assists interpretation of the differences between the landscapes, as compared with the other elevation-based metrics considered here. The topographic metric results calculated in this way are plotted in Figure 4.14.

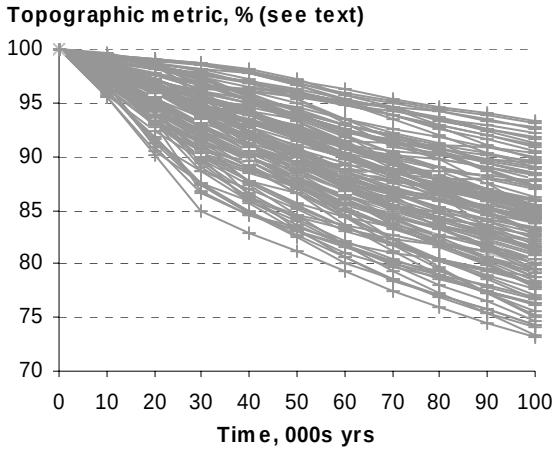

Figure 4.14: Results for the topographic difference metric for each factorial case in the central composite design sample.

The figure shows that the spread in the results for the topographic metric increases during the simulations. At 100,000 years, the topographic metric ranges between about 73% and 94%, so some of the landscapes appear to be very similar to the base case, whilst others

differ markedly from it. The higher sensitivity of the topographic metric, compared with the mean elevation and standard deviation of elevations (Figure 4.12), is clearly evident.

In summary, of the elevation metrics considered here, the author decided that the topographic metric was the probably the most useful, and chose this as a suitable subject for metamodelling. Discussion now turns to drainage density and related metrics.

4.3.3 Drainage density and related metrics

Figure 4.15, a and b, shows the temporal trends in the drainage density and bedrock channel percentage for the base case and factorial point cases. It will be noted that the base case response lies broadly in the middle of the range of results for both metrics. However, the split in the drainage density results is most curious, and is revealed later to be caused by the effects of two parameters in particular (section 4.4 *q.v.*). The reduction in the bedrock channel percentage continues throughout the simulation in all of the samples. Both metrics appear to be suitable candidates for metamodelling, the range in results (at 100,000 years) being *c.* 32% for the drainage density, and *c.* 130% for the bedrock percentage (a very high figure compared with the other metrics), when expressed as percentages of the respective base case values for these metrics.

a. Drainage density data, the base case shown by the bold black line.

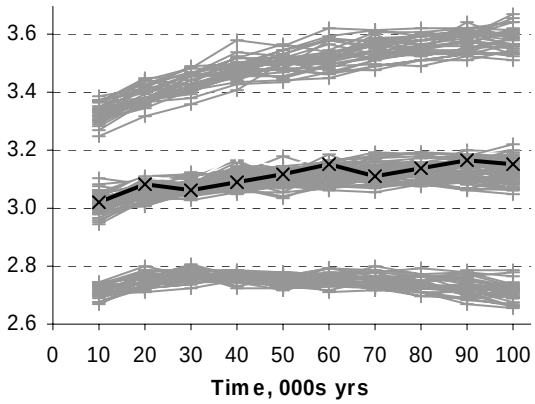

b. Change in the bedrock channel percentage over time, the base case shown by the bold black line.

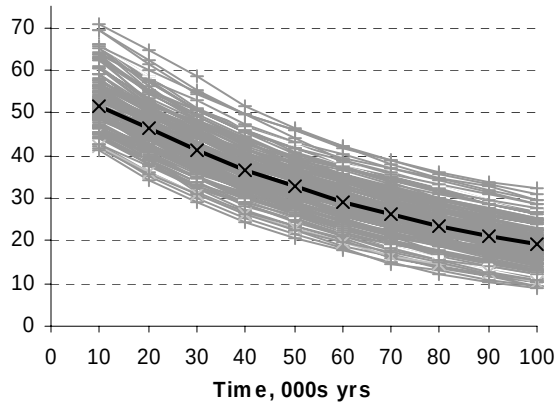

Figure 4.15, a and b: Drainage density and bedrock channel percentage for the base case and each factorial point case in the central composite design sample.

Other metrics related to the channel network were also considered, but rejected. For example, stream length is simply a variant of the drainage density, and the stream order was a coarse metric, showing little variation between the sample cases. Of the two metrics plotted above, the author decided to use drainage density, and to conduct analysis using the bedrock channel percentage later if time permitted.

4.3.4 Metrics related to sediment and its distribution

Figure 4.16 shows the results for the maximum and mean sediment depth, the sediment yield, and the sediment delivery ratio.

a. Maximum sediment depth at each time slice, the base case shown by the bold black line.

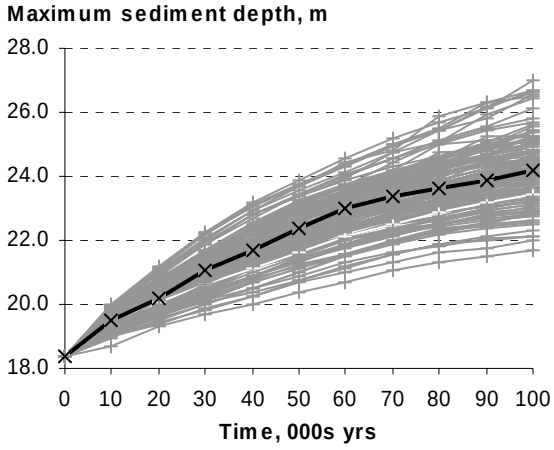

b. Mean sediment depth at each time slice, the base case shown by the bold black line.

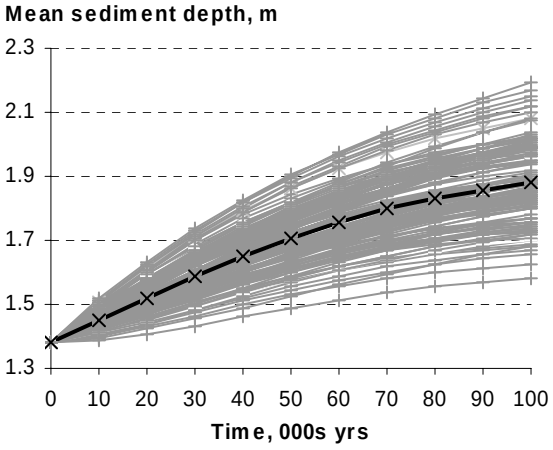

c. **Sediment delivery ratio data, the base case shown by the bold black line. The method of calculation is explained in Appendix F.**

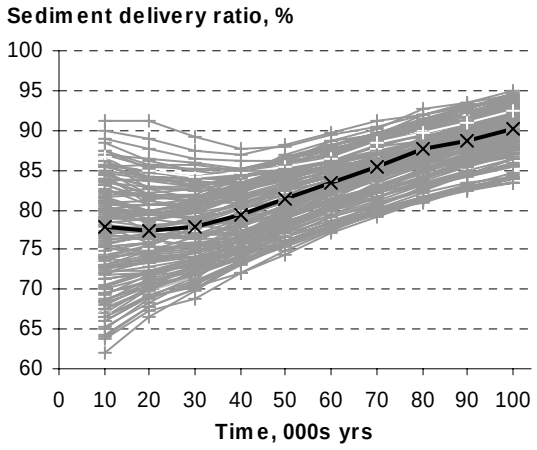

d. Sediment yield data, the base case shown by the bold black line. The method of calculation is explained in Appendix F.

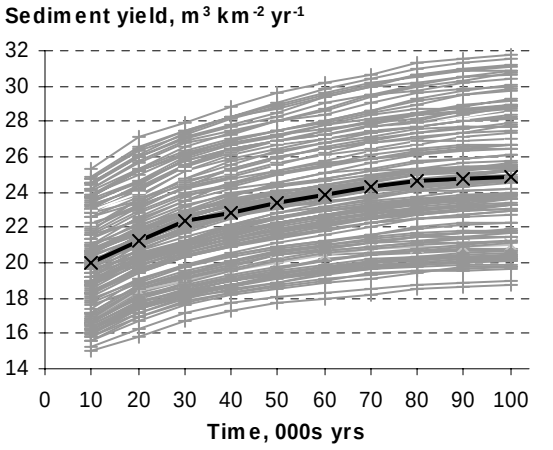

Figure 4.16, a-d: Maximum and mean sediment depths, and sediment yield and sediment delivery ratio, for the base and factorial point cases in the central composite design sample.

As with previous data, the base case lies in the middle of the range of results for each metric. All the metrics here show a scatter at 100,000 years, indicating the they may be used as discriminating measures of different model responses. The spreads in the results for the mean sediment depth and the sediment yield, at respectively *c.* 35% and *c.* 55% of the base case values, suggests that these two would be useful subjects for metamodelling. However, the author thought it would be useful to contrast sediment yield and sediment delivery ratio, as these are both metrics incorporating time as a physical dimension. Also, the sediment delivery ratio appears to be less sensitive than the sediment yield, with a spread of *c.* 13% (expressed as a percentage of the base case value), so a comparison of their relative equifinality would be of interest. Accordingly, sediment yield and sediment delivery ratio were therefore selected as subject metrics for metamodelling.

4.3.5 Gradients and other possible metrics

In addition to the metrics reviewed above, the author considered others which might be of interest. Figure 4.17 shows the maximum and mean gradient over time, and the hypsometric style curve (non-normalised) for gradients at 100,000 years. As with the previous metrics, the base case responses are broadly in the middle of the range for each metric. Since the author had already chosen four metrics for metamodelling work, none of these was actually selected for the main research, the author choosing to keep them in reserve, to use if required or time permitted. Nevertheless, the output is of interest, in that it indicates further the pattern of responses possible in LEM output metrics. In this respect, a gradient metric is used in support of a discussion point, in Chapter 6; similarly, the types of response seen here in all of the metrics, whether actually used in the metamodelling or not, are used in Chapter 7 as further evidence of LEM outputs and responses more generally.

a. Maximum gradients at each time slice, the base case shown by the bold black line.

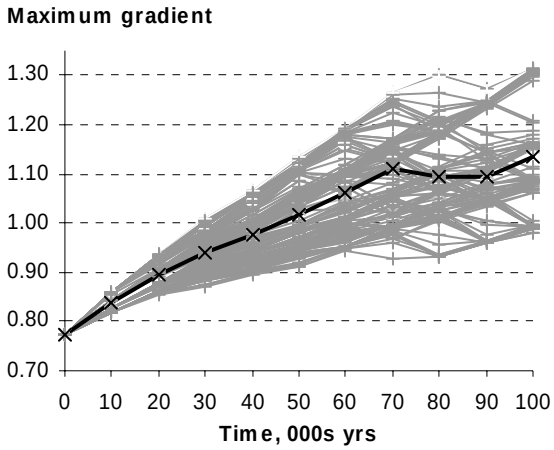

b. Mean gradients at each time slice, the base case shown by the bold black line.

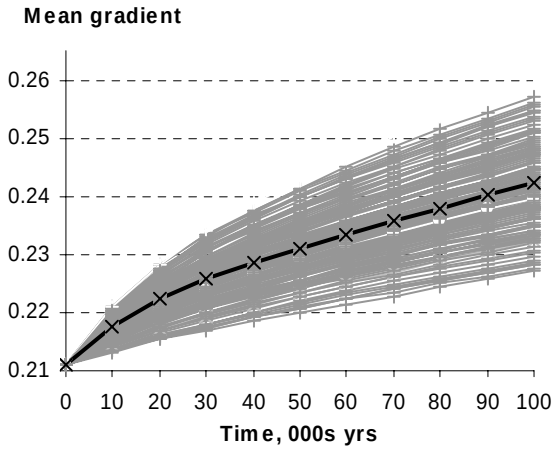

c. **Hypsometric style curves of gradient data (non-normalised), the base case shown by the bold black line. The small differences between the curves, particularly for gradients <0.3, will be noted.**

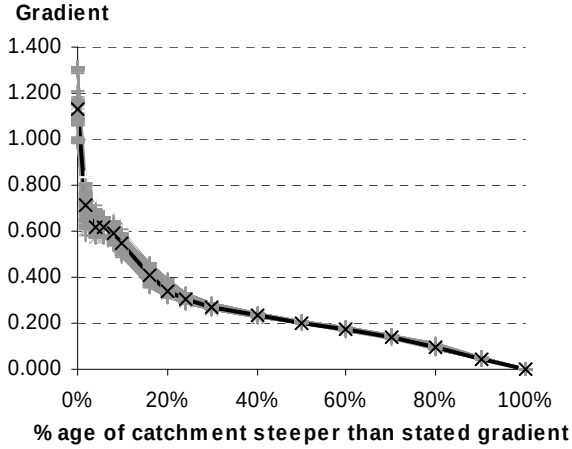

Figure 4.17, a to c: Maximum and mean gradients at each time slice, and hypsometric style curves of gradient (non-normalised data) at 100,000 years, for the base case and each factorial point case in the central composite design sample.

Besides the metrics discussed above, the author considered other metrics, and compound metrics based on manipulation of two or more landscape output descriptors, similar to the ideas discussed by Church (2003). These included hypsometric integral and equivalent integrals relating to sediment, slopes, and of differences and absolute differences in all of the foregoing. These were all rejected, however, as exploratory work on the results indicated that hypsometric integrals could be treated as proxies for mean values, and that they were generally insensitive to changes in parameter values in the factorial space.

Another possibility was to devise a metric summarising the log|area| v_s log|slope| relationships used by Willgoose and other workers. For example, Willgoose (1994a and b) discusses in detail the importance of area-slope curves of this kind, and their usefulness as indicators of differences in the processes acting on landscapes. However, the necessary data from each factorial point case produced wide scatters of points at 100,000 years, and simplification of the data, using for example the mean, appeared highly problematic. A metric based on slope-area relationships was therefore not considered further.

Having chosen therefore four metrics as subjects for metamodelling, the discussion now turns to derivation of the metamodels themselves.

4.4 DERIVATION OF METAMODELS

4.4.1 Main effects, all metrics

The analysis principles set out in subsection 3.3.1 indicate that, where possible, main effects should be identified before interactions, as the latter will in all likelihood turn out to be less powerful than the former. In trying to identify the main effects, the sample points of most interest are the central (base case) and star point values. Although the main focus on output is at 100,000 years, plots of the main effects of each parameter over time help to indicate the stability or otherwise of a parameter's main effect during the course of the simulation. The consideration of main effects therefore includes plots over time, and also main effects plots at 100,000 years. Each of the four selected metrics is considered in turn.

Sediment yield

Figure 4.18 shows that, with the exception of the parameter m_w, each parameter has a consistent effect on sediment yield during the simulation, the response to a star point value always being either above or below the base case response. The data also show that some main effects are clearly positive (for k_w, k_d, k_f, and k_b), with a high parameter value raising the sediment yield over time, and a low parameter value lowering it; similarly, other parameters clearly have a negative main effect (τ_c, n_{ci}, t_{ci}, s_{cr} and τ_b), so that the reverse applies.

To identify these effects more clearly, the output at 100,000 years is shown in Figure 4.19. This time, a common scaling is also used for the y-axis, so as to emphasise any differences in the size of each parameter's main effect, and any positive or negative trend. For equivalent reasons, the parameter values on the x-axis are stated in terms of their scaled design levels, defined from here onwards as follows:

$$x' = \frac{x - x_0}{x_{+1} - x_0}, \qquad 4.01$$

where x' is the scaled design level value, x is the actual value, and x_{+1} and x_0 are the values of x corresponding to the upper factorial and central points (base case) respectively, as listed in Table 3.5. Thus, the sediment transport coefficient, k_f, has by far the strongest main effect, the sediment yield ranging from about 14 $m^3 km^{-2} yr^{-1}$ at $-\alpha$ to about 33 $m^3 km^{-2} yr^{-1}$ at $+\alpha$. The positive trend is clearly shown, and there is a slight curvature in the relationship. Much smaller positive main effects are also shown by k_w, k_d and k_b. Of the negative main effects, the strongest is shown by the sediment transport threshold, τ_c, and appears to be nearly linear, the yield ranging from about 31 $m^3 km^{-2} yr^{-1}$ at $-\alpha$ to about 18 $m^3 km^{-2} yr^{-1}$ at $+\alpha$. Smaller negative effects are displayed by n_{ci}, t_{ci}, s_{cr} and τ_b, some with curvature.

Notes: 1. The letter above each plot denotes the parameter value being varied.
2. Sediment yield units throughout are m^3 km^{-2} yr^{-1}; the y-axis ranges for k_f and τ_c are extended to accommodate the size of their main effects.
3. Legend: +α ; base case ; −α

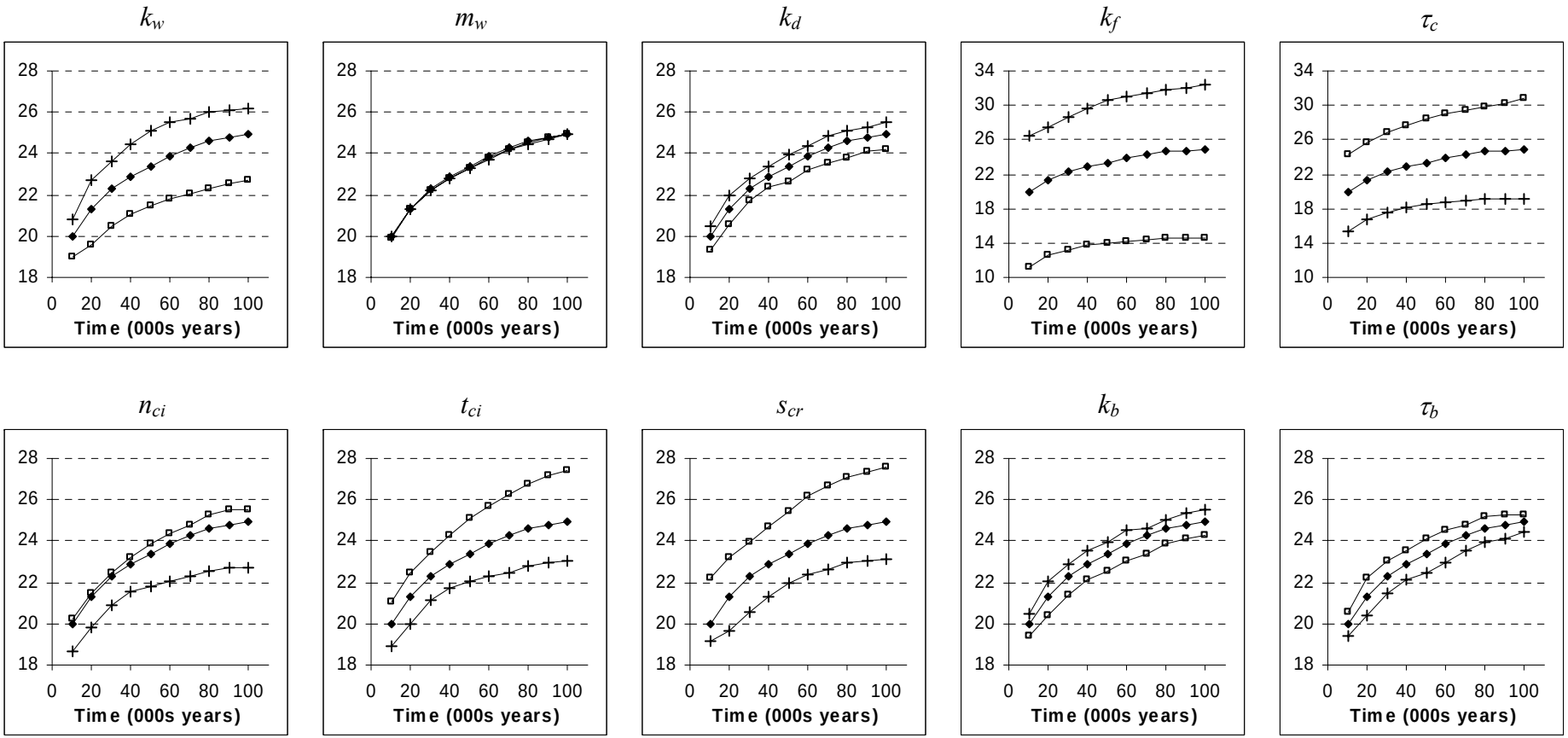

Figure 4.18: Plots for each parameter of sediment yield (y-axis) against time (x-axis), contrasting the star point simulations with the base case.

Notes: 1. The letter above each plot denotes the parameter value varied.
2. Sediment yield units throughout are m^3 km^{-2} yr^{-1}; the y-axis ranges are also common throughout, to emphasise differences between parameters in the main effects.

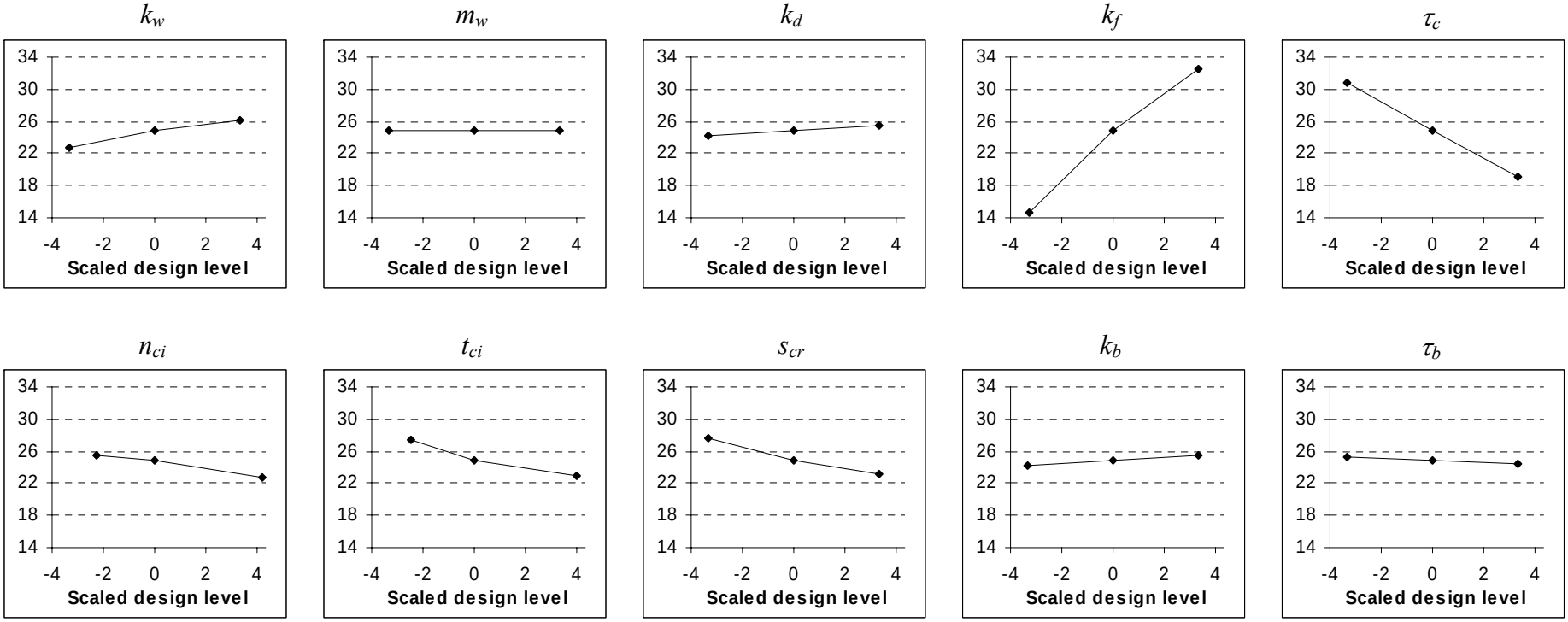

Figure 4.19: Plots showing the main effects of each parameter on sediment yield (y-axis) after 100,000 years. Note that only the star point and base case results are plotted, using parameter values (x-axis) given in terms of their scaled design levels (eq. 4.01 *q.v.*).

Drainage density

Plots of the temporal trend in the main effects of each parameter are shown in Figure 4.20. They show that apart from the effects exhibited by t_{ci} and n_{ci}, the effects of each parameter are quite small, the drainage densities ranging between about 3.0 km^{-1} and 3.25 km^{-1} only for these weaker parameters; response to changes in these parameters also appears somewhat erratic, so that for some parameters the star point curves actually cross each other at various times during the simulation (e.g. m_w, k_d, k_b and τ_b). The plots for these minor parameters (minor, at least, with respect to their effect on this metric) therefore track the base case line fairly closely, albeit with slight variation to either side.

Regarding the main effects of n_{ci} and t_{ci}, both are strongly negative, with that of t_{ci} being slightly greater than that for n_{ci}. This is well illustrated in Figure 4.21, which shows all the main effects at 100,000 years, using the scaled design levels on the x-axis (eq. 4.01, *q.v.*) and a common y-axis scale to emphasise differences between the parameters' effects. Most of the plotted lines are horizontal or very nearly so, whereas the plots for n_{ci} and t_{ci} by comparison are both steeply sloping, the drainage densities ranging respectively from about 3.7 km^{-1} to 2.2 km^{-1} and 4.3 km^{-1} to 2.45 km^{-1}. The main effect for t_{ci} also appears to be distinctly curved.

Notes: 1. The letter above each plot denotes the parameter value being varied.
2. Drainage density units throughout are km km^{-2} ; the y-axis ranges for n_{ci} and τ_{ci} are extended to accommodate the size of their main effects.
3. Legend: +α ; base case ; −α

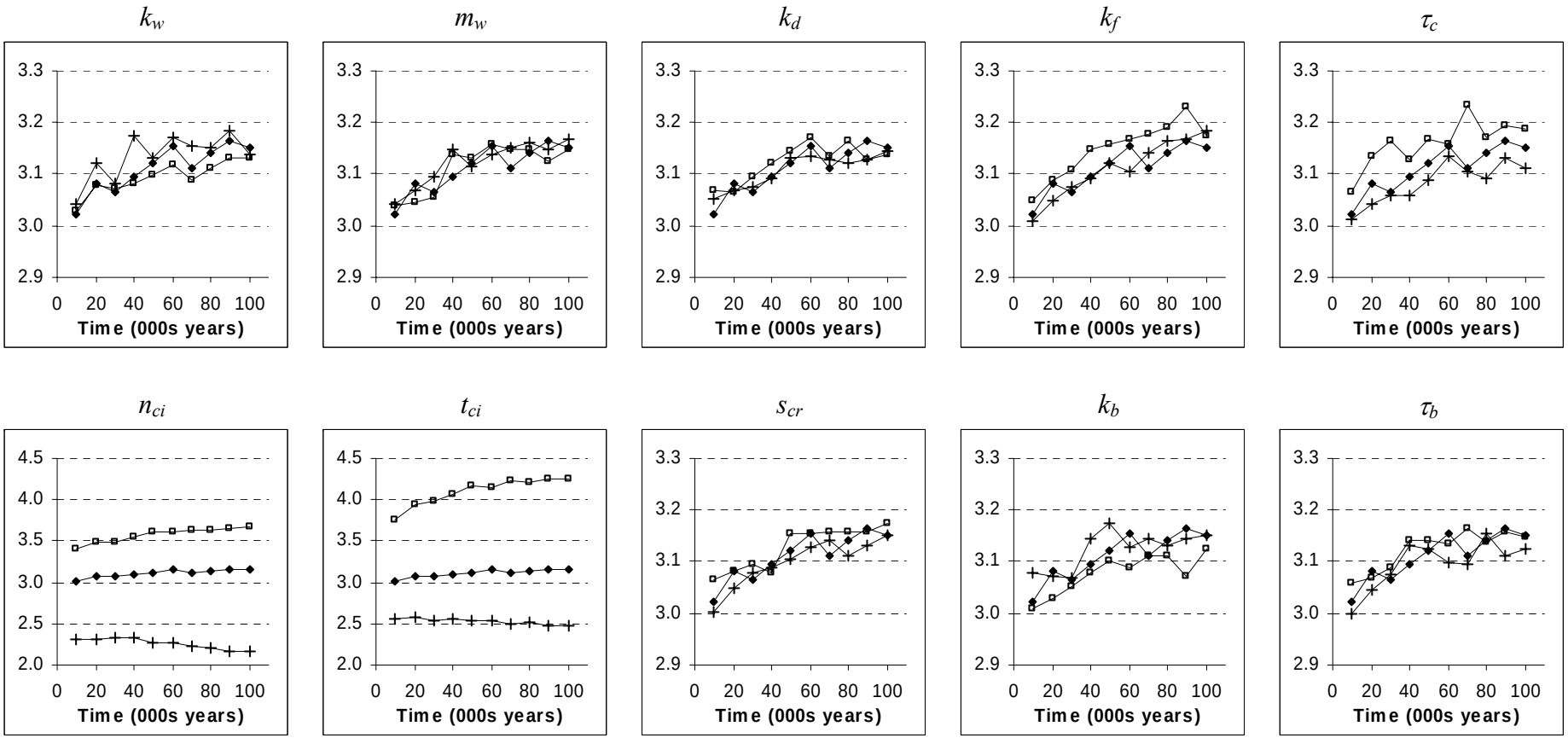

Figure 4.20: Plots for each parameter of drainage density (y-axis) against time (x-axis), contrasting the star point simulations with the base case.

Notes: 1. The letter above each plot denotes the parameter value varied.

2. Drainage density units throughout are km km^{-2} ; the y-axis ranges are also common throughout, to emphasise differences between parameters in the main effects.

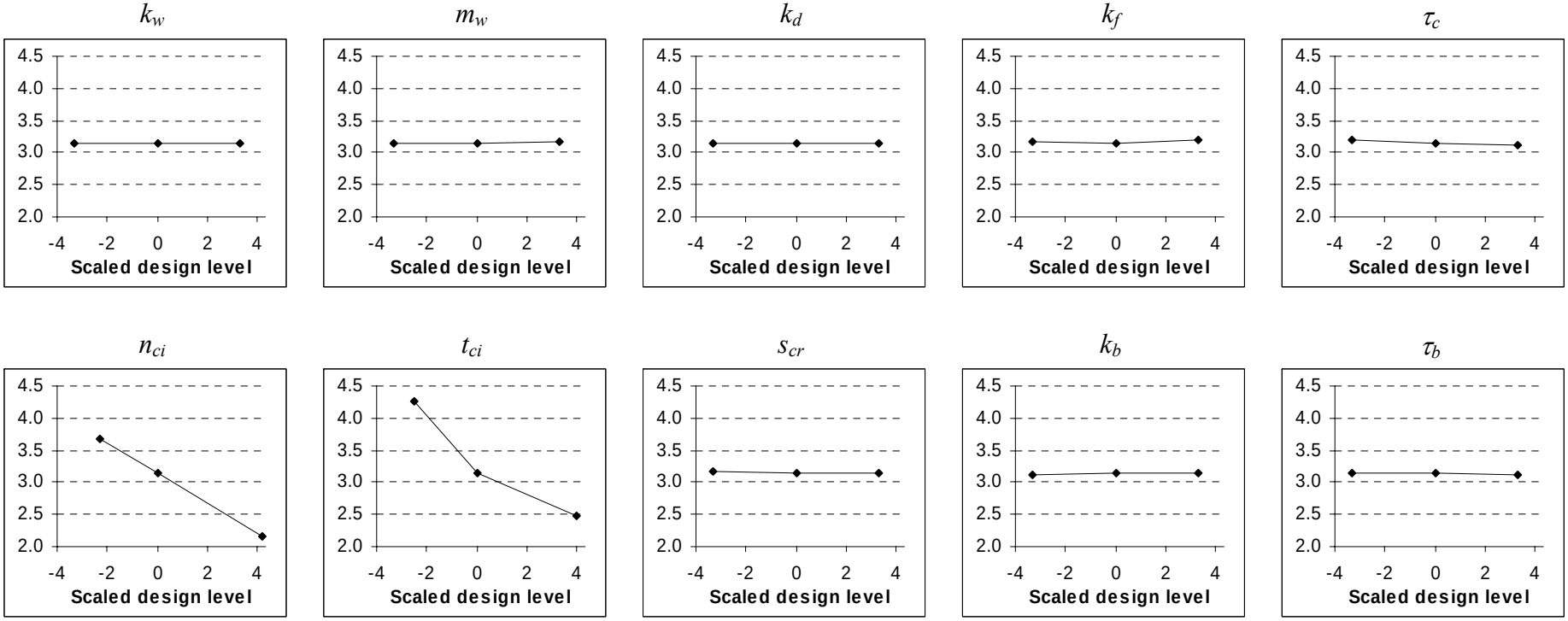

Figure 4.21: Plots showing the main effects of each parameter on drainage density (y-axis) after 100,000 years. Note that only the star point and base case results are plotted, using parameter values (x-axis) given in terms of their scaled design levels (eq. 4.01 *q.v.*).

Sediment delivery ratio

Figure 4.22 shows the temporal trend in the main effects of each parameter on sediment delivery ratio. The strongest main effect (evidenced by the spread in the data) is exhibited by k_f, followed by t_{ci} and n_{ci}, all of these showing a generally stable effect over time, albeit narrowing in range for k_f. The patterns for the other parameters are clearly more mixed, with the curves for k_b and τ_b crossing, thus exhibiting a reversal in the direction of each parameter's main effect. This in itself is a striking result, and one which the author had not seriously considered or would have predicted when planning the simulations. Similarly, the curves for k_w and τ_c appear to converge near 100,000 years but they do not cross, suggesting the strength of the main effects of these parameters declines over time, and could perhaps also undergo a reversal were the simulation to have continued for a longer period.

Turning to Figure 4.23, with the common y-axis scaling, and x-axis scaling by scaled design levels (eq. 4.01, *q.v.*), the main effects of k_f, t_{ci} and n_{ci} at 100,000 years are all positive, the first two showing distinct curvature. The other parameters, however, have much smaller main effects at this time.

Notes:
1. The letter above each plot denotes the parameter value being varied.
2. Sediment delivery ratio throughout reported in %; some of the y-axis ranges, in particular for k_f, are extended to accommodate the size of the main effects.
3. Legend: +α ; base case ; −α

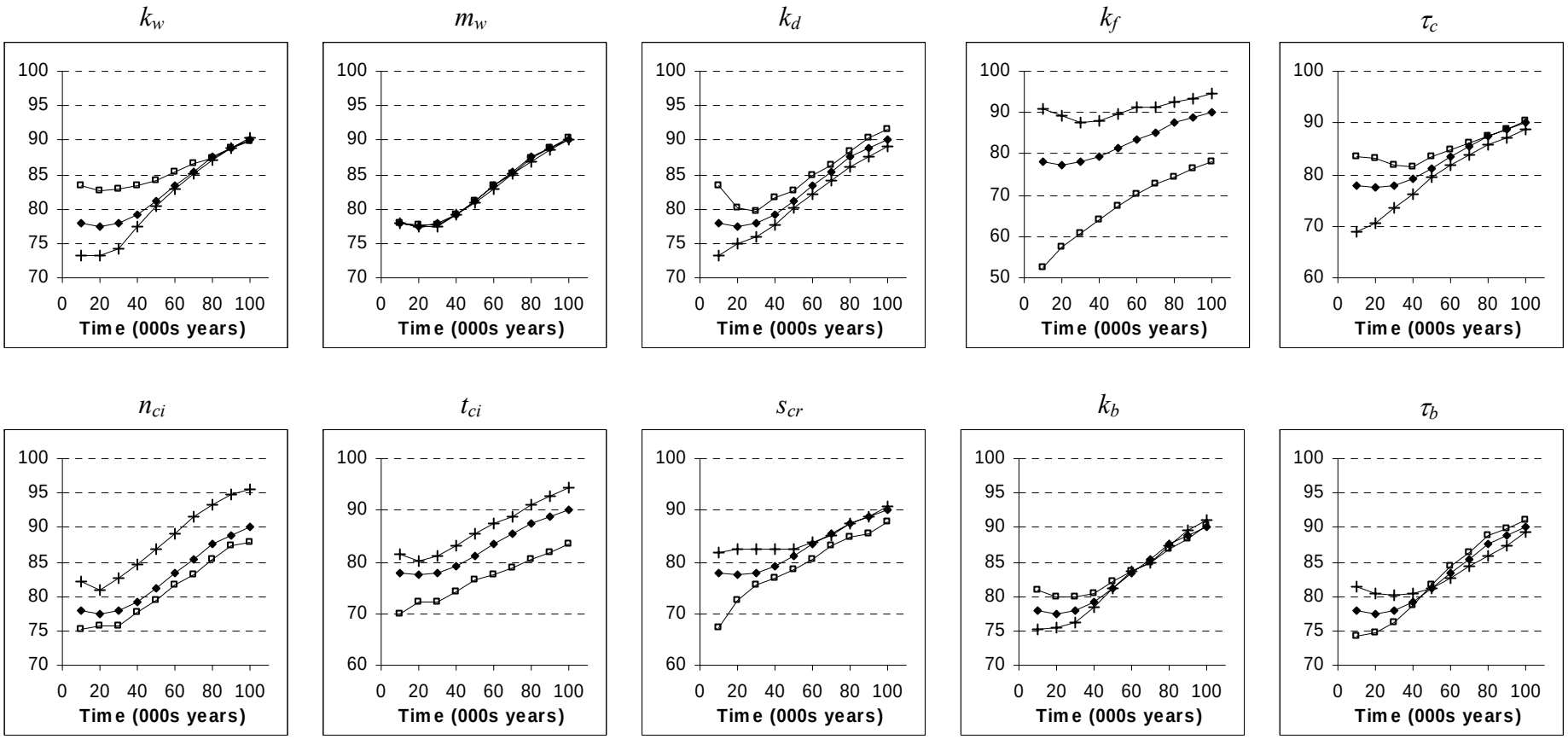

Figure 4.22: Plots for each parameter of sediment delivery ratio (y-axis) against time (x-axis), contrasting the star point and base case simulations.

Notes: 1. The letter above each plot denotes the parameter value varied.
2. Sediment delivery ratio throughout reported in %; y-axis ranges are also common throughout, to emphasise differences between parameters in the main effects.

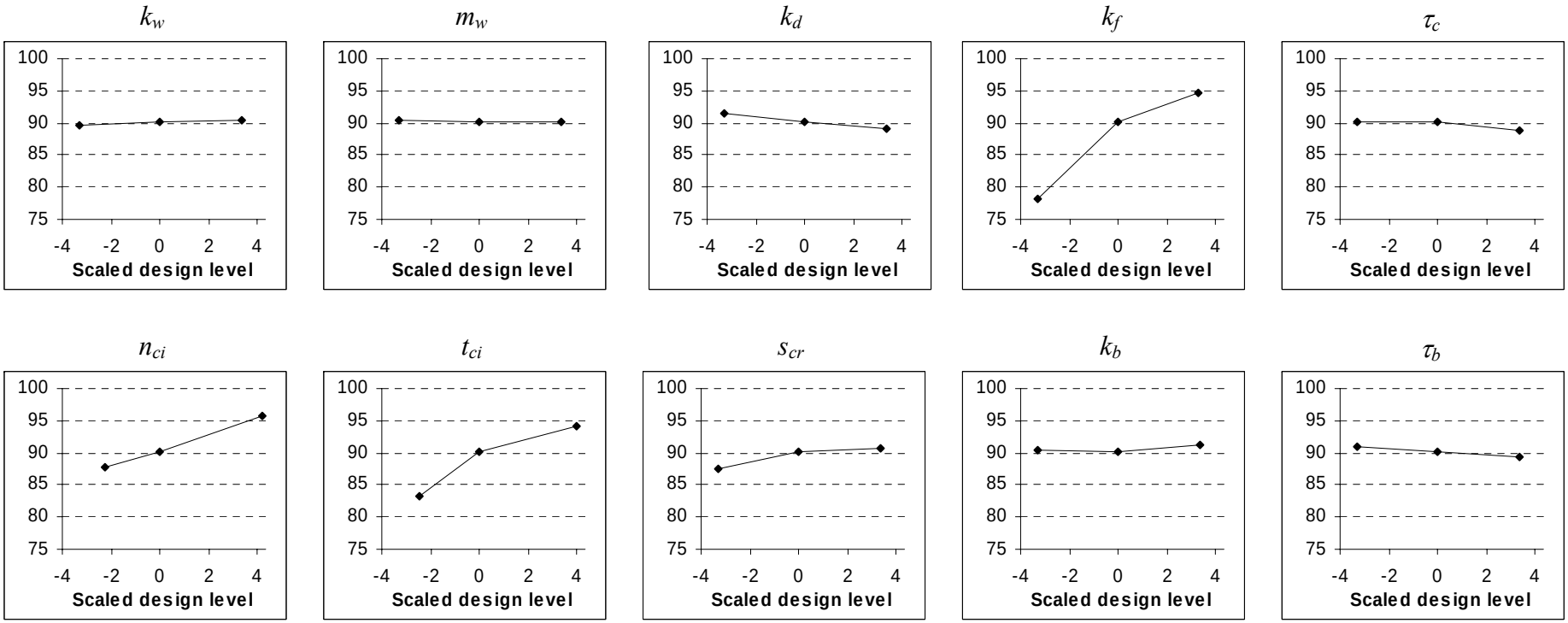

Figure 4.23: Plots showing the main effects of each parameter on sediment delivery ratio (y-axis) after 100,000 years. Note that only the star point and base case results are plotted, using parameter values (x-axis) given in terms of their scaled design levels (eq. 4.01 *q.v.*).

Topographic metric

Whereas the central composite sampling, with its star point simulations, was satisfactory for modelling the main effects of each parameter on the other metrics, this was far from true for the topographic metric. Indeed, inclusion of the star point results turned out to make the analysis more difficult rather than less. As explained later, in subsections 4.4.4-5, further simulations were run, in which only one parameter's value was varied at a time, the other parameters being held at their central (base case) values. The star point results were also subsequently dropped from the analysis. Figure 4.24 therefore shows the main effects of each parameter over time, but using simulations generated by parameter factorial level values for each parameter (Table 3.5, *q.v.*). Details of the additional main effects simulations are provided in Appendix J.

The main effects curves over time in these plots are very different from the ones seen for the other metrics. In this instance, the base case result is always (by definition of the metric) 100%, so the main effects must be viewed relative to this. Some of the plots are distinctly stepped, suggesting that the effects are rather unstable over time, particularly for k_w and k_b. Also, some parameters have almost no effect at all, particularly m_w and k_d, whereas others, such as k_f , k_w and s_{cr}, show an increase in the size of the main effect, with their landscapes becoming less and less like that of the base case landscape during the simulations.

Turning to the main effects curves at 100,000 years (Figure 4.25), with common y-axis scaling, and scaled design levels on the x-axis (eq. 4.01 *q.v.*), with the exception of m_w and k_d, which have very little effect at all, the unusual form of these main effects curves is well illustrated. The forms of the response for n_{ci} and t_{ci} appear particularly difficult to model, suggesting the need to include absolute values of each parameter in the regression analysis. Similarly, the step changes in the k_w, k_f and s_{cr} curves suggest the need for functions going beyond the usual quadratic or similar polynomial transformations used in regression.

Having considered the main effects of the four metrics, the chapter is now directed to the derivation of the metamodels, beginning with some comments on the general approach to the regression analyses.

Notes:
1. The letter above each plot denotes the parameter value being varied.
2. Topographic metric throughout reported in %; some of the y-axis ranges, in particular for k_f , are extended to accommodate the size of the main effects.
3. Legend: '+' upper factorial point level; '-□-' lower factorial point level.

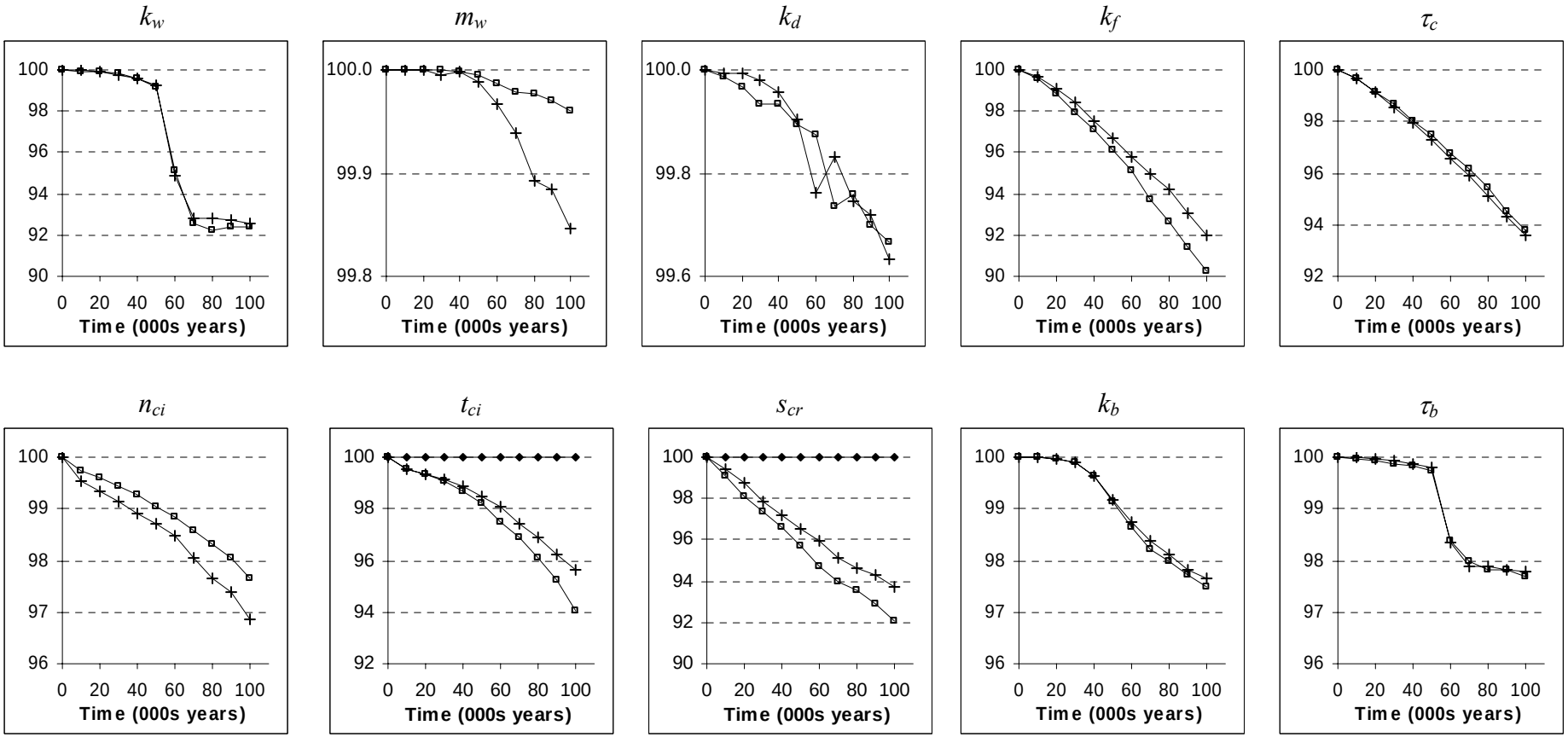

Figure 4.24: Plots for each parameter of the topographic metric (y-axis) against time (x-axis), each simulation using values corresponding to the factorial point levels for each parameter (see text).

Notes: 1. The letter above each plot denotes the parameter value varied.
2. The topographic metric throughout is reported in %; y-axis ranges are also common throughout, to emphasise differences between parameters in the main effects.

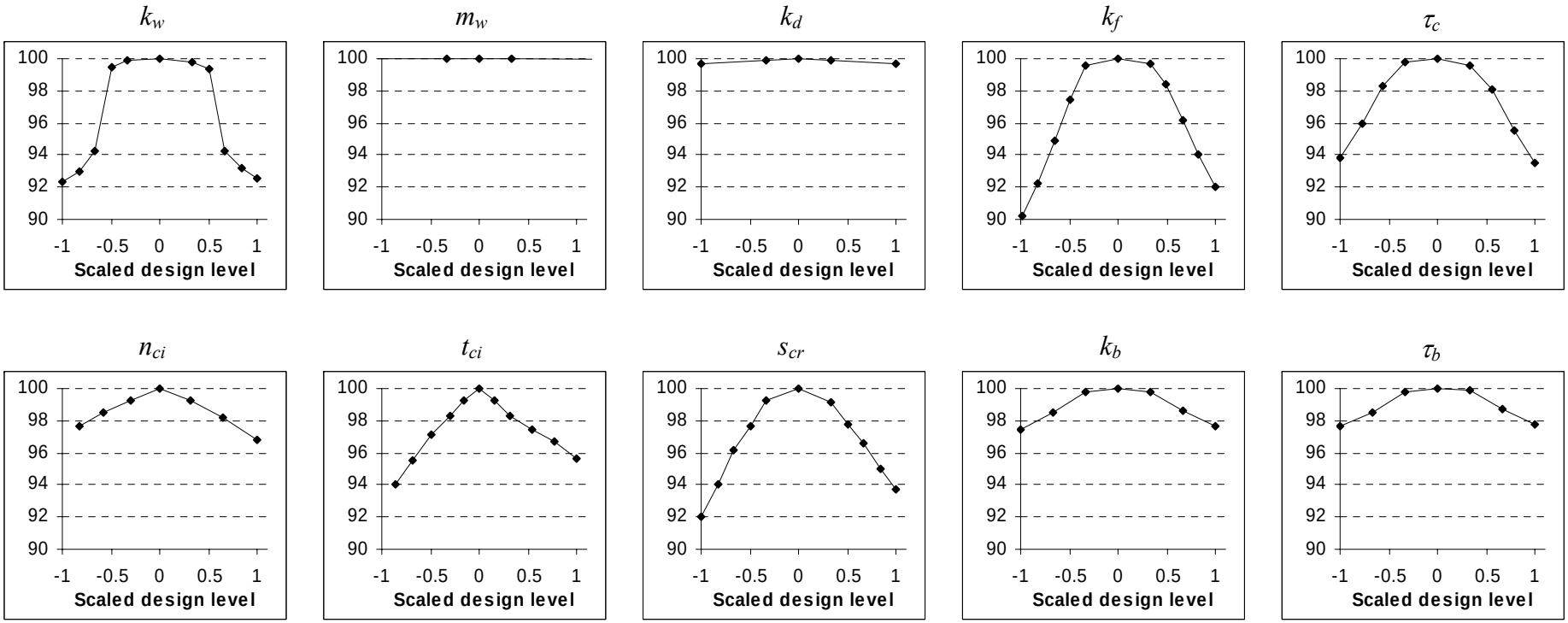

Figure 4.25: Plots showing the main effects of each parameter on the topographic metric (y-axis) after 100,000 years. Note that the parameter value ranges are bounded by their factorial space values, and the plots show data from additional sample points used to clarify these main effects. As with the plots in Figures 4.19, 4.21 and 4.23, the parameter values are given in terms of their scaled design levels (eq. 4.01 *q.v.*).

4.4.2 Approach to the regression analysis and preliminary metamodels

General approach

Before beginning the regression analysis, it was necessary to consider how the metamodels should be derived, and how many there should be for each metric. A common approach is to derive two or more different metamodels for the same metric, using independent subsets of the sample data, and check their predictive abilities against each other. Each metamodel is then used as a predictor, and differences between each model's predictions allow a confidence interval to be estimated. Alternatively, the regressions are repeated until the two models conform to the same basic structure, as represented by their regressor terms and any mathematical functions thereof. This procedure, called 'cross-validation', is well established in engineering and operational research and is served by a large, standard literature (e.g. Davison and Hinkley, 1997; Good, 1999; Marriott and Krzanowski, 1995; Webster and Oliver, 2001; and numerous others). An altogether different method of cross-validation could be used instead, however, in which one or more data points at a time are omitted from the whole set, and a different metamodel is derived from the remaining data (e.g. Davison and Hinkley, 1997). In the latter technique, the aim is to arrive at one 'best' metamodel form, which is used as the sole predictor for the metric.

For the purposes of this research, although cross-validation has some attractions, it was thought that it would be difficult to take subsets of the central composite design data without introducing aliasing, particularly between the two-factor interaction effects. This would compromise the analysis, defeating the object of conducting the initial experiment using a regular sampling design. Also, cross-validation did not appear to simplify derivation of the final metamodel forms nor did it eliminate the need for further simulations to sample unexplored areas of the parameter space. For these reasons, cross-validation was not adopted here.

Having excluded cross-validation, the approach to metamodel derivation follows the manner of model development and improvement outlined in the standard texts (e.g. Box *et al.*, 1978; Box and Draper, 1987). In particular, the aim initially was to derive preliminary linear regression models from the central composite design sample, test predictions made using these models by running further simulations, and then run additional simulations and improve the fit of the metamodels if required. A disadvantage of this approach is that each

set of test simulations needs to be quite large (10s of sample points) to test predictions across a 10-D parameter space. Moreover, it would not be appropriate to use data from the tests in deriving the final metamodel for each metric, which implies some wastage in the sampling. These points aside, the approach seemed to be suitable for the purposes here, and further comments on how it was implemented now follow.

Simplicity of preliminary metamodels and general form

The advantage of using metamodels over full simulations has been explained in Chapter 3, from which it is implicit that, for the metamodels to be representative a LEM's behaviour, they have to predict GOLEM's output to within an acceptable degree of error. When planning this phase of the research, although it was not expected that the error could be reduced to zero, it was thought important that it should be reduced so far as practical, and a number of principles were followed in order to achieve this.

Following recommendations in the standard texts (e.g. Box and Draper, 1987; Box *et al.*, 1978; Draper and Smith, 1981), these principles were, in the preliminary metamodelling analysis, to achieve high R^2 and adjusted R^2 scores (as evidence of a good fit with small errors), and balanced residuals plots (as evidence of correct model formulation and low bias). Furthermore, so far as possible, the metamodels should not include terms appearing to be only marginally significant in the regression. These principles were also followed in deriving the final metamodels, and an additional principle, that the constant term should be generally stable between regressions using different subsets of the data but the same model structure was also included at that stage (Box *et al.*, 1978)[3].

The initial analysis, therefore, was aimed at deriving metamodels employing a low number of regressor terms, each with high or very high significance[4], and using only simple transformations of the predictor variables. With regard to the latter point, the functions to be used should not produce points of inflexion within the range of interest, as recommended

[3] This is not essential, as high R^2 scores and balanced residuals plots are generally good evidence of a sound model. However, the stability of the constant term also provides some additional assurance that the basic model structure i.e. its mathematical formulation, is correct, and this may be useful where fitting of a more complex model form is being attempted (e.g. Box *et al.*, 1978).

[4] Defined for convenience as follows: probability of less than or equal to 0.01 – 'highly significant'; probability of less than or equal to 0.001 – 'very highly significant'.

for response surface investigations during early phases of analysis (e.g. Box and Draper, 1987; Wu and Hamada, 2000).

As an additional aim to the above, the author hoped to include as many of the parameters as possible in the models, so that each metamodel would be sensitive to changes in the values of most of the parameters rather than to changes in just a few of them. Finally, the preliminary metamodels were restricted to a linear (i.e. additive) form, with the possibility that they could be changed to non-linear forms after further sampling and analysis. In this respect, drawing on examples from standard works (e.g. Box and Draper, 1987; Draper and Smith, 1981), and taking into account the foregoing, each preliminary metamodel, ignoring the error term, was expected to have a structure conforming to the equation below:

$$\hat{y} = \beta_0 + \beta_1 x_1 + \gamma_1 f(x_1) + \beta_2 x_2 + \gamma_2 f(x_2) + \ldots + \beta_j x_j + \gamma_j f(x_j)$$

$$+ \beta_{12} x_1 x_2 + \gamma_{12} f(x_1 x_2) + \beta_{13} x_1 x_3 + \gamma_{13} f(x_1 x_3) + \ldots + \beta_{ij} x_i x_j + \gamma_{ij} f(x_i x_j), \quad 4.02$$

where $\hat{y}$ is the predicted value of the metric at a particular sample point positioned by the parameter values $\{x_1, x_2, \ldots, x_j\}$, assuming j parameters in the model, β_0 is a constant, and the other terms are understood as follows:

- β_1 to β_j are coefficients for the linear main effects terms of x_1 to x_j;
- β_{12} to β_{ij} are coefficients for the linear two-factor interaction effects terms of x_1x_2 to x_ix_j;
- γ_1 to γ_j are coefficients for the curvature terms of the main effects, expressed by the functions $f(x_1)$ to $f(x_j)$;
- γ_{12} to γ_{ij} are coefficients for the curvature terms of the two-factor interaction effects, expressed by the functions $f(x_1x_2)$ to $f(x_ix_j)$;
- the functions $f(\ldots)$, whether applied to a single parameter or a two-way interaction, may be quadric, power, log, hyperbolic, inverse or similar functions, without points of inflexion within the parameter value ranges of interest.

With these points in mind, the preliminary metamodels were derived for sediment yield, drainage density and sediment delivery ratio, using least squares multiple regression, and working many times through forward, backward and best subsets procedures. In deriving the metamodels, the analyses were all performed using a standard statistics software package (MINITAB 14 ®). Main effects were also 'tuned' to some extent, through trial of different functions and polynomials in the regressions, in order to obtain more balanced

residuals plots. The preliminary regression work was successfully completed on these three metrics, and the resulting metamodels and analysis details are now reported and commented on.

4.4.3 Preliminary models and example plots

The preliminary metamodels were first derived using normalised parameter values. Normalising is a simple form of scaling, which was thought suitable at this stage of the analysis following recommendations made in the standard texts (e.g. Draper and Smith, 1981) for avoiding problems in the regression that may arise where the independent variables have values ranging across several or more orders of magnitude. One advantage of using normalised scaling is that it allowed application of inverse, power and log functions, which would not have been possible if using scaled design levels, as defined by equation 4.01. The normalised scaling was therefore centred on 1 for each parameter, and found by dividing each parameter's value by its base case value, thus:

$$x' = \frac{x}{x_0}, \qquad 4.03$$

where x', x and x_0 are respectively the scaled, true and base case values of the parameter.

The full statistics relating to each preliminary metamodel, complete with coefficients and ANOVA tables, are provided in Appendix H, and the main features of each metamodel are summarised in Table 4.1. It will be noted that all of these preliminary metamodels conformed to the general linear model structure of equation 4.02. Unless stated otherwise in the notes, all curvature terms are quadric functions.

Table 4.1: Preliminary metamodels for sediment yield, drainage density and sediment delivery ratio. All curvature terms are quadric functions unless stated otherwise in the notes.

Model Summary:	**Sediment yield**		**Drainage density**		**Sediment delivery ratio**	
R^2 score (%)	99.9		99.5		99.1	
Adjusted R^2 (%)	99.9		99.5		98.9	
s	0.1181		.02289		0.3162	
No. of terms	23		11		25	
MAIN EFFECTS:						
Parameter	Linear term	Curvature term	Linear term	Curvature term	Linear term	Curvature term
k_w	+ vhs	- vhs	.	.	.	- vhs
k_f	+ vhs	- vhs (3)	.	.	- vhs	+ vhs(5)
τ_c	- vhs	.	.	.	.	- vhs
n_{ci}	+ vhs	- vhs	- vhs	.	+ vhs	.
t_{ci}	+ vhs	- vhs	.	- vhs (4)	.	- vhs (6)
s_{cr}	+ vhs	.	.	.	+ vhs	- vhs
k_b	.	.	.	.	.	.
2-FACTOR INTERACTIONS:						
Parameters	Linear term	Curvature term	Linear term	Curvature term	Linear term	Curvature term
$k_w \times k_d$	.	.	.	.	- hs	.
$k_w \times k_f$	+ vhs	.	.	.	.	.
$k_w \times \tau_c$	- vhs	.	.	.	.	.
$k_w \times n_{ci}$	.	.	+ vhs	- vhs	+ hs	.
$k_w \times t_{ci}$	.	.	.	- vhs	+ vhs	.
$k_w \times s_{cr}$	.	.	.	.	.	.
$k_w \times k_b$	.	.	.	.	- hs	.
$k_w \times t_b$	.	.	.	.	+ hs	.
$k_d \times k_f$	+ vhs	.	.	.	+ hs	.
$k_f \times \tau_c$	.	.	- vhs	.	+ hs	.
$k_d \times s_{cr}$	.	.	.	.	.	.
$k_f \times \tau_c$	- vhs	.	.	.	+ hs	.
$k_f \times n_{ci}$	- vhs	.	- vhs	+ vhs	- vhs	.
$k_f \times t_{ci}$	- vhs	+ vhs	.	.	- vhs	.
$k_f \times s_{cr}$	- vhs	+ vhs	.	.	- hs	.
$k_f \times k_b$	+ vhs	.	.	.	.	.
$k_f \times t_b$	- vhs	.	.	.	.	.
$\tau_c \times t_{ci}$	+ vhs	.	.	.	+ hs	.
$\tau_c \times s_{cr}$	+ vhs	.	.	.	.	.
$n_{ci} \times t_{ci}$	.	.	+ vhs	.	- vhs	.
$n_{ci} \times s_{cr}$	.	.	- s	+ s	.	.
$t_{ci} \times s_{cr}$	.	.	.	.	- hs	.
$t_{ci} \times t_b$	.	.	.	.	- vhs	.
$t_{ci} \times k_b$	.	.	.	.	+ vhs	.
$k_b \times t_b$	.	.	.	.	- s	.

Notes:

1. **'+' and '-' signs indicate a positive or negative coefficient.**
2. **'vhs'- very highly significant, p<=0.001; 'hs' - highly significant, p<=0.01; 's' -significant, p<=0.05.**
3. **Sediment yield – the k_f exponent in the main effect curvature term was 1.5.**
4. **Drainage density – the main effect of t_{ci} was modelled as $\ln|t_{ci} - 5{,}700|$.**
5. **Sediment delivery ratio – the k_f exponent for its main effect curvature was 0.355.**
6. **Sediment delivery ratio – the t_{ci} exponent for its main effect curvature was -1.08**

The table shows that high R^2 and adjusted R^2 scores were achieved for all of the preliminary metamodels for these three metrics, and also that most of the regressor terms in each metamodel were either highly or very highly significant. It was found that by tuning the most important main effects terms for each model, the fit, particularly as evidenced by the residual plots, could be improved compared with that obtained by limiting the modelling of curvature to quadratic functions only. This is reflected in the functions used to model the curvature terms for the main effects of k_f and t_{ci}, identified in notes 5 and 6 to the table. The plots in Figure 4.26 demonstrate the close fits achieved by each model, and also the scatters in the residuals. For clarity from here onwards, a residual will mean, in the context of a regression analysis, the simulated value (from GOLEM's output) minus the fitted value, and in the context of model testing, the value generated by GOLEM in a test simulation minus the value predicted by the metamodel for that test.

a. Sediment yield. All units are $m^3 km^{-2} yr^{-1}$.

i. Simulated vs fits, with 'perfect fit' line

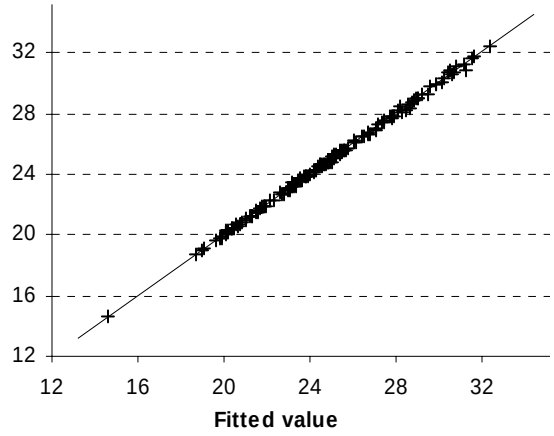

ii. Residuals vs fits.

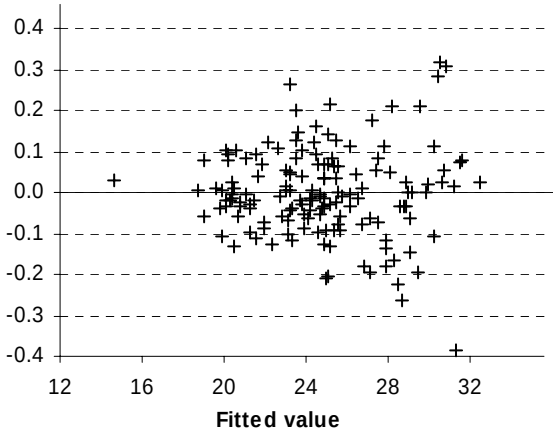

b. Drainage density. All units are km km^{-2}.

i. Simulated vs fits, with 'perfect fit' line

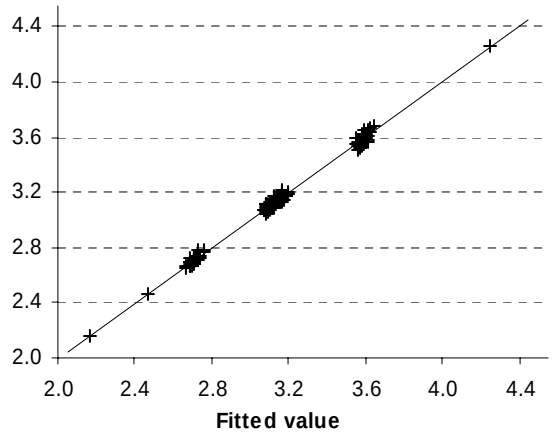

ii. Residuals vs fits.

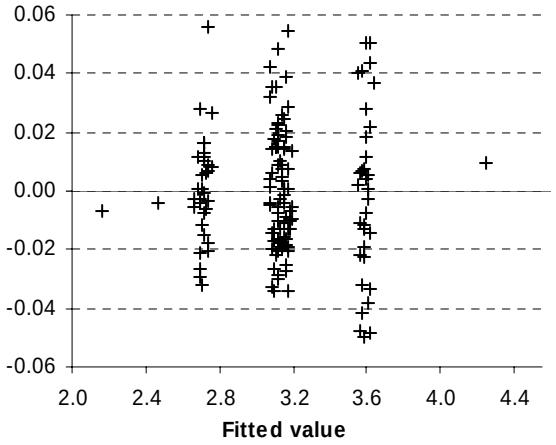

c. **Sediment delivery ratio. All units are %.**

i. Simulated vs fits, with 'perfect fit' line

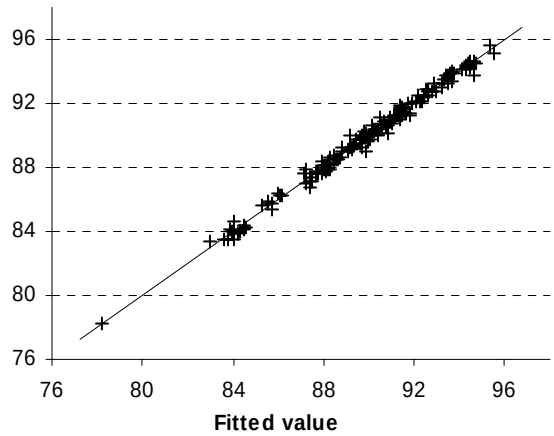

ii. Residuals vs fits.

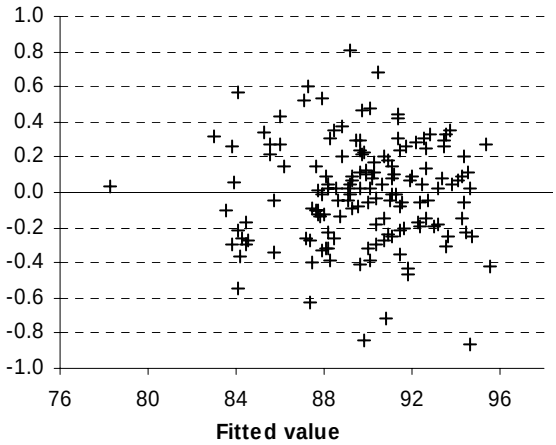

Figures 4.26, a to c: Plots of simulated output and residuals versus fitted values for the preliminary sediment yield, drainage density and sediment delivery ratio metamodels.

Although the scatter in each of the residual plots was generally satisfactory, the author thought that it was important to test the models for possible model misfit and bias, and these aspects are now discussed.

4.4.4 Tests of the preliminary metamodels and subsequent problems

The preliminary metamodels were tested strictly in order, that is, the metamodel for one metric was derived first and the tests on it were then conducted, before moving on to the next metric. The new sample points were all from within the factorial space, and were selected carefully so as to 'strain' each equation as much as possible i.e. in gaps left by the central composite sample, where the fitting of main or interaction effects appeared to be problematic. There were thirty two independent test simulations each for the sediment yield and drainage density metamodels, and twenty eight for the sediment delivery ratio metamodel. The results are summarised in Figure 4.27 and discussed briefly below.

Dealing first with sediment yield (Figure 4.27 a, (i) and (ii)), the plot of simulated versus predicted values emphasises the close fit obtained in the regression. The residuals plot, however, suggests a slope in the scatter, and a bias towards positive residuals, such that the metamodel is under predicting slightly[5]. On this basis, some further work was expected to be necessary to improve this model. The test results for the drainage density metamodel (Figure 4.27 b, (i) and (ii)) look satisfactory, although there is a suggestion of coning, and hence that the variance is not constant (e.g. Draper and Smith, 1981), and perhaps a small positive bias in the residuals, again indicating slight under prediction by the metamodel. The tests of the sediment delivery ratio model (Figure 4.27 c, (i) and (ii)) indicate a small bias of negative residuals, and that this metamodel is over predicting slightly. The scatter in the residuals also indicates a slight slope, perhaps caused by a strong influence of one of the k_f star points.

[5] As defined on page 153, in the context of testing the metamodels, a residual is the GOLEM output for the test simulation minus the value predicted for that simulation by the metamodel. Hence, positive residuals indicate an under prediction by the metamodel, and negative residuals an over prediction.

a. Sediment yield. All units are $m^3 km^{-2} yr^{-1}$.

i. Simulated vs predicted, with 'perfect fit' line

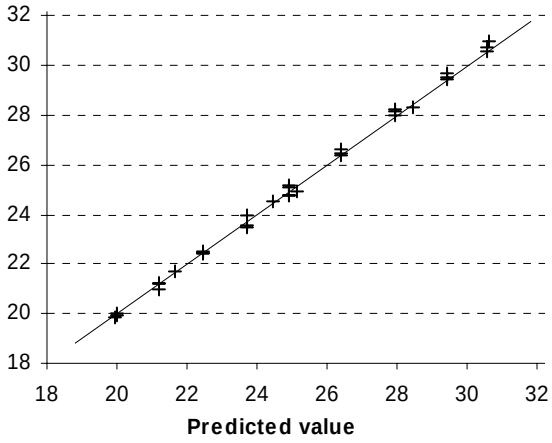

ii. Residuals vs predicted.

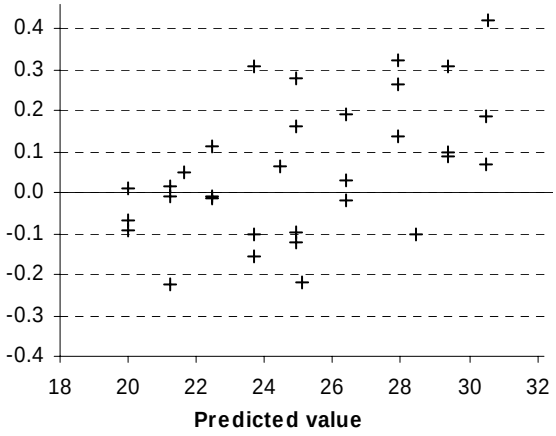

b. Drainage density. All units are km km^{-2}.

i. Simulated vs predicted, with 'perfect fit' line

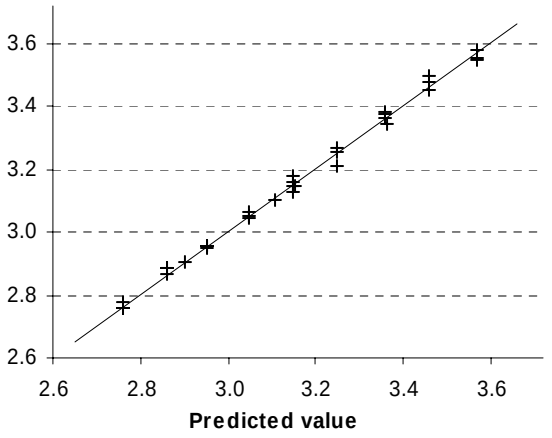

ii. Residuals vs predicted.

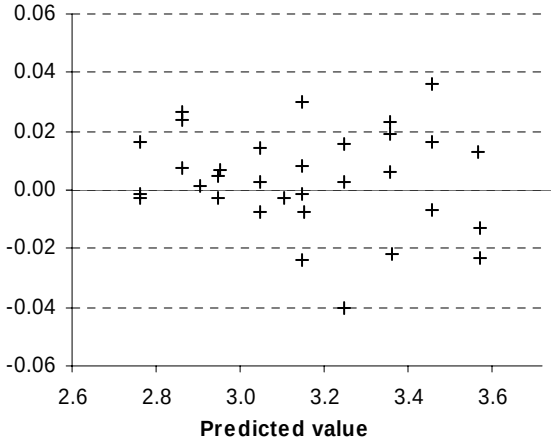

b. Sediment delivery ratio. All units are %.

i. Simulated vs predicted, with 'perfect fit' line

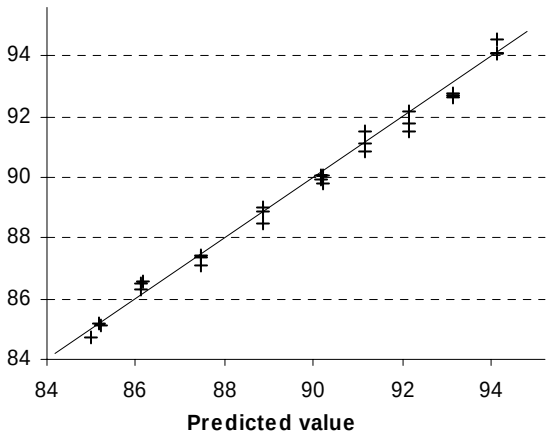

ii. Residuals vs predicted.

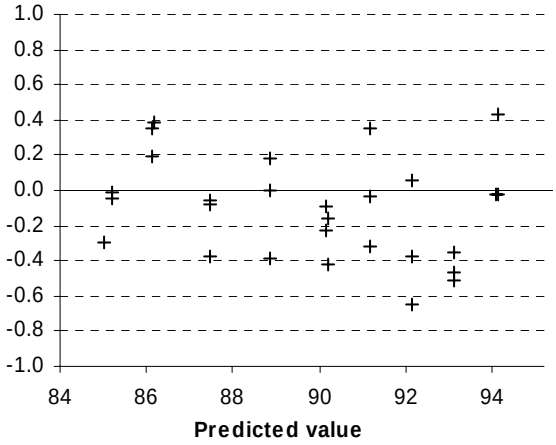

Figures 4.27, a to c: Plots of output and residuals versus predicted values for the tests run on the preliminary sediment yield, drainage density and sediment delivery ratio metamodels.

Notwithstanding these observations, the results of the preliminary regression and metamodelling work for these three metrics are considered highly satisfactory. However, problems were encountered when deriving a metamodel for the topographic metric, and these are now discussed.

Problems with the topographic metric prompting a revised approach to the regressions

Although the metamodelling work to this point had proved satisfactory, when conducting the analysis to derive the metamodel for the topographic metric, all initial attempts to fit a parsimonious model to the data failed. Either the R^2 scores were very low (< 50%) compared with what had been achieved for the other three metrics, or the model required a large number of regressors (> 40) to achieve a reasonable R^2 score (*c.* 70%), out of which some of the terms were only just statistically significant. It was concluded that these problems were caused by an unusual form of response surface, and additional simulations were run to clarify the form of each parameter's main effect. The new sample points were confined to the factorial point ranges of each parameter (the range of most interest), varying only one parameter's value at a time, the others' being held at their base case values. The additional sampling revealed stepped and pointed main effects, of a very different character from those seen in Figures 4.19, 4.21, and 4.23. These results have been shown already, in Figure 4.25, from which it has been seen that some parameters needed more additional sample points than others before the forms of their main effects could be clarified.

After conducting these simulations, the decision was made to drop the star point results from the analysis for this metric, and to concentrate on the data from the factorial space only. A wide variety of linear and non-linear model forms (e.g. Ratkowsky, 1990) were then tried, but none was found to be satisfactory. Additional sampling, in which only k_f and sc_r were varied, was also tried, in order to derive a generic function for interaction terms, but this proved successful only in part, and at the cost of using many k_f and s_{cr} regressor terms. Focus was therefore shifted to how a more loosely fitting metamodel, as compared with the other three, might be derived and used. At this stage, it was decided that a 'bootstrap' technique (e.g. Davison and Hinkley, 1997) would be assist in the calculations of equifinality, by allowing a confidence interval to be calculated. The possibility of using a bootstrap in the quantifications of equifinality also permit a different approach to the derivation of the metamodels for all four metrics, and this is now explained.

4.4.5 'Bootstrapping' and revising the approach to the regression analyses

Principles of the bootstrap

The idea of the 'bootstrap' is not new, and for the purposes of this section, the author has relied on certain standard works, in particular Davison and Hinkley (1997) and Vose (2000), with technical assistance provided by Professor Russell Cheng, Professor of Operational Research in the School of Mathematics at Southampton University, United Kingdom.

The bootstrap is related to another statistical procedure called the 'jackknife', and the two are sometimes used together in statistical work (Davison and Hinkley, 1997). Both are essentially resampling techniques, whereby for any set of sample data, *X*, a series of alternative sample sets, *X**, may be derived, on which statistical analysis can also be conducted. One of the main objects of such resampling schemes is to obtain a better estimation of the uncertainty around the value of a statistic of interest. If the bootstrap sample is obtained by drawing data from the original sample, then it is called a *non-parametric bootstrap* (Vose, 2000). Sometimes it is more useful to resample from a mathematically defined distribution, which models the original sample data or source population in some way, in which case it is called a *parametric bootstrap* (*ibid.*). Both techniques were used at different stages in this research.

The principle behind the bootstrap is to resample *with replacement*. The object is to construct a number of bootstrap sample sets, and calculate the statistic of interest from each sample. Using the mathematical notation adopted by Vose(2000), the steps in constructing a non-parametric bootstrap are straightforward, and are summarised below, assuming that the statistic of interest is denoted by θ:

1. obtain the sample of data, *X*, comprising *n* data points x_i, ordered from x_1 to x_n;

2. by resampling at random from *X*, with replacement, construct *B* bootstrap samples, labelled from X_1* to X_B*, each consisting of *n* data points;

3. for each bootstrap sample, X_j*, calculate the statistic of interest, $\hat{\theta}_j^*$;

4. analyse the distribution of all $\hat{\theta}_j^*$, from $\hat{\theta}_1^*$ to $\hat{\theta}_B^*$, and calculate the bootstrapped estimate of uncertainty as required.

The number of bootstrap samples is typically from hundreds to tens of thousands or more, and is dependent largely on the purpose of the analysis and properties of the sample data (Davison and Hinkley, 1997; Vose, 2000). A general property of the bootstrap, however, is that the confidence interval around the study statistic is inversely related to the number of bootstrap samples; thus, the bootstrap estimate becomes narrower with increasing B, and typically becomes broadly stable beyond a sufficiently large B (*ibid.*).

To construct a parametric bootstrap, the resampling in step 2 is achieved by taking data points at random from a distribution function stipulated for X, with a specified mean and standard deviation (*ibid.*). Both the parametric and non-parametric bootstrap have a wide variety of applications, and their application in this research and the practical consequences in the regression analyses are now explained.

Practical consequences of the application of bootstrapping for the regression analysis and final form of the metamodels

The reasoning underlying the application of a bootstrap in the calculations of equifinality using the metamodels is explained as follows. The fit of any of the metamodels will not be exact, and each regression will produce an associated set of residuals. The residuals may be considered, as a first approximation, to be representative of the range of possible errors to which any prediction may be subject in the parameter space, particularly within the factorial space (Russell Cheng, 2006, personal communication). Therefore, in calculating the proportion of equifinal results produced by GOLEM, errors in the predictions can be introduced by bootstrapping each metamodel's prediction using one of its associated regression residuals. This allows either a distribution of results to be formed from booted repeat predictions at any single sampled point, or from many such individual predictions across a range of points sampled across the parameter space generally. It is thence possible to calculate confidence intervals around the results.

In this research, a non-parametric bootstrap was applied to the main predictions made with the final metamodels (explained below). With the data from the additional simulations conducted to test each preliminary metamodel and to clarify parameter main effects, there were sets of over 300 residuals from each regression, which was considered a large enough number from which to draw bootstrap errors non-parametrically (R. Cheng, 2006, personal communication).

On this basis, the regression analyses and metamodels were revised, so that each regression would include all of the data points (although not the star points when deriving the topographic metric's metamodel). The metamodels would also not be tested separately, provided the residuals plots seemed satisfactory and the R^2 and adjusted R^2 scores remained high (*c.* 90% or over), since the application of the bootstrap would make allowances for the errors in the predictions. The final forms of the metamodels derived in this way are now presented and explained.

4.5 FINAL FORMS OF THE METAMODELS

4.5.1 Sediment yield and drainage density

Having made the decision to use all of the sample points, the regression analysis was re-worked in much more detail, using a wider range of main effects functions, and now including a selection of three-factor interactions. The inclusion of the latter was not considered a problem, given that the number of such interactions in any model was expected to be small, and the additional sample points – 160 in all – made aliasing with lower-way effects unlikely.

A concern with the sediment yield metamodel, despite the high adjusted R^2 score already obtained, was that the data were heteroscedastic (e.g. Box and Draper, 1987; Draper and Smith, 1981). Tests for appropriate transformation of the dependent variable, as described in Box and Draper (1987), indicated that a log transform was suitable[6]. Once this was applied, by exploring a number of different combinations of transformations of the independent variables, it was found that log compound terms worked very well, particularly in producing balanced residual plots, and in allowing regressions against subsets of the data to test for stability of the constant (after Box *et al.*, 1978, as explained in subsection 4.4.2). Use of log compound terms also made model fitting much easier, in that the author did not need to select from a potentially very large set of possible interaction terms, nor include a large number of these in the final model. In its final form, the metamodel therefore took on a structure rather different from that in equation 4.02, as follows:

[6] The results of the transformation test actually indicated a power transformation of about 0.2 i.e. that the dependent variable should be $y^{0.2}$. The log transform was used instead, as the effect of this is almost the same (Box and Draper, 1987), and it also allowed great simplification in structuring the final metamodel.

$$\ln|(\text{sediment yield})| = \beta_0 + \beta_1 \ln|M_1| + \beta_2 \ln|M_2| + ... + \beta_j \ln|M_j|, \qquad 4.04$$

where the terms M_1 to M_j refer to polynomial functions which modelled the main effects of the parameters 1 to j, the regressor terms are natural log values of these functions, and β_1 to β_j are the coefficients appropriate to each $\ln|M_i|$ regressor. The polynomials for each M_i term were themselves found by regression and each parameter's main effects sample data only, and balanced scaled values, given by

$$x' = 1 + 0 \cdot 2 \times \left[\frac{x - x_0}{x_{+1} - x_0} \right], \qquad 4.05$$

where x' is the scaled value of the parameter, x the true value, and x_{+1} and x_0 respectively the positive factorial point and central point values. The final (logarithmic) metamodel derived using this structure required only nine regressors, and is much simpler conceptually than the preliminary metamodel outlined in Table 4.1, in that the dependent variable has been reduced to a single, general function of the independent variables. This is approaching the mechanistic modelling described by Box and Draper (1987), by which more complete explanations of a system's response may be derived. It would certainly be of interest to see this approach repeated in other LEM studies, referring to this and other metrics, and to a range of different output reference times, as such tools could turn out to be of great use in explaining landscape responses to factor variations.

Following the same 'y' transformation test as that used above, it was found that a log transform was appropriate for the drainage density data. A variety of different model structures were also tried, after which the same general model structure, as given in equation 4.05, was found to work for the drainage density metamodel also. However, the parameters t_{ci} and n_{ci} so dominated the response that it was very difficult to find other parameters which were significant, and the final metamodel was formed using only four regressors. The summaries of the final sediment yield and drainage density metamodels are provided in Table 4.2, and the regression output and related data on these models in Appendix K.

Table 4.2: Final metamodels for sediment yield and drainage density, using the log compound regressor form (equation 4.04) and based on all of the available data points. Details of the regression output, fits and residuals are provided in Appendix K.

	Sediment yield		**Drainage density**	
	R^2 score 99.9 %, adjusted R^2 99.8 %		R^2 score 99.3 %, adjusted R^2 99.3 %	
	s = 0.004758		s = 0.006823	
	329 data points, d.f. = 328		329 data points, d.f. = 328	
	9 compound regressors, plus constant		4 compound regressors, plus constant	
Parameter, x	Constant, or coefficient for $\ln\|M_x\|$	Equation for main effect, 'sediment yield = M_x'	Constant, or coefficient for $\ln\|M_x\|$	Equation for main effect, 'drainage density = M_x'
Const.	-26.475	.	-2.5173	.
k_w	0.9561	$15.72 + 9.234k_w^{0.25}$	.	.
k_d	0.9638	$23.48 + 1.45k_d^{0.7}$	.	.
k_f	0.9974	$7.046 + 33.55k_f - 15.67k_f^{1.3}$	.	.
τ_c	1.0114	$33.664 - 8.711\,\tau_c$	1.1932	$3.206 - 0.063\,\tau_c$
n_{ci}	1.0193	$25.64 - 0.665n_{ci}^{2.4}$	0.9970	$5.043 - 1.832n_{ci}^{0.5} - 0.0635n_{ci}^{3}$
t_{ci}	0.9955	$34.05 - 18.77t_{ci} + 12.96t_{ci}^2 - 3.306t_{ci}^3$	1.0054	$2.952 - 0.433t_{ci} + 0.630t_{ci}^{-1.3}$
s_{cr}	0.9864	$31.17 - 6.219\,s_{cr}^{0.5}$	.	.
k_b	0.9561	$23.85 + 1.086k_b^{0.8}$	0.0063	k_b only (see notes)
τ_b	1.2615	$25.46 - 0.532\,\tau_b^{1.2}$	.	.

Notes:
1. The constants and all $\ln|M_x|$ regressor terms were very highly significant (p <= 0.001) except the $\ln|M_x|$ term for k_b in the drainage density metamodel, which was only highly significant (p <= 0.01).
2. The functions M_x were themselves found by regression, using scaled parameter values (eq. 4.05).

The detail in Table 4.2 allows the full metamodels, based on the form of equation 4.04, to be written for both metrics. Thus, for convenience here using the drainage density metamodel as the example, as this is the shorter of the two, the full metamodel equation is:

$$\ln\left|\text{drainage density}\right| = -2.5173 + 1.1932\ln\left|3.206 - 0.063\tau_c\right|$$
$$+ 0.997\ln\left|5.043 - 1.832n_{ci}^{0.5} - 0.0635n_{ci}^{3}\right| + 1.0054\ln\left|2.952 - 0.433t_{ci} + 0.63t_{ci}^{-1.3}\right|$$
$$+ 0.0063\ln\left|k_b\right| \qquad 4.06$$

It will be noted that despite the increase in the degrees of freedom, the adjusted R^2 scores for both metamodels are little different from the values obtained for their preliminary models (Table 4.1, *q.v.*). The plots of simulated versus fitted values, and residuals versus fitted values, are shown in Figure 4.28, from which it will be seen that the models appear balanced, with no evidence of significant model misfit or bias.

a. Sediment yield model, in logarithmic form. All plotted units are ln|(sediment yield)|, and source units $m^3\ km^{-2}\ yr^{-1}$.

i. Simulated vs fits, with 'perfect fit' line

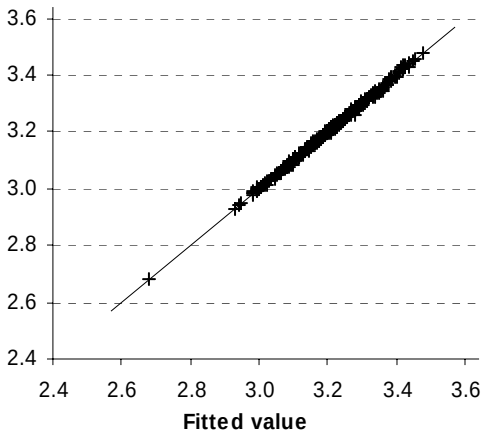

ii. Residuals vs fits.

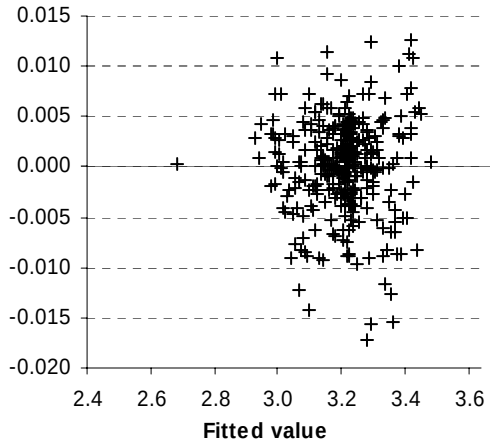

b. Drainage density model, in logarithmic form. All plotted units are ln|(drainage density)|, and source units km km^{-2}.

i. Simulated vs fits, with 'perfect fit' line

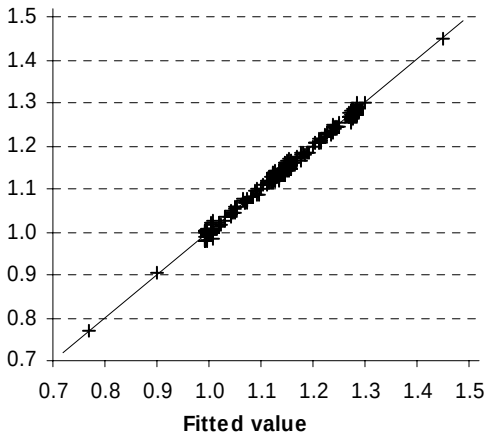

ii. Residuals vs fits.

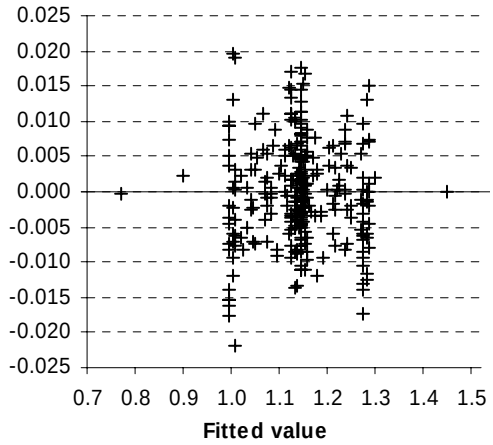

Figures 4.28, a to d: Output and residuals vs fitted values for the final metamodels of ln|(sediment yield)| and ln|(drainage density)|. Equation 4.04 gives the general model form, and Table 4.2 the components of each compound regressor term.

4.5.2 Sediment delivery ratio and the topographic metric

The final sediment delivery ratio metamodel proved quite problematical to derive. In particular, the 'y' transformation test (e.g. Box and Draper, 1987) did not prove helpful. Specifically, the main effect of k_f was difficult to model simply, particularly if the upper star point ($kf_{+\alpha}$) was included in the regression data. Eventually it was decided to treat this as an outlier, and to derive a simpler model of the form of equation 4.02. A final metamodel was then obtained using only five main effects and six interaction terms, all of the latter being

linear, although some were three-factor interactions. All of the regressions in deriving the final metamodel for sediment delivery ratio were conducted using scaled values calculated according to equation 4.05.

Regarding the topographic metric, no star points were used in the analysis, and the metamodel was restricted to an arbitrary number of regressors, in the manner outlined by Wu and Hamada (2000). The author was particularly concerned that adding too many regressor terms was merely 'patching' the model, rather like patching the holes in a dyke: each patch might cure a small part of the problem, but it could never substitute for having a better overall structure. Exhaustive testing, with forward and backward stepwise procedures, and using a wide range of two-factor and three-factor interaction terms, suggested that a reasonable final model, with an adjusted R^2 score of 90-95%, could be obtained using between 20 and 30 terms, and only linear, quadric or quadratic functions. By further extensive tests, this was reduced to a final metamodel of 20 regressors only, with an adjusted R^2 score of nearly 92%, a considerable improvement on the early regression efforts for this metric. It should be noted that all the regressions in deriving the final topographic metric metamodel were conducted using scaled design levels, calculated according to equation 4.01. These were found to work well, in that the regression could be forced through the origin, where the predicted value, by definition, should be zero. In the later regressions, a constant was incorporated, as this gave a slightly better model fit to the data.

The summaries of the two final metamodels for these metrics are provided in Table 4.3. Again, it will be noted that despite the increase in the degrees of freedom, the adjusted R^2 scores for both metamodels are high, with that for the sediment delivery ratio little different from the value obtained for its preliminary model. The plots of simulated values and residuals versus fitted values are shown in Figure 4.29, from which it will be seen that the models appear reasonably balanced, with no evidence of major misfit or bias. Possibly the sediment delivery ratio model is over-predicting slightly some of the lower values. Similarly, the scatter in the residuals for the topographic metric is rather wider than the author would have hoped to see, but this is probably as good a metamodel as can be derived from the data without using much more sophisticated mathematical functions, and quite possibly more output from additional GOLEM simulations.

Table 4.3: Final metamodels for sediment delivery ratio and the topographic metric, using the linear model form (eq. 4.02). All curvature terms are quadric functions unless noted otherwise, and all regressors were very highly significant (p <= 0.001) in both models.

	Sediment delivery ratio		**Topographic metric**	
	R^2 score 97.9 %, adjusted R^2 97.8 %		R^2 score 92.3 %, adjusted R^2 91.8 %	
	s = 0.3460		s = 2.009	
	328 data points, d.f. = 327 (1)		309 data points, d.f. = 308 (4)	
	11 regressors, plus constant (2)		20 regressors, plus constant (5)	
Parameter	Constant, linear term coefficient	Curvature or second term coefficient	Constant, linear term coefficient	Curvature or second term coefficient
Constant	103.944	.	98.8005	.
k_w	.	.	.	-7.7245
k_f	.	-12.4695 (3)	.	-7.0275
τ_c	.	-0.64724 (3)	.	-3.2006
n_{ci}	.	4.4700 (3)	.	.
t_{ci}	.	12.2402 (3)	1.1117	-3.9925 (6)
s_{cr}	.	-1.8176 (3)	.	-6.1646
INTERACTION EFFECTS				
$k_w \times k_f$	.	.	1.3665	.
$k_w \times k_f \times s_{cr}$	.	.	.	12.2212
$k_w \times \tau_c$	-4.3637	.	.	.
$k_w \times \tau_c \times n_{ci}$	2.0327	.	.	.
$k_w \times \tau_c \times t_{ci}$	2.8696	.	.	.
$k_w \times s_{cr}$	.	.	2.0325	.
$k_w \times t_{ci}$	.	.	.	.
$k_w \times s_{cr} \times k_b$	.	.	2.4705	.
$k_d \times t_{ci} \times s_{cr}$	.	.	-0.6702	.
$k_d \times t_{ci} \times \tau_b$	-1.6330	.	.	.
$k_f \times \tau_c$	.	.	2.4925	.
$k_f \times n_{ci}$	2.6974	.	-0.9912	.
$k_f \times n_{ci} \times t_{ci}$	-4.7859	.	.	.
$k_f \times t_{ci}$	.	.	-2.0197	.
$k_f \times s_{cr}$	.	.	-1.1439	.
$k_f \times k_b$	.	.	0.6937	.
$n_{ci} \times t_{ci}$	.	.	-4.6017	0.9647 (7)
$t_{ci} \times s_{cr}$	.	.	-0.8045	.

1. **All data points were used in the regression except the upper star point for k_f.**
2. **All parameter values were scaled, as defined by equation 4.05.**
3. **Sediment delivery ratio, main effects terms exponents or functions: k_f -1; τ_c 3; n_{ci} 1.3; ln|t_{ci}|; s_{cr} -0.8.**
4. **All star points omitted from the regression.**
5. **All parameter values were scaled to their scaled design levels, as defined by equation 4.01.**
6. **Topographic metric: second term for main effect of t_{ci} is abs(t_{ci}).**
7. **Topographic metric: second term for interaction of t_{ci} with n_{ci} is $n_{ci} \times$ abs(t_{ci}).**

a. Sediment delivery ratio. All units are in %.

i. Simulated vs fits, with 'perfect fit' line

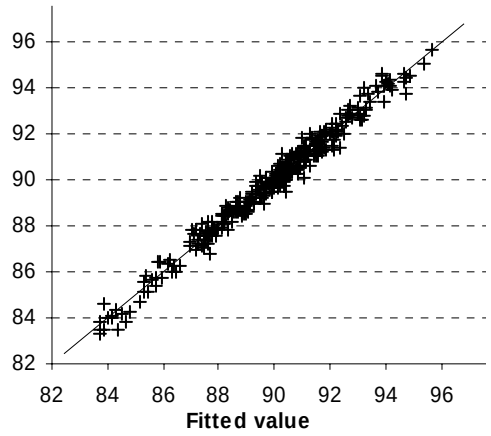

ii. Residuals vs fits.

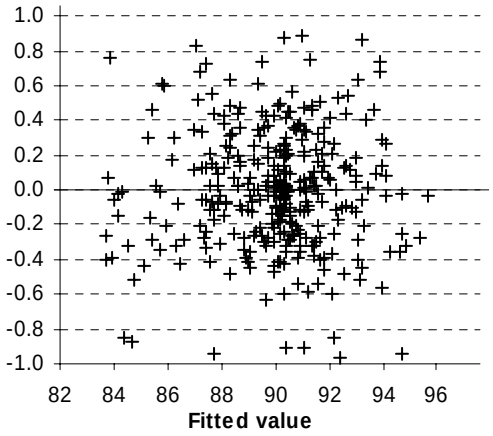

b. Topographic metric. All units are in %.

i. Simulated vs fits, with 'perfect fit' line

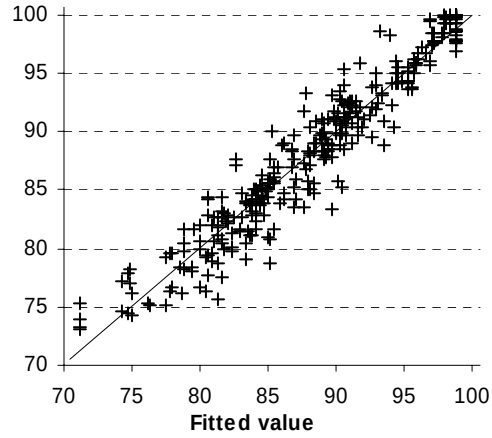

ii. Residuals vs fits.

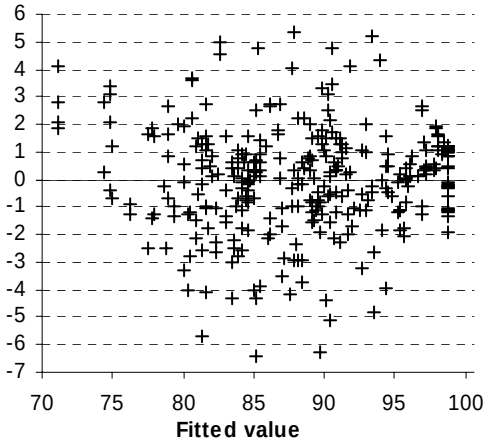

Figures 4.29, a and b: Output and residuals vs fitted values for the final metamodels of sediment delivery ratio and the topographic metric. (Regressors listed in Table 4.3)

This concludes the work of deriving the metamodels for the four chosen metrics. The main points in the chapter are now summarised.

4.6 CHAPTER SUMMARY

In this chapter, the output from the warm up simulation and the main experiment (using the central composite design) was reviewed in some detail as a basis for selecting four output metrics, representing output from GOLEM after 100,000 simulated years. In general, it was decided that there was little point in choosing metrics that were clearly insensitive to the

applied parameter sampling, as these would be highly equifinal, and metamodelling effort would reveal little more than could be reasonably inferred from plots of the output data. By contrast, using metrics which are more sensitive to the parameter sampling would be more informative of how model equifinality would be affected by sampling different combinations of the parameters, or using metrics in combination. The four chosen metrics, namely sediment yield, drainage density, sediment delivery ratio, and a topographic metric summarising elevation differences, were therefore selected after assessing their sensitivity to the parameter sampling represented by the factorial point simulations.

For three of the chosen metrics – sediment yield, drainage density and sediment delivery ratio - the output generated according to the central composite design proved very efficacious in forming preliminary metamodels. The preliminary metamodels all achieved high R^2 scores (>> 90%), with balanced residuals, and performed well in tests against output from new simulations. However, deriving the topographic metric's metamodel proved highly problematical using the same approach, and much additional sampling was needed to clarify the forms of the main effects of the parameters on this metric, many proving to be bowl or Christmas pudding shaped, or markedly stepped or pointed.

Consequently, the regression analysis was reattempted, but taking into account the proposed use of a (non-parametric) 'bootstrap'. The bootstrap allows error from the regressions (from the lists of residuals) to be added to metamodel predictions, and a confidence interval around the quantifications of model equifinality to be calculated. Accordingly, provided the metamodels are closely fitted ($R^2 > c.$ 90%), parsimonious, and the residuals plots balanced, all of the sample data, including the test simulation results and the additional main effects cases, can be used in deriving the final metamodels for each metric.

This revision in the approach to deriving the metamodels allowed parsimonious log form models (equation 4.04) to be derived for sediment yield and drainage density, and linear form models (equation 4.02) for the sediment delivery ratio and the topographic metric. The first three metrics' final metamodels achieved high R^2 scores in the regression analyses (*c.* 98% or more), which was considered very satisfactory. The final metamodel for the topographic metric achieved an R^2 score of *c.* 92%, despite being restricted for simplicity to only 20 regressors. Nevertheless, the fit was considered good enough for the research purpose herein. Having therefore derived the tools for predicting GOLEM's output across the parameter space, the method by which the metamodels were applied and the resulting quantifications of model equifinality are presented next.

CHAPTER 5: RESULTS (1) - QUANTIFYING EQUIFINALITY IN SINGLE METRICS AND POLYMETRIC COMBINATIONS

5.1 INTRODUCTION

Having explained how the metamodels were derived, it is now possible to turn to the results generated through their use, both in quantifying model equifinality and in mapping equifinal solution regions. It will be appreciated that the metamodels provide great flexibility in the way the parameter space may be explored; in particular, equifinality can be quantified using metrics singly or in combinations ('polymetric' equifinality), presented in this chapter, or the search can encompass subsets of the parameter space, to identify the influence on equifinality of the parameters individually and in combination, presented in Chapter 6. The main aim in this chapter is to present the more general situations, that is, where the exploration is conducted across the whole parameter space, regardless of whether only one metric or a polymetric combination is being considered.

As this part of the research necessitated running replicates of the calculations with each metamodel, large data sets were generated, so the results have had to be heavily summarised, with additional detail provided in the appendices. In mapping the equifinal solution regions, a further simplification has also been required, so the examples of mapping are limited to explorations of the parameter space using only two of the parameters. This permits much easier plotting and visualisation of the results, and also emphasises the main points of interest.

Besides the need to summarise and simplify, the ordering of ideas and main findings has been chosen carefully. Issues relating to replication and the robustness of the results are presented first, as the points raised apply to the all of the results, including those presented later, in Chapter 6. Similarly, it was thought more appropriate to present single metric equifinality before the polymetric examples, as understanding of the former is simpler to explain, and there are some general points which also apply to the latter. Regarding other matters of interest, the parameter space exploration is also applied to mapping equifinal solution regions of the parameter space, and this aids understanding of the difference between single metric and polymetric equifinality.

The use of the bootstrap, introduced in Chapter 4, was fundamental to all of the calculations, so the method of its application is considered first.

5.2 IMPLEMENTATION OF THE BOOTSTRAP METHOD

5.2.1 Basic calculations

The general procedure that was applied to obtain bootstrapped results for each of the metrics singly is shown in Figure 5.1. The first steps are quite straightforward: sample points are selected at random from within the 10-D factorial space and the value for the metric at that point is calculated using the metamodel (steps 1 and 2). An error term is then selected at random from the appropriate residuals list (subsection 4.4.5 *q.v.*), and used to 'boot' the prediction, either raising or lowering it according to the value of the error (steps 3 and 4). The booted solution is then compared with a reference value for the metric. In all of the calculations herein, the value of the reference was that metric's value obtained from the base case simulation at 100,000 years. It is accepted that different target values could have been chosen, but for simplicity the base case values seem the most appropriate. In particular, their use conforms with the idea of using a LEM to simulate the evolution of a landscape to the present day, such that there is only one reference condition – the present day landscape – with which to compare LEM outputs for equifinality. Also, as described in Chapter 4, the base case is used as the reference landscape in the calculation of the topographic metric, so use of the base case for the other metrics provides consistency across the reference conditions for all of the metrics. The reference results for each metric, therefore, are as follows:

- for sediment yield, 24.913 m km^{-2} yr^{-1};
- for drainage density, 3.150 km km^{-2};
- for sediment delivery ratio, 90.177%; and
- for the topographic metric, 100% (which is the value by definition).

Turning again to Figure 5.1, the bootstrapped solutions are therefore compared with the reference values for each metric, and differences between the two are expressed as a percentage of the latter's value (step 5). It will be realised that the percentage can be positive or negative, so it was decided for simplicity to use absolute percentage differences.

The use of absolute percentages also allows the introduction of a *tolerance band* to equifinality in the calculations. This permits a wider range of results to be compared with the reference, so that the exploration of equifinality can be extended to results which are

similar to it, rather than having to be exactly the same. Thus, provided the absolute percentage difference lies within the target tolerance band, the booted solution is treated as equifinal to the reference case (step 6).

The tolerance bands used in this research were chosen after trial and error, and are ranged from 1% to 10%, in 1% intervals, with an additional band of 0.05%. The latter was included primarily to allow equifinal response curves to be plotted near the origin, as obtaining exactly equifinal solutions for the sediment yield, drainage density and sediment delivery ratio seemed highly unlikely. However, the topographic metric metamodel, by reason of the definition of the metric, could be expected to generate results which are 100% equifinal. Such a result would mean that all the elevation differences between the base case landscape and the test landscape are predicted to be less than one metre. Rather than use a separate 0% band to detect these cases, the 0.05% band was considered close enough and was also used for this metric.

Although the treatment of negative and positive results has been explained above, a further adaptation was also required for the topographic metric, as booted results of over 100% could be generated. Accepting such a bootstrapped result would make no sense, however: either all the elevation differences between the landscapes are predicted to be less than one metre or they are not. Any booted solutions of greater than 100% were therefore truncated to 100% for the calculations herein.

Having described the selection of the tolerance bands and their use, the remaining calculations (steps 6 to 9) are essentially a matter of recording each result and updating the running totals. The procedure for polymetric calculations was also essentially the same as that shown in Figure 5.1. However, the predictions for each metric were made using the same sample point in the parameter space, whereas the bootstrap errors were still selected at random from each metric's list. The polymetric results are presented in this chapter, after the single metric results.

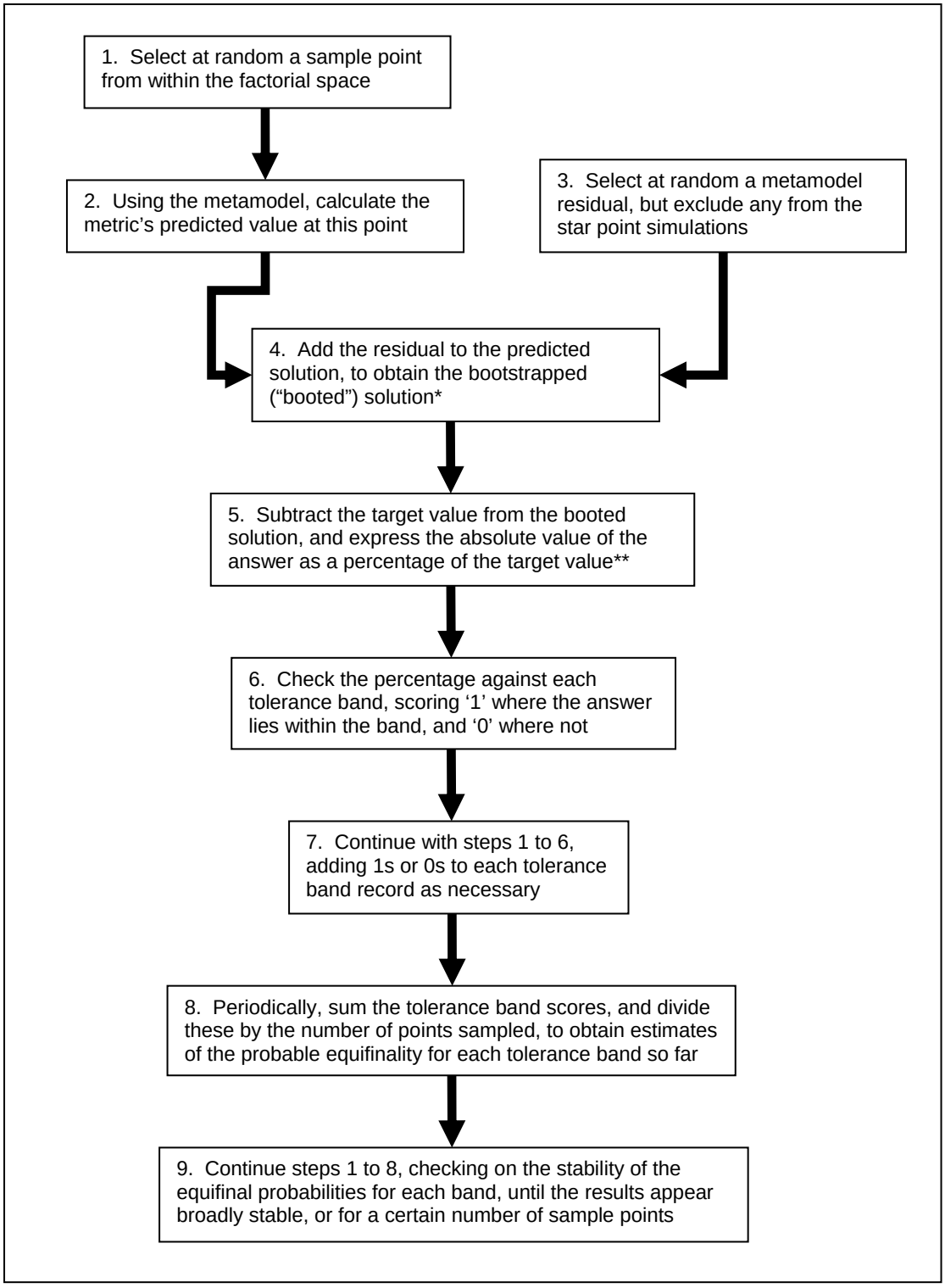

Figure 5.1: Flow chart outlining implementation of the bootstrap method for calculating equifinal proportions for each metric and tolerance band.

* Step 4. The sediment yield and drainage density calculations were made using the log model forms (equation 4.04). To effect the bootstrap, the predictions were first converted to actual values, and residuals were also added as actual values, as listed in Appendix K.

** Step 5. The target values are the base case results for the metrics, as explained in accompanying text.

To examine the effect of model size i.e. the differences in the equifinal response as one increases the number of parameters varied, the calculations were performed by varying at first only one of the parameters, then two, then three, and so on, in order of their importance as main effects, until all the parameters in the metamodel were allowed to vary together. No polymetric calculations of this kind were performed, however, as they were considered too numerous and complicated to set up. The model size calculations and results are described in Chapter 6.

Having explained the basic calculation method, some comments are needed on stability of the results and calculation of confidence intervals, and these matters are now considered.

5.2.2 Replication, stability and confidence intervals

Although the confidence interval around the results would be inversely related to the bootstrap sample size (subsection 4.4.5, *q.v.*), this still left a question over how large the bootstrap samples should be, and whether the results needed to be replicated. The algorithms allowed running totals to be stored, which could show - as a trace on a plot - how the results varied with size of the bootstrap run. Figure 5.2 is a typical example of such a trace, for sediment yield in the 2% equifinal tolerance band, and shows how the proportion of cases found to be equifinal changed as the number of bootstrapped sample points was increased. It also shows the upper and lower 95% confidence limits at any point, these being found by the binomial theorem (e.g. Box *et al.*, 1978) from the equation :

$$\sigma = \sqrt{\frac{pq}{n}}, \qquad 5.01$$

where σ is the standard deviation, p the number of solutions falling within the tolerance band, q the number falling outside the tolerance band, and n is the bootstrap run size[1].

The first thing to note from the plot is that the search of the parameter space has found equifinal solutions for this metric in the selected tolerance band. In this instance, the reference solution for sediment yield is 24.913 m^3 km^{-2} yr^{-1}, so the upper and lower values corresponding to the tolerance band are respectively *c.* 25.4 and 24.4 m^3 km^{-2} yr^{-1}. The

[1] Strictly speaking, the 95% confidence limits differ between the binomial and normal distributions, especially if n is small (< *c.*50), and p is near 0 or 1 (Box *et al.*, 1978). However, for large n, as here, the differences are negligible (*ibid.*), and the intervals may be calculated using $\pm 1.96\sigma$, based on σ as derived from equation 5.01.

result therefore shows that a proportion, equating to about 18.6% of the solutions, is equifinal to within this range of values. Given the large sample size, the 18.6% figure is also a reasonable estimate of the probability that the next sample point – selected at random - will also generate a solution equifinal to within the same band. The example result may therefore be expressed more specifically, saying that, in any simulation using parameter values selected at random from within the factorial space, there is approximately an 18.6% probability that the result generated will be equifinal to within 2% of the base case result. For simplicity, the author will generally talk in terms of *equifinal probability* (or probabilities) from here onwards. The example result may therefore be stated more succinctly, by saying that the equifinal probability is 18.6% in the 2% band.

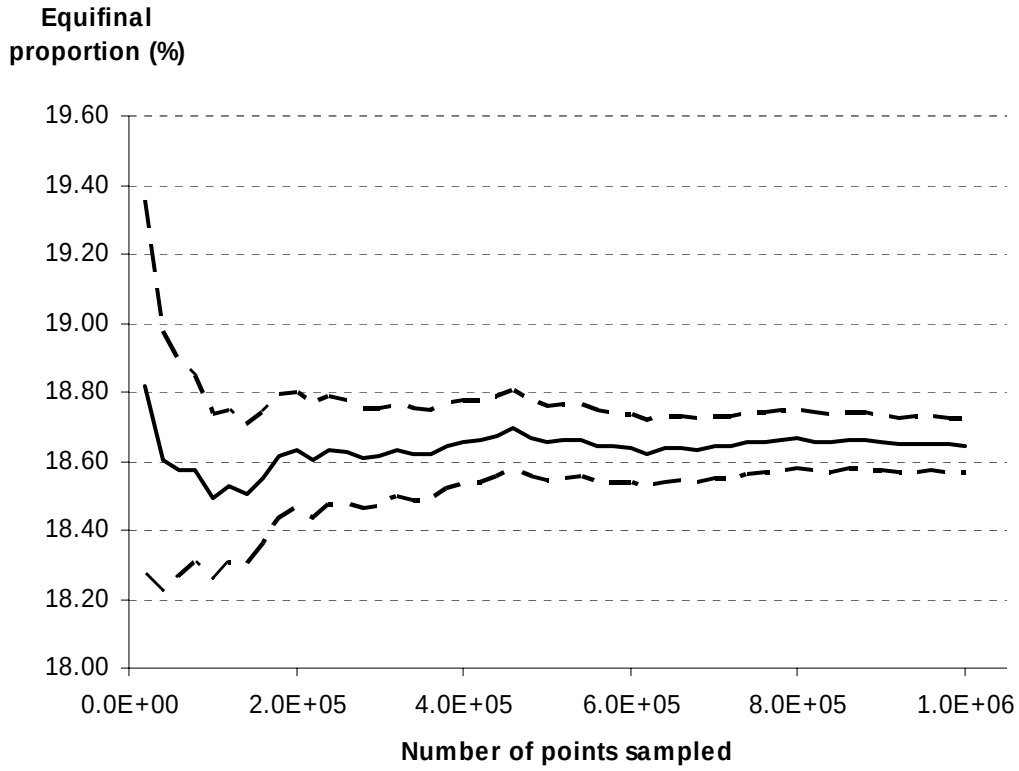

Figure 5.2: Example bootstrap trace (bold line), for sediment yield in the 2% tolerance band, updated after every 20,000 points. Dashed lines mark ±95% confidence limits (eq. 5.01).

Figure 5.2 also shows that the fluctuations in the probability become smaller, and the probability more nearly stable, as the bootstrap run size increases. In the example, the values range from between about 18.8 and 18.5% during the first 200,000 or so sample points, but then between about 18.6 and 18.7% during the next 400,000 points, and only between about 18.63 and 18.67% over the last 400,000 points. Similar comments can be

made about the confidence intervals, which also become narrower as the number of bootstrap samples increases. The limits are much narrower after 400,000 or so points compared with those near the start of the bootstrap set. However, after 400,000 points, the narrowing of the confidence interval is much less marked. This suggests that the confidence interval is also tending to a more nearly stable value, in this case at about ±0.08%.

Despite the foregoing, when conducting the calculations the author could not be sure whether the result above, and ones relating to the other metrics or polymetric cases, were in some way atypical, so as a precaution, all such results were replicated ten times, and unless otherwise stated herein, all bootstrap sets comprised run sizes of a million sample points each. Although the use of replicates may seem cautious, the bootstrap runs were not onerous computationally, taking about one hour each for a million sample points, which was a huge gain compared with the running time of the full simulations with GOLEM (from 28 to 42 hours per simulation). It should also be borne in mind that a sample of a million points from a 10-D parameter space, assuming the type of N^k structured sampling described in Chapter 3, is equivalent to about four levels per parameter, which does not seem excessive.

By adopting these measures, and taking the mean of the replicates, the equifinal probabilities and associated confidence intervals appeared to be much more nearly stable. This is illustrated in Figure 5.3, which shows the trace for each replicate and the overall mean, again using sediment yield and the 2% tolerance band as the example. A grey background is used to highlight the different traces left by each replicate.

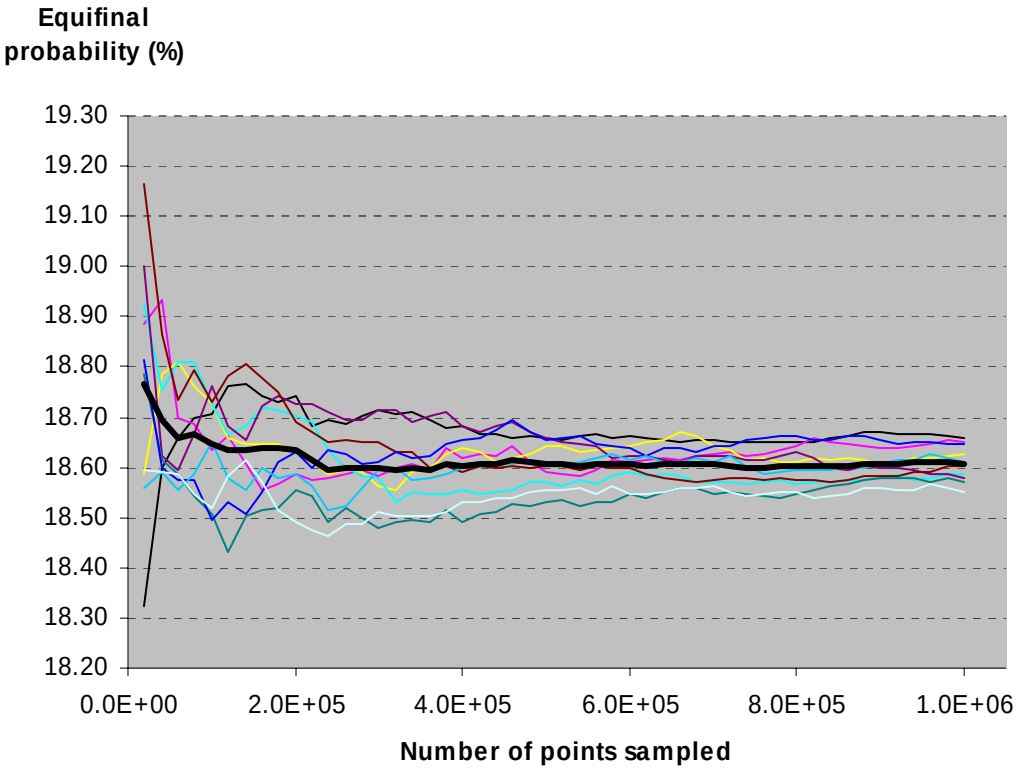

Figure 5.3: Estimated equifinal probabilities for sediment yield, in the 2% tolerance band, for ten replicate bootstrap sets, with the overall mean shown by the bold black line.

The traces for each replicate are very similar in general form to the one show in Figure 5.2. It is reassuring to note that each trace, despite any big differences between them near the start of the set, is tending towards the same general value, between 18.5% and 18.7%, with a mean of close to 18.6%. Variations in the mean equifinal probability are present throughout, but are generally very small after the first 300,000 or so sample points, and always smaller than in any of the individual probability traces. It should be borne in mind, however, that the example shown above is based on the sediment yield metamodel, which was the most closely fitting of the four (Table 4.2 *q.v.*). As the other metamodel predictions, particularly those for the topographic metric, were subject to larger errors, it was decided to use bootstrap run sizes of a million sample points in all of the basic calculations herein, replicated ten times, regardless of the metric.

The overall mean in the above example is also plotted in Figure 5.4, but this time with the two sets of upper and lower 95% confidence limits, one calculated using the replicate mean and the binomial formula, and the other based more simply on the standard deviation of the ten replicates themselves.

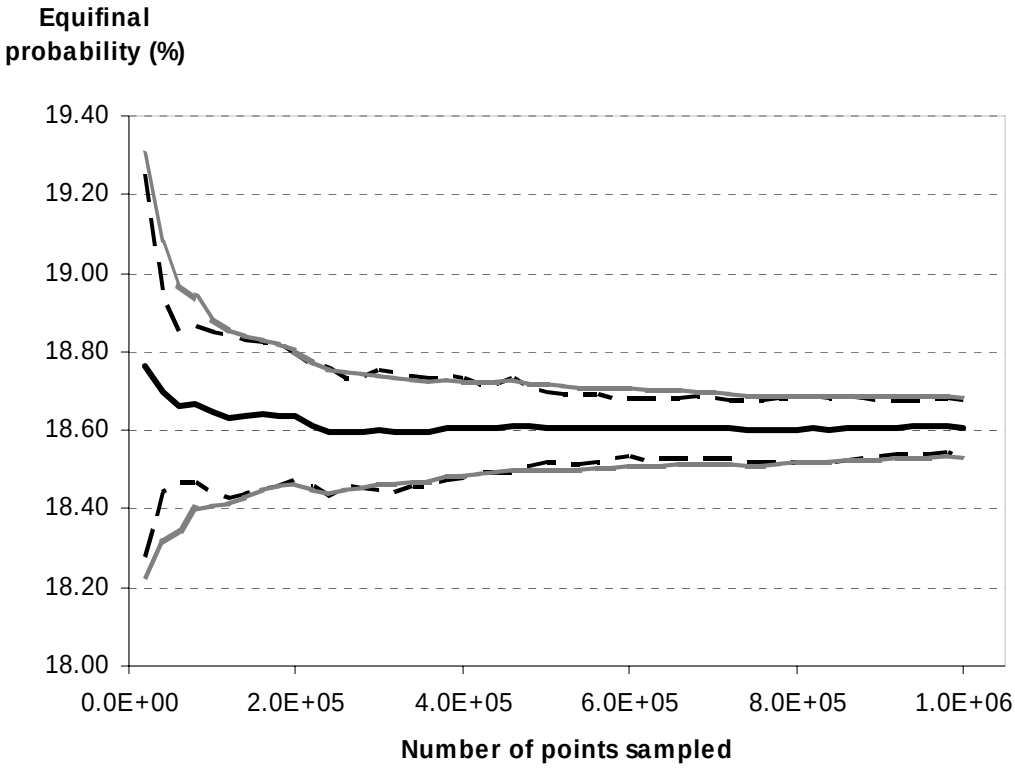

Figure 5.4: Mean equifinal probabilities for sediment yield, in the 2% tolerance band, based on ten replicate bootstrap sets, and showing upper and lower 95% confidence limits. The hatched line shows the limits calculated using the overall mean and binomial theorem formula (eq. 5.01); the dashed line shows the limits calculated directly from the replicates.

The data in Figure 5.4 show that there is little difference between the confidence intervals as calculated using either method, and this gives some comfort that the estimate based on the binomial theorem is generally acceptable. In the example above, at some points one interval is slightly narrower than the other, but both calculations show the same trend overall. This result was found to be repeated generally, throughout the calculations. In more detail, Figures 5.5 shows the 95% confidence intervals for each metric across all of the tolerance bands. Each confidence interval estimate is based on the standard deviation calculated by equation 5.01, this in turn using the overall mean from the ten replicates, with one million booted sample points per replicate.

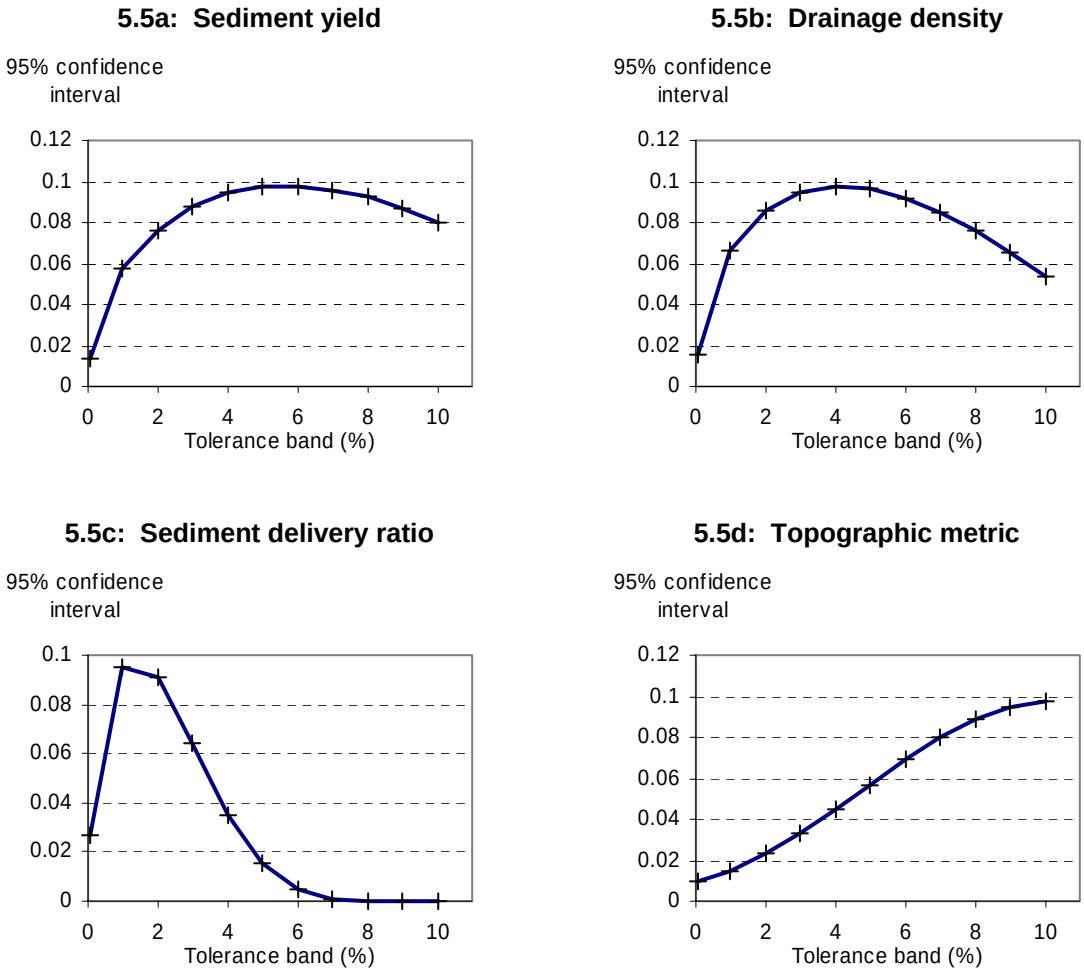

Figure 5.5, a-d: 95% confidence intervals, for each metric and tolerance band, calculated from the mean equifinal probabilities and using the binomial theorem formula (Eq. 5.01)

The humped appearances of plots a-c, and the rising trend in plot d, result from the relationship between the mean and standard deviation in the binomial distribution (e.g. Box *et al.*, 1978). This point aside, the plots show clearly that the confidence interval is small (< 0·1%) for all of the metrics and in all tolerance bands, a result that is repeated in all of the polymetric calculations. The results which are reported subsequently, therefore, are the mean equifinal probabilities only, as the confidence intervals are too narrow to be distinguished from the equifinal probability curves. Any confidence intervals quoted in the text are calculated using the binomial formula method (equation 5.01).

Having dealt with the general issue of the stability of the results and confidence intervals, results for the metrics singly are now presented.

5.3 SINGLE METRIC EQUIFINALITY – RESULTS FOR ALL FOUR METRICS

The results for all of the metrics are listed in Table 5.1, and plotted in Figure 5.6.

Table 5.1: Mean equifinal probabilities in each tolerance band, for each metric.

	Equifinal probabilities by metric (%)			
Tolerance band (%)	**Sediment yield**	**Drainage density**	**Sediment delivery ratio**	**Topographic metric**
0.05	0.47	0.66	1.94	0.23
1	9.36	13.13	37.62	0.59
2	18.61	25.84	68.35	1.39
3	27.68	37.75	87.92	2.93
4	36.45	48.63	96.70	5.50
5	44.85	58.46	99.36	9.32
6	52.76	67.24	99.94	14.49
7	60.14	74.97	100.00	20.98
8	66.93	81.63	100.00	28.64
9	73.08	87.24	100.00	37.20
10	78.55	91.81	100.00	46.30

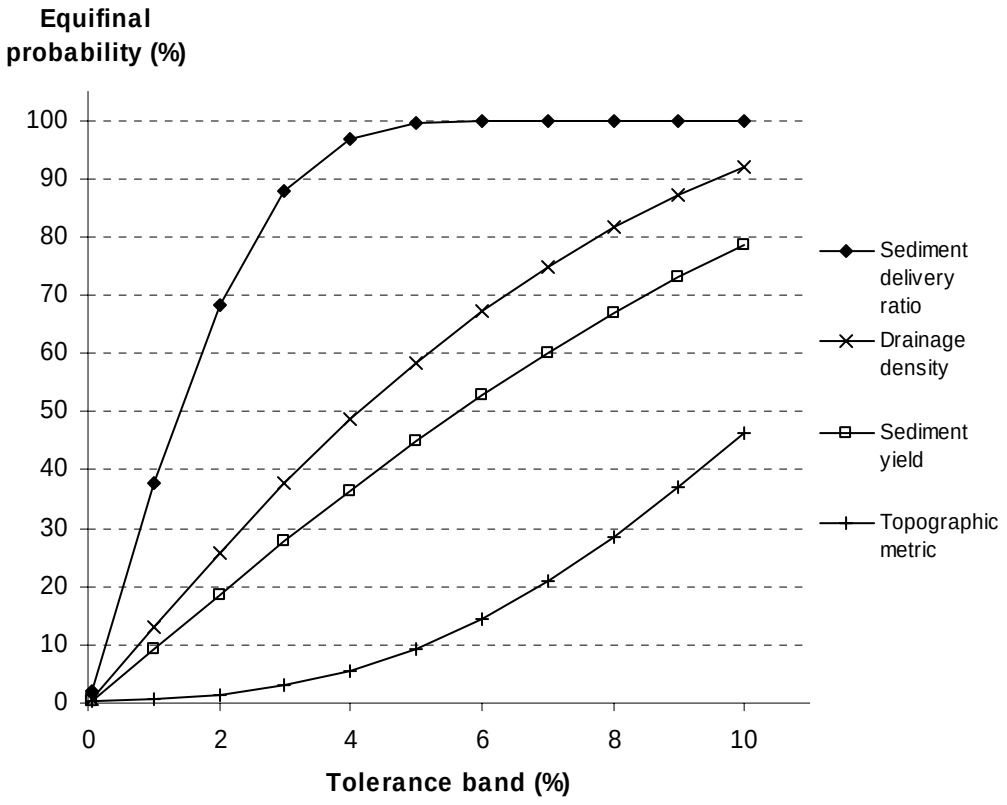

Figure 5.6: Equifinal probabilities for all metrics singly, in all tolerance bands. As discussed in the text, the confidence intervals are too narrow to be shown on the plot at this scale.

Figure 5.6 shows that the probability of obtaining an equifinal solution increases for all of the metrics as one increases the tolerance band. However, there are marked differences in the values and trends for each metric, and this needs some comment.

Dealing first with the sediment delivery ratio, the probability of obtaining an equifinal solution for this metric within the 1% tolerance band is estimated to be about 38%, rising to 68% for the 2% band, 88% for the 3% band, virtually 100% for the 4-6% bands, and 100% for all of the higher bands. Hence, there is, compared with the other metrics, a relatively high probability of an equifinal solution in this band. Indeed, for any tolerance band, this metric is clearly the most likely to be equifinal of the four considered here. Such a property would make model calibration using this metric on its own highly problematical. The matter is yet more problematic when the tolerance band is compared with the accuracy of typical field data on the same metric. For example, if estimating rates of sediment transport using different fluvial transport equations, it can be difficult to obtain an answer accurate to within one order of magnitude (e.g. Gomez and Church, 1989), let alone to within ± 5% or 10% of the true figure. Similarly, errors of ± 20-50% are likely in estimates of long term rates of erosion, depending upon the processes and setting (e.g. Saunders and Young, 1983; Young and Saunders, 1986; see also Selby, 1993, Chapter 19). There can also be large differences in sediment movement within a catchment, such that the sediment delivery ratio appears large near headwaters regions, but small near the outlet, adding further difficulties to accurate estimation of true figures (*ibid.*; see also Richards, 1993). These considerations help to put into perspective the tolerance bands being used for the sediment delivery ratio, and indeed for the other metrics treated here.

Regarding the shape of the probability curve, although the sediment delivery ratio displays high equifinality at low tolerances, the curvature of the trend is convex. This implies that it becomes increasingly difficult to find additional equifinal combinations of parameter values in the factorial space as the tolerance band is increased: such new solutions can be found, but they occupy a smaller proportion of the remaining, unused space.

Turning to drainage density and sediment yield, both of these metrics were found to have similar equifinal probabilities in each band, although those for drainage density are consistently somewhat higher than those for sediment yield. In the 5% tolerance band, the equifinal probabilities for sediment yield and drainage density are estimated to be about 45% and 58% respectively, and these rise to about 78.5% and 92% in the 10% band. Again, the high probability of obtaining an equifinal solution, even at quite low tolerances, will be

noted. Also, the low tolerances, compared with errors typical in field data, are striking, (even for the drainage density, as errors of ±20% are quite feasible, e.g. Heine *et al.*, 2004).

The curvature for each of these relationships is also convex, and each curve appears to be trending towards an upper limit. Having already seen how the sediment delivery ratio trends to 100%, it seems likely that the equifinality would approach 100% for both the drainage density and the sediment yield each at a tolerance band of about 15%. As with the sediment delivery ratio, the rate of change is seen to decline at the higher bands, presumably because the factorial space is taken up by more solutions for each increase in tolerance.

The model equifinality represented by the topographic metric was found to be lower throughout than it was for any of the other metrics, and markedly so for much of the range. Even in the 10% band, the probability of an equifinal solution is found to be about 46%, and roughly half that of the next most sensitive indicators (sediment yield and drainage density). At 5%, the topographic equifinal probability is estimated to be only 9% or so, barely a fifth of the figure for the sediment yield. The topographic metric is therefore the most sensitive of the metrics, and the least likely to be equifinal. However, to what extent the tolerance bands are significant or not compared with field data is more difficult to assess. Certainly, the insensitivity of the other metrics of elevation quantities was revealed clearly in Chapter 4, hence the main reason for having to devise the topographic metric for the purpose herein. Possibly a researcher using the topographic metric or a similar estimation of elevation differences would consider selecting *a priori* a target value, within which the results would be considered equifinal. Thus, 90% might be considered equifinal in one study, or 95% in another, and so on. It will be appreciated that the situation is not ideal, however, and the need to develop better elevation metrics generally is included in the recommendations, in Chapter 7.

The trend in the topographic metric curve was found also to be concave, rather than convex, which implies that it becomes easier to find equifinal solutions for this metric as the tolerance band is increased. This contrasts strongly with the results for the other metrics. Some deeper reasoning is required, taking into account the changes affecting the modelled landscape and how these are manifested as parameter effects, in order to explain why this should be so. An indication of how the shape of the curve may be accounted for is considered in the exploration of model size influences and metamodel archetypes, discussed in Chapter 6.

One of the other striking features from the probability curves in Figure 5.5 is just how devoid of feature they are, all of the curves appearing smooth and continuous, suggesting that each individual metric's equifinal probability can also be expressed by an equation in terms of the tolerance bands alone.

Having considered quantification of single metric equifinality, and introduced some ideas important to the wider topic, it is now possible to consider the polymetric calculations.

5.4 POLYMETRIC EQUIFINALITY

5.4.1 Introduction and a bimetric example

Illustration of bimetric equifinality, using sediment yield and the topographic metric

Although the single metric quantifications are straightforward to explain and visualise, matters become more complicated when considering polymetric equifinality. Regarding the calculations, the method is identical to that outlined in Figure 5.1, save that all four metrics' predictions are calculated simultaneously, using the same point in the parameter space. The predictions are then bootstrapped separately, selecting randomly from each metric's list of residuals.

Regarding the tolerance bands, these are also the same as those used in the single metric calculations. However, it was thought necessary to include an additional band, labelled 'unrestricted' to permit subsets of polymetric combinations to be calculated. Thus, if the sediment yield band was unrestricted, the polymetric results would refer to tolerance bands applied to the drainage density, the sediment delivery ratio and the topographic metric only. Similarly, if both the topographic metric and sediment yield bands were unrestricted, the polymetric results would apply to the drainage density and the sediment delivery ratio only. The inclusion of the unrestricted band provides twelve possible tolerance bands for each metric, and therefore 20,736 (i.e. 12^4) separate possible banded quantifications. Since each bootstrap set comprises a million sample points, and each set was replicated ten times, this presents a formidable data handling and visualisation problem.

The solution adopted herein is to focus firstly on the sediment yield and topographic metrics, and then examine how the equifinal response for these two metrics is affected by

applying tolerance band restrictions on the drainage density and sediment delivery ratio. Figure 5.7 therefore shows the bimetric equifinality for the topographic metric and sediment yield together. It should be noted here that the equifinal probability is now visualised as a surface. It is also useful to begin talking, with regard to the polymetric results, in terms of the 'tolerance space', and the equifinal probability 'zones' found within the tolerance band combinations.

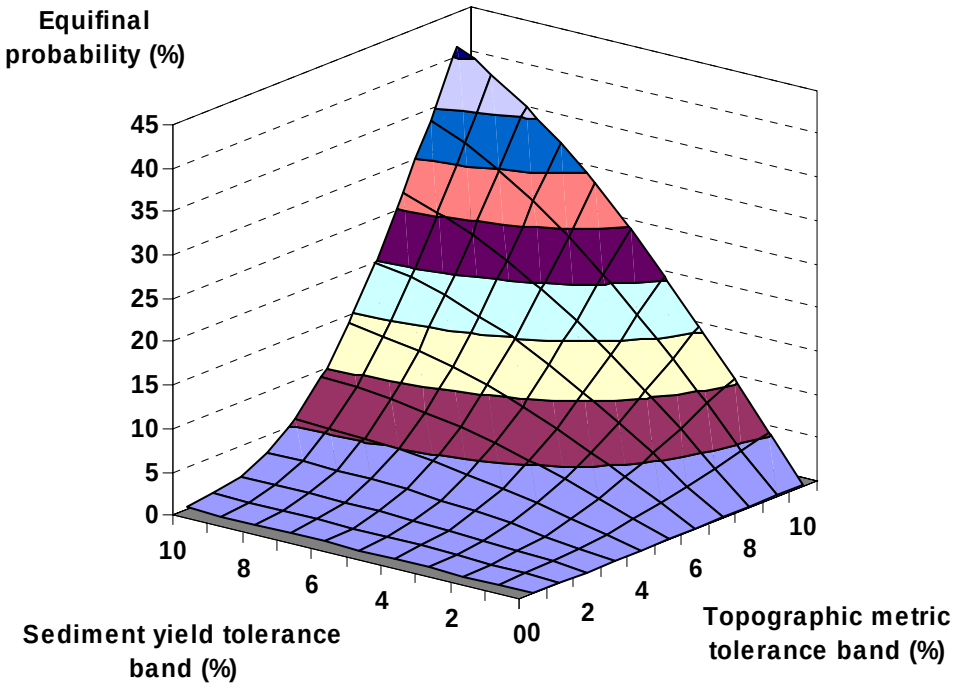

Figure 5.7: Bimetric equifinal probabilities for the topographic metric and sediment yield, topographic bands along the x axis, and sediment yield bands along the y axis. The surface is the overall mean from ten replicates, of one million bootstrapped sample points each, and is shaded in the 5% contour bands corresponding to the probability axis scale.

Figure 5.7 shows that as the tolerance band of one metric is reduced, the probability of obtaining an equifinal result for the other metric is also reduced. In this manner, each metric's individual curve becomes more flattened as the tolerance band applied to the other metric approaches zero. The probability, therefore, of obtaining an equifinal solution for both metrics together, each within a given tolerance band, is lower than the probability for these metrics singly within the same bands. This result is also shown in Figure 5.8, which is an overhead contour plot of the data in Figure 5.7. The contours help to emphasise the curvature of the bimetric probability surface, as well as bringing out other points which are of interest here.

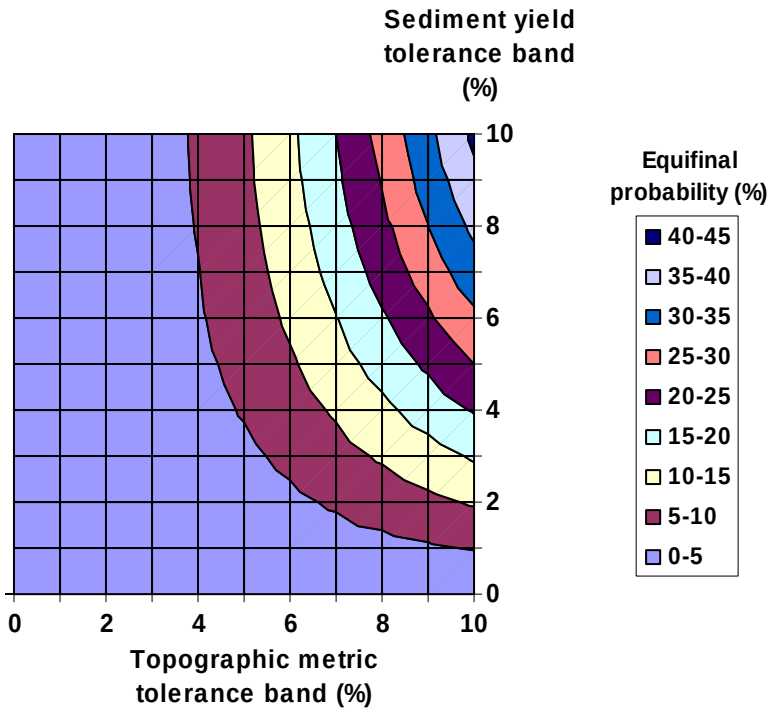

Figure 5.8: The same bimetric equifinality data for the topographic metric and sediment yield as plotted in Figure 5.7, but shown as an overhead contour plot to highlight the curvature of the surface. Note the area lying within the 0 - 5% probability zone.

Some useful comparisons can be made between Figures 5.6 and Figure 5.8. For example, from Figure 5.6, the probability of obtaining an equifinal solution for sediment yield in the 5% band is approximately 45%. However, from Figure 5.8, by also applying a tolerance band of 10% for the topographic metric, this probability falls to about 25%. By imposing a even tighter tolerance band on the topographic metric, say 6%, the probability is reduced even more, to about 9.5%. The same point can be made by considering the topographic metric first, and constraining it with a narrower and narrower tolerance band for the sediment yield.

Another way of considering the effect of using two metrics simultaneously is to note how much of the tolerance space lies in the 0 to 5% probability zone, roughly 55% in this example; similarly, about 68% of the tolerance space lies in the 0 to 10% probability zone. This is strikingly different from the results found for the metrics singly, as shown in Figure 5.6. Thus, to ensure that the probability of obtaining an equifinal sediment yield solution was 10% or less, the tolerance band allowable in the single metric calculations would have to be approximately 1% (from Figure 5.6). By contrast, by simultaneously applying a tolerance band of 10% (or less) for the topographic metric, the tolerance band for the

sediment yield can be allowed to range between from 2% and 10%, yet the probability of an equifinal solution still remains within the 10% zone i.e. at 10% or less.

Confidence intervals in the bimetric and polymetric examples

Before closing this introductory section, some comments are needed on the stability of the solutions and the confidence intervals. These were checked thoroughly, not simply in the example bimetric case, but also for the polymetric cases generally, and were found to be materially no different from what was observed in the single metric calculations. The polymetric solutions all tended to a more nearly stable probability, for each combination of bands, as the number of sample points was increased. Likewise, the mean value from the replicates was also very stable, indeed more so than for any of the polymetric replicates individually. The standard deviations calculated using the binomial formula and from the replicates direct also matched each other very closely, and were very small when compared with the equifinal probabilities themselves. Overall, as in the single metric examples, the confidence intervals were too small to be distinguishable from the mean probability surfaces at the scale of interest, and are not plotted in the results which follow. However, it should be noted that the confidence limits, rather than being a zone either side of the probability curve, in this case encompass a region bounded by two surfaces either side of the mean probability surface. As an example, Figure 5.9 shows a plot of the confidence interval for the bimetric equifinality data plotted in Figures 5.7 and 5.8. The interval has been calculated using the binomial theorem formula, and varies with the mean equifinal probability in the manner explained in subsection 5.2.2.

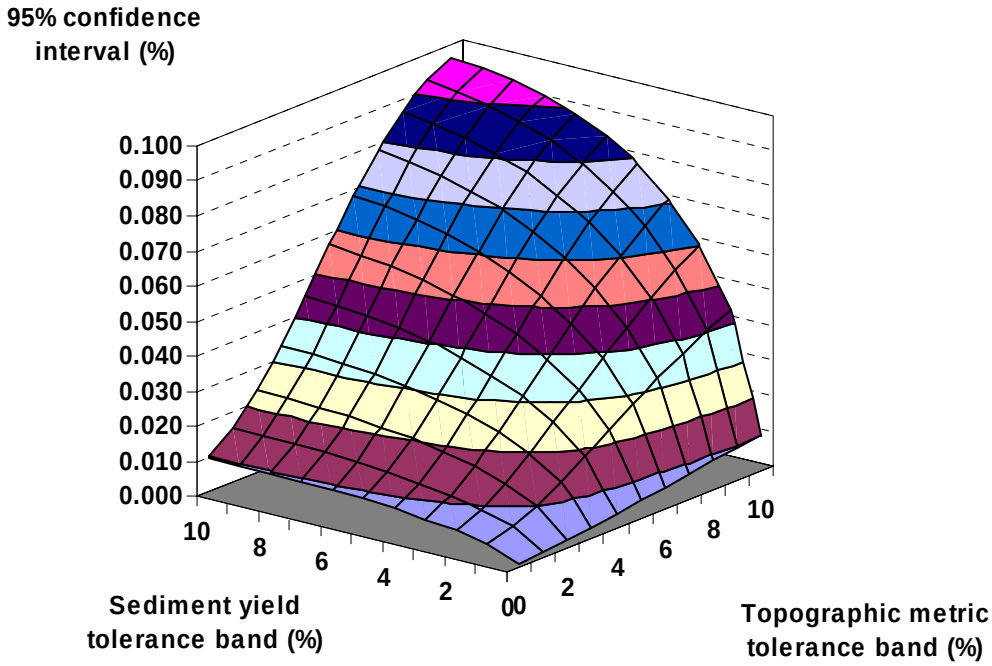

Figure 5.9: Confidence intervals for the combined sediment yield and topographic metric equifinality data shown in Figures 5.7 and 5.8.

Having considered in some detail a bimetric example, presentation of the polymetric results for all four of the metrics now follows.

5.4.2 Polymetric results

The results here are shown, in Figures 5.10 and 5.11, in the same manner as for the bimetric example above, with surface and contour plots of the equifinality probabilities for the topographic metric and sediment yield. However, each equifinality probability surface is itself further constrained by tolerance bands imposed on the drainage density and sediment delivery ratio, and a range of combinations is shown by arraying the plots by the different tolerance bands applied to the latter two metrics. The drainage density and sediment delivery ratio tolerance bands are therefore listed in the corresponding column headings or left hand row labels.

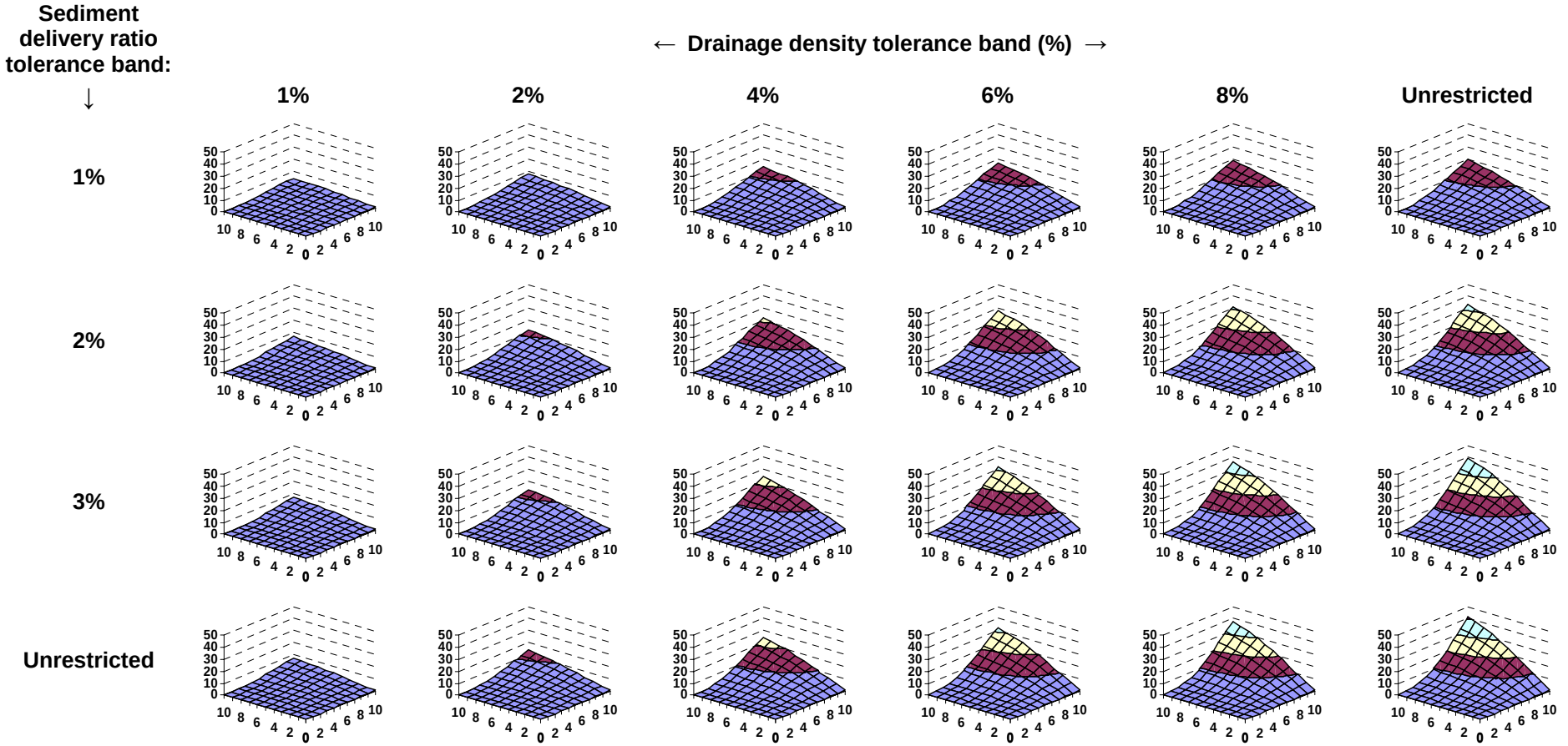

Figure 5.10: Polymetric equifinality probability surfaces. Each plot shows the probability of obtaining an equifinal solution for all four metrics simultaneously i.e. from the same point in the parameter space, subject to tolerance bands for each. As in Figure 5.7, the x axis is the tolerance band for the topographic metric, and the y axis the tolerance band for the sediment yield. Tolerance bands for the drainage density and sediment delivery ratio are shown respectively in the column headings and row labels. The probability zones are shaded in 10% intervals.

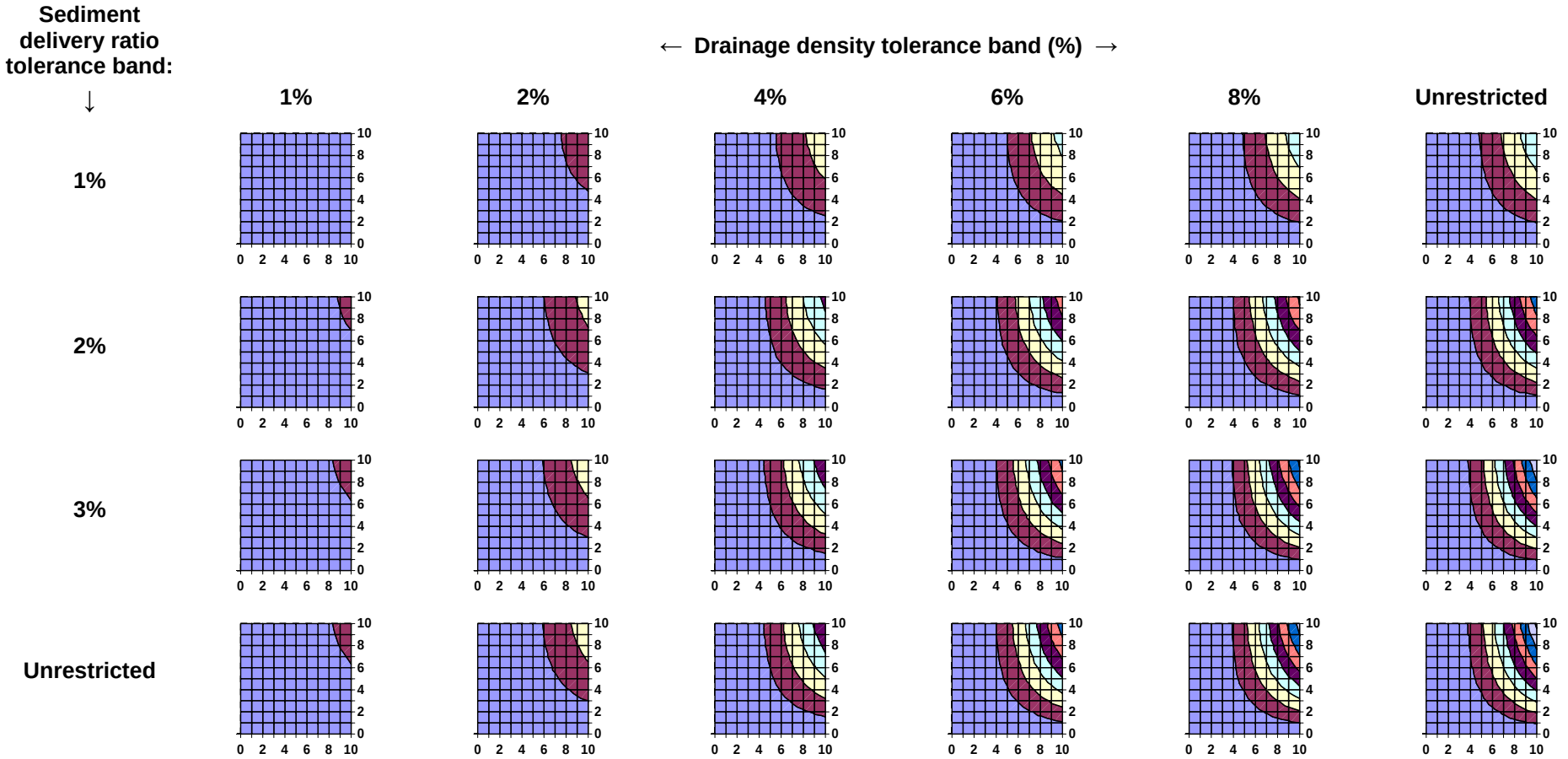

Figure 5.11: Contour plots of the polymetric equifinal probability surfaces in Figure 5.10, showing the probability of obtaining an equifinal solution for all four metrics simultaneously. Probability zones are shaded here in 5% intervals, to emphasis the curvature in the probability surfaces. The x and y axes are the tolerance bands for the topographic metric and sediment yield respectively, and the tolerance bands for drainage density and sediment delivery ratio are shown as before in the column headings and left hand row labels.

As with the bimetric example, the plots show clearly that as the tolerance band for each metric is increased, the probability of obtaining an equifinal solution also increases. However, as was previously shown, the probability of generating two or more equifinal solutions together is usually less than the probability of doing so if using a single metric alone. As a corollary to this point, some metrics appear to impose more of a constraint than others, particularly at the lower tolerance bands. For example, there was very little difference between any of the results where the sediment delivery ratio tolerance band was held at 3% and where it was unrestricted. Similarly, the drainage density tolerance band constrained the polymetric equifinality less and less as the former band tended towards 10%. In both instances, the upper limit of the constraint appears to coincide with the band at which the equifinal probability of the constraining metric on its own reaches 100%. Thus, it would appear that generally, one or more of the component metrics in a polymetric combination needs to have an equifinal probability of less than 100% in the tolerance band of interest if it is to constrain the equifinal probability of the combination.

Figure 5.11 reinforces this point, showing that much of the tolerance space is occupied by a probability zone of 10% or lower. In general, this demonstrates how the combination of metrics and tolerance bands, using at least two metrics simultaneously, may reduce the equifinal probability compared with the situation in which any metric is used on its own, or in some smaller combination.

This concludes the main points to be made regarding overall quantification of equifinality in single metric and polymetric cases. However, there are some interesting issues relating to why polymetric equifinality should be less generally than it is for single metrics. This can be examined by plotting the equifinal solution regions for each metric, and examples of this are now presented.

5.5 MAPPING EQUIFINAL SOLUTION REGIONS

5.5.1 Introduction to 'two-parameter' examples

The results shown here are restricted to two parameters only, that is for the situation of a 2-D parameter space. This is for ease of presentation, as mapping 3-D or higher spaces,

although possible, would require more plots and explanation, without necessarily making the general points any clearer.

The 'two-parameter' example calculations were performed using the full metamodels and the method shown in figure 5.1, but varying only the two most important parameters in each metamodel. These were selected according to the size of their main effects, and the other parameters were fixed at their base case values. The bootstrap runs were generally conducted using 10,000 sample points per bootstrap set and without replication, which was considered sufficient for a two parameter exploration and the purposes here. For each solution within the required tolerance, the sample point values were stored, so that in due course, all the points could be plotted. The general solution patterns for each metric at example tolerance bands are shown in Figure 5.12, the parameter values being scaled to their scaled design levels (eq. 4.01).

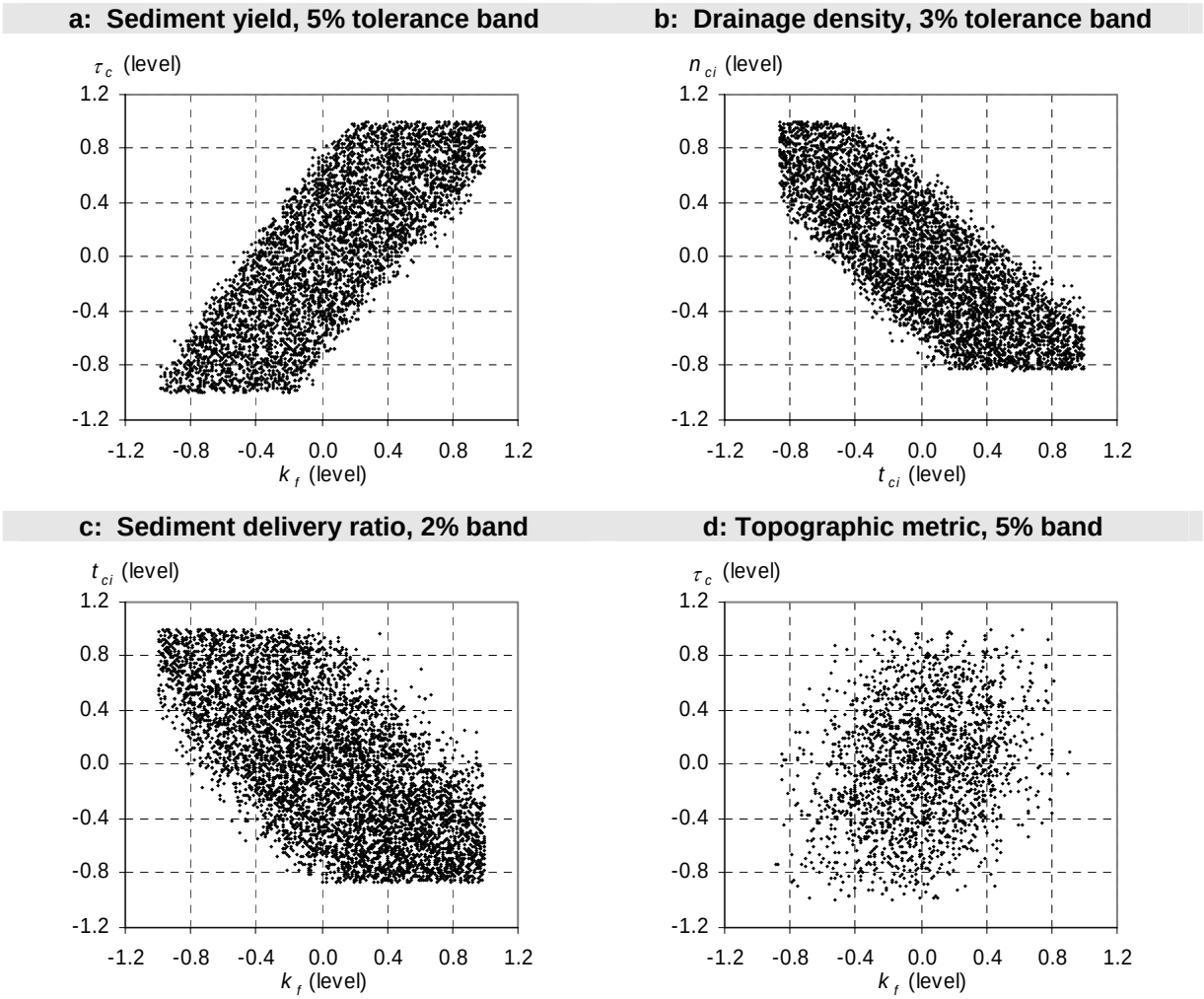

Figure 5.12, a-d: Equifinal solution spaces for two dominant parameters for each metric, at example tolerance bands, based on 10,000 sample points per calculation set.

In the sediment yield example (figure 5.12a), the two dominant parameters are k_f and τ_c. The plot of the points lying within the solution space shows a general trend with a positive slope i.e. that positive values of k_f and τ_c together, or negative values together, have produced most of the equifinal solutions. This trend can be understood by referring to the main effects of each parameter (Figure 4.19). The main effect of k_f is strongly positive, and that of τ_c strongly negative. When both parameters are positive or negative, therefore, the main effect of one works in opposition to the main effect of the other, so the results are more likely to be equifinal. Similarly, when both parameters are valued at opposite levels (k_f negative and τ_c positive, and vice versa), the main effect of one reinforces the main effect of the other, so the results are much less likely to be equifinal. The other point to note from this plot is that the general area bounding the solutions occupies about 47% of the factorial space, which represents the equifinal probability for the sediment yield in this tolerance band due to these two parameters[2]. Similarly, for drainage density, the area bounding the solutions occupies *c.* 40% of the space, corresponding to an equifinal probability of 40% in the 3% tolerance band due to the parameters t_{ci} and n_{ci}. The equivalent figure for the sediment delivery ratio is *c.* 68% (due to k_f and t_{ci}) in the 2% band, and for the topographic metric *c.* 40% (due to k_f and τ_c) in the 5% band. Thus, the proportion of the area occupied by equifinal solutions corresponds to the equifinal probability in each case.

Turning to the drainage density and sediment delivery ratio (figures 5.12b and 5.12c), the two most important parameters for drainage density are t_{ci} and n_{ci}, and in the sediment delivery ratio example, k_f and t_{ci}. The trend in the points in each of these plots is negative, showing that solutions are most likely to be equifinal where one parameter has a high value and the other a low value. Referring as before to the main effects plots in Figures 4.21 and 4.23, the main effects of t_{ci} and n_{ci} on drainage density are both negative, whereas the main effects of k_f and t_{ci} on sediment delivery ratio are both positive. It follows that the effects of the parameters on their respective metrics tend to offset each other when the parameter levels for each have opposite signs, thus making equifinal solutions more likely. Similarly, if the parameter levels are of the same sign, then the effects of each reinforce the other, and the likelihood of obtaining an equifinal solution is reduced.

Turning to the topographic metric (figure 5.12d), the situation is rather different. As with sediment yield, the two dominant factors chosen are k_f and τ_c. In this instance, the pattern is

[2] This particular result is also demonstrated by the model size results, in Chapter 6, in Figure 6.2a.

less easy to see at first glance, mainly because the edge to the equifinal solution is less well defined than it is for the other three metrics. This results from the poorer fit of the metamodel in this instance, at *c.* 92%, compared with *c.* 99% for the other three (section 4.5, *q.v.*). However, the general shape bounding the solution space approximates an ellipse, with its semi-major axis pointing up the page and tilted slightly to the right. Again, referring to Figure 4.25, the main effects of these two parameters are strongly curved, and in the metamodel were approximated by quadric equations, with an additional interaction effect term (Table 4.3, *q.v.*). In this case, any increase or decrease in the level of each parameter, compared with the central or base case level, makes the results less likely to be equifinal. This can be likened to slicing through a domed surface. The shape of the solution region is elliptical rather than circular because the main effect of k_f is stronger than that of τ_c; the region is therefore longer along the τ_c axis, and shorter along the k_f axis.

Another point to note from the plots in Figure 5.12 is that although the addition of the second parameter has always reduced the equifinal probability compared with that generated by either parameter on its own, the range of parameter values over which equifinal solutions have been found has been extended for each parameter. For example, in the case of sediment yield, the equifinal solution range for k_f on its own (i.e. with τ_c and all of the parameters at their base level values) lies approximately between -0.5 to 0.5; similarly, the equifinal solution range for τ_c on its own lies approximately between -0.7 to 0.8. However, varying the two parameters together increases the range of values over which both k_f and τ_c need to be varied in order to obtain equifinal solutions, both pairs of ranges being extended to their factorial space limits, at -1 to +1. Despite this, the *overall* equifinal probability is still less for the two together than it is for either separately.

The same quality of result is seen for drainage density and sediment delivery ratio: the equifinal solution range for each parameter on its own, when the other is kept at base level, is less than the equifinal solution range when both parameters are varied together. Again, this is because both parameters need to be varied over a wider range of values to obtain the equifinal solutions within the target tolerance band.

Looking at the topographic metric, the position is rather less clear, not helped by the fuzzy edge to the solution space. However, even here, the equifinal solution range for k_f appears to have increased, from about -0.6 to 0.6, to -0.7 to 0.7, because of the influence of the main effect of and interaction effect with τ_c. To identify what is happening here more clearly, and indeed to obtain an idea of how the equifinal solution region varies in size and orientation

for different tolerance bands, it is helpful to calculate and plot the estimated edges to each solution region, and this is now considered.

5.5.2 Boundaries to equifinal solution spaces

The edges to the equifinal solution spaces cannot be found exactly, but had to be estimated by bracketing the upper and lower limits of the tolerance bands, using a bracket of 0.05%. For example, if trying to find the boundary to equifinal solutions for sediment yield in the 5% tolerance band, solutions were sought in the zones from -4.95% to -5.05%, and from 4.95% to 5.05%. The metamodel was run to obtain at least two hundred solutions in each bracket, and the bootstrap error was held constant at the base case residual, so as to reduce the scatter in the points. A combination of line fit tools and regression was then used to derive functions which would approximate the solution space limits as lines. The procedure was repeated for a range of tolerance bands, for each metric, and the results are shown in Figure 5.13. As with the previous figure, each parameter's value is given in terms of its scaled design level (equation 4.01). It will also be appreciated from the method of calculation that the results should be subject to greater error, as the full residuals set was not used for each metric. However, the main intention here is to demonstrate patterns of result rather than the more precise solutions already presented. The potential error is in any event not thought to be great enough in these examples to detract from such patterns and general points being made here.

Having plotted the lines marking the limits to the solution space in various tolerance bands, the results appear as contours, which clarify the trends seen in the plots in Figure 5.13, a-d, particularly for the topographic metric. More importantly, the contours also allow us to examine the influence on equifinality of using two or more metrics in combination, and this is discussed next.

a. Sediment yield, k_f vs τ_c

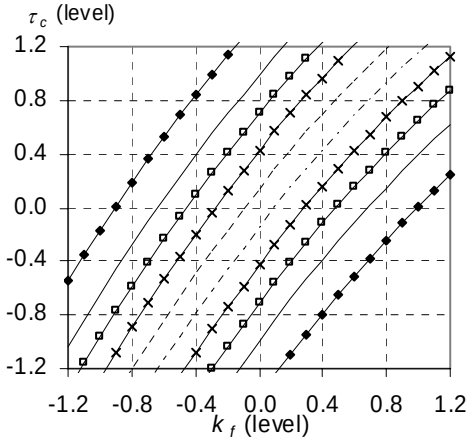

b. Drainage density, t_{ci} vs n_{ci}

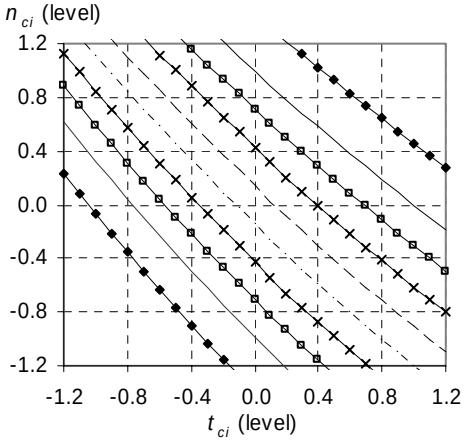

c. Sediment delivery ratio, k_f vs t_{ci}

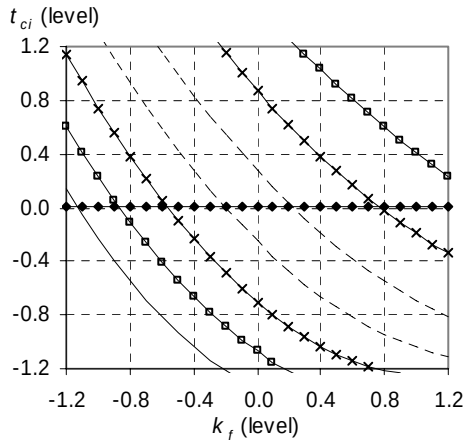

d. Topographic metric, k_f vs τ_c

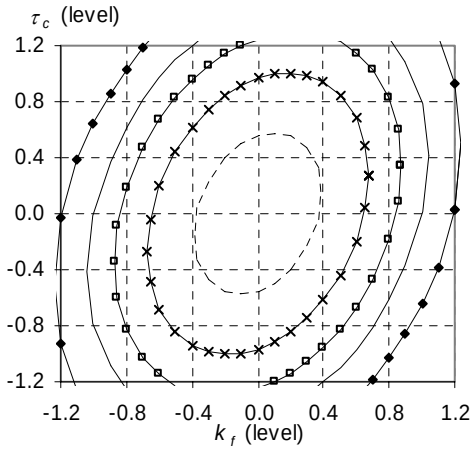

Legend for tolerance band contours (%):

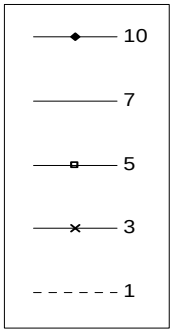

Figure 5.13, a-d: Contoured limits to the equifinal solution spaces of each metric, for the two-parameter examples. Each 'contour' is derived from *c.* 200 sample points, found by bracketing ±0.05% either side of each band, and using the base case residual only in the bootstrap.

5.5.3 Mapping the combined equifinal solution space for two metrics

Having delineated the 2-D equifinal solution spaces, it is possible to make a direct comparison of those plotted for two different metrics using the same parameters. The examples for sediment yield and the topographic metric, in Figures 5.12 and 5.13 above, are both presented showing the equifinal solution spaces formed by k_f and τ_c, so the comparison can be made by laying one metric's solution space directly over the other. Any intersection of the two between stipulated tolerance bands then marks the bimetric equifinality solution space for those bands. An example of this is shown in Figure 5.14, using the solution space for each metric in its 3% tolerance band.

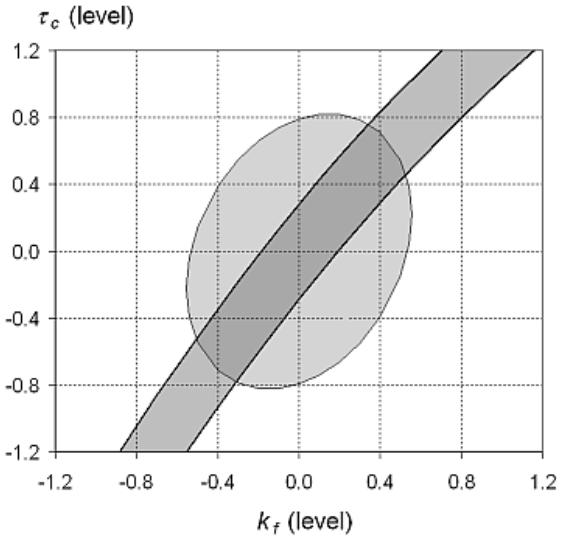

Figure 5.14: Combined biparameter plots of k_f versus τ_c, showing the intersection of the sediment yield (darker grey) and topographic metric (paler grey) equifinal solution spaces, both metrics in their 3% equifinal tolerance bands.

It can be seen from Figure 5.14 that the intersection – the bimetric equifinal solution space - is smaller than either of the individual metric's solution spaces. In fact, this is only one of a range of possible bimetric results which the author could have presented, in which the general finding, that the intersection is often smaller (and never bigger) than the components, always holds. Figure 5.14 therefore illustrates how the use of two or more metrics in combination may reduce the equifinal probability. The result also helps to explain the more general situation, which is now considered.

5.5.4 A general explanation of the polymetric results

As discussed in subsection 1.2.1, Bras *et al.* (2003) hypothesise that equifinality should be very rare if model outcomes are defined by a complete description of the landscape in question. They also comment that the problem is really a practical one, namely of finding and using appropriate statistical measures, so that model results can be more clearly discriminated from each other. Not only do the polymetric results in this chapter conform to Bras *et al*'s hypothesis, but they also permit an explanation of why it should be correct.

Viewing the problem as it has been approached above, and as illustrated in Figure 5.14, the use of many metrics helps to confine more tightly the regions in the parameter space which will allow equifinal solutions to be generated. Specifically, the region of the parameter space which generates equifinal solutions for one metric will almost certainly not coincide exactly with the region generating equifinal solutions for another, unless the solution space for one metric is a subset of that for the other in the tolerance bands of interest. That this should be so can be inferred from the metamodels derived for the metrics in this research. For example, parameters which have large main effects in the sediment yield metamodel are largely absent from, or of only modest influence in, the drainage density metamodel (Table 4.2, *q.v.*); similarly, even where two different metamodels utilise the same parameters, their coefficients and functional forms will differ, so that each draws on a different region of the parameter space in order to generate equifinal output. This is strikingly shown by the differences between the sediment delivery ratio and topographic metrics' metamodels, which use mostly the same parameters, but are of completely different form, and have very different individual equifinal probability curves (Table 4.3, and Figures 5.13 c and d, *q.v.*).

The general polymetric situation can be shown conceptually in a Venn diagram, as in Figure 5.15, using a bimetric example. In the diagram, the solution region – which may be hyper-dimensional – is the area within the box. For metric A, in tolerance band 'x' %, the parameter values generating an equifinal solution are bounded in a specific part of the parameter space. A similar situation is shown for metric B, in its 'y' % tolerance band. A speckled line marks the boundaries to each metric's solution space, which are assumed not to be known exactly.

In the example, each solution space occupies about 20% of the whole parameter space, so the equifinal probabilities for these metrics individually would be about 20%. However, if trying to find solutions which generate results which are equifinal for both metrics

simultaneously, within the same targeted tolerance bands, the bimetric solution space is confined to the intersection of the two individual spaces. The bimetric equifinal probability will therefore be much less than it is for the two metrics individually, as the intersection is much smaller than either metric's individual solution space.

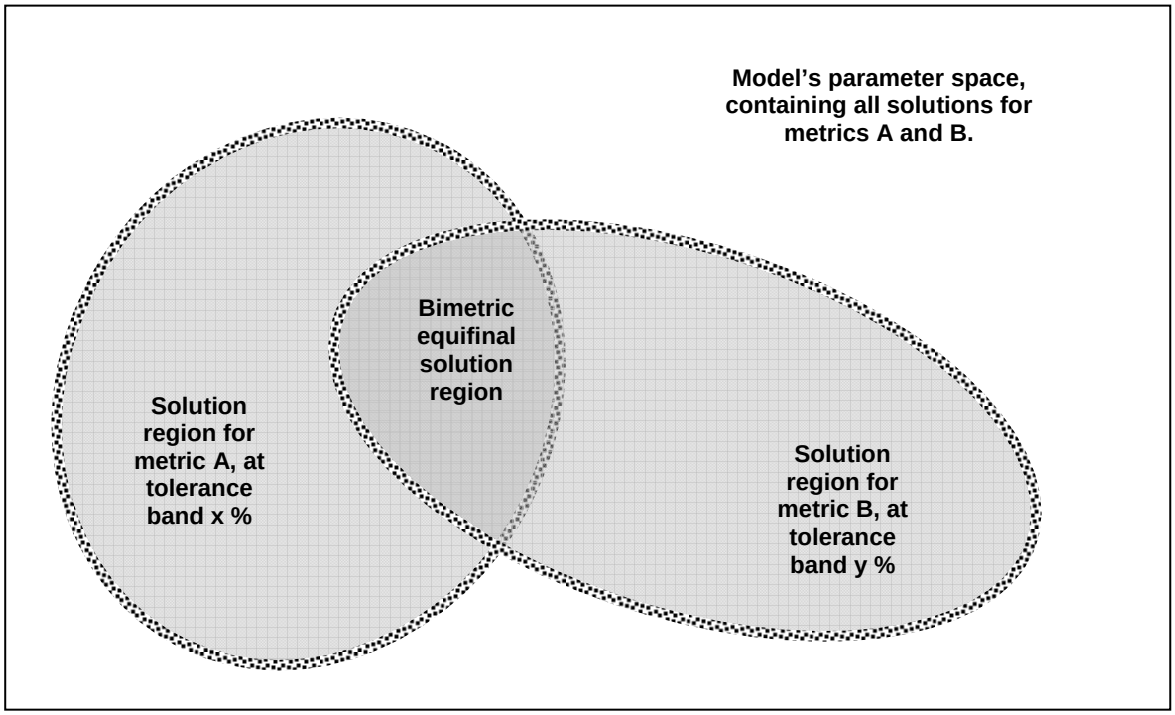

Figure 5.15: Venn diagram illustrating the difference between single metric and bimetric equifinality. The bimetric case is a simplification of the general polymetric situation.

The diagram also illustrates how subsetting may affect polymetric equifinality. If the solution region for one metric is entirely bound within the solution region for another, then the polymetric equifinality is not constrained by the tolerance band of the more equifinal metric. In such a situation, the bimetric equifinal probability is simply the probability represented by the smaller of the two solution spaces. Similarly, if both metrics of interest are targeted in tolerance bands where individually their equifinal probabilities are 100%, then their combined equifinality will also be 100%, since neither component metric constrains the equifinality of the other. As a general statement, therefore, polymetric equifinality will always be either less than or equal to the lowest equifinality amongst the component metrics in the polymetric combination, within the tolerance bands of interest.

This completes presentation of the general results relating to quantification of single metric and polymetric equifinality. The main points in this chapter are now summarised.

5.6 CHAPTER SUMMARY

The results reported in this chapter comprise the main findings from the quantifications carried out in this part of the research. The results show that equifinal solutions can be generated for all of the metrics, both singly and in combination, across a range of tolerance bands, although some metrics are more likely to be equifinal than others. In particular, the sediment delivery ratio is highly likely to provide equifinal results, whereas the topographic metric is least likely to be equifinal.

The polymetric equifinality calculations show clearly that for specified tolerance bands, bimetric or higher-metric equifinal probabilities may be lower, and are never higher, than they are for any of the component metrics on their own or used in smaller combinations, and subject to the same tolerance bands. In this way, the inclusion of a second or further metric is always likely to constrain the size of the region in the parameter space from which equifinal solutions may be generated. This was illustrated through the use of two-parameter examples, and a particular combination of two metrics. The results together showed that the equifinal probability for all four metrics can be understood as the proportion of the factorial space occupied by the zone of the equifinal solutions for each metric. Moreover, for different metrics but the same parameters, these zones are unlikely to coincide exactly, unless one is in some way a subset of the other. It follows that the intersection of two or more solution spaces is likely to be smaller than the solution space for any single metric, hence the reduction observed in the polymetric equifinality.

The equifinal probabilities calculated in the chapter range generally from near 0% to 100%, depending upon the selected metric and tolerance band. More generally, the equifinal probability curves are smooth and continuous.

These summary points have been made with regard to exploration of the parameter space generally, but the two-parameter results, reported in section 5.5, hint at the importance of also understanding the influence of the parameters singly, and in smaller combinations than the full 10-D space. The focus is now therefore shifted to a consideration of the parameter influences, and how these may be better quantified and understood.

CHAPTER 6: RESULTS (2) – UNDERSTANDING THE INFLUENCE OF THE PARAMETERS ON EQUIFINALITY

6.1 INTRODUCTION

Whereas the results presented in Chapter 5 are focused mainly on estimation of equifinal probabilities calculated by exploring the whole factorial space, it is evident from the two-parameter examples that the equifinality of the LEM's output is influenced differently by different parameters. The aim in this chapter therefore is to explore the parameters' influences in more detail. Accordingly, the chapter begins by considering the influence of each parameter singly on the equifinality of each metric, and the results are contrasted with the evidence of each parameter's main effect, reported in Chapter 4. The parameter results are then extended to tests demonstrating how equifinality in the metrics is affected by introducing more parameters, increasing the dimensions of the parameter space by one parameter at a time. These results together suggest that there are equifinal properties in all metamodels, and that these may be explored through the use of generic metamodels, or 'metamodel archetypes'. Regression analysis to derive metamodels for three additional metrics, and further consideration of the regression work in Chapter 4, further suggest that most metamodels that might be derived from LEM output can be expected to conform to a general structure. A simple archetype based on that structure is then used to explore a hypothetical, two-dimensional parameter space, and the results obtained thereby are found to illustrate certain equifinal properties of metamodels which are likely to be general. More specifically, results from explorations with the archetypes highlight how equifinal behaviour is determined largely by parameter main effects and interactions. This finding permits consideration what of should be expected of LEM metamodels - and hence LEM equifinality - more generally. The structure of the chapter is therefore as follows:

- equifinality arising from single parameter variations;
- the influence of model size (the number of parameters varied) on equifinality;
- main effects, interactions and the idea of metamodel archetypes;
- new regressions and a basic LEM metamodel archetype;
- example results with the archetype and main findings; and
- chapter summary.

The first stage is to consider the influence of the parameters singly on each metric, and this is now discussed.

6.2 CONTRIBUTION TO EQUIFINALITY BY INDIVIDUAL PARAMETERS

6.2.1 Modification of the bootstrap calculation method

To calculate the influence of each parameter on its own, it is necessary to sample the parameter space varying one parameter value only, and this requires running separate bootstrap sets for each parameter. This presents something of a problem, as the main four metamodels, although generally well fitting across the whole factorial space, are not necessarily the best tools to contrast the equifinal probabilities generated by *individual* parameters with each another. It will be appreciated that some parameters do not appear as terms in the general metamodels because their effects were found to be less significant than the terms including the other parameters. However, lower significance, or even marginal insignificance, in a general metamodel does not mean that a parameter has no effect at all on the metric in question; rather, the parameter's effect is simply too small to contribute to the explanatory power of the general metamodel. Accordingly, it was decided that individual parameter metamodels should be derived so that a fairer comparison could be made between the influences of each of them singly, no matter how large or small their main effects might be, and irrespective of whether they were eventually included in the general metamodels or not.

Having made this decision, single parameter models were derived by regression using a standard spreadsheet and data from each parameter's main effects cases and the base case. For the most part, well fitting metamodels were obtained (R^2 from 95-99%), using polynomials and power functions, but the topographic metric presented some difficulties, and the star point results were omitted, and more complex, non-linear functions had to be used (e.g. Ratkowsky, 1990). All of the regressions and individual metamodel forms are reported in detail in Appendix L.

Having obtained the individual parameter metamodels for each metric, the predicted value of the metric for a particular sample point was then calculated and bootstrapped, to obtain a proxy actual value. In this instance, a parametric bootstrap was used (subsection 4.4.5 *q.v.*).

To achieve this, for each parameter the bootstrap error was selected at random from a normal distribution, with the mean of the predicted value of the metric, and the standard deviation of the regression residuals, found from the sum of squares of the residuals in each parameter's regression ANOVA table (Appendix L, *q.v.*). By repeating the sequence of calculations in the manner outlined in Figure 5.1, and bootstrapping the solutions as described, equifinal probabilities were calculated for each parameter, metric, and tolerance band. As only one parameter was being sampled in each run, the calculation sets comprised 10,000 sample points only, without replication, this number being found to produce near stable solutions.

6.2.2 Single parameter results, and associations with parameter main effects

The single parameter equifinal probabilities are shown as spider plots in Figure 6.1. Each parameter axis is labelled with a letter corresponding to a particular parameter, as explained in the legend. Also, for greater clarity, only the results for the 0.05%, 1%, 2% and 4% tolerance bands are shown.

The plots highlight how the different influences on equifinal probability exerted be each parameter are manifested. The shaded areas for each tolerance band can be likened to shading the areas between contour lines on a map: reading from the central point outwards, along one of the parameter axes, crossing more shaded bands means that there is a 'steeper' change in equifinal probability for a given change in the tolerance band. Conversely, crossing few lines shows that there is a much flatter response, so that changes in the tolerance band have a lesser influence on the equifinal probability. It should be noted that a flat response does not have to mean that the probability is itself high or low, although generally the flatter areas are associated with the higher equifinal probabilities. The contrast between the flatter and steeper equifinal responses is most striking between figures 6.1c and 6.1d. The former shows the results for the sediment delivery ratio. The plot appears largely 'flat', with an equifinal probability of 100% in the 1% tolerance band for the parameters s_{cr}, k_b, τ_b, k_w, m_w, k_d and τ_c. By contrast, in figure 6.1d, showing results for the topographic metric, the equifinal probability associated with eight of the parameters in the 1% tolerance band is around 50% or less.

6.1a: Sediment yield

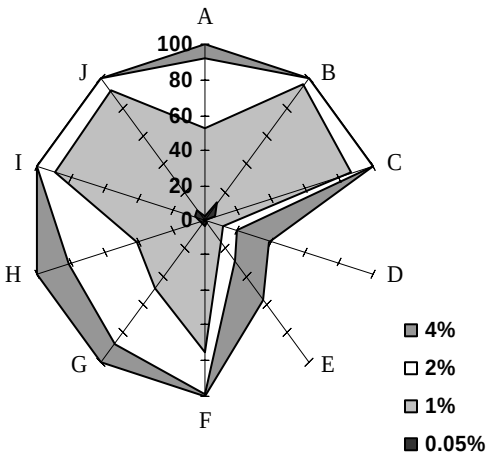

6.1b: Drainage density

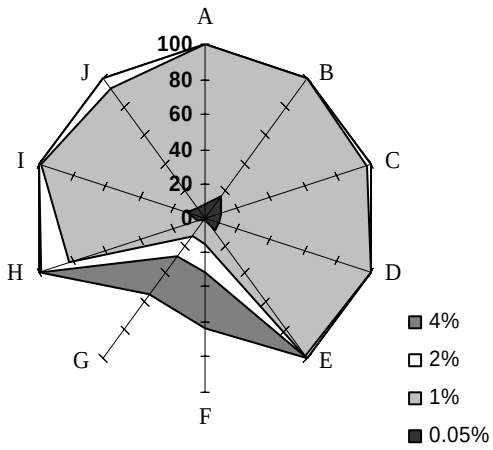

6.1c: Sediment delivery ratio

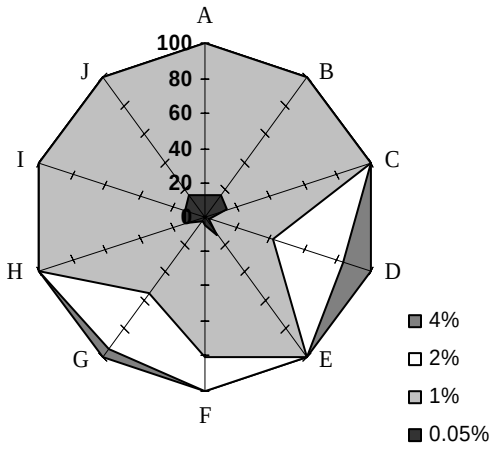

6.1d: Topographic metric

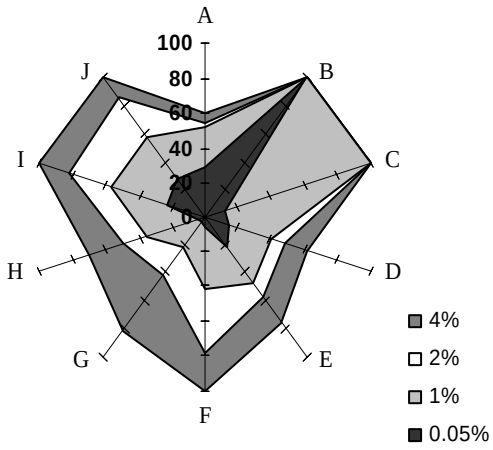

Legend:

Letter	Parameter	Letter	Parameter
A	k_w	F	n_{ci}
B	m_w	G	t_{ci}
C	k_d	H	s_{cr}
D	k_f	I	k_b
E	τ_c	J	τ_b

Figure 6.1, a-d: Equifinal probabilities attributable to each individual parameter for each metric in example tolerance bands, calculated using single parameter metamodels and 10,000 bootstrapped sample points per parameter (see text).

Summarising the four plots in turn, the sediment yield is least equifinal to changes in k_f and τ_c, the drainage density to changes in t_{ci} and n_{ci}, the sediment delivery ratio to changes in k_f, t_{ci} and n_{ci}, and the topographic metric to changes in k_f, s_{cr}, t_{ci}, τ_c and k_w. It is highly interesting to note how these patterns are broadly in agreement with the strength of the main

effects of each of these parameters on the metrics in question, as reported in Chapter 4. For example, referring to Figure 4.19, it can be seen that parameters k_f and τ_c have strong main effects on sediment yield. Similarly, from Figures 4.21 and 4.23, drainage density is most sensitive to changes in t_{ci} and n_{ci}, and sediment delivery ratio to changes in k_f, t_{ci} and n_{ci}, matching the patterns in the individual parameter equifinal probabilities plotted above. In this way, it can be seen that, with regard to the influences of these parameters on GOLEM's response, equifinality and sensitivity are in essence opposite relations: the highly equifinal results are generally associated with parameters having weak main effects, whereas the less equifinal results are associated with the parameters which have strong main effects.

Having considered the equifinality associated with each parameter on its own, the equifinality associated with combinations of parameters may be investigated. This can be likened to exploring the influence of using different numbers of parameters in a model, and the problem is approached in this manner.

6.3 INFLUENCE OF MODEL SIZE ON EQUIFINAL PROBABILITIES

6.3.1 Equifinality as a function of the number of parameters

The results presented above begin to provide the type of data which may assist a researcher in deciding how complex a model should be for a particular purpose, and also how equifinal will be the results generated using that model. Some LEM studies in the literature list dozens of parameters (e.g. Lancaster *et al.*, 2001), and the version of GOLEM used in this research includes over twenty. Given the number of possible simulations that are possibly required to explore such parameter spaces (Table 3.1, *q.v.*), it becomes important to consider whether it really is necessary to vary all of them. The results reported above suggest that the problem can be approached, at least as a first approximation, by identifying which parameters have the strongest main effects. This is similar in some respects to the 'Dominant Processes Concept' in hydrology (e.g. Sivakumar, 2004), which is also beginning to arouse interest in the geosciences (e.g. Phillips, 2006). In many respects these ideas are not new; rather, they reflect practices and developments from other disciplines, in particular engineering, where screening and similar designs – often of resolution IV or similarly constructed - are frequently used in initial sampling to reduce subsequent experimental complexity (e.g. Box and Draper, 1987; Wu and Hamada, 2000). However, at

least from the reviews the author has conducted as part of this research, such designs have not been applied in the experiments and studies conducted using LEMs.

Regarding clarification of parameter influences and model size, given the inference from the previous subsection, that strong main effects are associated with lower equifinal probabilities, a logical way to calculate the influence of model size is to introduce new parameters in order of their main effect, beginning with the 'strongest' parameter. The results reported below derive from calculations performed in this way, all calculations being performed with the general metamodel in each case and bootstrapping as outlined in Figure 5.1, and taking the most important parameter first. The calculations were then run again, including the next most important parameter, and then again with the next important parameter, and so on, until all the parameters used in the metamodel had been employed. The order of inclusion of the parameters herein is listed in Table 6.1, and the results obtained are plotted in Figure 6.2. It should be noted that a bootstrap set of a million sample points was used in each set of model size calculations, but without replication.

Table 6.1: Order of inclusion of parameters in the successive model size calculations, arranged by the relative strength of each parameter's main effects (Tables 4.19-4.25 *q.v.*), the biggest first and smallest last.

	Parameters included in the model, by metric			
Model size (no. of parameters included)	**Sediment yield**	**Drainage density**	**Sediment delivery ratio**	**Topographic metric**
1	k_f	t_{ci}	k_f	k_f
2	As above, + τ_c	As above, + n_{ci}	As above, + t_{ci}	As above, + k_w
3	" " , + t_{ci}	" " , + τ_c	" " , + n_{ci}	" " , + s_{cr}
4	" " , + s_{cr}	" " , + k_b	" " , + s_{cr}	" " , + τ_c
5	" " , + k_w	Not applicable	" " , + k_d	" " , + t_{ci}
6	" " , + n_{ci}	-	" " , + τ_b	" " , + n_{ci}
7	" " , + k_d	-	" " , + τ_c	" " , + k_b
8	" " , + k_b	-	" " , + k_w	" " , + k_d
9	" " , + τ_b	-	Not applicable	Not applicable

Figure 6.2a: Sediment yield

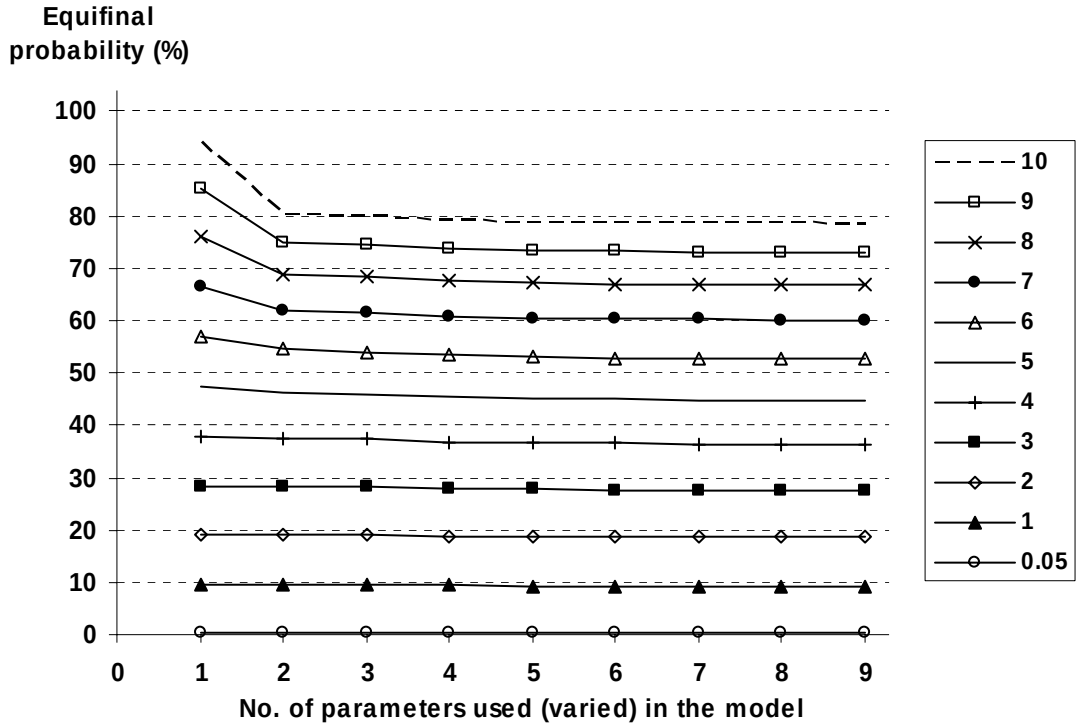

Figure 6.2b: Drainage density

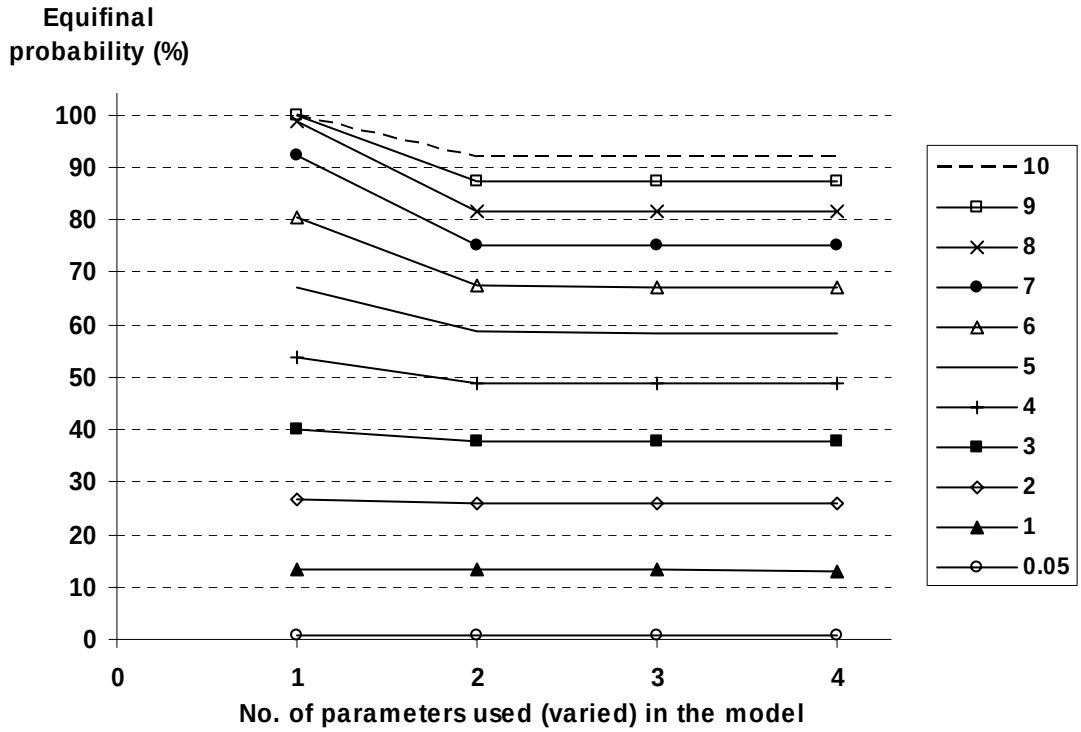

Figure 6.2, a and b: Equifinal probabilities for sediment yield and the drainage density, shown for different model sizes at example tolerance bands. The legend shows the tolerance band in each instance, and the parameters varied in the different models are as listed in Table 6.1.

Figure 6.2c: Sediment delivery ratio

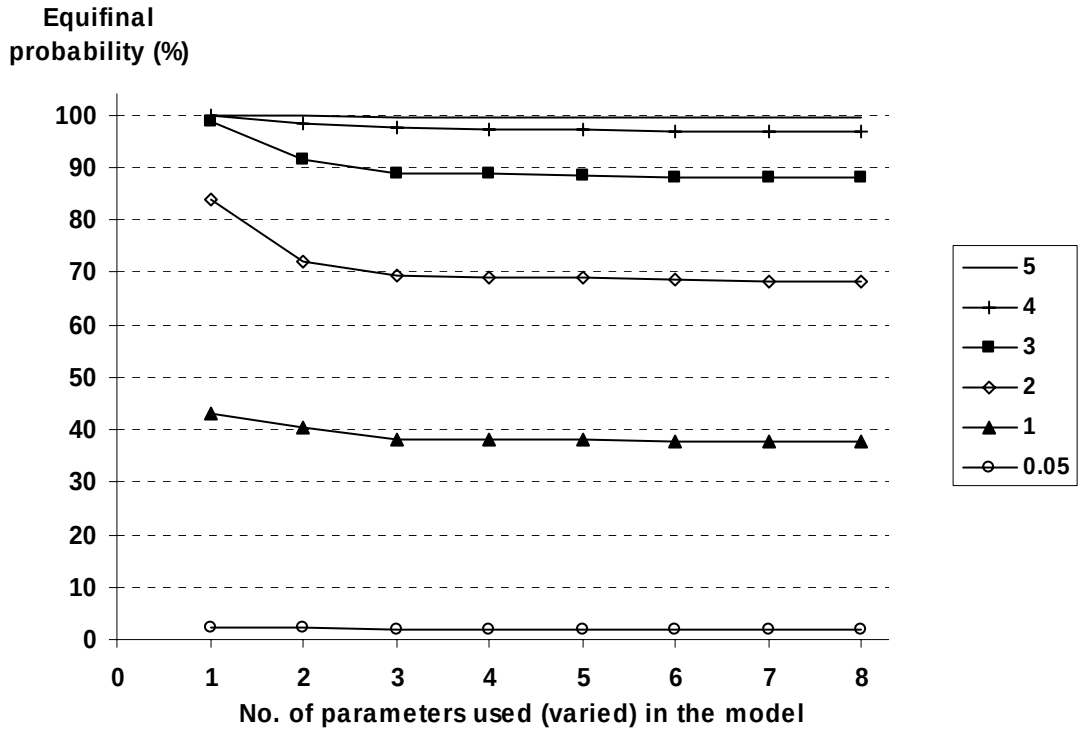

Figure 6.2d: Topographic metric

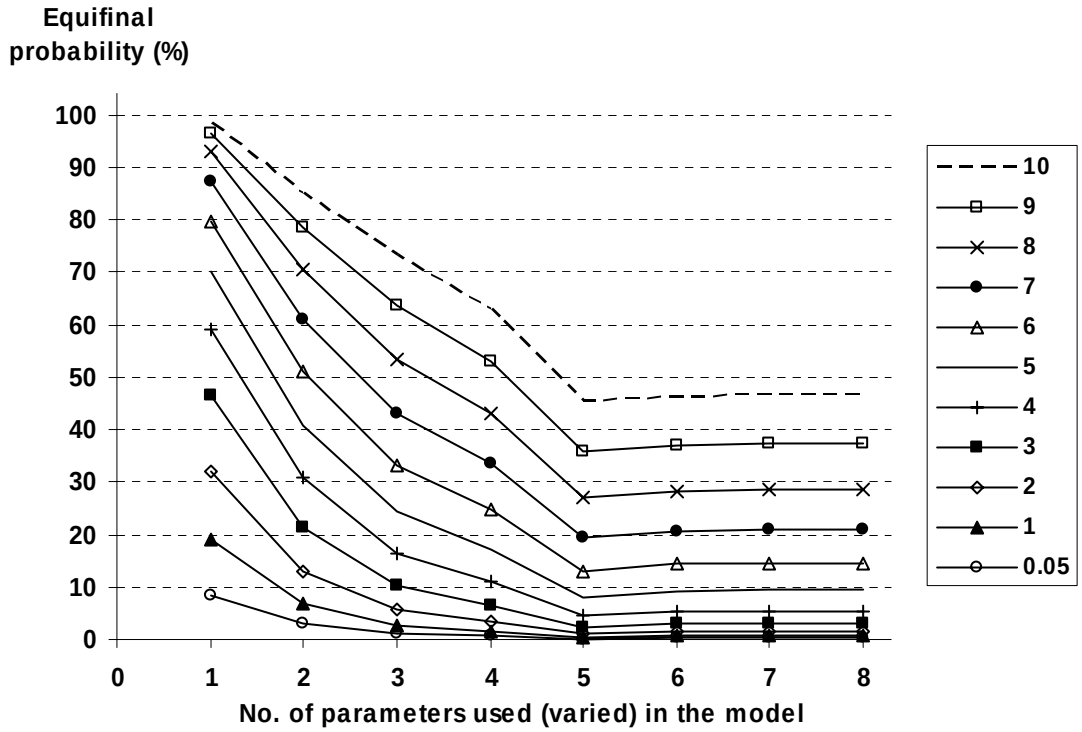

Figure 6.2 (cntd), c and d: Equifinal probabilities for the sediment delivery ratio and topographic metric, shown for different model sizes at example tolerance bands. The legend shows the tolerance band in each instance, and the parameters varied in the different models are as listed in Table 6.1.

The figures all reveal that, in general, the probability of obtaining an equifinal solution declines as one increases the number of parameters included in the model. However, the reduction in equifinality is not linear, and each curve quickly approaches a stable value after including the first three or four parameters (five in the case of the topographic metric). This was initially considered a very surprising discovery, as the author had supposed that increasing the number of parameters in a model would also increase the likelihood of the LEM generating equifinal output. There appears to be no doubt about these results, however, as it was repeated for all the metrics across all tolerance bands, with just a minor exception for the topographic metric, after the model size for the latter is increased beyond five parameters. The slight increase (*c.* 2%) in equifinal probabilities for the topographic metric could be down to some misfit in the metamodel and the greater error in the predictions, as the R^2 score for this metamodel was *c.* 92%, compared the *c.* 98% or greater values achieved for the other models. Another possibility is that the reduction in equifinality associated with introduction of parameters with strong main effects is partly offset by introducing the weaker parameters as interaction terms. The influence of interaction effect terms on equifinality is commented on later in this chapter, in the explorations using metamodel archetypes.

Regarding the results more generally, Figure 6.2 shows that the effect of each newly introduced parameter is generally less than that of those previously included. Thus, the parameters with the stronger main effects, when used in combination, are the most effective at reducing equifinality in a particular tolerance band.

Although the effect of increasing the number of parameters is found generally to reduce the equifinal probability, the effect is more marked for some of the metrics than for others. For example, looking at Figure 6.2a, although the sediment yield metamodel uses nine of the parameters in its full version, the equifinal probabilities when including just two are only slightly higher than the probabilities found when including three, four, or, for that matter, all nine. Likewise, in Figures 6.2b and c, the equifinal probabilities for drainage density and sediment delivery ratio only decline fractionally after including respectively the first two and the first three parameters. Similarly, looking at Figure 6.2d, the topographic metric metamodel uses eight of the parameters, and the equifinal probabilities are found to decline steeply by including the first five, but there is found to be almost no change (a slight increase in probability) by including the remaining three. Again, this shows how the

reduction in equifinality is greatest in response to inclusion of the strongest three or four parameters, but declines thereafter.

6.3.2 Probabilities and tolerance bands

The results presented above may also be presented as equifinal probability curves (Figure 5.6 *q.v.*). However, as different model sizes are being compared, a separate curve is needed for each model. The curves are plotted in Figure 6.3, and further demonstrate the differences in equifinality arising between models of different size.

Figure 6.3a: Sediment yield

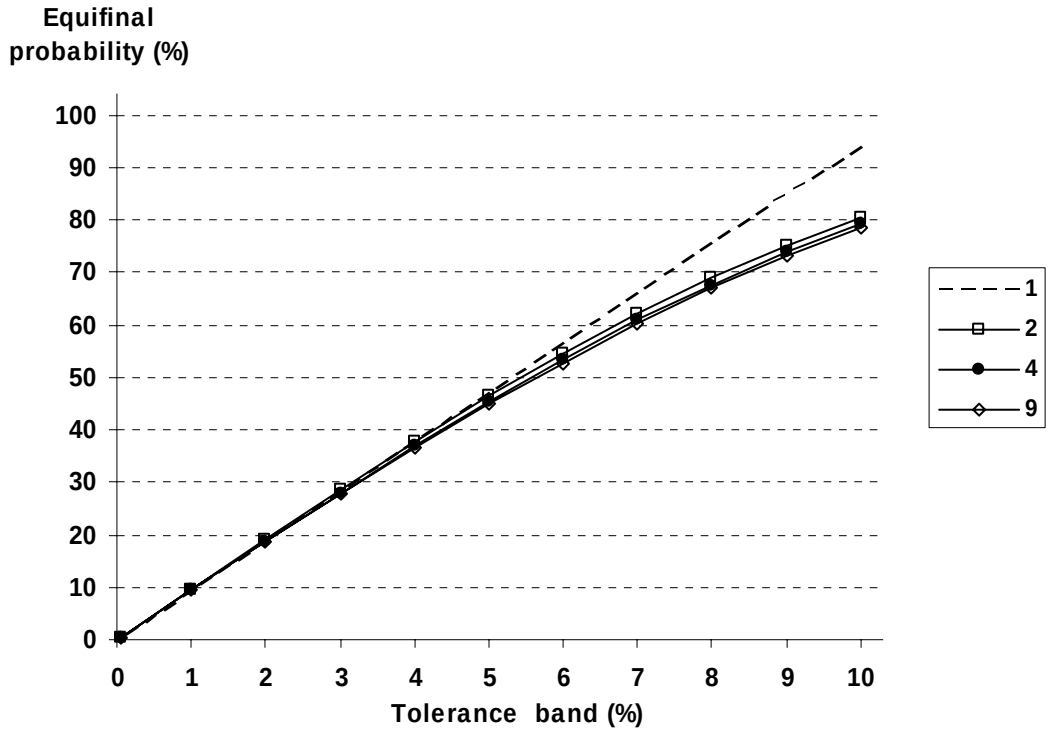

Figure 6.3, a: Equifinal probability curves for sediment yield for different model sizes. The legend shows the model size for each curve, and the number of parameters varied in each model is increased according to the order listed in Table 6.1.

Figure 6.3b: Drainage density

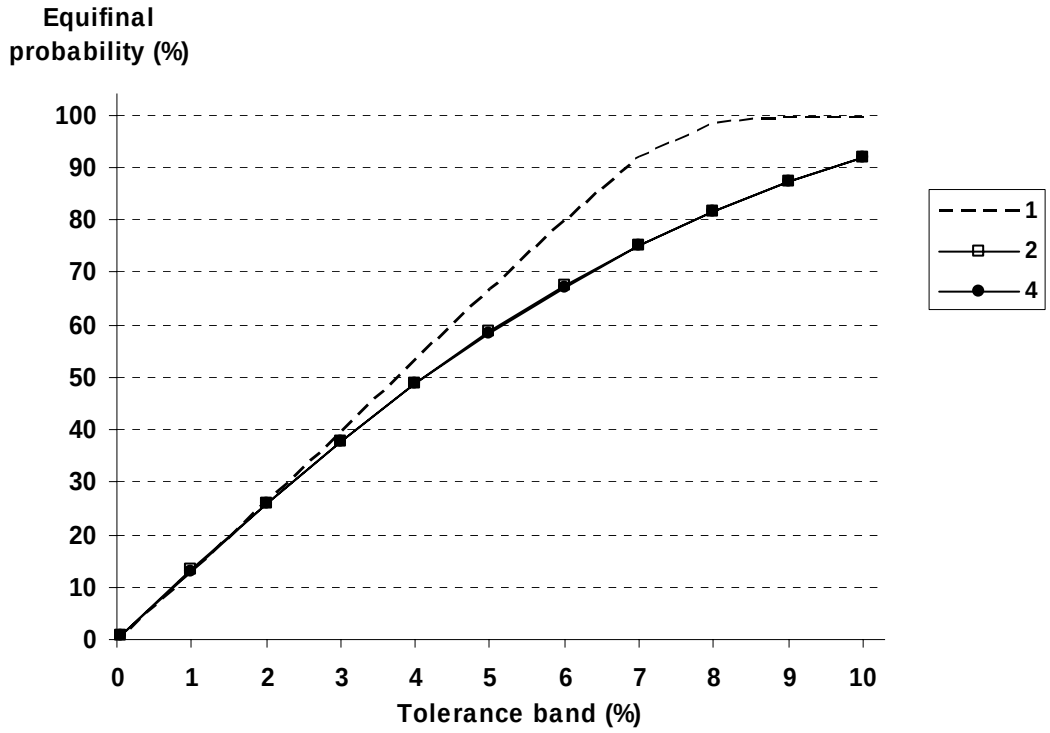

Figure 6.3c: Sediment delivery ratio

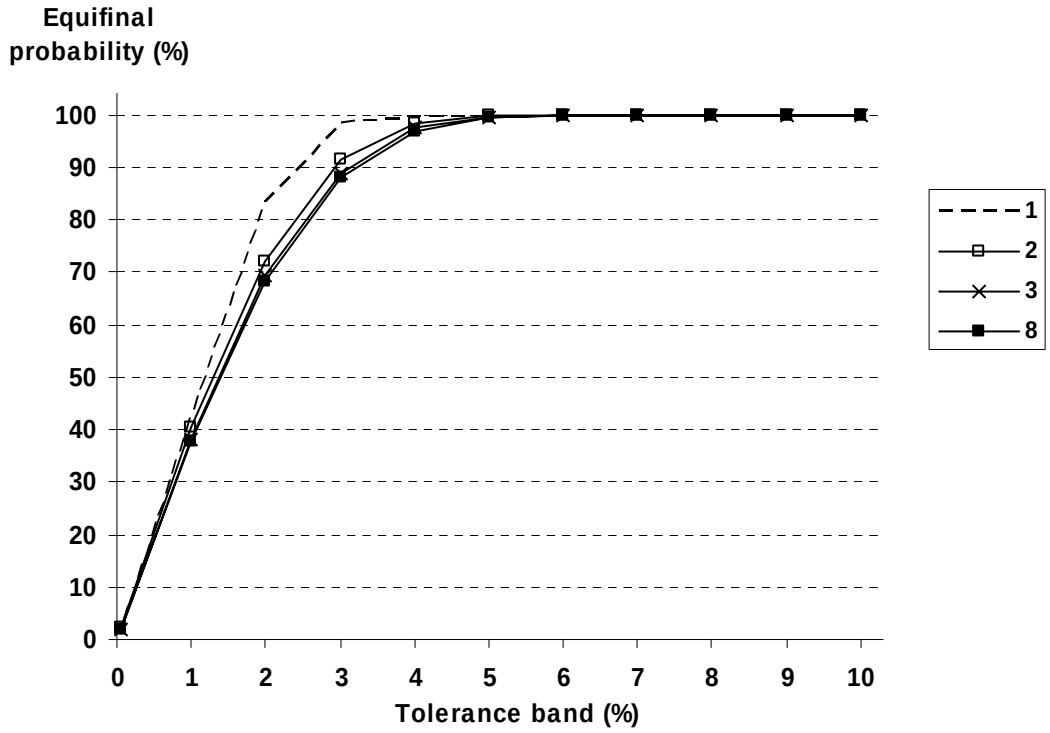

Figure 6.3 (cntd), b and c: Equifinal probability curves for the drainage density and sediment delivery ratio, for different model sizes. The legend shows the model size for each curve, and the no. of parameters varied in each model is increased according to the order in Table 6.1.

Figure 6.3d: Topographic metric

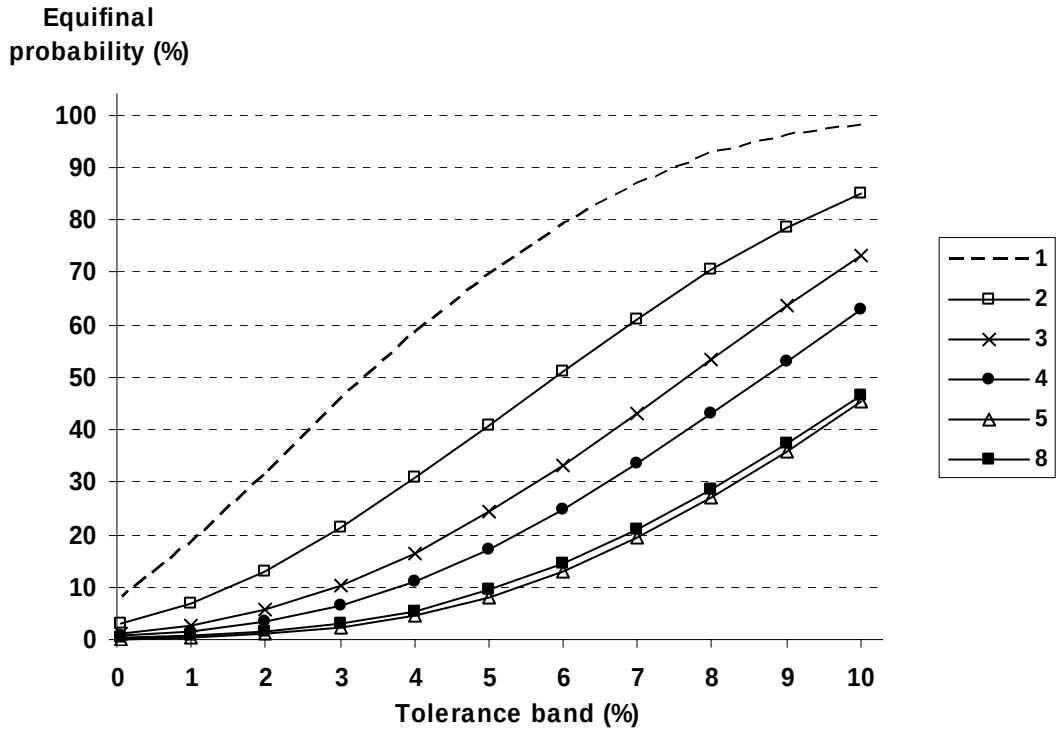

Figure 6.3 (cntd), d: Equifinal probability curves for the topographic metric for different model sizes. The legend shows the model size for each curve, and the number of parameters varied in each model is increased according to the order listed in Table 6.1.

The plots reinforce the points already made. The drainage density results with the two-parameter model (Figure 6.3b) are hardly different from those with the whole model; similarly, the four-parameter sediment yield and three-parameter sediment delivery ratio models are almost no more equifinal than their complete versions. The plot for the topographic metric (Figure 6.3d) shows that the equifinality is little changed after including the first five parameters, but there is also an interesting difference in the overall form of the probability curves. The four, five and eight parameter model curves are distinctly concave, curving upwards, whereas the one, two and three parameter model curves are broadly sigmoidal, the former two showing distinct convex curvature at the higher tolerance bands. It would of interest to explore this more deeply, and relate it to changes in the modelled landscape itself.

In conclusion of this section, the most important parameters to include, in order to reduce equifinality, were found to be as follows:

- for sediment yield, k_f and τ_c;
- for drainage density, t_{ci} and n_{ci};

- for sediment delivery ratio, k_f, t_{ci} and n_{ci}; and
- for the topographic metric, k_f, k_w, s_{cr}, τ_c and t_{ci}.

One implication of this result is that the evolution of the chosen landscape (under the climatic and other conditions used in the simulations) could have been modelled almost as well with the six parameters listed above as it was with the ten actually used. There is therefore clear potential to design a more parsimonious LEM for the simulations herein, with little impact on its predictive ability (as measured by these metrics after 100,000 years). It is also interesting to note how the sediment transport coefficient, k_f, and the channel initiation threshold, t_{ci}, appear three times each in the list. This reflects the importance of fluvial sediment transport, via channelled processes, as an agent of denudation in the modelled landscape.

A subtler inference from the list, and indeed from the results generally in this chapter so far, is that equifinality may be controlled to some extent by a researcher including variations in the 'stronger' parameters in preference to the 'weaker' ones. The parameters listed above all demonstrate strong main effects (Figures 4.18-4.25 *q.v.*), whereas the main effects of the others on each metric are either smaller, or too small to be included in a general metamodel, except perhaps as interaction terms. If this pattern can be shown to be common to most metrics and metamodels that might be used in LEM studies, it would suggest powerfully a means by which researchers could limit the possibility of equifinality in LEMs in general. The remainder of the chapter is therefore focused on this issue, beginning with a broader assessment of how parameter main effects and interactions can be expected to be represented in metamodels.

6.4 MAIN EFFECTS, INTERACTIONS, AND THEIR ROLE IN METAMODELS

6.4.1 A test of repeatability - deriving metamodels for other metrics

Before looking at possible generic patterns in metamodel structures, and what these may mean for equifinality in LEMs in general, a core question must be to what extent derivation of metamodels, of the kind seen herein, is feasible. More simply, although it was possible to derive well fitting metamodels in this study, was this only because of good luck in the

choice of the metrics? The possibility arises that the high R^2 values are in fact most unusual. If this were so, any patterns emerging from the quantifications would have to be seen to apply only to these four metrics, or at best to a very limited class of metric. Such a result would imply that that predictive quantification (via a metamodel) of a LEM's output could only be conducted using very few output measures. It would also suggest that relating output from LEMs to the driving conditions and other parameter value variations used in any simulation is highly problematic, and quite possibly infeasible in many LEM studies. This would be a major obstacle to quantifying equifinality more generally, and researchers would have to run very many simulations (*c.* 10^4-10^5, or more, as reviewed in Chapter 3) in order to obtain LEM responses across even quite modestly sized parameter spaces[1].

As a step towards clarifying matters, the question of whether closely fitting metamodels can be obtained for other metrics has also been addressed, in particular for some of the alternative metrics that were discussed as part of the selection of the metrics, in section 4.3. In the original appraisal of which metrics to use, it was noted that most of the metrics, as evidenced by plots of model response over time, looked suitable subjects for metamodelling. The evidence to support this view was largely qualitative, however, based on a visual inspection of the plots for each metric. To test whether this judgment was justified, and hence whether like judgements could be justified more generally, three alternative metrics were selected randomly from those reviewed in section 4.3, and metamodels for them were derived through a series of regression analyses. The metrics chosen were median gradient, mean regolith depth and the standard deviation of elevation differences with the base case. To be consistent with how the other metamodels were derived, the data used in the regressions were from the last time slice i.e. at 100,000 simulated years; similarly, the parameter values were rescaled to level values according to either equation 4.01 or 4.05 (*q.v.*), as listed in Table 6.2.

To see which parameters were likely to be significant, the author repeated the plots of main effects over time and at 100,000 years for each parameter and alternative metric, in the manner of Figures 4.19 to 4.25, and these are provided in Appendix O. The regression analyses were then carried out using a series of stepwise procedures. In assessing the success or otherwise of the regressions, it should be emphasised that the author was not intending to obtain the most closely fitting models; rather the aim was to assess whether

[1] By LEM standards, that is, taking into account the number of parameters likely to used in a LEM, as reviewed in Chapter 2 and summarised in Table 2.2.

first approximation models could be fitted, and what R^2 scores could be achieved by doing so. For this reason, curvature terms were limited to quadric or quadratic functions, and interactions to two factors only. For the standard deviations metric, as the main effects of some parameters were distinctly spiked (Appendix O, *q.v.*), absolute value terms were also used in modelling their main effects. Fuller details of the regressions are given in Appendix P, but for the purposes here, the main results are summarised in Table 6.2.

Table 6.2: Summary of regressions to derive metamodels for three alternative metrics.

Metric	Number of sample points and source	R^2 (adj. R^2) achieved, %	Number of regressors, notes
Median gradient	149 – all of the central composite design sample	98.7 (98.6)	9 terms, of which 7 used to model 6 main effects; 7 of the parameters used in all. All terms very highly significant. Used balance-scaled values (eq. 4.05)
Mean sediment depth	149 - all of the central composite design sample	99.1 (99.0)	15 terms, of which 12 used to model main effects; all of the ten parameters used. All terms very highly significant. Used scaled values (eq. 4.05)
Standard deviation of elevation differences	201 – the centre point, all factorial points, and all additional main effects points	97.5 (97.2)	18 terms, of which 7 used to model main effects; 9 of the parameters used in all. All terms very highly significant. Used scaled values, (eq. 4.01), and some absolute value terms to model main effects.

The results demonstrate that the qualitative impression given by plots, namely that metamodelling should be possible, has been borne out convincingly. The high R^2 scores are particularly striking, and suggest that close fitting models of this kind should be more usual than not in LEM studies. Admittedly, the use of stochastic forcing, in climate drivers for example, could confuse matters somewhat, leading to a wider scatter and poorer metamodel fits, and this is commented on in the discussion, in Chapter 7.

It is also of interest to note that the models dominated by main effects terms are the more closely fitted, with fewer regressors, as was found with the main four metamodels derived in Chapter 4. Therefore, taking the analyses in that chapter and these tests together, there appears to be a more general finding, namely that the likely form of any metamodel can be inferred qualitatively, at least as a first approximation, by referring to main effects and factorial points plots of the kind provided in Chapter 4 and Appendix O. If the stronger main effects, as revealed by the star point simulations, demonstrate a greater spread in their results than the spread of values seen in the factorial point samples, then the metamodel is likely to be dominated by main effects terms and contain few interaction terms, and the R^2 score is likely to be high. This is the mode of LEM response exhibited by the sediment

yield, drainage density and sediment delivery ratio metrics, and it has been repeated here by the median gradient and mean sediment depth metrics. However, where the spread in the factorial point sample results is greater than or similar to the spread in the main effects results, than the output comprises a more complex combination of interactions and main effects, with a lower R^2 score likely. This mode of model response is exhibited by the topographic metric, and is also seen here in the standard deviations metric. Either way, however, both response modes permit metamodelling, and that in turn highlights the more important parameter combinations driving the response of the LEM and its equifinality.

As a proviso to the above, there is still a question over how widely the patterns of response observed here would be repeated in other studies with LEMs. In particular, the possibility arises that in some situations, LEM output is not dominated by main effects, but is the result of high factor interactions, perhaps with complicated curvature terms, which would be difficult to model. Another possibility is that LEM output, particularly under certain combinations of geology, sediment cover and stochastic climate, is chaotic or non-linear in some way, evidenced by steps, ridges and spikes in the response, such that metamodelling of the kind used here is not possible. Regarding the latter point, it should be borne in mind that the chaotic response being considered in this research is that measured *at a time,* rather than *over time,* the latter being the more usual manner in which chaotic effects are discussed (e.g. Phillips, 1996, 1999, 2006). A chaotic or non-linear at a time response could also be confused with a noisy response generally, as would occur perhaps under strong stochastic forcing. It is not possible to deal with these points definitively based on this research alone, but the problems can at least be approached qualitatively, by referring to findings from previous researchers, and this is considered in sections 7.6 and 7.7.

Finally, the forms of the preliminary metamodels, listed in Table 4.1, and those for the new metrics, listed in Table 6.2, suggest a means of exploring parameter effects and the resulting equifinality in a generic manner, and this is now discussed.

6.4.2 Generic patterns of equifinality, and the use of 'metamodel archetypes'

The foregoing results and discussion suggest that equifinality can be explored in a theoretical way using example metamodels, or *metamodel archetypes*. Such archetypes could be applied in a range of numerical explorations of a hypothetical parameter space, in

the same manner as the four metamodels in this thesis have been used to explore GOLEM's parameter space. It must be emphasised here that the archetypes cannot be used to predict *which* of the LEM's parameters would be significant as main effects or interactions, only the patterns of equifinality to expect assuming those effects have been identified and modelled. Moreover, provided the range of structures of the archetypes conforms to the metamodel structures considered realistic to model LEM output metrics generally, then the types and ranges of equifinal behaviour that LEMs should exhibit can be demonstrated.

By approaching the understanding of equifinality in this way, it becomes feasible to test how different combinations of the parameters, main effects and interactions influence the equifinal behaviour of the archetype, and hence of any LEM metric modelled satisfactorily using an equivalent to the archetype. To illustrate a possible geomorphological application of a metamodel archetype, and how its use extends our understanding of equifinal behaviour in LEMs for the purposes of this thesis, it is helpful to consider what is revealed using a simple two parameter archetypal metamodel, of the form:

$$Z = \beta_0 + \beta_1 x_1 + \beta_2 x_2 + \gamma_1 x_1^2 + \gamma_2 x_2^2 + \beta_{12} x_1 x_2 + \gamma_{12} x_1^2 x_2^2 , \qquad 6.01$$

where Z is the equivalent conceptually of any LEM output metric, β_0 is a constant, x_1 and x_2 are the hypothetical LEM parameters, and β_1, β_2, β_{12}, γ_1, γ_2, and γ_{12} are coefficients appropriate for the fitted metamodel. It should be noted that metamodel error is assumed here to be negligible, but in a more comprehensive research programme, presumably different sizes and distributions of error could be applied. Also, the parameters x_1 and x_2 are assumed to be varied across their scaled factorial space values of ± 1, with a base case value of zero for each, and the constant β_0 has a value of 100, which makes the assessment of percentage differences and tolerances somewhat easier.

Regarding the use of simple quadratic terms, since these were found to be adequate for most of the terms in the initial metamodels and the alternative trials (Tables 4.1 and 6.2, *q.v.*), their inclusion here is considered an adequate way to include curvature in the main effects and interactions. Although only a limited parameter space and model structure exploration can be conducted using this archetype, results were obtained in like manner to the method explained in Chapter 5, albeit with no error term or bootstrap. By sampling the hypothetical parameter space randomly, 1,000 points at a time, and replicating the results 10 times, a number of interesting results were quickly obtained. Some of these are shown in the plots

below, the first, Figure 6.4, dealing with the equifinal probability curves generated by linear and bilinear models, with no interaction terms.

a. Bilinear examples (no curvature or interaction terms), β_0 =100, showing the influence of stronger main effects.

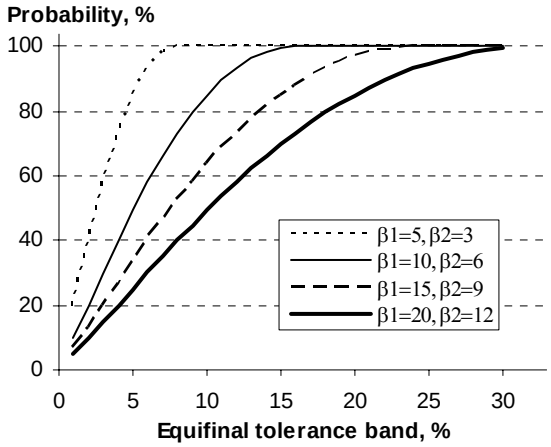

b. Bilinear model example (no curvature or interaction terms), β_0 =100, β_1 = 20 and β_2 =12, showing the influence of model size.

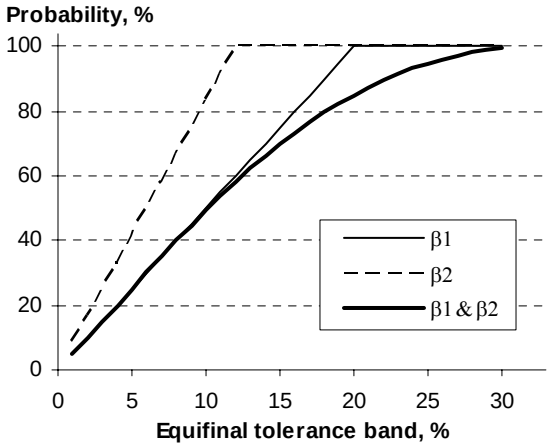

Figures 6.4, a and b: Equifinal probability curves for a two-parameter archetypal metamodel (eq. 6.01), demonstrating the influence of linear main effects on equifinal likelihood. Results are based on 1,000 random sample points, replicated ten times.

The first thing to note is the similarity between the general forms of the probability curves shown in Figure 6.4 and the forms seen for three of the metrics in the main study in this research, in Figure 5.6. In addition, in Figure 6.4a, the archetype shows clearly how increasing the strength of the main effects is associated with reducing the likelihood of an equifinal result being generated. In Figure 6.1b, it can be seen that the equifinality of the result where both parameters are varied together is less than either result where the parameters are varied singly.

These are striking results, not least for their similarity to those found already in this research, but also for their clarity in explaining the general forms and patterns of equifinal probability found herein using the main metamodels. More specifically, the result with the bilinear archetype was repeated using up to 10 parameters, all modelled as linear functions, and the pattern of result in Figure 6.4b was found in each instance. This suggests that where the response of a LEM metric is strongly dominated by linear main effects, varying more of the parameters in a simulation is always likely to reduce the probability of the LEM generating equifinal results. This conforms to some extent with theoretical inferences made by Phillips (e.g. Phillips 2006), who proposes that including more factors should make

model results more singular. However, the matter could be made more complicated here by the presence of curvature in the main effects, and the possibility of strong interaction effects, which may themselves be curved. These possibilities can also be explored using the same archetype. Figure 6.5 therefore shows examples of how main effect curvature may influence equifinality. Regarding Figure 6.5a, which is a biquadric model example, it will remembered that in the topographic metric metamodel, most of the main effects were modelled using quadric functions, all with the same sign, so there is clearly a possibility of such a metamodel being derived for other metrics. Regarding Figure 6.5b, quadratic models are clearly another possibility, but in the biquadratic example shown here particularly strong curvature terms have been used, to simulate the situation of a local maximum or minimum within the factorial space, but not at the origin.

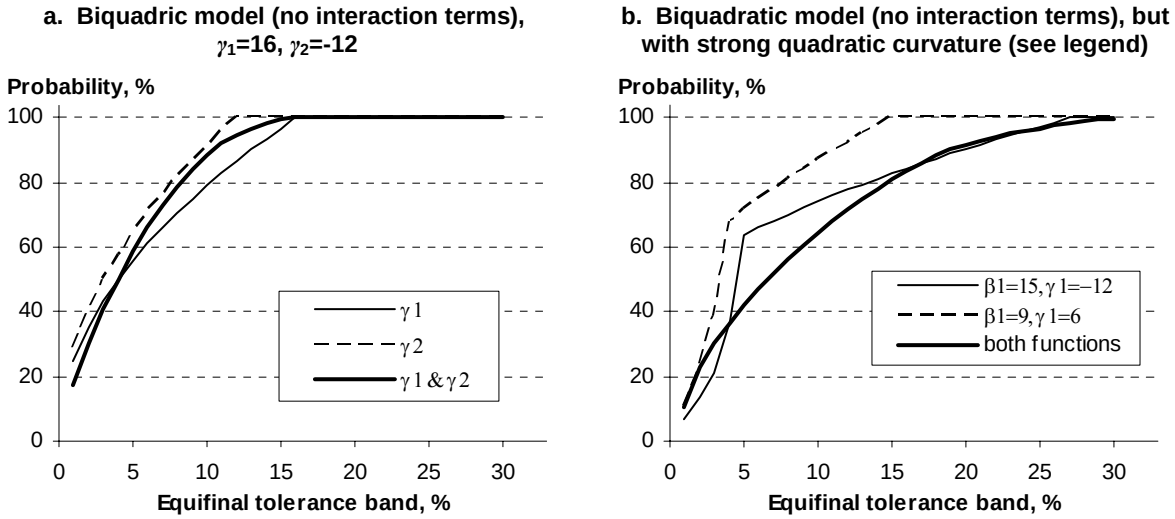

Figures 6.5, a and b: Equifinal probability curves for two archetypal two-parameter metamodels (eq. 6.01), demonstrating the association of equifinal probability with curvature in the parameter main effects. (Results based on ten replicates, of 10,000 points each)

When testing the biquadric archetype, it was found that if the signs of the coefficients were the same (i.e. both positive or both negative) then the patterns of result were the same as shown in the bilinear model examples above (Figure 6.4). In particular, increasing the number of parameters varied always reduced the equifinality, provided the coefficients' signs were the same. Moreover, further testing with mixed models, of up to ten parameters, and comprising only linear and quadric terms, produced the same general results, again provided that the quadric term signs were all positive or all negative. The same general patterns of result were also found if the quadric term functions were replaced by absolute value functions.

However, if opposite signs were used for the quadric terms, a different result was obtained. This is shown in Figure 6.2a, where for some tolerance bands, the equifinality arising through varying both parameters together is greater than it is when varying the stronger parameter (x_1) on its own. The effect here is weak, however, even when using coefficients which are quite high compared with the base case result. It would be interesting to see under what circumstances and by using how many parameters the result might be made more marked, and whether such circumstances would ever arise in simulations using LEMs.

In Figure 6.5b, the biquadratic example, the equifinality of the combined curve is greater than that for the stronger (more curved) parameter (x_1) at low and high tolerance bands, but much less than the curves for either parameter singly in the intermediate tolerance bands. The results in Figure 6.5 a and b, taken together, suggest that main effect curvature terms influence the equifinality of the output, but more so at some tolerance bands than others, depending upon the types of curvature and the relative strength of each parameter's effect.

The next examples show how a parameter interaction may affect equifinality. As before, the results are based on a run of 1,000 sample points per parameter, replicated ten times. In Figure 6.6a, the plot shows the equifinal probabilities generated by a bilinear model which includes a linear interaction term. In this instance, the interaction term has increased the likelihood of obtaining an equifinal result for the combined curve in low to medium tolerance bands. However, the effect here is not especially strong, so it would be of interest to see a more thorough investigation, using more parameters and greater variation in the comparative strengths of the main effects and interactions. Figure 6.6b shows curves generated by a biquadratic model, also including a linear interaction. Again, the interaction has altered the combined response somewhat, so that between tolerance bands of about 5 and 10%, the combined curve lies above that for the strongest parameter (x_1).

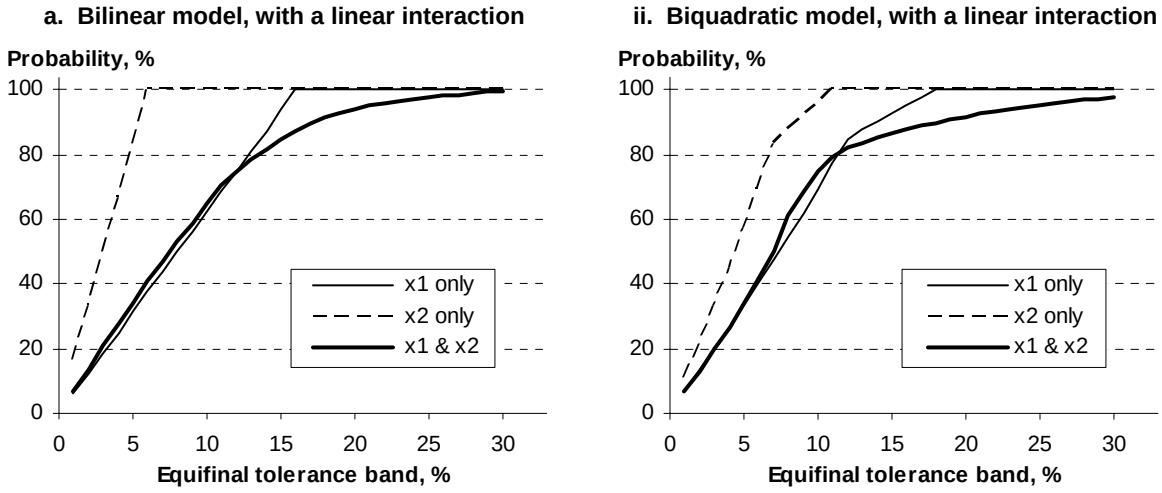

Figures 6.6, a and b: Equifinal probability curves for two archetypal two-parameter metamodels (eq. 6.01), showing the influence of a linear interaction term.

In the final example, Figure 6.7, the influence of the signs of the interaction terms is shown.

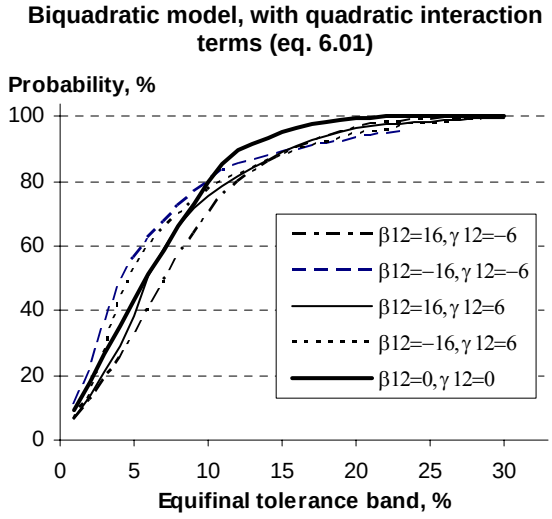

Figures 6.7: Equifinal probability curves for archetypal two-parameter metamodels. The main effects are quadratic functions, held constant. The other curves are generated by adding a quadratic interaction, with different combinations of same coefficient values, as shown in the legend (see text).

The bold line in the figure shows the combined equifinal probability curve for a biquadratic model, with no interactions. The other curves all incorporate the same parameter main effects, but also a quadratic interaction term. In each curve, the same absolute values are used for the interaction term coefficients, but different combinations of signs for those coefficients are applied. It is interesting to note that two of the curves demonstrate a lower equifinal probability across all of the tolerance bands than is found for the model without

the interaction. These are therefore instances where inclusion of interactions *reduces* equifinal probabilities rather than increasing them.

All of the examples above help to illustrate how parameter main effects and interactions can combine to influence equifinality in a LEM's output, and how archetypes can be used to explore more thoroughly the properties and equifinal behaviour of wide ranges of such main and interaction effect combinations. Moreover, the explorations can be conducted with as many parameters as desired, with or without error and use of a bootstrap. There is clearly a need for further work in this respect, as it could be of great use in LEM studies.

These comments complete the second results chapter, and the main points are now summarised.

6.5 CHAPTER SUMMARY

In this chapter, the influence of the parameters on equifinality has been explored, beginning with the calculation of the equifinal probabilities for each parameter individually and each metric. The results for all four metrics indicated clearly that some parameters are much more likely to generate equifinal output than others. In particular, by contrasting the equifinal probabilities for each parameter with their main effects on the metric of interest, a close association was identified between the strength of a parameter's main effect and its propensity to generate equifinal outcomes. This showed that the stronger parameters exhibit little equifinality, whereas the weaker exhibit much more.

Next, the influence of varying two or more parameters was then explored, introducing one additional parameter in each new set of calculations, starting with those parameters with the strongest main effects. These results showed clearly that equifinal probability was reduced as more of the parameters were introduced into the calculations. The reduction in equifinal probabilities was generally most marked for the parameters with the strongest main effects. Before treating this as a generally applicable result, however, it was necessary to conduct further tests.

A first step was to see whether the general structure of the metamodels, as a combination of main effects and interactions, was in some way simply a matter of good luck, or something that could reasonably be expected. To this end, regression analyses were conducted to derive preliminary metamodels for three alternative metrics, these being median gradient,

mean sediment depth and standard deviation of elevation differences. The regression analyses produced three closely fitting metamodels, with R^2 and adjusted R^2 scores of between *c.*97% and 99%, from combinations of main effect and interaction effect terms. Main effects terms were found to be dominant in the metamodels for median gradient and mean sediment depth, whereas more interaction terms were needed in the metamodel for the standard deviations metric. These results together were taken to imply a general result, which should be expected in most LEM studies, namely that metamodels of the type considered in this research should be capable of being fitted to a wide variety of metrics.

Using the results from the metamodelling in Chapter 4, and for the three trial metrics, it was then proposed that general forms of metamodel, called 'metamodel archetypes' can be used to explore equifinal behaviour. Using a particular two-parameter version of an archetype, it was possible to explain how the forms of the equifinal probability curves reported in Chapter 5, and how the strength of main effects and interactions, and also the presence of curvature, influence the equifinal probability at different tolerance bands. Specifically, it was possible to show that introducing more parameters into a model always *reduces* equifinal probabilities provided that there are no interaction terms and all the main effects are linear. A similar result was obtained using main effects modelled as quadric terms, provided the signs of those terms are either all positive or negative[2]. Further results showed how interactions and curvature modify equifinal response, although for the most part the differences are small provided the main effects curvature and interaction effects are also small.

These remarks conclude presentation of the quantifications of equifinality in this thesis. The discussion of the research and statement of the main conclusions now follows.

[2] It should be borne in mind here that the effects are modelled using scaled design levels, centred on zero, as obtained using equation 4.01 (*q.v.*).

CHAPTER 7: DISCUSSION AND CONCLUSIONS

7.1 INTRODUCTION

This chapter is divided broadly into two parts. The purpose in the first is to present a summary and critical appraisal of the results of this research, focusing particularly on the quantifications of equifinality, which were conducted in pursuit of research aims 1 to 5. The discussion here therefore comprises an assessment of the methods used to obtain the quantifications, including in particular a consideration of the sampling strategy, and of the derivation and adequacy of the metamodels. The influences on equifinality which have been revealed in the parameter main effects and interactions are also appraised and discussed. The points arising from this part of the discussion are then applied and more widely assessed in the second main part of the chapter, in which the requirements of research aim 6 are also considered. This involves reappraising the results of the LEM studies reviewed in Chapter 1 (Table 1), to examine whether equifinality is likely to affect materially the findings from those studies. The ways in which equifinality may be better identified and controlled in LEMs in general are also considered, this allowing the thesis to be placed in the context of geomorphology and model equifinality more generally.

At the end of the discussion, there is a summary of the main discussion points, and the author makes some recommendations for further work. This is followed by a statement of the conclusions, and some final remarks to bring the thesis to a close. In broad outline, therefore, this concluding chapter is structured as follows:

- summary of the main results and review of the quantifications and method;
- patterns of LEM output and their implications;
- consideration of possible equifinality in other LEM studies;
- summary of main discussion points and general assessment of the research;
- recommendations for further work; and finally
- research conclusions, and closing remarks.

7.2 SUMMARY OF MAIN RESULTS

The author presented a range of results in Chapters 5 and 6, firstly denoting in different ways the equifinality of the model's output, and thence - in each chapter - further results

which could be expected to apply to LEMs generally. In all cases, a clear result was found, namely that equifinal output was readily obtained once one began to look for it. Notwithstanding inaccuracies in the metamodels and the calculations, discussed here in section 7.3, it appears that this is a general finding, to be expected of all LEMs. It is also consistent with the conclusions of Beven (1996) regarding equifinality in LEMs, based on understanding of the causes of equifinal behaviour in hydrological and environmental models[1]. Although the likely emergence of equifinal behaviour was indicated in Chapter 1, that it should have been found with such ease is important evidence of its presence in both LEMs and similar types of numerical simulation models. It also demonstrates the need for researchers to consider means of identifying and controlling equifinality in LEM studies.

Regarding the other key results from the research, these are summarised as follows:

1. For a given metric, the likelihood of obtaining an equifinal result depends upon the tolerance band permitted for the metric (section 5.3, Table 5.1 and Figure 5.6, *q.v.*). For example, in the 1% , 2% and 5% tolerance bands, the equifinal probabilities for sediment yield are estimated to be *c.* 9%, 19% and 45% respectively. Similarly, in the same tolerance bands, the equifinal probabilities for drainage density are estimated to be *c.* 13%, 26% and 58%; for the sediment delivery ratio, in the same bands, *c.* 38%, 68% and 99%; and for the topographic metric in the same bands, *c.* 0.6%, 1.4% and 9.3%.
2. Within the same tolerance band, some metrics are much more likely to be equifinal than others (section 5.3). This is shown in particular in Figure 5.6, from which it can be seen that the equifinal probabilities for the sediment delivery ratio are consistently the highest across all the tolerance bands, and those for the topographic metric consistently the lowest, with those for the drainage density and the sediment yield lying at values in between these extremes (Figure 5.6).
3. Where for a particular metric and tolerance band the likelihood of obtaining an equifinal solution is less than 100%, an increase in tolerance generally increases the likelihood of the model generating an equifinal result, and never reduces it; likewise a reduction in tolerance generally reduces equifinal probability, and never increases it (sections 5.3, 5.4 and 6.4). This result is also clearly evident from Figure 5.6.

[1] By extension, Beven's point can also be seen to apply to all numerical models relying on empirical or semi-empirical processes formulations, and not simply to those used in the geosciences.

4. Where metrics are used in combination, each subject to a tolerance band, the probability of obtaining an equifinal solution for the combination is generally lower (and never higher) than it would have been for any of the component metrics used singly, or together in some smaller combination, and in their same respective tolerance bands. This is a general result, caused by the way that polymetric equifinal solution spaces are formed by the intersection of their contributing parameters' equifinal solution spaces (sections 5.4 and 5.5). The general situation is also pictured in the Venn diagram, in Figure 5.15.
5. For a given metric and tolerance band, the probability of obtaining an equifinal result is much higher if one varies some parameters than it is if one varies others (sections 6.2 and 6.3). In this regard, equifinality and parameter sensitivity are in essence opposite relations, but also see result 6 below.
6. For a given metric and tolerance band, the likelihood of obtaining an equifinal result generally decreases as the number of parameters employed in the model increases, although the exact pattern of equifinal response depends upon the contribution made by each parameter's main and interaction effects (sections 6.3 and 6.4);
7. Correspondingly with point 6, in order to generate an equifinal solution, the range of values over which each parameter has to be varied generally increases with any increase in the number of parameters varied overall (section 5.5).
8. LEM responses and equifinal probabilities may be understood generally from the combinations of parameter main effects and interactions they display, tempered by any stochastic, non-linear, or chaotic responses. This allows LEM equifinality to be explored in a generic way, through the use of metamodel archetypes, and permits general statements to be made regarding the influences on equifinality of different parameter functional responses. For example, by exploring with a particular archetype (equation 6.01), and expressing parameter values always in terms of their scaled design levels (equation 4.01), it is possible to show that inclusion of parameters with linear main effects, but negligible interaction effects, will reduce the likelihood of equifinal outcomes being generated across the tolerance bands. This is also found to be true of parameters with quadric or absolute value main effects, provided that the signs of the quadric or absolute value functions are all the same (i.e. all positive or negative), but again provided any interaction effects are negligible. However, introduction of curved main effects, such as may be produced by quadratic functions, may increase or reduce equifinal probabilities in some tolerance bands (e.g. Figure 6.6); similarly, introduction

of linear or quadratic interaction terms may increase or reduce equifinal probabilities, although again, the pattern of equifinal response depends upon the strength and form of the interaction effects (e.g. Figure 6.7).

The quantifications need to be examined for their robustness, but before doing so, further comment on some of the above is useful. More specifically, regarding results 1 and 2, it is noted that this is in keeping with what one would expect. What was unclear at the start of this research, however, was how small or large the equifinal probabilities would be, and how the patterns of equifinal behaviour would differ between metrics. The quantifications have therefore been successful in showing - for the first time in a LEM - how equifinal outcomes may occur in different metrics, and how the probability of such outcomes varies across tolerance bands, and between one metric and another (e.g. Figure 5.6).

Regarding result number 3, this is deduced from the equifinal probability curves and surfaces reported in Chapters 5 and 6, for both single metrics and combinations, and as demonstrated by the metamodel archetypes. Although results obtained using the two-parameter archetypes did display some kinked probability curves, the curves or surfaces for the larger metamodels generally exhibited no flat spots or undulations[2]. Though the result certainly seems to be correct, and perhaps rather simple, it should be borne in mind that stepped or oddly shaped surfaces could not have been ruled out before the research was conducted. It is interesting therefore to see that no such irregular curves or surfaces were found.

Result 4 was reported and discussed in detail in Chapter 5, and will not be commented on further here. Regarding result number 5, this makes sense intuitively, as some model responses should be expected to be very sensitive to parameter value changes, whilst others would not be. Result 6, on the other hand, was not expected when the author first began the research. It was assumed then that the inclusion of many parameters, of uncertain value, would raise the chances of generating equifinal output. Indeed, the use of many parameters in a model is argued against partly for the same reason, namely that the likelihood of generating equifinal output increases with the number of parameters, and this makes calibration work especially difficult (e.g. Beven, 1996, 2006). Initially, therefore, result 6 seemed intuitively *incorrect*, but there appears to be no doubting it, and the quantifications

[2] Note that the author distinguishes here between the curves or surfaces relating to equifinal probabilities, and those used to display factor-response relationships, as in Figures 4.18-4.25.

were clear for all of the metrics. There is also some theoretical support for a reduction in equifinality if more factors are included in a model (e.g. Phillips, 2006). However, the theoretical analysis, using the metamodel archetype studies in Chapter 6, indicated that the result is rather more complicated than this, as the equifinal response is driven by the strength and form of the parameter main effects and interactions together. As discussed in Chapter 6, provided interaction effects are not strong, and the metamodel does not include strong or conflicting forms of curvature in the main effects, then result 6 should have general applicability. However, particularly strong curvature or interactions modify the equifinal probabilities in some tolerance bands, perhaps raising them or lowering them depending upon the situation, and further research is clearly required to explore this behaviour more thoroughly.

Result 7 was demonstrated using the two-parameter solution mapping, and result 8 is related to result 6 and the comments made thereon.

With these points made, the discussion now turns to a consideration of the method.

7.3 CRITICAL ASSESSMENT OF THE METHOD

7.3.1 Deriving the metamodels

The task of obtaining model output for use in this study was discussed in Chapter 3, and the method of summarising the output in metrics and of deriving metamodels to predict their values was described in Chapters 3 and 4. The advantage of using metamodels over full simulations was also described in Chapter 3. In particular, LEMs typically have large parameter spaces (Chapter 2), necessitating potentially very large numbers of simulations (*c.* 10^4 or more, Table 3.1, *q.v.*) if those spaces are to be explored thoroughly. In addition, each individual LEM simulation typically takes from many hours to days, or even weeks, to complete. The large simulation run sizes and long simulation times together form a computational burden which is quite infeasible given usual computing resources. The use of a metamodel approach here has drastically reduced that burden. More specifically, the initial sampling, using the central composite design, required only 149 simulations with GOLEM to sample the selected 10-D parameter space (subsection 3.5.3). This is to be compared with the *c.* 10^5 or much larger run sizes likely to be needed to sample a parameter

space of such dimensions if using a GLUE methodology (e.g. Beven and Binley, 1992; Beven and Freer, 2001), or possibly the even larger run sizes if relying on the N^k factorial type of sampling summarised in Table 3.1. Additional simulations, to test the preliminary metamodels and assist in the derivation of more balanced final metamodels, increased the total number of simulations in this research to 329 runs, still an enormous saving on the potential run sizes required by GLUE or N^k sampling methods.

In applying the metamodel approach, it was implicit that, for the quantifications to be representative of model behaviour, the metamodels would have to predict GOLEM's output to within an acceptable degree of error. Although it was not expected that the error could be reduced to zero, it was important that it should be reduced so far as practical. The inclusion of the bootstrap technique in all of the quantifications also allowed for inclusion of the estimated errors after deriving the models, so this permitted some relaxation in the effort to achieve very closely fitting models.

The general principles adopted in deriving the preliminary metamodels were explained in subsection 4.4.2, namely to achieve:

i. high R^2 and adjusted R^2 scores (as evidence of a good fit with small errors);
ii. balanced residuals plots (as evidence of correct model formulation and low bias);
iii. and if possible, stable constant terms for different sub-samples of the data (as further evidence of a more correct model formulation).

These measures were adopted following recommendations in the standard texts (e.g. Box and Draper, 1987; Draper and Smith, 1981; Box *et al.*, 1978). The need to keep metamodel structures simple was also explained, using terms of high significance where possible, but also as many of the parameters as possible subject to those requirements.

Finally, the use of the bootstrap is an important aspect of this work, as it permitted prediction errors to be incorporated in the calculations in a systematic way; it was also a way of openly acknowledging that the metamodels were not perfect predictors, however well-fitting they appeared to be. The bootstrap runs were conducted for a large number (10^6) of sample points in the parameter space, and these runs were replicated ten times, so as to reduce any likelihood of bias through under-sampling of the parameter space. The use of the bootstrap also allowed estimation of the confidence intervals around the estimated equifinal probabilities, but these were found generally to be very narrow (*c.* 0.2% or less) and were ignored for the purposes of reporting the results. Although Davison and Hinkley

(1997) point out that confidence intervals may be underestimated in bootstrap calculations and suggest certain ways in which they may be adjusted, such adjustments are not considered material here, nor would they affect any of the general patterns of result for the metrics or parameters.

With respect to the metamodel formulations, for the most part, the general metamodels were considered adequate for all of the calculations, but the author did have some concerns about accuracy of the results where only one parameter was being varied at a time, particularly if using the topographic metric metamodel. For this reason, metamodels for parameters individually were employed in Chapter 6, using the same principles as described above, but this time employing a parametric bootstrap (discussed in subsection 6.2.1).

7.3.2 General assessment of the regressions and metamodels

Working to the principles summarised above, the R^2 and adjusted R^2 scores of all of the general metamodels (Tables 4.2 and 4.3) were well above 90% (the lowest, for the topographic metric, being an R^2 of 92.3%, and an adjusted R^2 of 91.8%), and the residuals plots looked balanced and satisfactory (e.g. Box and Draper, 1987; Draper and Smith, 1981). There were especial difficulties obtaining a good metamodel for the topographic metric, but the generally good fit, with eight parameters in the model and 20 regressor terms, was considered satisfactory for the purpose herein. Similarly, the R^2 scores for the individual parameter models were generally all 90% or over for the more important parameters i.e. those where a main effect was identifiable in the regression. For reasons of space, these individual metamodels are not listed here, but full details of each of these models are provided in Appendix L. Although some of the individual parameter regressions indicated a poor fit of the metamodel to the data, and marginally significant or non-significant regressors, this occurred only for those parameters which had a weak main effect on the metric in question (Appendix L, *q.v.*). The individual results for these minor parameters are therefore thought not to affect materially the generality of how the equifinal response may differ between one parameter and another.

Given the generally high R^2 scores for the metamodels, the balanced residuals plots, and the high significance of the regressor terms, stabilisation of the constant in each metamodel was not considered important here. Moreover, use of the central composite design would make

subsetting of the initial sample data problematic, introducing the risk of aliasing in any two-factor or higher-way interaction terms. A Latin Hypercube sampling design would be better in this respect, although it would also have disadvantages, as discussed in Chapter 3.

Regarding the significance of each regressor, nearly all of the terms used in the final metamodels were very highly significant ($p < 0.001$) or highly significant ($p < 0.01$), so it seems doubtful that the terms were inappropriate or misapplied in any material way. As a further comment on the types of model that were fitted, although the general sediment yield and drainage density metamodels were of a more sophisticated type, employing logarithms of polynomials rather than a simpler, linear model structure, closer inspection shows that they are really only adaptations non-linear model forms, but cast as log terms, as reported in the standard literature (e.g. Draper and Smith, 1981; Ratkowsky, 1990).

Regarding the aim to include as many of the parameters as possible, this was subordinated to the requirements for high significance for each of the regressors. There is not much to add here, other than the author thought one should not force inclusion of a parameter merely for the sake of it: if a parameter could be omitted, it was, and there is no reason to suppose that the quantifications obtained were materially less representative as a consequence. In addition, the use of the non-parametric bootstrap for the main calculations takes into account the errors that may arise through omission of the less significant terms and parameters in the general metamodels. Of these, none included all of the parameters, although two of them included eight out of the ten (for both the sediment delivery ratio and the topographic metric, as shown in Table 4.3), whether in main effects or interaction terms, and the sediment yield metamodel nine of the ten (as listed in Table 4.2). However, for the drainage density metamodel, it was difficult to justify including more than a few parameters in addition to the main two, as the effects of the additional parameter terms were so small and always of marginal significance or insignificant. This metamodel therefore included only four of the parameters (also listed in Table 4.2). The differences seen here are thought to reflect what should be expected in other studies with LEMs, namely that some metamodels will need far fewer of the parameters in the regressor terms, whereas others will need more, this depending upon the relative strengths of their effects on the metric in question. It would certainly be interesting to explore in more detail how these differences between metamodel parameter structures are related to the morphology of the landscape and the processes shaping it.

In addition to the above, it needs to be emphasised that the metamodels were used to *interpolate* model output within the factorial space. In this respect, besides the factorial point simulations, additional simulations were also run using points lying at various intervening positions within the factorial space, in order to test the preliminary metamodels, and to improve fits of the main effects and interactions, as described in subsections 4.4.4 and 4.4.5. It follows that in the quantifications made with the metamodels, there was always a high degree of anchoring of the predicted values to output from the simulations. Had the metamodels been used to extrapolate beyond the sampled ranges, which in this instance would mean beyond the limits of the factorial space, the predictions would then clearly be more speculative (notwithstanding the use of the bootstrap), and detracted from the robustness of any results reported here. Extrapolation beyond the sampled region would also have been likely if using a Latin Hypercube ('LH') type of sampling, as it would be inevitable that a proportion of the sample points would have lain nearer to the centre than to the corner points of the parameter space, and almost none of them would have been positioned exactly at any single corner point. Although this problem could have been corrected to some extent by forcing the LH design to include points at or very near the corners, doing this would largely obviate the use of a LH scheme. However, the use of Latin Hypercube sampling is certainly not dismissed here, and it would be of interest to see it used in other LEM metamodelling studies.

Taking into account all the foregoing, the quantifications and results that were obtained and reported in Chapters 5 and 6, and summarised above, appear to be robust and reliable for the purposes of this research. In addition, the metamodels are not unusual in some way, as tests to derive preliminary metamodels for three alternative metrics, in Chapter 6, were strikingly successful, even though the regression analyses were by no means sophisticated or exhaustive. The similarity in the structures of the four main metamodels and the three trials, that is in the mix of parameter main effects and interactions, indicates clearly that the patterns of equifinal behaviour are not unusual, but rather should be expected from any metamodels with these or similar structures. Consequently, it is evident that equifinality can be quantified using this method, with a degree of confidence, provided the experiment design permits the more important influences and effects to be themselves quantified and modelled.

7.3.3 Wider limitations in the methodology

The critique so far has focused mainly on the technical aspects of the sampling, regression and quantifications. However, there are more general criticisms which need to be considered, relating primarily to the choices of the output time, the LEM, the simulation scenario and the chosen landscape.

Regarding the chosen output time, that is, the choice of metrics at 100,000 years, ideally, a range of other times would have been used, and metamodels would also be derived from metrics referenced to those times. Quantifications of equifinality would then be made from those metamodels also, and a more complete set of equifinal probability responses generated by the LEM would be provided thereby. Quite possibly, these calculations would show differences in equifinal probabilities for each metric at the different times, and under different metamodel structures, as some parameters become more important or less so over time, following changes in their main and interaction effects. Temporal change in the equifinality of the LEM metrics is discussed in detail below, in section 7.4, but for the purposes here, it is not thought to alter the general findings of the research, as reported in section 7.2. In particular, temporal variation in equifinality does not impinge on the theoretical relationships between parameter effects and equifinal response, outlined in Chapter 6, as these relationships apply to all equivalent metamodel structures, where main effects and interactions contribute to the response of the LEM, and regardless of either the time of the output from which the data are taken or the metric to which they refer.

The use of GOLEM only, and the particular processes within it used here, is ostensibly a important limitation, as the possibility arises that there could be major differences between equifinal responses of LEMs. Quite probably the specific quantifications of equifinality would be different between LEMs for the same metrics. However, it is difficult to see how the general patterns found in the research would be different in any material degree if using a different LEM. For example, as reviewed in Chapter 2, many LEMs use the same or very similar process formulations to the ones used in GOLEM (Tables 2.1 and 2.2, *q.v.*). Also, as reviewed in Chapter 2, many LEMs use an orthogonal grid (Table 2.1). Therefore, although there may be specific differences in the equifinal probabilities generated by different LEMs for the same metric, in simulations of the same landscape and driving conditions, the metamodels derived from different LEMs and metrics should still be a mix of parameter main effects and interactions, of the kind found in this research; indeed, it is

difficult to see why it should be otherwise, unless the response is very noisy for some reason, thus making derivation of a metamodel problematic. Possibly the shapes of the equifinal response curves would be somewhat different for the same metrics generated by different LEMs, for example convex rather than concave, but even in this situation, the underlying competition between parameter effects should be broadly the same from one LEM to another, and exhibited between different LEMs in similar ways. This should also be the case for different architectures, although again, the equifinal probability curves may well have slightly different shapes from those produced here by GOLEM. For these reasons, the general findings here, as summarised in subsection 7.2, are thought to apply to other LEMs also. However, further research is clearly required with other LEMs to test this hypothesis.

Regarding the specific landscape and scenario (constant climate and no uplift), again, there are likely to be different specific quantifications of equifinality from one landscape to another, but these differences do not override the generality of the main findings in subsection 7.2. The importance of parameter main effects and interactions in determining LEM output still applies, and hence the patterns of equifinal response those parameters generate for the landscape and scenario in question.

With these general points made, further comment is now needed on patterns in the output and the implications of these patterns on equifinality in LEMs generally. The first part of the discussion deals with the observed patterns in parameter main effects and interactions.

7.4 PARAMETER MAIN EFFECTS, INTERACTIONS AND PATTERNS OF EQUIFINALITY

7.4.1 Changes over time

In the foregoing section, the author has commented on the mix of main effects and interactions which are likely to drive a LEM's response. With reference to the main effects plots in Figures 4.18-4.25 and in Appendix O, and taking into account the discussion above, there would appear to be at least four modes of LEM response to parameter variation, namely:

i. a main effects dominated response;

ii. a more complex response in which the interactions and main effects are more nearly balanced;
iii. another, yet more complex response in which the interactions are dominant; and
iv. a noisy or chaotic (non-linear) response, in which no patterns of effects are identifiable.

As commented in Chapter 6, the first two have been observed in this research, and the plotted data provide an insight into how main effects and interactions may change over time. It is of interest to examine the way these changes are manifested, and what they imply for the equifinal behaviour of a LEM.

Dealing first with trends in the parameter main effects in Figures 4.19-4.25 and Appendix O, it can be seen that for any parameter, the spread between the $+\alpha$ and $-\alpha$ responses may increase over time, indicating an increase in the main effect, or it may reduce over time, indicating a reduction in the main effect, or the lines may converge, cross and diverge, indicating a reversal in the main effect. The plots do not indicate clearly whether several or more reversals in the main effect of a parameter can occur, but it seems reasonable to suppose that under different simulation conditions, of geology and climate for example, multiple reversals over time might be possible, and indeed, the same might also be found for interaction effects.

The data also demonstrate another key point, which is that the *mean* effect, that is, of the effect of all the parameters together at their base values, also changes over time. In some metrics, it increases (e.g. for sediment yield, in Figures 4.16d and 4.18, and for median gradient and mean sediment depth, in Appendix O, Figures 1a and 2a respectively), whilst in others it declines (e.g. for the bedrock channel percentage, in Figure 4.15b). The mean effect of the parameters is rather more interesting on the sediment delivery ratio, where it declines during the first 20,000 years of the simulation, and then increases (Figures 4.16c and 4.22). As with fluctuations in the main effects, presumably multiple increases or decreases in the mean effect can also be experienced, depending upon the circumstances.

Given therefore that the mean, main and interaction effects over time can be expected to vary, it follows that the equifinality of the model is itself not a constant property but also varies over time. Moreover, the temporal effect may well be quantifiable, in that it could be possible to include time in some way as a variable in a metamodel. Thus, a series of *at a time* main effects plots, presumably sampled at a suitable temporal resolution, could be used to demonstrate the changes *over time* in parameter main effects. Admittedly, some of the

main effects responses over time seem to be noisy or erratic, with steps or undulations, and it would probably be very difficult to include time in these metamodels. For example the weaker parameters have a rather erratic effect on the drainage density (Figure 4.20, *q.v.*), and the main effects of two parameters, k_w and τ_b, over time on the topographic metric are distinctly stepped. However, responses over time for other metrics and parameters seemed much smoother, suggesting that incorporation of a temporal dimension in the metamodels for those metrics is feasible. The matter could be of use in understanding model output more generally, and deserves further research.

Whether or not time were incorporated in a metamodel, it is interesting to consider how changing equifinality over time might be manifested. Quite possibly, metrics found to be very equifinal at some times would be found to be much less so at others. As a possible corollary to this, it might also be found that for a particular metric and under certain conditions, the dominant main and interaction effects shift over time from some parameters to others without any change in the overall response, so that the equifinality of the metric itself is not seen to vary. More generally, the contrast between *'over time'* and *'at a time'* model responses is also made in the review of LEMs in section 7.5, where it is considered further. In any event, the whole topic suggests a range of new questions which have implications for understanding equifinality and landscape evolution, and it clearly merits further research.

7.4.2 From parameters in particular to factors in general: the role of experimental factors in understanding equifinality

So far in this research, much attention been concentrated on parameter values, whether these occur in a LEM as the coefficients, thresholds or exponents in process formulations, or as governing quantities in the driving conditions of a simulation. The research itself was directed to using coefficients and thresholds for exploratory purposes, with the intention of seeking patterns of model response and equifinality that could reasonably be expected to represent the behaviour of LEMs in general. In this respect, for experimental purposes, the standard texts make clear that there is in principle no limitation on the sort of experimental variations that can be treated as factors (e.g. Box and Draper, 1987; Wu and Hamada, 2000). It should be remembered here that the words 'experiment' and 'experimental' are being used in accordance with their meaning in response surface methodology studies (*ibid.*),

rather than in their more usual meaning in geomorphology. Thus, the variation of two different parameters in suite of simulations constitutes a two-factor experiment, and the variation of three a three-factor experiment, and so on; similarly, the variation of two process classes in the simulations gives rise to two sets of factors, one for the experiments with process 'A', and another for experiments with process 'B'. That they are factors in general rather than parameters in particular makes no qualitative difference from the experimental viewpoint. Moreover, the modes of response of a LEM to variations in the factors, whatever their nature, should be no different qualitatively to the modes of response discussed above, namely that the LEM's response at any time is identifiably determined either by some combination of factor main effects and interactions, or by a 'noisy' response around those effects, perhaps in response to stochastic forcings, or by some form of chaotic emergent behaviour. In any event, provided the noise in the response at any time is not so great as to hide underlying associations of the factor variations with the LEM's response, then it should always be possible in a LEM study to explore equifinal behaviour through an understanding of the main and interaction effects of all of the experimental factors.

Although this would seem to be a very simple point, it is argued here that it is fundamental to an understanding of equifinality in LEMs. Indeed, it was the main reason for approaching the research herein using the methods of designed sampling and metamodelling. There are complications to conducting fully factored experiments, however, not the least being the increase in the number of simulations required to explore the 'factor space' (as distinct from simply the parameter space), the treatment of changes over time and space, and the way some types of factoring necessitate a modified approach to calculating equifinality. The issues relating to the size of the experiment have been reviewed and discussed in Chapter 3, but the other two points will be considered below, beginning with a consideration of how temporal and spatial changes in the factors can be incorporated in a designed experiment.

7.4.3 The influence of factors over time and space

Factor changes over time

Temporal changes in factors are used in many LEM studies, particularly those which are used to explore the effects of climate changes, and examples were reported in the model

review in Chapter 1 (section 1.3, *q.v.*). One particular study is here discussed in more detail, to illustrate how such temporal changes are amenable to treatment as different factors.

In the example, Rinaldo *et al.* (1995), the authors were able to make a strong case for the persistence of evidence of past climates in many landscapes. As a core part of their study, they equated wetter and drier climates with difference resistances to fluvial erosion, expressed by the fluvial sediment transport threshold parameter τ_c, arguing that a low τ_c could be used to represent wetter conditions (as it would allow more fluvial erosion), and a high τ_c drier conditions (as it would allow less fluvial erosion). In their study, τ_c was varied over time as a sine wave, and output from the simulations was summarised using three metrics, drainage density, valley density and a fractal measure of topography[3]. Their results showed that all of the metrics varied strongly in response to the changes in τ_c over time, although the response was lagged slightly behind the climate cycle, and responses appeared relatively greater for two of the metrics.

Given the need for 'at a time' analysis in understanding equifinality, the author would argue that the findings presented by Rinaldo *et al.* (1995) could be extended in their scope by treating the climate changes, as expressed by τ_c, as a number of separate factors, rather than just one. Careful consideration shows that the variation can be approached as a four factor experiment, and possibly a five factor experiment if continuous time is included. To explain this, if we assume that the climate variation is never to be varied from its general sinusoidal form, then the influence of climate change on the modelled landscape may be made accountable according to the following:

- the 'base case' or central value of τ_c;
- the amplitude of the oscillation either side of the central value;
- the period (wavelength) of the climate oscillation; and
- the phase shift of the sine wave at $t = 0$.

It is argued that such an approach to the temporal variation would greatly assist in the identification of 'at a time' main effects and interactions, and also in the temporal progression of changes in the same. It would also permit analysis, perhaps through metamodels, of the equifinality pertaining to the results from the study.

[3] The original authors do no specify how their topographic metric was calculated, so it was not possible to repeat its use in this research.

Similar comments can be made regarding other studies which have used temporal variations of some kind, whether these be in climate, land cover, uplift and so on. Again, it would be very interesting to see what was revealed by such an approach if it was applied in LEM studies generally, and what equifinal patterns might emerge from it.

Factor changes over space, including differences in initial forms and sediment distribution

The need for these is perhaps rather subtler than temporal changes, and seldom explored in LEM studies. Armstrong (1987) considered the effects of initial forms very specifically, and some other studies have incorporated more limited initial differences (Table 1, *q.v.*). Similarly, orientation and depth of the geology and strata could be expected to have a strong influence on the evolution of landscapes, and the work by Ahnert (1976) still represents some of the best examples we have of studies incorporating these variations. Moglen and Bras (1995) considered sediment and smaller scale variations also, and again, their work is a thought-provoking study demonstrating the importance of these influences. Could such variations, and similar ones relating to sediment sizes or initial depths of sediment, be incorporated as factors?

Probably the most important attribute of these variations is that they should, if possible, be factored as *ratio* quantities, so that main effects and interactions can be quantified in the manner achieved herein. Regarding variations in geology and strata, presumably the spatial differences can be expressed in terms of the depth of each layer, its dip and strike, the position in space of its outcrop at the surface, and so on. Regarding initial forms, again, it may be possible to express the differences in the gradients or elevations, or through the use of composite initial metrics in some manner, as described for example by Church (2003). Similar considerations can also be made regarding the initial sediment cover and its spatial erodibility or other properties.

It will be appreciated from the above, however, that each new factor increases the size of the factor space that has to be explored. The author would argue that this awareness is good in itself: either it will prompt the use of suitable screening designs, to eliminate from the study the weaker factors, so that the study may be made more manageable; or it will generate a wider discussion of whether a different model or type of experiment is needed, so that the problem is a tractable one. In general, it would seem undesirable to include many factors in

an experiment if their effects are not to be tested methodically. If attempts to clarify the number and nature of the temporal and spatial factors helps also to promote experimental clarity, this surely is a good thing.

Although the foregoing points describe how temporal and spatial factor variations can be accommodated, attempting to assess the equifinality resulting from other types of factor variation can be more problematic, in particular if these include the use of different process classes or process formulations, or even different LEMs altogether. This is an important topic and is considered next.

7.4.4 Calculating equifinality arising from different process classes, different formulations, or different LEMs

The factoring of experiments and the use of efficient experiment designs may greatly assist in the understanding of equifinal behaviour, but matters become more complicated when variations between process classes, formulations and the LEMs themselves are considered. Besides the practical difficulty of greatly increasing the run sizes required, the factoring of these variations changes the way equifinality itself has to be quantified.

To understand why this should be so, it is helpful as an example to contrast the situation in which parameters alone are being varied with one in which process formulations are being varied. In the former, the parameters are almost always likely to be ratio quantities, with meaningful high, central and low values. This can be appreciated readily by considering the parameters and parameter values listed in Tables 2.2 and 2.3 respectively.

By contrast, where LEM runs are designed to explore the effects of using two different process formulations, what is the 'level' of each process formulation? The fact that one formulation is different from the other can be indicated in the analysis afterwards, using 'dummy' variables for example (Draper and Smith, 1981), but there is no design *level* as such for either formulation. It follows that there is also no meaningful equivalent of a centre point or 'base case' level for the whole experiment, as we are unable to assign a meaningful middle condition between the formulations. Moreover, although there is no unique base case result for the experiment, there will be two separate base case results for the output sets corresponding to the simulations generated by each process formulation.

The situation described here would also arise if two LEMs were being contrasted with each other, or if different process classes (aeolian versus glacial for example) were being contrasted with each other using the same LEM. It could also arise if a researcher were unable or unwilling to describe properties of other experimental factors in a satisfactory way as ratio data, for example those pertaining to different initialising forms, or to different grid cell arrangements.

Clearly, the absence of a unique base case result appears to frustrate the very idea of being able to quantify equifinality. Drawing on the findings in this thesis, however, it is suggested that the problem is not as bad as it appears. At its simplest, it may be possible, for theoretical or other reasons, to say that one result is preferable to use as the base case reference. For example, if one of the formulations is thought to have been reliable in a wide range of model studies, whereas the other is more experimental, then it might be decided to use the base case result from the former as the reference. Therefore, if base case 'A' is the reference result, one would then use metamodel 'B', sampling across its factor space, to assess how frequently simulations using process formulation B were able to generate the base case result 'A'. The equifinality probability curve derived by doing this could then be compared with the curve for metamodel 'A' against base case 'A', to see which of the two formulations generates the more discriminating result.

In some cases, it may be that neither formulation's base case is preferred, so it may then be more useful to use metamodel 'A' to try to generate base case result 'B' and also use metamodel 'B' to generate base case result 'A'. This would give rise to two *co-equifinal* probability curves, which could be displayed on the same plot. This could also be extended to more comprehensive explorations, comparing all possible results generated by one model or formulation with all possible results generated by the other. Presumably, bootstrapping could also be used, as described in Chapter 5, to calculate co-equifinality confidence intervals, and other presentations of equifinality, such as those shown in Chapters 5 and 6, could also be adapted to show how one model formulation's results differed from the other's. In addition, there is no need to confine the analysis to just two LEMs or formulations, and perhaps a wide range of LEMs could be used in this way to explore equifinal outcomes encompassing the study of a set of exemplar landscapes. The subject certainly seems worth exploring, either through the use of metamodels derived from simulation data, or through the use of suitable metamodel archetypes.

Continuing with the difficulty of having no unique base case from the LEM or LEMs, perhaps the most desirable reference case of all is a real landscape, or perhaps an archetype of a real landscape if a suitable one can be devised. Of course, this is not always possible, and depends much upon the type of study to which the LEM is being applied. Either way, the whole subject area is rich with possibilities for further research.

This ends the first part of the chapter, and the points discussed and research findings together provide most of the elements required for an assessment of whether the aims of this research have been met, although there is still a need to put the research in a wider context. This part of the discussion now follows, beginning with a return to Chapter 1 and the review of example LEM studies listed in Table 1.

7.5 EQUIFINALITY IN LEMs GENERALLY

7.5.1 Table 1 revisited: problems identifying factors and factor effects

It has been argued in the foregoing discussion that the potential for equifinality in the output from a LEM will in many situations be best understood by analysing the 'at a time' factor main effects and interactions driving the LEM's response. Table 1, however, refers to 'scenarios' or 'variables' rather than 'factors'. The appreciation of how general classes of variables may be treated as factors, or broken down into component factors, has been described above, and this idea is followed in discussing the broader implications of the issues raised by Table 1. Clearly, some of the variables listed in the table may present particular difficulties in the way they may be factored. For example, as discussed above, the differences in process formulations are not describable as ratio quantities. In addition, temporal and spatial variations may need to be disaggregated as different component factors if the effects of their variation are to be more clearly understood. Notwithstanding these difficulties, apart from the factors which cannot be expressed as ratio data, there appear to be few limitations in principle on being able to estimate the main effects and interactions of any of the variables listed in the example LEM studies in Table 1. Regrettably, however, it turns out that for the most part, the effects of these variables cannot be quantified in many of the studies, and it is important here to explain why this is so.

Many of the example studies have a temporal development focus, that is, on the progression of change, rather than on the condition reached after a certain time, or at a series of different reference times. This means that in almost all of the studies, 'at a time' factor responses are not reported, or if they are, then the manner of their presentation does not allow a main effect or interaction effect to be quantified. There are a few exceptions. For example, the main effect of uplift is estimable from the data presented by Rinaldo *et al.* (1995); similarly, Clevis *et al.* (2003), in their figure 12b, show the response of sedimentation rate to changes in a certain thrust displacement rate over time, plotting three different traces of the dependent variable corresponding to the three different factor levels used in their simulations. For the most part, this form or presentation is not used in LEM studies, researchers preferring to present their results in the form of spatial plots, such as those used herein in Chapter 4 when presenting output from the warm up simulation and base case simulation. Quantified estimation of equifinality in other LEMs is therefore not possible based on the data presented in the published papers reviewed in Chapter 1.

In addition to this difficulty, it is noteworthy that designed experiments, of the kind used herein, are generally not used. Certainly, there are no examples of the application of screening designs, of resolution III or IV for example, and most studies only apply limited and targeted variations in a small number of factors (subsection 1.3, *q.v.*). The lack of factorial or fractional factorial designs is probably for very understandable reasons, such as limitations in computing resources. However, as explained in Chapter 3, these types of design are still computationally less burdensome - *by two or more orders of magnitude* - than methods (e.g. GLUE) that require exploration using full simulations. Despite the absence of use of these types of design, and also of the presentation of LEM output is a way that allows main effects and interactions to be estimated, it is argued here that there are consistencies in the factor influences, as listed in Table 1, and that these allow a qualitative view to be formed of factor effects within LEMs more generally. This in turn suggests ways in which equifinality in LEM studies may be controlled, and these matters are now considered.

7.5.2 Consistencies in the output

Closer inspection of the results listed in Table 1 reveals that there are some consistencies across the studies in the responses of LEMs to the main experimental factors. The most

basic of these is that model response as viewed over time is generally less erratic or noisy as the spatial scale of interest increases, or the interval of time between which metrics are reported increases. Interestingly, this result appears to apply not only to the deterministic studies, but also to those in which temporally or spatially stochastic forcings have been applied. This is an important point, because if it is representative of LEM studies generally then it implies that where the response appears noisy or non-linear, it may be smoothed somewhat by increasing the time interval over which the metric is calculated, or where possible the spatial extent of the same. In addition, it suggests that the possible 'noisy response' or 'chaotic response' at a time problems posited in Chapter 6 are not common. Moreover, as described by Phillips (2006), the presence of chaotic or non-linear responses over time does not preclude estimable main effects and interactions *at a time*. The matter clearly needs further research in LEM studies, however.

7.5.3 Identifying common influences: factor groups and metric groups

In Chapter 1, the author referred to Bras *et al.* (2003), who argued that reference to every facet of a modelled landscape should prevent results from different simulations being treated as equifinal. Alternatively, Phillips (2006) has argued that inclusion of more factors should make results more singular, and presumably less equifinal. In Chapter 6, it was also demonstrated, via the metamodel archetypes, that strong factors, especially those having linear or near linear main effects, or quadric or absolute value form main effects, tended to dominate equifinal responses, even if interactions were present but provided the latter were not themselves strong. It is therefore argued that it is also possible to propose the factor variations most likely to reduce the likelihood of equifinality in a LEM study. Similarly, it is possible to propose the best metrics to use if the factor variations have been decided upon and one wishes to be more discriminating between one simulation and another. In addition, the change in model response over time suggests that the most appropriate factors and metrics to use to reduce equifinal outcomes at any time will themselves change over time. The problem or predicting and controlling LEM equifinal behaviour is therefore closely related to the time frame of the study, and to the question of which metrics to use to reduce the equifinality associated with certain factors, or conversely, which factors to vary if one wishes to reduce the equifinality that may be generated in certain metrics.

To make the problem more tractable, and to focus the discussion in a way that will allow general and useful statements to be made, the factor influences and output metrics reviewed in Table 1 have been divided into groups. Thus, each factor group is assumed to be a set of all of the factors that one might need to include in an experiment to test for the effects of conditions or variables with similar attributes, such as climate, geology or process formulation. Likewise, each metric group is assumed to be a set of all of the metrics of similar landscape relations calculated when quantifying the output of a simulation with a LEM. For the purposes of this discussion, selection of metric and factor groups has been made somewhat restrictive here, including particularly only those metric groups which appear to be the most useful in describing certain classes of landscape properties.

Taking these points together, and drawing on the review of variables and influences listed in Table 1, it is possible to summarise, as a first approximation, how each factor group would be expected to influence each metric group in a LEM study, and also how that influence would be expected to change over time (Table 7.1). It should be noted that sediment yield and drainage density are treated as separate metrics in their own right, and are not grouped, as these metrics seem to be particularly useful descriptors and sensitive to most factors, whether in short term or long term studies (Table 1, *q.v.*). In deriving the table, efforts were made (by reference to the time frames reported in the studies) to take into account whether the greatest influence of any factor group is over the short term, including transient landscapes, or over the long term, which would include steady declining relief and landscapes in equilibrium or approaching equilibrium. Regarding the factor influences, it should be emphasised here that, unless noted otherwise, the influence of each factor group is assumed to be primarily in response to that group only. Therefore, when considering the influence of climate variations, it has been assumed that no other factor groups are being varied; similarly, when considering the influences of geological spatial variation, it has been assumed that no other factor variations are being used.

Table 7.1: Influences on metrics - according to simulation reference time – of factors commonly used in LEM simulations.

Factor group ↓	Reference time ↓	METRIC OR METRIC GROUP: Sediment yield	Deposition, other sediment movement	Drainage density	Other channel network	Morphology	Topography and relief
Uplift, tectonics (a): spatial variation	Short-term/transient ↓ Long-term/to equilibrium	Weak ↓ **Strong**	Weak ↓ **Strong**	Weak ↓ **Strong**	Weak ↓ **Strong**	Weak ↓ **Strong**	Weak ↓ **Strong**
Uplift, tectonics (b): temporal variation	Short-term/transient ↓ Long-term/to equilibrium	Weak ↓ **Strong**	Weak ↓ **Strong**	Weak ↓ **Strong**	Weak ↓ **Strong**	Weak ↓ **Strong**	Weak ↓ **Strong**
Climate (a): spatial variation	Short-term/transient ↓ Long-term/to equilibrium	**Strong** ↓ **Strong**	**Strong** ↓ **Strong**	**Strong** ↓ **Strong**	**Strong** ↓ **Strong**	Weak ↓ **Strong**	Weak ↓ **Strong**
Climate (b): temporal variation	Short-term/transient ↓ Long-term/to equilibrium	**Strong** ↓ **Strong**	**Strong** ↓ **Strong**	**Strong** ↓ **Strong**	**Strong** ↓ **Strong**	Weak ↓ **Strong**	Weak ↓ **Strong**
Geology (spatial variation only)	Short-term/transient ↓ Long-term/to equilibrium	**Strong** ↓ **Strong**	Weak ↓ **Strong**	Weak ↓ **Strong**	Weak ↓ **Strong**	Weak ↓ **Strong**	Weak ↓ **Strong**
Initial form	Short-term/transient ↓ Long-term/to equilibrium	**Strong** ↓ Weak	**Strong** ↓ Weak	**Strong** ↓ Weak	**Strong** ↓ Weak	**Strong** ↓ Weak	**Strong** ↓ Weak
Initial sediment distribution (also sediment classes)	Short-term/transient ↓ Long-term/to equilibrium	**Strong** ↓ Weak	**Strong** ↓ Weak	Weak ↓ Weak	Weak ↓ **Strong**	Weak ↓ **Strong**	Weak ↓ **Strong**
Process formulations	Short-term/transient ↓ Long-term/to equilibrium	Weak ↓ **Strong**	**Strong** ↓ **Strong**	Weak ↓ **Strong**	Weak ↓ **Strong**	Weak ↓ **Strong**	Weak ↓ **Strong**
Process rate parameters (also basal removal)	Short-term/transient ↓ Long-term/to equilibrium	**Strong** ↓ **Strong**	**Strong** ↓ **Strong**	**Strong** ↓ **Strong**	**Strong** ↓ **Strong**	Weak ↓ **Strong**	Weak ↓ **Strong**

Table 7.1 indicates that the influence of some factors on certain metrics (e.g. uplift and process formulations, on sediment yield and drainage density) grows stronger over time, whereas that of others on the same metrics weakens over time (e.g. initial form, also on sediment yield and drainage density). These observations may now be used, with a hypothesis based on the findings in this thesis, to propose, as a first approximation, the combinations of factors and metrics which are most likely to reduce the equifinality of a LEM's output.

7.5.4 A 'strong factors' hypothesis

Based on the results reported in Chapter 6, including those generated by the parameter explorations with the metamodel archetype, it is proposed that the equifinality associated with the factor groups listed in Table 7.1 may be predicted, as a first approximation, by applying a 'strong factors' hypothesis, which is stated:

"For any time reference and metric of interest, results are much less likely to be equifinal if, in the simulations, strong factors are varied rather than weak ones, and if more factors are varied rather than fewer."

The hypothesis is bound by conditions, listed below:

1. A strong factor is likely to be a component in a 'strong' factor group, as listed in Table 7.1.

2. Strong factor main effects are assumed to be generally linear, gently curved, or conversely of the quadric or absolute value type[4], the latter all with the same sign.

3. Interaction effects associated with each strong factor are assumed to be small and their influence on equifinal likelihood negligible.

4. Predictions where non-ratio data factors are varied are made comparing model results with metrics derived from a common reference, whether this be a real landscape or a landscape archetype.

[4] All effects are assumed to be calculated here using their scaled design levels, as defined in equation 4.01.

Using this hypothesis, it possible to predict which combinations of factors and metrics are likely to exhibit lower likelihoods of equifinality at the time reference and for the metrics of interest. In general, therefore, *for short term and transient studies*, it is predicted that researchers, as a first preference, should find a lower likelihood of equifinal output across most metrics by using factor variations of one or more of the process rate parameters (e.g. Table 2.2), the initial form and the climate (whether spatially or temporally). Conversely, for long term, near equilibrium and equilibrium studies, it is predicted that researchers should find a lower likelihood of equifinal output across most metrics by using factor variations of one or more of uplift and tectonics (whether spatially or temporally), climate (spatially or temporally), geology, process formulations and process rate parameters. The equifinality associated with initial sediment distribution and incorporation of different sediment classes appears to be less clear across the metrics and time periods. Overall, the combination of the tabled information and the strong factors hypothesis together suggests that LEM output may be made less equifinal if more of the strong factors are varied in the simulations experiments.

In closing this section, it will be appreciated that the summary proposed here is qualitative, and only intended to be used as a first approximation. As such, it is most important that it is subjected to further research and testing.

7.6 FINAL ASSESSMENT OF THE RESEARCH AND SUMMARY OF RECOMMENDATIONS FOR FURTHER WORK

The research aims were set out in section 1.4, as follows:

1. To quantify the extent to which a LEM generates equifinal results;
2. To assess how LEM equifinality may be affected by using different measures of output;
3. To quantify whether LEM equifinality is due more to some parameters than to others;
4. To quantify how LEM equifinality varies with the number of introduced parameters;
5. To identify those parts of the parameter space emerging as equifinal solution regions; and

6. Based on the results relating to the above and their wider implications, to comment on factors which seem to increase or reduce the likelihood of equifinality in LEM studies, and hence to form a view on the extent to which equifinality is a problem in LEMs generally.

Taking into account the discussion points in this chapter, and also the supporting remarks in Chapters 5 and 6, research aims 1 to 5 have been satisfied. However, with regard to research aim 6, this has only been satisfied in part, and a quantified understanding of equifinality in LEMs more generally, relating to much broader classes of factor variation, has not been possible. Even so, the results relating to application of more metrics and strong factors appear to have wide applicability, and suggest that equifinality in LEMs generally may be controlled to some extent, so that it is not a severe problem, particularly if more factors and metrics are used in the research.

Recommendations for further work have been proposed throughout the text, and are summarised as follows:

1. Research is required to explore equifinal behaviour in other LEMs and other metrics, and to explore the use of different process classes and formulations as well as different parameter values. Work testing the efficacy or otherwise of the 'strong factors' hypothesis would also be useful, as this would indicate whether its wider applicability is justified.

2. Researchers using LEMs should, so far as practically possible, use factored, designed experiments, which permit estimation of factor main effects and interactions, and thence the derivation of metamodels by which equifinal probabilities may be quantified. Researchers should also consider the use of screening designs, to reduce factor space exploration to tractable dimensions, and to allow fractional factorial or Latin Hypercube designs to be used later to sample variation in the more important factors.

3. The use of metamodel archetypes appears particularly interesting, and generic work on equifinal behaviour with models of this type could be especially informative of the patterns of equifinality to expect in response to particular factor effects, statistical distributions of the factors, and error distributions in any metamodel fitted to the hypothetical LEM output data.

4. The examination of main effects over time may permit changes in such effects to be modelled not simply as a function of the factors themselves, but also as a function of time. Associations between the changes in the modelled landscape and these temporal shifts in main effects could be of particular use in clarifying the main drivers of landscape evolution, and explorations focusing on such associations are recommended.

5. Finally, researchers should try, where possible, to include presentations of results which permit estimation of factor effects from their published data. In particular, although plots of spatial data or output are often of interest, they are difficult to relate to particular factor variations quantitatively, and further work is needed to develop suitable suites of metrics to represent the most informative aspects of these spatial data. The insensitivity of metrics quantifying elevation characteristics of the landscape was noted in particular, in Chapter 4, so the development of more sensitive metrics to described elevation attributes would be very useful.

With these recommendations made, the thesis is brought to a close in the next section.

7.7 CONCLUSIONS AND FINAL REMARKS

Subject to the discussion points and recommendations made above, the main conclusions of the research are as follows:

I. Equifinality is much more likely for some metrics than for others, and as a response to some factor variations than to others, the probability of obtaining an equifinal result depending upon the tolerance permitted in assessing similarity between the outcomes.

II. The likelihood of obtaining equifinal output can be reduced, and is never increased, by considering equifinality in two or more metrics simultaneously.

III. The likelihood of obtaining an equifinal solution may also be reduced by increasing the number of factors varied in the simulations. Generally, the weaker the factor interaction effects and the more nearly linear the factor main effects, the lower will be the probability of obtaining an equifinal solution as one introduces (varies) more of the factors. The same holds true of quadric or similar form main effects provided these are centred at the base case and the signs for the effects are the same (all positive or negative).

IV. In general, equifinality can be understood in terms of the 'at-a-time' modes of a LEM's response to the factors used in any simulation. In this respect, for any metric, there appear to be four general modes of LEM response, grading from one into the next as follows: (i) dominance by factor main effects; (ii) more balanced response between factor

main effects and interactions; (iii) dominance by factor interaction effects; and (iv), dominance by stochastic or chaotic (non-linear) response, overriding any underlying main or interaction effects. Reviews of LEM studies show that chaotic at-a-time responses are likely to be rare; on the other hand, dominance by stochastic response is more likely to be dependent on the strength of stochastic forcings used in the simulation

V. Given the importance of factor effects, the likelihood of a LEM generating equifinal output should be expected to vary over time, in response to changes in the strength, form and trend of the factor main effects and interactions.

VI. Regarding equifinality in LEMs generally, as a first approximation, a 'strong factors' hypothesis allows prediction of the relative likelihood of equifinal outcomes for certain metrics in response to particular factors. Corresponding with this hypothesis, for short term and transient from studies, researchers should find a lower likelihood of equifinal output across most metrics by varying factors relating to process rate parameters (Table 2.2, *q.v.*), the initial landscape form and the climate (whether spatially or temporally). Similarly, in long term, near equilibrium and equilibrium studies, researchers should find a lower likelihood of equifinal output across most metrics by using factor variations relating to uplift and tectonics (whether spatially or temporally), climate (also spatially or temporally), geology, process formulations (sections 2.4-2.6, *q.v.*) and process rate parameters (Table 2.2, *q.v.*).

In closing, research into the problem of equifinality in LEMs has revealed that there is a rich pattern of model responses at different times and to different experimental factors, each of which has an influence on equifinal behaviour in a LEM. The overriding impression from this research is that the risk of obtaining equifinal output is significant generally, but that it may be made smaller through careful experiment design, and use of appropriate factor variations and output metrics. Equifinality is therefore ever present, but it is also quantifiable and treatable, unlike the 'ogre lurking in the dark' of Chapter 1. More subtly, it represents another aspect of the efforts in geomorphology to devise better theories of landscape evolution, and better models to demonstrate the consequences of those theories. The use of designed sampling and metamodels has proved to be a powerful approach to

these problems. More mysteriously, perhaps, the curves and surfaces of equifinal response are rather like landscapes themselves, as if these modelled ‘landscapes of equifinality’ had helped to clarify the equifinality of modelled landscapes. By such means, and with suitable combinations of field data and modelling studies, we shall surely come closer to a more complete understanding of the real landscapes in the world around us, and of the story hidden at any time in those varieties of form and feature presented to the eye.

REFERENCES

Ahnert F. 1976. Brief description of a comprehensive three-dimensional process-response model of landform development. *Zeitschrift für Geomorphologie, N.F.* Supplementband **25**. 29-29.

Ahnert F. 1987. Approaches to dynamic equilibrium in theoretical simulations of slope development. *Earth Surface Processes and Landforms.* **12**. 3-15.

Armstrong AC. 1976. A three-dimensional simulation of slope forms. *Zeitschrift für Geomorphologie, N.F.* Supplementband **25**. 20-28.

Armstrong AC. 1987. Slopes, boundary conditions, and the development of convexo-concave forms - some numerical experiments. *Earth Surface Processes and Landforms*. **12**. 17-30.

Bagnold RA. 1966. An Approach to the Sediment Transport Problem from General Physics. *United States Geological Survey, Professional Paper no*. **422-I**. 37 pages.

Baker VR. 1996. Hypotheses and Geomorphological Reasoning. Chapter 3 in: *The Scientific Nature of Geomorphology*, Proceedings of the 27th Binghampton Symposium in Geomorphology, held 27th-29th September, 1996, BL Rhoads and CE Thorn (editors). John Wiley and Sons, Chichester.

Beringer J, McIlwaine S, Lynch AH, Chapin FS, Bonan GB. 2002. The use of a reduced form model to assess the sensitivity of a land surface model to biotic surface parameters. *Climate Dynamics.* **19**(5-6). 455-466.

Beven K. 1996. Equifinality and Uncertainty in Geomorphological Modelling. Chapter 12 in: *The Scientific Nature of Geomorphology*, Proceedings of the 27th Binghampton Symposium in Geomorphology, held 27th-29th September, 1996, BL Rhoads and CE Thorn (editors). John Wiley and Sons, Chichester.

Beven K. 2002. Towards a coherent philosophy for modelling the environment. *Proceedings of The Royal Society*, series A. **458**. 2,465-2,484.

Beven K. 2006. A manifesto for the equifinality thesis. *Journal of Hydrology.* **320**. 18-36.

Beven K and Binley AM. 1992. The future of distributed models: Model calibration and uncertainty prediction. *Hydrological Processes.* **6**. 279-298.

Beven K and Freer J. 2001. Equifinality, data assimilation, and uncertainty estimation in mechanistic modelling of complex environmental systems using the GLUE methodology. *Journal of Hydrology.* **249**. 11-29.

Beven K and Kirkby MJ. 1979. A physically-based variable contributing area model of basin hydrology. *Hydrological Science Bulletin*. **24**. 43-69.

Bogaart PW, Tucker GE and de Vries JJ. 2003a. Channel network morphology and sediment dynamics under alternating periglacial and temperate regimes: a numerical simulation study. *Geomorphology*. **54**. 257-277.

Bogaart PW, Van Balen RT, Kasse C and Vandenberghe J. 2003b. Process-based modelling of fluvial system response to rapid climate change – I: model formulation and generic applications. *Quaternary Science Reviews*. **22**. 2,077-2,095.

Bowman KP, Sacks J and Chang Y-F. 1993. Design and Analysis of Numerical Experiments. *Journal of the Atmospheric Sciences*. **50**(9). 1,267-1,278.

Box GEP and Draper NR. 1987. *Empirical Model-Building and Response Surfaces*. John Wiley and Sons, New York. 669 pages.

Box GEP and Hunter JS. 1957. Multifactor Experiment Designs for Exploring Response Surfaces. *Annals of Mathematical Statistics*. **28**. 195-241.

Box GEP, Hunter WG and Hunter JD. 1978. *Statistics for Experimenters: An Introduction to Design, Data Analysis, and Model Building*. John Wiley, New York.

Box GEP and Wilson KB. 1951. On the Experimental Attainment of Optimum Conditions. *Journal of the Royal Statistical Society*, Series B. **13**. 1-45.

Bras RL, Tucker GE and Teles V. 2003. Six Myths About Mathematical Modeling in Geomorphology. Pages 63-82 in: *Prediction in Geomorphology*. Geophysical Monograph Series, number 135, PR Wilcock and RM Iverson (editors). American Geophysical Union, Washington D.C.

Braun J and Sambridge M. 1997. Modelling landscape evolution on geological time scales: a new method based on irregular spatial discretization. *Basin Research*. **9**. 27-52.

Brunsden D. 1993. The persistance (*sic*) of landforms. *Zeitschrift für Geormorphologie N.F*. Supplementband **93**. 13-28.

Carson MA and Kirkby MJ. 1972. *Hillslope Form and Process*. Cambridge University Press. 476 pages.

Chapman WL, Welch WJ, Bowman KP, Sacks J and Walsh JE. 1994. Arctic sea-ice variability – model sensitivities and a multidecadal simulation. *Journal of Geophysical Research*. **99**(C1). 919-935.

Chen VCP, Tsui K-L, Barton RR and Meckesheimer M. 2006. A review on design, modelling and applications of computer experiments. *IIE Transactions*. **38**. 273-291.

Chorley RJ and Kennedy BA. 1971. *Physical Geography: A Systems Approach.* Prentice-Hall International Inc., London. 370 pages.

Chorley RJ, Schumm SA and Sugden DE. 1984. *Geomorphology.* Methuen & Co. Ltd, London. 607 pages.

Church M. 2003. What Is a Geomorphological Prediction? Pages 183-194 in: *Prediction in Geomorphology*. Geophysical Monograph 135, PR Wilcock and RM Iverson (editors). American Geophysical Union, Washington D.C.

Clevis Q, de Boer P and Wachter M. 2003. Numerical modelling of drainage basin evolution and three-dimensional alluvial fan stratigraphy. *Sedimentary Geology.* **163**. 85-110.

Codilean AT, Bishop P and Hoey TB. 2006. Surface process models and the links between tectonics and topography. *Progress in Physical Geography.* **30**(3). 307-333.

Coulthard TJ. 2001. Landscape evolution models: a software review. *Hydrological Processes*. **15**. 165-173.

Coulthard TJ, Kirkby MJ and Macklin MG. 1999. Modelling the impacts of Holocene environmental change on the fluvial and hillslope morphology of an upland landscape, using a cellular automaton approach. Pages 31-47 in: *Fluvial Processes and Environmental Change*, AG Brown and TM Quine (editors). Wiley, New York.

Coulthard TJ, Kirkby MJ and Macklin MG. 2000. Modelling geomorphic response to in an upland catchment. *Hydrological Processes*. **14**. 2,031-2,045.

Coulthard TJ, Lewin J and Macklin MG. 2005. Modelling differential catchment response to environmental change. *Geomorphology*. **69**. 222-241.

Coulthard TJ, Macklin MG and Kirkby MJ. 2002. A cellular model of Holocene upland river basin and alluvial fan evolution. *Earth Surface Processes and Landforms.* **27**. 269-288.

Cox NJ. 1980. On the relationship between bedrock lowering and regolith thickness. *Earth Surface Processes.* **5**. 271-274.

Craig RG. 1982. The ergodic principle in erosional models. Chapter 5 in: *Space and Time in Geomorphology*, CE Thorn (editor). George Allen and Unwin, London.

Culling WEH. 1987. Equifinality: modern approaches to dynamical systems and their potential for geographical thought. *Transactions of the Institute of British Geographers.* N.S. **12**. 57-72.

Dade WB and Friend PF. 1998. Grain-Size, Sediment-Transport Regime, and Channel Slope in Alluvial Rivers. *Journal of Geology*. **106**. 661-675.

Davis WM. 1899. The geographical cycle. *Geographical Journal*. **14**. 481-504.

Davis WM. 1902. Base level, grade and peneplain. *Journal of Geology*. **10**. 77-111.

Davis WM. 1909. *Geographical Essays*. Ginn, New York. 777 pages.

Davison, AC, and Hinkley, DV. 1997. *Bootstrap methods and their application.* Cambridge University Press, Cambridge.

De Boer DH. 2001. Self-organization in fluvial landscapes: sediment dynamics as an emergent property. *Computers & Geosciences.* 27. 995-1003.

Dietrich WE, Bellugi DG, Sklar LS, Stock JD and Heimsath AM. 2003. Geomorphic Transport Laws for Predicting Landscape Form and Dynamics. Pages 103 to 132 in: *Prediction in Geomorphology*. Geophysical Monograph Series, number 135, PR Wilcock and RM Iverson (editors). American Geophysical Union, Washington D.C.

Dietrich WE and Dunne T. 1993. The Channel Head. Chapter 7 in: *Channel Network Hydrology*, K Beven and MJ Kirkby (editors). John Wiley, Chichester.

Draper NR and Smith H. 1981. *Applied Regression Analysis.* (2nd edition). John Wiley & Sons, Inc., New York. 709 pages.

Duijsings JJHM. 1987. A sediment budget for a forested catchment in Luxembourg and its implications for channel development. *Earth Surface Processes and Landforms*. **12**. 173-184.

Embleton C and Whalley WB. 1979. Energy, forces, resistances and responses. Chapter 2 in: *Process in Geomorphology*, C Embleton and J Thornes (editors). Edward Arnold, London.

Fagherazzi S, Howard AD and Wiberg PL. 2004. Modeling fluvial erosion and deposition on continental shelves during sea level changes. *Journal of Geophysical Research.* 109(F3). Article number F03010, 16 pages.

Fischer KD, Jahr T and Jentzsch G. 2004. Evolution of the Variscan foreland-basin: modelling the interactions between tectonics and surface processes. *Physics and Chemistry of the Earth.* **29**. 665-671.

Fishman GS. 1996. *Monte Carlo – Concepts, Algorithms and Applications*. Springer Series in Operations Research, Springer-Verlag, New York. 698 pages.

Flew A. 1983. *A Dictionary of Philosophy* (2nd revised edition). Pan Books Ltd, London. 380 pages.

Freer J, Beven K and Ambroise B. 1996. Bayesian estimation of uncertainty in runoff prediction and the value of data: An application of the GLUE approach. *Water Resources Research*. **32**(7). 2,161-2,173.

Gargani J, Stab O, Cojan I and Brulhet J. 2006. Modelling the long-term fluvial erosion of the River Somme during the last million years. *Terra Nova.* **18**. 118-129.

Gasparini NM, Tucker GE and Bras RL. 1999. Downstream fining through selective particle sorting in an equilibrium drainage network. *Geology*. **27**(12). 1,079-1,082.

Gasparini NM, Tucker GE and Bras RL. 2004. Network-scale dynamics of grain-size sorting: implications for downstream fining, stream-profile concavity, and drainage basin morphology. *Earth Surface Processes and Landforms.* **29**. 401-421.

Gendaszek AS, Balco G, Montgomery DR, Stone JOH and Thompson N. 2005. Long-term Erosion Rates and Styles of Erosion in the Coastal Ranges of the Pacific Northwest. Unpublished report, Quaternary Research Center and Department of Earth and Space Sciences, University of Washington, Seattle.

Giere RN. 1999. *Science without laws.* The University of Chicago Press. Chicago and London. 285 pages.

Gomez B and Church M. 1989. An Assessment of Bed Load Sediment Transport Formulae for Gravel Bed Rivers. *Water Resources Research*. **25**(6). 1,161-1,186.

Good PI. 1999. *Resampling Methods: A Practical Guide to Data Analysis*. Birkhauser, Boston. 269 pages.

Goudie AS (editor). 1997. *The Encyclopaedic Dictionary of Physical Geography.* Blackwell, Oxford.

Haff PK. 1996. Limitations on Predictive Modeling in Geomorphology. Chapter 14 in: *The Scientific Nature of Geomorphology*, Proceedings of the 27th Binghampton Symposium in Geomorphology, held 27th-29th September, 1996, BL Rhoads and CE Thorn (editors). John Wiley and Sons, Chichester.

Haines-Young RH and Petch JR. 1983. Multiple working hypotheses: equifinality and the study of landforms. *Transactions of the Institute of British Geographers.* N.S. **8**. 458-466.

Haines-Young RH and Petch JR. 1986. *Physical geography: its nature and methods.* Paul Chapman Publishing Ltd, London. 230 pages.

Hairsine PB and Rose CW. 1992. Modeling Water Erosion Due to Overland Flow Using Physical Principles: 1. Sheet Flow. *Water Resources Research*. **28**(1). 237-243.

Hancock GR. 2003. Effect of Catchment Aspect Ratio on Geomorphological Descriptors. Pages 217-230 in: *Prediction in Geomorphology.* Geophysical Monograph 135, PR Wilcock and RM Iverson (editors). American Geophysical Union, Washington D.C.

Heimsath AM, Dietrich WE, Nishiizumi K, and Finkel RC. 1997. The soil production function and landscape equilibrium. *Nature*. **388**. 358-361.

Heimsath AM, Dietrich WE, Nishiizumi K and Finkel RC. 2001. Stochastic processes of soil production and transport: Erosion rates, topographic variation and cosmogenic nuclides in the Oregon Coast Range. *Earth Surface Processes and Landforms.* **26**(5). 531-552.

Heine RA, Lant CL and Sengupta RR. 2004. Development and Comparison of Approaches for Automated Mapping of Stream Channel Networks. *Annals of the Association of American Geographers.* **94**(3). 477-490.

Helton JC. 2004. Alternative representations of epistemic uncertainty. *Reliability Engineering and System Safety.* **85**. 1-10.

Helton JC and Davis FJ. 2003. Latin hypercube sampling and the propagation of uncertainty in analyses of complex systems. *Reliability Engineering and System Safety.* **81**. 23-69.

Howard AD. 1994. A detachment-limited model of drainage basin evolution. *Water Resources Research.* **30**(7). 2,261-2,285.

Howard AD. 1997. Badland morphology and evolution: Interpretation using a simulation model. *Earth Surface Processes and Landforms.* **22**. 211-227.

Iman RL and Helton JC. 1988. An Investigation of Uncertainty and Sensitivity Analysis Techniques for Computer Models. *Risk Analysis.* **8**(1). 71-90.

Inkpen R. 2005. *Science, Philosophy and Physical Geography.* Routledge, Abingdon. 164 pages.

Kalos MH and Whitlock PA. 1986. *Monte Carlo Methods, Volume 1: Basics.* John Wiley and Sons, New York. 186 pages.

King LC. 1957. The uniformitarian nature of hillslopes. *Transactions of the Edinburgh Geological Society*. **17**. 81-102.

King LC. 1962. *The morphology of the Earth.* Oliver and Boyd, Edinburgh. 699 pages.

Kirkby MJ. 1971. Hillslope process-response models based on the continuity equation. Chapter 2 in: *Slopes - form and process,* Institute of British Geographers Special Publication No. 3, C Embleton and JT Coppock (editors). Institute of British Geographers, London.

Kirkby MJ. 1989. A model to esti*mate the impact of climatic change on hillslope and regolith form.* Catena. **16**. 321-341.

Kirkby MJ. 1996. A role for theoretical models in geomorphology? Chapter 10 in: *The Scientific Nature of Geomorphology*, Proceedings of the 27th Binghampton Symposium in Geomorphology, held 27th-29th September, 1996, BL Rhoads and CE Thorn (editors). John Wiley and Sons, Chichester.

Kirkby MJ. 2000. Limits to modelling in the Earth and environmental sciences. Chapter 15 in: *Geocomputation*, S Openshaw and RJ Abrahart (editors). Taylor and Francis, London and New York.

Kleijnen JPC. 1998. Experimental Design for Sensitivity Analysis, Optimization, and Validation of Simulation Models. Pages 173-223 in: *Handbook of Simulation: Principles, Methodology, Advances, Applications, and Practice*, J Banks (editor). John Wiley and Sons, Inc., New York.

Kleijnen JPC, Sanchez SM, Lucas TW and Cioppa TM. 2005. A User's Guide to the Brave New World of Designing Simulation Experiments. *INFORMS Journal on Computing*. **17**(3). 263-289.

Knighton AD. 1998. *Fluvial Forms and Processes: A new perspective*. Hodder Headline Group, London. 383 pages.

Knighton AD. 1999. Downstream variation in stream power. *Geomorphology*. **29**. 293-306.

Kobor JS and Roering JJ. 2004. Systematic variation of bedrock channel gradients in the central Oregon Coast Range: implications for rock uplift and shallow landsliding. *Geomorphology*. **62**. 239-256.

Kooi H and Beaumont C. 1996. Large-scale geomorphology: classical concepts reconciled and integrated with contemporary ideas via a surface processes model. *Journal of Geophysical Research*. **101**(B2). 3,361-3,386.

Lancaster ST, Hayes SK and Grant GE. 2001. Modeling Sediment and Wood Storage and Dynamics in Small Mountainous Watersheds. Pages 85-102 in: *Geomorphic Processes and Riverine Habitat*, Water Science and Application Volume 4, JM Dorava, DR Montgomery, BB Palcsak and FA Fitzpatrick (editors). American Physical Union, Washington D.C.

Law AM and Kelton WD. 1991. *Simulation Modeling and Analysis*, Second Edition. McGraw-Hill Inc., New York. 759 pages.

Leeder M. 1999. *Sedimentology and Sedimentary Basins: From Turbulence to Tectonics*. Blackwell Science, London. 592 pages.

Leopold LB and Maddock T. 1953. The hydraulic geometry of stream channels and some physiographic implications. *U.S. Geological Survey Professional Paper no.* **252**. 56 pages.

Leopold LB, Wolman MG and Miller JP. 1964. *Fluvial processes in geomorphology*. W.H.Freeman, San Francisco. 1995 Dover edition reprint by Constable and Company, London. 522 pages.

Luke JC. 1972. Mathematical Models for Landform Evolution. *Journal of Geophysical Research*. **77**(14). 2,460-2,464.

Luke JC. 1974. Special Solutions for Nonlinear Erosion Problems. *Journal of Geophysical Research*. **79**(26). 4,035-4,040.

Lynch AH, McIlwaine S, Beringer J and Bonan GB. 2001. An investigation of the sensitivity of a land surface model to climate change using a reduced form model. *Climate Dynamics.* **17**(8). 643-652.

Madras N. 2002. *Lectures on Monte Carlo Methods. Fields Institute Monographs no. 16,* The Fields Institute for Research in Mathematical Sciences. American Mathematical Society, Providence, Rhode Island. 103 pages.

Marriott FHC and Krzanowski WJ. 1995. *Multivariate Analysis, Part 2: Classification, Covariance Structures and Repeated Measurements.* Edward Arnold, London. 288 pages.

Martin Y. 2000. Modelling hillslope evolution: linear and nonlinear transport relations. *Geomorphology*. **34**. 1-21.

Martin Y and Church M. 1997. Diffusion in landscape development models: on the nature of basic transport relations. *Earth Surface Processes and Landforms*. **22**. 273-279.

Martin Y and Church M. 2004. Numerical modelling of landscape evolution: geomorphological perspectives. *Progress in Physical Geography.* **28**(3). 317-339.

McKean JA, Dietrich WE, Finkel RC, Southon JR and Caffee MW. 1993. Quantification of soil production and downslope creep rates from cosmogenic ^{10}Be accumulations on a hillslope profile. *Geology*. **21**. 343-346.

Moglen GE and Bras RL. 1995. The effect of spatial heterogeneities on geomorphic expression in a model of basin development. *Water Resources Research*. **31**(10). 2,613-2,623.

Montgomery DR and Dietrich WE. 1988. Where do channels begin? *Nature*. **336**. 232-234.

Montgomery DR and Dietrich WE. 1989. Source areas, drainage density, and channel initiation. *Water Resources Research*. **25**. 1907-1918.

Montgomery DR and Dietrich WE. 1992. Channel initiation and the problem of landscape scale. *Science*. **255**(5046). 826-830.

Morris PH and Williams DJ. 1999. Worldwide correlations for subaerial aqueous flows with exponential longitudinal profiles. *Earth Surface Processes and Landforms*. **24**. 867-879.

Niemann JD, Gasparini NM, Tucker GE and Bras RL. 2001. A quantitative evaluation of Playfair's Law and its use in testing long-term erosion models. *Earth Surface Processes and Landforms.* **26**. 1,317-1,332.

Oberkampf WL, Helton JC, Joslyn CA, Wojtkiewicz SF and Ferson S. 2004. Challenge problems: uncertainty in system response given uncertain parameters. *Reliability Engineering and System Safety*. **85**. 11-19.

Ollier CD. 1984. *Weathering*. (2nd edition) Longman, White Plains, New York. 270 pages.

Oreskes N, Shrader-Frechette K and Belitz K. 1994. Verification, Validation and Confirmation of Numerical Models in the Earth Sciences. *Science*. **263**. Pages 641-646.

Phillips JD. 1996. Deterministic Complexity, Explanation, and Predictability in Geomorphic Systems. Chapter 13 in: *The Scientific Nature of Geomorphology*, Proceedings of the 27th Binghampton Symposium in Geomorphology, held 27th-29th September, 1996, BL Rhoads and CE Thorn (editors). John Wiley and Sons, Chichester.

Phillips JD. 1997. Simplexity and the Reinvention of Equifinality. *Geographical Analysis*. **29**(1). 1-15.

Phillips JD. 1999. Divergence, Convergence, and Self-Organization in Landscapes. *Annals of the Association of American Geographers*. **89**(3). 466-488.

Phillips JD. 2006. Evolutionary geomorphology: thresholds and nonlinearity in landform response to environmental change. *Hydrology and Earth System Sciences Discussions*. **3**. 365-394.

Pitty A. 1971. *Introduction to Geomorphology*. Methuen & Co. Ltd, London. 526 pages.

Platt JR. Strong Inference. *Science*. **146**(3642). 347-353.

Pollack HN. 2003. *Uncertain Science … Uncertain World*. Cambridge University Press, Cambridge. 243 pages.

Popper K. 1969. *Conjectures and Refutations.* Routledge and Kegan Paul, London. 412 pages.

Prosser IP and Rustomji P. 2000. Sediment transport capacity relations for overland flow. *Progress in Physical Geography*. **24**(2). 179-193.

Ratkowsky, DA. 1990. *Handbook of nonlinear regression models.* M Decker, New York.

Reid I, Bathurst JC, Carling PA, Walling DE, and Webb BW. 1997. Sediment Erosion, Transport and Deposition. Chapter 5 in: *Applied Fluvial Geomorphology for River Engineering and Management*, CR Thorne, RD Hey and MD Newson (editors). John Wiley and Sons, Chichester.

Reneau SL and Dietrich WE. 1991. Erosion Rates in the Southern Oregon Coast Range: Evidence for an Equilibrium Between Hillslope Erosion and Sediment Yield. *Earth Surface Processes and Landforms.* **16**. 307-322.

Richards KS. 1993. Sediment Delivery and the Drainage Network. Chapter 8 in: *Channel Network Hydrology*, K Beven and MJ Kirkby (editors). John Wiley, Chichester.

Rinaldo A, Dietrich WE, Rigon R, Vogel G, and Rodriguez Iturbe I. 1995. Geomorphological signatures of varying climate. *Nature*. **374**. 632-634.

Roering JJ, Kirschner JW and Dietrich WE. 1999. Evidence for nonlinear, diffusive sediment transport on hillslopes and implications for landscape morphology. *Water Resources Research*. **35**(3). 853-870.

Rosenbloom NA and Anderson RS. 1994. Hillslope and channel evolution in a marine terraced landscape, Santa Cruz, California. *Journal of Geophysical Research.* **99**(B7). 14,013-14,029.

Sacks J, Welch WJ, Mitchell TJ and Wynn HP. 1989. Design and Analysis of Computer Experiments. S*tatistical Science.* **4**(4). 409-435.

Sanchez SM. 2006. Work smarter, not harder: guidelines for designing simulation experiments. Pages 47 to 57 in: *Proceedings of the 2006 Winter Simulation Conference*, LF Perrone, FP Wieland, J Liu, BG Lawson, DM Nicol and RM Fujimoto (editors). Institute of Electrical and Electronics Engineers. Electronic publication no. 1-4244-0501-7/06.

Saunders I and Young A. 1983. Rates of surface processes on slopes, slope retreat and denudation. *Earth Surface Processes and Landforms*. **8**. 473-501.

Scheidegger AE. 1970. *Theoretical Geomorphology* (Second revised edition). George Allen and Unwin Ltd, London. 435 pages.

Schlunegger F, Melzer J and Tucker GE. 2001. *International Journal of Earth Sciences.* **90**(3). 484-499.

Schumm SA. 1991. *To interpret the Earth: ten ways to be wrong.* Cambridge University Press, Cambridge. 133 pages.

Selby MJ. 1993. *Hillslope Materials and Processes*, 2nd Edition. Oxford University Press, Oxford. 451 pages.

Sexton DMH, Grubb H, Shine KP and Folland CK. 2003. Design and analysis of climate model experiments for the efficient estimation of anthropogenic signals. *Journal of Climate.* **16**(9). 1320-1336.

Sivakumar B. 2004. Dominant processes concept in hydrology: moving forward. *Hydrological Processes.* **18**. 2,349-2,353.

Smith TR and Bretherton FP. 1972. Stability and the Conservation of Mass in Drainage Basin Evolution. *Water Resources Research*. **8**(6). 1506-1529.

Spear RC. 1997. Large simulation models: calibration, uniqueness and goodness of fit. *Environmental Modelling & Software.* **12**(2-3). 219-228.

Summerfield MA. 1991. *Global Geomorphology*. Prentice Hall, Harrow, England. 537 pages.

Talling PJ and Sowter MJ. 1998. Erosion, deposition and basin-wide variations in stream power and bed shear stress. *Basin Research*. **10**. 87-108.

Thomas MF. 2001. Landscape sensitivity in time and space – an introduction. *Catena.* **42**. 83-98.

Thorn CE. 1988. *An Introduction to Theoretical Geomorphology*. Unwin Hyman, Boston. 247 pages.

Thornes J. 1979. Fluvial processes. Chapter 7 in: *Process in Geomorphology*, C Embleton and J Thornes (editors). Edward Arnold, London.

Trudgill ST and Wise S. 1997. Long-term spatially distributed solution erosion: how do we put solutes on the map? *Earth Surface Processes and Landforms*. **22**. 281-285.

Tucker GE. 2004. Drainage basin sensitivity to tectonic and climate forcing: implications of a stochastic model for the role of entrainment and erosion thresholds. *Earth Surface Processes and Landforms.* **29**. 185-205.

Tucker GE and Bras RL. 1998. Hillslope processes, drainage density, and landscape morphology. *Water Resources Research*. **34**(10). 2,751-2,764.

Tucker GE and Bras RL. 2000. A stochastic approach to modelling the role of rainfall variability in drainage basin evolution. *Water Resources Research*. **36**(7). 1,953-1,964.

Tucker GE, Gasparini NM, Lancaster ST and Bras RL. 1997. An Integrated Hillslope and Channel Evolution Model as an Investigation and Prediction Tool, Technical Report prepared for the U.S. Army Corps of Engineers Construction Engineering Research Laboratories.

Tucker GE, Lancaster ST, Gasparini NM, Bras RL and Rybarczyk SM. 2001a. An object-oriented framework for hydrologic and geomorphic modelling using triangulated irregular networks. *Computers and Geosciences.* **27**. 959-973.

Tucker GE, Lancaster ST, Gasparini NM and Bras RL. 2001b. The Channel-Hillslope Integrated Landscape Development Model (CHILD). Chapter 12 in: *Landscape Erosion and Evolution Modeling*, RS Harmon and WM Doe III (editors). Kluwer Academic/Plenum Publishers, Springer-Verlag, New York.

Tucker GE and Slingerland RL. 1994. Erosional dynamics, flexural isostacy, and long-lived escarpments: A numerical modeling (*sic*) study. *Journal of Geographical Research*. **99**(B6). 12,229-12,243.

Tucker GE and Slingerland R. 1996. Predicting sediment flux from fold and thrust belts. *Basin Research*. **8**. 329-349.

Tucker GE and Slingerland RL. 1997. Drainage basin response to climate change. *Water Resources Research*. **33**(8). 2,031-2,047.

Tucker GE and Whipple KX. 2002. Topographic outcomes predicted by stream erosion models: Sensitivity analysis and intermodel comparison. *Journal of Geophysical Research.* **107**(B9). Article number 2179, 16 pages.

Van Asch ThWJ, Deimal MS, Haak WJC and Simon J. 1989. The viscous creep component in shallow clayey soil and the influence of tree load on creep rates. *Earth Surface Processes and Landforms.* **14**. 557-564.

Van Laningham S, Meigs A and Goldfinger C. 2006. The effects of rock uplift and rock resistance on river morphology in a subduction zone forearc, Oregon, USA. *Earth Surface Processes and Landforms.* **31**. 1,257-1,279.

Veldkamp A and Van Dijke JJ. 1998. Modelling Long-term Erosion and Sedimentation Processes in Fluvial Systems: A Case Study for the Allier/Loire System. Chapter 5 in: *Palæohydrology and Environmental Change*, G Benito, VR Baker and KJ Gregory (editors). John Wiley and Sons, Chichester.

von Bertalanffy, L. 1968. *General System Theory – Foundations, Development, Applications* (Revised edition). George Braziller, New York. 295 pages.

Vose, D. 2000. *Risk analysis: a quantitative guide* (2nd edition). Wiley, Chichester.

Walker GW and Macherd NS. 1991. Geologic Map of Oregon, USGS 1:500,000 series.

Webster R and Oliver MA. 2001. *Geostatistics for Environmental Scientists.* John Wiley, New York. 271 pages.

Whipple KX and Tucker GE. 1999. Dynamics of the stream-power river incision model: Implications for the height limits of mountain ranges, landscape response timescales, and research needs. *Journal of Geophysical Research.* **104**(B8). 17,661-17,674.

Willgoose G. 1994a. A physical explanation for an observed area-slope-elevation relationship for catchments with declining relief. *Water Resources Research*. **30**(2). 151-159.

Willgoose G. 1994b. A statistic for testing the elevation characteristics of landscape simulation models. *Journal of Geophysical Research.* **99**(B7). 13,987-13,996.

Willgoose G. 2005. Mathematical Modeling (*sic*) of Whole Landscape Evolution. *Annual Review of Earth and Planetary Sciences.* **33**. 443-459.

Willgoose G, Bras RL and Rodriguez-Iturbe I. 1991a. A coupled channel network growth and hillslope evolution model, 1. Theory. *Water Resources Research*. **27**(7). 1,671-1,684.

Willgoose G, Bras RL and Rodriguez-Iturbe I. 1991b. A coupled channel network growth and hillslope evolution model, 2. Nondimensionalization and Applications. *Water Resources Research*. **27**(7). 1,685-1,696.

Willgoose G, Bras RL and Rodriguez-Iturbe I. 1991c. A Physical Explanation of an Observed Link Area-Slope Relationship. *Water Resources Research*. **27**(7). 1,697-1,702.

Willgoose G, Bras RL and Rodriguez-Iturbe I. 1991d. Results from a new model of river basin evolution. *Earth Surface Processes and Landforms.* **16**. 237-254.

Willgoose G and Hancock G. 1998. Revisiting the hypsometric curve as an indicator of form and process in transport-limited catchment. *Earth Surface Processes and Landforms.* **23**. 611-623.

Willgoose G, Hancock GR and Kuczera GA. 2003. A Framework for the Quantitative Testing of Landform Evolution Models. Pages 195-216 in: *Prediction in Geomorphology*. Geophysical Monograph 135, PR Wilcock and RM Iverson (editors). American Geophysical Union, Washington D.C.

Young A. 1972. *Slopes*. Geomorphology Texts no. 3, KM Clayton (general editor). Longman Group, London and New York. 288 pages.

Young A. 1978. A twelve-year record of soil movement on a slope. *Zeitschrift für Geomorphologie N.F*. Supplementband **29**. 104-110.

Young A and Saunders I. 1986. Rates of surface processes and denudation. Chapter 1 in: *Hillslope Processes*, AD Abrahams (editor). Allen and Unwin, Boston.

Wu CFJ and Hamada M. 2000. *Experiments: Planning, Analysis and Parameter Design Optimization*. John Wiley and Sons, Inc., New York. 630 pages.

APPENDIX A

Notes to Table 2.1

Column 2: Time scale; time step	CAESAR, Coulthard *et al.* (1999, 2000) - In this model, calculations are performed by cellular automata, and the length of the time step is automatically adjusted so as to keep solutions numerically stable.
"	Howard (1994, 1997), Moglen and Bras (1995) and Rinaldo *et al.* (1995) - time is dimensionless in these models, so the graded/cyclic label is used to indicate the extent of landscape change expected during a model simulation
"	SIBERIA, Willgoose *et al.* (1991) - time was dimensionless in this paper, but Coulthard (2001), in a model review, indicates the normal scale and time step.
Column 3: Spatial scale; cell no.	Howard (1994, 1997), Moglen and Bras (1995) and Rinaldo *et al.* (1995) - space is dimensionless in these models, so the graded/cyclic label is used to indicate the extent of landscape change expected during a model simulation
"	SIBERIA, Willgoose *et al.* (1991) - space was dimensionless in this model, but Coulthard (2001), in a model review, indicates the expected spatial scale
Column 4: State variables	CAESAR, Coulthard *et al.* (1999, 2000) - calculations are performed for up to nine different class sizes of sediment, so each class is a state variable in its own right.
Column 7: Climate; land cover	CASCADE, Braun & Sambridge (1997) - this model can cover large areas, and allows the possibility of variable climate across the spatial domain and also with altitude. Climate variations in the other listed models is temporally varied, but not spatially.
"	CAESAR, Coulthard *et al.* (1999, 2000) - water discharge and depth are calculated by a separate version of TOPMODEL (Beven and Kirkby, 1979), which allows simulations to be made event by event rather than as aggregates within a particular continuous climate regime.
"	Rinaldo *et al.* (1995) - climate and land cover are varied simultaneously, by changing the critical shear stress resisting entrainment by fluvial processes.
"	GOLEM, Tucker and Slingerland (1994, 1996, 1997), and Tucker and Bras (1998), and CHILD, Tucker *et al.* (2001) - these models include vegetation options, although they were not used in the papers reviewed (G. Tucker, personal communication)
Column 8: Weathering	'Physical' here means a detachment process, whether brought about by physical or chemical means.
Column 9: Mass movement	Howard (1994, 1997) uses a single representation to combine the effects of both slow and fast mass movements. This is covered in more detail in section 2.2.5.
"	Martin (2000) compares results from separate and combined process representations of fast and slow mass movements, so both types of representation are used.
Column 10: Fluvial transport	Where fluvial processes are included, the model always includes erosion and transport, but not necessarily deposition. Whether or not deposition is allowed is therefore stated, but erosion and transport are taken as read.
"	'Fixed channels' - Armstrong (1976, 1980) In this model, channels are pre-set, as part of the model's initialisation procedures; channel extension or meandering is not possible.
"	'Inferred channels' – CASCADE (Braun & Sambridge, 1997), Howard (1994, 1997), Moglen and Bras (1995), GOLEM (Tucker and Slingerland, 1994, 1996, 1997; Tucker and Bras, 1998), FLUVER2 (Veldkamp & van Dijke, 1999), SIBERIA (Willgoose *et al.*,1991) - In these models, the presence of a channel in a cell is inferred from the local conditions, such as discharge, slope and contour curvature, and rules imposed by the researcher; such channels may extend upslope, but there is no meandering.
"	'Explicit channels' – CAESAR (e.g Coulthard *et al.*, 1999), CHILD (e.g. Tucker *et al.*, 2001) In these models, the channels are represented as separate entities, which may extend upslope and meander. In CAESAR, the channel width is modelled as well as the channel's direction or course, and may extend across more than one cell's width; in CHILD, the route of the channel is modelled, but not its width, this being inferred from hydraulic geometry relationships.

APPENDIX B. RUNOFF RATE CALCULATIONS FOR USE IN THE SMITH RIVER CATCHMENT SIMULATIONS

Runoff data were obtained from the USGS web pages at http://waterdata.usgs.gov/or/nwis/annual/calendar_year/?site_no= …., and then using the USGS gauging station site codes, as below:

USGS code	14311300	14323100	14311200
Gauging station site name	Tenmile Creek, Tenmile, Oregon	Smith R. nr Gardiner, Oregon	Olalla Creek, nr Tenmile, Oregon
Latitude	43 deg. 05'27"	43 deg 47'05"	43 deg 02'20"
Longitude	123 deg 34'09"	123 deg 48'50"	123 deg 32'35"
Area (sq. miles)	29.6	206	61.3
Year	**Mean annual discharges, in cubic feet per second**		
1957			120.0
1958			136.0
1959			82.1
1960			87.2
1961			122.0
1962			76.8
1963			91.1
1964			138.0
1965			83.2
1966		715.0	125.0
1967		601.0	65.8
1968		818.0	89.3
1969		662.0	97.3
1970	72.1	724.0	99.1
1971	100.0	1007.0	161.0
1972	67.4	771.0	105.0
Mean	79.8	834.0	121.7
	Constants for conversion to SI units		
Seconds per year	3.15E+07	3.15E+07	3.15E+07
Cubic feet per cubic metre	35.315	35.315	35.315
Square metres per square mile	2.59E+06	2.59E+06	2.59E+06
Annual runoff in cubic feet (mean x seconds in year)	2.52E+09	2.63E+10	3.84E+09
Equivalent in cubic metres	7.13E+07	7.45E+08	1.09E+08
Upstream gauging area, in square metres	7.67E+07	5.34E+08	1.59E+08
Run off rate in metres per year	**0.93**	**1.40**	**0.68**
	Value used in simulations: 1 metre per year.		

APPENDIX C. MORPHOMETRIC DATA USED IN DERIVING THE AREA-SLOPE CHANNEL FORMATION PARAMETERS t_{ci} AND n_{ci}

I. Method of abstraction and analysis:

1. A catchment map was derived, showing the gradients.
2. The cumulative runoff at each cell in the catchment was then calculated, using a steepest downslope flow path algorithm.
3. The positions of maximum gradient which coincided with strong flow convergence where then identified, the latter based on curvature in the elevation contours. These points were treated as the locations of notional channel heads.
4. The gradients and cumulative flows in the 3 cells nearest to the notional channel heads were then noted, and the mean areas and gradients at each location were then calculated.
5. Altogether, some 60 or so possible channel head locations were identified. After exploratory analysis, this was reduced to a core set of 58 locations, which were used in the regression analysis from which the parameter values for t_{ci} and n_{ci} were obtained.

II. Table of data:

Logarithms are to base 10.

Pt no.	Mean gradient	Area - $m^2 \times 10^3$	log of mean gradient	log of mean area	Pt no.	Mean gradient	Area - $m^2 \times 10^3$	log of mean gradient	log of mean area
1	0.2453	40.2	-0.6102	4.6042	30	0.1333	31.5	-0.8751	4.4983
2	0.1577	37.8	-0.8023	4.5775	31	0.1890	22.8	-0.7235	4.3579
3	0.2040	17.1	-0.6904	4.2330	32	0.1357	42.6	-0.8675	4.6294
4	0.2123	24.9	-0.6730	4.3962	33	0.1583	21.9	-0.8004	4.3404
5	0.2833	18.9	-0.5477	4.2765	34	0.1923	16.8	-0.7159	4.2253
6	0.2343	27.0	-0.6302	4.4314	35	0.1220	48.6	-0.9136	4.6866
7	0.2040	19.2	-0.6904	4.2833	36	0.1330	64.2	-0.8761	4.8075
8	0.1930	29.1	-0.7144	4.4639	37	0.0617	26.4	-1.2099	4.4216
9	0.1657	15.9	-0.7808	4.2014	38	0.1743	24.6	-0.7586	4.3909
10	0.1883	29.1	-0.7251	4.4639	39	0.1220	17.4	-0.9136	4.2405
11	0.1853	23.7	-0.7320	4.3747	40	0.0980	33.6	-1.0088	4.5263
12	0.2150	20.1	-0.6676	4.3032	41	0.1470	15.0	-0.8327	4.1761
13	0.2453	15.0	-0.6102	4.1761	42	0.1333	26.1	-0.8751	4.4166
14	0.2200	14.4	-0.6576	4.1584	43	0.0863	26.1	-1.0638	4.4166
15	0.1110	40.8	-0.9547	4.6107	44	0.1280	33.9	-0.8928	4.5302
16	0.1847	18.6	-0.7336	4.2695	45	0.1670	31.5	-0.7773	4.4983
17	0.2787	15.0	-0.5549	4.1761	46	0.1333	17.1	-0.8751	4.2330
18	0.1853	11.1	-0.7320	4.0453	47	0.1853	26.1	-0.7320	4.4166
19	0.2270	20.4	-0.6440	4.3096	48	0.1330	27.3	-0.8761	4.4362
20	0.2330	14.7	-0.6326	4.1673	49	0.1853	46.5	-0.7320	4.6675
21	0.1663	38.7	-0.7790	4.5877	50	0.2567	17.1	-0.5906	4.2330
22	0.1930	32.7	-0.7144	4.5145	51	0.2317	28.2	-0.6351	4.4502
23	0.3443	21.3	-0.4630	4.3284	52	0.3447	17.1	-0.4626	4.2330
24	0.1577	19.5	-0.8023	4.2900	53	0.1853	29.4	-0.7320	4.4683
25	0.2260	21.0	-0.6459	4.3222	54	0.2617	24.0	-0.5823	4.3802
26	0.2040	24.3	-0.6904	4.3856	55	0.1170	26.7	-0.9318	4.4265
27	0.1550	34.8	-0.8097	4.5416	56	0.2557	17.1	-0.5923	4.2330
28	0.1280	18.6	-0.8928	4.2695	57	0.2330	32.1	-0.6326	4.5065
29	0.2110	21.9	-0.6757	4.3404	58	0.1247	25.2	-0.9042	4.4014

III. Regression analysis and inferred base case values and value ranges for t_{ci} and n_{ci}.

1. The regression was conducted using a standard spreadsheet.
2. The basic relationship, after equations 2.71 and 3.06, is $\log|A| = \log|t_{ci}| - n_{ci} \log|S|$, where A is the area draining into the notional channel head and S is the gradient.
3. Summary regression output is shown below.

SUMMARY OUTPUT

Regression Statistics

Multiple R	0.3655
R Square	0.1336
Adjusted R Square	0.1181
Standard Error	0.1454
Observations	58

ANOVA

	df	*SS*	*MS*	*F*	*Significance F*
Regression	1	0.18256	0.18256	8.63378	0.00478
Residual	56	1.18414	0.02115		
Total	57	1.36670			

	Coefficients	*Standard Error*	*t Stat*	*P-value*	*Lower 95%*	*Upper 95%*
Intercept (t_{ci})	4.08765	0.1031	39.648	1.1E-42	3.8811	4.2942
X Variable (slope term – n_{ci})	-0.39565	0.13465	-2.938	0.00478	-0.665	-0.126

4. Direct values for the intercept (t_{ci}) and the slope (n_{ci}) are estimated from the regression output, using the lower and upper 95% limits to indicate the star point values. The proper values, and those actually used in the simulations, are summarised below:

From regression:	**Lower 95% value**	**Mean value**	**Upper 95% value**
t_{ci}	7,605.4	12,236.4	19,687.4
n_{ci}	0.2161	0.4021	0.7483
	↓	↓	↓
Used in simulations:	**- α**	**Base case**	**+ α**
t_{ci}	7,600	12,236	19,700
n_{ci}	0.216	0.402	0.748

APPENDIX D. DESIGN MATRIX OF THE CENTRAL COMPOSITE DESIGN

Levels corresponding to base case values are denoted by zero, those corresponding to upper and lower factorial point values are denoted respectively +1 and -1, and the upper and lower star point levels are shown as $+\alpha$ and $-\alpha$. Design levels of s_{cr}, k_b and τ_b are found using the design generators, as explained in subsection 3.5.3.

Para-meter	k_w	m_w	k_d	k_f	τ_c	n_{ci}	t_{ci}	s_{cr}	k_b	τ_b
No.	**1**	**2**	**3**	**4**	**5**	**6**	**7**	**8**	**9**	**10**
Case no.										
1	0	0	0	0	0	0	0	0	0	0
2	α	0	0	0	0	0	0	0	0	0
3	$-\alpha$	0	0	0	0	0	0	0	0	0
4	0	α	0	0	0	0	0	0	0	0
5	0	$-\alpha$	0	0	0	0	0	0	0	0
6	0	0	α	0	0	0	0	0	0	0
7	0	0	$-\alpha$	0	0	0	0	0	0	0
8	0	0	0	α	0	0	0	0	0	0
9	0	0	0	$-\alpha$	0	0	0	0	0	0
10	0	0	0	0	α	0	0	0	0	0
11	0	0	0	0	$-\alpha$	0	0	0	0	0
12	0	0	0	0	0	α	0	0	0	0
13	0	0	0	0	0	$-\alpha$	0	0	0	0
14	0	0	0	0	0	0	α	0	0	0
15	0	0	0	0	0	0	$-\alpha$	0	0	0
16	0	0	0	0	0	0	0	α	0	0
17	0	0	0	0	0	0	0	$-\alpha$	0	0
18	0	0	0	0	0	0	0	0	α	0
19	0	0	0	0	0	0	0	0	$-\alpha$	0
20	0	0	0	0	0	0	0	0	0	α
21	0	0	0	0	0	0	0	0	0	$-\alpha$
22	1	1	1	1	1	1	1	1	1	1
23	-1	1	1	1	1	1	1	1	-1	-1
24	1	-1	1	1	1	1	1	1	1	-1
25	-1	-1	1	1	1	1	1	1	-1	1
26	1	1	-1	1	1	1	1	-1	-1	1
27	-1	1	-1	1	1	1	1	-1	1	-1
28	1	-1	-1	1	1	1	1	-1	-1	-1
29	-1	-1	-1	1	1	1	1	-1	1	1
30	1	1	1	-1	1	1	1	-1	-1	-1
31	-1	1	1	-1	1	1	1	-1	1	1
32	1	-1	1	-1	1	1	1	-1	-1	1
33	-1	-1	1	-1	1	1	1	-1	1	-1
34	1	1	-1	-1	1	1	1	1	1	-1
35	-1	1	-1	-1	1	1	1	1	-1	1
36	1	-1	-1	-1	1	1	1	1	1	1
37	-1	-1	-1	-1	1	1	1	1	-1	-1
38	1	1	1	1	-1	1	1	-1	-1	1
39	-1	1	1	1	-1	1	1	-1	1	-1
40	1	-1	1	1	-1	1	1	-1	-1	-1
41	-1	-1	1	1	-1	1	1	-1	1	1
42	1	1	-1	1	-1	1	1	1	1	1
43	-1	1	-1	1	-1	1	1	1	-1	-1

Para-meter	k_w	m_w	k_d	k_f	τ_c	n_{ci}	t_{ci}	s_{cr}	k_b	τ_b
44	1	-1	-1	1	-1	1	1	1	1	-1
45	-1	-1	-1	1	-1	1	1	1	-1	1
46	1	1	1	-1	-1	1	1	1	1	-1
47	-1	1	1	-1	-1	1	1	1	-1	1
48	1	-1	1	-1	-1	1	1	1	1	1
49	-1	-1	1	-1	-1	1	1	1	-1	-1
50	1	1	-1	-1	-1	1	1	-1	-1	-1
51	-1	1	-1	-1	-1	1	1	-1	1	1
52	1	-1	-1	-1	-1	1	1	-1	-1	1
53	-1	-1	-1	-1	-1	1	1	-1	1	-1
54	1	1	1	1	1	-1	1	-1	1	-1
55	-1	1	1	1	1	-1	1	-1	-1	1
56	1	-1	1	1	1	-1	1	-1	1	1
57	-1	-1	1	1	1	-1	1	-1	-1	-1
58	1	1	-1	1	1	-1	1	1	-1	-1
59	-1	1	-1	1	1	-1	1	1	1	1
60	1	-1	-1	1	1	-1	1	1	-1	1
61	-1	-1	-1	1	1	-1	1	1	1	-1
62	1	1	1	-1	1	-1	1	1	-1	1
63	-1	1	1	-1	1	-1	1	1	1	-1
64	1	-1	1	-1	1	-1	1	1	-1	-1
65	-1	-1	1	-1	1	-1	1	1	1	1
66	1	1	-1	-1	1	-1	1	-1	1	1
67	-1	1	-1	-1	1	-1	1	-1	-1	-1
68	1	-1	-1	-1	1	-1	1	-1	1	-1
69	-1	-1	-1	-1	1	-1	1	-1	-1	1
70	1	1	1	1	-1	-1	1	1	-1	-1
71	-1	1	1	1	-1	-1	1	1	1	1
72	1	-1	1	1	-1	-1	1	1	-1	1
73	-1	-1	1	1	-1	-1	1	1	1	-1
74	1	1	-1	1	-1	-1	1	-1	1	-1
75	-1	1	-1	1	-1	-1	1	-1	-1	1
76	1	-1	-1	1	-1	-1	1	-1	1	1
77	-1	-1	-1	1	-1	-1	1	-1	-1	-1
78	1	1	1	-1	-1	-1	1	-1	1	1
79	-1	1	1	-1	-1	-1	1	-1	-1	-1
80	1	-1	1	-1	-1	-1	1	-1	1	-1
81	-1	-1	1	-1	-1	-1	1	-1	-1	1
82	1	1	-1	-1	-1	-1	1	1	-1	1
83	-1	1	-1	-1	-1	-1	1	1	1	-1
84	1	-1	-1	-1	-1	-1	1	1	-1	-1
85	-1	-1	-1	-1	-1	-1	1	1	1	1
86	1	1	1	1	1	1	-1	1	-1	-1
87	-1	1	1	1	1	1	-1	1	1	1
88	1	-1	1	1	1	1	-1	1	-1	1
89	-1	-1	1	1	1	1	-1	1	1	-1
90	1	1	-1	1	1	1	-1	-1	1	-1
91	-1	1	-1	1	1	1	-1	-1	-1	1
92	1	-1	-1	1	1	1	-1	-1	1	1
93	-1	-1	-1	1	1	1	-1	-1	-1	-1
94	1	1	1	-1	1	1	-1	-1	1	1
95	-1	1	1	-1	1	1	-1	-1	-1	-1
96	1	-1	1	-1	1	1	-1	-1	1	-1
97	-1	-1	1	-1	1	1	-1	-1	-1	1

Para-meter	k_w	m_w	k_d	k_f	τ_c	n_{ci}	t_{ci}	s_{cr}	k_b	τ_b
98	1	1	-1	-1	1	1	-1	1	-1	1
99	-1	1	-1	-1	1	1	-1	1	1	-1
100	1	-1	-1	-1	1	1	-1	1	-1	-1
101	-1	-1	-1	-1	1	1	-1	1	1	1
102	1	1	1	1	-1	1	-1	-1	1	-1
103	-1	1	1	1	-1	1	-1	-1	-1	1
104	1	-1	1	1	-1	1	-1	-1	1	1
105	-1	-1	1	1	-1	1	-1	-1	-1	-1
106	1	1	-1	1	-1	1	-1	1	-1	-1
107	-1	1	-1	1	-1	1	-1	1	1	1
108	1	-1	-1	1	-1	1	-1	1	-1	1
109	-1	-1	-1	1	-1	1	-1	1	1	-1
110	1	1	1	-1	-1	1	-1	1	-1	1
111	-1	1	1	-1	-1	1	-1	1	1	-1
112	1	-1	1	-1	-1	1	-1	1	-1	-1
113	-1	-1	1	-1	-1	1	-1	1	1	1
114	1	1	-1	-1	-1	1	-1	-1	1	1
115	-1	1	-1	-1	-1	1	-1	-1	-1	-1
116	1	-1	-1	-1	-1	1	-1	-1	1	-1
117	-1	-1	-1	-1	-1	1	-1	-1	-1	1
118	1	1	1	1	1	-1	-1	-1	-1	1
119	-1	1	1	1	1	-1	-1	-1	1	-1
120	1	-1	1	1	1	-1	-1	-1	-1	-1
121	-1	-1	1	1	1	-1	-1	-1	1	1
122	1	1	-1	1	1	-1	-1	1	1	1
123	-1	1	-1	1	1	-1	-1	1	-1	-1
124	1	-1	-1	1	1	-1	-1	1	1	-1
125	-1	-1	-1	1	1	-1	-1	1	-1	1
126	1	1	1	-1	1	-1	-1	1	1	-1
127	-1	1	1	-1	1	-1	-1	1	-1	1
128	1	-1	1	-1	1	-1	-1	1	1	1
129	-1	-1	1	-1	1	-1	-1	1	-1	-1
130	1	1	-1	-1	1	-1	-1	-1	-1	-1
131	-1	1	-1	-1	1	-1	-1	-1	1	1
132	1	-1	-1	-1	1	-1	-1	-1	-1	1
133	-1	-1	-1	-1	1	-1	-1	-1	1	-1
134	1	1	1	1	-1	-1	-1	1	1	1
135	-1	1	1	1	-1	-1	-1	1	-1	-1
136	1	-1	1	1	-1	-1	-1	1	1	-1
137	-1	-1	1	1	-1	-1	-1	1	-1	1
138	1	1	-1	1	-1	-1	-1	-1	-1	1
139	-1	1	-1	1	-1	-1	-1	-1	1	-1
140	1	-1	-1	1	-1	-1	-1	-1	-1	-1
141	-1	-1	-1	1	-1	-1	-1	-1	1	1
142	1	1	1	-1	-1	-1	-1	-1	-1	-1
143	-1	1	1	-1	-1	-1	-1	-1	1	1
144	1	-1	1	-1	-1	-1	-1	-1	-1	1
145	-1	-1	1	-1	-1	-1	-1	-1	1	-1
146	1	1	-1	-1	-1	-1	-1	1	1	-1
147	-1	1	-1	-1	-1	-1	-1	1	-1	1
148	1	-1	-1	-1	-1	-1	-1	1	1	1
149	-1	-1	-1	-1	-1	-1	-1	1	-1	-1

APPENDIX E. PLANNING MATRIX OF THE CENTRAL COMPOSITE DESIGN

I. Translation of design levels into parameter values for the planning matrix.

1. Base values, factorial point values and star point values are listed in Table 3.5.

2. Ideally, each parameter's base case value lies exactly mid way between both its star point and its factorial point values. There are some slight exceptions, explained in point 4 below.

3. For the 2_{V}^{10-3} design used in this research, the star point values, by the Box and Hunter (1957) criterion (eq. 3.05), should be scaled to approximately 3.363 times the spacing of the factorial points from the base case. To do this, it is necessary to use the correct scaled design levels corresponding to the factorial points. Thus, if a parameter's base value is x_0, and the upper factorial value is x_{+1}, the scaled design level for a parameter is given by (equation 4.01 *q.v.*):

$$x' = \frac{x - x_0}{x_{+1} - x_0}, \qquad \text{E1.01}$$

where x′ is the scaled design level. Hence, for the upper star point, and using the Box and Hunter scaling, we have:

$$x' = 3.363 = \frac{x_{+\alpha} - x_0}{x_{+1} - x_0}, \qquad \text{E1.02}$$

where $x_{+\alpha}$ is the actual value to use for the upper star point. This value can now be found by recasting E1.02, to give:

$$x_{+\alpha} = x_0 + 3.363\left(x_{+1} - x_0\right), \qquad \text{E1.03}$$

for the upper star point, and:

$$x_{+\alpha} = x_0 - 3.363\left(x_{+1} - x_0\right), \qquad \text{E1.04}$$

for the lower star point.

4. Because of their derivation from logarithmic relationships, as explained in Appendix C, the base case values of t_{ci} and n_{ci} are rather less than mid way between the star or factorial points. This means that the upper and lower scaled design levels are slightly different from the Box-Hunter scale levels shown in point 3 here. Similarly, the lower factorial point scalings for these parameters are also slightly different from their nominal -1 levels. The differences from the 'ideal' are not great, however, and do not affect the efficacy of the central composite design. There are also one other slight variation, for k_f, caused by rounding a value when setting up the experiment. For convenience otherwise, all the other star point and factorial point scaled design levels are respectively ± 3.333, which is only a little less than the Box-Hunter criterion, and ± 1. In detail, the full details for all the parameter scaled levels for the star points and factorial points are shown below:

	k_w	m_w	k_d	k_f	τ_c	n_{ci}	t_{ci}	s_{cr}	k_b	τ_b
+ star pt	3.333	3.333	3.333	3.313	3.333	4.220	3.972	3.333	3.333	3.333
+ fact. pt	1.000	1.000	1.000	1.000	1.000	1.000	1.000	1.000	1.000	1.000
- fact. pt	-1.000	-1.000	-1.000	-0.985	-1.000	-0.829	-0.867	-1.000	-1.000	-1.000
- star pt	-3.333	-3.333	-3.333	-3.299	-3.333	-2.268	-2.467	-3.333	-3.333	-3.333

5. The full planning matrix - a table of all the actual values used in each parameter case - is given over the next few pages. Note that the values for k_b are stated $\times 10^{-6}$.

Planning matrix for the central composite design:

Para-meter	k_w	m_w	k_d	k_f	τ_c	n_{ci}	t_{ci}	s_{cr}	k_b $\times 10^{-6}$	τ_b
Design no. Case no.	**1**	**2**	**3**	**4**	**5**	**6**	**7**	**8**	**9**	**10**
1	0.00024	0.33	0.0036	0.000442	6	0.402	12236	0.62	15	4
2	0.00030	0.33	0.0036	0.000442	6	0.402	12236	0.62	15	4
3	0.00018	0.33	0.0036	0.000442	6	0.402	12236	0.62	15	4
4	0.00024	0.43	0.0036	0.000442	6	0.402	12236	0.62	15	4
5	0.00024	0.23	0.0036	0.000442	6	0.402	12236	0.62	15	4
6	0.00024	0.33	0.0052	0.000442	6	0.402	12236	0.62	15	4
7	0.00024	0.33	0.0020	0.000442	6	0.402	12236	0.62	15	4
8	0.00024	0.33	0.0036	0.000664	6	0.402	12236	0.62	15	4
9	0.00024	0.33	0.0036	0.000221	6	0.402	12236	0.62	15	4
10	0.00024	0.33	0.0036	0.000442	12	0.402	12236	0.62	15	4
11	0.00024	0.33	0.0036	0.000442	0	0.402	12236	0.62	15	4
12	0.00024	0.33	0.0036	0.000442	6	0.748	12236	0.62	15	4
13	0.00024	0.33	0.0036	0.000442	6	0.216	12236	0.62	15	4
14	0.00024	0.33	0.0036	0.000442	6	0.402	19700	0.62	15	4
15	0.00024	0.33	0.0036	0.000442	6	0.402	7600	0.62	15	4
16	0.00024	0.33	0.0036	0.000442	6	0.402	12236	0.76	15	4
17	0.00024	0.33	0.0036	0.000442	6	0.402	12236	0.48	15	4
18	0.00024	0.33	0.0036	0.000442	6	0.402	12236	0.62	26.25	4
19	0.00024	0.33	0.0036	0.000442	6	0.402	12236	0.62	3.75	4
20	0.00024	0.33	0.0036	0.000442	6	0.402	12236	0.62	15	8
21	0.00024	0.33	0.0036	0.000442	6	0.402	12236	0.62	15	0
22	0.000258	0.36	0.00408	0.0005086	7.8	0.484	14115	0.662	18.375	5.2
23	0.000222	0.36	0.00408	0.0005086	7.8	0.484	14115	0.662	11.625	2.8
24	0.000258	0.3	0.00408	0.0005086	7.8	0.484	14115	0.662	18.375	2.8
25	0.000222	0.3	0.00408	0.0005086	7.8	0.484	14115	0.662	11.625	5.2
26	0.000258	0.36	0.00312	0.0005086	7.8	0.484	14115	0.578	11.625	5.2
27	0.000222	0.36	0.00312	0.0005086	7.8	0.484	14115	0.578	18.375	2.8
28	0.000258	0.3	0.00312	0.0005086	7.8	0.484	14115	0.578	11.625	2.8

29	0.000222	0.3	0.00312	0.0005086	7.8	0.484	14115	0.578	18.375	5.2
30	0.000258	0.36	0.00408	0.0003757	7.8	0.484	14115	0.578	11.625	2.8
31	0.000222	0.36	0.00408	0.0003757	7.8	0.484	14115	0.578	18.375	5.2
32	0.000258	0.3	0.00408	0.0003757	7.8	0.484	14115	0.578	11.625	5.2
33	0.000222	0.3	0.00408	0.0003757	7.8	0.484	14115	0.578	18.375	2.8
34	0.000258	0.36	0.00312	0.0003757	7.8	0.484	14115	0.662	18.375	2.8
35	0.000222	0.36	0.00312	0.0003757	7.8	0.484	14115	0.662	11.625	5.2
36	0.000258	0.3	0.00312	0.0003757	7.8	0.484	14115	0.662	18.375	5.2
37	0.000222	0.3	0.00312	0.0003757	7.8	0.484	14115	0.662	11.625	2.8
38	0.000258	0.36	0.00408	0.0005086	4.2	0.484	14115	0.578	11.625	5.2
39	0.000222	0.36	0.00408	0.0005086	4.2	0.484	14115	0.578	18.375	2.8
40	0.000258	0.3	0.00408	0.0005086	4.2	0.484	14115	0.578	11.625	2.8
41	0.000222	0.3	0.00408	0.0005086	4.2	0.484	14115	0.578	18.375	5.2
42	0.000258	0.36	0.00312	0.0005086	4.2	0.484	14115	0.662	18.375	5.2
43	0.000222	0.36	0.00312	0.0005086	4.2	0.484	14115	0.662	11.625	2.8
44	0.000258	0.3	0.00312	0.0005086	4.2	0.484	14115	0.662	18.375	2.8
45	0.000222	0.3	0.00312	0.0005086	4.2	0.484	14115	0.662	11.625	5.2
46	0.000258	0.36	0.00408	0.0003757	4.2	0.484	14115	0.662	18.375	2.8
47	0.000222	0.36	0.00408	0.0003757	4.2	0.484	14115	0.662	11.625	5.2
48	0.000258	0.3	0.00408	0.0003757	4.2	0.484	14115	0.662	18.375	5.2
49	0.000222	0.3	0.00408	0.0003757	4.2	0.484	14115	0.662	11.625	2.8
50	0.000258	0.36	0.00312	0.0003757	4.2	0.484	14115	0.578	11.625	2.8
51	0.000222	0.36	0.00312	0.0003757	4.2	0.484	14115	0.578	18.375	5.2
52	0.000258	0.3	0.00312	0.0003757	4.2	0.484	14115	0.578	11.625	5.2
53	0.000222	0.3	0.00312	0.0003757	4.2	0.484	14115	0.578	18.375	2.8
54	0.000258	0.36	0.00408	0.0005086	7.8	0.334	14115	0.578	18.375	2.8
55	0.000222	0.36	0.00408	0.0005086	7.8	0.334	14115	0.578	11.625	5.2
56	0.000258	0.3	0.00408	0.0005086	7.8	0.334	14115	0.578	18.375	5.2
57	0.000222	0.3	0.00408	0.0005086	7.8	0.334	14115	0.578	11.625	2.8
58	0.000258	0.36	0.00312	0.0005086	7.8	0.334	14115	0.662	11.625	2.8
59	0.000222	0.36	0.00312	0.0005086	7.8	0.334	14115	0.662	18.375	5.2
60	0.000258	0.3	0.00312	0.0005086	7.8	0.334	14115	0.662	11.625	5.2
61	0.000222	0.3	0.00312	0.0005086	7.8	0.334	14115	0.662	18.375	2.8
62	0.000258	0.36	0.00408	0.0003757	7.8	0.334	14115	0.662	11.625	5.2
63	0.000222	0.36	0.00408	0.0003757	7.8	0.334	14115	0.662	18.375	2.8

64	0.000258	0.3	0.00408	0.0003757	7.8	0.334	14115	0.662	11.625	2.8
65	0.000222	0.3	0.00408	0.0003757	7.8	0.334	14115	0.662	18.375	5.2
66	0.000258	0.36	0.00312	0.0003757	7.8	0.334	14115	0.578	18.375	5.2
67	0.000222	0.36	0.00312	0.0003757	7.8	0.334	14115	0.578	11.625	2.8
68	0.000258	0.3	0.00312	0.0003757	7.8	0.334	14115	0.578	18.375	2.8
69	0.000222	0.3	0.00312	0.0003757	7.8	0.334	14115	0.578	11.625	5.2
70	0.000258	0.36	0.00408	0.0005086	4.2	0.334	14115	0.662	11.625	2.8
71	0.000222	0.36	0.00408	0.0005086	4.2	0.334	14115	0.662	18.375	5.2
72	0.000258	0.3	0.00408	0.0005086	4.2	0.334	14115	0.662	11.625	5.2
73	0.000222	0.3	0.00408	0.0005086	4.2	0.334	14115	0.662	18.375	2.8
74	0.000258	0.36	0.00312	0.0005086	4.2	0.334	14115	0.578	18.375	2.8
75	0.000222	0.36	0.00312	0.0005086	4.2	0.334	14115	0.578	11.625	5.2
76	0.000258	0.3	0.00312	0.0005086	4.2	0.334	14115	0.578	18.375	5.2
77	0.000222	0.3	0.00312	0.0005086	4.2	0.334	14115	0.578	11.625	2.8
78	0.000258	0.36	0.00408	0.0003757	4.2	0.334	14115	0.578	18.375	5.2
79	0.000222	0.36	0.00408	0.0003757	4.2	0.334	14115	0.578	11.625	2.8
80	0.000258	0.3	0.00408	0.0003757	4.2	0.334	14115	0.578	18.375	2.8
81	0.000222	0.3	0.00408	0.0003757	4.2	0.334	14115	0.578	11.625	5.2
82	0.000258	0.36	0.00312	0.0003757	4.2	0.334	14115	0.662	11.625	5.2
83	0.000222	0.36	0.00312	0.0003757	4.2	0.334	14115	0.662	18.375	2.8
84	0.000258	0.3	0.00312	0.0003757	4.2	0.334	14115	0.662	11.625	2.8
85	0.000222	0.3	0.00312	0.0003757	4.2	0.334	14115	0.662	18.375	5.2
86	0.000258	0.36	0.00408	0.0005086	7.8	0.484	10607	0.662	11.625	2.8
87	0.000222	0.36	0.00408	0.0005086	7.8	0.484	10607	0.662	18.375	5.2
88	0.000258	0.3	0.00408	0.0005086	7.8	0.484	10607	0.662	11.625	5.2
89	0.000222	0.3	0.00408	0.0005086	7.8	0.484	10607	0.662	18.375	2.8
90	0.000258	0.36	0.00312	0.0005086	7.8	0.484	10607	0.578	18.375	2.8
91	0.000222	0.36	0.00312	0.0005086	7.8	0.484	10607	0.578	11.625	5.2
92	0.000258	0.3	0.00312	0.0005086	7.8	0.484	10607	0.578	18.375	5.2
93	0.000222	0.3	0.00312	0.0005086	7.8	0.484	10607	0.578	11.625	2.8
94	0.000258	0.36	0.00408	0.0003757	7.8	0.484	10607	0.578	18.375	5.2
95	0.000222	0.36	0.00408	0.0003757	7.8	0.484	10607	0.578	11.625	2.8
96	0.000258	0.3	0.00408	0.0003757	7.8	0.484	10607	0.578	18.375	2.8
97	0.000222	0.3	0.00408	0.0003757	7.8	0.484	10607	0.578	11.625	5.2
98	0.000258	0.36	0.00312	0.0003757	7.8	0.484	10607	0.662	11.625	5.2

99	0.000222	0.36	0.00312	0.0003757	7.8	0.484	10607	0.662	18.375	2.8
100	0.000258	0.3	0.00312	0.0003757	7.8	0.484	10607	0.662	11.625	2.8
101	0.000222	0.3	0.00312	0.0003757	7.8	0.484	10607	0.662	18.375	5.2
102	0.000258	0.36	0.00408	0.0005086	4.2	0.484	10607	0.578	18.375	2.8
103	0.000222	0.36	0.00408	0.0005086	4.2	0.484	10607	0.578	11.625	5.2
104	0.000258	0.3	0.00408	0.0005086	4.2	0.484	10607	0.578	18.375	5.2
105	0.000222	0.3	0.00408	0.0005086	4.2	0.484	10607	0.578	11.625	2.8
106	0.000258	0.36	0.00312	0.0005086	4.2	0.484	10607	0.662	11.625	2.8
107	0.000222	0.36	0.00312	0.0005086	4.2	0.484	10607	0.662	18.375	5.2
108	0.000258	0.3	0.00312	0.0005086	4.2	0.484	10607	0.662	11.625	5.2
109	0.000222	0.3	0.00312	0.0005086	4.2	0.484	10607	0.662	18.375	2.8
110	0.000258	0.36	0.00408	0.0003757	4.2	0.484	10607	0.662	11.625	5.2
111	0.000222	0.36	0.00408	0.0003757	4.2	0.484	10607	0.662	18.375	2.8
112	0.000258	0.3	0.00408	0.0003757	4.2	0.484	10607	0.662	11.625	2.8
113	0.000222	0.3	0.00408	0.0003757	4.2	0.484	10607	0.662	18.375	5.2
114	0.000258	0.36	0.00312	0.0003757	4.2	0.484	10607	0.578	18.375	5.2
115	0.000222	0.36	0.00312	0.0003757	4.2	0.484	10607	0.578	11.625	2.8
116	0.000258	0.3	0.00312	0.0003757	4.2	0.484	10607	0.578	18.375	2.8
117	0.000222	0.3	0.00312	0.0003757	4.2	0.484	10607	0.578	11.625	5.2
118	0.000258	0.36	0.00408	0.0005086	7.8	0.334	10607	0.578	11.625	5.2
119	0.000222	0.36	0.00408	0.0005086	7.8	0.334	10607	0.578	18.375	2.8
120	0.000258	0.3	0.00408	0.0005086	7.8	0.334	10607	0.578	11.625	2.8
121	0.000222	0.3	0.00408	0.0005086	7.8	0.334	10607	0.578	18.375	5.2
122	0.000258	0.36	0.00312	0.0005086	7.8	0.334	10607	0.662	18.375	5.2
123	0.000222	0.36	0.00312	0.0005086	7.8	0.334	10607	0.662	11.625	2.8
124	0.000258	0.3	0.00312	0.0005086	7.8	0.334	10607	0.662	18.375	2.8
125	0.000222	0.3	0.00312	0.0005086	7.8	0.334	10607	0.662	11.625	5.2
126	0.000258	0.36	0.00408	0.0003757	7.8	0.334	10607	0.662	18.375	2.8
127	0.000222	0.36	0.00408	0.0003757	7.8	0.334	10607	0.662	11.625	5.2
128	0.000258	0.3	0.00408	0.0003757	7.8	0.334	10607	0.662	18.375	5.2
129	0.000222	0.3	0.00408	0.0003757	7.8	0.334	10607	0.662	11.625	2.8
130	0.000258	0.36	0.00312	0.0003757	7.8	0.334	10607	0.578	11.625	2.8
131	0.000222	0.36	0.00312	0.0003757	7.8	0.334	10607	0.578	18.375	5.2
132	0.000258	0.3	0.00312	0.0003757	7.8	0.334	10607	0.578	11.625	5.2
133	0.000222	0.3	0.00312	0.0003757	7.8	0.334	10607	0.578	18.375	2.8

134	0.000258	0.36	0.00408	0.0005086	4.2	0.334	10607	0.662	18.375	5.2
135	0.000222	0.36	0.00408	0.0005086	4.2	0.334	10607	0.662	11.625	2.8
136	0.000258	0.3	0.00408	0.0005086	4.2	0.334	10607	0.662	18.375	2.8
137	0.000222	0.3	0.00408	0.0005086	4.2	0.334	10607	0.662	11.625	5.2
138	0.000258	0.36	0.00312	0.0005086	4.2	0.334	10607	0.578	11.625	5.2
139	0.000222	0.36	0.00312	0.0005086	4.2	0.334	10607	0.578	18.375	2.8
140	0.000258	0.3	0.00312	0.0005086	4.2	0.334	10607	0.578	11.625	2.8
141	0.000222	0.3	0.00312	0.0005086	4.2	0.334	10607	0.578	18.375	5.2
142	0.000258	0.36	0.00408	0.0003757	4.2	0.334	10607	0.578	11.625	2.8
143	0.000222	0.36	0.00408	0.0003757	4.2	0.334	10607	0.578	18.375	5.2
144	0.000258	0.3	0.00408	0.0003757	4.2	0.334	10607	0.578	11.625	5.2
145	0.000222	0.3	0.00408	0.0003757	4.2	0.334	10607	0.578	18.375	2.8
146	0.000258	0.36	0.00312	0.0003757	4.2	0.334	10607	0.662	18.375	2.8
147	0.000222	0.36	0.00312	0.0003757	4.2	0.334	10607	0.662	11.625	5.2
148	0.000258	0.30	0.00312	0.000376	4.2	0.334	10607	0.662	18.375	5.2
149	0.000222	0.30	0.00312	0.000376	4.2	0.334	10607	0.662	11.625	2.8

APPENDIX F. CALCULATION OF SEDIMENT YIELD AND SEDIMENT DELIVERY RATIO METRICS

I. Sediment yield

Sediment yield is calculated from the difference in the mean elevations of the catchment at the 90,000 and 100,000 years time slices. This is then multiplied by the area of the catchment in square metres, to give a volume in cubic metres, and divided by the area in square kilometres and the time interval, to give a rate expressed in cubic metres per square kilometre per year. This can be expressed mathematically and simplified, as follows:

$$\text{sediment yield} = \frac{38.7 \times 10^6 \times \left(\bar{x}_{90} - \bar{x}_{100}\right)}{38.7 \times 10 \times 10^3}$$

$$= 100 \Delta \bar{x}_{90:100}, \qquad \text{F1.01}$$

where $\bar{x}_{90}$ and $\bar{x}_{100}$ are the mean elevations of the catchment at 90,000 and 100,000 years respectively, and $\Delta \bar{x}_{90:100}$ is the difference between these two quantities.

II. Sediment delivery ratio

The sediment delivery ratio calculation is slightly more complicated than the sediment yield calculation above. An algorithm is used to sum the elevation changes in all of the cells experiencing net erosion between the 90,000 and 100,000 year time slices, and similarly the elevation changes in all of the cells experiencing net deposition over the same period. The volume of sediment represented by both quantities is then calculated (using 900 m^2, the area of each cell), and thence the difference between the sediment volumes is found, equivalent to the overall erosion of the catchment. The sediment delivery ratio is then equal to the overall erosion divided by the net erosion, multiplying by 100 to convert this to a percentage. This complete calculation may be expressed mathematically as follows:

$$\text{sediment delivery ratio (\%)} = 100 \times \frac{900 \times \left(\Sigma x_{net-} - \Sigma x_{net+}\right)}{900 \times \Sigma x_{net-}}$$

$$= 100 \times \left(1 - \frac{\Sigma x_{net+}}{\Sigma x_{net-}}\right), \qquad \text{F1.02}$$

where Σx_{net-} and Σx_{net+} are respectively the sums of the elevation changes experienced by cells experiencing net erosion and net deposition.

APPENDIX G. DATA FOR MAIN EFFECTS PLOTS, FIGURES 4.18 TO 4.25 INCLUSIVE

I. Sediment yield ($m^3\,km^{-2}\,yr^{-1}$)

Time (000s yrs)		k_w		m_w		k_d		k_f		τ_c		n_{ci}		t_{ci}		s_{cr}		k_b		τ_b	
	Base case	+ α	- α	+ α	- α	+ α	- α	+ α	- α	+ α	- α	+ α	- α	+ α	- α	+ α	- α	+ α	- α	+ α	- α
10	19.95	20.78	18.98	19.96	19.94	20.48	19.33	26.51	11.22	15.41	24.22	18.63	20.21	18.92	21.05	19.13	22.22	20.44	19.41	19.40	20.55
20	21.30	22.70	19.55	21.32	21.30	21.94	20.56	27.47	12.62	16.71	25.71	19.78	21.50	19.99	22.45	19.63	23.20	22.02	20.40	20.37	22.22
30	22.32	23.63	20.44	22.23	22.22	22.78	21.73	28.74	13.25	17.61	26.90	20.93	22.48	21.14	23.45	20.56	23.96	22.88	21.40	21.45	23.02
40	22.85	24.42	21.04	22.83	22.79	23.38	22.36	29.69	13.69	18.07	27.58	21.52	23.21	21.71	24.28	21.34	24.70	23.54	22.11	22.12	23.56
50	23.34	25.10	21.48	23.29	23.33	23.97	22.66	30.55	13.96	18.49	28.36	21.79	23.84	22.04	25.09	21.93	25.44	23.99	22.54	22.47	24.13
60	23.86	25.54	21.82	23.71	23.82	24.40	23.18	31.12	14.20	18.72	28.98	22.06	24.40	22.32	25.70	22.37	26.15	24.52	23.00	22.96	24.56
70	24.26	25.70	22.06	24.23	24.21	24.90	23.51	31.37	14.35	18.93	29.47	22.31	24.81	22.47	26.28	22.61	26.68	24.62	23.37	23.50	24.82
80	24.61	26.00	22.29	24.44	24.53	25.12	23.82	31.77	14.47	19.06	29.88	22.54	25.27	22.79	26.74	22.98	27.07	25.02	23.84	23.91	25.19
90	24.76	26.13	22.55	24.72	24.76	25.29	24.09	32.03	14.58	19.07	30.32	22.68	25.51	22.99	27.16	23.04	27.32	25.35	24.08	24.12	25.31
100	24.91	26.21	22.74	24.91	24.94	25.54	24.17	32.46	14.62	19.14	30.75	22.72	25.56	23.01	27.45	23.15	27.57	25.50	24.30	24.48	25.31

II. Drainage density ($km\,km^{-2}$)

Time (000s yrs)		k_w		m_w		k_d		k_f		τ_c		n_{ci}		t_{ci}		s_{cr}		k_b		τ_b	
	Base case	+ α	- α	+ α	- α	+ α	- α	+ α	- α	+ α	- α	+ α	- α	+ α	- α	+ α	- α	+ α	- α	+ α	- α
10	3.02	3.04	3.03	3.04	3.04	3.05	3.07	3.01	3.05	3.01	3.07	2.32	3.40	2.55	3.75	3.00	3.06	3.08	3.01	3.00	3.06
20	3.08	3.12	3.08	3.07	3.04	3.07	3.07	3.05	3.09	3.04	3.13	2.30	3.49	2.57	3.95	3.05	3.08	3.07	3.03	3.05	3.07
30	3.07	3.08	3.07	3.10	3.06	3.08	3.09	3.08	3.11	3.06	3.17	2.33	3.49	2.53	3.98	3.08	3.10	3.07	3.05	3.07	3.09
40	3.09	3.17	3.08	3.15	3.14	3.09	3.12	3.09	3.15	3.06	3.13	2.33	3.55	2.56	4.07	3.09	3.08	3.14	3.08	3.13	3.14
50	3.12	3.13	3.10	3.11	3.13	3.13	3.15	3.12	3.16	3.09	3.17	2.28	3.60	2.53	4.18	3.10	3.16	3.18	3.10	3.13	3.14
60	3.15	3.17	3.12	3.14	3.16	3.14	3.17	3.10	3.17	3.13	3.16	2.26	3.62	2.53	4.15	3.13	3.16	3.13	3.09	3.10	3.14
70	3.11	3.15	3.09	3.15	3.15	3.13	3.13	3.14	3.18	3.10	3.24	2.22	3.64	2.50	4.23	3.14	3.16	3.14	3.11	3.09	3.16
80	3.14	3.15	3.11	3.16	3.15	3.12	3.17	3.16	3.19	3.09	3.17	2.20	3.63	2.51	4.21	3.11	3.16	3.13	3.11	3.15	3.14
90	3.17	3.18	3.13	3.15	3.12	3.13	3.13	3.17	3.23	3.13	3.20	2.17	3.65	2.47	4.26	3.13	3.16	3.14	3.07	3.11	3.16
100	3.15	3.14	3.13	3.17	3.15	3.14	3.14	3.18	3.17	3.11	3.19	2.16	3.68	2.47	4.26	3.15	3.17	3.15	3.12	3.12	3.15

III. Sediment delivery ratio (%)

Time (000s yrs)		k_w		m_w		k_d		k_f		τ_c		n_{ci}		t_{ci}		s_{cr}		k_b		τ_b	
	Base case	+ α	- α	+ α	- α	+ α	- α	+ α	- α	+ α	- α	+ α	- α	+ α	- α	+ α	- α	+ α	- α	+ α	- α
10	77.91	73.28	83.48	77.85	77.97	73.20	83.31	91.04	52.43	68.94	83.55	82.17	75.13	81.34	69.88	81.67	67.42	75.27	81.02	81.30	74.26
20	77.45	73.30	82.63	77.37	77.64	74.88	80.07	89.36	57.56	70.69	83.07	81.00	75.64	80.03	72.16	82.36	72.69	75.40	80.03	80.36	74.82
30	77.98	74.15	83.01	77.48	77.76	75.98	79.76	87.56	60.56	73.57	81.79	82.53	75.69	81.19	72.36	82.48	75.37	76.25	79.86	80.23	76.24
40	79.27	77.53	83.31	79.14	79.14	77.58	81.63	87.86	64.22	76.31	81.61	84.56	77.67	83.05	74.26	82.39	77.00	78.41	80.49	80.43	78.66
50	81.26	80.32	84.13	81.00	81.21	80.14	82.67	89.57	67.56	79.62	83.33	86.87	79.52	85.52	76.41	82.50	78.52	81.10	82.08	81.28	81.77
60	83.47	83.00	85.42	82.83	83.45	82.10	84.81	91.13	70.41	81.72	84.94	88.98	81.70	87.58	77.67	83.88	80.45	83.65	83.71	82.65	84.49
70	85.32	85.20	86.64	85.15	85.20	84.23	86.45	91.45	72.53	83.91	86.12	91.52	83.15	88.64	78.78	85.12	83.05	84.88	84.89	84.42	86.46
80	87.56	87.10	87.35	86.90	87.31	86.07	88.30	92.54	74.55	85.85	87.59	93.41	85.50	91.01	80.63	87.43	84.65	87.44	86.80	85.91	88.73
90	88.76	88.96	88.74	88.59	88.79	87.60	90.28	93.30	76.44	87.06	88.80	94.76	87.24	92.85	81.95	88.70	85.51	89.57	88.46	87.24	89.91
100	90.18	90.40	89.72	90.06	90.33	89.21	91.46	94.62	78.29	88.79	90.27	95.65	87.81	94.27	83.32	90.58	87.62	91.18	90.39	89.38	91.06

IV. Topographic metric (%)

N.B. The design levels are the factorial points rather than the star points.

Time (000s yrs)		k_w		m_w		k_d		k_f		τ_c		n_{ci}		t_{ci}		s_{cr}		k_b		τ_b	
	Base case	+ 1	- 1	+ 1	- 1	+ 1	- 1	+ 1	- 1	+ 1	- 1	+ 1	- 1	+ 1	- 1	+ 1	- 1	+ 1	- 1	+ 1	- 1
10	19.95	20.78	18.98	19.96	19.94	20.48	19.33	26.51	11.22	15.41	24.22	18.63	20.21	18.92	21.05	19.13	22.22	20.44	19.41	19.40	20.55
20	21.30	22.70	19.55	21.32	21.30	21.94	20.56	27.47	12.62	16.71	25.71	19.78	21.50	19.99	22.45	19.63	23.20	22.02	20.40	20.37	22.22
30	22.32	23.63	20.44	22.23	22.22	22.78	21.73	28.74	13.25	17.61	26.90	20.93	22.48	21.14	23.45	20.56	23.96	22.88	21.40	21.45	23.02
40	22.85	24.42	21.04	22.83	22.79	23.38	22.36	29.69	13.69	18.07	27.58	21.52	23.21	21.71	24.28	21.34	24.70	23.54	22.11	22.12	23.56
50	23.34	25.10	21.48	23.29	23.33	23.97	22.66	30.55	13.96	18.49	28.36	21.79	23.84	22.04	25.09	21.93	25.44	23.99	22.54	22.47	24.13
60	23.86	25.54	21.82	23.71	23.82	24.40	23.18	31.12	14.20	18.72	28.98	22.06	24.40	22.32	25.70	22.37	26.15	24.52	23.00	22.96	24.56
70	24.26	25.70	22.06	24.23	24.21	24.90	23.51	31.37	14.35	18.93	29.47	22.31	24.81	22.47	26.28	22.61	26.68	24.62	23.37	23.50	24.82
80	24.61	26.00	22.29	24.44	24.53	25.12	23.82	31.77	14.47	19.06	29.88	22.54	25.27	22.79	26.74	22.98	27.07	25.02	23.84	23.91	25.19
90	24.76	26.13	22.55	24.72	24.76	25.29	24.09	32.03	14.58	19.07	30.32	22.68	25.51	22.99	27.16	23.04	27.32	25.35	24.08	24.12	25.31
100	24.91	26.21	22.74	24.91	24.94	25.54	24.17	32.46	14.62	19.14	30.75	22.72	25.56	23.01	27.45	23.15	27.57	25.50	24.30	24.48	25.31

APPENDIX H. DETAILS OF REGRESSION ANALYSIS FOR PRELIMINARY METAMODELS (Table 4.1 *q.v.*).

All regressions were carried out using normalised values (equation 4.03).

I. Sediment yield – list of predictors and analysis of variance

Predictor	Coef	SE Coef	T	P
Constant	-127.25	15.72	-8.10	0.000
kw	12.576	3.079	4.08	0.000
kw^2	-6.869	1.448	-4.74	0.000
kf	296.39	29.92	9.91	0.000
kf^1.5	-124.73	13.19	-9.46	0.000
tauc	-3.2075	0.7710	-4.16	0.000
nci	2.3310	0.5308	4.39	0.000
nci^2	-0.9874	0.1761	-5.61	0.000
tci	123.27	18.24	6.76	0.000
tci^2	-29.264	4.451	-6.57	0.000
scr	17.512	3.498	5.01	0.000
kw.kf	10.8608	0.9257	11.73	0.000
kw.tauc	-3.1010	0.4643	-6.68	0.000
kd.kf	1.48515	0.07156	20.75	0.000
kf.tauc	-3.2949	0.2314	-14.24	0.000
kf.nci	-2.0047	0.3719	-5.39	0.000
kf.tci	-136.77	18.86	-7.25	0.000
(kf.tci)^2	32.874	4.660	7.05	0.000
kf.scr	-48.150	6.802	-7.08	0.000
(kf.scr)^2	9.170	1.679	5.46	0.000
kf.kb	0.77897	0.04241	18.37	0.000
kf.tb	-0.52404	0.03180	-16.48	0.000
tauc.tci	0.9980	0.2428	4.11	0.000
tauc.scr	2.7921	0.5140	5.43	0.000

S = 0.118179 R-Sq = 99.9% R-Sq(adj) = 99.9%

Analysis of Variance

Source	DF	SS	MS	F	P
Regression	23	1666.457	72.455	5187.81	0.000
Residual Error	125	1.746	0.014		
Total	148	1668.202			

II. Drainage density – list of predictors and analysis of variance

Predictor	Coef	SE Coef	T	P
Constant	3.76525	0.04880	77.16	0.000
nci	-1.7345	0.1140	-15.22	0.000
f(tci)	-0.96062	0.02844	-33.78	0.000
kw.nci	0.8816	0.1481	5.95	0.000
(kw.nci)^2	-0.31716	0.05788	-5.48	0.000
(kw.tci)^2	-0.11571	0.02616	-4.42	0.000
kd.tauc	-0.050118	0.005661	-8.85	0.000
kf.nci	-0.27047	0.06783	-3.99	0.000
(kf.nci)^2	0.12657	0.03110	4.07	0.000
nci.tci	0.40185	0.06593	6.10	0.000
nci.scr	-0.2949	0.1281	-2.30	0.023
(nci.scr)^2	0.14821	0.05841	2.54	0.012

S = 0.0229225 R-Sq = 99.5% R-Sq(adj) = 99.5%

Analysis of Variance

Source	DF	SS	MS	F	P
Regression	11	15.3142	1.3922	2649.58	0.000
Residual Error	137	0.0720	0.0005		
Total	148	15.3862			

III. Sediment delivery ratio – list of predictors and analysis of variance

Predictor	Coef	SE Coef	T	P
Constant	-46.875	7.702	-6.09	0.000
kw^2	-6.676	1.588	-4.20	0.000
kf	-14.093	4.335	-3.25	0.001
kf^0.355	126.000	7.308	17.24	0.000
tauc^2	-1.0513	0.2202	-4.77	0.000
nci	11.887	2.419	4.91	0.000
tci^-1.08	-11.5893	0.8977	-12.91	0.000
scr	72.09	10.15	7.10	0.000
scr^2	-26.118	4.702	-5.55	0.000
kw.kd	-4.127	1.318	-3.13	0.002
kw.nci	5.138	1.940	2.65	0.009
kw.tci	14.447	2.029	7.12	0.000
kw.kb	-2.7162	0.8193	-3.32	0.001
kw.tb	1.9702	0.6508	3.03	0.003
kd.kf	3.415	1.241	2.75	0.007
kd.tauc	-1.8728	0.5658	-3.31	0.001
kf.tauc	1.2658	0.5350	2.37	0.020
kf.nci	-5.5912	0.9951	-5.62	0.000
kf.tci	-7.132	1.239	-5.76	0.000
kf.scr	-8.608	2.742	-3.14	0.002
tauc.tci	1.8314	0.5455	3.36	0.001
nci.tci	-5.612	1.014	-5.53	0.000
tci.scr	-6.456	2.196	-2.94	0.004
tci.kb	3.8528	0.7552	5.10	0.000
tci.tb	-2.0609	0.5743	-3.59	0.000
kb.tb	-0.9601	0.3875	-2.48	0.015

S = 0.316214 R-Sq = 99.1% R-Sq(adj) = 98.9%

Analysis of Variance

Source	DF	SS	MS	F	P
Regression	25	1392.234	55.689	556.94	0.000
Residual Error	123	12.299	0.100		
Total	148	1404.533			

IV. Output (from central composite design), metamodel fits and residuals.

	Sediment yield			Drainage density			Sediment delivery ratio		
Case no.	Output	Fit	Resid.	Output	Fit	Resid.	Output	Fit	Resid.
1 (Base)	24.91	24.88	0.04	3.150	3.143	0.007	90.18	90.36	-0.18
2	26.21	26.10	0.11	3.137	3.120	0.017	90.40	90.28	0.11
3	22.74	22.80	-0.06	3.133	3.112	0.021	89.72	89.60	0.11
4	24.91	24.88	0.04	3.169	3.143	0.026	90.06	90.36	-0.30
5	24.94	24.88	0.07	3.146	3.143	0.003	90.33	90.36	-0.03
6	25.54	25.54	0.00	3.144	3.121	0.023	89.21	89.21	-0.01
7	24.17	24.22	-0.04	3.138	3.165	-0.027	91.46	91.51	-0.05
8	32.46	32.44	0.03	3.185	3.166	0.019	94.62	94.50	0.12
9	14.62	14.59	0.03	3.173	3.183	-0.010	78.29	78.25	0.04
10	19.14	19.06	0.08	3.110	3.093	0.017	88.79	88.43	0.35
11	30.75	30.69	0.05	3.188	3.193	-0.005	90.27	90.19	0.08
12	22.72	22.73	-0.01	2.157	2.164	-0.007	95.65	95.37	0.28
13	25.56	25.43	0.13	3.680	3.643	0.037	87.81	87.67	0.14
14	23.01	22.99	0.01	2.468	2.472	-0.004	94.28	94.33	-0.06
15	27.45	27.40	0.05	4.258	4.249	0.009	83.32	83.00	0.32
16	23.15	23.20	-0.04	3.152	3.151	0.001	90.58	90.11	0.47
17	27.57	27.49	0.08	3.175	3.150	0.025	87.62	87.95	-0.32

	Sediment yield			Drainage density			Sediment delivery ratio		
Case no.	Output	Fit	Resid.	Output	Fit	Resid.	Output	Fit	Resid.
18	25.50	25.46	0.04	3.152	3.143	0.009	91.18	90.49	0.68
19	24.30	24.29	0.00	3.124	3.143	-0.019	90.40	90.23	0.17
20	24.48	24.35	0.12	3.124	3.143	-0.019	89.38	89.31	0.07
21	25.31	25.40	-0.09	3.148	3.143	0.005	91.06	91.41	-0.35
22	24.66	24.67	-0.01	2.687	2.687	0.000	93.83	93.78	0.05
23	23.61	23.53	0.08	2.722	2.712	0.010	93.39	93.64	-0.25
24	24.82	25.03	-0.21	2.699	2.687	0.012	94.66	94.64	0.02
25	23.43	23.17	0.26	2.728	2.712	0.016	93.20	92.86	0.33
26	25.38	25.16	0.22	2.690	2.694	-0.004	94.16	94.10	0.06
27	24.82	24.83	-0.01	2.704	2.719	-0.015	94.26	94.49	-0.23
28	25.45	25.52	-0.08	2.665	2.694	-0.029	94.45	94.70	-0.25
29	24.63	24.47	0.16	2.735	2.719	0.016	93.75	93.45	0.30
30	20.80	20.82	-0.02	2.659	2.664	-0.005	90.04	89.91	0.12
31	20.23	20.25	-0.02	2.662	2.689	-0.027	89.20	88.82	0.37
32	20.66	20.55	0.10	2.661	2.664	-0.003	89.39	89.31	0.09
33	20.38	20.51	-0.13	2.668	2.689	-0.021	90.09	89.86	0.22
34	19.90	19.90	0.01	2.689	2.692	-0.003	92.13	92.04	0.09
35	18.73	18.72	0.01	2.729	2.717	0.012	90.12	90.10	0.02
36	19.64	19.63	0.01	2.719	2.692	0.027	91.28	91.18	0.10
37	18.93	18.99	-0.06	2.716	2.717	-0.001	90.64	90.88	-0.24
38	29.78	29.57	0.21	2.703	2.711	-0.008	94.06	93.71	0.35
39	28.96	28.96	0.00	2.718	2.736	-0.018	94.12	94.26	-0.15
40	29.95	29.93	0.02	2.722	2.711	0.011	94.41	94.31	0.09
41	28.56	28.59	-0.03	2.744	2.736	0.008	93.25	93.22	0.02
42	27.75	27.93	-0.18	2.724	2.730	-0.006	93.79	94.66	-0.86
43	26.50	26.52	-0.01	2.764	2.755	0.009	94.56	94.35	0.21
44	28.13	28.30	-0.17	2.736	2.730	0.006	95.09	95.52	-0.42
45	26.12	26.15	-0.03	2.782	2.755	0.027	93.90	93.57	0.33
46	23.24	23.36	-0.12	2.676	2.708	-0.032	91.40	91.61	-0.21
47	21.82	21.91	-0.09	2.730	2.733	-0.003	88.99	89.83	-0.84
48	23.03	23.09	-0.07	2.714	2.708	0.006	90.59	90.74	-0.15
49	22.30	22.18	0.12	2.712	2.733	-0.021	90.66	90.61	0.05
50	23.81	23.84	-0.03	2.709	2.708	0.001	91.28	91.29	-0.01
51	22.99	22.98	0.01	2.788	2.732	0.056	89.98	90.04	-0.06
52	23.72	23.57	0.15	2.696	2.708	-0.012	90.90	90.69	0.21
53	23.30	23.25	0.05	2.739	2.732	0.007	91.16	91.08	0.08
54	26.93	27.12	-0.20	3.073	3.069	0.004	92.48	92.62	-0.14
55	25.35	25.26	0.08	3.067	3.071	-0.004	91.28	91.13	0.14
56	26.68	26.76	-0.08	3.071	3.069	0.002	92.02	91.76	0.26
57	25.56	25.62	-0.06	3.066	3.071	-0.005	91.98	91.91	0.07
58	24.88	24.91	-0.03	3.096	3.081	0.015	93.45	93.36	0.09
59	23.81	23.86	-0.05	3.068	3.083	-0.015	92.34	92.40	-0.06
60	24.62	24.55	0.07	3.048	3.081	-0.033	92.71	92.76	-0.05
61	24.21	24.22	-0.01	3.119	3.083	0.036	93.70	93.44	0.26
62	20.26	20.18	0.08	3.121	3.079	0.042	87.57	87.69	-0.13
63	20.11	20.14	-0.04	3.061	3.081	-0.020	88.55	88.53	0.02
64	20.46	20.45	0.01	3.111	3.079	0.032	88.60	88.29	0.30
65	19.77	19.87	-0.10	3.087	3.081	0.006	87.10	87.50	-0.40
66	21.03	21.03	0.00	3.137	3.102	0.036	88.21	88.18	0.02
67	20.38	20.39	-0.02	3.118	3.104	0.015	87.86	88.17	-0.31

	Sediment yield			Drainage density			Sediment delivery ratio		
Case no.	Output	Fit	Resid.	Output	Fit	Resid.	Output	Fit	Resid.
68	21.20	21.30	-0.10	3.116	3.102	0.015	89.07	89.05	0.02
69	20.11	20.13	-0.02	3.082	3.104	-0.022	86.77	87.39	-0.62
70	28.95	29.09	-0.15	3.064	3.098	-0.034	92.78	92.97	-0.19
71	27.87	27.76	0.11	3.087	3.100	-0.013	92.45	92.17	0.28
72	28.70	28.73	-0.03	3.080	3.098	-0.018	92.18	92.37	-0.19
73	28.17	28.12	0.05	3.073	3.100	-0.027	93.03	93.21	-0.18
74	30.64	30.62	0.03	3.102	3.113	-0.011	93.19	93.50	-0.31
75	28.25	28.48	-0.22	3.123	3.115	0.008	91.41	91.85	-0.43
76	30.37	30.26	0.11	3.135	3.113	0.022	92.77	92.64	0.13
77	28.86	28.84	0.03	3.098	3.115	-0.017	92.88	92.62	0.25
78	24.67	24.72	-0.05	3.111	3.118	-0.007	87.76	87.75	0.01
79	23.91	23.81	0.10	3.139	3.120	0.019	88.44	87.90	0.54
80	24.90	24.99	-0.09	3.088	3.118	-0.030	88.56	88.61	-0.05
81	23.67	23.54	0.13	3.091	3.120	-0.029	87.64	87.12	0.52
82	23.03	22.97	0.05	3.102	3.122	-0.020	89.03	89.07	-0.04
83	22.76	22.65	0.11	3.122	3.124	-0.002	90.22	89.75	0.47
84	23.25	23.24	0.00	3.137	3.122	0.015	89.97	89.67	0.29
85	22.26	22.39	-0.13	3.106	3.124	-0.018	88.57	88.71	-0.14
86	25.76	25.77	-0.01	3.153	3.144	0.009	91.67	91.36	0.31
87	24.71	24.71	-0.01	3.163	3.148	0.015	90.48	90.75	-0.27
88	25.47	25.41	0.06	3.124	3.144	-0.020	91.10	91.11	-0.01
89	25.22	25.08	0.14	3.163	3.148	0.015	91.22	91.43	-0.22
90	27.01	27.07	-0.06	3.135	3.151	-0.016	91.36	91.44	-0.08
91	25.18	25.21	-0.03	3.130	3.156	-0.026	90.92	90.97	-0.05
92	26.72	26.71	0.01	3.133	3.151	-0.018	91.12	90.93	0.19
93	25.64	25.57	0.07	3.147	3.156	-0.009	91.81	91.39	0.42
94	21.71	21.67	0.04	3.170	3.121	0.049	85.74	85.52	0.21
95	21.11	21.03	0.08	3.113	3.126	-0.013	86.30	86.15	0.15
96	21.86	21.94	-0.07	3.115	3.121	-0.006	86.31	86.03	0.28
97	20.73	20.76	-0.03	3.136	3.126	0.010	85.39	85.73	-0.34
98	20.24	20.15	0.09	3.149	3.149	0.000	87.88	87.89	-0.01
99	20.21	20.10	0.10	3.152	3.153	-0.001	88.14	88.05	0.09
100	20.41	20.41	0.00	3.144	3.149	-0.005	88.18	88.14	0.04
101	19.80	19.84	-0.04	3.142	3.153	-0.011	87.10	87.37	-0.27
102	31.72	31.65	0.08	3.175	3.168	0.007	91.80	91.36	0.44
103	29.31	29.50	-0.19	3.173	3.172	0.001	90.80	91.06	-0.25
104	30.90	31.28	-0.39	3.196	3.168	0.028	90.14	90.86	-0.71
105	29.87	29.87	0.00	3.152	3.172	-0.020	91.73	91.48	0.24
106	29.21	29.21	0.00	3.180	3.187	-0.007	92.85	92.55	0.31
107	27.76	27.87	-0.12	3.182	3.192	-0.010	91.31	91.78	-0.47
108	28.81	28.84	-0.03	3.174	3.187	-0.013	92.13	92.30	-0.17
109	28.45	28.23	0.21	3.206	3.192	0.014	92.51	92.46	0.05
110	23.82	23.78	0.04	3.186	3.165	0.021	87.63	87.77	-0.14
111	23.66	23.46	0.20	3.151	3.170	-0.019	87.78	88.10	-0.32
112	23.99	24.05	-0.06	3.147	3.165	-0.018	87.90	88.02	-0.12
113	23.24	23.19	0.04	3.157	3.170	-0.013	87.33	87.41	-0.09
114	24.73	24.86	-0.13	3.203	3.164	0.039	86.96	87.22	-0.26
115	23.85	23.94	-0.09	3.224	3.169	0.055	87.58	87.68	-0.10
116	24.99	25.12	-0.13	3.148	3.164	-0.016	87.62	87.73	-0.11
117	23.65	23.67	-0.02	3.135	3.169	-0.034	87.86	87.26	0.60

	Sediment yield			Drainage density			Sediment delivery ratio		
Case no.	Output	Fit	Resid.	Output	Fit	Resid.	Output	Fit	Resid.
118	27.43	27.50	-0.07	3.537	3.569	-0.032	87.86	88.24	-0.38
119	27.35	27.17	0.18	3.553	3.551	0.002	89.06	88.85	0.21
120	27.73	27.86	-0.14	3.528	3.569	-0.041	88.23	88.49	-0.26
121	26.63	26.81	-0.18	3.591	3.551	0.040	87.94	88.17	-0.23
122	26.09	26.10	-0.01	3.562	3.581	-0.019	89.16	89.24	-0.09
123	24.75	24.96	-0.21	3.569	3.563	0.006	89.68	89.99	-0.31
124	26.50	26.46	0.05	3.569	3.581	-0.012	89.97	89.75	0.22
125	24.50	24.60	-0.10	3.541	3.563	-0.022	89.48	89.57	-0.08
126	21.45	21.56	-0.11	3.619	3.579	0.040	83.52	84.07	-0.55
127	20.42	20.39	0.03	3.550	3.560	-0.010	84.62	84.05	0.57
128	21.27	21.30	-0.03	3.585	3.579	0.006	83.45	83.56	-0.11
129	20.60	20.66	-0.06	3.513	3.560	-0.047	84.18	84.47	-0.29
130	21.88	21.82	0.07	3.599	3.601	-0.002	84.04	84.30	-0.26
131	21.20	21.24	-0.04	3.534	3.583	-0.049	83.51	83.81	-0.30
132	21.64	21.55	0.09	3.563	3.601	-0.038	83.83	84.05	-0.22
133	21.49	21.51	-0.02	3.561	3.583	-0.022	84.33	84.50	-0.17
134	30.73	30.45	0.29	3.602	3.598	0.004	89.97	89.17	0.80
135	28.97	29.03	-0.06	3.587	3.580	0.007	89.69	90.08	-0.39
136	31.12	30.81	0.31	3.590	3.598	-0.008	89.91	89.67	0.24
137	28.40	28.67	-0.26	3.567	3.580	-0.013	89.25	89.66	-0.41
138	31.18	31.17	0.02	3.564	3.612	-0.048	89.73	89.43	0.29
139	30.87	30.56	0.32	3.645	3.594	0.051	89.99	89.88	0.11
140	31.60	31.53	0.07	3.656	3.612	0.044	89.70	89.68	0.02
141	30.09	30.19	-0.11	3.622	3.594	0.028	89.24	89.20	0.04
142	25.59	25.68	-0.09	3.604	3.618	-0.014	83.82	84.18	-0.36
143	24.79	24.82	-0.04	3.611	3.600	0.011	84.12	83.86	0.26
144	25.39	25.41	-0.02	3.585	3.618	-0.033	83.98	83.93	0.05
145	25.16	25.09	0.07	3.618	3.600	0.018	84.26	84.54	-0.28
146	24.62	24.53	0.09	3.644	3.622	0.022	85.71	85.76	-0.05
147	22.97	23.07	-0.10	3.609	3.604	0.005	85.85	85.58	0.27
148	24.24	24.26	-0.02	3.673	3.622	0.051	85.59	85.25	0.34
149	23.30	23.34	-0.04	3.605	3.604	0.001	86.43	86.00	0.43

APPENDIX I. TESTS OF THE PRELIMINARY METAMODELS – PLANNING MATRIX FOR EACH TEST SET AND RESULTS

I. Cases run to test the sediment yield metamodel

Para-meter	k_w	m_w	k_d	k_f	τ_c	n_{ci}	t_{ci}	s_{cr}	k_b $\times 10^{-6}$	τ_b	Result (GOLEM output)	Predicted	Difference
Case													
201	0.000252	0.345	0.00384	0.0004009	4.65	0.3747	11610	0.648	13.31	3.4	24.790	24.911	-0.121
202	0.000234	0.345	0.00336	0.0004799	7.35	0.4293	11610	0.606	13.31	3.4	25.076	24.913	0.164
203	0.000234	0.315	0.00384	0.0004342	6.45	0.3567	11610	0.606	16.69	3.4	24.814	24.913	-0.099
204	0.000246	0.345	0.00336	0.0004176	4.65	0.4293	13489	0.606	13.31	3.4	25.194	24.914	0.280
205	0.000234	0.345	0.00336	0.0003802	7.50	0.4567	13489	0.648	13.31	4.6	19.953	20.020	-0.067
206	0.000228	0.345	0.00336	0.0003885	7.65	0.4567	13489	0.648	13.31	4.6	20.031	20.020	0.011
207	0.000228	0.345	0.00336	0.0003802	7.65	0.4567	12862	0.648	13.31	4.6	19.876	19.967	-0.091
208	0.000228	0.315	0.00336	0.0003885	6.60	0.3747	13489	0.648	13.31	4.6	21.192	21.201	-0.009
209	0.000234	0.345	0.00336	0.0003968	7.65	0.4567	13489	0.592	13.31	3.4	21.216	21.200	0.015
210	0.000246	0.315	0.00384	0.0003802	7.50	0.4567	11610	0.634	16.69	4.6	20.976	21.202	-0.226
211	0.000228	0.345	0.00384	0.0003926	5.70	0.4293	12862	0.648	13.31	3.4	22.424	22.439	-0.016
212	0.000246	0.315	0.00336	0.0004176	7.50	0.3747	11610	0.648	13.31	4.6	22.431	22.441	-0.010
213	0.000234	0.345	0.00336	0.0004300	6.90	0.4293	12862	0.648	13.31	4.6	22.551	22.439	0.112
214	0.000246	0.315	0.00384	0.0003843	4.65	0.3747	12862	0.648	13.31	3.4	23.523	23.679	-0.156
215	0.000246	0.345	0.00336	0.0004799	7.65	0.4567	13489	0.634	13.31	3.4	23.986	23.679	0.307
216	0.000228	0.315	0.00384	0.0004217	7.20	0.4293	11150	0.592	16.69	3.4	23.577	23.679	-0.103
217	0.000252	0.315	0.00336	0.0004259	4.35	0.4293	11150	0.634	16.69	3.4	26.392	26.411	-0.019
218	0.000246	0.315	0.00384	0.0004799	6.60	0.3747	12862	0.592	16.69	3.4	26.441	26.410	0.031
219	0.000252	0.345	0.00336	0.0004508	5.25	0.3747	13489	0.592	16.69	3.4	26.603	26.409	0.193
220	0.000246	0.345	0.00384	0.0005048	5.70	0.4293	13489	0.592	16.69	3.4	28.037	27.899	0.138
221	0.000234	0.315	0.00336	0.0004841	4.35	0.3567	11610	0.648	16.69	3.4	28.222	27.901	0.321
222	0.000252	0.345	0.00384	0.0004799	4.80	0.4567	12862	0.592	13.31	3.4	28.163	27.900	0.263
223	0.000252	0.315	0.00336	0.0005007	5.10	0.3567	11150	0.592	13.31	3.4	29.499	29.400	0.099
224	0.000252	0.315	0.00384	0.0004882	4.35	0.4293	11150	0.606	16.69	4.6	29.489	29.399	0.090
225	0.000252	0.345	0.00336	0.0004965	4.35	0.3747	12862	0.592	16.69	3.4	29.710	29.399	0.311
226	0.000252	0.315	0.00336	0.0005048	4.35	0.3567	11150	0.592	16.69	3.4	31.000	30.578	0.422

227	0.000252	0.315	0.00384	0.0005048	4.35	0.3747	11150	0.592	13.31	3.4	30.597	30.525	0.071
228	0.000252	0.315	0.00384	0.0005048	4.35	0.3567	11150	0.606	16.69	3.4	30.710	30.526	0.185
229	0.000249	0.345	0.00384	0.0004753	5.10	0.3664	11392	0.599	16.69	3.4	28.362	28.464	-0.102
230	0.000231	0.315	0.00336	0.0004089	6.90	0.4411	13142	0.641	13.31	4.6	21.677	21.626	0.052
231	0.000231	0.345	0.00384	0.0004753	6.90	0.3664	13142	0.641	13.31	3.4	24.519	24.454	0.065
232	0.000249	0.315	0.00336	0.0004089	5.10	0.4411	11392	0.599	16.69	4.6	24.898	25.117	-0.219

II. Cases run to test the drainage density metamodel

Para-meter Case	k_w	m_w	k_d	k_f	τ_c	n_{ci}	t_{ci}	s_{cr}	k_b $\times 10^{-6}$	τ_b	Result (GOLEM output)	Predicted	Difference
301	0.000229	0.31	0.00322	0.000487	7.08	0.4567	11116	0.592	16.12	4.4	3.180	3.150	0.030
302	0.000229	0.35	0.00389	0.000420	4.92	0.3793	12706	0.606	13.88	3.2	3.148	3.150	-0.002
303	0.000251	0.32	0.00350	0.000487	6.36	0.4088	12032	0.592	12.75	4.4	3.126	3.150	-0.024
304	0.000254	0.34	0.00389	0.000465	4.92	0.3510	13293	0.634	12.75	3.2	3.158	3.150	0.008
305	0.000233	0.31	0.00398	0.000420	7.44	0.4772	13645	0.634	12.75	3.6	2.776	2.760	0.016
306	0.000244	0.31	0.00389	0.000420	7.08	0.4635	13998	0.634	16.12	3.6	2.757	2.760	-0.003
307	0.000251	0.34	0.00379	0.000420	5.64	0.4703	13880	0.606	16.12	4.4	2.758	2.760	-0.002
308	0.000226	0.35	0.00341	0.000398	7.44	0.4293	13998	0.592	16.12	3.2	2.867	2.860	0.007
309	0.000226	0.34	0.00379	0.000487	4.56	0.4703	13176	0.592	12.75	4.4	2.887	2.860	0.027
310	0.000251	0.32	0.00398	0.000398	5.64	0.4430	13645	0.634	12.75	3.2	2.884	2.860	0.024
311	0.000251	0.35	0.00370	0.000398	5.28	0.4362	13058	0.592	13.88	4.4	2.947	2.950	-0.003
312	0.000251	0.34	0.00389	0.000420	7.08	0.3907	13998	0.648	16.12	3.2	2.955	2.950	0.005
313	0.000254	0.31	0.00350	0.000465	4.56	0.4703	12353	0.634	12.75	3.2	2.957	2.950	0.007
314	0.000226	0.32	0.00331	0.000487	7.44	0.4225	12471	0.634	13.88	4.8	3.053	3.050	0.003
315	0.000233	0.34	0.00379	0.000420	7.44	0.3623	13763	0.648	12.75	3.6	3.042	3.050	-0.008
316	0.000244	0.32	0.00331	0.000487	6.36	0.4567	11829	0.606	12.75	3.6	3.064	3.050	0.014
317	0.000233	0.34	0.00341	0.000420	6.36	0.3397	12706	0.634	17.25	4.8	3.210	3.250	-0.040
318	0.000244	0.31	0.00322	0.000398	5.28	0.4498	10709	0.634	12.75	3.6	3.253	3.250	0.003
319	0.000251	0.34	0.00398	0.000420	7.08	0.3793	11829	0.606	17.25	4.4	3.266	3.250	0.016
320	0.000251	0.34	0.00350	0.000420	4.56	0.3952	11014	0.592	17.25	4.8	3.383	3.360	0.023
321	0.000251	0.31	0.00389	0.000465	6.72	0.3397	11829	0.634	16.12	3.2	3.366	3.360	0.006

322	0.000254	0.34	0.00398	0.000487	6.72	0.3737	11218	0.606	16.12	3.2	3.379	3.360	0.019
323	0.000233	0.32	0.00331	0.000420	4.92	0.3397	11320	0.634	13.88	4.4	3.453	3.460	-0.007
324	0.000236	0.31	0.00398	0.000420	4.56	0.3397	11320	0.592	12.75	4.8	3.476	3.460	0.016
325	0.000247	0.35	0.00322	0.000420	4.56	0.3737	10811	0.592	17.25	3.6	3.496	3.460	0.036
326	0.000254	0.32	0.00379	0.000398	5.28	0.3397	10709	0.592	12.75	4.8	3.583	3.570	0.013
327	0.000254	0.35	0.00322	0.000398	4.56	0.3385	10788	0.606	13.88	4.8	3.557	3.570	-0.013
328	0.000254	0.32	0.00331	0.000398	4.56	0.3385	10788	0.592	17.25	3.2	3.547	3.570	-0.023
329	0.000231	0.345	0.00336	0.000409	5.10	0.3680	11422	0.641	13.31	4.6	3.342	3.364	-0.022
330	0.000249	0.315	0.00384	0.000475	6.90	0.4430	13176	0.599	16.69	3.4	2.904	2.903	0.001
331	0.000249	0.345	0.00384	0.000409	6.90	0.3680	13176	0.641	16.69	4.6	3.105	3.108	-0.002
332	0.000231	0.315	0.00336	0.000475	5.10	0.4430	11422	0.599	13.31	3.4	3.146	3.154	-0.008

III. Cases run to test the sediment yield metamodel

Para-meter Case	k_w	m_w	k_d	k_f	τ_c	n_{ci}	t_{ci}	s_{cr}	k_b $\times 10^{-6}$	τ_b	Result (GOLEM output)	Predicted	Difference
401	0.000249	0.305	0.00392	0.000502	4.8	0.3680	10879	0.606	13.30	3.2	89.770	90.188	-0.419
402	0.000249	0.325	0.00328	0.000406	7.2	0.4430	12549	0.606	16.70	3.6	90.038	90.193	-0.156
403	0.000231	0.345	0.00376	0.000435	5.4	0.3680	12862	0.592	16.70	3.2	89.945	90.173	-0.229
404	0.000231	0.335	0.00328	0.000435	5.4	0.4430	11422	0.648	16.70	4.8	90.087	90.174	-0.087
405	0.000231	0.355	0.00392	0.000391	7.2	0.3510	10879	0.592	16.70	4.8	84.705	84.996	-0.291
406	0.000249	0.315	0.00392	0.000383	6.6	0.3510	11150	0.592	16.70	4.4	85.171	85.181	-0.010
407	0.000249	0.305	0.00392	0.000383	7.2	0.3680	10879	0.592	16.70	3.2	85.148	85.193	-0.045
408	0.000231	0.325	0.00344	0.000383	5.4	0.3510	11422	0.592	16.70	4.8	86.320	86.122	0.198
409	0.000231	0.345	0.00344	0.000383	6.6	0.3510	10879	0.648	13.30	3.6	86.477	86.124	0.353
410	0.000249	0.335	0.00392	0.000406	6.6	0.3680	10879	0.592	13.30	4.8	86.547	86.161	0.386
411	0.000231	0.355	0.00392	0.000383	5.4	0.3680	12862	0.592	13.30	4.8	87.388	87.473	-0.085
412	0.000249	0.315	0.00328	0.000420	6.6	0.3815	10879	0.592	16.70	4.4	87.424	87.478	-0.054
413	0.000249	0.305	0.00392	0.000383	7.2	0.4635	10879	0.634	13.30	3.2	87.097	87.474	-0.378
414	0.000231	0.325	0.00328	0.000465	7.2	0.3510	10879	0.634	13.30	4.8	88.844	88.841	0.003
415	0.000231	0.345	0.00344	0.000391	4.8	0.3510	13802	0.606	13.30	4.8	89.019	88.838	0.181
416	0.000249	0.335	0.00376	0.000406	4.8	0.4635	11422	0.592	16.70	4.8	88.464	88.847	-0.383

417	0.000231	0.355	0.00344	0.000465	5.4	0.4430	11422	0.634	13.30	3.6	90.851	91.169	-0.318
418	0.000231	0.315	0.00376	0.000465	5.4	0.3510	13176	0.606	16.70	3.6	91.521	91.171	0.350
419	0.000249	0.305	0.00392	0.000435	6.6	0.4430	12862	0.634	13.30	3.6	91.117	91.156	-0.039
420	0.000231	0.325	0.00344	0.000487	6.6	0.4635	11693	0.648	13.30	3.6	91.498	92.144	-0.645
421	0.000249	0.345	0.00376	0.000494	6.6	0.3680	13802	0.592	16.70	4.8	92.196	92.135	0.061
422	0.000249	0.335	0.00392	0.000435	4.8	0.4430	13802	0.648	13.30	3.6	91.764	92.136	-0.372
423	0.000231	0.355	0.00344	0.000502	6.6	0.4225	13802	0.648	16.70	4.8	92.670	93.138	-0.468
424	0.000249	0.315	0.00344	0.000487	4.8	0.4635	12862	0.634	13.30	4.4	92.783	93.133	-0.350
425	0.000249	0.305	0.00376	0.000457	5.4	0.4635	13802	0.634	13.30	3.2	92.610	93.123	-0.513
426	0.000249	0.325	0.00328	0.000487	4.8	0.4635	13802	0.634	13.30	3.2	94.086	94.112	-0.026
427	0.000249	0.345	0.00328	0.000502	5.4	0.4635	13489	0.592	16.70	3.2	94.548	94.121	0.427
428	0.000249	0.305	0.00344	0.000502	7.2	0.4430	13802	0.648	16.70	3.2	94.101	94.119	-0.019

APPENDIX J. PLANNING MATRIX - ADDITIONAL SIMULATIONS (originally run to aid estimation of parameter main effects and to derive more complete mathematical formulation of interaction terms for the topographic metric metamodel)

Para-meter	k_w	m_w	k_d	k_f	τ_c	n_{ci}	t_{ci}	s_{cr}	k_b $\times 10^{-6}$	τ_b
Case no.										
233	0.000240	0.33	0.00360	0.000442	6.0	0.402	10607	0.62	15	4.0
234	0.000240	0.33	0.00360	0.000442	6.0	0.402	14115	0.62	15	4.0
235	0.000240	0.33	0.00360	0.000442	6.0	0.402	12236	0.578	15	4.0
236	0.000240	0.33	0.00360	0.000442	6.0	0.402	12236	0.662	15	4.0
237	0.000258	0.33	0.00360	0.000442	6.0	0.402	12236	0.62	15	4.0
238	0.000222	0.33	0.00360	0.000442	6.0	0.402	12236	0.62	15	4.0
239	0.000240	0.33	0.00408	0.000442	6.0	0.402	12236	0.62	15	4.0
240	0.000240	0.33	0.00312	0.000442	6.0	0.402	12236	0.62	15	4.0
241	0.000240	0.33	0.00360	0.000509	6.0	0.402	12236	0.62	15	4.0
242	0.000240	0.33	0.00360	0.000376	6.0	0.402	12236	0.62	15	4.0
243	0.000240	0.33	0.00360	0.000442	7.8	0.402	12236	0.62	15	4.0
244	0.000240	0.33	0.00360	0.000442	4.2	0.402	12236	0.62	15	4.0
245	0.000240	0.33	0.00360	0.000442	6.0	0.484	12236	0.62	15	4.0
246	0.000240	0.33	0.00360	0.000442	6.0	0.334	12236	0.62	15	4.0
247	0.000240	0.33	0.00360	0.000442	6.0	0.402	12236	0.62	18.375	4.0
248	0.000240	0.33	0.00360	0.000442	6.0	0.402	12236	0.62	11.625	4.0
249	0.000240	0.33	0.00360	0.000442	6.0	0.402	12236	0.62	15	5.2
250	0.000240	0.33	0.00360	0.000442	6.0	0.402	12236	0.62	15	2.8
251	0.000246	0.33	0.00360	0.000442	6.0	0.402	12236	0.62	15	4.0
252	0.000234	0.33	0.00360	0.000442	6.0	0.402	12236	0.62	15	4.0
253	0.000240	0.34	0.00360	0.000442	6.0	0.402	12236	0.62	15	4.0
254	0.000240	0.32	0.00360	0.000442	6.0	0.402	12236	0.62	15	4.0
255	0.000240	0.33	0.00376	0.000442	6.0	0.402	12236	0.62	15	4.0
256	0.000240	0.33	0.00344	0.000442	6.0	0.402	12236	0.62	15	4.0
257	0.000240	0.33	0.00360	0.000464	6.0	0.402	12236	0.62	15	4.0
258	0.000240	0.33	0.00360	0.000420	6.0	0.402	12236	0.62	15	4.0
259	0.000240	0.33	0.00360	0.000442	6.6	0.402	12236	0.62	15	4.0
260	0.000240	0.33	0.00360	0.000442	5.4	0.402	12236	0.62	15	4.0

261	0.000240	0.33	0.00360	0.000442	6.0	0.428	12236	0.62	15	4.0
262	0.000240	0.33	0.00360	0.000442	6.0	0.378	12236	0.62	15	4.0
263	0.000240	0.33	0.00360	0.000442	6.0	0.402	12833	0.62	15	4.0
264	0.000240	0.33	0.00360	0.000442	6.0	0.402	11667	0.62	15	4.0
265	0.000240	0.33	0.00360	0.000442	6.0	0.402	12236	0.634	15	4.0
266	0.000240	0.33	0.00360	0.000442	6.0	0.402	12236	0.606	15	4.0
267	0.000240	0.33	0.00360	0.000442	6.0	0.402	12236	0.62	16.13	4.0
268	0.000240	0.33	0.00360	0.000442	6.0	0.402	12236	0.62	13.88	4.0
269	0.000240	0.33	0.00360	0.000442	6.0	0.402	12236	0.62	15	4.4
270	0.000240	0.33	0.00360	0.000442	6.0	0.402	12236	0.62	15	3.6
501	0.000255	0.33	0.00360	0.000442	6.0	0.402	12236	0.62	15	4.0
502	0.000252	0.33	0.00360	0.000442	6.0	0.402	12236	0.62	15	4.0
503	0.000249	0.33	0.00360	0.000442	6.0	0.402	12236	0.62	15	4.0
504	0.000231	0.33	0.00360	0.000442	6.0	0.402	12236	0.62	15	4.0
505	0.000228	0.33	0.00360	0.000442	6.0	0.402	12236	0.62	15	4.0
506	0.000225	0.33	0.00360	0.000442	6.0	0.402	12236	0.62	15	4.0
507	0.000240	0.33	0.00360	0.000497	6.0	0.402	12236	0.62	15	4.0
508	0.000240	0.33	0.00360	0.000486	6.0	0.402	12236	0.62	15	4.0
509	0.000240	0.33	0.00360	0.000475	6.0	0.402	12236	0.62	15	4.0
510	0.000240	0.33	0.00360	0.000409	6.0	0.402	12236	0.62	15	4.0
511	0.000240	0.33	0.00360	0.000398	6.0	0.402	12236	0.62	15	4.0
512	0.000240	0.33	0.00360	0.000387	6.0	0.402	12236	0.62	15	4.0
513	0.000240	0.33	0.00360	0.000442	7.4	0.402	12236	0.62	15	4.0
514	0.000240	0.33	0.00360	0.000442	7.0	0.402	12236	0.62	15	4.0
515	0.000240	0.33	0.00360	0.000442	5.0	0.402	12236	0.62	15	4.0
516	0.000240	0.33	0.00360	0.000442	4.6	0.402	12236	0.62	15	4.0
517	0.000240	0.33	0.00360	0.000442	6.0	0.455	12236	0.62	15	4.0
518	0.000240	0.33	0.00360	0.000442	6.0	0.355	12236	0.62	15	4.0
519	0.000240	0.33	0.00360	0.000442	6.0	0.402	13674	0.62	15	4.0
520	0.000240	0.33	0.00360	0.000442	6.0	0.402	13248	0.62	15	4.0
521	0.000240	0.33	0.00360	0.000442	6.0	0.402	12531	0.62	15	4.0
522	0.000240	0.33	0.00360	0.000442	6.0	0.402	11948	0.62	15	4.0
523	0.000240	0.33	0.00360	0.000442	6.0	0.402	11302	0.62	15	4.0
524	0.000240	0.33	0.00360	0.000442	6.0	0.402	10949	0.62	15	4.0
525	0.000240	0.33	0.00360	0.000442	6.0	0.402	12236	0.655	15	4.0

526	0.000240	0.33	0.00360	0.000442	6.0	0.402	12236	0.648	15	4.0
527	0.000240	0.33	0.00360	0.000442	6.0	0.402	12236	0.641	15	4.0
528	0.000240	0.33	0.00360	0.000442	6.0	0.402	12236	0.599	15	4.0
529	0.000240	0.33	0.00360	0.000442	6.0	0.402	12236	0.592	15	4.0
530	0.000240	0.33	0.00360	0.000442	6.0	0.402	12236	0.585	15	4.0
531	0.000240	0.33	0.00360	0.000442	6.0	0.402	12236	0.62	17.25	4.0
532	0.000240	0.33	0.00360	0.000442	6.0	0.402	12236	0.62	12.75	4.0
533	0.000240	0.33	0.00360	0.000442	6.0	0.402	12236	0.62	15	4.8
534	0.000240	0.33	0.00360	0.000442	6.0	0.402	12236	0.62	15	3.2
535	0.000240	0.33	0.00360	0.000509	6.0	0.402	12236	0.662	15	4.0
536	0.000240	0.33	0.00360	0.000375	6.0	0.402	12236	0.662	15	4.0
537	0.000240	0.33	0.00360	0.000509	6.0	0.402	12236	0.578	15	4.0
538	0.000240	0.33	0.00360	0.000375	6.0	0.402	12236	0.578	15	4.0
539	0.000240	0.33	0.00360	0.000475	6.0	0.402	12236	0.662	15	4.0
540	0.000240	0.33	0.00360	0.000409	6.0	0.402	12236	0.662	15	4.0
541	0.000240	0.33	0.00360	0.000475	6.0	0.402	12236	0.578	15	4.0
542	0.000240	0.33	0.00360	0.000409	6.0	0.402	12236	0.578	15	4.0
543	0.000240	0.33	0.00360	0.000509	6.0	0.402	12236	0.641	15	4.0
544	0.000240	0.33	0.00360	0.000375	6.0	0.402	12236	0.641	15	4.0
545	0.000240	0.33	0.00360	0.000509	6.0	0.402	12236	0.599	15	4.0
546	0.000240	0.33	0.00360	0.000375	6.0	0.402	12236	0.599	15	4.0
547	0.000240	0.33	0.00360	0.000475	6.0	0.402	12236	0.641	15	4.0
548	0.000240	0.33	0.00360	0.000409	6.0	0.402	12236	0.641	15	4.0
549	0.000240	0.33	0.00360	0.000475	6.0	0.402	12236	0.599	15	4.0
550	0.000240	0.33	0.00360	0.000409	6.0	0.402	12236	0.599	15	4.0

APPENDIX K. REGRESSION ANALYSES FOR THE FINAL METAMODELS (Tables 4.2 and 4.3 *q.v.*).

I. Notes

1. All of the regressions for the sediment yield, drainage density and sediment delivery ratio metamodels, including those by which the components used in the former two were derived (subsection 4.5.1 *q.v.*), were conducted using 1-centred, 0.2-scaled values, calculated according to equation 4.05.
2. M_x components (equation 4.04 *q.v.*) of the sediment yield and drainage density metamodels are listed in Table 4.2 and were derived from the base case and relevant main effects parameter cases for each parameter.
3. The topographic metric metamodel was derived using 0-centred, 1-scaled values, calculated according to equation 4.01.

II. Sediment yield – list of predictors and analysis of variance

Predictor	Coef	SE Coef	T	P
Constant	-26.4751	0.3252	-81.42	0.000
ln(Mkf)	0.997412	0.00310	321.04	0.000
ln(Mtauc)	1.01142	0.00495	204.28	0.000
ln(Mtci)	0.99548	0.01597	62.35	0.000
ln(Mscr)	0.98644	0.01365	72.24	0.000
ln(Mkw)	1.03899	0.01845	56.31	0.000
ln(Mnci)	1.01930	0.02628	38.79	0.000
ln(Mkd)	0.95609	0.04331	22.07	0.000
ln(Mkb)	0.96383	0.05107	18.87	0.000
ln(Mtb)	1.26152	0.06966	18.11	0.000

S = 0.004758 R-Sq = 99.8% R-Sq(adj) = 99.8%

Analysis of Variance

Source	DF	SS	MS	F	P
Regression	9	3.91817	0.43535	19229.23	0.000
Residual Error	319	0.00722	0.00002		
Total	328	3.92539			

III. Drainage density – list of predictors and analysis of variance

Predictor	Coef	SE Coef	T	P
Constant	-2.5173	0.1417	-17.77	0.000
ln(Mtci)	1.00543	0.00657	153.02	0.000
ln(Mnci)	0.996994	0.007371	135.26	0.000
ln(Mtauc)	1.1932	0.1238	9.64	0.000
ln(kb)	0.006305	0.002436	2.59	0.010

S = 0.006823 R-Sq = 99.3% R-Sq(adj) = 99.3%

Analysis of Variance

Source	DF	SS	MS	F	P
Regression	4	2.09079	0.52270	11229.37	0.000
Residual Error	324	0.01508	0.00005		
Total	328	2.10587			

IV. Sediment delivery ratio – list of predictors and analysis of variance

Predictor	Coef	SE Coef	T	P
Constant	103.944	0.890	116.84	0.000
kf^-1	-12.4695	0.5957	-20.93	0.000
nci^1.3	4.4700	0.6280	7.12	0.000
ln(tci)	12.2402	0.6742	18.15	0.000
scr^-0.8	-1.8176	0.1336	-13.61	0.000
tauc^3	-0.64724	0.05376	-12.04	0.000
kd*tci*tb	-1.63302	0.08994	-18.16	0.000
kf*nci*tci	-4.7859	0.5164	-9.27	0.000
kw*tauc*nci	2.0327	0.5621	3.62	0.000
kw*tauc	-4.3637	0.7745	-5.63	0.000
kw*tauc*tci	2.8696	0.5114	5.61	0.000
kf*nci	2.6974	0.8143	3.31	0.001

S = 0.3460 R-Sq = 97.9% R-Sq(adj) = 97.8%

Analysis of Variance

Source	DF	SS	MS	F	P
Regression	11	1759.34	159.94	1335.76	0.000
Residual Error	316	37.84	0.12		
Total	327	1797.17			

V. Topographic metric – list of predictors and analysis of variance

Predictor	Coef	SE Coef	T	P
Constant	98.8005	0.2632	375.35	0.000
kf^2	-7.0275	0.5372	-13.08	0.000
abs(tci)	-3.9925	0.5880	-6.79	0.000
kf*tauc	2.4925	0.1709	14.58	0.000
kw*scr	2.0325	0.1727	11.77	0.000
kf*tci	-2.0197	0.1823	-11.08	0.000
nci*tci	-4.6017	0.6584	-6.99	0.000
kw*kf	1.3665	0.1724	7.93	0.000
tci	1.1117	0.1770	6.28	0.000
kf*scr	-1.1439	0.1682	-6.80	0.000
kw*scr*kb	2.4705	0.5785	4.27	0.000
scr^2	-6.1646	0.6272	-9.83	0.000
(kw*kf*scr)^2	12.2212	0.9335	13.09	0.000
kw^2	-7.7245	0.8364	-9.23	0.000
kf*nci	-0.9912	0.1866	-5.31	0.000
tauc^2	-3.2006	0.6399	-5.00	0.000
nci*abs(tci)	0.9647	0.2041	4.73	0.000
tci*scr	-0.8045	0.1830	-4.39	0.000
kw*tci	0.7852	0.1831	4.29	0.000
kf*kb	0.6937	0.1732	4.01	0.000
kd*tci*scr	-0.6702	0.1876	-3.57	0.000

S = 2.009 R-Sq = 92.3% R-Sq(adj) = 91.8%

Analysis of Variance

Source	DF	SS	MS	F	P
Regression	20	13926.03	696.30	172.44	0.000
Residual Error	288	1162.90	4.04		
Total	308	15088.93			

VI. Output (all sample points), metamodel fits and residuals.

Notes:
1. These residuals are calculated as ln|metric| - fitted.
2. These residuals are calculated as actual metric - exp(fitted).
3. Cases dropped from the regression analyses are indicated by '*'.
4. Residuals used in the bootstrap calculations are indicated by background shading.

	Sediment yield						Drainage density						Sediment delivery ratio			Topographic metric		
Case no.	GOLEM (yield)	ln|yield|	Model fit, ln|yield|	Residual (note 1)	Model fit, yield	Residual (notes 2 & 4)	GOLEM (ddens)	ln|ddens|	Model fit, ln|ddens|	Residual (note 1)	Model fit, ddens	Residual (note 2 & 4)	GOLEM Sed. del. ratio	Model fit	Residual (notes 3 & 4)	GOLEM Topog. Metric	Model fit	Residual (notes 3 & 4)
1 (Base)	24.91	3.22	3.22	0.00	24.92	0.00	3.15	1.15	1.15	0.00	3.14	0.01	90.18	90.30	-0.12	100.00	98.80	1.20
2	26.21	3.27	3.27	0.00	26.22	-0.01	3.14	1.14	1.15	0.00	3.14	-0.01	90.40	90.66	-0.26	*	12.97	*
3	22.74	3.12	3.12	0.01	22.62	0.12	3.13	1.14	1.15	0.00	3.14	-0.01	89.72	89.94	-0.22	*	12.97	*
4	24.91	3.22	3.22	0.00	24.92	0.00	3.17	1.15	1.15	0.01	3.14	0.02	90.06	90.30	-0.24	*	98.80	*
5	24.94	3.22	3.22	0.00	24.92	0.03	3.15	1.15	1.15	0.00	3.14	0.00	90.33	90.30	0.03	*	98.80	*
6	25.54	3.24	3.24	0.00	25.51	0.03	3.14	1.15	1.15	0.00	3.14	0.00	89.21	89.21	0.00	*	98.80	*
7	24.17	3.19	3.19	0.00	24.17	0.00	3.14	1.14	1.15	0.00	3.14	-0.01	91.46	91.39	0.07	*	98.80	*
8	32.46	3.48	3.48	0.00	32.45	0.01	3.18	1.16	1.15	0.01	3.14	0.04	94.62	93.88	0.74	*	21.65	*
9	14.62	2.68	2.68	0.00	14.62	0.00	3.17	1.15	1.15	0.01	3.14	0.03	*	*	*	*	22.34	*
10	19.14	2.95	2.95	0.00	19.06	0.08	3.11	1.13	1.13	0.01	3.09	0.02	88.79	88.31	0.48	*	63.24	*
11	30.75	3.43	3.43	0.00	30.79	-0.04	3.19	1.16	1.16	0.00	3.19	-0.01	90.27	90.56	-0.29	*	63.24	*
12	22.72	3.12	3.12	0.00	22.66	0.06	2.16	0.77	0.77	0.00	2.16	0.00	95.65	95.68	-0.03	*	98.80	*
13	25.56	3.24	3.24	0.00	25.43	0.12	3.68	1.30	1.30	0.00	3.67	0.01	87.81	87.89	-0.08	*	98.80	*
14	23.01	3.14	3.14	0.00	22.99	0.02	2.47	0.90	0.90	0.00	2.46	0.01	94.28	94.63	-0.36	*	87.36	*
15	27.45	3.31	3.31	0.00	27.41	0.04	4.26	1.45	1.45	0.00	4.26	0.00	83.32	83.72	-0.41	*	86.21	*
16	23.15	3.14	3.14	0.00	23.13	0.02	3.15	1.15	1.15	0.00	3.14	0.01	90.58	90.91	-0.32	*	30.31	*
17	27.57	3.32	3.31	0.00	27.50	0.07	3.17	1.16	1.15	0.01	3.14	0.03	87.62	87.74	-0.11	*	30.31	*
18	25.50	3.24	3.24	0.00	25.44	0.05	3.15	1.15	1.15	0.00	3.15	0.00	91.18	90.30	0.88	*	98.80	*
19	24.30	3.19	3.19	0.00	24.31	-0.01	3.12	1.14	1.14	0.00	3.12	0.00	90.40	90.30	0.10	*	98.80	*
20	24.48	3.20	3.19	0.01	24.35	0.13	3.12	1.14	1.15	-0.01	3.14	-0.02	89.38	89.21	0.17	*	98.80	*

	Sediment yield						Drainage density						Sediment delivery ratio			Topographic metric		
Case no.	GOLEM (yield)	ln|yield|	Model fit, ln|yield|	Residual (note 1)	Model fit, yield	Residual (notes 2 & 4)	GOLEM (ddens)	ln|ddens|	Model fit, ln|ddens|	Residual (note 1)	Model fit, ddens	Residual (note 2 & 4)	GOLEM Sed. del. ratio	Model fit	Residual (notes 3 & 4)	GOLEM Topog. Metric	Model fit	Residual (notes 3 & 4)
21	25.31	3.23	3.24	0.00	25.41	-0.10	3.15	1.15	1.15	0.00	3.14	0.00	91.06	91.39	-0.33	*	98.80	*
22	24.66	3.21	3.21	0.00	24.69	-0.03	2.69	0.99	1.00	-0.01	2.71	-0.02	93.83	93.74	0.09	84.22	84.60	-0.38
23	23.61	3.16	3.17	-0.01	23.74	-0.13	2.72	1.00	0.99	0.01	2.70	0.02	93.39	93.95	-0.56	78.21	74.84	3.37
24	24.82	3.21	3.22	-0.01	25.01	-0.19	2.70	0.99	1.00	0.00	2.71	-0.01	94.66	94.68	-0.02	84.97	84.60	0.37
25	23.43	3.15	3.15	0.00	23.43	0.00	2.73	1.00	0.99	0.01	2.70	0.03	93.20	93.01	0.19	76.93	74.84	2.08
26	25.38	3.23	3.23	0.01	25.20	0.18	2.69	0.99	0.99	0.00	2.70	-0.01	94.16	94.08	0.09	82.64	83.04	-0.40
27	24.82	3.21	3.21	0.00	24.88	-0.07	2.70	0.99	1.00	0.00	2.71	-0.01	94.26	93.98	0.28	83.06	84.19	-1.13
28	25.45	3.24	3.24	0.00	25.52	-0.08	2.66	0.98	0.99	-0.01	2.70	-0.04	94.45	94.71	-0.26	84.62	83.04	1.58
29	24.63	3.20	3.20	0.00	24.57	0.06	2.74	1.01	1.00	0.01	2.71	0.03	93.75	93.35	0.40	81.64	84.19	-2.55
30	20.80	3.03	3.04	-0.01	20.99	-0.19	2.66	0.98	0.99	-0.02	2.70	-0.04	90.04	90.39	-0.36	82.68	81.65	1.03
31	20.23	3.01	3.01	0.00	20.20	0.03	2.66	0.98	1.00	-0.02	2.71	-0.05	89.20	88.72	0.47	86.93	85.47	1.46
32	20.66	3.03	3.03	0.00	20.72	-0.06	2.66	0.98	0.99	-0.02	2.70	-0.04	89.39	89.45	-0.06	83.25	81.65	1.59
33	20.38	3.01	3.02	0.00	20.46	-0.08	2.67	0.98	1.00	-0.02	2.71	-0.04	90.09	89.66	0.42	86.11	85.47	0.64
34	19.90	2.99	2.99	0.00	19.93	-0.03	2.69	0.99	1.00	-0.01	2.71	-0.02	92.13	91.62	0.51	84.32	85.00	-0.67
35	18.73	2.93	2.93	0.00	18.68	0.05	2.73	1.00	0.99	0.01	2.70	0.03	90.12	90.27	-0.15	79.12	83.42	-4.30
36	19.64	2.98	2.98	0.00	19.68	-0.04	2.72	1.00	1.00	0.00	2.71	0.01	91.28	90.99	0.28	85.12	85.00	0.12
37	18.93	2.94	2.94	0.00	18.92	0.02	2.72	1.00	0.99	0.01	2.70	0.01	90.64	90.89	-0.25	80.39	83.42	-3.03
38	29.78	3.39	3.38	0.01	29.48	0.29	2.70	0.99	1.00	-0.01	2.73	-0.02	94.06	93.20	0.86	78.04	79.40	-1.36
39	28.96	3.37	3.37	-0.01	29.12	-0.16	2.72	1.00	1.01	-0.01	2.74	-0.02	94.12	93.65	0.47	79.37	80.55	-1.18
40	29.95	3.40	3.40	0.00	29.87	0.08	2.72	1.00	1.00	0.00	2.73	-0.01	94.41	94.14	0.27	78.45	79.40	-0.95
41	28.56	3.35	3.36	-0.01	28.74	-0.18	2.74	1.01	1.01	0.00	2.74	0.01	93.25	92.71	0.54	77.73	80.55	-2.81
42	27.75	3.32	3.33	-0.01	28.00	-0.25	2.72	1.00	1.01	0.00	2.74	-0.01	93.79	94.74	-0.95	78.83	80.95	-2.12
43	26.50	3.28	3.29	-0.02	26.92	-0.42	2.76	1.02	1.00	0.01	2.73	0.04	94.56	94.88	-0.32	74.01	71.20	2.81
44	28.13	3.34	3.35	-0.01	28.37	-0.24	2.74	1.01	1.01	0.00	2.74	0.00	95.09	95.37	-0.27	79.51	80.95	-1.45
45	26.12	3.26	3.28	-0.02	26.57	-0.45	2.78	1.02	1.00	0.02	2.73	0.05	93.90	94.25	-0.35	73.08	71.20	1.88
46	23.24	3.15	3.15	0.00	23.32	-0.08	2.68	0.98	1.01	-0.02	2.74	-0.06	91.40	91.05	0.34	88.98	88.57	0.41
47	21.82	3.08	3.08	0.00	21.85	-0.03	2.73	1.00	1.00	0.00	2.73	0.00	88.99	89.63	-0.63	83.48	86.99	-3.51
48	23.03	3.14	3.14	0.00	23.02	0.00	2.71	1.00	1.01	-0.01	2.74	-0.02	90.59	90.11	0.48	90.81	88.57	2.24
49	22.30	3.10	3.10	0.01	22.14	0.16	2.71	1.00	1.00	-0.01	2.73	-0.02	90.66	90.57	0.09	85.29	86.99	-1.70
50	23.81	3.17	3.17	0.00	23.80	0.01	2.71	1.00	1.00	-0.01	2.73	-0.02	91.28	91.08	0.20	85.51	85.22	0.29

	Sediment yield						Drainage density						Sediment delivery ratio			Topographic metric		
Case no.	GOLEM (yield)	ln|yield|	Model fit, ln|yield|	Residual (note 1)	Model fit, yield	Residual (notes 2 & 4)	GOLEM (ddens)	ln|ddens|	Model fit, ln|ddens|	Residual (note 1)	Model fit, ddens	Residual (note 2 & 4)	GOLEM Sed. del. ratio	Model fit	Residual (notes 3 & 4)	GOLEM Topog. Metric	Model fit	Residual (notes 3 & 4)
51	22.99	3.13	3.13	0.00	22.91	0.08	2.79	1.03	1.01	0.02	2.74	0.05	89.98	89.96	0.01	89.35	89.04	0.31
52	23.72	3.17	3.16	0.01	23.50	0.22	2.70	0.99	1.00	-0.01	2.73	-0.03	90.90	90.45	0.45	85.92	85.22	0.70
53	23.30	3.15	3.14	0.00	23.21	0.10	2.74	1.01	1.01	0.00	2.74	0.00	91.16	90.59	0.57	89.91	89.04	0.87
54	26.93	3.29	3.29	0.00	26.93	0.00	3.07	1.12	1.13	0.00	3.08	-0.01	92.48	92.21	0.27	87.84	89.30	-1.46
55	25.35	3.23	3.23	0.00	25.23	0.12	3.07	1.12	1.12	0.00	3.08	-0.01	91.28	90.90	0.38	87.34	87.67	-0.33
56	26.68	3.28	3.28	0.00	26.58	0.10	3.07	1.12	1.13	0.00	3.08	-0.01	92.02	91.27	0.75	89.31	89.30	0.02
57	25.56	3.24	3.24	0.00	25.56	0.01	3.07	1.12	1.12	0.00	3.08	-0.01	91.98	91.84	0.14	91.72	87.67	4.05
58	24.88	3.21	3.21	0.00	24.90	-0.02	3.10	1.13	1.12	0.01	3.08	0.02	93.45	93.44	0.01	87.08	88.08	-1.00
59	23.81	3.17	3.18	-0.01	23.96	-0.16	3.07	1.12	1.13	-0.01	3.08	-0.02	92.34	92.44	-0.10	80.57	81.10	-0.53
60	24.62	3.20	3.20	0.00	24.58	0.04	3.05	1.11	1.12	-0.01	3.08	-0.03	92.71	92.81	-0.10	85.12	88.08	-2.96
61	24.21	3.19	3.19	0.00	24.27	-0.07	3.12	1.14	1.13	0.01	3.08	0.03	93.70	93.07	0.63	82.57	81.10	1.48
62	20.26	3.01	3.01	0.00	20.21	0.05	3.12	1.14	1.12	0.01	3.08	0.04	87.57	87.74	-0.18	85.27	84.95	0.32
63	20.11	3.00	2.99	0.01	19.96	0.15	3.06	1.12	1.13	-0.01	3.08	-0.02	88.55	88.31	0.24	84.21	80.64	3.57
64	20.46	3.02	3.02	0.00	20.47	-0.01	3.11	1.13	1.12	0.01	3.08	0.03	88.60	88.68	-0.09	85.55	84.95	0.60
65	19.77	2.98	2.98	0.00	19.70	0.07	3.09	1.13	1.13	0.00	3.08	0.00	87.10	87.37	-0.27	84.28	80.64	3.64
66	21.03	3.05	3.05	-0.01	21.19	-0.16	3.14	1.14	1.13	0.02	3.08	0.05	88.21	88.08	0.12	79.68	78.87	0.81
67	20.38	3.01	3.01	0.00	20.37	0.01	3.12	1.14	1.12	0.01	3.08	0.04	87.86	88.34	-0.48	85.75	85.42	0.32
68	21.20	3.05	3.07	-0.01	21.46	-0.26	3.12	1.14	1.13	0.01	3.08	0.03	89.07	88.71	0.36	78.18	78.87	-0.69
69	20.11	3.00	3.00	0.00	20.11	0.00	3.08	1.13	1.12	0.00	3.08	0.01	86.77	87.71	-0.94	85.52	85.42	0.09
70	28.94	3.37	3.37	-0.01	29.13	-0.19	3.06	1.12	1.13	-0.01	3.11	-0.04	92.78	93.23	-0.45	83.03	81.75	1.28
71	27.87	3.33	3.33	-0.01	28.04	-0.17	3.09	1.13	1.14	-0.01	3.11	-0.03	92.45	92.04	0.41	74.37	74.77	-0.40
72	28.70	3.36	3.36	0.00	28.76	-0.06	3.08	1.12	1.13	-0.01	3.11	-0.03	92.18	92.29	-0.11	80.00	81.75	-1.75
73	28.17	3.34	3.35	-0.01	28.40	-0.24	3.07	1.12	1.14	-0.01	3.11	-0.04	93.03	92.98	0.05	77.90	74.77	3.13
74	30.64	3.42	3.42	0.00	30.54	0.10	3.10	1.13	1.14	0.00	3.11	-0.01	93.19	93.25	-0.06	81.61	82.97	-1.36
75	28.25	3.34	3.35	-0.01	28.61	-0.36	3.12	1.14	1.13	0.01	3.11	0.02	91.41	92.38	-0.96	78.80	81.34	-2.55
76	30.37	3.41	3.41	0.01	30.15	0.22	3.13	1.14	1.14	0.01	3.11	0.02	92.77	92.63	0.14	81.40	82.97	-1.57
77	28.86	3.36	3.37	0.00	28.99	-0.12	3.10	1.13	1.13	0.00	3.11	-0.01	92.88	93.00	-0.13	81.76	81.34	0.42
78	24.67	3.21	3.21	0.00	24.79	-0.12	3.11	1.13	1.14	0.00	3.11	0.00	87.76	87.56	0.21	80.83	85.12	-4.29
79	23.91	3.17	3.17	0.00	23.83	0.08	3.14	1.14	1.13	0.01	3.11	0.03	88.44	88.25	0.19	90.41	91.68	-1.26
80	24.90	3.21	3.22	-0.01	25.11	-0.21	3.09	1.13	1.14	-0.01	3.11	-0.03	88.56	88.50	0.07	78.69	85.12	-6.43

	Sediment yield						Drainage density						Sediment delivery ratio			Topographic metric		
Case no.	GOLEM (yield)	ln|yield|	Model fit, ln|yield|	Residual (note 1)	Model fit, yield	Residual (notes 2 & 4)	GOLEM (ddens)	ln|ddens|	Model fit, ln|ddens|	Residual (note 1)	Model fit, ddens	Residual (note 2 & 4)	GOLEM Sed. del. ratio	Model fit	Residual (notes 3 & 4)	GOLEM Topog. Metric	Model fit	Residual (notes 3 & 4)
81	23.67	3.16	3.16	0.01	23.53	0.14	3.09	1.13	1.13	0.00	3.11	-0.01	87.64	87.31	0.34	89.70	91.68	-1.97
82	23.03	3.14	3.13	0.00	22.92	0.11	3.10	1.13	1.13	0.00	3.11	0.00	89.03	89.10	-0.07	92.17	91.20	0.97
83	22.76	3.13	3.12	0.01	22.64	0.13	3.12	1.14	1.14	0.00	3.11	0.01	90.22	89.48	0.74	89.59	86.89	2.70
84	23.24	3.15	3.14	0.00	23.22	0.03	3.14	1.14	1.13	0.01	3.11	0.03	89.97	89.73	0.24	92.51	91.20	1.31
85	22.26	3.10	3.11	0.00	22.35	-0.09	3.11	1.13	1.14	0.00	3.11	-0.01	88.57	88.85	-0.28	87.68	86.89	0.80
86	25.76	3.25	3.25	0.00	25.73	0.03	3.15	1.15	1.14	0.00	3.14	0.01	91.67	91.73	-0.07	93.37	90.25	3.12
87	24.70	3.21	3.21	0.00	24.76	-0.06	3.16	1.15	1.15	0.00	3.15	0.02	90.48	90.87	-0.39	84.77	86.20	-1.43
88	25.47	3.24	3.23	0.00	25.40	0.07	3.12	1.14	1.14	-0.01	3.14	-0.02	91.10	91.09	0.01	92.78	90.25	2.53
89	25.22	3.23	3.22	0.01	25.08	0.13	3.16	1.15	1.15	0.00	3.15	0.02	91.22	91.52	-0.30	88.90	86.20	2.70
90	27.00	3.30	3.29	0.00	26.97	0.03	3.14	1.14	1.15	0.00	3.15	-0.01	91.36	91.56	-0.21	85.50	88.46	-2.97
91	25.18	3.23	3.23	0.00	25.27	-0.09	3.13	1.14	1.14	0.00	3.14	-0.01	90.92	90.92	0.00	88.48	89.77	-1.29
92	26.72	3.29	3.28	0.00	26.63	0.09	3.13	1.14	1.15	0.00	3.15	-0.02	91.12	91.13	-0.01	88.26	88.46	-0.20
93	25.63	3.24	3.24	0.00	25.60	0.04	3.15	1.15	1.14	0.00	3.14	0.01	91.81	91.35	0.46	93.06	89.77	3.29
94	21.71	3.08	3.09	-0.01	21.89	-0.19	3.17	1.15	1.15	0.01	3.15	0.02	85.74	85.95	-0.21	77.13	74.33	2.80
95	21.11	3.05	3.05	0.00	21.05	0.06	3.11	1.14	1.14	-0.01	3.14	-0.03	86.30	86.38	-0.08	84.55	83.81	0.74
96	21.86	3.08	3.10	-0.01	22.18	-0.32	3.12	1.14	1.15	-0.01	3.15	-0.03	86.31	86.59	-0.29	74.58	74.33	0.25
97	20.73	3.03	3.03	0.00	20.78	-0.05	3.14	1.14	1.14	0.00	3.14	0.00	85.39	85.73	-0.34	84.25	83.81	0.43
98	20.24	3.01	3.01	0.00	20.24	0.00	3.15	1.15	1.14	0.00	3.14	0.01	87.88	87.20	0.69	84.02	83.41	0.61
99	20.21	3.01	3.00	0.01	19.99	0.22	3.15	1.15	1.15	0.00	3.15	0.00	88.14	87.41	0.73	82.13	82.03	0.10
100	20.41	3.02	3.02	0.00	20.50	-0.09	3.14	1.15	1.14	0.00	3.14	0.00	88.18	87.63	0.56	83.82	83.41	0.41
101	19.80	2.99	2.98	0.00	19.73	0.07	3.14	1.14	1.15	0.00	3.15	-0.01	87.10	86.98	0.12	82.88	82.03	0.85
102	31.72	3.46	3.45	0.01	31.56	0.16	3.18	1.16	1.16	0.00	3.18	0.00	91.80	91.70	0.10	80.04	82.31	-2.28
103	29.31	3.38	3.39	-0.01	29.57	-0.26	3.17	1.15	1.15	0.00	3.17	0.00	90.80	90.91	-0.11	81.14	83.62	-2.48
104	30.90	3.43	3.44	-0.01	31.15	-0.26	3.20	1.16	1.16	0.01	3.18	0.02	90.14	91.06	-0.91	81.27	82.31	-1.05
105	29.87	3.40	3.40	0.00	29.95	-0.08	3.15	1.15	1.15	-0.01	3.17	-0.02	91.73	91.56	0.16	83.71	83.62	0.09
106	29.21	3.37	3.37	0.00	29.18	0.03	3.18	1.16	1.15	0.00	3.17	0.01	92.85	92.74	0.11	85.00	84.10	0.90
107	27.76	3.32	3.34	-0.01	28.08	-0.33	3.18	1.16	1.16	0.00	3.18	0.00	91.31	92.16	-0.85	76.74	80.05	-3.31
108	28.81	3.36	3.36	0.00	28.80	0.01	3.17	1.15	1.15	0.00	3.17	0.00	92.13	92.31	-0.17	82.34	84.10	-1.76
109	28.44	3.35	3.35	0.00	28.45	0.00	3.21	1.17	1.16	0.01	3.18	0.03	92.51	92.60	-0.09	80.60	80.05	0.55
110	23.82	3.17	3.16	0.01	23.68	0.14	3.19	1.16	1.15	0.01	3.17	0.02	87.63	87.12	0.51	91.05	89.48	1.57

	Sediment yield						Drainage density						Sediment delivery ratio			Topographic metric		
Case no.	GOLEM (yield)	ln|yield|	Model fit, ln|yield|	Residual (note 1)	Model fit, yield	Residual (notes 2 & 4)	GOLEM (ddens)	ln|ddens|	Model fit, ln|ddens|	Residual (note 1)	Model fit, ddens	Residual (note 2 & 4)	GOLEM Sed. del. ratio	Model fit	Residual (notes 3 & 4)	GOLEM Topog. Metric	Model fit	Residual (notes 3 & 4)
111	23.66	3.16	3.15	0.01	23.39	0.27	3.15	1.15	1.16	-0.01	3.18	-0.03	87.78	87.63	0.15	87.93	88.10	-0.18
112	23.99	3.18	3.18	0.00	23.99	0.00	3.15	1.15	1.15	-0.01	3.17	-0.02	87.90	87.77	0.13	88.52	89.48	-0.97
113	23.24	3.15	3.14	0.01	23.09	0.15	3.16	1.15	1.16	-0.01	3.18	-0.02	87.33	86.98	0.35	90.36	88.10	2.25
114	24.73	3.21	3.21	0.00	24.83	-0.10	3.20	1.16	1.16	0.01	3.18	0.03	86.96	87.17	-0.21	79.16	80.40	-1.24
115	23.85	3.17	3.17	0.00	23.87	-0.02	3.22	1.17	1.15	0.02	3.17	0.05	87.58	87.46	0.13	91.67	89.89	1.78
116	24.99	3.22	3.22	-0.01	25.15	-0.16	3.15	1.15	1.16	-0.01	3.18	-0.03	87.62	87.60	0.02	76.39	80.40	-4.01
117	23.65	3.16	3.16	0.00	23.56	0.09	3.14	1.14	1.15	-0.01	3.17	-0.03	87.86	87.02	0.83	91.16	89.89	1.27
118	27.43	3.31	3.31	0.00	27.35	0.08	3.54	1.26	1.27	-0.01	3.57	-0.04	87.86	87.83	0.03	83.18	83.84	-0.66
119	27.34	3.31	3.30	0.01	27.01	0.34	3.55	1.27	1.28	-0.01	3.58	-0.03	89.06	88.62	0.44	84.97	87.92	-2.95
120	27.73	3.32	3.32	0.00	27.70	0.02	3.53	1.26	1.27	-0.01	3.57	-0.05	88.23	88.48	-0.25	81.04	83.84	-2.80
121	26.63	3.28	3.28	0.00	26.66	-0.04	3.59	1.28	1.28	0.00	3.58	0.01	87.94	87.97	-0.03	88.26	87.92	0.34
122	26.09	3.26	3.26	0.00	25.97	0.12	3.56	1.27	1.28	-0.01	3.58	-0.02	89.16	89.08	0.07	88.99	88.40	0.60
123	24.75	3.21	3.22	-0.01	24.97	-0.22	3.57	1.27	1.27	0.00	3.57	-0.01	89.68	89.66	0.02	84.28	81.57	2.70
124	26.50	3.28	3.27	0.01	26.31	0.19	3.57	1.27	1.28	0.00	3.58	-0.01	89.97	89.51	0.45	84.69	88.40	-3.70
125	24.50	3.20	3.20	-0.01	24.65	-0.15	3.54	1.26	1.27	-0.01	3.57	-0.03	89.48	89.22	0.26	80.50	81.57	-1.08
126	21.45	3.07	3.07	-0.01	21.63	-0.18	3.62	1.29	1.28	0.01	3.58	0.04	83.52	84.36	-0.85	75.06	77.53	-2.47
127	20.42	3.02	3.01	0.01	20.27	0.15	3.55	1.27	1.27	-0.01	3.57	-0.02	84.62	83.85	0.76	81.55	78.89	2.66
128	21.27	3.06	3.06	0.00	21.36	-0.09	3.59	1.28	1.28	0.00	3.58	0.00	83.45	83.71	-0.26	79.17	77.53	1.64
129	20.60	3.03	3.02	0.00	20.53	0.07	3.51	1.26	1.27	-0.02	3.57	-0.06	84.18	84.50	-0.32	80.50	78.89	1.61
130	21.88	3.09	3.09	-0.01	22.08	-0.19	3.60	1.28	1.27	0.01	3.57	0.02	84.04	84.19	-0.15	73.28	71.19	2.10
131	21.20	3.05	3.06	0.00	21.25	-0.04	3.53	1.26	1.28	-0.01	3.58	-0.05	83.51	83.90	-0.39	79.51	77.94	1.57
132	21.64	3.07	3.08	-0.01	21.79	-0.15	3.56	1.27	1.27	0.00	3.57	-0.01	83.83	83.76	0.07	75.30	71.19	4.12
133	21.49	3.07	3.07	0.00	21.52	-0.03	3.56	1.27	1.28	-0.01	3.58	-0.02	84.33	84.33	-0.01	76.71	77.94	-1.23
134	30.73	3.43	3.41	0.01	30.39	0.34	3.60	1.28	1.29	0.00	3.62	-0.02	89.97	89.36	0.61	86.16	84.58	1.58
135	28.97	3.37	3.37	-0.01	29.22	-0.25	3.59	1.28	1.28	-0.01	3.61	-0.02	89.69	90.11	-0.41	79.58	77.75	1.83
136	31.12	3.44	3.43	0.01	30.79	0.33	3.59	1.28	1.29	-0.01	3.62	-0.03	89.91	90.01	-0.10	84.48	84.58	-0.09
137	28.40	3.35	3.36	-0.02	28.84	-0.44	3.57	1.27	1.28	-0.01	3.61	-0.04	89.25	89.46	-0.21	76.37	77.75	-1.38
138	31.18	3.44	3.43	0.01	31.01	0.17	3.56	1.27	1.28	-0.01	3.61	-0.05	89.73	89.41	0.32	81.93	80.02	1.91
139	30.87	3.43	3.42	0.01	30.63	0.24	3.64	1.29	1.29	0.01	3.62	0.03	89.99	89.94	0.05	83.81	84.10	-0.29
140	31.60	3.45	3.45	0.01	31.42	0.18	3.66	1.30	1.28	0.01	3.61	0.05	89.70	89.84	-0.14	79.91	80.02	-0.10

	Sediment yield						Drainage density						Sediment delivery ratio			Topographic metric		
Case no.	GOLEM (yield)	ln|yield|	Model fit, ln|yield|	Residual (note 1)	Model fit, yield	Residual (notes 2 & 4)	GOLEM (ddens)	ln|ddens|	Model fit, ln|ddens|	Residual (note 1)	Model fit, ddens	Residual (note 2 & 4)	GOLEM Sed. del. ratio	Model fit	Residual (notes 3 & 4)	GOLEM Topog. Metric	Model fit	Residual (notes 3 & 4)
141	30.09	3.40	3.41	0.00	30.24	-0.15	3.62	1.29	1.29	0.00	3.62	0.00	89.24	89.50	-0.26	84.15	84.10	0.05
142	25.58	3.24	3.25	-0.01	25.83	-0.25	3.60	1.28	1.28	0.00	3.61	-0.01	83.82	84.69	-0.87	74.23	74.93	-0.70
143	24.79	3.21	3.21	0.00	24.86	-0.07	3.61	1.28	1.29	0.00	3.62	-0.01	84.12	84.13	-0.02	80.72	81.69	-0.96
144	25.39	3.23	3.24	0.00	25.50	-0.11	3.58	1.28	1.28	-0.01	3.61	-0.02	83.98	84.04	-0.06	76.15	74.93	1.22
145	25.16	3.23	3.23	0.00	25.18	-0.02	3.62	1.29	1.29	0.00	3.62	0.00	84.26	84.78	-0.52	77.56	81.69	-4.12
146	24.62	3.20	3.20	0.00	24.54	0.08	3.64	1.29	1.29	0.01	3.62	0.03	85.71	85.72	-0.01	75.59	81.28	-5.69
147	22.97	3.13	3.13	0.00	22.99	-0.02	3.61	1.28	1.28	0.00	3.61	0.00	85.85	85.38	0.46	87.64	82.64	5.01
148	24.24	3.19	3.19	0.00	24.22	0.02	3.67	1.30	1.29	0.02	3.62	0.05	85.59	85.29	0.30	81.14	81.28	-0.14
149	23.30	3.15	3.15	0.00	23.28	0.02	3.60	1.28	1.28	0.00	3.61	0.00	86.43	85.82	0.61	87.15	82.64	4.52
201	24.79	3.21	3.21	0.00	24.78	0.01	3.32	1.20	1.20	0.00	3.32	0.00	88.43	88.18	0.25	93.20	87.86	5.34
202	25.08	3.22	3.22	0.00	24.99	0.08	3.16	1.15	1.15	0.00	3.14	0.01	91.26	91.04	0.22	98.51	93.31	5.20
203	24.81	3.21	3.21	0.00	24.83	-0.01	3.35	1.21	1.21	0.00	3.36	-0.01	88.60	88.58	0.02	90.35	94.32	-3.97
204	25.19	3.23	3.22	0.01	25.03	0.16	2.93	1.07	1.08	0.00	2.93	0.00	91.82	91.33	0.49	92.37	93.12	-0.75
205	19.95	2.99	2.99	0.00	19.92	0.03	2.83	1.04	1.04	0.00	2.84	-0.01	89.45	89.72	-0.27	84.80	84.80	0.01
206	20.03	3.00	2.99	0.00	19.97	0.06	2.85	1.05	1.04	0.01	2.84	0.02	89.68	89.97	-0.29	85.02	83.94	1.08
207	19.88	2.99	2.98	0.00	19.78	0.09	2.94	1.08	1.07	0.01	2.91	0.03	88.62	89.06	-0.44	84.41	84.60	-0.19
208	21.19	3.05	3.05	0.00	21.14	0.05	3.05	1.12	1.12	0.00	3.05	0.00	88.69	89.05	-0.36	88.22	89.07	-0.85
209	21.22	3.05	3.06	0.00	21.24	-0.02	2.83	1.04	1.04	0.00	2.84	0.00	89.76	90.36	-0.60	88.74	86.10	2.64
210	20.98	3.04	3.05	0.00	21.08	-0.10	3.12	1.14	1.12	0.01	3.07	0.05	87.19	87.61	-0.42	86.88	86.81	0.07
211	22.42	3.11	3.11	0.00	22.33	0.10	2.97	1.09	1.10	-0.01	2.99	-0.02	89.25	89.55	-0.30	90.57	90.42	0.15
212	22.43	3.11	3.11	0.00	22.35	0.08	3.26	1.18	1.19	-0.01	3.29	-0.03	88.92	88.29	0.63	87.90	89.12	-1.22
213	22.55	3.12	3.12	0.00	22.55	0.00	3.01	1.10	1.09	0.01	2.98	0.03	90.30	90.84	-0.54	89.51	92.70	-3.19
214	23.52	3.16	3.16	0.00	23.54	-0.02	3.14	1.15	1.15	0.00	3.15	0.00	88.83	88.67	0.16	95.34	90.56	4.78
215	23.99	3.18	3.18	0.00	23.96	0.02	2.85	1.05	1.04	0.00	2.84	0.01	93.10	93.30	-0.20	90.99	88.99	2.00
216	23.58	3.16	3.16	0.00	23.52	0.06	3.23	1.17	1.17	0.00	3.22	0.01	88.74	88.42	0.33	88.26	89.40	-1.14
217	26.39	3.27	3.27	0.00	26.28	0.11	3.27	1.18	1.18	0.01	3.24	0.03	90.08	89.71	0.37	92.53	90.40	2.14
218	26.44	3.27	3.28	0.00	26.55	-0.11	3.14	1.15	1.14	0.00	3.13	0.01	90.66	91.25	-0.59	91.86	93.01	-1.15
219	26.60	3.28	3.28	0.00	26.60	0.00	3.09	1.13	1.12	0.01	3.07	0.02	91.56	91.58	-0.02	89.76	89.98	-0.22
220	28.04	3.33	3.33	0.00	28.04	0.00	2.92	1.07	1.07	0.00	2.93	-0.01	93.10	93.02	0.08	84.25	86.20	-1.95
221	28.22	3.34	3.34	0.00	28.08	0.14	3.37	1.21	1.22	0.00	3.38	-0.01	91.84	90.95	0.89	86.44	85.50	0.94

	Sediment yield						Drainage density						Sediment delivery ratio			Topographic metric		
Case no.	GOLEM (yield)	ln|yield|	Model fit, ln|yield|	Residual (note 1)	Model fit, yield	Residual (notes 2 & 4)	GOLEM (ddens)	ln|ddens|	Model fit, ln|ddens|	Residual (note 1)	Model fit, ddens	Residual (note 2 & 4)	GOLEM Sed. del. ratio	Model fit	Residual (notes 3 & 4)	GOLEM Topog. Metric	Model fit	Residual (notes 3 & 4)
222	28.16	3.34	3.33	0.00	28.06	0.11	2.91	1.07	1.07	-0.01	2.93	-0.02	92.68	92.55	0.13	84.22	87.09	-2.87
223	29.50	3.38	3.38	0.00	29.41	0.09	3.44	1.23	1.24	0.00	3.44	0.00	90.33	90.37	-0.04	84.95	84.29	0.66
224	29.49	3.38	3.38	0.00	29.39	0.10	3.23	1.17	1.18	0.00	3.24	-0.01	91.12	90.78	0.34	83.82	85.94	-2.12
225	29.71	3.39	3.39	0.00	29.56	0.15	3.16	1.15	1.15	0.00	3.15	0.00	92.23	92.23	0.00	82.83	84.66	-1.83
226	31.00	3.43	3.42	0.01	30.61	0.39	3.47	1.25	1.24	0.01	3.45	0.02	91.03	90.58	0.45	82.81	80.58	2.23
227	30.60	3.42	3.42	0.00	30.57	0.03	3.40	1.22	1.22	0.00	3.39	0.00	90.47	90.57	-0.10	82.00	81.27	0.73
228	30.71	3.42	3.42	0.00	30.59	0.12	3.48	1.25	1.24	0.01	3.45	0.03	90.15	90.44	-0.29	82.67	81.38	1.30
229	28.36	3.35	3.35	0.00	28.46	-0.10	3.35	1.21	1.22	-0.01	3.38	-0.03	89.47	89.94	-0.47	87.67	89.20	-1.52
230	21.68	3.08	3.08	0.00	21.67	0.01	2.93	1.07	1.07	0.00	2.92	0.00	89.52	90.43	-0.91	88.91	91.16	-2.26
231	24.52	3.20	3.21	-0.01	24.70	-0.18	3.11	1.13	1.14	0.00	3.11	0.00	91.08	91.46	-0.38	90.67	91.24	-0.58
232	24.90	3.21	3.22	0.00	24.97	-0.07	3.16	1.15	1.15	0.00	3.17	0.00	88.51	88.90	-0.39	89.84	90.41	-0.57
233	25.51	3.24	3.24	0.00	25.50	0.00	3.40	1.22	1.22	0.00	3.40	0.00	88.61	88.58	0.03	94.05	94.38	-0.33
234	24.40	3.19	3.20	0.00	24.46	-0.06	2.94	1.08	1.07	0.01	2.92	0.01	91.36	91.82	-0.46	95.66	95.92	-0.26
235	25.54	3.24	3.24	0.00	25.56	-0.02	3.17	1.15	1.15	0.01	3.14	0.02	89.51	89.94	-0.43	92.07	92.64	-0.56
236	24.32	3.19	3.19	0.00	24.33	-0.02	3.15	1.15	1.15	0.00	3.14	0.01	90.36	90.54	-0.18	93.73	92.64	1.10
237	25.45	3.24	3.23	0.00	25.36	0.08	3.17	1.15	1.15	0.01	3.14	0.03	90.63	90.40	0.23	92.60	91.08	1.52
238	24.52	3.20	3.19	0.01	24.40	0.13	3.16	1.15	1.15	0.01	3.14	0.02	90.68	90.19	0.49	92.37	91.08	1.29
239	25.18	3.23	3.22	0.00	25.11	0.07	3.16	1.15	1.15	0.01	3.14	0.02	90.11	89.97	0.14	99.63	98.80	0.83
240	24.65	3.20	3.21	0.00	24.72	-0.07	3.14	1.14	1.15	0.00	3.14	-0.01	90.36	90.62	-0.26	99.67	98.80	0.87
241	27.42	3.31	3.31	0.00	27.43	-0.01	3.16	1.15	1.15	0.01	3.14	0.02	92.03	91.96	0.07	92.01	91.77	0.24
242	22.15	3.10	3.10	0.00	22.20	-0.05	3.15	1.15	1.15	0.00	3.14	0.00	87.58	87.65	-0.07	90.26	91.98	-1.72
243	23.30	3.15	3.14	0.01	23.16	0.14	3.12	1.14	1.14	0.00	3.13	-0.01	90.36	89.93	0.43	93.56	95.60	-2.04
244	26.68	3.28	3.28	0.00	26.68	0.00	3.16	1.15	1.15	0.00	3.16	0.00	90.49	90.50	-0.01	93.82	95.60	-1.79
245	24.76	3.21	3.20	0.01	24.55	0.21	2.93	1.08	1.07	0.00	2.92	0.00	91.71	91.48	0.23	96.86	98.80	-1.94
246	25.17	3.23	3.23	0.00	25.16	0.02	3.35	1.21	1.20	0.01	3.33	0.02	89.37	89.37	0.00	97.66	98.80	-1.14
247	25.10	3.22	3.22	0.00	25.08	0.02	3.17	1.15	1.15	0.01	3.15	0.03	90.44	90.30	0.14	97.65	98.80	-1.15
248	24.78	3.21	3.21	0.00	24.75	0.03	3.13	1.14	1.14	0.00	3.14	-0.01	90.29	90.30	-0.01	97.50	98.80	-1.30
249	24.78	3.21	3.21	0.00	24.75	0.03	3.13	1.14	1.15	0.00	3.14	-0.01	89.94	89.97	-0.03	97.78	98.80	-1.02
250	25.04	3.22	3.22	0.00	25.07	-0.03	3.15	1.15	1.15	0.00	3.14	0.01	90.43	90.62	-0.19	97.69	98.80	-1.11
251	25.10	3.22	3.22	0.00	25.07	0.03	3.14	1.14	1.15	0.00	3.14	0.00	90.30	90.33	-0.03	99.80	97.94	1.86

	Sediment yield						Drainage density						Sediment delivery ratio			Topographic metric		
Case no.	GOLEM (yield)	ln|yield|	Model fit, ln|yield|	Residual (note 1)	Model fit, yield	Residual (notes 2 & 4)	GOLEM (ddens)	ln|ddens|	Model fit, ln|ddens|	Residual (note 1)	Model fit, ddens	Residual (note 2 & 4)	GOLEM Sed. del. ratio	Model fit	Residual (notes 3 & 4)	GOLEM Topog. Metric	Model fit	Residual (notes 3 & 4)
252	24.77	3.21	3.21	0.00	24.75	0.02	3.13	1.14	1.15	0.00	3.14	-0.02	90.14	90.26	-0.12	99.88	97.94	1.94
253	25.03	3.22	3.22	0.00	24.92	0.11	3.14	1.14	1.15	0.00	3.14	0.00	90.56	90.30	0.26	99.98	98.80	1.18
254	24.92	3.22	3.22	0.00	24.92	0.00	3.15	1.15	1.15	0.00	3.14	0.00	90.25	90.30	-0.05	99.99	98.80	1.19
255	25.01	3.22	3.22	0.00	24.98	0.03	3.14	1.14	1.15	0.00	3.14	0.00	90.15	90.19	-0.04	99.87	98.80	1.07
256	24.87	3.21	3.21	0.00	24.85	0.01	3.13	1.14	1.15	0.00	3.14	-0.02	90.42	90.41	0.01	99.86	98.80	1.06
257	25.83	3.25	3.25	0.00	25.77	0.06	3.11	1.13	1.15	-0.01	3.14	-0.03	90.97	90.93	0.04	99.72	98.04	1.68
258	24.14	3.18	3.18	0.00	24.04	0.10	3.14	1.14	1.15	0.00	3.14	-0.01	89.92	89.56	0.36	99.58	98.04	1.54
259	24.29	3.19	3.19	0.00	24.33	-0.04	3.13	1.14	1.14	0.00	3.14	-0.01	89.94	90.19	-0.25	99.62	98.45	1.17
260	25.57	3.24	3.24	0.00	25.50	0.07	3.15	1.15	1.15	0.00	3.15	0.00	90.41	90.38	0.03	99.83	98.45	1.39
261	24.91	3.22	3.21	0.00	24.81	0.10	3.08	1.12	1.12	0.00	3.07	0.00	91.02	90.67	0.35	99.21	98.80	0.41
262	25.02	3.22	3.22	0.00	25.01	0.01	3.20	1.16	1.17	0.00	3.21	-0.01	90.04	89.96	0.08	99.27	98.80	0.47
263	24.90	3.21	3.21	0.01	24.75	0.15	3.05	1.12	1.12	-0.01	3.07	-0.01	91.20	90.83	0.37	98.31	97.89	0.43
264	25.11	3.22	3.22	0.00	25.10	0.01	3.24	1.18	1.17	0.00	3.22	0.01	89.83	89.75	0.08	98.33	97.26	1.08
265	24.70	3.21	3.21	0.00	24.72	-0.02	3.18	1.16	1.15	0.01	3.14	0.04	90.31	90.39	-0.08	99.17	98.12	1.05
266	25.22	3.23	3.22	0.00	25.12	0.10	3.19	1.16	1.15	0.01	3.14	0.05	90.43	90.19	0.24	99.30	98.12	1.18
267	24.97	3.22	3.22	0.00	24.97	0.00	3.15	1.15	1.15	0.00	3.15	0.00	90.24	90.30	-0.06	99.77	98.80	0.97
268	24.87	3.21	3.21	0.00	24.86	0.01	3.14	1.14	1.15	0.00	3.14	-0.01	90.33	90.30	0.03	99.82	98.80	1.02
269	24.85	3.21	3.21	0.00	24.86	-0.01	3.16	1.15	1.15	0.01	3.14	0.01	90.10	90.19	-0.09	99.92	98.80	1.12
270	25.06	3.22	3.22	0.00	24.97	0.09	3.15	1.15	1.15	0.00	3.14	0.01	90.71	90.41	0.30	99.81	98.80	1.01
301	25.53	3.24	3.24	0.00	25.59	-0.06	3.18	1.16	1.15	0.01	3.15	0.03	90.57	90.93	-0.36	95.87	91.75	4.12
302	25.08	3.22	3.22	0.00	25.08	0.00	3.15	1.15	1.15	0.00	3.15	0.00	89.67	89.70	-0.03	98.24	93.93	4.31
303	27.00	3.30	3.29	0.01	26.81	0.19	3.13	1.14	1.15	-0.01	3.15	-0.02	91.49	91.16	0.33	91.99	91.22	0.77
304	27.00	3.30	3.30	0.00	27.07	-0.07	3.16	1.15	1.15	0.00	3.15	0.01	91.03	91.57	-0.54	91.17	90.81	0.36
305	21.89	3.09	3.08	0.00	21.79	0.10	2.78	1.02	1.02	0.00	2.77	0.01	91.12	91.44	-0.32	88.76	89.48	-0.72
306	22.45	3.11	3.11	0.00	22.49	-0.04	2.76	1.01	1.02	-0.01	2.78	-0.02	91.42	91.81	-0.39	92.40	90.89	1.51
307	24.22	3.19	3.19	0.00	24.23	-0.01	2.76	1.01	1.02	-0.01	2.78	-0.02	91.35	91.63	-0.28	90.96	89.92	1.04
308	21.45	3.07	3.07	0.00	21.44	0.01	2.87	1.05	1.05	0.00	2.86	0.01	90.06	90.38	-0.32	90.06	85.33	4.73
309	27.29	3.31	3.31	-0.01	27.44	-0.14	2.89	1.06	1.05	0.01	2.86	0.03	92.04	92.52	-0.48	82.37	81.86	0.51
310	23.18	3.14	3.14	0.00	23.17	0.01	2.88	1.06	1.05	0.00	2.87	0.01	90.55	90.76	-0.21	93.99	90.53	3.47
311	24.14	3.18	3.18	0.00	24.04	0.10	2.95	1.08	1.08	0.00	2.96	-0.01	89.88	89.69	0.19	89.87	89.18	0.69

	Sediment yield						Drainage density						Sediment delivery ratio			Topographic metric		
Case no.	GOLEM (yield)	ln|yield|	Model fit, ln|yield|	Residual (note 1)	Model fit, yield	Residual (notes 2 & 4)	GOLEM (ddens)	ln|ddens|	Model fit, ln|ddens|	Residual (note 1)	Model fit, ddens	Residual (note 2 & 4)	GOLEM Sed. del. ratio	Model fit	Residual (notes 3 & 4)	GOLEM Topog. Metric	Model fit	Residual (notes 3 & 4)
312	22.84	3.13	3.13	0.00	22.81	0.04	2.95	1.08	1.08	0.00	2.96	0.00	91.16	91.14	0.02	91.56	90.10	1.46
313	27.23	3.30	3.30	0.01	27.00	0.23	2.96	1.08	1.08	0.00	2.95	0.00	93.05	92.61	0.44	89.03	89.48	-0.45
314	23.93	3.18	3.18	-0.01	24.10	-0.17	3.05	1.12	1.11	0.00	3.05	0.01	91.28	91.68	-0.40	83.45	87.59	-4.14
315	22.08	3.09	3.09	0.01	21.95	0.13	3.04	1.11	1.11	0.00	3.05	-0.01	90.09	90.24	-0.15	88.49	90.64	-2.15
316	26.40	3.27	3.27	0.00	26.27	0.13	3.06	1.12	1.11	0.01	3.05	0.02	92.12	92.06	0.06	94.91	94.40	0.51
317	23.35	3.15	3.15	0.00	23.34	0.00	3.21	1.17	1.18	-0.01	3.25	-0.04	89.04	89.07	-0.03	93.51	95.36	-1.85
318	23.80	3.17	3.17	0.00	23.80	-0.01	3.25	1.18	1.18	0.00	3.24	0.01	88.61	88.30	0.31	93.96	92.98	0.98
319	23.82	3.17	3.17	0.00	23.87	-0.05	3.27	1.18	1.18	0.00	3.26	0.01	88.09	88.17	-0.08	83.41	89.71	-6.30
320	26.49	3.28	3.28	0.00	26.54	-0.05	3.38	1.22	1.21	0.01	3.36	0.02	87.93	88.08	-0.15	83.63	84.39	-0.76
321	25.77	3.25	3.25	0.00	25.79	-0.02	3.37	1.21	1.21	0.00	3.37	0.00	89.75	89.71	0.04	90.82	93.48	-2.66
322	27.26	3.31	3.31	0.00	27.27	-0.01	3.38	1.22	1.21	0.00	3.37	0.01	89.68	89.87	-0.19	86.82	87.77	-0.95
323	25.01	3.22	3.22	0.00	24.95	0.06	3.45	1.24	1.24	0.00	3.46	-0.01	88.46	88.08	0.38	91.23	90.86	0.37
324	26.10	3.26	3.27	0.00	26.18	-0.08	3.48	1.25	1.24	0.00	3.46	0.01	87.21	87.27	-0.06	88.19	88.15	0.04
325	26.65	3.28	3.28	0.00	26.66	-0.01	3.50	1.25	1.24	0.01	3.46	0.04	87.62	87.93	-0.31	80.95	84.99	-4.04
326	25.12	3.22	3.22	0.00	25.14	-0.03	3.58	1.28	1.27	0.01	3.56	0.02	85.62	85.59	0.03	78.37	78.59	-0.22
327	25.26	3.23	3.23	-0.01	25.41	-0.15	3.56	1.27	1.27	0.00	3.56	0.00	85.98	86.31	-0.33	81.58	79.59	1.99
328	25.98	3.26	3.26	0.00	26.06	-0.08	3.55	1.27	1.27	-0.01	3.57	-0.02	86.03	86.45	-0.42	75.30	76.17	-0.87
329	24.01	3.18	3.18	0.00	24.01	0.00	3.34	1.21	1.21	-0.01	3.36	-0.02	88.50	88.08	0.42	91.28	90.64	0.64
330	25.75	3.25	3.24	0.00	25.64	0.11	2.90	1.07	1.07	0.00	2.92	-0.01	92.87	92.34	0.53	91.46	90.98	0.48
331	22.61	3.12	3.12	0.00	22.67	-0.06	3.11	1.13	1.13	0.00	3.11	0.00	88.96	89.23	-0.27	91.37	92.51	-1.14
332	27.12	3.30	3.30	0.00	27.16	-0.04	3.15	1.15	1.15	0.00	3.15	-0.01	91.33	91.26	0.07	91.26	91.62	-0.36
401	29.68	3.39	3.40	-0.01	29.83	-0.15	3.43	1.23	1.24	-0.01	3.46	-0.02	89.77	90.19	-0.42	84.06	84.16	-0.10
402	22.48	3.11	3.11	0.00	22.52	-0.04	2.96	1.09	1.09	-0.01	2.99	-0.03	90.04	90.04	-0.01	85.24	90.38	-5.14
403	25.62	3.24	3.24	0.00	25.61	0.01	3.15	1.15	1.15	0.00	3.16	-0.01	89.95	90.13	-0.18	95.43	94.51	0.92
404	24.49	3.20	3.20	0.00	24.50	-0.02	3.14	1.14	1.15	0.00	3.15	-0.01	90.09	90.13	-0.05	91.04	92.05	-1.01
405	22.45	3.11	3.12	-0.01	22.59	-0.14	3.48	1.25	1.25	0.00	3.49	-0.01	84.71	85.14	-0.44	82.01	80.84	1.17
406	22.99	3.13	3.14	-0.01	23.20	-0.21	3.47	1.24	1.24	0.01	3.45	0.02	85.17	85.34	-0.16	76.21	78.74	-2.53
407	22.62	3.12	3.13	-0.01	22.83	-0.21	3.41	1.23	1.23	-0.01	3.44	-0.03	85.15	85.43	-0.28	75.05	76.29	-1.24
408	23.50	3.16	3.16	0.00	23.52	-0.02	3.43	1.23	1.23	0.01	3.41	0.01	86.32	86.14	0.18	86.99	85.80	1.19
409	21.92	3.09	3.09	0.00	21.89	0.04	3.50	1.25	1.25	0.00	3.49	0.01	86.48	85.88	0.60	82.68	82.51	0.17

	Sediment yield						Drainage density						Sediment delivery ratio			Topographic metric		
Case no.	GOLEM (yield)	ln|yield|	Model fit, ln|yield|	Residual (note 1)	Model fit, yield	Residual (notes 2 & 4)	GOLEM (ddens)	ln|ddens|	Model fit, ln|ddens|	Residual (note 1)	Model fit, ddens	Residual (note 2 & 4)	GOLEM Sed. del. ratio	Model fit	Residual (notes 3 & 4)	GOLEM Topog. Metric	Model fit	Residual (notes 3 & 4)
410	23.95	3.18	3.18	0.00	24.02	-0.07	3.44	1.24	1.24	0.00	3.44	0.00	86.55	86.24	0.30	81.37	83.60	-2.23
411	23.10	3.14	3.14	0.00	23.09	0.02	3.17	1.15	1.15	0.00	3.16	0.01	87.39	87.44	-0.06	92.24	90.53	1.71
412	24.45	3.20	3.20	0.00	24.53	-0.08	3.41	1.23	1.23	0.00	3.40	0.01	87.42	87.54	-0.12	81.60	85.50	-3.90
413	21.66	3.08	3.08	0.00	21.77	-0.10	3.21	1.17	1.15	0.02	3.16	0.04	87.10	87.43	-0.33	85.93	87.00	-1.07
414	24.37	3.19	3.20	0.00	24.46	-0.09	3.47	1.24	1.25	0.00	3.48	-0.01	88.84	88.65	0.20	89.60	88.82	0.78
415	23.50	3.16	3.15	0.00	23.43	0.07	3.10	1.13	1.13	0.00	3.09	0.01	89.02	88.98	0.04	94.92	92.91	2.01
416	25.18	3.23	3.23	0.00	25.25	-0.07	3.10	1.13	1.13	0.00	3.10	0.00	88.46	88.81	-0.35	88.22	88.97	-0.75
417	25.78	3.25	3.26	-0.01	25.93	-0.14	3.17	1.15	1.15	0.01	3.15	0.02	90.85	91.12	-0.27	88.72	93.52	-4.80
418	26.57	3.28	3.28	0.00	26.51	0.06	3.16	1.15	1.15	0.00	3.17	-0.01	91.52	91.05	0.47	94.22	94.85	-0.63
419	23.94	3.18	3.17	0.00	23.85	0.09	2.95	1.08	1.08	0.00	2.95	0.00	91.12	91.21	-0.09	95.92	94.35	1.57
420	24.91	3.22	3.22	-0.01	25.13	-0.22	3.06	1.12	1.11	0.01	3.04	0.02	91.50	92.10	-0.60	85.79	90.16	-4.37
421	26.78	3.29	3.28	0.00	26.70	0.08	3.04	1.11	1.11	0.00	3.04	0.00	92.20	91.84	0.35	90.94	90.07	0.87
422	25.16	3.23	3.22	0.00	25.15	0.02	2.84	1.04	1.05	-0.01	2.86	-0.02	91.76	92.13	-0.36	90.60	89.07	1.53
423	25.14	3.22	3.23	-0.01	25.27	-0.13	2.92	1.07	1.07	0.01	2.90	0.01	92.67	93.07	-0.40	79.72	82.36	-2.64
424	27.24	3.30	3.30	0.00	27.20	0.04	2.91	1.07	1.07	0.00	2.91	0.00	92.78	93.07	-0.28	85.65	87.98	-2.33
425	25.47	3.24	3.24	0.00	25.53	-0.05	2.79	1.03	1.03	-0.01	2.80	-0.01	92.61	93.13	-0.52	89.66	90.25	-0.59
426	27.05	3.30	3.30	0.00	27.06	-0.01	2.81	1.03	1.03	0.00	2.81	0.00	94.09	94.12	-0.03	83.80	84.65	-0.85
427	28.07	3.33	3.33	0.00	27.94	0.13	2.82	1.04	1.04	-0.01	2.84	-0.02	94.55	93.87	0.68	82.82	83.81	-0.99
428	25.17	3.23	3.23	0.00	25.27	-0.10	2.84	1.04	1.05	0.00	2.85	0.00	94.10	93.97	0.14	87.63	85.12	2.51
501	25.42	3.24	3.23	0.00	25.29	0.13	3.12	1.14	1.15	-0.01	3.14	-0.02	90.80	90.39	0.41	93.18	93.44	-0.26
502	25.24	3.23	3.23	0.00	25.22	0.02	3.14	1.14	1.15	0.00	3.14	-0.01	90.39	90.37	0.02	94.27	95.37	-1.10
503	25.05	3.22	3.22	0.00	25.15	-0.10	3.14	1.14	1.15	0.00	3.14	0.00	89.93	90.35	-0.42	99.39	96.87	2.52
504	24.72	3.21	3.21	0.00	24.67	0.05	3.15	1.15	1.15	0.00	3.14	0.01	90.27	90.24	0.03	99.51	96.87	2.64
505	24.62	3.20	3.20	0.00	24.58	0.04	3.12	1.14	1.15	-0.01	3.14	-0.02	90.22	90.22	0.00	94.26	95.37	-1.11
506	24.53	3.20	3.20	0.00	24.49	0.04	3.14	1.14	1.15	0.00	3.14	-0.01	90.25	90.21	0.04	93.01	93.44	-0.43
507	27.04	3.30	3.30	0.00	26.99	0.05	3.15	1.15	1.15	0.00	3.14	0.01	91.92	91.71	0.21	94.05	94.07	-0.02
508	26.64	3.28	3.28	0.00	26.59	0.04	3.14	1.14	1.15	0.00	3.14	0.00	91.50	91.47	0.03	96.21	95.77	0.44
509	26.18	3.27	3.27	0.00	26.18	0.00	3.16	1.15	1.15	0.01	3.14	0.01	91.09	91.21	-0.12	98.43	97.10	1.34
510	23.54	3.16	3.16	0.00	23.59	-0.05	3.16	1.15	1.15	0.01	3.14	0.01	89.01	89.14	-0.13	97.40	97.10	0.30
511	23.14	3.14	3.14	0.00	23.14	0.00	3.14	1.14	1.15	0.00	3.14	0.00	88.82	88.69	0.13	94.93	95.77	-0.84

	Sediment yield						Drainage density						Sediment delivery ratio			Topographic metric		
Case no.	GOLEM (yield)	ln|yield|	Model fit, ln|yield|	Residual (note 1)	Model fit, yield	Residual (notes 2 & 4)	GOLEM (ddens)	ln|ddens|	Model fit, ln|ddens|	Residual (note 1)	Model fit, ddens	Residual (note 2 & 4)	GOLEM Sed. del. ratio	Model fit	Residual (notes 3 & 4)	GOLEM Topog. Metric	Model fit	Residual (notes 3 & 4)
512	22.62	3.12	3.12	0.00	22.67	-0.05	3.15	1.15	1.15	0.00	3.14	0.01	88.12	88.19	-0.07	92.25	94.07	-1.82
513	23.55	3.16	3.16	0.00	23.55	0.01	3.14	1.14	1.14	0.00	3.13	0.01	89.94	90.03	-0.09	95.57	96.86	-1.29
514	23.98	3.18	3.18	0.00	23.94	0.04	3.12	1.14	1.14	-0.01	3.14	-0.02	90.14	90.12	0.02	98.11	97.81	0.30
515	25.96	3.26	3.25	0.00	25.89	0.07	3.15	1.15	1.15	0.00	3.15	0.00	90.53	90.43	0.10	98.35	97.81	0.53
516	26.36	3.27	3.27	0.00	26.29	0.07	3.15	1.15	1.15	0.00	3.16	0.00	90.68	90.47	0.21	95.91	96.86	-0.96
517	24.78	3.21	3.21	0.00	24.69	0.09	3.01	1.10	1.10	0.00	3.00	0.01	91.11	91.05	0.06	98.19	98.80	-0.61
518	24.99	3.22	3.22	0.00	25.09	-0.09	3.26	1.18	1.19	0.00	3.27	-0.02	89.33	89.65	-0.32	98.50	98.80	-0.30
519	24.58	3.20	3.20	0.00	24.55	0.03	2.99	1.10	1.09	0.01	2.97	0.02	91.52	91.50	0.02	96.69	96.60	0.09
520	24.70	3.21	3.20	0.00	24.65	0.05	3.03	1.11	1.10	0.00	3.02	0.01	91.10	91.17	-0.07	97.47	97.25	0.22
521	24.80	3.21	3.21	0.00	24.83	-0.04	3.09	1.13	1.13	-0.01	3.11	-0.01	90.44	90.56	-0.12	99.23	98.35	0.89
522	25.08	3.22	3.22	0.00	25.00	0.07	3.20	1.16	1.16	0.01	3.18	0.02	90.25	90.02	0.23	99.26	98.02	1.24
523	25.31	3.23	3.23	0.00	25.22	0.09	3.27	1.18	1.19	0.00	3.28	-0.01	89.72	89.37	0.35	97.10	96.26	0.83
524	25.30	3.23	3.23	0.00	25.36	-0.06	3.35	1.21	1.21	0.00	3.34	0.01	88.86	88.98	-0.12	95.52	95.30	0.21
525	24.41	3.19	3.20	0.00	24.43	-0.02	3.11	1.13	1.15	-0.01	3.14	-0.04	90.33	90.51	-0.18	95.02	94.52	0.50
526	24.55	3.20	3.20	0.00	24.52	0.03	3.14	1.14	1.15	0.00	3.14	-0.01	90.47	90.47	0.00	96.59	96.06	0.53
527	24.72	3.21	3.20	0.00	24.62	0.10	3.13	1.14	1.15	0.00	3.14	-0.02	90.63	90.43	0.20	97.77	97.26	0.51
528	25.28	3.23	3.23	0.00	25.23	0.05	3.14	1.14	1.15	0.00	3.14	0.00	89.96	90.14	-0.18	97.64	97.26	0.38
529	25.39	3.23	3.23	0.00	25.34	0.05	3.13	1.14	1.15	0.00	3.14	-0.01	89.94	90.08	-0.14	96.20	96.06	0.14
530	25.55	3.24	3.24	0.00	25.45	0.10	3.16	1.15	1.15	0.01	3.14	0.02	90.06	90.01	0.05	94.06	94.52	-0.46
531	25.06	3.22	3.22	0.00	25.03	0.03	3.15	1.15	1.15	0.00	3.15	0.00	90.55	90.30	0.25	98.60	98.80	-0.20
532	24.87	3.21	3.21	0.00	24.80	0.06	3.16	1.15	1.14	0.01	3.14	0.02	90.48	90.30	0.18	98.53	98.80	-0.27
533	24.85	3.21	3.21	0.00	24.81	0.04	3.11	1.13	1.15	-0.01	3.14	-0.03	90.19	90.08	0.11	98.69	98.80	-0.12
534	24.98	3.22	3.22	0.00	25.02	-0.04	3.13	1.14	1.15	0.00	3.14	-0.01	90.37	90.51	-0.14	98.56	98.80	-0.24
535	26.54	3.28	3.29	-0.01	26.78	-0.24	3.15	1.15	1.15	0.00	3.14	0.01	91.95	92.20	-0.25	85.39	84.47	0.93
536	21.64	3.07	3.07	0.00	21.64	0.00	3.17	1.15	1.15	0.01	3.14	0.03	87.94	87.84	0.10	88.36	86.75	1.61
537	28.33	3.34	3.34	0.01	28.14	0.19	3.15	1.15	1.15	0.00	3.14	0.01	91.92	91.60	0.32	88.51	86.75	1.76
538	22.70	3.12	3.12	0.00	22.74	-0.04	3.18	1.16	1.15	0.01	3.14	0.04	87.37	87.24	0.13	83.86	84.47	-0.61
539	25.47	3.24	3.24	0.00	25.57	-0.10	3.14	1.14	1.15	0.00	3.14	-0.01	91.56	91.46	0.10	90.65	90.37	0.28
540	23.09	3.14	3.14	0.00	23.04	0.05	3.15	1.15	1.15	0.00	3.14	0.00	89.54	89.39	0.15	92.61	91.49	1.11
541	26.90	3.29	3.29	0.00	26.86	0.04	3.15	1.15	1.15	0.00	3.14	0.01	90.62	90.85	-0.23	91.71	91.49	0.21

	Sediment yield						Drainage density						Sediment delivery ratio			Topographic metric		
Case no.	GOLEM (yield)	ln|yield|	Model fit, ln|yield|	Residual (note 1)	Model fit, yield	Residual (notes 2 & 4)	GOLEM (ddens)	ln|ddens|	Model fit, ln|ddens|	Residual (note 1)	Model fit, ddens	Residual (note 2 & 4)	GOLEM Sed. del. ratio	Model fit	Residual (notes 3 & 4)	GOLEM Topog. Metric	Model fit	Residual (notes 3 & 4)
542	24.25	3.19	3.19	0.00	24.20	0.04	3.17	1.15	1.15	0.01	3.14	0.03	88.67	88.78	-0.11	88.82	90.37	-1.55
543	27.05	3.30	3.30	0.00	27.10	-0.05	3.14	1.14	1.15	0.00	3.14	0.00	92.30	92.09	0.21	88.86	89.66	-0.80
544	21.98	3.09	3.09	0.00	21.89	0.08	3.20	1.16	1.15	0.02	3.14	0.05	88.17	87.73	0.44	89.63	90.80	-1.17
545	27.90	3.33	3.32	0.00	27.77	0.12	3.16	1.15	1.15	0.01	3.14	0.01	92.07	91.80	0.27	90.31	90.80	-0.49
546	22.34	3.11	3.11	0.00	22.44	-0.10	3.14	1.14	1.15	0.00	3.14	0.00	87.20	87.44	-0.24	87.74	89.66	-1.92
547	25.94	3.26	3.25	0.00	25.87	0.07	3.14	1.14	1.15	0.00	3.14	0.00	91.80	91.34	0.46	95.16	95.27	-0.11
548	23.29	3.15	3.15	0.00	23.31	-0.02	3.17	1.15	1.15	0.01	3.14	0.02	89.03	89.27	-0.24	95.82	95.84	-0.02
549	26.54	3.28	3.28	0.00	26.51	0.02	3.14	1.14	1.15	0.00	3.14	0.00	90.92	91.05	-0.13	95.86	95.84	0.03
550	23.85	3.17	3.17	0.00	23.89	-0.04	3.14	1.14	1.15	0.00	3.14	-0.01	88.57	88.98	-0.41	94.06	95.27	-1.21

APPENDIX L. REGRESSION ANALYSES AND OTHER DETAILS RELATING TO THE INDIVIDUAL PARAMETER METAMODELS (Section 6.2 *q.v.*).

1. The individual parameter metamodels for sediment yield, drainage density and sediment delivery ratio were derived using data generated by the base case simulation, the star point simulations and all of the additional parameter main effects simulations. Parameter case numbers and other details are provided for each parameter in the appropriate sections below. Regressions were conducted using 1-centred, 0.2-scaled values, as per equation 4.05. The metamodel chosen in each instance was the best from a large range of alternatives tried for that parameter and metric, even if the R^2 was rather poor or the regressors just non-significant, as these data were thought to provide a better estimate than the general metamodel. In a few cases, however, no reasonable model was derivable, so the general metamodel was used with the general metamodel bootstrap routine and prediction errors. These instances are noted below.
2. The individual parameter metamodel for the topographic metric was derived using data generated by the base case simulation and all of the additional parameter main effects simulations. Star point results were also used in deriving the model for m_w, but only for this parameter. Parameter case numbers and other details are provided below. Where possible, regressions were conducted using 0-centred, 1-scaled values, as per equation 4.01. However, for a number of the metrics, it was necessary first to use Gompertz functions (Ratkowsky, 1990) to model each 'side' of the parameter's main effect i.e. the responses exhibited to positive design level values were modelled using one function, and those exhibited to negative design level values were modelled using a separate function. The regressions incorporating these double Gompertz functions were then conducted using the combined terms as the regressors.
3. In calculating the equifinal probabilities (Figure 6.1 and Appendix M), generally a parametric bootstrap was used, assuming a normal distribution of errors. The standard deviation for each parameter's error distribution was calculated from the mean sum of squares of the residuals in each regression, simply taking the square root of the value in the regression ANOVA table in each instance. In few instances, however, as explained in point 1 above, no reasonable model was derivable for the individual parameter, so the general metamodel was used with the general metamodel bootstrap routine and prediction errors.

I. Source data for all metrics and parameters.

A. k_w

Case no.	Scaled value (eq. 4.05)	Sediment yield	Drainage density	Sediment deliv^y ratio	Scaled value (eq. 4.01)	Topographic metric
1	1.000	24.913	3.150	90.177	0.000	100.000
2	1.667	26.211	3.137	90.397	3.333	Not used
3	0.333	22.742	3.133	89.718	-3.333	Not used
237	1.200	25.447	3.173	90.631	1.000	92.599
238	0.800	24.525	3.161	90.685	-1.000	92.369
251	1.067	25.099	3.141	90.300	0.333	99.802
252	0.933	24.771	3.126	90.136	-0.333	99.884
501	1.167	25.419	3.123	90.798	0.833	93.177
502	1.133	25.242	3.138	90.389	0.667	94.271
503	1.100	25.053	3.140	89.927	0.500	99.388
504	0.900	24.720	3.152	90.271	-0.500	99.509
505	0.867	24.616	3.125	90.222	-0.667	94.255
506	0.833	24.533	3.139	90.249	-0.833	93.007

B. m_w

Case no.	Scaled value (eq. 4.05)	Sediment yield	Drainage density	Sediment deliv^y ratio	Scaled value (eq. 4.01)	Topographic metric
1	1.000	24.913	3.150	90.177	0.000	100.000
4	1.667	24.913	3.169	90.061	3.333	99.846
5	0.333	24.944	3.146	90.330	-3.333	99.960
253	1.067	25.028	3.143	90.560	0.333	99.984
254	0.933	24.917	3.148	90.248	-0.333	99.986

C. k_d

Case no.	Scaled value (eq. 4.05)	Sediment yield	Drainage density	Sediment deliv^y ratio	Scaled value (eq. 4.01)	Topographic metric
1	1.000	24.913	3.150	90.177	0.000	100.000
6	1.667	25.540	3.144	89.207	3.333	Not used
7	0.333	24.174	3.138	91.457	-3.333	Not used
239	1.200	25.180	3.160	90.114	1.000	99.632
240	0.800	24.648	3.137	90.357	-1.000	99.665
255	1.067	25.007	3.142	90.154	0.333	99.865
256	0.933	24.866	3.125	90.416	-0.333	99.860

D. k_f

Case no.	Scaled value (eq. 4.05)	Sediment yield	Drainage density	Sediment deliv^y ratio	Scaled value (eq. 4.01)	Topographic metric
1	1.000	24.913	3.150	90.177	0.000	100.000
8	1.663	32.462	3.185	94.622	3.313	Not used
9	0.340	14.623	3.173	78.287	-3.299	Not used
241	1.200	27.422	3.159	92.029	1.000	92.008
242	0.803	22.151	3.147	87.583	-0.985	90.260
257	1.066	25.832	3.113	90.968	0.328	99.718
258	0.934	24.140	3.136	89.923	-0.328	99.581
507	1.164	27.042	3.155	91.923	0.821	94.050
508	1.131	26.636	3.142	91.496	0.657	96.212
509	1.099	26.182	3.157	91.093	0.493	98.431
510	0.901	23.539	3.159	89.008	-0.493	97.400
511	0.869	23.140	3.145	88.820	-0.657	94.930
512	0.836	22.623	3.150	88.121	-0.821	92.250

E. τ_c

Case no.	Scaled value (eq. 4.05)	Sediment yield	Drainage density	Sediment deliv^y ratio	Scaled value (eq. 4.01)	Topographic metric
1	1.000	24.913	3.150	90.177	0.000	100.000
10	1.667	19.142	3.110	88.786	3.333	Not used
11	0.333	30.745	3.188	90.270	-3.333	Not used
243	1.200	23.302	3.116	90.360	1.000	93.563
244	0.800	26.676	3.157	90.488	-1.000	93.815
259	1.067	24.288	3.132	89.940	0.333	99.616
260	0.933	25.574	3.154	90.412	-0.333	99.832
513	1.156	23.554	3.138	89.935	0.778	95.570
514	1.111	23.978	3.119	90.139	0.556	98.112
515	0.889	25.963	3.150	90.534	-0.556	98.347
516	0.844	26.358	3.153	90.680	-0.778	95.905

F. n_{ci}

Case no.	Scaled value (eq. 4.05)	Sediment yield	Drainage density	Sediment deliv^y ratio	Scaled value (eq. 4.01)	Topographic metric
1	1.000	24.913	3.150	90.177	0.000	100.000
12	1.844	22.716	2.157	95.649	4.220	Not used
13	0.546	25.557	3.680	87.811	-2.268	Not used
245	1.200	24.757	2.925	91.712	1.000	96.860
246	0.834	25.173	3.345	89.371	-0.829	97.663
261	1.063	24.911	3.077	91.015	0.317	99.206
262	0.941	25.023	3.203	90.036	-0.293	99.269
517	1.129	24.777	3.007	91.111	0.646	98.194
518	0.885	24.994	3.256	89.330	-0.573	98.496

G. t_{ci}

Case no.	Scaled value (eq. 4.05)	Sediment yield	Drainage density	Sediment deliv^y ratio	Scaled value (eq. 4.01)	Topographic metric
1	1.000	24.913	3.150	90.177	0.000	100.000
14	1.794	23.009	2.468	94.275	3.972	Not used
15	0.507	27.451	4.258	83.318	-2.467	Not used
233	0.827	25.505	3.399	88.611	-0.867	94.047
234	1.200	24.402	2.938	91.356	1.000	95.663
263	1.064	24.899	3.054	91.204	0.318	98.310
264	0.939	25.108	3.237	89.829	-0.303	98.333
519	1.153	24.582	2.986	91.519	0.765	96.690
520	1.108	24.700	3.028	91.101	0.539	97.470
521	1.031	24.796	3.093	90.439	0.157	99.234
522	0.969	25.079	3.201	90.253	-0.153	99.255
523	0.901	25.312	3.270	89.719	-0.497	97.097
524	0.863	25.297	3.351	88.860	-0.685	95.516

H. s_{cr}

Case no.	Scaled value (eq. 4.05)	Sediment yield	Drainage density	Sediment deliv^y ratio	Scaled value (eq. 4.01)	Topographic metric
1	1.000	24.913	3.150	90.177	0.000	100.000
16	1.667	23.154	3.152	90.584	3.333	Not used
17	0.333	27.574	3.175	87.623	-3.333	Not used
235	0.800	25.539	3.167	89.514	-1.000	92.073
236	1.200	24.315	3.154	90.362	1.000	93.731
265	1.067	24.697	3.180	90.305	0.333	99.169
266	0.933	25.225	3.193	90.428	-0.333	99.295
525	1.167	24.408	3.106	90.327	0.833	95.023
526	1.133	24.554	3.135	90.473	0.667	96.590
527	1.100	24.721	3.128	90.631	0.500	97.772
528	0.900	25.278	3.139	89.963	-0.500	97.639
529	0.867	25.389	3.133	89.941	-0.667	96.201
530	0.833	25.550	3.163	90.058	-0.833	94.061

I. k_b

Case no.	Scaled value (eq. 4.05)	Sediment yield	Drainage density	Sediment deliv^y ratio	Scaled value (eq. 4.01)	Topographic metric
1	1.000	24.913	3.150	90.177	0.000	100.000
18	1.667	25.497	3.152	91.177	3.333	Not used
19	0.333	24.296	3.124	90.395	-3.333	Not used
247	1.200	25.102	3.174	90.441	1.000	97.646
248	0.800	24.776	3.132	90.289	-1.000	97.497
267	1.067	24.969	3.147	90.243	0.335	99.770
268	0.934	24.874	3.136	90.332	-0.332	99.818
531	1.133	25.062	3.149	90.548	0.667	98.599
532	0.867	24.868	3.160	90.481	-0.667	98.533

J. τ_b

Case no.	Scaled value (eq. 4.05)	Sediment yield	Drainage density	Sediment deliv^y ratio	Scaled value (eq. 4.01)	Topographic metric
1	1.000	24.913	3.150	90.177	0.000	100.000
20	1.667	24.476	3.124	89.379	3.333	Not used
21	0.333	25.309	3.148	91.059	-3.333	Not used
249	1.200	24.781	3.129	89.943	1.000	97.781
250	0.800	25.044	3.153	90.431	-1.000	97.688
269	1.067	24.853	3.157	90.104	0.333	99.923
270	0.933	25.058	3.152	90.710	-0.333	99.807
533	1.133	24.849	3.112	90.195	0.667	98.685
534	0.867	24.983	3.134	90.367	-0.667	98.559

II. Sediment yield – list of predictors and analysis of variance

A. k_w

```
Predictor              Coef   SE Coef         T         P
Constant             15.726     0.196    80.355     0.000
kw^0.25               9.230     0.197    46.875     0.000

S = 0.058337          R-Sq = 99.5%       R-Sq(adj) = 99.5%

Analysis of Variance
Source                   DF        SS        MS         F           P
Regression                1     7.478     7.478   2197.31     0.00000
Residual Error           11   0.03743   0.00340
Total                    12     7.515
```

B. m_w – No individual parameter model derived; used general metamodel (notes 1 and 3).

C. k_d

Predictor	Coef	SE Coef	T	P
Constant	23.478	0.061	387.541	0.000
kd^0.7	1.450	0.059	24.420	0.000

S = 0.042599 R-Sq = 99.2% R-Sq(adj) = 99%

Analysis of Variance

Source	DF	SS	MS	F	P
Regression	1	1.082	1.082	596.33	0.00000
Residual Error	5	0.00907	0.00181		
Total	6	1.091			

D. k_f

Predictor	Coef	SE Coef	T	P
Constant	7.046	0.126	55.780	0.000
kf	33.549	0.563	59.585	0.000
kf^1.3	-15.669	0.438	-35.812	0.000

S = 0.049271 R-Sq = 100% R-Sq(adj) = 100%

Analysis of Variance

Source	DF	SS	MS	F	P
Regression	2	196.818	98.409	40536.43	0.00000
Residual Error	10	0.02428	0.00243		
Total	12	196.842			

E. τ_c

Predictor	Coef	SE Coef	T	P
Constant	33.664	0.054	618.496	0.000
tauc	-8.710	0.052	-167.49	0.000

S = 0.053307 R-Sq = 100% R-Sq(adj) = 100%

Analysis of Variance

Source	DF	SS	MS	F	P
Regression	1	79.720	79.720	28054.14	0.00000
Residual Error	9	0.02557	0.00284		
Total	10	79.746			

F. n_{ci}

Predictor	Coef	SE Coef	T	P
Constant	25.637	0.047	540.635	0.000
nci^2.4	-0.666	0.027	-24.400	0.000

S = 0.092486 R-Sq = 98.8% R-Sq(adj) = 98.7%

Analysis of Variance

Source	DF	SS	MS	F	P
Regression	1	5.093	5.093	595.38	0.00000
Residual Error	7	0.05988	0.00855		
Total	8	5.153			

G. t_{ci}

Predictor	Coef	SE Coef	T	P
Constant	34.055	0.607	56.088	0.000
tci	-18.772	1.905	-9.855	0.000
tci^2	12.964	1.843	7.033	0.000
tci^3	-3.306	0.544	-6.083	0.000

S = 0.068302 R-Sq = 99.6% R-Sq(adj) = 99.5%

Analysis of Variance

Source	DF	SS	MS	F	P
Regression	3	11.070	3.690	790.95	0.00000
Residual Error	9	0.04199	0.00467		
Total	12	11.112			

H. s_{cr}

Predictor	Coef	SE Coef	T	P
Constant	31.170	0.086	362.220	0.000
scr^0.5	-6.221	0.086	-72.289	0.000

S = 0.048056 R-Sq = 99.8% R-Sq(adj) = 99.8%

Analysis of Variance

Source	DF	SS	MS	F	P
Regression	1	12.068	12.068	5225.73	0.00000
Residual Error	11	0.02540	0.00231		
Total	12	12.094			

I. k_b

Predictor	Coef	SE Coef	T	P
Constant	23.853	0.031	778.281	0.000
kb^0.8	1.087	0.030	36.422	0.000

S = 0.024525 R-Sq = 99.5% R-Sq(adj) = 99.4%

Analysis of Variance

Source	DF	SS	MS	F	P
Regression	1	0.798	0.798	1326.54	0.00000
Residual Error	7	0.00421	0.00060		
Total	8	0.802			

J. τ_b

Predictor	Coef	SE Coef	T	P
Constant	25.458	0.035	725.615	0.000
taub^1.2	-0.532	0.032	-16.537	0.000

S = 0.038489 R-Sq = 97.5% R-Sq(adj) = 97.1%

Analysis of Variance

Source	DF	SS	MS	F	P
Regression	1	0.405	0.405	273.48	0.00000
Residual Error	7	0.01037	0.00148		
Total	8	0.416			

III. Drainage density – list of predictors and analysis of variance

A. k_w - No individual model parameter derived; used general metamodel (notes 1 and 3).

B. m_w

Predictor	Coef	SE Coef	T	P
Constant	3.135	0.009	365.007	0.000
mw	0.016	0.008	2.031	0.135

S = 0.007494 R-Sq = 57.9% R-Sq(adj) = 43.9%

Analysis of Variance

Source	DF	SS	MS	F	P
Regression	1	0.000	0.000	4.13	0.13516
Residual Error	3	0.00017	0.00006		
Total	4	0.000			

C. k_d

Predictor	Coef	SE Coef	T	P
Constant	3.133	0.012	257.471	0.000
kd	0.010	0.011	0.849	0.434

S = 0.01127 R-Sq = 12.6% R-Sq(adj) = -4.9%

Analysis of Variance

Source	DF	SS	MS	F	P
Regression	1	0.000	0.000	0.72	0.43448
Residual Error	5	0.00064	0.00013		
Total	6	0.001			

D. k_f - No individual model parameter derived; used general metamodel (notes 1 and 3).

E. τ_c

Predictor	Coef	SE Coef	T	P
Constant	3.206	0.009	342.687	0.000
tauc	-0.063	0.009	-7.098	0.000

S = 0.009163 R-Sq = 84.8% R-Sq(adj) = 83.2%

Analysis of Variance

Source	DF	SS	MS	F	P
Regression	1	0.004	0.004	50.39	0.00006
Residual Error	9	0.00076	0.00008		
Total	10	0.005			

F. n_{ci}

Predictor	Coef	SE Coef	T	P
Constant	5.052	0.046	110.969	0.000
nci^0.5	-1.845	0.051	-36.046	0.000
nci^3	-0.062	0.005	-13.402	0.000

S = 0.010149 R-Sq = 100% R-Sq(adj) = 99.9%

Analysis of Variance

Source	DF	SS	MS	F	P
Regression	2	1.361	0.680	6605.37	0.00000
Residual Error	6	0.00062	0.00010		
Total	8	1.361			

G. t_{ci}

Predictor	Coef	SE Coef	T	P
Constant	2.953	0.037	79.920	0.000
tci	-0.433	0.022	-19.467	0.000
tci^-1.3	0.630	0.014	44.282	0.000

S = 0.011845 R-Sq = 99.9% R-Sq(adj) = 99.9%

Analysis of Variance

Source	DF	SS	MS	F	P
Regression	2	1.900	0.950	6770.38	0.00000
Residual Error	10	0.00140	0.00014		
Total	12	1.901			

H. s_{cr}

Predictor	Coef	SE Coef	T	P
Constant	3.179	0.023	135.666	0.000
scr	-0.027	0.023	-1.184	0.261

S = 0.023485 R-Sq = 11.3% R-Sq(adj) = 3.2%

Analysis of Variance

Source	DF	SS	MS	F	P
Regression	1	0.001	0.001	1.40	0.26123
Residual Error	11	0.00607	0.00055		
Total	12	0.007			

I. k_b

Predictor	Coef	SE Coef	T	P
Constant	3.149	0.004	776.011	0.000
ln(kb)	0.023	0.010	2.367	0.050

S = 0.011993 R-Sq = 44.5% R-Sq(adj) = 36.5%

Analysis of Variance

Source	DF	SS	MS	F	P
Regression	1	0.001	0.001	5.60	0.04982
Residual Error	7	0.00101	0.00014		
Total	8	0.002			

J. τ_b

Predictor	Coef	SE Coef	T	P
Constant	3.163	0.015	210.915	0.000
taub	-0.023	0.014	-1.633	0.146

S = 0.014313 R-Sq = 27.6% R-Sq(adj) = 17.2%

Analysis of Variance

Source	DF	SS	MS	F	P
Regression	1	0.001	0.001	2.67	0.14649
Residual Error	7	0.00143	0.00020		
Total	8	0.002			

IV. Sediment delivery ratio – list of predictors and analysis of variance

A. k_w

Predictor	Coef	SE Coef	T	P
Constant	90.324	0.071	1269.75	0.000
ln(kw)	0.458	0.198	2.312	0.041

S = 0.253667 R-Sq = 32.7% R-Sq(adj) = 26.6%

Analysis of Variance

Source	DF	SS	MS	F	P
Regression	1	0.344	0.344	5.35	0.04114
Residual Error	11	0.70782	0.06435		
Total	12	1.052			

B. m_w

Predictor	Coef	SE Coef	T	P
Constant	90.451	0.222	407.752	0.000
mw	-0.176	0.204	-0.862	0.452

S = 0.193528 R-Sq = 19.9% R-Sq(adj) = -6.8%

Analysis of Variance

Source	DF	SS	MS	F	P
Regression	1	0.028	0.028	0.74	0.45189
Residual Error	3	0.11236	0.03745		
Total	4	0.140			

C. k_d

Predictor	Coef	SE Coef	T	P
Constant	92.448	0.189	488.458	0.000
kd^0.7	-2.216	0.186	-11.942	0.000

S = 0.133085 R-Sq = 96.6% R-Sq(adj) = 95.9%

Analysis of Variance

Source	DF	SS	MS	F	P
Regression	1	2.526	2.526	142.62	0.00007
Residual Error	5	0.08856	0.01771		
Total	6	2.615			

D. k_f - **NOTE:** the lower star point was omitted from the regression

Predictor	Coef	SE Coef	T	P
Constant	101.039	0.262	385.236	0.000
kf^-1	-10.738	0.263	-40.889	0.000

S = 0.159098 R-Sq = 99.4% R-Sq(adj) = 99.3%

Analysis of Variance

Source	DF	SS	MS	F	P
Regression	1	42.319	42.319	1671.88	0.00000
Residual Error	10	0.25312	0.02531		
Total	11	42.572			

E. τ_c

Predictor	Coef	SE Coef	T	P
Constant	90.649	0.102	887.002	0.000
tauc^3	-0.383	0.059	-6.483	0.000

S = 0.22665 R-Sq = 82.4% R-Sq(adj) = 80.4%

Analysis of Variance

Source	DF	SS	MS	F	P
Regression	1	2.159	2.159	42.03	0.00011
Residual Error	9	0.46233	0.05137		
Total	10	2.621			

F. n_{ci}

Predictor	Coef	SE Coef	T	P
Constant	85.812	0.176	488.114	0.000
nci^1.3	4.498	0.149	30.120	0.000

S = 0.205185 R-Sq = 99.2% R-Sq(adj) = 99.1%

Analysis of Variance

Source	DF	SS	MS	F	P
Regression	1	38.193	38.193	907.19	0.00000
Residual Error	7	0.29471	0.04210		
Total	8	38.488			

G. t_{ci}

Predictor	Coef	SE Coef	T	P
Constant	90.125	0.135	665.270	0.000
ln(tci)	8.645	0.502	17.223	0.000

S = 0.488202 R-Sq = 96.4% R-Sq(adj) = 96.1%

Analysis of Variance

Source	DF	SS	MS	F	P
Regression	1	70.698	70.698	296.62	0.00000
Residual Error	11	2.62176	0.23834		
Total	12	73.320			

H. s_{cr}

Predictor	Coef	SE Coef	T	P
Constant	92.015	0.155	593.357	0.000
scr^-0.8	-1.815	0.133	-13.648	0.000

S = 0.193579 R-Sq = 94.4% R-Sq(adj) = 93.9%

Analysis of Variance

Source	DF	SS	MS	F	P
Regression	1	6.980	6.980	186.26	0.00000
Residual Error	11	0.41220	0.03747		
Total	12	7.392			

I. k_b

Predictor	Coef	SE Coef	T	P
Constant	90.806	0.257	353.425	0.000
kb	-1.482	0.507	-2.923	0.027
kb^2	1.015	0.245	4.142	0.006

S = 0.130735 R-Sq = 85.3% R-Sq(adj) = 80.4%

Analysis of Variance

Source	DF	SS	MS	F	P
Regression	2	0.597	0.298	17.46	0.00315
Residual Error	6	0.10255	0.01709		
Total	8	0.699			

J. τ_b

Predictor	Coef	SE Coef	T	P
Constant	91.527	0.165	553.143	0.000
taub	-1.264	0.157	-8.057	0.000

S = 0.157913 R-Sq = 90.3% R-Sq(adj) = 88.9%

Analysis of Variance

Source	DF	SS	MS	F	P
Regression	1	1.619	1.619	64.92	0.00009
Residual Error	7	0.17456	0.02494		
Total	8	1.793			

V. Topographic metric – list of predictors and analysis of variance; also component Gompertz function details where appropriate (note 2)

A. k_w

Derived from regression of the sum 100 + two Gompertz functions of k_w:

$-7.45\exp[-\exp(7.85 + 13.74k_w)]$, for values of $k_w <= 0$; and

$-7.27\exp[-\exp(7.83 - 13.87k_w)]$, for values of $k_w >= 0$.

Predictor	Coef	SE Coef	T	P
Constant	0.832	1.445	0.576	0.579
Sum Gompertz f(kw)	0.991	0.015	66.035	0.000

S = 0.163339 R-Sq = 99.8% R-Sq(adj) = 99.8%

Analysis of Variance

Source	DF	SS	MS	F	P
Regression	1	116.338	116.338	4360.56	0.00000
Residual Error	9	0.24012	0.02668		
Total	10	116.578			

B. m_w

Predictor	Coef	SE Coef	T	P
Constant	99.996	0.003	28621.7	0.000
mw	-0.017	0.001	-14.265	0.005
abs(mw)	-0.028	0.002	-16.933	0.003

S = 0.005638 R-Sq = 99.6% R-Sq(adj) = 99.2%

Analysis of Variance

Source	DF	SS	MS	F	P
Regression	2	0.016	0.008	245.11	0.00406
Residual Error	2	0.00006	0.00003		
Total	4	0.016			

C. k_d

Derived from regression of the sum of 100 + two Gompertz functions of k_d:

$-181.43\exp[-\exp(2.135 + 0.297k_d)]$, for values of $k_d <= 0$; and

$-17.72\exp[-\exp(1.838 - 0.484k_d)]$, for values of $k_d >= 0$.

Predictor	Coef	SE Coef	T	P
Constant	-0.125	17.834	-0.007	0.995
Sum Gompertz f(kd)	1.001	0.179	5.603	0.011

S = 0.052334 R-Sq = 91.3% R-Sq(adj) = 88.4%

Analysis of Variance

Source	DF	SS	MS	F	P
Regression	1	0.086	0.086	31.40	0.01123
Residual Error	3	0.00822	0.00274		
Total	4	0.094			

D. k_f

Derived from regression of the sum of 100 + two Gompertz functions of k_f:

$-12.67\exp[-\exp(2.334 + 3.715k_f)]$, for values of $k_f <= 0$; and

$-10.83\exp[-\exp(2.443 - 3.622k_f)]$, for values of $k_f >= 0$.

Predictor	Coef	SE Coef	T	P
Constant	-0.353	0.843	-0.419	0.685
Sum Gompertz f(kf)	1.004	0.009	114.210	0.000

S = 0.095215 R-Sq = 99.9% R-Sq(adj) = 99.9%

Analysis of Variance

Source	DF	SS	MS	F	P
Regression	1	118.254	118.254	13043.84	0.00000
Residual Error	9	0.08159	0.00907		
Total	10	118.336			

E. τ_c

Derived from regression of the sum of 100 + two Gompertz functions of τ_c:

-8.526exp[-exp(2.550 + 3.684τ_c)], for values of τ_c <=0; and

-9.020exp[-exp(2.336 – 3.428τ_c)], for values of τ_c >=0.

Predictor	Coef	SE Coef	T	P
Constant	0.030	0.453	0.067	0.948
Sum Gompertz f(tauc)	1.000	0.005	214.460	0.000

S = 0.033549 R-Sq = 100% R-Sq(adj) = 100%

Analysis of Variance

Source	DF	SS	MS	F	P
Regression	1	51.767	51.767	45992.91	0.00000
Residual Error	7	0.00788	0.00113		
Total	8	51.775			

F. n_{ci}

Predictor	Coef	SE Coef	T	P
Constant	100.119	0.082	1225.68	0.000
nci	-0.119	0.070	-1.697	0.165
abs(nci)	-3.038	0.135	-22.508	0.000

S = 0.111199 R-Sq = 99.3% R-Sq(adj) = 98.9%

Analysis of Variance

Source	DF	SS	MS	F	P
Regression	2	6.772	3.386	273.82	0.00005
Residual Error	4	0.04946	0.01237		
Total	6	6.821			

G. t_{ci}

Predictor	Coef	SE Coef	T	P
Constant	100.078	0.135	740.357	0.000
tci	1.038	0.129	8.055	0.000
abs(tci)	-5.588	0.238	-23.459	0.000

S = 0.240982 R-Sq = 98.6% R-Sq(adj) = 98.3%

Analysis of Variance

Source	DF	SS	MS	F	P
Regression	2	33.202	16.601	285.86	0.00000
Residual Error	8	0.46458	0.05807		
Total	10	33.666			

H. s_{cr}

Derived from regression of the sum of 100 + two Gompertz functions of s_{cr}:

$-14.47\exp[-\exp(1.807 + 2.310 s_{cr})]$, for values of $s_{cr} <= 0$; and

$-9.62\exp[-\exp(1.704 - 2.546 s_{cr})]$, for values of $s_{cr} >= 0$.

Predictor	Coef	SE Coef	T	P
Constant	-0.559	1.513	-0.369	0.720
Sum Gompertz f(scr)	1.006	0.016	64.154	0.000

S = 0.126103 R-Sq = 99.8% R-Sq(adj) = 99.8%

Analysis of Variance

Source	DF	SS	MS	F	P
Regression	1	65.447	65.447	4115.69	0.00000
Residual Error	9	0.14312	0.01590		
Total	10	65.590			

I. k_b

Derived from regression of the sum of 100 + two Gompertz functions of k_b:

$-3.011\exp[-\exp(2.387 + 4.071 k_b)]$, for values of $k_b <= 0$; and

$-2.885\exp[-\exp(2.186 - 3.774 k_b)]$, for values of $k_b >= 0$.

Predictor	Coef	SE Coef	T	P
Constant	-0.097	0.108	-0.898	0.411
X Variable 1	1.001	0.001	917.492	0.000

S = 0.002789 R-Sq = 100% R-Sq(adj) = 100%

Analysis of Variance

Source	DF	SS	MS	F	P
Regression	1	6.546	6.546	8.42E+05	0.00000
Residual Error	5	0.00004	0.00001		
Total	6	6.546			

J. τ_b

Derived from regression of the sum of 100 + two Gompertz functions of τ_b:

$-2.672\exp[-\exp(2.405 + 4.328\tau_b)]$, for values of $\tau_b <= 0$; and

$-2.507\exp[-\exp(2.905 - 5.006\tau_b)]$, for values of $\tau_b >= 0$.

Predictor	Coef	SE Coef	T	P
Constant	-0.163	0.096	-1.688	0.152
X Variable 1	1.002	0.001	1029.04	0.000

S = 0.002372 R-Sq = 100% R-Sq(adj) = 100%

Analysis of Variance

Source	DF	SS	MS	F	P
Regression	1	5.958	5.958	1.06E+06	0.00000
Residual Error	5	0.00003	0.00001		
Total	6	5.958			

APPENDIX M. INDIVIDUAL PARAMETER EQUIFINAL PROBABILITIES (Section 6.2 and Figure 6.1*q.v.*).

Full details of each individual parameter's metamodel, including source data for the regressions, model structure, R^2 score etc., are provided in Appendix L. Each prediction was booted using a parametric bootstrap, as explained in section 6.2 and Appendix L.

I. Sediment yield

	← Tolerance band, % →										
	0.05	**1**	**2**	**3**	**4**	**5**	**6**	**7**	**8**	**9**	**10**
k_w	2.47	52.65	97.39	100.00	100.00	100.00	100.00	100.00	100.00	100.00	100.00
m_w	12.54	95.82	100.00	100.00	100.00	100.00	100.00	100.00	100.00	100.00	100.00
k_d	5.97	98.55	100.00	100.00	100.00	100.00	100.00	100.00	100.00	100.00	100.00
k_f	0.46	9.15	18.79	27.91	37.50	47.16	56.08	65.78	75.51	85.02	94.34
τ_c	0.75	14.59	28.25	42.60	57.34	71.27	85.62	98.39	100.00	100.00	100.00
n_{ci}	3.72	76.84	99.85	100.00	100.00	100.00	100.00	100.00	100.00	100.00	100.00
t_{ci}	2.61	49.48	90.49	99.98	100.00	100.00	100.00	100.00	100.00	100.00	100.00
s_{cr}	2.04	39.27	79.72	99.76	100.00	100.00	100.00	100.00	100.00	100.00	100.00
k_b	7.28	99.98	100.00	100.00	100.00	100.00	100.00	100.00	100.00	100.00	100.00
τ_b	9.61	100.00	100.00	100.00	100.00	100.00	100.00	100.00	100.00	100.00	100.00

II. Drainage density

	← Tolerance band, % →										
	0.05	**1**	**2**	**3**	**4**	**5**	**6**	**7**	**8**	**9**	**10**
k_w	7.96	84.47	99.77	100.00	100.00	100.00	100.00	100.00	100.00	100.00	100.00
m_w	16.01	100	100	100	100	100	100	100	100	100	100
k_d	9.11	98.23	100	100	100	100	100	100	100	100	100
k_f	7.96	84.47	99.77	100.00	100.00	100.00	100.00	100.00	100.00	100.00	100.00
τ_c	8.79	97.99	100	100	100	100	100	100	100	100	100
n_{ci}	0.59	14.77	31.41	47.71	63.49	79.2	92.37	98.43	100	100	100
t_{ci}	0.66	13.18	26.77	40.51	54.33	67.3	81.19	93.55	99.37	100	100
s_{cr}	5.04	81.89	99.38	99.99	100	100	100	100	100	100	100
k_b	10.08	98.9	100	100	100	100	100	100	100	100	100
τ_b	6.8	92.43	100	100	100	100	100	100	100	100	100

III. Sediment delivery ratio

	← Tolerance band, % →										
	0.05	**1**	**2**	**3**	**4**	**5**	**6**	**7**	**8**	**9**	**10**
k_w	12.16	99.81	100.00	100.00	100.00	100.00	100.00	100.00	100.00	100.00	100.00
m_w	15.57	100.00	100.00	100.00	100.00	100.00	100.00	100.00	100.00	100.00	100.00
k_d	13.62	100.00	100.00	100.00	100.00	100.00	100.00	100.00	100.00	100.00	100.00
k_f	2.29	41.26	83.69	99.78	100.00	100.00	100.00	100.00	100.00	100.00	100.00
τ_c	12.96	99.97	100.00	100.00	100.00	100.00	100.00	100.00	100.00	100.00	100.00
n_{ci}	4.56	80.71	99.99	100.00	100.00	100.00	100.00	100.00	100.00	100.00	100.00
t_{ci}	2.83	54.28	92.78	99.86	100.00	100.00	100.00	100.00	100.00	100.00	100.00
s_{cr}	13.08	99.97	100.00	100.00	100.00	100.00	100.00	100.00	100.00	100.00	100.00
k_b	12.78	100.00	100.00	100.00	100.00	100.00	100.00	100.00	100.00	100.00	100.00
τ_b	14.79	99.99	100.00	100.00	100.00	100.00	100.00	100.00	100.00	100.00	100.00

IV. Topographic metric

	← Tolerance band, % →										
	0.05	**1**	**2**	**3**	**4**	**5**	**6**	**7**	**8**	**9**	**10**
k_w	28.27	51.33	54.32	57.07	59.77	63.29	67.58	80.06	100.00	100.00	100.00
m_w	97.97	100.00	100.00	100.00	100.00	100.00	100.00	100.00	100.00	100.00	100.00
k_d	11.45	100.00	100.00	100.00	100.00	100.00	100.00	100.00	100.00	100.00	100.00
k_f	14.66	39.73	48.72	55.78	62.24	68.99	75.67	83.45	91.88	96.12	99.99
τ_c	20.15	46.74	57.37	66.10	74.57	84.35	95.69	100.00	100.00	100.00	100.00
n_{ci}	6.21	40.89	78.09	98.92	100.00	100.00	100.00	100.00	100.00	100.00	100.00
t_{ci}	3.21	21.05	41.23	60.79	79.98	93.86	99.95	100.00	100.00	100.00	100.00
s_{cr}	4.49	36.09	49.81	60.80	70.09	80.02	90.49	96.41	99.96	100.00	100.00
k_b	22.91	56.74	82.53	100.00	100.00	100.00	100.00	100.00	100.00	100.00	100.00
τ_b	27.10	57.61	85.57	100.00	100.00	100.00	100.00	100.00	100.00	100.00	100.00

APPENDIX N. EQUIFINAL PROBABILITIES FOR EACH METRIC ACCORDING TO MODEL SIZE (Section 6.3 *q.v.*)

The order of inclusion of parameters is listed in Table 6.1.

I. Sediment yield

No. of params	← Tolerance band, % →										
	0.05	**1**	**2**	**3**	**4**	**5**	**6**	**7**	**8**	**9**	**10**
1	0.47	9.48	18.93	28.43	37.91	47.41	56.92	66.45	75.94	85.42	94.09
2	0.47	9.49	19.03	28.46	37.64	46.34	54.55	62.02	68.82	74.99	80.45
3	0.48	9.48	18.96	28.27	37.29	45.94	54.01	61.53	68.32	74.43	79.94
4	0.47	9.45	18.80	27.95	36.85	45.35	53.37	60.82	67.61	73.76	79.23
5	0.48	9.35	18.67	27.76	36.62	45.05	53.03	60.42	67.24	73.38	78.85
6	0.47	9.33	18.59	27.69	36.55	44.95	52.92	60.32	67.10	73.25	78.73
7	0.45	9.35	18.59	27.68	36.50	44.91	52.82	60.25	67.03	73.16	78.67
8	0.46	9.31	18.57	27.64	36.49	44.85	52.75	60.20	66.98	73.11	78.60
9	0.46	9.34	18.54	27.65	36.44	44.83	52.72	60.17	66.93	73.08	78.54

II. Drainage density

No. of params	← Tolerance band, % →										
	0.05	**1**	**2**	**3**	**4**	**5**	**6**	**7**	**8**	**9**	**10**
1	0.68	13.39	26.78	40.18	53.56	66.94	80.24	92.20	98.53	99.87	100.00
2	0.68	13.16	25.87	37.82	48.72	58.52	67.28	74.95	81.58	87.25	91.85
3	0.67	13.14	25.86	37.78	48.68	58.48	67.22	74.91	81.55	87.23	91.81
4	0.67	13.14	25.87	37.76	48.67	58.47	67.22	74.90	81.55	87.23	91.80

III. Sediment delivery ratio

No. of params	← Tolerance band, % →										
	0.05	**1**	**2**	**3**	**4**	**5**	**6**	**7**	**8**	**9**	**10**
1	2.15	42.97	83.64	98.84	100.00	100.00	100.00	100.00	100.00	100.00	100.00
2	2.12	40.52	72.12	91.46	98.38	99.92	100.00	100.00	100.00	100.00	100.00
3	1.97	38.13	69.22	88.93	97.34	99.56	99.98	100.00	100.00	100.00	100.00
4	1.99	38.03	69.02	88.71	97.18	99.51	99.97	100.00	100.00	100.00	100.00
5	1.96	37.91	68.77	88.45	97.03	99.48	99.97	100.00	100.00	100.00	100.00
6	1.95	37.73	68.51	88.17	96.90	99.45	99.96	100.00	100.00	100.00	100.00
7	1.96	37.63	68.36	88.02	96.75	99.38	99.94	100.00	100.00	100.00	100.00
8	1.95	37.61	68.31	87.96	96.72	99.37	99.94	100.00	100.00	100.00	100.00

IV. Topographic metric

No. of params	← Tolerance band, % →										
	0.05	**1**	**2**	**3**	**4**	**5**	**6**	**7**	**8**	**9**	**10**
1	8.45	18.89	32.15	46.51	59.12	69.98	79.57	87.37	93.05	96.49	98.33
2	2.95	6.75	13.05	21.38	30.88	40.85	51.06	61.09	70.39	78.42	84.89
3	1.15	2.71	5.66	10.28	16.54	24.19	33.11	42.91	53.22	63.45	73.06
4	0.61	1.47	3.25	6.33	10.98	17.19	24.74	33.54	43.10	53.07	62.94
5	0.17	0.45	1.07	2.37	4.61	8.15	13.13	19.54	27.22	35.95	45.37
6	0.24	0.59	1.37	2.88	5.44	9.25	14.32	20.75	28.36	36.88	46.06
7	0.24	0.60	1.39	2.91	5.50	9.34	14.45	20.95	28.60	37.16	46.29
8	0.24	0.60	1.39	2.92	5.50	9.34	14.46	20.95	28.61	37.17	46.29

APPENDIX O. MAIN EFFECTS PLOTS FOR THE THREE ALTERNATIVE METRICS (Subsection 6.4.1 and table 6.2*q.v.*).

Notes:
1. These plots are presented over the next eight pages in the same format as those for the four main metrics, in Figures 4.19 to 4.25.
2. Factorial points plots of mean sediment depth and the standard deviation of elevation differences, over time, are provided in Figures 4.16b and 4.13b respectively.
3. The factorial points results for median gradient were not plotted separately, as they are very similar to the data plotted in the graph of mean gradient, in Figure 4.17b.

Notes: 1. The letter above each graph denotes the parameter value being varied.
2. Median gradient reported throughout as tangent of the slope angle.
3. Legend: +α ; base case ; −α

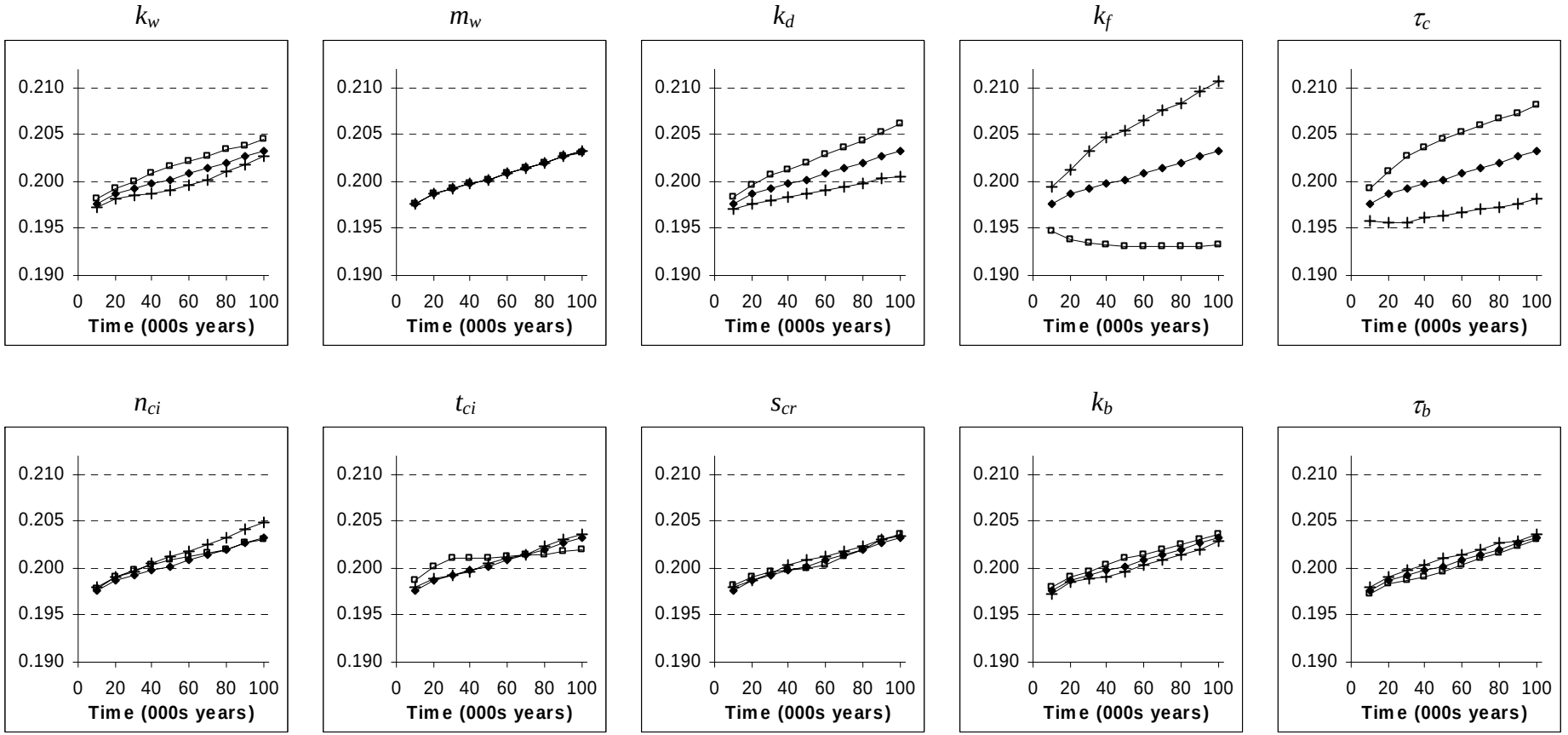

Figure Appendix O, 1a: Plots for each parameter of median gradient (y-axis) against time (x-axis), contrasting the star point and base case simulations.

Notes: 1. The letter above each graph denotes the parameter value varied.
2. Median gradient shown as tangent of the slope angle; y-axis ranges are common throughout, to emphasise differences between parameters in the main effects.

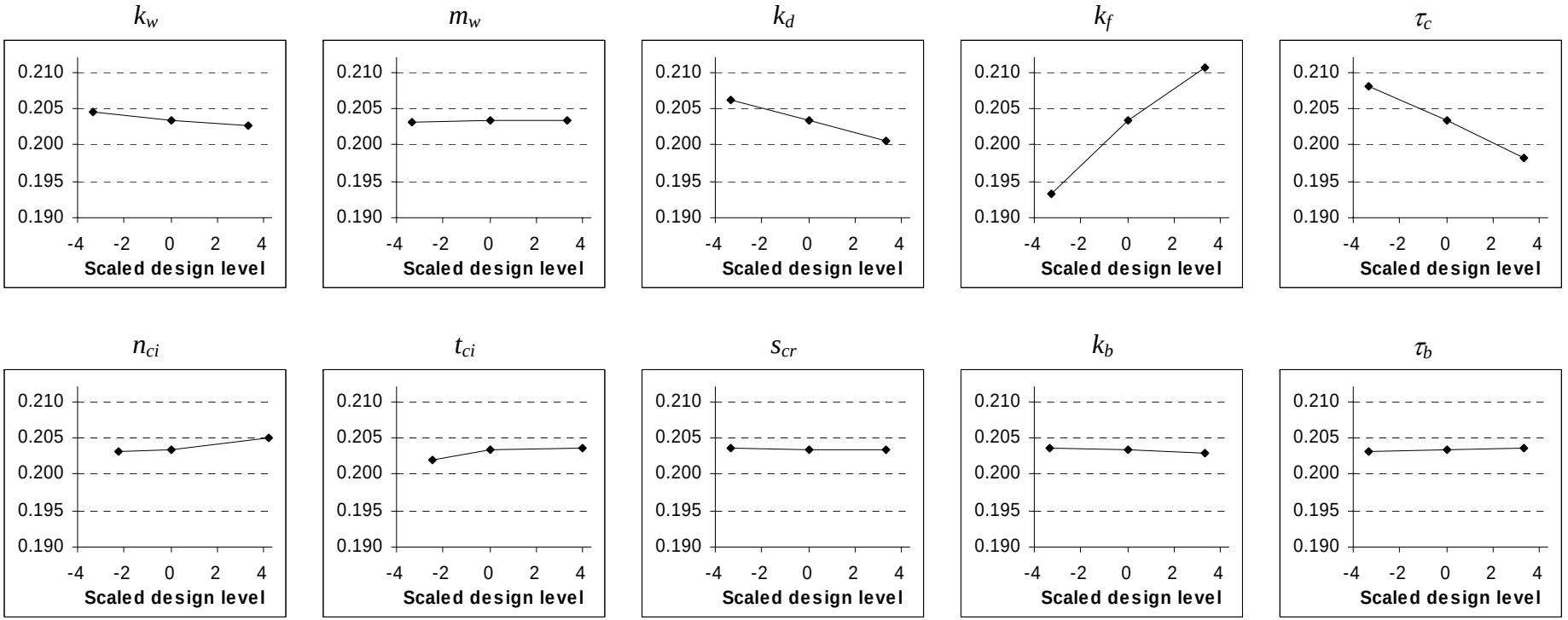

Figure Appendix O, 1b: Plots showing the main effects of each parameter on median gradient (y-axis) after 100,000 years. As with the similar plots in Chapter 4, only the star point and base case results are plotted, using scaled design levels for the parameter values (x-axis) (eq. 4.01 *q.v.*).

Notes: 1. The letter above each graph denotes the parameter value being varied.
2. Mean sediment depth throughout reported in metres.
3. Legend: +α ; base case ; −α

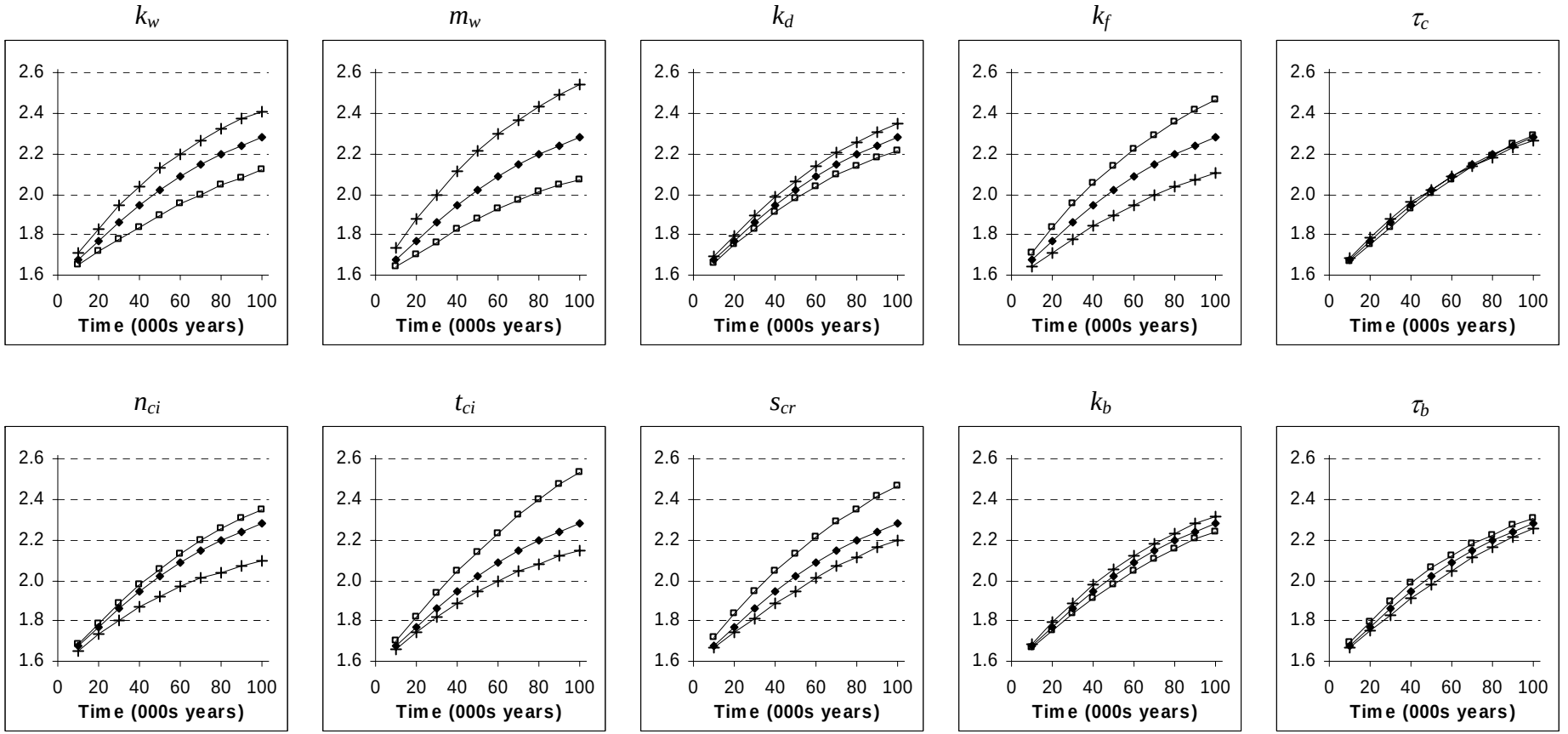

Figure Appendix O, 2a: Plots for each parameter of mean sediment depth (y-axis) against time (x-axis), contrasting the star point and base case simulations.

Notes: 1. The letter above each graph denotes the parameter value varied.
2. Mean sediment depth is shown in metres; y-axis ranges are common throughout, to emphasise differences between parameters in the main effects.

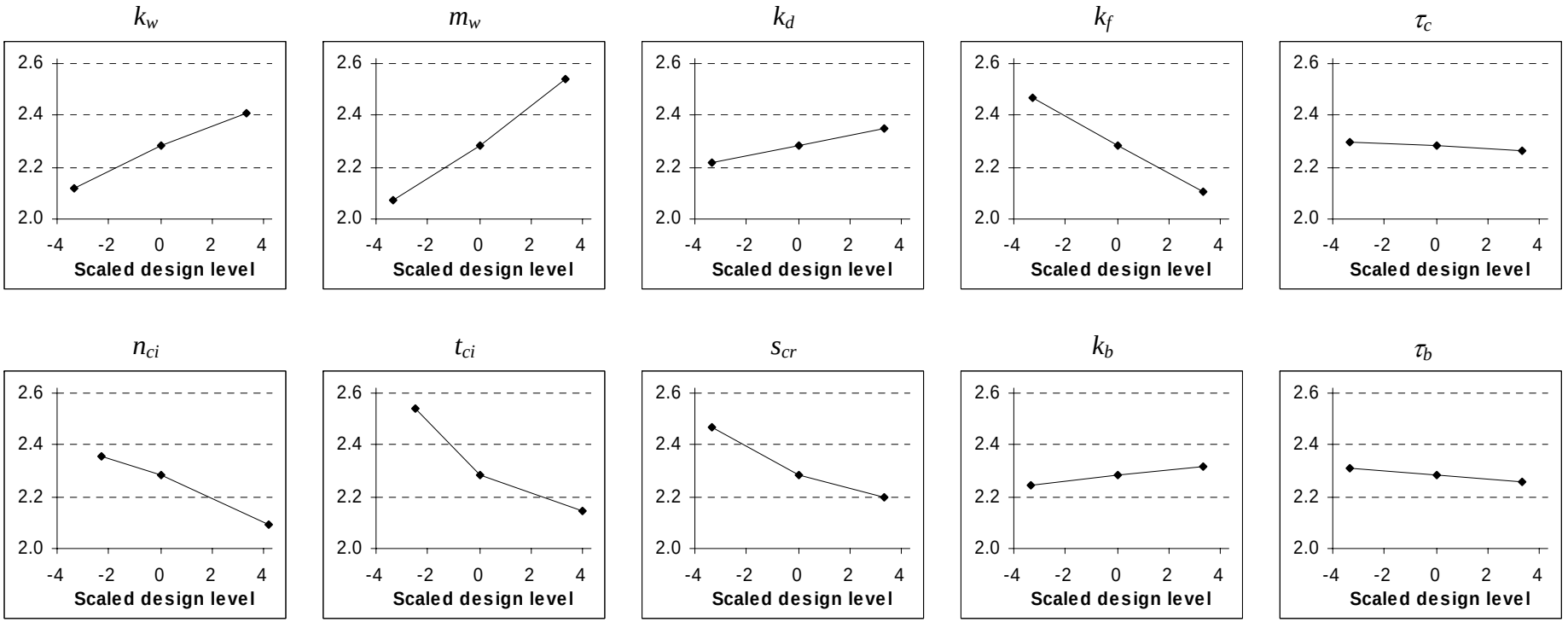

Figure Appendix O, 2b: Plots showing the main effects of each parameter on mean sediment depth (y-axis) after 100,000 years. As with the similar plots in Chapter 4, only the star point and base case results are plotted, using scaled design levels for the parameter values (eq. 4.01 *q.v.*).

Notes: 1. The letter above each graph denotes the parameter value being varied.
2. Standard deviation units are in metres.
3. Legend: '+' lower factorial point level; '-□-' upper factorial point level.

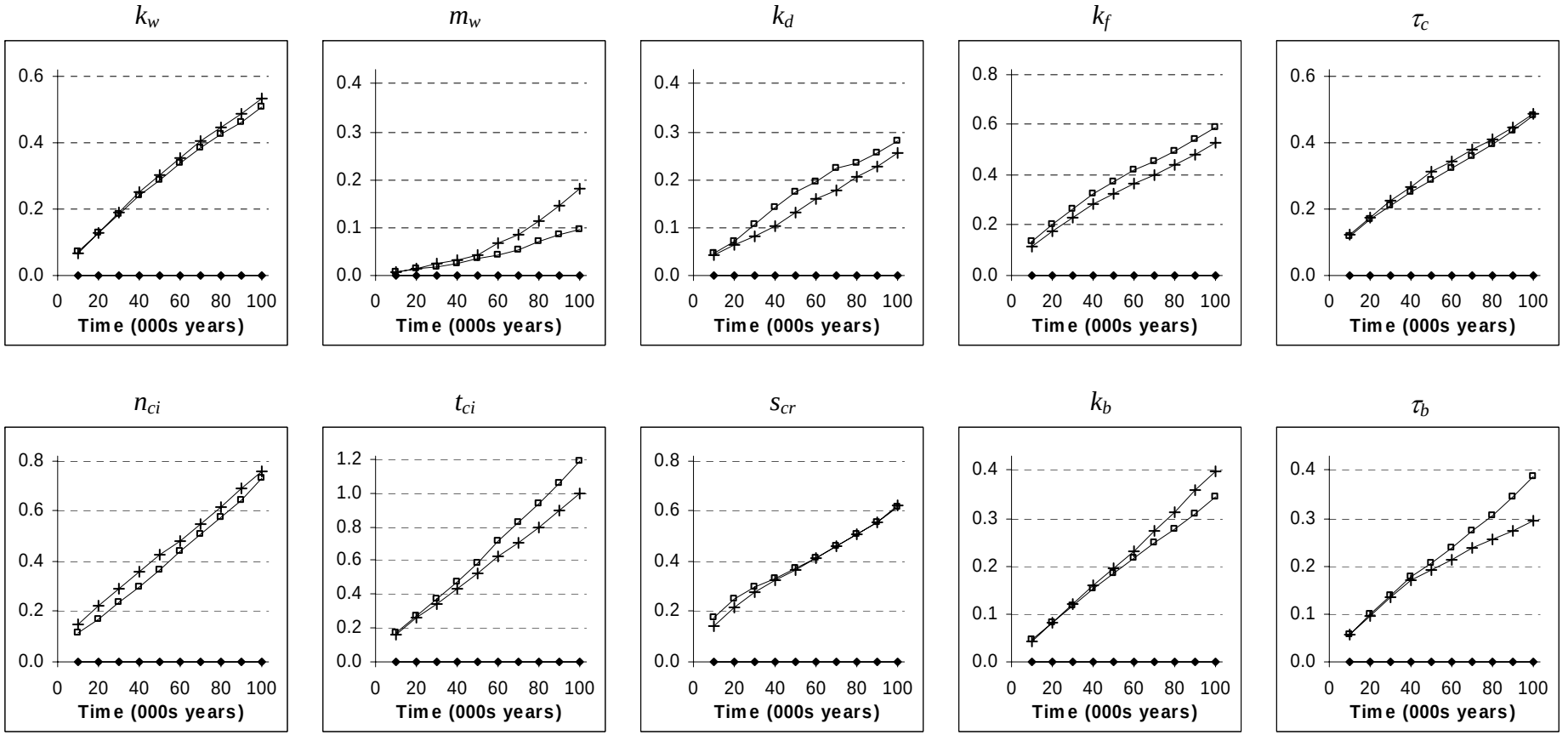

Figure Appendix O, 3a: Plots for each parameter of the standard deviation of elevation differences with the base case (y-axis) vs time (x-axis). Each plot shows the results generated using parameter values corresponding to the parameter's ± 1 design levels.

Notes: 1. The letter above each graph denotes the parameter value varied.
2. The topographic metric throughout is reported in %; y-axis ranges are also common throughout, to emphasise differences between parameters in the main effects.

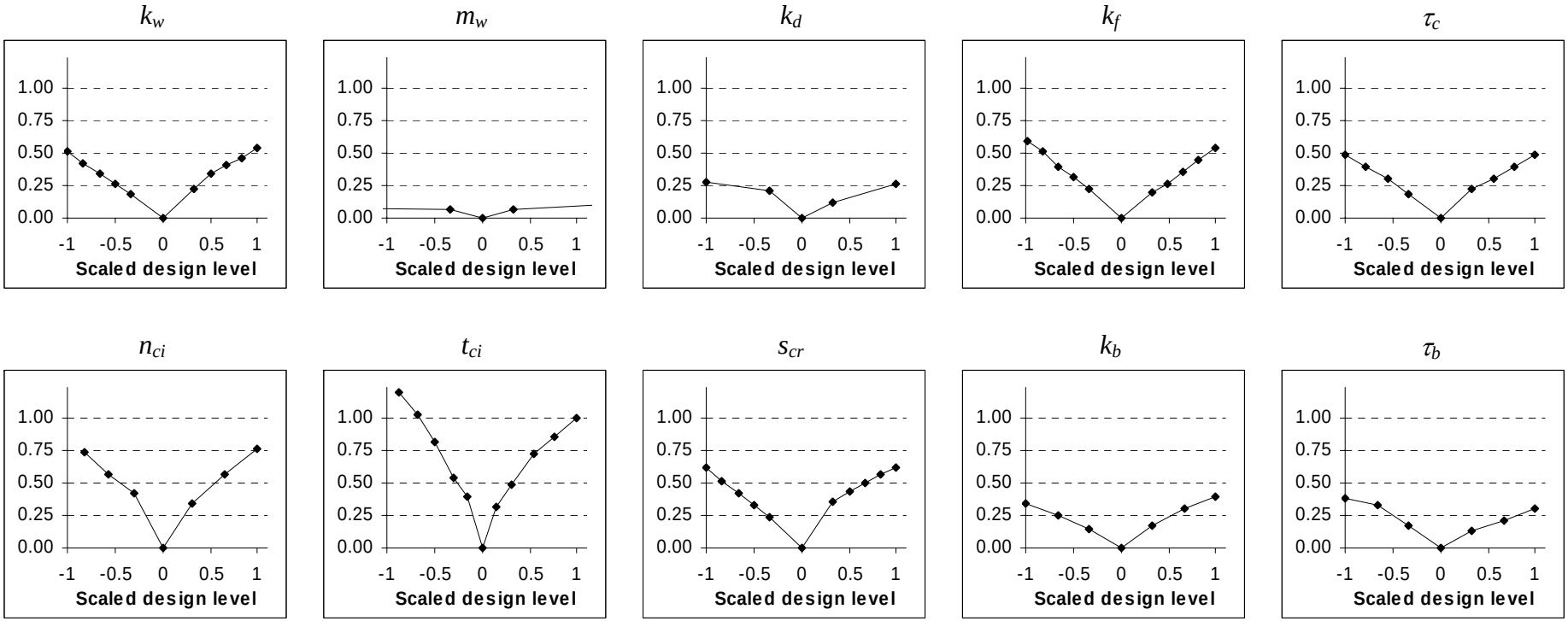

Figure Appendix O, 3b: Plots showing the main effects of each parameter on the standard deviation of elevation differences with the base case (y-axis) after 100,000 years. Note that the parameter value ranges are bounded by their factorial space values, and the plots show data from additional sample points used to clarify the main effects of each parameter. Parameter values are shown as scaled design levels (eq. 4.01 *q.v.*).

APPENDIX P. DETAILS OF REGRESSION ANALYSES FOR THE THREE ALTERNATIVE METRICS' METAMODELS (Table 6.2*q.v.*).

I. Median gradient – list of predictors and analysis of variance

The regression was conducted using scaled parameter values as per equation 4.05 and all of the central composite design results.

```
Predictor        Coef     SE Coef       T      P
Constant     0.203867    0.000958  212.86  0.000
kw          -0.0014534   0.0001529   -9.51  0.000
kd          -0.0050098   0.0002129  -23.53  0.000
kf           0.0151922   0.0004239   35.84  0.000
tauc        -0.0050507   0.0004237  -11.92  0.000
nci          -0.004825    0.001215   -3.97  0.000
nci^2        0.0023318   0.0005673    4.11  0.000
kb          -0.0011428   0.0001529   -7.47  0.000
(kd*tci)^2  0.00045617  0.00007040   6.48  0.000
(kf*tauc)^2 -0.0011659   0.0001907   -6.11  0.000

S = 0.000374764   R-Sq = 98.7%   R-Sq(adj) = 98.6%

Analysis of Variance

Source           DF          SS          MS        F      P
Regression        9  0.00143429  0.00015937  1134.69  0.000
Residual Error  139  0.00001952  0.00000014
Total           148  0.00145381
```

II. Mean sediment depth - list of predictors and analysis of variance

The regression was conducted using scaled parameter values as per equation 4.05 and all of the central composite design results.

```
Predictor       Coef   SE Coef       T      P
Constant     2.66326   0.05718   46.58  0.000
kw           0.24953   0.01389   17.97  0.000
mw          0.363683  0.005036   72.21  0.000
kd          0.100296  0.005036   19.92  0.000
kf           -0.42354   0.02795  -15.15  0.000
tauc         -0.11212   0.03082   -3.64  0.000
nci^2       -0.080097  0.002530  -31.66  0.000
tci          -0.48592   0.05156   -9.43  0.000
tci^2         0.16304   0.02015    8.09  0.000
scr          -0.37924   0.04191   -9.05  0.000
scr^2         0.10042   0.02080    4.83  0.000
kb            0.16709   0.02997    5.58  0.000
tb          -0.044822  0.005036   -8.90  0.000
(kw*tauc)^2 -0.023661  0.006257   -3.78  0.000
kf*tauc       0.13780   0.02748    5.01  0.000
tci*kb       -0.10444   0.02921   -3.58  0.000

S = 0.0123451   R-Sq = 99.1%   R-Sq(adj) = 99.0%

Analysis of Variance

Source           DF       SS       MS        F      P
Regression       15  2.31712  0.15447  1013.60  0.000
Residual Error  133  0.02027  0.00015
Total           148  2.33739
```

III. Standard deviation of elevation differences - list of predictors and analysis of variance

The regression was conducted using scaled parameter values as per equation 4.01, the base case and factorial point results from the central composite design sample, and all of the additional main effects test points.

Regression Analysis: std elev diffs versus kw, abskw, ...

Predictor	Coef	SE Coef	T	P
Constant	0.25957	0.01379	18.82	0.000
kw	0.036269	0.009035	4.01	0.000
abskw	0.16229	0.04225	3.84	0.000
abskf	0.19525	0.04268	4.57	0.000
absnci	0.52120	0.05612	9.29	0.000
abstci	0.82270	0.04847	16.97	0.000
absSCR	0.28177	0.04225	6.67	0.000
kb	0.055127	0.009100	6.06	0.000
kw*kf	-0.048718	0.009256	-5.26	0.000
kw*tci	-0.078802	0.009841	-8.01	0.000
kw*SCR	-0.097849	0.009187	-10.65	0.000
kw*kb	0.044765	0.009187	4.87	0.000
kw*tb	-0.045529	0.009187	-4.96	0.000
kf*tauc	-0.112733	0.009256	-12.18	0.000
kf*SCR	0.034771	0.009256	3.76	0.000
nci*tci	0.35550	0.01099	32.35	0.000
(nci*tci)^2	-0.86185	0.06318	-13.64	0.000
tci*kb	-0.066685	0.009841	-6.78	0.000
tci*tb	0.060305	0.009817	6.14	0.000
kb*tb	-0.040277	0.009187	-4.38	0.000

S = 0.103941 R-Sq = 97.5% R-Sq(adj) = 97.2%

Analysis of Variance

Source	DF	SS	MS	F	P
Regression	19	75.9284	3.9962	369.90	0.000
Residual Error	181	1.9555	0.0108		
Total	200	77.8839			